

The Water Uptake of Experimental Soft Lining Materials

Riggs, Paul David

The copyright of this thesis rests with the author and no quotation from it or information derived from it may be published without the prior written consent of the author

For additional information about this publication click this link.

<http://qmro.qmul.ac.uk/jspui/handle/123456789/1889>

Information about this research object was correct at the time of download; we occasionally make corrections to records, please therefore check the published record when citing. For more information contact scholarlycommunications@qmul.ac.uk

**The Water Uptake of Experimental
Soft Lining Materials.**

By Paul David Riggs.

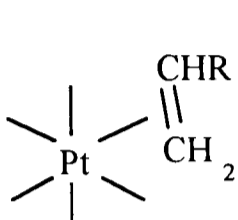
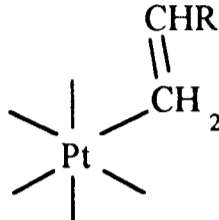
**A Thesis submitted to the University of London
for the degree of Doctor of Philosophy.**

**Department of Biomaterials in Relation to Dentistry,
St. Bartholomew's and the Royal London
School of Medicine and Dentistry,
Turner Street, London, E1 2AD.**

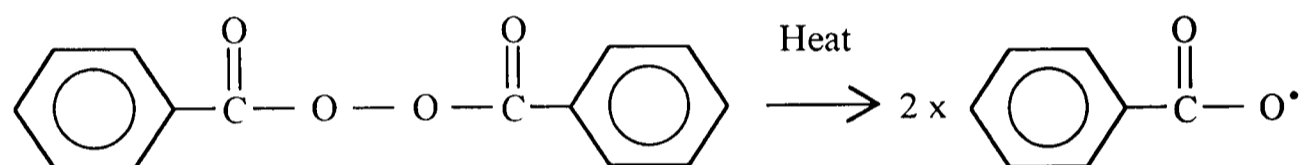
Errata Sheet.

1. Throughout the thesis the isotopes used for NMR experiments are referred to as H¹ and C¹³ rather than the correct IUPAC nomenclature of ¹H and ¹³C.

2. Nuclear magnetic resonance imaging is more properly known as magnetic resonance imaging (MRI).

3. Figure 4.3. (page 77) should be  , rather than .

4. Figure 5.1. (page 119) should have the initial decomposition of benzoyl peroxide as,



5. Benzoyl peroxide is wrongly referred to as benzol peroxide throughout the thesis.

6. Table 5.1 (page 123) has an incorrect caption for the units of molecular weight as g rather than molecular mass in g mol⁻¹.

7. In the references and the main text the author S. Downes is incorrectly spelt as Downs.

8. Two citations in the references the incorrect abbreviation Phd is used rather than PhD.

Abstract.

In order to develop a successful soft lining material various factors have to be considered; physical strength, adhesion to the denture base (or prosthetic) and the durability of the material's properties when in the mouth. It has been recognised that in order to fulfil these criteria the material must be stable and have a low water uptake from the aqueous environments of the mouth.

In the dental field comparatively little work has focused on how soft lining materials behave in water where as water in polymers has received a considerable amount of interest, with many different types of behaviour being observed and explained. It has been realised by previous authors that the water uptake of elastomers is primarily driven by soluble impurities, these form solution droplets within the material. The nature of the growth is somewhat more debatable, with both Fickian and dual sorption kinetics being reported.

Two basic types of materials were used in the study; silicone polymers and elastomer / methacrylate materials. Silicone polymers are characterised by a low water uptake and form the basis of perhaps the most successful soft lining material ('Molloplast B'). The elastomer / methacrylate materials were based on those developed by Parker (1982), Parker and Braden (1990) which showed considerable promise but suffered from an extensive protracted uptake. Water uptake at 37°C in conjunction with the tensile strength were used to evaluate the materials produced as these simple tests enabled the behaviour of the material in service to be estimated.

Three different types of silicone polymers were used during the study classified by the curing mechanism (condensation, peroxide and hydrosilanised), various fillers and additives (such as calcium stearate) were incorporated into the materials and different uptakes observed. The condensation silicones demonstrated large weight losses (up to 20 wt%) in water which is attributed to hydrolytic instability of the siloxane bridge in the presence of an organo tin compound leading to a leaching of siloxane. The pure peroxide and hydrosilanised materials both demonstrated a low water uptake but when doped they form solution droplets in a similar way to that described in the literature. Other additives showed different behaviour with the formation of cracks within the silicone due to failure of the material around the droplets, the action of hydrophilic but insoluble fillers also promotes the uptake. The hydrosilanised silicone polymers showed considerable promise as soft lining materials with low water uptake and good tensile strength.

The elastomer / methacrylate materials were based initially on butadiene styrene copolymer and a higher methacrylate monomer which formed a gel this was then free radically cured. The water uptake of these materials was attributed to soluble separating agent added to the butadiene styrene (to prevent particle agglomeration) during the production of the powdered elastomer. The extent of the uptake could be controlled by improving the strength of the material but the overall uptake remained too high. When the material was placed in an osmotic solution (Na Cl or glucose) the water uptake was significantly reduced and the behaviour could be described by a modified (for small strains) version of the Thomas and Muniandy (1987) theory for the growth of water droplets in a elastomer.

In order to reduce the water uptake of the elastomer / methacrylate materials butadiene styrene copolymers without separating agent was used. The emulsion polymerised material contained soluble impurities from the polymerisation (i.e. soap) which acted to drive the water uptake. Solution polymerised butadiene styrene also demonstrated a high uptake but this is attributed to a clustering behaviour of carboxylic and hydroxyl groups which formed post production. Similar behaviour is also seen for a solution polymerised isoprene styrene elastomer. The role of crosslinking the material in restraining the growth of the droplets is also investigated with dramatic reductions in the uptake being observed as the crosslink density increased. The employment of a reinforcing silica filler proved more effective than simply using a dimethacrylate. Oxidation is another problem (characterised by an upturn in the absorption), although not observed in every case it was a problem for all of the unsaturated elastomers and was found to be promoted by ions present within saliva. Saturated butyl based (including chloro and bromo butyl) elastomers were used instead and did not show any tendency for oxidation but they still showed an uptake of approximately 3 to 4 wt%. Their stability however and reasonable strength makes them suitable for further development as soft lining materials.

Theoretical considerations were investigated by H^1 NMR imaging with the formation of droplets being observed, the profiles seen indicating the absorption to be two stage rather than Fickian. The role of creep or stress relaxation is also identified as a mechanism for extending the uptake by reducing the restraining force. Further reasoning on all the data presented here concluded the role of chemical potential change associated with the water into the matrix or the droplets will determine the nature of the uptake observed.

Acknowledgements.

Firstly I would like to thank my supervisor Dr Sandra Parker for guidance, patience, and friendship over the last few years. Professor Michael Braden for his inspiration, experience and assistance in all areas of the project particularly the mathematical aspects. Together with all the other members of the department (past and present) who have helped greatly with the project, always provided a diversion and never been short of an opinion on any subject.

Most of all I should also thank the people who have supported and provided much needed diversion in recent years and over the course of my life so far. Especially Eve, my mother, Andy, Kumar, Saj and all my family, to name a few.

I am also very grateful to Dr Paul Kinchesh (Dept. of Chemistry, Queen Mary Westfield College), Mrs Jane Hawkes (Dept. of Chemistry, King's College) and U.L.I.R.S. (University of London Intercollegiate Research Services) for assistance and enabling the nuclear magnetic resonance studies. Dr Sid Kalachandra (Dept. of Chemistry, Virginia Tech, Blacksburg, Virginia, U.S.A.) and the National Institute of Health for funding the project (NIH Grant No. DE 094250). Finally all the companies and people who have given samples or information for the project.

Contents.

	Page
Title Page.....	i
Abstract.....	ii
Acknowledgements.....	iii
Contents	iv
List of figures.....	ix
List of tables	xvi
1. Introduction	1
1.1. Forward	2
1.2. Soft lining materials.....	2
1.2.1. Plasticised methacrylate materials.....	4
1.2.2. Silicone based materials	5
1.2.3. Elastomer based systems.....	6
1.3. Summary.....	8
1.4. Scope of thesis	9
2. Literature review	12
2.1. Water absorption into polymers.....	13
2.2. Diffusion	14
2.2.1. Fick's laws	14
2.2.2. Solutions to Fick's second law.....	15
2.2.3. Concentration dependence of the diffusion coefficient	18
2.3. Hydroscopic properties of polymers	22
2.3.1. Free volume or micro voids within the polymer.....	23
2.3.2. The states of water within polymers.....	25
2.3.3. Water clusters within polymers	29
2.3.4. Dual sorption models (Flory-Huggins, Langmuir and Zimm Lundberg)	33
2.3.5. Modelling of the formation of droplets within elastomers	38
2.3.6. Permeation of elastomers	49
2.4. Crack formation	52
2.5. Oxidation and diffusion	56
2.6. Case II diffusion.....	58
2.6.1. Hydrogels and ionizable gels.....	62
2.7. Monte-carlo simulation.....	63
2.8. Drug delivery	67

Contents continued.

	Page
3. Methodology	67
3.1. Sample Preparations	68
3.2. Tensile strength	68
3.3. Water absorption	70
3.4. Other tests	70
4. Silicone polymers	72
4.1. Introduction	73
4.2. Curing of silicone polymers	74
4.2.1. Acetoxy curing silicones	74
4.2.2. Condensation silicone polymers	75
4.2.3. Peroxide addition	76
4.2.4. Hydrosilanised silicones	76
4.3. General formulation of silicone polymers	78
4.3.1. Fillers for silicone polymers	79
4.3.2. Degradation of silicone polymers	83
4.4. Development of silicone polymers	84
4.5. Condensation silicone polymers	86
4.5.1. Formulation of condensation silicone polymers	86
4.5.2. Results for the condensation silicone materials	87
4.6. Peroxide silicone polymers	93
4.6.1. Formulation of peroxide silicone polymers	93
4.6.2. Results for the peroxide silicone polymers	94
4.7. Hydrosilanised silicone polymers	104
4.7.1. Formulation of hydrosilanised silicone polymers	104
4.7.2. Results for the hydrosilanised silicones	105
4.8. Summary of silicone polymer results	114
5. Elastomer / methacrylate materials	116
5.1. Overview	117
5.2. Methacrylates	121
5.2.1. Water uptake of the methacrylate homopolymers	123
5.3. Powdered butadiene styrene samples (PBS)	127
5.3.1. Tensile strength of PBS based materials	129
5.3.2. Water uptake of PBS materials	132

Contents continued.

	Page
5.4. Water uptake of PBS materials from solutions of different osmotic pressures	139
5.4.1. Formulation of an artificial saliva	139
5.4.2. Behaviour of PBS based materials in NaCl solutions	141
5.4.3. Behaviour of PBS5+ in other solutions	144
5.5. Osmotic pressure and the small strain theory.....	146
5.5.1. Small strain theory for droplet formulation.....	146
5.5.2. Application of the small strain theory to the PBS based materials	149
6. Development of the elastomer /methacrylate materials.....	156
6.1. Introduction	157
6.2. Comparison of different elastomers.....	157
6.2.1. Tensile results from the different elastomers.....	159
6.2.2. Water uptake of emulsion elastomer based materials (HBS)	160
6.2.3. Water uptake of the solution polymerised elastomers	162
6.3. Oxidation of the elastomers	165
6.3.1. Oxidation of SBS from different environments	168
6.3.2. Acetone extraction of the materials	171
6.3.3. Suitability of the elastomer methacrylates.....	173
6.4. Butyl elastomers.....	174
6.4.1. Tensile strength of butyl based materials	176
6.4.2. Water uptake of butyl based materials.....	176
6.5. Re formulation of the elastomer methacrylate materials.....	180
6.5.1. Reinforcement of elastomer by silica fillers.....	180
6.5.2. Results from the filled EBS5+ samples	181
6.5.3. Re formulation of SIS based materials.....	186
6.5.4. Results of the SIS based materials.....	187
6.5.5. Re formulation of PBB based materials	193
6.5.6. Results of the reformulated PBB based materials.....	193
7. Nuclear magnetic resonance imaging.....	198
7.1. Introduction	199
7.2. Methodology.....	200
7.3. Results of NMR imaging experiments.....	203
7.3.1. The kinetics of the absorption	207
7.3.2. Results of Si NB A	211

Contents continued.

	Page
7.3.3. Correlation of the intensity with water uptake	214
7.3.4. Crack formation.....	217
8. Discussion and Conclusions.....	219
8.1. Stress relaxation, creep and the restraining force.....	220
8.2. The desorption diffusion coefficient.....	223
8.3. The absorption coefficient	228
8.4. The nature of the water uptake into elastomers.....	236
8.4.1. The initial kinetics.....	237
8.4.2. The later stages of water absorption.....	239
8.4.3. Free energy and water absorption.....	240
8.5. Clustering during water uptake.....	244
8.6. Summary of diffusion into elastomers	245
8.7. Implications for soft lining materials	249
8.8. Recommendations for further study.....	251
References	253
Appendices	276
I. The formulation of Molloplast B	277
II. Diffusion.....	280
II.a. Fick's laws	280
II.b. Solutions to Fick's second law.....	282
II.c. The equations of Muniandy and Thomas	287
III. Nuclear magnetic resonance (NMR) imaging.....	294
IV. Polymer Solubility and Miscibility	296
V. Modification of theory of water uptake into elastomers for small strains.....	302

List of Figures.

	Page
1.1. Illustration of the application of a soft lining material to a lower denture.	3
2.1. A typical water uptake of elastomer	13
2.2. Concentration profile of diffusion into a semi-infinite media as predicted by equation 2.3, at different times.	15
2.3. Concentration profile as predicted by equation 2.5 at different times with respect to distance though sample, x	16
2.4. M_t/M_∞ against time as predicted by equation 2.6, (solid line) and equation 2.6 (dotted line)	17
2.5. Concentration dependence of diffusion coefficient as a function of c for various functions of f(c) based on equation 2.10, based on Crank, 1975, for diffusion into a semi-infinite media.....	19
2.6. Graph of the diffusion coefficient (D) as a finction of c/c_0 where c_0 is equilibrium concentration, based on Blackband and Mansfield, 1986	20
2.7. Dependence of diffusion coefficient on concentration of water for a series of halogen-containing epoxies, based on Barrie et al, 1985	20
2.8. Effect of partial pressure of water on concentration and the resultant effect on the diffusion coefficient for a rubbery polyurethane, based on Schinder et al, 1968	21
2.9. Schematic of polyethylene chain with planar zig zag resulting in two free volumes available for water absorption (based on Pace and Datyner, 1980).....	24
2.10. Variation of projected intensity though a sample of Nylon 6,6 with different T_e times after 8 hours exposure to water at 100°C. Based on Fyfe et al, 1993	26
2.11. DSC melting endotherms of water in grafted Nylon-6 membranes, based on Takigami et al, 1993	28
2.12. Dielectric relaxation spectra of polyimide film at a frequency of 1Khz after saturation in different relative humidities, based on Lim et al, 1993.....	29
2.13. Schematic of expansion of water droplets within a material.	31
2.14. The miscibility of different polymer solutions with a range of different χ values..	35
2.15. The prediction of water uptake from solutions of different activities using the dual sorption model (equation 2.17) , data from for Nylon 6 at 5°C, Hernandez and Gavara, 1994.....	36
2.16. Prediction of equation 2.40, using the data of Barrie et al, 1975, the full line indicating the predicted values, based on Muniandy and Thomas, 1987	46
2.17. Model of absorbance profile inside membrane, based on Harrison et al, 1991	48

List of figures continued.

	Page
2.18. Permeation rate with time for a Neoprene rubber from distilled water and simulated sea water (3.45 % NaCl) at different temperatures, based on data in Cassidy et al, 1983	51
2.19. Formation of cracks within polymer due to osmotic pressure from droplet solutions	53
2.20. Water uptake and salt release from a silicone rubber doped with 11.5 wt% NaCl and a drug (sulphanilamide), based on Di Colo, 1992.	53
2.21. Type of results obtained for Case II diffusion into polymer in terms of concentration with distance into polymer and time.....	58
2.22. Change of Case II to Fickian, based on Thomas and Windle, 1982.....	60
3.1. Moulding of a sample between two plates.	69
3.2. Schematic of dumbbell used in tensile tests.....	69
4.1. Typical condensation curing reaction.....	75
4.2. Hydrosilation curing reaction.....	76
4.3. Action of platinum catalyst.....	77
4.4. Relationship between stress/strain curves and molecular weight of unfilled vinyl siloxane polymer of a hydrosilanised silicone (k = 1000) based on Bontems et al 1993.....	79
4.5. Effect of silica (200 m ² /g) loading (parts per hundred) on peroxide cured silicone (based on Cochrane and Lin, 1993).	80
4.6. The possible orientation and surface states of silica.	81
4.7. Hydrogen bonding of siloxane to silica surface.	81
4.8. Silanation of a silica.	82
4.9. The structure of L77.	86
4.10. UTS results for the condensation silicones.....	88
4.11. Absorption results for condensation silicones.	89
4.12. C ¹³ NMR spectrum of leached from CB972, scan performed by Mrs J. Hawkes, Department of. Chemistry, King College London. The lower spectrum is a magnification of the low intensity peaks.	90
4.13. Tensile properties of peroxide cure silicone polymers.	95
4.14. The effect of hydrophilic and hydrophobic fillers on the water uptake of peroxide silicone polymers.....	97
4.15. The effect of additives on the water absorption of P200	98
4.16. Initial period of the uptake of P200 based CS doped materials.....	98
4.17. The effect of NaF on water uptake of P974.....	99

List of figures continued.

	Page
4.18. Initial period of the water uptake of P974 NF plotted against time $\frac{1}{2}$ for the first and second absorption cycles	100
4.19. Initial period of water uptake of P974 NF plotted against time for the first and second absorption cycles	100
4.20. The effect of additives on the water uptake of P974	101
4.21. Initial water uptake of P974 based doped materials	102
4.22. Tensile strength of hydrosilanised silicone materials.....	106
4.23. Water absorption of the stoichiometrically balanced silicone materials	107
4.24. Initial period of water absorption of the stoichiometrically balanced silicone materials	108
4.25. Water absorption characteristics of H200 5	113
5.1. Possible reactions of the methacrylate monomer and elastomer within due to the peroxide radical	119
5.2. The effect of powder liquid ratio on the viscoelastic properties of Pulvatex based materials. Reproduced from Parker (1982), figure 4.2 page 124, or Parker and Braden, 1990	120
5.3. Plot of energy to rupture (w) as a function of concentration of the cross linking agent, for a series of elastomeric poly (alkyl methacrylate)s. Reproduced from Davy and Braden (1987).....	122
5.4. Water uptake of soft mono methacrylates.....	124
5.5. Water uptake of di methacrylates	125
5.6. Equilibrium water uptake of the methacrylate materials against the δ_p	127
5.7. Breakdown of AZBN.....	128
5.8. Summary of the strength data for of the initial formulations of the PBS materials	129
5.9. Initiation rates of Benzol peroxide and Lauryl peroxide in benzene, based on data in Brandrup and Immergut, 1975.....	131
5.10. Strength of 50:50 PBS and EHM based materials.....	132
5.11. Water uptake of PBS based materials.....	134
5.12. Water uptake of PBS based materials up to 10 wt%.....	134
5.13. Water uptake of the PBS materials over the initial period	135
5.14. Water uptake of the cast and purified PBS	136
5.15. Desorption of the PBS materials after 196 days.....	137
5.16. First and second water uptakes of the HM based PBS materials removed from the first absorption after 196 days	137

List of figures continued.

	Page
5.17. Initial period of first and second water uptakes of the HM based PBS materials removed from the first absorption after 196 days.	138
5.18. First and second water absorption of EHM based PBS samples of the samples removed from first cycle after 196 days.....	138
5.19. Initial period of first and second water absorption of EHM based PBS samples of the samples removed from first cycle after 196 days	139
5.20. Water uptake of PBS5+ from NaCl solutions	142
5.21. Water uptake of PBS1 from NaCl solutions	142
5.22. Water uptake of PBS2 from NaCl solutions	143
5.23. Water uptake of PBS5+ from different solutions	145
5.24. Graphical representation of equation 5.3	147
5.25. Small strain theory in comparison with predicted values of c_w from small strains theory equation 5.3, and the full theory i.e. equations 5.1. and 5.4	148
5.26. Comparison of equation 5.3, 5.5 and 5.6, for predicting the c_w dependence on π_o	149
5.27. PBS5+ equilibrium uptake from different solutions.....	150
5.28. Correlation between data and calculated figures	151
5.29. Relationship between D_{abs} size of droplets c_w -s.....	152
5.30. Relationship between log D against log c_w -s.....	153
5.31. Correlation between the experimental and calculated diffusion coefficients	154
6.1. Strength results for the elastomers.....	159
6.2. First absorption of emulsion elastomer based materials	160
6.3. Water uptake of the pure elastomers	161
6.4. Comparison of the first and second absorption cycles for the emulsion polymerised elastomer based materials	162
6.5. Water absorption of solution polymerised elastomer based materials	163
6.6. Comparison of first and second absorption cycles of solution polymerised elastomers.....	165
6.7. Infra red spectra of PBS1 from different environments, range 400 to 2000 cm^{-1}	166
6.8. Infra red spectra of PBS1 from different environments, range 2000 to 4000 cm^{-1}	166
6.9. Oxidation of butadiene, as illustrated by Brydson (1978)	167
6.10. Water uptake of SBS5+ in NaCl solutions.....	169
6.11. Initial water uptake of SBS5+ in NaCl solutions.....	169
6.12. Water uptake of SBS5+ from artificial saliva and de ionised water	170

List of figures continued.

	Page
6.13. Water uptake of acetone extracted samples	172
6.14. Initial water uptake of acetone extracted samples	173
6.15. Water uptake of butyl based materials	177
6.16. First and second water uptake of butyl based elastomers	178
6.17. Comparison of acetone extracted and normal PCB5+	178
6.18. Water uptake of pure butyl elastomers	179
6.19. Tensile strength of filled EBS5+ materials	182
6.20. Water uptake of filled EBS5+ materials	183
6.21. First and second absorption of filled EBS5+ materials	183
6.22. Initial first and second absorption of filled EBS5+ materials	184
6.23. Relationship between modulus and the water uptake	186
6.24. Tensile strength of SIS based materials reformulations: Part I	188
6.25. Water absorption of SIS based materials: Part I	189
6.26. Initial water absorption of SIS based materials: Part I	189
6.27. Tensile strength of SIS based materials reformulations: Part II	190
6.28. Water absorption of SIS based materials: Part II	191
6.29. Tensile strength of the PBB B based materials with different levels of elastomer	194
6.30. Tensile strength of the reinforced PBB B based materials	195
6.31. The loading rate dependence of the strength of PBBB 80/20 C2.5	196
6.32. Water absorption of PBBB based materials	197
7.1. Simplified pulse sequence of H ¹ NMR used in imaging experiments	201
7.2. NMR Pulse sequence for T _e 40 ms experiment	202
7.3. NMR Pulse sequence for T _e 9 ms experiment	203
7.4. Image of droplets within a NaBr doped silicone sample at approximately 6 months	204
7.5. Initial image of the samples before immersion in water (t _e 40 ms)	204
7.6. Water uptake of the silicone cylinders used in this study	205
7.7. Image of samples after 9 days immersion in water (t _e 40 ms)	206
7.8. Average of samples 8 slices of the samples after 9 days immersion in water (t _e 40 ms)	207
7.9. Profiles of Si NB A at different times of the averaged t _e 40 ms experiment	208
7.10. Profiles of Si NB A at different times of the averaged data t _e 9 ms experiment ..	208
7.11. Fickian distribution for diffusion in a cylinder using equation 7.1	209
7.12. Profiles of Si CS at different times of the averaged data t _e 9 ms experiment	210
7.13. Profiles of Si L77 at different times of the averaged data t _e 9 ms experiment	211

List of figures continued.

	Page
7.14. The intensity of the value calculated from the averaged images of Si NB A	212
7.15. The normalised intensity of the value calculated from the averaged images of Si NB A.....	213
7.16. Decay of NMR signal intensity with time.....	214
7.17. Correlation between average intensity for the T_e 40 ms experiment and water absorption.....	215
7.18. Correlation between average intensity for the T_e 9 ms experiment and water absorption.....	216
7.19. Normalised intensity at T_e 9 ms against time.....	217
7.20. Formation of crack in the Si NB B sample shown as a series of slices along the sample at 158 days with a T_e of 40 ms.....	218
8.1. Comparative water uptake of materials of different types.....	220
8.2. Relationship between $\tan \delta$ (0.2, 0.1, 0.05 and 0.01) and water uptake as predicted by equation 8.2, and 8.3, assuming small strains applies (i.e. $\lambda = 1+\epsilon$)	222
8.3. The relationship between total water uptake and desorption diffusion coefficient	224
8.4. The relationship between total water uptake and desorption diffusion coefficient, ignoring extreme point	225
8.5. The relationship between total water uptake and desorption diffusion coefficient, for the slower diffusion materials.....	225
8.6. The relationship between total water uptake and desorption diffusion coefficient, as a logarithmic relationship	226
8.7. The logarithmic relationship between total water uptake and desorption diffusion coefficient of Southern and Thomas (1980) for natural rubber and NaCl doped poly isoprene from NaCl solutions.....	228
8.8. The relationship between total water uptake and absorption diffusion coefficient for silicone materials	229
8.9. The relationship between total water uptake and absorption diffusion coefficient for silicone materials, enlargement of the lower absorbencies.....	229
8.10. The relationship between total water uptake and absorption diffusion coefficient for silicone materials, as a logarithmic relationship.....	230
8.11. Comparison of observed desorption data (M_t/M_∞) against normalised time ($[t.D]^{1/2}$) for the PBS5+ material in saline solutions.....	231
8.12. Comparison of observed absorption data (M_t/M_∞) against normalised time($[t.D]^{1/2}$) for the PBS5+ material in saline solutions.	232

List of figures continued.

	Page
8.13. Comparison of observed absorption and desorption data (M_t/M_∞) against normalised time($[t.D]^{1/2}$) for the P200 CS material.....	232
8.14. Correlation of equation 8.9 and the true data as calculated from equation 2.6.....	234
8.15. Correlation of equation 8.9, and PBS5+ absorption data from water	236
8.16. The change in chemical potential with the increasing volume fraction of water as predicted by equations 8.11, 8.12 and 8.13, using χ of 2	241
8.17. The change in chemical potential with the increasing volume fraction of water as predicted by equations 8.11 and 8.13, using χ of 5.31 for silicone and water (Favre et al, 1994) with NaCl as the impurity	243
8.18. The change in chemical potential with the increasing volume fraction of water as predicted by equations 8.11 and 8.13, using χ of 5.31 for silicone and water (Favre et al, 1994) with calcium stearate as the impurity.....	243
8.19. Illustration of sequence of water moving into the elastomer and the concentration profile across the material.	246
8.20. Illustration of different types of water uptake into the elastomer and the subsequent mass uptake profile	248
I.1. Infra red spectrum of Molloplast B and RTV 108.....	278
II.1. Element for diffusion model	280
IV.1. Equilibrium swelling as a function of solubility parameter of the solvent for linear and cross linked polymers (Based on figure 7.1, page 130, Van Krevelen, 1976)	297

List of Tables.

	Page
1.1. Water uptake of soft lining materials after long periods (at least a year).....	10
2.1. Barrie et al, 1975, data for a NaCl doped poly isoprene.....	46
4.1. Codes for the materials used in the formulation of silicone polymers.....	85
4.2. Composition of condensation silicones, based on SOH.....	87
4.3. Composition of CB972 as two part paste	87
4.4. Summary of absorption data for condensation silicones	89
4.5. Intensities of NMR spectra from CB972 leachant from D ₂ O.....	91
4.6. Formulation of peroxide cure silicone polymers, the siloxane used was SCC.....	94
4.7. Summary of absorption data for the peroxide cured silicone polymers	103
4.8. Summary of second absorption data for the peroxide cured silicone polymers...	103
4.9. Formulations of Hydrosilanised materials	104
4.10. Formulation for 20g of H974 V as two part paste	105
4.11. Summary of absorption data of hydrosilanised silicone polymers at 196 day	108
4.12. Water absorption attributed to different elements of the composition for the stoichiometrically balanced Hydrosilanised silicone polymers.....	109
4.13. Mechanical properties of matrix relative to droplet for the H974 H and H974 CS.....	111
4.14. Diffusion coefficients calculated from Muniandy and Thomas for the H974 H and H974 CS	112
5.1. The codes of the methacrylates used	123
5.2. Summary of water uptake of methacrylates	124
5.3. Initial formulation of the PBS based materials, the percentages are expressed in terms of the monomer. These monomer formulations were then mixed with the elastomer to monomer in the ratio's 50:50, 60:40 and 70:30	128
5.4. Second formulations based on the PBS elastomer and EHM monomer 50 : 50 ratio	131
5.5. PBS based materials for absorption	133
5.6. Summary of the first absorption and desorption results for the PBS samples after 196 days	135
5.7. Composition of artificial saliva as used by Avidson and Johansson (1985)	141
5.8. Summary of absorption data of PBS5+ from NaCl solutions.....	144
5.9. Summary of absorption of PBS1 and PBS2 from NaCl solutions.....	144
5.10. Summary of absorption data of PBS5+ from different solutions.....	145
5.11. Summary of PBS5+ data from different solutions.....	150
5.12. Summary of PBS1 and PBS2 data from different solutions.....	151

List of tables continued.

	Page
5.13. Values calculated from small strains theory using equation 5.6, from PBS based materials	151
5.14. Regression of log diffusion coefficient against concentration of water within the polymer.....	153
6.1. Specification of HBS elastomer, supplied by Shell chemicals Ltd.....	158
6.2. Specification of EBS, SBS and SIS elastomers, supplied by Enichem elastomeric Ltd and Shell chemicals Ltd	158
6.3. Summary of water uptake for the elastomer based materials.....	161
6.4. Summary of water absorption data for SBS5+ in different solutions	168
6.5. Summary of the acetone extraction samples and the ash testing of the elastomer materials	171
6.6. Composition of butyl based materials	175
6.7. Tensile strength of butyl based materials.....	176
6.8. Summary of water uptake of butyl based materials	177
6.9. Silicas used for reinforcement of elastomers	181
6.10. Formulation of EBS 5+ materials with a 50/50 ratio of monomer to elastomer	181
6.11. Summary of water absorption data for the reinforced EBS5+ materials, first absorption values at 203 days and 2nd absorption value at 238.....	182
6.12. Modulus and $\tan \delta$ of filled EBS5+ materials at 37 °C, data supplied by S.Kalachandra and D.Xu.....	184
6.13. Re formulation of SIS based materials formulations.....	187
6.14. Summary of water uptake of SIS based materials	192
6.15. Formulation of the PBB and BM based materials	193
6.16. Summary of absorption of PBB B based materials.....	196
7.1. Formulation of unfilled stoichiometrically balanced silicone polymers catalysed with VPT	200
7.2. Selective parameters used in the imaging experiments	202
7.3. Averages of the Control and Si Pure profile data at different times during the experiment.....	213
8.1. Dynamic mechanical properties of some materials at 37°C, data obtained by Dr. S. Kalachandra and Dr. D.Xu, using a frequency of 1 Hz	221
8.2. Summary of logarithmic (base 10) regression data for the relationship between desorption diffusion coefficient and total absorption.....	227

List of tables continued.

	Page
8.3. Summary of logarithmic (base 10) regression data for the relationship between absorption diffusion coefficient and total absorption for the silicone materials	231
8.4. Prediction of the diffusion coefficient from equation 8.9 using theoretical data	234
8.5. Prediction of diffusion coefficient from different time periods for the PBS5+ materials in different solutions	235
IV.1. The calculation of the solubility parameter of methyl methacrylate monomer from Small's (1953) and Hoy's (1970) group molar attraction constants.....	298
IV.2. Solubility parameters calculated from Small (1953) and Hoy (1970) values for the group molar attractions with comparison to experimental values were available.....	299
IV.3. Calculation of the solubility parameter components from parts based on Van Krevlen (1976).....	301
IV.4. The calculated data of the solubility parameter and its different components as calculated from Van Kevelen, 1976.....	301

Chapter 1.

Introduction.

1.1. Foreword.

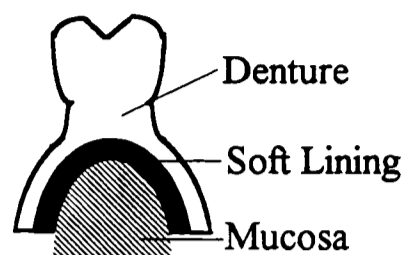
The use of full and partial dentures in dentistry is widespread, these have to be made from hard rigid materials. In a proportion of patients the prosthetic denture applies an intolerable force to the mucosa during mastication; this can result in ulceration (Lyttle, 1957) or resorption of the bone (Badway and El-Sherbiny, 1992). In such cases a soft lining material may be prescribed to act as a cushioning interface between the hard denture and mucosa. These materials benefit the patient by absorbing energy and distributing stresses of mastication more evenly across the mucosa (Parker, 1966, Woelfel and Paffenbarger, 1968, Wendt, 1974, Kawano et al, 1993). Tissue conditioners are also employed to fulfil a similar function but here the materials are used as a temporary measure primarily in the treatment of sensitised or traumatised tissue.

1.2. Soft lining materials.

Soft lining materials are most commonly prescribed for complete lower dentures where the patient cannot tolerate the poly (methylmethacrylate) (PMMA) denture (Lammie and Storer, 1958, Travaglini et al, 1960, Gonzales and Laney, 1966, Braden et al, 1995). They may however also be used on removable partial dentures (Whitstill et al, 1984, Todd and Holt, 1987) and as obturators (Lammie and Storer, 1958, Gonzales and Laney, 1966), as well as treatment to overcoming anatomically undercut areas (Lammie and Storer, 1958, Bell 1970) or to retain dentures to implants (Adrian et al, 1992). Additionally they are used for maxiofacial prostheses (such as cleft palate devices) and in the treatment of oral cancers (Ryan, 1991).

The application of a soft lining material to a lower mandibular denture may be performed on the original denture by removal of material from the underside (the side against the mucosa) to produce a channel for the lining or by fabricating a new denture designed to incorporate the soft lining. In either case the lining acts as an interface between the PMMA denture and the mucosa as shown in figure 1.1. It should be noted that the design of the lining is important in establishing its success (Kawano et al, 1993), the thickness being particularly important as this has a dramatic effect on the effective compliance of the lining (Jepson et al, 1993,a).

Figure 1.1. Illustration of the application of a soft lining material to a lower denture.



Initially it may seem that the formulation of material for a soft lining should be fairly straight forward. A soft compliant material that will bond to the denture base, retain its softness over the lifetime of the denture and be biocompatible. History has shown that the development of a successful soft liners is not as straight forward as may be supposed.

A primary concern to the dentist or dental technician is ease of fabrication of the denture lining. The conventional production of a denture or lining involves taking an impression of the oral mucosa and casting a model, which can then be invested in a dental flask containing dental stone ($\text{CaSO}_4 \cdot \frac{1}{2}\text{H}_2\text{O}$). This forms the mould for the denture and lining. The PMMA or lining material is then placed in the mould and compressed by hand or hydraulic press. Curing is conventionally performed by slow heating of the flask held in a clamp under water or in dry oven up to 95 to 100 °C, or via a room temperature cold cure depending on the material. Other methods of curing have been successfully used for soft lining materials, such as microwave curing (McKinstry, 1991) and light curing (Olge et al, 1986, Polyzois, 1992, Jepson et al, 1995), although the acceptance in general dentistry is limited. The limitations imposed by dental technology need to be considered during the selection of appropriate materials.

Over the years a wide selection of materials have been used as soft lining materials; some have been more successful than others. The first materials used as soft lining materials were based on natural rubber and plasticised PVC. The natural rubber material experienced a large water uptake which caused the material to swell and distort thus increasing the tendency for fouling (Lammie and Storer, 1958, Quadah et al, 1990). The plasticised PVC proved difficult to stabilise and was prone to leaching out of the plasticiser (dibutyl phthalate) causing the material to harden and crack (Lammie and Storer, 1958, Wright, 1976, Quadah et al, 1990). The plasticiser was then changed to

dioctyl phthalate which being a larger molecule was less prone to leaching; this served only to delay the leaching rather than solve the problem.

1.2.1. Plasticised methacrylate materials.

The idea behind the plasticised methacrylates is very simple in that they originally were based on PMMA (used in a denture base) plasticised with a di butyl or di octyl phthalate (as previously used with the PVC material). These materials are supplied in two parts, a powder and liquid component which are mixed together so they form a dough which may then be processed. The powder component is a methacrylate polymer powder (e.g. PMMA) which contains residual peroxide (normally benzoyl peroxide) from its polymerisation process. The liquid is one or more methacrylate monomers (e.g. methyl methacrylate) and a plasticiser (e.g. di octyl phthalate). When mixed the monomer and plasticiser swell the powder particles this forms a dough and releases the residual peroxide from the powder. The dough can then be moulded and cured by heat as a result of the residual peroxide free radical polymerisation.

There are many variations on this type of material, the results being generally similar with 'Super Soft' probably being the most widely accepted. These materials bond well to the PMMA denture (Wright, 1982) and initially fulfil the strength and softness criteria. Immersion in water however leads to a hardening and possible rupture of the material due to the leaching out of the plasticiser (Wilson and Thomlin, 1969, Suchatlampong and Davies, 1975, Wright, 1976, Robinson and McCabe, 1982, Jepson et al, 1993,b). Improvements can be made by using ethyl methacrylate or butyl methacrylate, rather than methyl methacrylate, this is beneficial as the higher methacrylates are generally more biocompatible, have lower exotherms and lower Tg's (so less plasticiser can be used). Other changes have primarily focused on using different plasticisers (such as citrates) to try and limit the leaching out of plasticiser when the material is in an aqueous environment. As yet no material seems immune from the problems associated with the leaching out of the plasticiser although some materials seem better than others. The leaching out of plasticisers is described in great detail by Zieminski and Peppas (1983) for a phthalate/PVC based materials. Another cause for concern is ingestion of the plasticiser by the patient as there are questions over the toxicity of the phthalates commonly used (Autian, 1973, Harsanyi et al, 1991).

An interesting development in these materials is the use of higher methacrylates in conjunction with a polymerisable plasticiser. These materials, originally developed by

Litchfield and Wood (1965), utilise diethyl hexyl maleate as the plasticiser, which polymerises independently of the methacrylate component. Unfortunately the methacrylate monomer chosen was 2-ethoxy ethyl methacrylate which has since proven biologically suspect (ICI chemical safety sheet, Aiken, 1988). Parker and Braden (1982), developed this system further using tri decyl methacrylate rather than then 2-ethoxy ethyl methacrylate. Although the plasticiser did prove virtually unextractable the material failed clinically due to an excessive water uptake which causing the formation of blisters within the material and mechanical failure (Parker and Braden, 1989).

An alternative approach to limiting the leaching of the plasticiser is to apply a sealant to the surface of the material which prevents the diffusion of the plasticiser through surface of the materials, e.g. 'Softerex'. Here however the results are disappointing with the material showing a high water uptake (Parker, 1996). There is also concern over how the surface coating would remain intact when material is swollen by water ingress and exposed to physical wear from the handling of the material.

1.2.2 Silicone based materials.

Silicone elastomers were identified as a potential soft lining material from an early stage due to their low water uptake; their development was hampered by the absence of a suitable curing mechanism as this either involved high temperature processing or use of a lead based catalyst (Lammie and Storer, 1958). These problems have since been overcome by the development of peroxide, organo tin based and platinum based catalysts for silicone polymers. The siloxane chemistry involved in the different curing mechanisms is described in a later section.

These materials have been generally quite successful as soft lining materials with 'Molloplast B' being generally widely accepted as the most successful material yet available. With long term reports (25 and 9 years) showing the material performing well (Ryan 1991, Wright 1994) This seems to be due to its long term low water uptake (Braden and Wright, 1983, Kazanji and Watkinson, 1988) in conjunction with reasonable mechanical properties which are maintained after immersion in water (Jepson et al, 1993,b,c, Jepson et al, 1995, Kalachandra et al, 1995). The major problem with this material is the poor adhesion to the PMMA denture base (Kawano et al, 1992, Kutay, 1994, Kutay et al, 1994); this decreases further when the material is immersed in water (Sinobad et al, 1992). The bond failure normally occurs cohesively (through the material) rather than adhesively (along the interface), indicating that the material is rupturing before the bond

strength is exceeded (Wright, 1982, Kutay et al, 1994), this is confirmed by the poor tear resistance (Wright, 1980). The composition of 'Molloplast B' is unclear with different authors describing the material differently, Appendix I describes its formulation with the discrepancies and contradictions. The wetting behaviour of 'Molloplast B' is another problem as the poorly wetted material (Wright, 1981) can lead to soreness (Wright, 1994), caused by frictional damage to the oral mucosa (Braden et al, 1995).

Another silicone material ('Flexibase') which is a condensation (organo tin catalyst) silicone, shows an unexpectedly high water uptake of 60 wt% and a high solubility which has been attributed to the breakdown of bond within the rubber (Wright, 1976). A new fluoro silicone material, 'Flexor', has recently been introduced which seems to be physically superior to many of the materials being used (Dootz et al, 1992). It also has a low water uptake (Braden et al, 1995) and hence shows promise for the future.

There has been comparatively little written about the development of new silicone based soft lining materials. Wright (1981) and Parker (1994) have both studied a acetoxy silicone RTV 108 and RTV 106 (manufactured by GE Silicones) which is quoted as the major constituent of 'Molloplast B' (see appendix I). These material produced some very promising results although the production of acetic acid during curing remains a problem. A alternative material produced by Nishiyama and Kato (1987) is based on a addition hydrosilanised rubber utilising a chloroplatinic acid catalyst. It is formulated as a two part system with involves mixing two siloxane fluids together immediately prior to application to the denture base. The results show the material to have sufficient strength and adhesion to PMMA (by forming a interpenetrating network of PMMA and silicone at the interlayer) together with little change in any of the mechanical properties after water storage at 37°C for 5 years (water uptake 0.02 mg/cm²). Clinical results are also favourable with the authors reporting positive 3 year results. Despite the apparent potential of this system little else seems to be published on this material and what there is prior to this date.

1.2.3. Elastomer based systems.

Early in the development of soft lining materials natural rubber was used as a soft lining material as discussed earlier. Early failures were attributed to excessively high water uptake of the material and generally poor processing characteristics (Lammie and Storer, 1958). Natural rubber was re-introduced as a soft lining material in conjunction with methyl methacrylate to form a graft co-polymer (Braden et al, 1995), this showed

promise although the water uptake was disconcertingly high (Wright, 1976). This material was however cured by a sulphur/zinc dimethyldithiocarbamate system the later being biologically suspect (IARC).

'Novus' is a well accepted commercially available material based on poly(fluoro alkoxy) phosphazine elastomer (Firestone PNF-200) which is milled with methacrylate and dimethacrylate monomers (May et al, 1981, Gettleman and Gebert, 1987) and an initiator (lauryl peroxide initially and later changed to benzoyl peroxide). The resultant material comes in the form of a very viscous gel which is moulded and then cured by conventional dental technology. This material performs well in vitro (Dootz et al, 1992, Polyzois, 1992, Collis, 1993) and in vivo (Gettleman et al, 1987, Gettleman et al, 1990). There is however concern over the materials water uptake as over 25 wt% has been reported (Kawano et al, 1994, Braden et al, 1995), although such high uptakes do not seem to be repeated clinically, due to the effect of osmolarity of the saliva (Parker et al, 1995, Parker et al, 1997). Collis (1993) looked at 'Novus' using a radiographic analytic probe on a scanning electron microscope to look at small white flecks present on the surface of 'Novus', formed on curing and showed these to contain the elements barium, potassium, chlorine, sulphur and silicone. These elements are unattributable to the material formulation and are liable to stem from impurities.

An alternative system has been developed by Parker and Braden in the early 80's, this system used a powdered high molecular weight elastomer (such as natural, butadiene-styrene or butadiene acrylonitrile rubbers) being gelled with a higher methacrylate monomer (2-ethoxy ethyl methacrylate, 1 tridecyl methacrylate, 2-ethyl hexyl methacrylate, lauryl methacrylate or nonyl methacrylate) containing benzoyl peroxide (Parker and Braden, 1982). The materials had promising physical properties and the absence of a plasticiser meaning that the material should be stable in aqueous environments. The materials were then the subject of a patent application (Braden and Parker, 1985) where the same materials were described using a ratio of elastomer to monomer ratio of between 1:2 to 2:1. Additional cold curing compositions using N,N-dimethyl p-toluidene and benzoyl peroxide as the initiating system were described. Again all the properties described in this patent application showed the material to be very promising.

Parker and Braden (1990) published a detailed evaluation of these systems, showing results for all three types of powdered elastomer from many different sources and a range of monomers (2-ethoxy ethyl methacrylate, 2-ethyl hexyl methacrylate, lauryl

methacrylate, tridecyl methacrylate and nonyl methacrylate). These materials showed excellent strength and bonding characteristics, with the acrylonitrile rubber/2-ethoxy ethyl methacrylate material showing the best results. The water uptake of these materials was however unexpectedly high with between 5 and 15 wt% uptake being observed, this water uptake was also accompanied by a reduction in the bond strength. A further complication was the toxicity of the 2-ethoxy ethyl methacrylate (Aikien, 1988, ICI). Further work focused on materials based on butadiene styrene using n-hexyl methacrylate and ethyl hexyl methacrylate with a small percentage of ethylene glycol dimethacrylate with a benzoyl peroxide catalyst. These materials also showed considerable promise although the water uptake was again a cause of concern (Parker, 1993)

There are materials that have become available recently, which cannot be classified simply, these include 'Triad' a poly ether based polymer with methacrylate end groups, and fluoro ethylene co-polymers. 'Triad' is a light cured material which exhibits a low water uptake but there is some concern over the residual iso cyanate remaining after manufacture (Saber-Sheikh, 1996). The fluoro ethylene co-polymers combine fluoro alkyl methacrylate monomers with vinylidene fluoride/hexa fluoropropylene or vinylidene fluoride/tetrafluoroethylene/hexa fluoropropylene copolymer. These materials seem to behave well in water but limited data in the ^{literature} prevents a full assessment (Braden et al, 1995).

1.3. Summary.

The long term application of a soft lining material is of proven benefit to the patient but such materials have long been recognised as unsuitable for protracted use (Lammie and Storer, 1958, Combe and Grant, 1973, Wright, 1976), a situation still true to this day (Brown, 1988, Quadah et al, 1990, Braden et al, 1995). Although over the years Molloplast B has proved itself to be possibly the most satisfactory material it still remains far from ideal. Its key advantage over many of the many of the other materials seems to stem from its low water uptake and low solubility (Kawano et al, 1994) which enables the material to maintain its physical properties and remain dimensionally stable over the years. It is felt that in order for a material to be successful the material should have low water uptake characteristics.

It should be realised that the oral environment is complex and the in vitro testing of the material in water will not necessarily predict how it will behave in vivo. Comparison of soft lining materials in vivo with in vitro results show differing effects on the compliance of the material, with great reductions being observed in saliva (Ellis et al, 1980, Jepson et al, 1993,b, Jepson et al, 1993,c), although the ranking tended to be the same.

Differences between the laboratory and clinical results tend to reflect the inconstant nature of the mouth. Personal habits have a profound effect on some properties, such as smoking and drinking on the compliance (Jepson et al, 1993c) and colour (Wright, 1994 and Ryan 1991). Temperature cycling the denture similar to that which would be experienced (from hot and cold drinks etc.) has also been shown to be detrimental to the compliance of the soft lining (Quadah et al, 1991). The patients treatment of the denture during cleaning etc. affects the longevity of some materials with some denture cleaning fluids leading to surface degradation (Collis, 1993) or, in the case of hypochlorites (bleach), denture discolouration (Ryan, 1991). Tests performed in artificial saliva rather than water have also shown that the solubility of the material tends to be higher (Kazanji, and Watkinson, 1988). Despite this the use of in vitro testing enables some assessment of the materials behaviour in the mouth to be determined.

1.4. Scope of thesis.

In order to develop new soft lining materials water uptake has been used as a primary section criteria although the strength is also considered in detail. The ideal water uptake characteristics were suggested to be that of the denture base PMMA (Bates and Smith, 1965), i.e. a water uptake of about 2 wt% and a diffusion coefficient of $1.7 \times 10^{-10} \text{ m}^2 \text{ sec}^{-1}$ (Braden, 1964).

Table 1.1 summarises the water uptake characteristics of some commercial and experimental materials available. Some of the silicone polymers exhibit a very small water uptake ('Molloplast B'), although 'Flexibase' an alternative silicone system, shows a very high uptake. Silicone materials therefore seem to be one reasonable starting point the development of a future soft lining material. The elastomer methacrylate materials are promising but the high water uptake of some of them makes their suitability doubtful. Studies in other areas on the water uptake into elastomers have shown soluble agents and impurities are primarily responsible for high absorption. By removing such soluble impurities low uptake elastomers may be produced. The application of these theories to

the elastomer methacrylate based materials should improve there long term prospects in the mouth.

Table 1.1 Water uptake of soft lining materials after long periods (at least a year).

Material	Water uptake at 37°C.	Solubility	Source
Molloplast B	1 wt%	2.17 wt%	Braden and Wright, 1983
Flexibase	60 wt%	7.6 wt%	Braden and Wright, 1983
Novus	26.5 wt%*	-0.38 wt%*‡	Kawano et al, 1994
Flexor	3.18 wt%*	0.32 wt%*	Kawano et al, 1994
Coe Supersoft	-†	15.18 wt%	Braden and Wright, 1983
Parker and Braden's Elastomer/methacrylates	5 to 15 wt %	1 to 2 wt%	Parker and Braden, 1990
Parker and Braden's Polymerisable plasticiser	8 to 11 wt %	1.3 to 2.3 wt%	Parker and Braden, 1989
Parker's butadiene styrene/methacrylates	7 to 9 wt %	-	Parker, 1993

* Kawano et al , (1994) used the units mg/cm² this implies that water absorption is a surface condition which it is not. The results have therefore been converted to wt% using a assumed density of the polymer of 1 g/cm³.

† The Coe Supersoft sample did not have any observable water uptake due to the leaching of the plasticiser.

‡ The negative solubility of the water uptake indicates that the final dry weight of the material was greater than the initial weight of the material.

The polymerisable plasticiser material has been dramatically improved recently with the absorption now being between 2 and 3 percent after 3 months (Parker, 1996). These materials and the fluoro ethylene co-polymers therefore have considerable promise as soft lining materials, although they are not included in this study.

In order to try and minimise the water uptake of a potential soft lining material the processes that govern the uptake have to be understood. Despite a large body literature on the subject of water absorption into polymers (described in chapter 2) much remains controversial or unexplained. The aim of this study is therefore two fold, firstly to produce low uptake elastomeric materials for soft lining materials, and secondly help

explain the experimental phenomena seen. It is felt that only through understanding of the second part may the first be achieved.

While most of the study used simple gravimetric measurements of the absorption process, it was recognised that visualisation of the water inside the material should form part of this study. To this effect nuclear magnetic resonance imaging has been employed to study the absorption in a series of elastomers. This technique has proved itself as a potent tool in studies on the diffusion of water and solvents into other polymer systems.

Chapter 2.

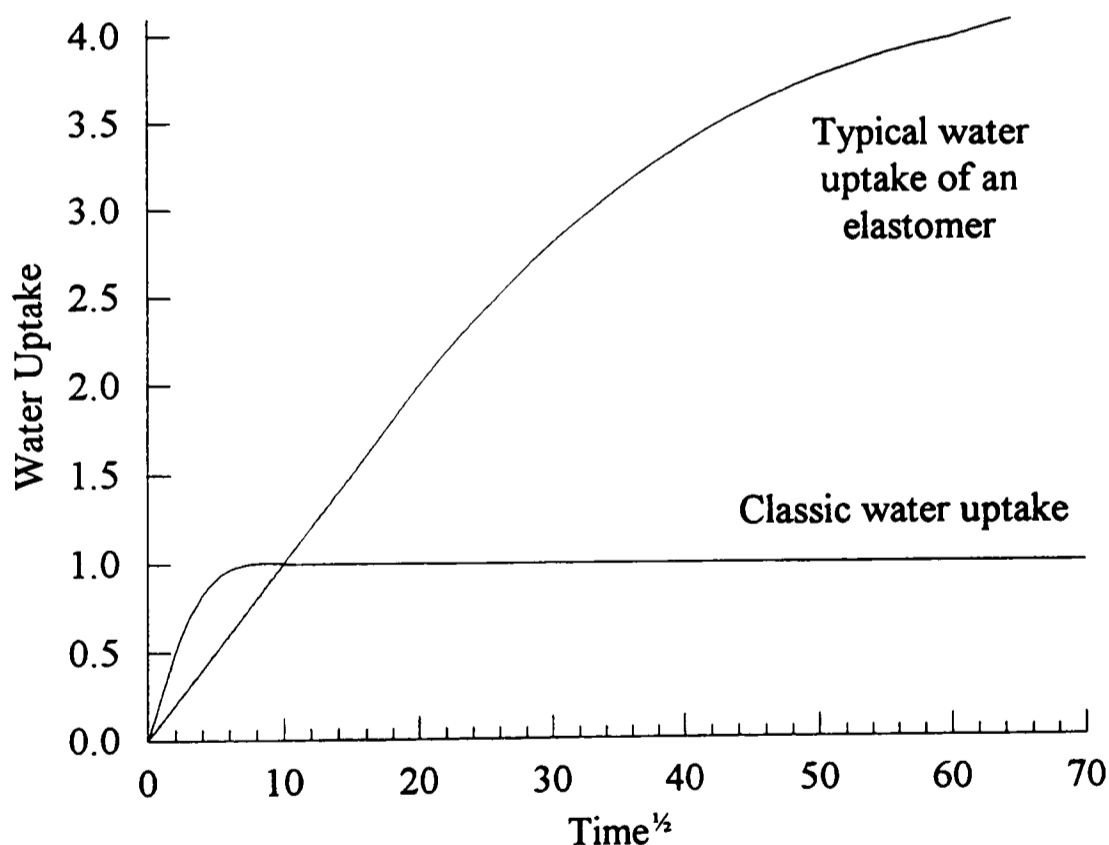
Literature Review.

2.1. Water absorption into polymers.

The absorption of water into polymers may occur in different ways depending on the composition and properties of the material. The environment also plays an important role in the determining the water uptake of the polymer with the temperature and activity (partial pressure or osmolarity) of the water determining the extent and type of uptake seen.

The classical water uptake profile into a material is seen in figure 2.1, with the material reaching a equilibrium via Fickian kinetics with the initial period of the uptake being linear with respect to the square root of time. Typically, this sort of uptake is seen for most rigid glassy polymer systems although even here there can be quite a lot of deviation from the classical behaviour. Elastomers, by contrast, show a higher more protracted uptake which may continue to increase over many months or indeed years.

Figure 2.1. A typical water uptake of elastomer.



2.2. Diffusion.

'Diffusion is the process by which matter is transported from one part of the system to another as a result of random molecular motions.'

Crank, 1975.

Diffusion occurs in many different types of system, from the mixing of gases to the ingress of a solvent into a solid, and results in many equations to describe the different characteristics and limits of the various processes. In order to predict the random molecular motions the overall effect is modelled rather than the individual molecular motion, this not only simplifies the problem but results in a more useful solution. Fick proposed a mathematical continuum theory (Crank, 1975) based on earlier work on heat conduction by Fourier (1822). This work forms the basis for current diffusion theories for liquids and gases in different media, although it originally was used for heat or energy movement. The extensive body of equations which have been derived for diffusion (Barrer, 1951, Crank, 1975) and heat transfer (Carslaw and Jaeger, 1959) makes a complete survey of all the aspects of diffusion beyond the scope of this thesis, hence only the most applicable equations for water absorption will be considered here.

2.2.1. Fick's laws.

Fick's first law (equation 2.1) describes the rate of diffusion or flux (F) through a section of unit area as proportional to the concentration gradient measured normal to the section (x), where D is the diffusion coefficient and c is concentration.

$$F = -D \frac{\partial c}{\partial x} \quad \text{Equation 2.1.}$$

It should be noted that the diffusion coefficient may be constant (i.e. dilute solutions and gases) or may vary with the concentration (c). The negative sign within the equation is required as the direction of the diffusion is opposite to the direction of increasing concentration.

This gives rise to Fick's second law (see appendix II.a. for the full details) for one dimension,

$$\frac{\partial c}{\partial t} = D \frac{\partial^2 c}{\partial x^2} \quad \text{Equation 2.2.}$$

2.2.2. Solutions to Fick's second law.

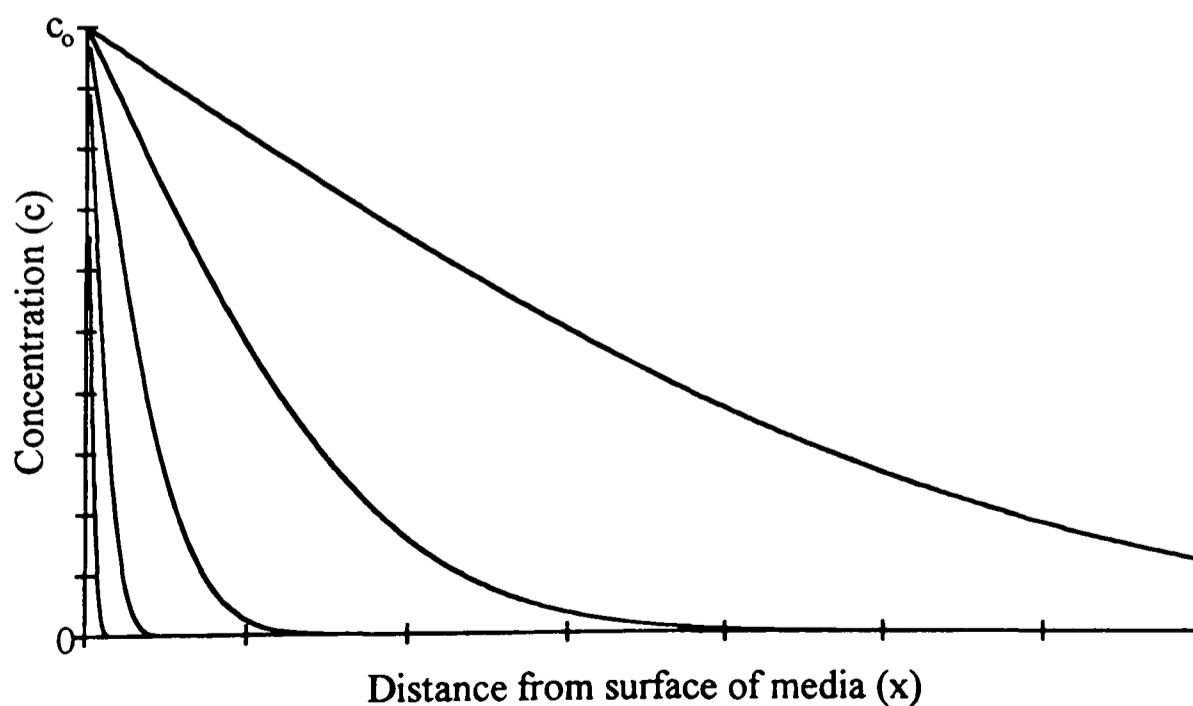
In general, and particularly for the theories of diffusion into polymers, the diffusion coefficient is assumed constant with concentration of diffusing species. Whilst this is a significant assumption, and as frequently not the case, experimentally it simplifies the problem to a solvable form in terms of explicit mathematical functions. Fick's second law is solved for the individual geometry and boundary conditions. For a semi infinite media when the diffusion occurs from one surface (i.e. is one dimensional) and is unrestricted in this direction, the material is effectively infinite in this direction to ignore surface contributions. The surface adsorption is ignored as the concentration of the penetrant or solvent (c_0) in the material at the boundary is assumed constant. The diffusion coefficient is assumed constant as in equation 2.2 which leads to (see appendix II.b),

$$c = c_0 \operatorname{erfc} \frac{x}{2\sqrt{Dt}} \quad \text{Equation 2.3.}$$

where $\operatorname{erfc} \frac{x}{2\sqrt{Dt}} = \frac{2}{\pi} \int_{x/2}^{\infty} \frac{e^{-z^2}}{2\sqrt{Dt}} dz$, where z is a dummy variable.

Figure 2.2, shows the shape of the profiles this equation predicts with increasing time, as time progresses the concentration throughout the sample tends to c_0 .

Figure 2.2. Concentration profile of diffusion into a semi-infinite media as predicted by equation 2.3, at different times.



The uptake may be expressed in terms of mass as a function of time by integrating equation 2.3, (see appendix II.b) which, when diffusion is occurring from only one direction into the sample, gives,

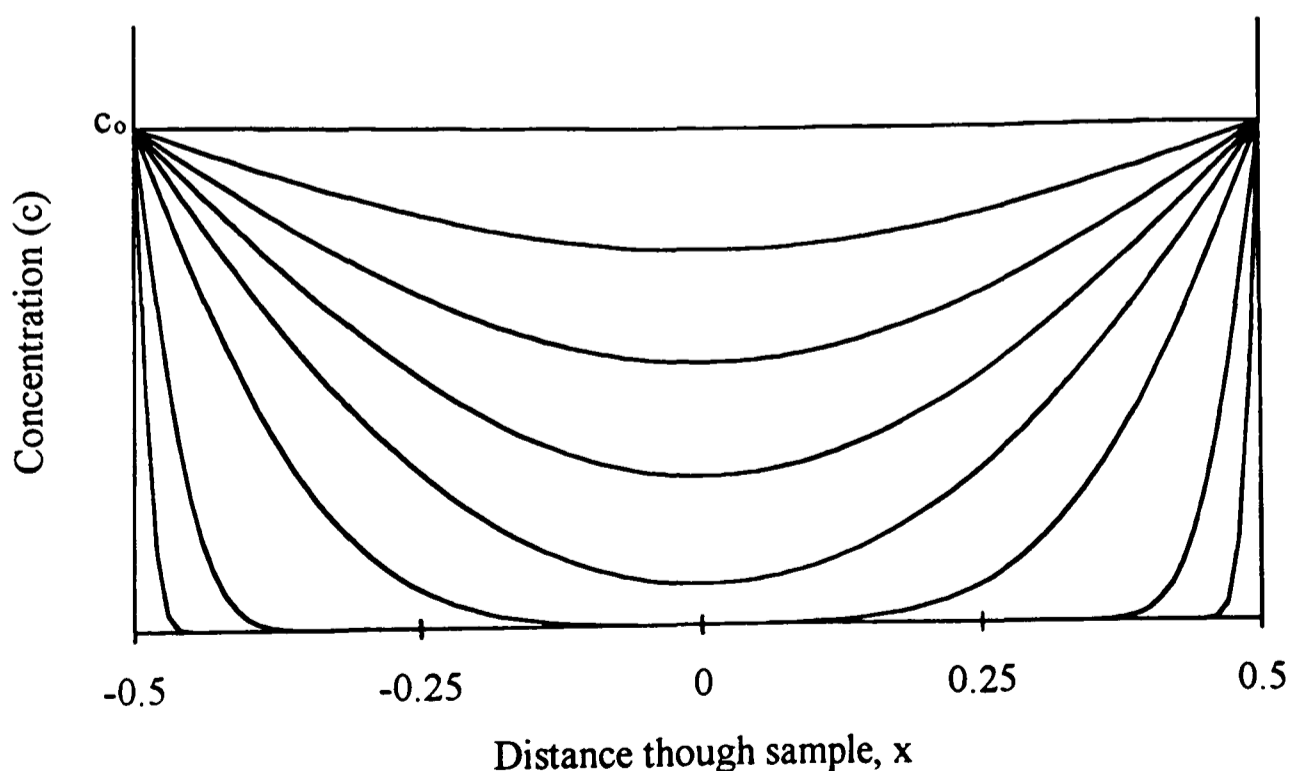
$$\frac{M_t}{M_\infty} = 2\sqrt{\frac{Dt}{\pi l^2}} \quad \text{Equation 2.4.}$$

where M_t is mass at time t and M_∞ is mass at equilibrium and l is the thickness of the media perpendicular to the surface. It should be noted that this will only apply until the diffusing species reaches the outer edge of the sample. In a similar way it will also apply to the early stages of diffusion in a plane sheet when diffusion occurs through two opposite surfaces provided the two diffusing fronts do not interfere with each other, here however l should be half the thickness.

The equation for diffusion into a plane sheet at longer times is a little more complex due to the fronts meeting (see appendix II.b), Equation 2.5. Here l is again half the thickness of the sheet and x is defined as distance from the mid point, the profiles for a series of different times predicted from this equation are shown in figure 2.3.

$$C = C_o - \frac{4C_o}{\pi} \sum_{n=0}^{\infty} \frac{(-1)^n}{2n+1} \exp\left[\frac{-D(2n+1)^2 \pi^2 t}{4l^2}\right] \cos\frac{(2n+1)\pi x}{2l} \quad \text{Equation 2.5.}$$

Figure 2.3. Concentration profile as predicted by equation 2.5 at different times with respect to distance through sample, x .



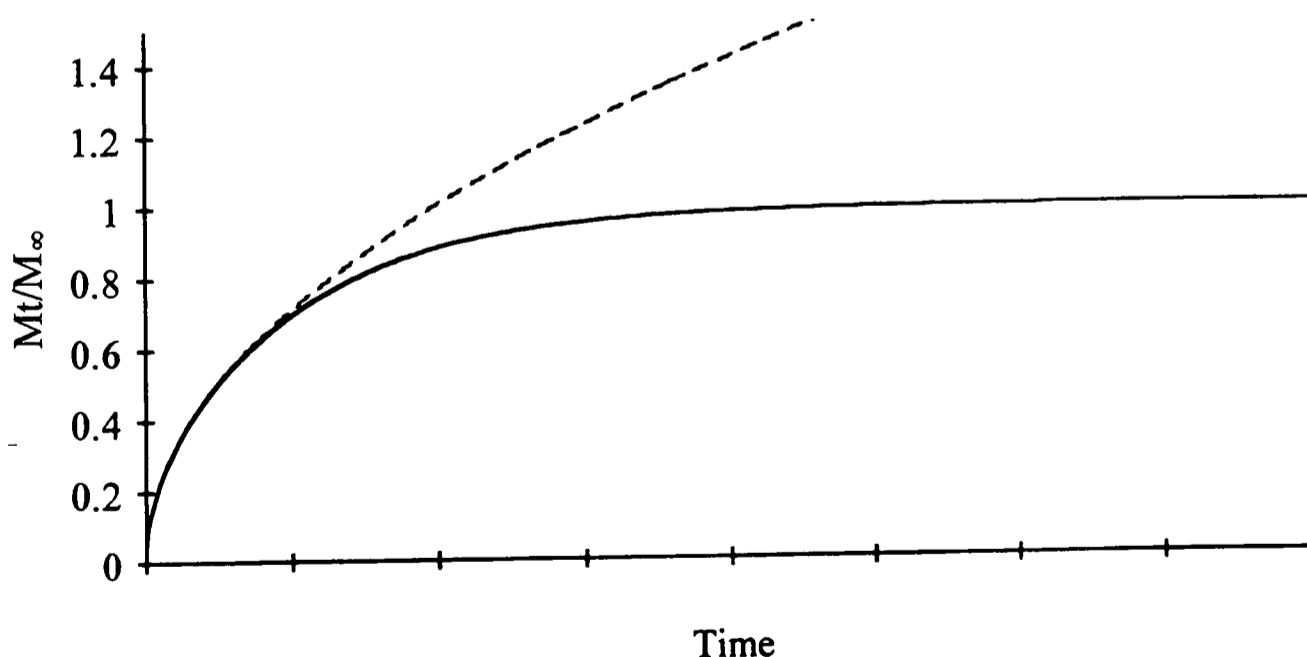
M_t/M_∞ will be given by integrating equation 2.5 with respect to x (see appendix II.b) to yield equation 2.6. Figure 2.4, shows the prediction this makes for absorption in comparison to the formula for the semi infinite media (Equation 2.4); from this it is apparent that the semi infinite media equation predicts the early part of the absorption process fairly accurately up until approximately $M_t/M_\infty = 0.5$, when the fronts meet. Indeed an alternative form of equation 2.6 is equation 2.7 (Crank, 1975) which approximates to equation 2.4, when the \sum term is small (i.e. during the early stages of the absorption process).

$$\frac{M_t}{M_\infty} = 1 - \frac{8}{\pi^2} \sum_{n=0}^{\infty} \frac{1}{(2n+1)^2} \exp\left[\frac{-\pi^2 D(2n+1)^2 t}{4l^2}\right] \quad \text{Equation 2.6.}$$

$$\frac{M_t}{M_\infty} = 2\sqrt{\frac{Dt}{l^2}} \left\{ \frac{1}{\sqrt{\pi}} + 2 \sum_{n=1}^{\infty} (-1)^n \operatorname{ierfc} \frac{n l}{\sqrt{Dt}} \right\} \quad \text{Equation 2.7.}$$

The application of the simpler equation 2.4, to the early stages enables the calculation of the diffusion coefficient by plotting of M_t/M_∞ against $t^{1/2}$, and calculating the gradient.

Figure 2.4. M_t/M_∞ against time as predicted by equation 2.6, (solid line) and equation 2.4 (dotted line).



Generally these equations (2.4, and 2.6,) predict the kinetics of the absorption process of water into polymers reasonably well. There is normally a deviation to reduce M_t/M_∞

values during the later stages of water uptake (i.e the higher values of M_t/M_∞). This is attributed to the relaxation of the polymer (due to swelling from the formation of clusters) being important in determining the later part of the diffusion cycle (Wong and Broutman, 1985), although this is function of film thickness. However, although Fick's laws predict much about water uptake into polymers, they do not explain many aspects such as the long protracted uptake of elastomers as commented on previously.

In the derivation of equations 2.4, and 2.6, it was assumed that the diffusion coefficient was constant, in practice it is not. The diffusion coefficient is in fact dependent on temperature and concentration. The dependence on temperature is only noted here as all experiments in this study were conducted at 37°C. Its importance is, however, recognised and has been described by other authors (Park, 1950, Schneider et al, 1968, Crank, 1975, Barrie et al, 1985) and it has been used to calculate the activation energy (using equation 2.8) when absorption measurements are conducted over a range of temperatures (Barrie et al, 1985, Rathna et al, 1994). The activation energy (E_a) being calculated by applying a Arrhenius type relationship,

$$D = D_0 \exp(-E_a / RT) \quad \text{Equation 2.8.}$$

where D_0 is a constant associated with the entropy of the diffusion.

2.2.3. Concentration dependence of the diffusion coefficient.

The dependence of the diffusion coefficient on concentration has been demonstrated in a number of ways, the most widely reported being conduction of experiments over a range of activities or partial pressures (Barrer, 1951, Barrie et al, 1985). The relationship now being expressed in a slightly different form of equation 2.2, with takes account of the diffusion coefficients dependence.

$$\frac{\partial c}{\partial t} = \frac{\partial}{\partial x} \left[D \frac{\partial c}{\partial x} \right] \quad \text{Equation 2.9.}$$

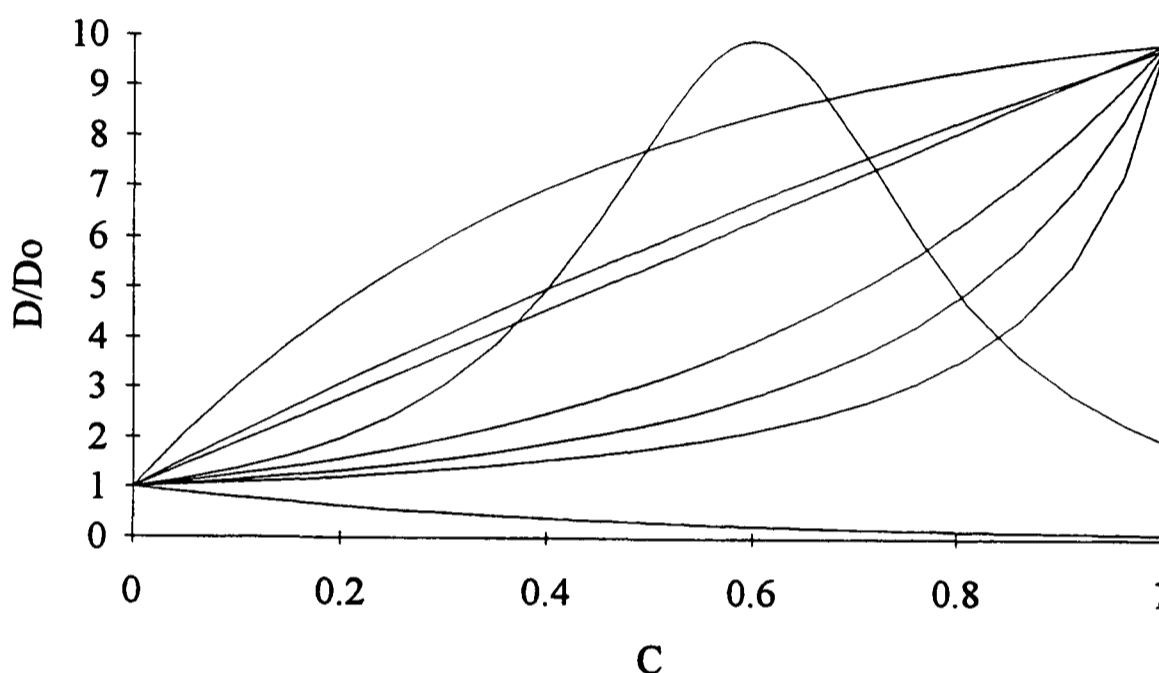
There are numerous different types of diffusion coefficient concentration dependence many of which are described in Crank (1975). Generally the diffusion coefficient, D , is expressed as a function of concentration, C ,

$$D = D_0 (1 + f(C)) \quad \text{Equation 2.10.}$$

where D_0 is the diffusion coefficient when C equals 0. This enables a wide range of predictions of the dependence, figure 2.5 demonstrates a few of these relationships.

Clearly a full account of all these theories is beyond what is required in this thesis but some relevant parts will be considered. Whether the dependence increases, decreases or has maximum depends on the nature of polymer and diffusing species.

Figure 2.5. Concentration dependence of diffusion coefficient as a function of c for various functions of $f(c)$ based on equation 2.10, based on Crank, 1975, for diffusion into a semi-infinite media.



A particularly interesting result is that of Blackband and Mansfield (1984 and 1986) on water diffusion (at 100°C) into Nylon 6,6 (Nylon being a trade name of the Du Pont company for poly amides) using NMR imaging (appendix III.a) with a T_e of 2.7 ms. Here dependence was shown to be exponential with respect to the relative concentration as shown in Figure 2.6. This demonstrates the change in diffusion coefficient with concentration within the polymer for a single absorption cycle rather than the more usual series of tests under different conditions, thus clarifying the dependence in a unequivocal way.

Sreenivansan (1993) showed a similar effect by grafting hydrophilic groups onto a rubbery polyurethane and found that as the water absorption increased (with increasing hydrophilicity) so did the diffusion coefficient. Barrie et al (1985) found the diffusion coefficient to increase with increasing concentration (figure 2.7) by altering the activity of the solution. Many different relationships have been observed but the effect has proven difficult to quantify.

Figure 2.6. Graph of the diffusion coefficient (D) as a function of c/c_0 where c_0 is equilibrium concentration, based on Blackband and Mansfield, 1986.

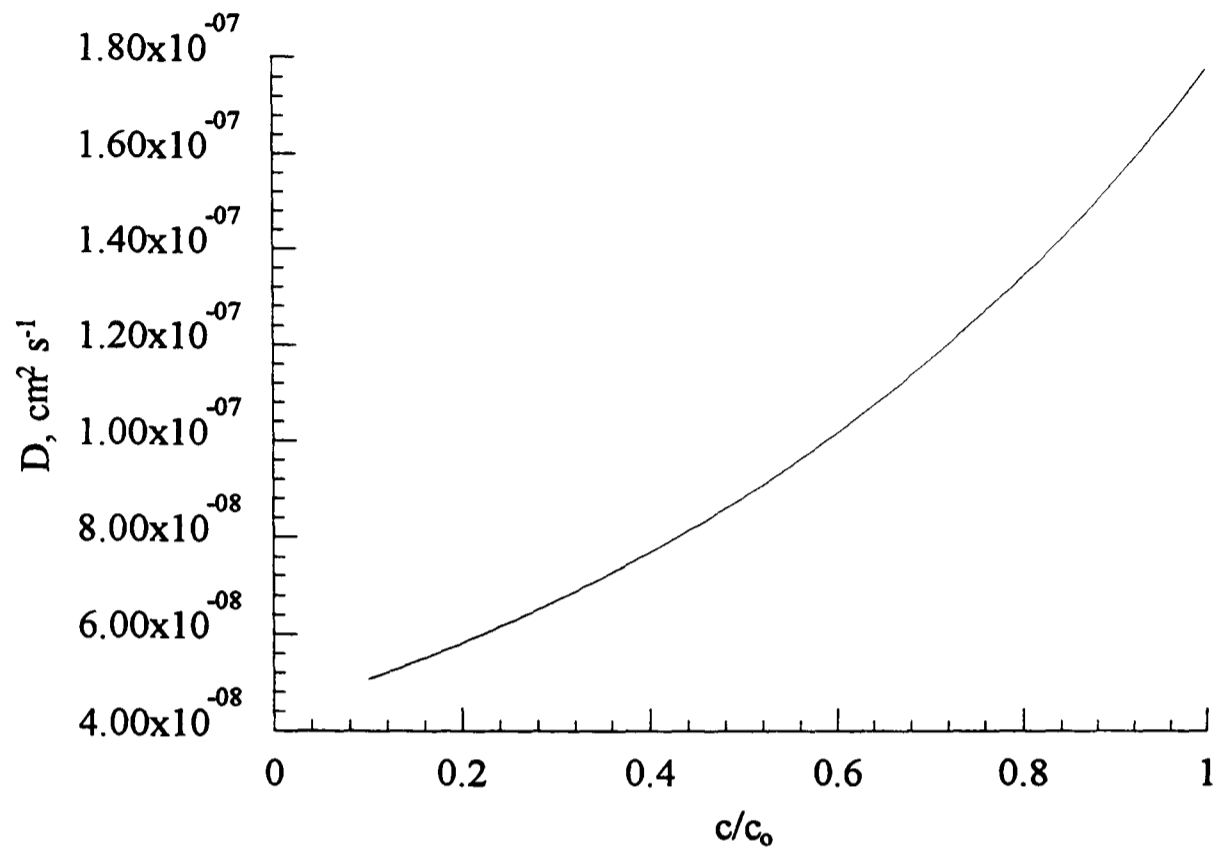
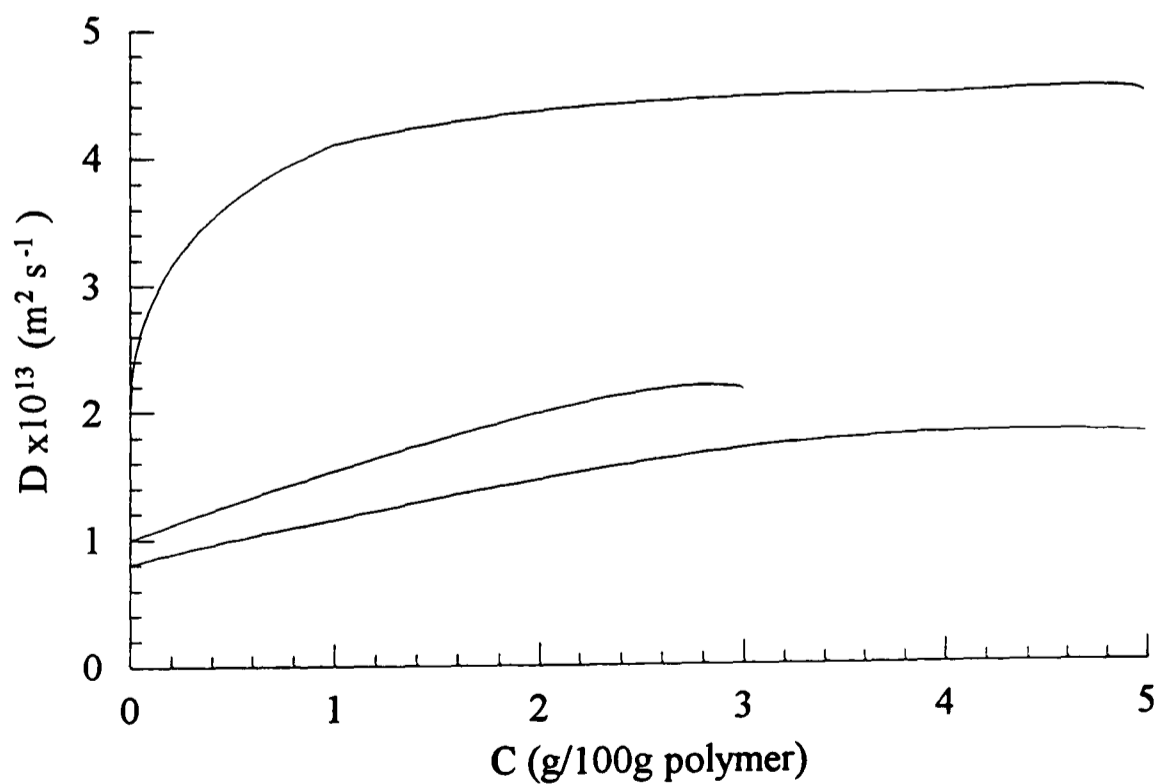
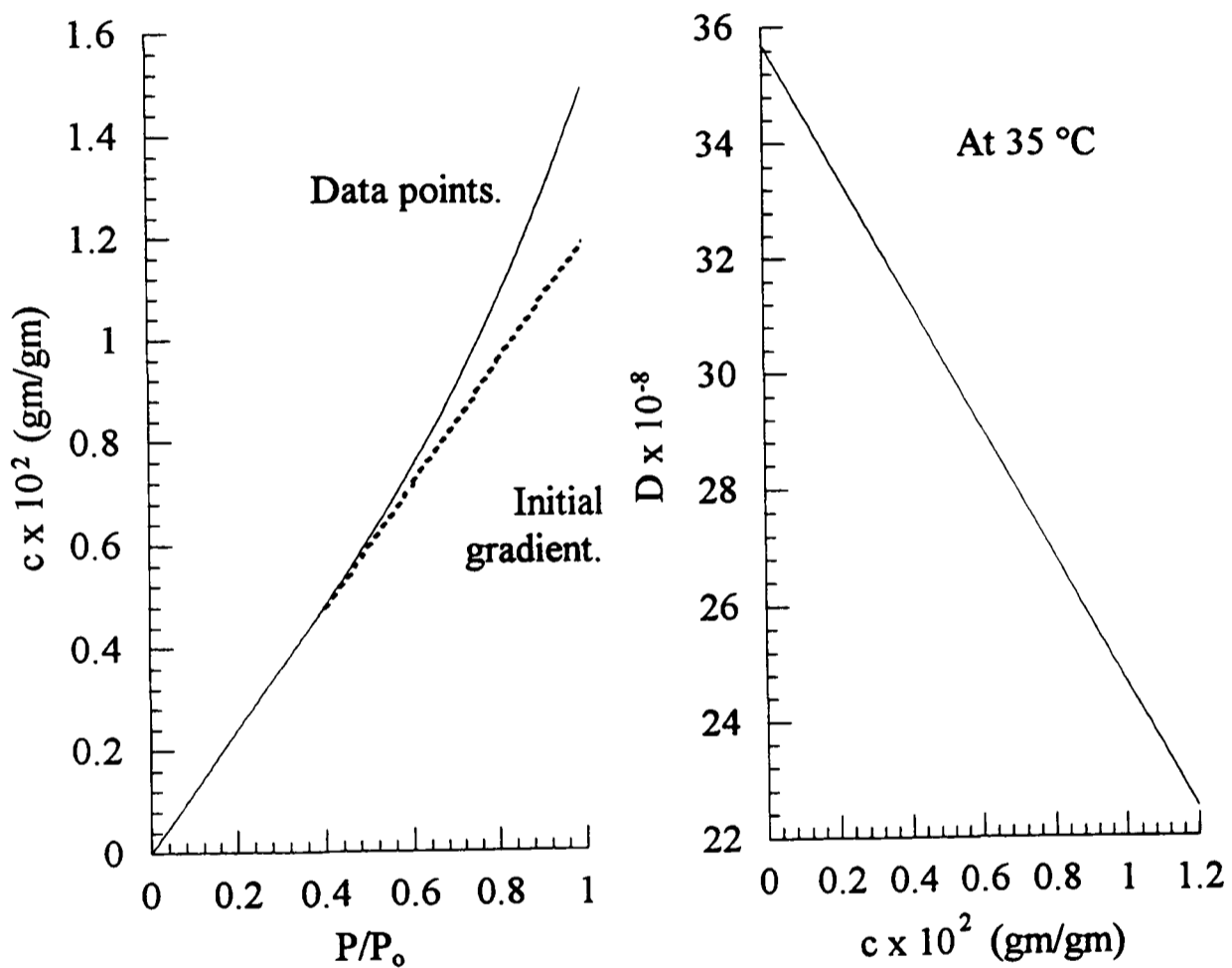


Figure 2.7. Dependence of diffusion coefficient on concentration of water for a series of halogen-containing epoxies, based on Barrie et al, 1985.



Alternatively, a decreasing trend was observed by others noticeably by Schinder et al (1968), on a rubbery polyurethane as shown in Figure 2.8. Such a trend was also observed for by Barrie and Platt (1963) for a silicone rubber and PMMA, and by Hsu et al (1993) for poly (styrene-co-*p*-hydroxystyrene). Both of these results are attributed to cluster formation within the materials acting to slow the absorption process of the material.

Figure 2.8. Effect of partial pressure of water on concentration and the resultant effect on the diffusion coefficient for a rubbery polyurethane, based on Schinder et al, 1968.



This decrease in diffusion coefficient with increasing concentration is well reported (Barrie and Platt, 1963, Crank and Park, 1968) and accounts for a quicker desorption diffusion coefficient than the absorption diffusion coefficient (Crank and Park, 1968, Braden et al 1976). This stems from the concentration at the surface during absorption being C_0 and in desorption the concentration at the surface is zero. Therefore the rate of ingress into the sample during absorption will be less than the rate of ingress out of the sample in desorption if the diffusion rate decreases with increasing concentration.

2.3. Hygroscopic properties of polymers.

The amount of water absorbed by a polymer is dependant on many factors; these will be considered in turn. Different authors have approached this in different ways and tend to report specific elements of the absorption process.

The polarity of the polymer has been shown to be very important in determining the water uptake. The action of hydrophilic groups has been shown to increase the water uptake (Sreenivasan, 1993), with a linear increase in uptake being observed for effective increase in the density of hydroxyl (Baddour et al, 1965, Diamant et al, 1981), carboxyl (Turner and Abell, 1987, Kalachandra and Kusy, 1991) and amide groups (Auerbach and Carnicom, 1991). The type of groups control the relative hydrophilicity of the polymer, with hydroxyl groups being particularly hydrophilic (Diamant et al, 1981). Such hydrophilic groups are capable of intermolecular bonding which seems to reduce their overall effect (Kalachandra and Kusy, 1991). Some evidence tends to contradict this by indicating water may break intra molecular bonded amide groups (causing a weakening of the material) and increase the water uptake (Rowland, 1980).

There are some theories for predicting the water uptake of a particular polymer system (Kalachandra and Kusy, 1991, Auerbach and Carnicom, 1991) but they rely, at present, on simple relationships between density of one or more hydrophilic groups. Whilst they work well when applied to a specific group of materials their application is limited.

The structure of the polymer is also very important with different isomers of the same material having different uptakes (the iso- form rather than the n- showing a higher uptake). This is attributed to differences in the accessibility of the hydrophilic groups and the density of the packing of the chains which leads to microvoids (or free volume) from inter molecular gaps between the polymer chains (Kalachandra and Kusy, 1991). Phase structure may also have an effect with glassy/crystalline state showing a lower absorption than plastic/amorphous structure (Marom et al, 1981, Hirschinger et al, 1990, Auerbach and Carnicom, 1991, Fyfe et al, 1993, Lim et al, 1993). Phase transformations may themselves be initiated by the ingress of water into the material (Cohen and Cohen, 1995). Such phase transformations will themselves be accompanied by an increase in the water uptake. Crosslink density may also effect the water uptake of a material with the more cross linked material expected to show the lower uptake (Baddour et al, 1965, Wong and Broutman, 1985, a and c) due the more rigid, less viscoelastic structure and

the crosslinks restricting the swelling. This seems to apply to a certain extent to chain entanglements and intra molecular bonds as well (Peppas et al, 1994).

Molecular weight is also a factor with high molecular weight polymer chains showing higher uptakes (Turner, 1987). This is also attributed to the packing as the higher molecular weight chains pack less efficiently than smaller chains leading to a greater free volume (or micro-voids) within the polymer; this free volume is available to the water. This seems a little questionable as the chain ends are usually responsible for determining the free volume of the polymer. The curing system used may also influence the number of micro-voids within the material and hence the water uptake (Söderholm, 1984).

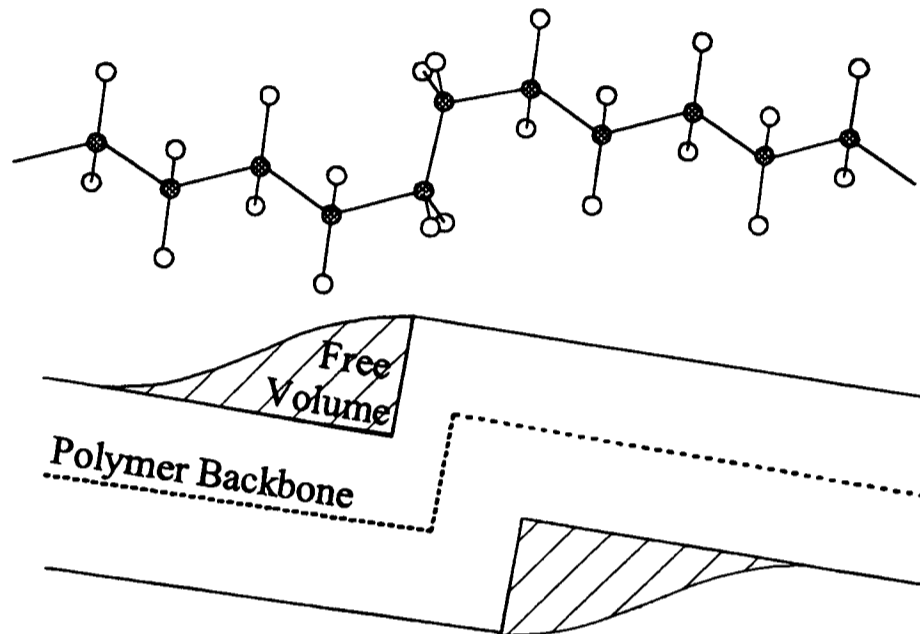
2.3.1. Free volume or micro-voids within the polymer.

The free volume or micro-void theories are based on the gaps within the polymer resulting from the polymerisation process and is probably the first major explanation for deviation from classical absorption behaviour as predicted by Fick's laws. These may be a result of polymerisation shrinkage or imperfect packing of the polymer chains. This was dealt with quite efficiently by Pace and Datyner (1980) in a study of gas absorption on a wide range of different polymers. Here the free volume is described as stemming from the polymerisation shrinkage, thermal expansion and contraction, and disturbances in the local microstructure, figure 2.9. This results in the penetrant being present in the polymer in 2 states, on the polymer chain (due to hydrophilic groups etc. for water) or in the free volume of the material. These different states are considered separately and give rise to the term dual sorption theory (Pace and Datyner, 1980, Labarr and Turner, 1982).

This type of theory has been quite widely applied to water absorption to explain some of the observed phenomena. The swelling characteristics frequently do not correlate with the mass uptake, with the mass uptake being greater than degree of swelling that is observed. This is attributed to the filling of the free volume during the absorption process and only the water on the polymer chains acting to swell the polymer (Marom et al, 1981, Labarr and Turner, 1982). The free volume is also used to explain difference in the absorption for different molecular weights (Turner, 1987) and isomeric forms (Kalachandra and Kusy, 1991) of a material, as mentioned in the previous section. The action of free volume in the polymer is particularly important in composites when free volume may be present along the interface (Lee and Peppas, 1993). The increase in

water absorption when a fibre composite is stressed has also been attributed to the increase in available volume of the polymer due to crazing of the material (Sancaktar and Baechtle, 1993).

Figure 2.9. Schematic of polyethylene chain with planar zig zag resulting in two free volumes available for water absorption (based on Pace and Datyner, 1980).



While the free volume theory explains some of the elements of water uptake it has limitations, it fails to explain the water uptake of some rigid systems (Turner and Abell, 1987) and is inapplicable to polymers above the T_g as the polymer chains are more mobile which enables the formation of new holes or voids (Pace and Datyner, 1980).

Neogi (1993) uses a variation of Fick's first law in terms of chemical potential (equation 2.31) to propose a model to express the kinetics of hole filling theories,

$$J = -D \left[1 + \frac{V_1 E}{\rho 3RT} c \right] \frac{\partial c}{\partial x} \quad \text{Equation 2.11.}$$

where c is the concentration, V_1 is the molar volume of the solute and E is Young's modulus. He also acknowledges that other factors such as relaxation, post yield deformation and viscous flow or creep will affect the diffusion process and be irreversible. An alternative approach to the kinetics was suggested by Wong and Broutman (1985,b) using effectively a dual version of Fick's laws where the total flux, J , was made of two components the flux into the matrix, and flux into the voids. The matrix flux dominates the absorption in the early stages and in the later stages the flux into the voids dominates.

2.3.2. The states of water within polymers.

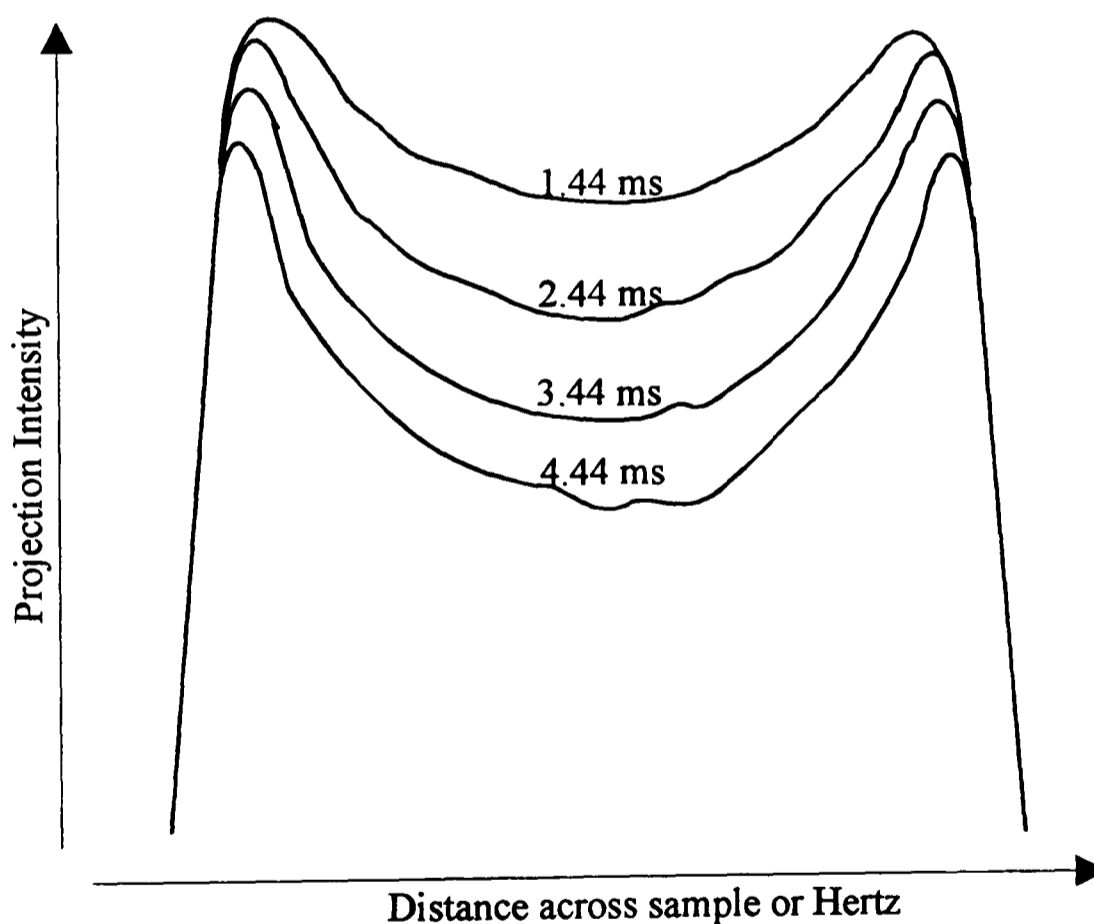
It has been recognised for many years (since the 1960's) that water may exist in different states (degree of intra molecular bonding) within the polymer (Schneider et al, 1968). Over the years many studies have been conducted using techniques such as nuclear magnetic resonance (NMR) (Fyfe 1993), (see appendix III.a.), differential scanning calorimetry (DSC) (Nakamura et al, 1981, Nakamura et al, 1983, Khare and Peppas, 1993, Takigami et al, 1993), dielectric measurements (Briggs et al, 1962, Bordeleau et al, 1986, Lim et al, 1993) and infra red or near infra red spectrometry (Gilbert et al, 1977, Venz and Dickens, 1991, Boakye and Yeager, 1992, Best et al, 1993). These techniques have enabled the state of the water to be determined, as the mobility (measured in NMR, dielectric's and IR.) and melting/boiling point (used in DSC) of the water will depend on the degree of bonding of the water. The recognition of the states of water within a polymer and their description has aided the development of theories of water sorption (Diamant et al, 1981, Venz and Dickens, 1991, Hsu et al, 1992, Lim et al, 1993, Takigami et al, 1993, Hernandez and Gavara, 1994).

The properties of water depend on the extent of hydrogen bonding and polar interactions with the polymer chains. Strong physicochemical interactions with hydrophilic groups give rise to bound (or non-freezing) water. Whereas hydrophobic groups produce slight interactions and hence are characterised by relatively free (or freezing) water (Khare and Peppas, 1993), which have the same properties as bulk water. There is some disagreement over the number of states of water possible within a polymer (Hernandez and Gavara, 1994) with the two reported above being widely accepted. Others (Sung et al, 1981, Takigami et al 1993) report a third type of intermediate water which freezes below zero (freezing bound water). In explaining the states of water and how they may appear three excellent recent papers, which illustrate the potential of some modern techniques, will be briefly summarised. These particular papers are chosen to illustrate those aspects of the work which enable visualisation of the states of water, although many other authors have made significant contributions to our understanding.

Fyfe et al, (1993) used NMR to look at the ingress of water (at 100°C) into Nylon 6,6, and found the T_2 increased with progressive absorption from 0.71 ms (at 5 hours) to 1.2 ms at 17 hours. These processes were much faster than the relaxation processes observed for bulk water of 2700 ms. Thus the water within the Nylon 6,6 is highly restricted or involved in strong interactions with the polymer (i.e. is bound). This was followed up by imaging experiments using a T_e of 1.44 ms. Although this T_e is greater

than the T_2 reported above, good images were obtained (when a T_e of 3.66 ms was used a poor inconclusive image was obtained). The absorption process was followed over time and a Fickian type of absorption observed as would have been expected from the gravimetric data also presented. Figure 2.10, shows the relationship between T_e and the image formed, with the intensity of the central region (with respect to the edge) reducing as T_e increases, thus indicating the T_2 and hence the mobility of the water increases with increasing concentration of water in the sample. This is attributed to a reduction in hydrogen bonding between the water and polymer due to the swelling of the polymer. The same experiment repeated at 48 hours exposure to water at 100°C showed no difference in profile for the different T_e 's.

Figure 2.10. Variation of projected intensity through a sample of Nylon 6,6 with different T_e times after 8 hours exposure to water at 100°C. Based on Fyfe et al, 1993.



Note, the x axis is marked in both distance and Hertz as the frequency applied to the sample controls the sampling position across the sample.

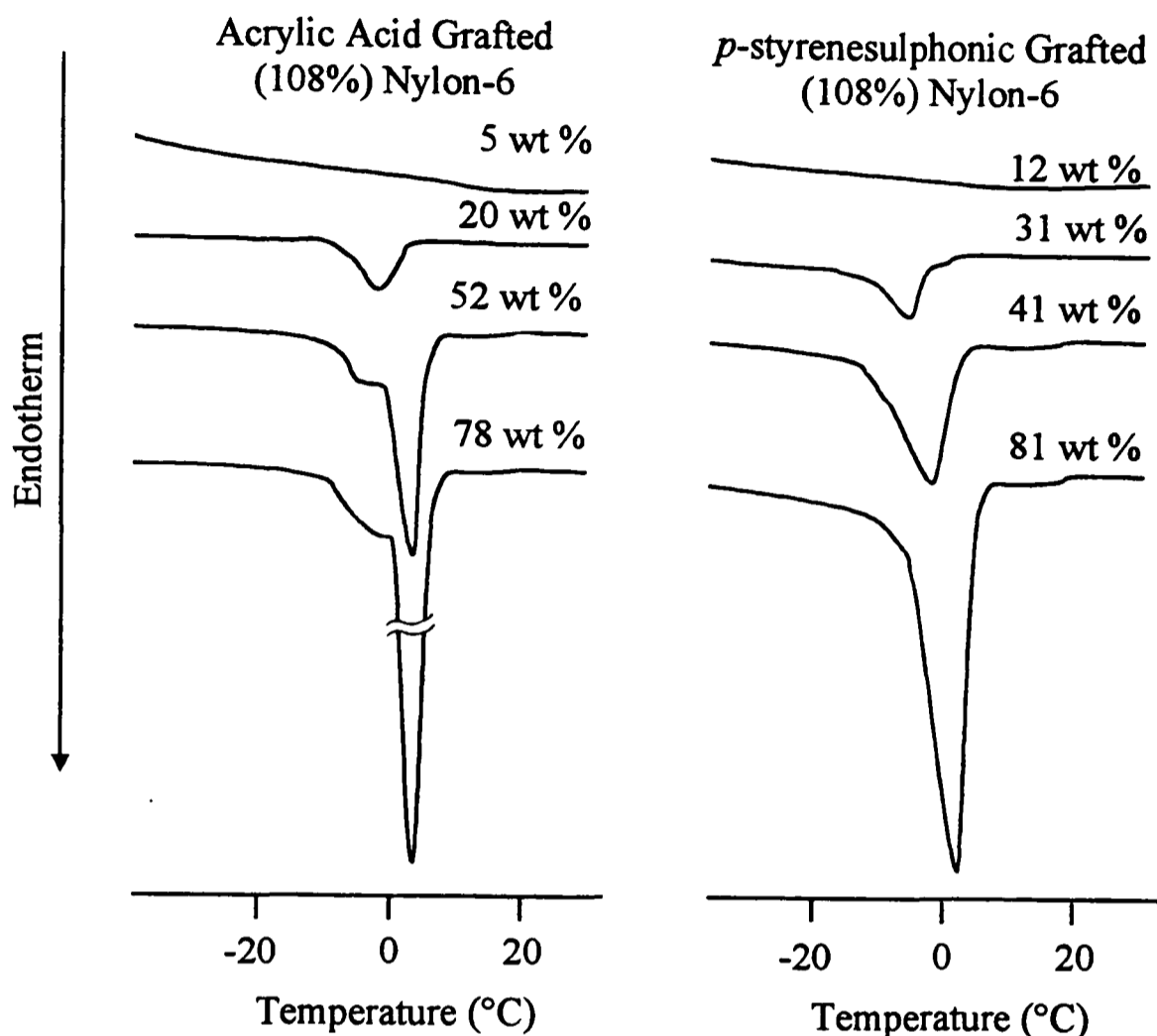
There is a particularly interesting point raised in this excellent paper; it shows water moving into the polymer in a Fickian manner (as also seen by Artemov et al, 1988) and shows a series of fronts relating to different concentrations at different degrees of mobility of the water (T_e times). This indicates that the bound water may exist within a

polymer in a range of states, and that during the continued ingress or diffusion of water in the polymer the highly bound water becomes less tightly bound.

Comparison of this result to that of Blackband and Mansfield (1986) for Nylon 6,6 shown in figure 2.6 reveals a problem with the NMR technique. Blackband and Mansfield (1986) used a T_e of 2.7 ms whereas Fyfe et al (1993) showed that the same material at the same temperature (100°C) has a considerable relaxation before this time during the early stages of absorption (figure 2.10), thus indicating that Blackband and Mansfield (1986) missed a portion of the relaxation of the water in the Nylon 6,6. This does not invalidate the result but it is worth noting. Unfortunately little is known about the temperature and condition of the Blackband and Mansfield (1986) samples. The test temperature effects the T_2 time with lower temperatures resulting in shorter T_2 times which may cause confusion when comparing results obtained from different conditions or by different investigators.

Takigami et al (1993), conducted a very interesting study on the influence of grafting on the states of water in Nylon 6 using a DSC. Figure 2.11, reproduces some of the data, for an acrylic acid grafted Nylon 6. At low concentrations (5 wt% water) a smooth curve is produced (non-freezing or bound water) for higher concentrations (20 wt%) a broad endotherm below 0°C appears associated with intermediate water. As the concentration increases (52 and 78 wt %) a second sharp peak appears (free water peak) with the broad peak becoming a shoulder of this new peak. *p*-styrenesulphonic grafted Nylon-6 shows an initial smooth bound water curve at low concentrations and an intermediate bound peak which sharpens and peaks at higher temperatures towards 0°C indicating a gradual transition between intermediate and free water. Clearly these results show that water in some materials exists in two states and in others three; the corresponding energy of these endotherms is then used to calculate the relative proportion of the water in each of the states. The differences are then attributed to poly (*p*-styrenesulphonate) being a strong poly acid, hence capable of producing strong repulsive electrostatic forces whereas poly (acrylic acid) is a weak poly acid and incapable of such interactions. Takigami et al, (1993) results also show the water being taken up in the bound state initially until a saturation is reached then intermediate and free water forming as the concentration increases. Similar results to these are also reported by Nakamura et al (1983) for a poly (hydroxystyrene), partially hydrolysed and unhydrolysed poly (4-acetoxystyrene) system. Here they also correlate the sum of the enthalpies of the materials with the overall water uptake and find a linear relationship.

Figure 2.11. DSC melting endotherms of water in grafted Nylon-6 membranes, based on Takigami et al, 1993.

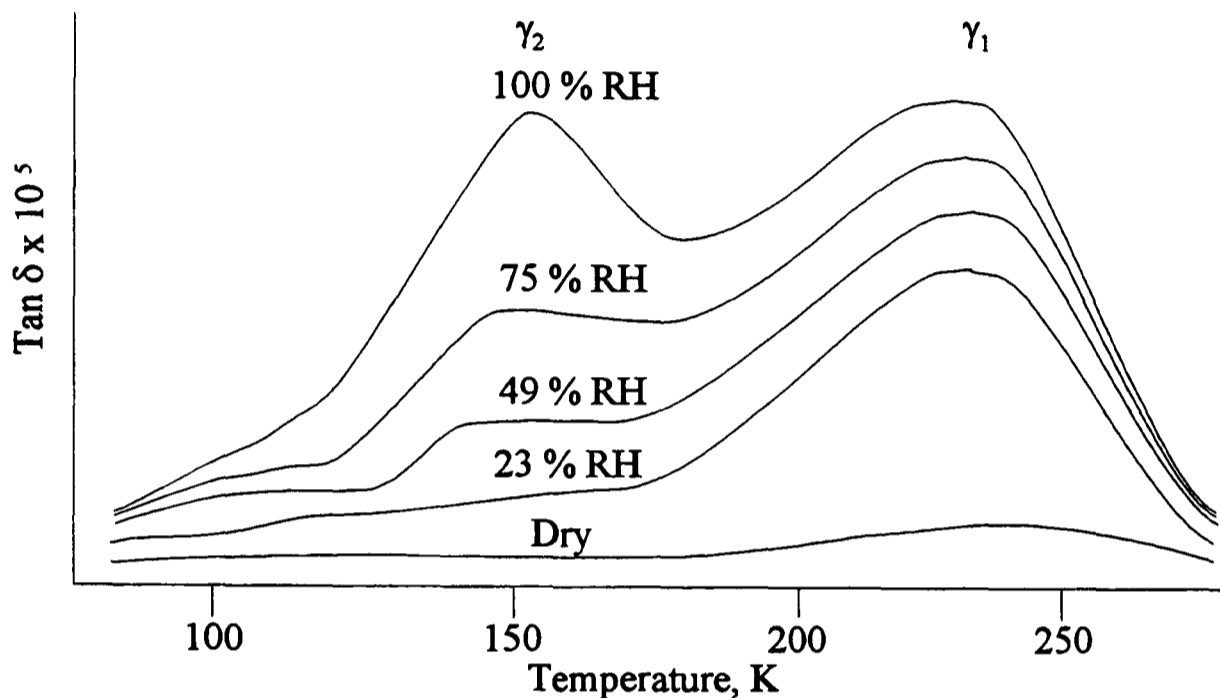


Lim et al (1993) conducted a study on ingress of water and other solvents into polyimide films using dielectric relaxation. He termed the two relaxation states observed for water γ_1 , homogeneously distributed water loosely bound to the polymer structure (bound water), and γ_2 , as specific sites involved in clusters with a lower associated activation energy (intermediate or free water). Figure 2.12, reproduces some of Lim et al (1993) data; note the similarity to the form of figure 2.11. with comparatively little change in γ_1 (bound) compared to γ_2 (intermediate or free water). The authors then show results for various solvents showing them forming bound (acetic acid), free (methanol and ethanol) and both (methylene chloride). They attribute the γ_2 water as being in small clusters within the polymer.

These clusters form during the absorption process due to co-operative reorientation of large dipolar groups leading to a magnification of the groups effect. This hypothesis they support with a considerable amount of data on the dipole moments and activation energies of water and the other solvents. Nakamura et al (1983) observed a similar

situation on the DSC where the free water peak only forms when the material has absorbed enough water so it may be considered saturated (no change in enthalpy associated with the first bound water peak).

Figure 2.12. Dielectric relaxation spectra of polyimide film at a frequency of 1Khz after saturation in different relative humidities, based on Lim et al, 1993.



Comparison to the results of Fyfe et al (1993), Takigami et al (1993) and Lim et al (1993), is interesting as the front of more bound water followed by less bound water diffusing indicates a gradual gradient of the state of water within a polymer during absorption. This seems to be followed by a second stage in the absorption process, the development of intermediate and free water within the sample, the importance of the concentration and energetic's in this stage can not be understated. Indeed the significance of these results to the previous sections should be apparent as the ingress of water moves further away from the simple Fickian model initially described.

2.3.3. Water clusters within polymers.

The previous sections have shown that water may not be uniformly distributed within a sample. While voids present initially and different structural regions (amorphous or crystalline) may account for some of these occurrences they do not account for all of

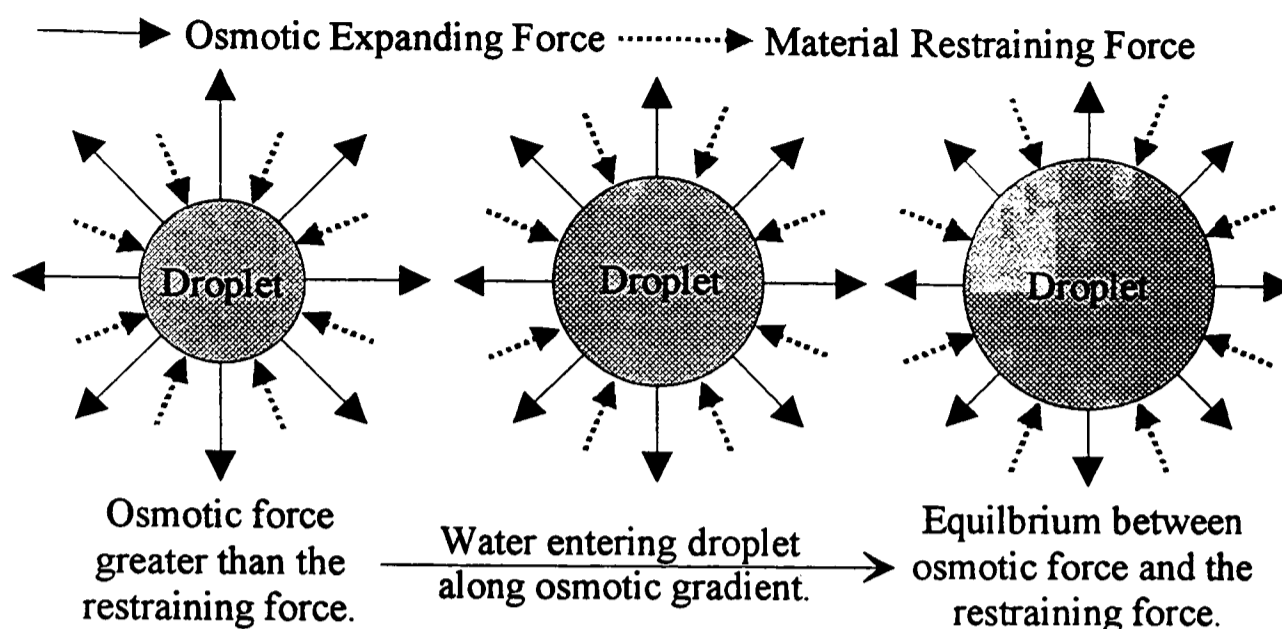
them. Voids or droplets may develop within material during the absorption process itself and this may be seen as the sample becomes opaque during the absorption process, when the droplets/clusters reach a certain size they will start to scatter light hence making the sample opaque. Although some mechanisms for the formation of droplets are now well accepted others remain quite debatable.

Probably the most accepted mechanism for cluster or droplet formation is the presence of a soluble impurity within the material, this being particularly well documented for elastomers (Barrer, 1951, Briggs et al, 1962, Yashuda and Stannett, 1962, Barrie et al 1975, Fedors, 1980, Southern and Thomas, 1980, Edwards, 1985, Thomas and Muniandy, 1987, Tillekeratne et al 1987, Harrison et al, 1991, Watson and Baron, 1996), but can occur in other materials. Soluble impurities (particularly left over from the production of the elastomer) within a material, once wetted by water diffusing into the material, form a solution droplet.

This solution droplet has an osmotic potential which depends on the size of the concentration of impurity in the droplet and type of impurity. The external solution also has an osmotic potential, the difference between these gives rise to an osmotic gradient between the two solutions. Water will then move along this gradient into the droplet expanding it. This results in a reduction in the osmotic gradient as the concentration of the impurity in the solution droplet is reduced. The deformation of the material around the droplet results in a force opposing this deformation exerted by the material on the droplet. The expansion will continue until this restraining force is equal to the force from the osmotic gradient. Figure 2.13 illustrates this expansion process of the droplets within the material. The nature of the restraining force is therefore critical in determining when the water uptake will reach equilibrium.

There is evidence of droplet formation in rigid polymers, but the materials have greater moduli which prevents the formation of the droplets, cracking or crazing of the polymer can then result (Bucknall et al, 1994). As elastomers stretch and deform more than rigid materials the effect of soluble agents or impurities will be more pronounced.

Figure 2.13. Schematic of expansion of water droplets within a material.



The ability of some polymers to form clusters by the reorganisation of the molecular structure or self attraction of water molecules within the polymer has been regarded as a somewhat of a contentious point. There is however a considerable body of evidence in favour of their formation (Lundberg, 1956, Barrie and Platt, 1963, Schneider et al, 1968, Gilbert et al 1977, Nakamura et al, 1983, Migliaresi et al, 1984, Smith and Fisher, 1984, Barrie et al, 1985, Venz and Dickens, 1991, Lee et al, 1992, Best et al, 1993, Lim et al. 1993, Patel and Braden, 1993, Hernandez and Gavara, 1994). While it is felt that some of these authors (particularly in the early work) may have wrongly attributed the formation of clusters to the action of soluble impurities, there is a considerable body of work which cannot be dismissed as easily, but the mechanisms for their formation are more open to debate. Lim et al (1993) describes a reorganisation of dipolar groups as previously mentioned. Bordeleau et al (1986) attributed it to oxygenated groups within the polymer. Barrie et al (1985) describes a similar process with the formation of the clusters being due to a reorganisation of polar groups near micro-voids, similar to the way groups cluster on the surface on contact with water and lower the contact angle (Noda, 1991). The freedom of such hydrophilic groups is recognised as being important in determining their effect on the diffusion coefficient and absorption characteristics (Davidson and Deen, 1988).

Lee et al (1992) describes the formation of clusters which result in cracks as being due to the polymer being locally in a 'supersaturated' state due to differences in the solubility (of the water in the polymer) within the polymer (possibly attributed to different degrees of conversions or heterogeneous morphology). Once the polymer has reached 'supersaturation' structural relaxation enables the formation of a second phase (the water

clusters), the growth of these being attributed to osmotic difference (due to hydrolysis) between the water cluster and external solution. Lee et al (1992) stresses the importance in hydrolysis of the polymer in generating the osmotic potential in expanding the clusters but not in the 'supersaturation' as he observes the formation of small (80 μm) solution domains within a unhydrolysable material (vinyl polyester resin). The 'supersaturated state' and how it forms seems a little open to interpretation but the work Lee et al (1992) shows the polymer only to form these clusters after saturation is obtained is fairly conclusive.

Nakamura et al (1983) attribute the formation of clusters within poly hydroxystyrene derivatives to the bound water attaching to hydroxyl groups (in the amorphous portion of the material). This breaks the intra molecular hydrogen bonding that existed between neighbouring hydroxyl groups; water then gathers at these sites in the free state (or clusters).

Gilbert et al (1977) used acoustic attenuation (to monitor the effect of the water on plasticization of the polymer) and infra red spectrometry (monitoring the shifts in the intensity of OH associated peaks) to study PMMA. In ambient conditions there was only one peak associated with water, when the test was repeated at 100°C however a second side peak was observed. This was attributed to the formation of clusters within the material at the higher temperature as the material was capable of relaxing (the PMMA was near its T_g). No other changes (shifting) were observed in the spectrum (including for the carbonyl group) of the PMMA. It was concluded that the formation of internal clusters was due to the self hydrogen bonding potential of water being sufficient to cause the formation of small clusters (of 3 or 4 molecules of water) within the PMMA. These small clusters were only weakly associated to the polar groups of the polymer. This was also reported to occur in other methacrylate polymers (Venz and Dickens, 1991) as well as ability of micro-voids and the interface between polymer and filler to initiate such clusters. These may be similar to the clusters between water and ethanol or acetic acid which are reported for pervaporation through a membrane (Uchytel et al, 1996).

Favre et al (1994) notes an increased tendency to cluster with increasing hydroxyl group density on the solvent (a range of alcohol's and water) for silicone materials. Links are also drawn to the aggregated water structures associated around polypeptides (Teeter, 1989). The strongest effect is with water due to its small size and high number of potential hydrogen bonds.

Garcia-Ferro and Aleman (1982) present a theory of a slow change in the state of water from being bound to hydroxyl groups on flexible polymer side chains (glycerine ether groups grafted on pre polymer of an epoxide). These hydroxyl groups then gradually reorientate to associate with more water; this leads to a lowering of the energy associated with the attraction of water onto the hydroxyl group and the formation of clusters. The gradual reorientation leads to a gradual reduction on the binding of the water to the hydroxyl groups during the absorption process. Similarities could perhaps be drawn to the *p*-styrenesulphonic grafted Nylon-6 shown in figure 2.11, which shows a gradual transition decreasing the degree of bonding of the water.

Smith and Fisher (1984) attribute the formation of clusters to residual stress within the material (melamine-formaldehyde, which is a highly cross linked thermosetting plastic) forming a network of stress variations throughout the sample. Water diffusing into the material blocks the intra molecular bonding between the polymer chains by hydrogen bonding to the chain enabling the local relaxation of the polymer so forming clusters. Hydrolysis of the polymer is noted as important in the growth of these droplets along with the stress relaxation of the polymer being involved in the formation and subsequent growth of the droplets.

Boakye and Yeager (1992) approached the area from studying ion diffusion into and through PTFE ionomers (sulphonate groups); they observe an association of ion concentration and water in micro regions within the material. IR spectrometry is then employed to study the interaction between the hydrated ionic groups on the polymer and ions; they observed a series of different states from the IR absorbance (shifting wavelengths) of OH with that attributed to the self associated water being most volatile (lost quickest during desorption). The sulphonate groups are responsible for the binding of the water and the clustering characteristics of the polymer.

2.3.4. Dual sorption models (Flory-Huggins, Langmuir and Zimm Lundberg).

Dual sorption theories are primarily concerned with predicting the extent of the water absorption of the polymer. The basis of these theories is the addition of two contributing equations, the first is normally based on Flory Huggins equation, although Henry's law has also been applied (Yasuda and Stannett, 1962, Vieth and Sladek, 1965, Vieth et al, 1966, Schneider et al, 1968, Pace and Datyner 1980, Garcia-Ferro and Aleman, 1982),

to describe the uniform distribution of water in the material using an additional term based on Langmuir. The second describes the onset of clustering as described by Zimm Lundberg for the self association of water in a binary media.

The Flory Huggins equation (Flory, 1942, Huggins 1942) is widely known and derived (Patel, 1987, Gedde, 1995), hence will not be derived here, but a few of the steps in the approach should be noted. The model uses a lattice of points which for each may be occupied by either one 'segment' of polymer or a solvent molecule, the polymer being connected within the model and the total volume is unchanged during mixing. The entropy terms and enthalpy term are each considered separately and then summed to give the total energy change in free energy (ΔG) on mixing as,

$$\frac{\Delta G}{N} = RT \left(v_1 \ln v_1 + \frac{v_2}{x} \ln v_2 + \chi v_1 v_2 \right) \quad \text{Equation 2.12.}$$

where N is the total number of moles of components 1 and 2, v is the volume fraction, x is number of lattice positions each polymer chains occupies (or the number segments in the chain) and χ is the interaction parameter between the components 1 and 2. This may be further refined into terms of activity of the solution of the solvent (a_1) by applying the Gibbs - Duhem equation ($x_1 d\mu_1 + x_2 d\mu_2 = 0$) which stems from consideration of the mixing of two solutions, where μ is the chemical potential.

$$\frac{\Delta G}{NRT} = \frac{\mu_1 - \mu_1^0}{RT} = \ln a_1 = \ln v_1 + \left(1 - \frac{1}{x}\right) v_2 + \chi v_2^2 \quad \text{Equation 2.13.}$$

For a polymer x is large therefore $1/x$ is very small and is neglected, and expressing purely in terms of v_1 as ($v_2 = 1 - v_1$),

$$\ln a_1 = \ln v_1 + (1 - v_1) + \chi(1 - v_1)^2 \quad \text{Equation 2.14.}$$

The activity of the solvent (a_1) is the free energy of the solution (μ_1) in comparison to the solution in the standard state (μ_1^0) as seen in equation 2.13. It is frequently defined as the partial pressure of the solution $a_1 = P_1/P_1^0$ where P_1 is the partial pressure and P_1^0 is the partial pressure in the standard state (Robinson and Stokes, 1959). The activity is also related to the osmotic pressure of the solution (π) via,

$$-\pi V_1 = RT \ln a_1 = \mu_1^0 - \mu_1 \quad \text{Equation 2.15.}$$

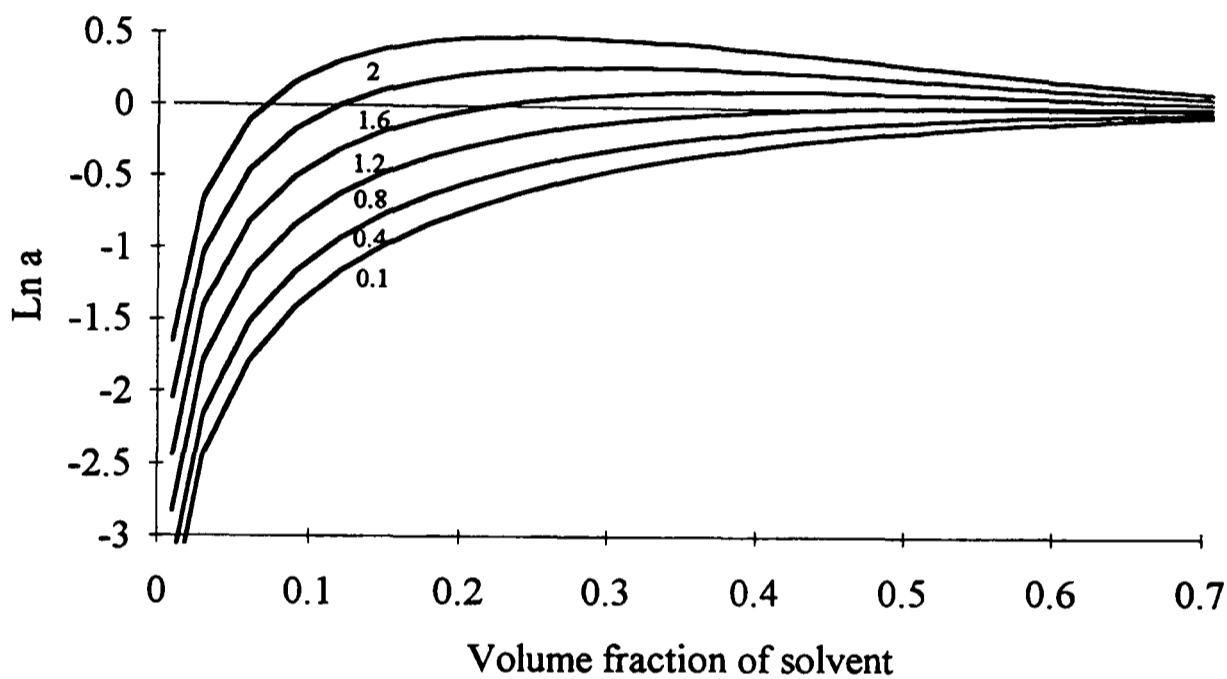
The solvent interaction parameter (χ) controls the limit of the miscibility of the solvent in the polymer as seen in figure 2.14. If χ is less than 0.5 the system will be miscible in all proportions, as $\ln a_1$ ($\Delta G/NRT$) is negative. When χ is greater than 0.5, $\ln a_1$ will become positive when a critical volume fraction of solvent is reached thus limiting the miscibility of the solvent and polymer. In theory χ is related to the solubility parameters

(δ) of the individual components by equation 2.16, (Van Krevelen, 1976), although this approach does not apply to all polymer systems (Favre et al 1994),

$$\chi \approx 0.34 + \frac{(\delta_1 - \delta_2)^2 V_1}{RT} \quad \text{Equation 2.16.}$$

The high values of χ for water and the different polymers (typically 1.5 to 2) demonstrate the limited miscibility or sorption expected to occur into the polymer.

Figure 2.14. The miscibility of different polymer solutions with a range of different χ values.



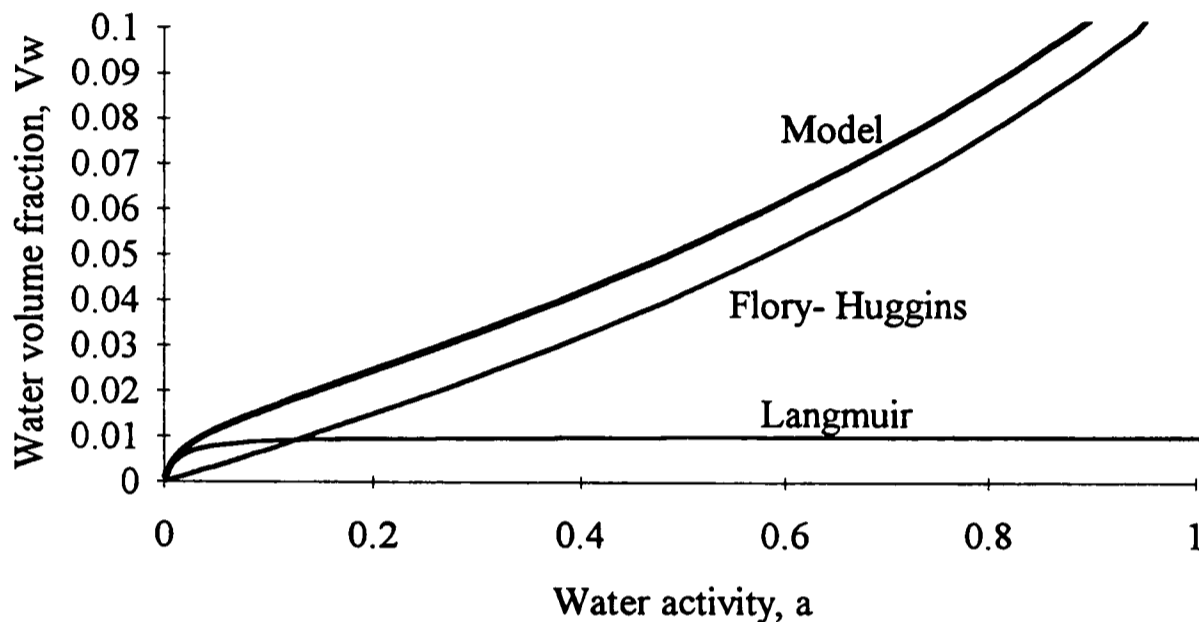
The second part of the dual sorption theories is based on the Langmuir equation to describe the formation of clusters as chemisorption onto active sites.

$$v_w = v_w^F + v_w^L = f(a, \chi) + \frac{Ka}{1 + Ba} \quad \text{Equation 2.17.}$$

where $v_w^F = f(a, \chi)$ is the contribution of the Flory Huggins equation and v_w^L is the Langmuir contribution, K and B are modified Langmuir parameters put in terms of activation rather than pressure. For the Henry Langmuir model v_w^F is replaced by the contribution from Henry, namely $k_D a$ where k_D is the Henry's law dissolution constant (Vieth and Sladek, 1965, and Vieth et al 1966). Figure 2.15, shows an illustration of equation 2.17, this demonstrates the different contributions of the Flory Huggins and Langmuir components of the model. The correlation with experimental data is

reportedly very good (Hernandez and Gavara, 1994). The approach taken above is generally applied but many different variations have been developed by different authors.

Figure 2.15. The prediction of water uptake from solutions of different activities using the dual sorption model (equation 2.17), data from for Nylon 6 at 5°C, Hernandez and Gavara, 1994.



Favre et al (1994) for example uses a semi empirical approach based on Koningsveld and Kleinjteins (1974) for a hydrophobic silicone system which considers the surface interaction as well as the volume,

$$\chi = \alpha + \frac{\beta(1-\omega)}{(1-\omega v_2)^2} \quad \text{Equation 2.18.}$$

where α, β and ω are adjustable parameters. This shows a good correlation with the more polar solvents used (2-methyl-2-propanol, 2-butanol, 1-butanol, ethanol, methanol and water) which tended to be lower at higher activities than predicted by the standard Flory-Huggins equation. Although α, β and ω show trends with the increasing polarity of the solvents little can be drawn from this data due to its semi empirical nature.

There is another element in this overall philosophy, namely the Zimm Lundberg's (Zimm and Lundberg, 1956) cluster function (G_{II}) which is used to calculate the self-association of the water / solvent molecules in binary systems. This was originally derived to describe the clustering behaviour of gases and solvents in non-polar polymers (Lundberg, 1956, Zimm and Lundberg, 1956). This is based on consideration of the Flory Huggins

Guggenheim theories and incorporates a term to describe the formation of a space for the penetrant between the chains within the matrix. This is expressed as,

$$\frac{G_{II}}{V_1} = -(1 - v_w) \frac{\partial \left(\frac{a}{v_w} \right)}{\partial a} - 1 \quad \text{Equation 2.19.}$$

Where $v_1 G_{II}/V_1$ is the mean number of gas / solvent molecules in excess of the mean concentration of gas / solvent molecules in the neighbouring sites, thus measuring the tendency of the gas / solvent molecules to cluster, assuming constant pressure and temperature (Lundberg, 1956). The water or solvent is said have a tendency to cluster when G_{II}/V_1 is greater than -1 (Lundberg, 1956, Yashuda and Stannett, 1962, Barrie and Platt, 1963, Schneider et al, 1968, Garcia-Fierro and Aleman, 1982, Hernandez and Gavara, 1994), below this value the dual sorption model as detailed above (equation 2.17) applies. The limitations of this equation are also detailed by Zimm and Lundberg (1956) who find the theory to apply well to some systems but not to others. Clearly the differential term (particularly a_1 / v_w) is very important, unfortunately there does not seem to be a simple answer to this as different authors use different methods to solve the equation. Lundberg (1956) considers different systems, including using Henry, Raoult's, Flory Huggins, Langmuir, and BET isotherms, to solve this term but none of these seem to be particularly applicable to water in polymers. Schneider et al (1968) used a curve fitting approach to determine a_1 / v_w . Hernandez and Gavara (1994) derived an expression based on equation 2.17, and 2.18, as,

$$\frac{G_{II}}{V_w} = \frac{(1 - V_w)}{V_w^2} \left\{ \frac{Ka}{(1 + Ba)^2} + \frac{v_w^F}{1 - v_w^F [1 + 2\chi(1 - v_w^F)]} \right\} - \frac{1}{V_w} \quad \text{Equation 2.20.}$$

For a particular polymer the overall model predicts that equation 2.17 will apply until a critical water uptake or activity is reached determined by equation 2.18, then clusters will start to form due to the self association of water. The kinetics of the process are normally assumed to be Fickian. Hernandez and Gavara (1994) do imply that the diffusion coefficient calculated at different solution activities is a polynomial expression reaching a maximum (highest diffusion rate) at the onset of water clustering activity (about $a = 0.5$). In theory this illustrates that a change in the concentration dependence of the diffusion coefficient occurs, from increasing with water concentration to

decreasing with concentration when the onset of clustering occurs. However the authors admit that the correlation is dubious with the onset of clustering.

A major drawback with this approach is that the factors K , B and χ need to be determined for each individual material. Although χ may be determined using equation 2.16, this relationship is not ideal as its applicability to polar solutions (capable of hydrogen bonding) such as water is questionable. When the Koningsveld and Kleinjans (1974) theory is applied the results at best can be semi empirical and say little about the inherent processes behind the absorption.

Whilst the Flory Huggins equations have proved very capable of predicting the mixing for good (polymer and solvent mutually miscible) solvents with a polymer system it fails to predict adequately when the solvent is poor (not miscible with the polymer), (Favre et al, 1994). The overall impression of the dual sorption theories is that they may work well in individual cases but when they are applied to a wider range of materials they tend to break down. This seems to be due to the different variations being applied in different cases to explain the results of a particular experiment rather than the absorption of water or solvents as a whole. Vieth et al (1966) approach the kinetics of the diffusion process and correlate, with reasonable accuracy theoretical and experimental data for methane in polystyrene. In general the dual sorption models say nothing or little about the kinetics of the process itself; Fickian kinetics are often assumed to be close enough fit (Lee and Peppas, 1993). Other methods have also been considered (Tamai et al, 1994, detailed in a later section). Although these theories have had some success with predicting the behaviour of water in elastomers (Yashuda and Stannett, 1962, Schneider et al, 1968, Favre et al 1994) generally they have limited applicability (Barrie et al, 1975, Fedors, 1980, Watson and Baron 1996).

2.3.5. Modelling of the formation of droplets within elastomers.

The following is a description of the results of Muniandy and Thomas (although the initial paper was published by Southern and Thomas, 1980) and a possible derivation (based on that derived by Professor M. Braden) is given in appendix II.c. Muniandy and Thomas published a series of papers (1984,a, 1984,b, 1988, Thomas and Muniandy, 1987) on the water uptake of elastomers, these papers represent probably the most comprehensive mathematical model yet derived for absorption into elastomers although

it should be recognised that other derivations were shown previously by other authors (particularly Fedors, 1980).

Consider an ideal elastomer containing an impurity which has reached an equilibrium water uptake. There is a balance between the osmotic force to expand the droplet and the elastic restraining force. As previously described the osmotic force is attributable to the difference between the osmotic pressure of the external solution (π_o) and the osmotic pressure of the internal solution droplet (π_i). Therefore,

$$P = \pi_i - \pi_o \quad \text{Equation. 2.21.}$$

where P is the pressure being applied by the droplet. Although Raoult's law is only applicable to dilute solutions it is used to calculate π_o and π_i (this seems reasonable when the system is at equilibrium, although at earlier times this is questionable for π_i). Hence,

$$\pi_o = \frac{c_o RT}{M_o} \quad \text{and} \quad \pi_i = \frac{c_i RT \rho_w}{(c_w - s) M_i} \quad \text{Equation. 2.22. \& 2.23.}$$

where c_o is the concentration and M_o the molecular weight of salt in external solution, R is the gas constant, T is temperature, c_i is the concentration and M_i the molecular weight of impurity/salt in rubber, ρ_w is the density of water, c_w is the overall concentration of water in material and s is the concentration of water in rubber matrix. Here, $c_w - s$, is the concentration of water in droplets within the material and so, $c_i \rho_w / (c_w - s)$, is the concentration of the impurity/salt within the droplets.

It is worth noting that Fedors (1980) approached this problem in a similar manner although he used a version of Raoult's law which used an osmotic coefficient to represent a correction for non-ideality (of the salt/impurity solution),

$$\pi = \frac{nRT\Phi}{V_2} \left(\frac{S_2}{1 - S_2} \right) \quad \text{Equation 2.24.}$$

where n is the number of moles of particles formed when one mole of the salt/impurity goes into solution and Φ is the osmotic coefficient. The use of S_2 (volume fraction of solute or salt in solution) and V_2 (molar volume of solute) rather than M and c is only a matter of algebra. This approach uses published (Robinson and Stokes, 1959, Harned and Owens, 1958) tables for the osmotic coefficient of common salts at different concentrations, where the data was not available unity was used. Although this approach is more accurate the practical problems in dealing with the tables particularly for calculations of unknowns as in the later equations makes it if not unfeasible certainly less attractive.

The droplets are assumed to be spherical and the rubber to obey statistical theory and hence the pressure required to enlarge a spherical droplet (Gent and Lindley, 1958) is,

$$P = \frac{G}{2} \left(5 - \frac{4}{\lambda} - \frac{1}{\lambda^4} \right) \quad \text{Equation. 2.25,}$$

where G is the shear modulus and λ is the principle extension ratio. Kaelble (1971) describes the limitations of this equation to be when the initial size of the particle is insufficient to overcome the surface energy effects, and when centre of the particles are too close for the assumption of isolation in a block of infinite rubber (distance of separation of centres is less or equal to 4 times the radii of the two particles) this will occur at approximately 1% (Fedors, 1980).

The pressure to enlarge the droplet is equal to the restraining pressure exerted by the material. Hence substituting into Equation 2.21,

$$\frac{G}{2} \left(5 - \frac{4}{\lambda} - \frac{1}{\lambda^4} \right) = \frac{c_i RT \rho_w}{(c_w - s) M_i} - \frac{c_o RT}{M_o} \quad \text{Equation 2.26.}$$

A similar equation to this was derived by Fedors (1980) apart from the exception of the π_o term and slightly different notation. A term is then calculated for the growth of the droplets in the elastomer by considering the growth of the individual droplets (Appendix II.c) which yields the relationship,

$$c_w - s = c_i (\lambda^3 - 1) \frac{\rho_w}{\rho_i} \quad \text{Equation 2.27.}$$

Although assumptions are made during this derivation (that the droplets are spherical, the volume of the material is constant and the rubber obeys statistical theory), which in reality are unlikely to be met, they establish an ideal model for the absorption process.

In the original paper by Southern and Thomas (1980) it was assumed that all the water was present in the droplets (the s term therefore disappears). They then derive an expression for c_w in a slightly simpler form by considering the individual droplets where the density of the water and impurity are neglected hence $\lambda^3 - 1 = c_w / c_i$.

The fit of equation 2.26 using equation 2.27 to calculate λ (or by substituting equation 2.27 into 2.26) to experimental data is reportedly good. Indeed the initial equations derived by Southern and Thomas, (1980) for a doped (10% NaCl) polyisoprene showed the model tending to predict 15-20 % more than the experimental value. This level of error was also observed in the later papers by Muniandy and Thomas (1984,a, 1984,b

and 1988, Thomas and Muniandy, 1987) for a range of different soluble agents in polyisoprene immersed in different saline solutions. This difference was initially attributed to leaching of the dopant during the absorption process, but later it was discovered that on average of only 80 % (between 73-87 %) of the salt was successfully being incorporated into the poly isoprene during the milling (Thomas and Muniandy, 1987 and Muniandy and Thomas, 1988). This improves the correlation, the experimental values being typically 8 % higher than the theoretical prediction.

Fedors (1980) approach is a little different in that from equation 2.26 he substitutes in for λ in terms of volume fractions of solute and solvent within the droplets. Based on $\lambda = r/r_0$ (the increase in radius of the droplet) hence $\lambda^3 = V/V_0$ (the increase in volume of the

droplets) and volume fraction of solute in cavity (ϕ_2) = $\frac{V_{v2,t}}{V_{v1} + V_{v2,t}}$ (where $V_{v2,t}$ is volume

of solute/salt and V_{v1} is volume of solvent/penetrant in the cavity) so $\lambda^3 = 1/\phi_2$. When this is combined with Equation 2.24, and 2.25, assuming that π_0 is zero, ignoring s , the general solution is

$$\frac{nRT\Phi}{V_2G} = \frac{1}{2} \left(5 - 4\phi_2^{1/3} - \phi_2^{4/3} \right) \left(\frac{1 - S_2}{S_2} \right) \quad \text{Equation 2.28.}$$

If the solute is completely miscible ($S_2 = \phi_2 < S_2^*$, volume fraction in saturated solution) the expression for equilibrium becomes.

$$\frac{nRT\Phi}{V_2G} = \frac{1}{2} \left(5 - 4\phi_2^{1/3} - \phi_2^{4/3} \right) \left(\frac{1 - \phi_2}{\phi_2} \right) \quad \text{Equation 2.29.}$$

Which is fundamentally a way of re-stating equation 2.26, without the s or π_0 . This equation is then solved graphically assuming the dilution's is high i.e. $\phi_2 < S_2^* < 0.1$. Here the agreement with experimental data (a *cis*-polybutadiene doped NaCl and Na₂SO₄) is very good as previously described by the results of Southern and Thomas (1980), Muniandy and Thomas(1984, 1984, 1988) and Thomas and Muniandy (1987).

Fedors (1980) also proposes a solution when the solute is incompletely miscible ($\phi_2 > S_2^*$), here $S_2 = S_2^*$ as solution saturated by solute, hence,

$$\frac{nRT\Phi}{V_2G} = \frac{1}{2} \left(5 - 4\phi_2^{1/3} - \phi_2^{4/3} \right) \left(\frac{1 - S_2^*}{S_2^*} \right) \quad \text{Equation 2.30.}$$

Here the agreement between theoretical and experimental (*cis*-butadiene doped with PbCl₂) is apparently 'excellent' (according to Fedors, 1980) apart from two high modulus

samples at a high temperature. However, inspection of the data shows good agreement for the three of the higher modulus and low temperature test samples, but the other samples (in good agreement) had not reach equilibrium (one of the samples showing a uptake of 64 % wt where as the calculated value is 355 wt%) seems this conclusion is a little premature.

Muniandy and Thomas consider the actual rate of the diffusion and define an 'apparent diffusion coefficient'; the potential of this approach was first demonstrated by Southern and Thomas (1980) using a more relaxed derivation (but still gave good correlation with experimental results). Fedors (1980) also briefly considers this but does not try to derive a solution for the problem. Muniandy and Thomas's approach is based on the previously derived equations and a variation on Fick's Laws (for chemical potential), to describe the protracted uptake observed for the elastomers. The actual philosophy behind their approach assumes that there is a decrease in the droplet size with increasing depth into the material this then enables the establishing of a chemical potential gradient (stemming from the dilution of impurity/salt particles) through the material. The next part is best described in their own words;

'The droplets near the surface of the rubber sample will thus generally be larger than those further inside the bulk of the rubber.'

Muniandy and Thomas, 1984,a.

and

'It is assumed that the water in the rubber phase immediately adjacent to the impurity droplet is in local equilibrium with the water in the droplet solution. The free energy of the water in the rubber phase in the neighbourhood of a droplet which in the rubber surface will be higher than that for a droplet nearer the rubber surface. Hence a free-energy gradient exists for the water dissolved in the rubber phase favouring movement of water into the body of the rubber.'

Muniandy and Thomas, 1984,b.

The approach assumes that Fick's Laws are obeyed within the system, in that M_t/M_∞ is still linear with respect to $t^{1/2}$, hence being modelled by equation 2.6 (Southern and Thomas, 1980). A similar approach is also described but not solved by Barrer (1951) where the diffusion coefficient is concentration dependant equation 2.9, the dependence being controlled by the osmotic pressure of the internal and external solution.

There is however a further problem. The growth of the droplets gives rise to stresses in the rubber which lead to complex stress fields within the material. The effect of this stress field on the concentration of the water in the rubber is complex and is avoided by using the chemical potential (μ) gradient rather than the normal concentration gradient as dealt with in the previously sections. This approach is based on a thermodynamic diffusion coefficient quoted by Park (1950) using the modified expression for flux,

$$F = -D_T \left(\frac{s}{RT} \right) \left(\frac{\partial \mu}{\partial x} \right) \quad \text{Equation 2.31.}$$

where s the concentration of water in the rubber phase. D_T is defined as the thermodynamic diffusion coefficient but as the concentration of water dissolved in the rubber is small it is taken to be the ordinary diffusion coefficient as used previously by equation 2.6. The problem is now somewhat simplified to that of determining the dependence of the chemical potential on the water present in the rubber matrix and in the droplets.

As the system is not in a state of equilibrium equation 2.21 has to be modified to,

$$P = \pi_i - \pi_o - p \quad \text{Equation 2.32}$$

where p is the elastic pressure restraining the droplet exerted by the material and P is the pressure applied by the droplet. With the chemical potential being,

$$\mu = -PV_w \quad \text{Equation 2.33}$$

where V_w is the molecular volume of water. Equation 2.31. can therefore be written as,

$$F = D_T \left(\frac{sV_w}{RT} \right) \left(\frac{\partial P}{\partial x} \right) \quad \text{Equation 2.34.}$$

The apparent diffusion coefficient (D_a) is then defined as the diffusion coefficient as for Fick's first law (equation 2.1), so,

$$F = -D_a \frac{\partial c_w}{\partial x} \quad \text{Equation 2.35}$$

Hence combining equations 2.34 and 2.35 gives, when put in terms of the extension ratio (λ),

$$D_a = -D_T \frac{sV_w}{RT} \frac{\partial P}{\partial c_w} = -D_T \frac{sV_w}{RT} \frac{\partial P}{\partial \lambda} \frac{\partial \lambda}{\partial c_w} \quad \text{Equation 2.36.}$$

There is however one further complication concerning the concentration of water in the rubber phase (s). As the rubber is stressed (under pressure) the water concentration will be less than that in the pure rubber. This is dealt with by applying Raoult's and Henry's laws assuming the system acts as an ideal gas. Which yields,

$$s = \frac{s_o}{1 + \frac{M_w \rho_i}{M_i \rho_w} (\lambda^3 - 1)} \quad \text{Equation 2.37}$$

The derivation (Appendix II.c.) of s in terms of s_o creates a problem in that as λ tends to 1, (i.e. for increasingly pure systems) s tends to zero rather than s_o. Additionally it should be remembered that the effect of the stressing of the matrix was assumed insignificant when dealing with the difference it would have on D_T. It is therefore apparent that this is a weak point in the overall argument.

Now returning to equation 2.36, it is apparent that we need to find ∂P/∂λ and ∂λ/∂c_w. The expression for ∂λ/∂c_w is derived by substituting equation 2.37 into a reordered version of equation 2.27 and differentiating. Which gives,

$$\frac{\partial c_w}{\partial \lambda} = 3\lambda^2 \frac{\left\{ \frac{\rho_w}{\rho_i} c_i \left[(\lambda^3 - 1) + \frac{M_w \rho_i}{M_i \rho_w} \right]^2 + s_o \frac{M_w \rho_i}{M_i \rho_w} \right\}}{\left[(\lambda^3 - 1) + \frac{M_w \rho_i}{M_i \rho_w} \right]^2} \quad \text{Equation 2.38.}$$

For the ∂P/∂λ equation 2.32 is used and equation 2.22, 2.23 and 2.25 (for p rather than P) substituted, and then differentiating to yield,

$$\frac{\partial P}{\partial \lambda} = \frac{-3\lambda^2 RT \rho_i}{(\lambda^3 - 1) M_i} - 2G \left(\frac{1}{\lambda^2} + \frac{1}{\lambda^5} \right) \quad \text{Equation 2.39.}$$

Here the first term stems from the elastic pressure and the second from the osmotic pressure. Equations 2.38 and 2.39 are then substituted into equation 2.36, to give the solution for D_a as,

$$D_a = \frac{(\lambda^3 + A - 1)(\lambda^3 - 1)}{\left[(\lambda^3 + A - 1)^2 + s_o A / kc_i \right]} \left[\frac{K_2}{(\lambda^3 - 1)^2} + K_1 \left(\frac{1}{\lambda^4} + \frac{1}{\lambda^7} \right) \right] \quad \text{Equation 2.40}$$

Where A and k are,

$$A = \frac{M_w \rho_i}{M_i \rho_w} \quad \text{and} \quad k = \frac{\rho_w}{\rho_i} \quad \text{Equation 2.41, and 2.42.}$$

and K_1 and K_2 are,

$$K_2 = \frac{D_T s_o V_w \rho_w}{c_i k^2 M_i} \quad \text{and} \quad K_1 = \frac{2GD_T s_o V_w}{3c_i kRT} \quad \text{Equation 2.43 and 2.44.}$$

Alternatively this may be expressed a ratio of D_a and D_T ,

$$\frac{D_a}{D_T} = \frac{\left[\frac{3\rho_i V_w}{(\lambda^3 - 1)M_i} + \frac{2GV_w}{RT} \left(\frac{1}{\lambda^4} + \frac{1}{\lambda^7} \right) (\lambda^3 - 1) \right] \left[(\lambda^3 - 1) + \frac{M_w \rho_i}{M_i \rho_w} \right]^3}{3 \left\{ \frac{\rho_w c_i}{\rho_i s_o} \left[(\lambda^3 - 1) + \frac{M_w \rho_i}{M_i \rho_w} \right]^2 + \frac{M_w \rho_i}{M_i \rho_w} \right\}} \quad \text{Equation 2.45.}$$

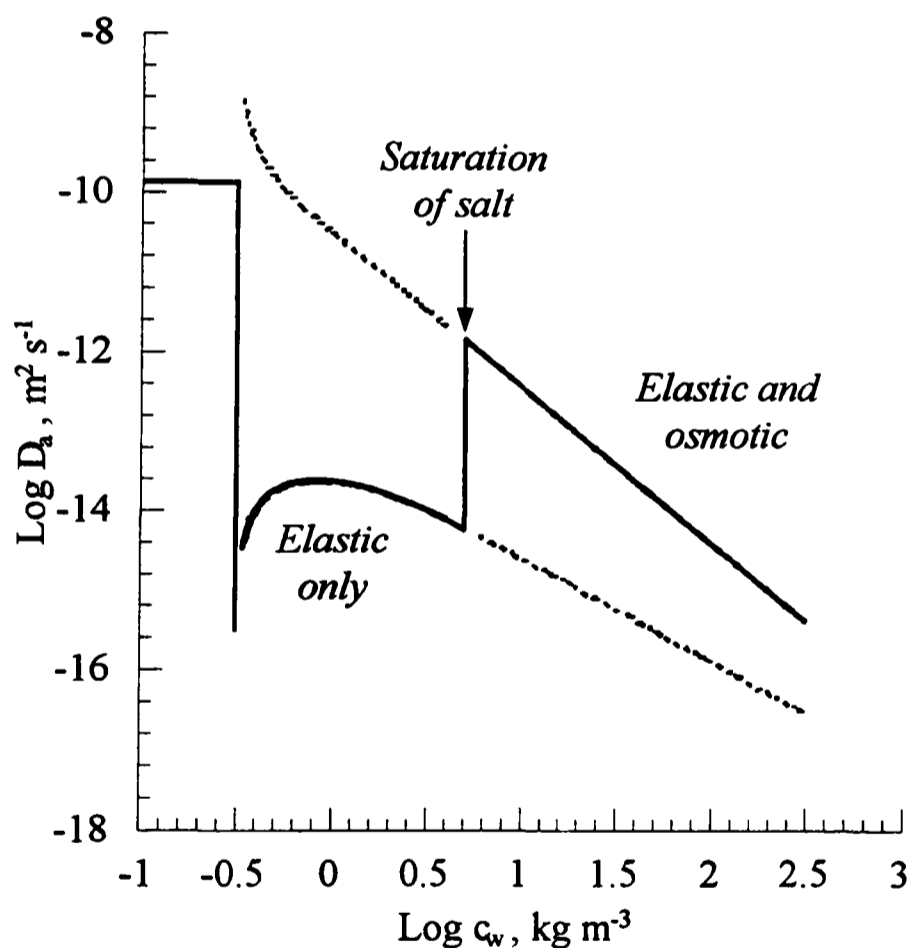
From equation 2.40 it is important to note that the K_1 term governs the elastic pressure and the K_2 the osmotic pressure. There is another stage in this process which considers the salt going into solution; here the only term considered is the elastic one (i.e. K_2 is taken to be zero and hence may be ignored). The application of Barrie et al 's (1975) data shown in table 2.1 to this overall theory, taking D_a to be equal to D_T until c_w equals $3/4$ of s_o , is shown in figure 2.16. Here the dependence of D_a on C_w is shown as the solid line with the predictions of the relative parts as broken lines. The change from the purely elasticity controlled to osmotic and elastic occurs when the NaCl (in this case) becomes saturated. This occurs when c_w equals 4.054 kg m^{-3} using the saturation of the proportion of NaCl in water as 370 kg m^{-3} . It is worth noting the prediction that as c_w (small λ) approaches s_o , s tends to positive or negative ∞ depending on the formula (elastic or elastic and osmotic) used, this seems to stem from the flaw in the correction for s and s_o .

Muniandy and Thomas go further with this work to describe the kinetics of the initial absorption process in terms of the predicted shape of the profile of water in the material and absorption and desorption of the water. This is not discussed here as the basic philosophy of this work is covered by the above and it is felt that it would add little to the overall understanding and discussion within this thesis.

Table 2.1. Barrie et al, 1975, data for a NaCl doped polyisoprene.

Variable	Value
G	0.37 MNm ⁻²
c _i	1.50 kg m ⁻³
D _T	1.32x10 ⁻¹⁰ m ² s ⁻¹
s _o	0.32 kg m ⁻³
ρ _i	2200 kg m ⁻³
M _i	0.0265 kg mole ⁻¹

Note: M_i half that of NaCl, 0.053 kg mole⁻¹.

Figure 2.16. Prediction of equation 2.40, using the data of Barrie et al ,1975, the full line indicating the predicted values, based on Muniandy and Thomas, 1987.

The experimental agreement for the doped polyisoprene used by Muniandy and Thomas is good with the experimental values being on average 8 % higher than the theoretical. The application of the theory to the Barrie et al (1975) data also shows good agreement with the theoretical values being approximately 12 % higher than those observed experimentally. The reduction in D_a with increasing water content is in agreement with many other authors as previously mentioned and shown in figure 2.8, although the

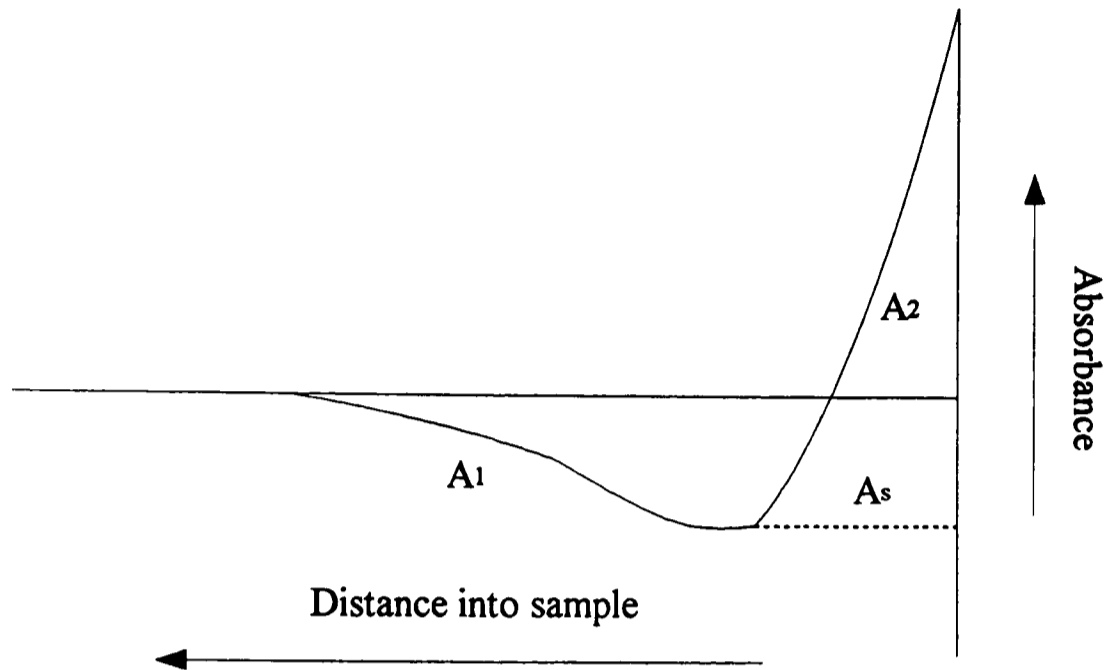
reduction is somewhat different (in figure 2.8, it is linear and figure 2.16, it is logarithmic). Generally this formula, bearing in mind the assumptions made, seems to predict the absorption characteristics quite accurately.

The same sort of pattern is seen in the Aminabhavi et al (1984) data on absorption from distilled water and sea water. With the rubbers (styrene butadiene, neoprene and ethylene propylene diene terpolymer) in the sea water (higher osmolarity solution) exhibiting a lower faster uptake than those in the distilled water.

There is an alternative approach to the problem of water uptake into elastomers which, rather than using a modified diffusion coefficient (D_a) in Fickian kinetics, uses a dual sorption type approach (Harrison et al, 1991). Here the absorption is two stage the first stage being the diffusion into the polymer by the water in a Fickian manner, the second being the diffusion controlled growth of the droplets. Here the growth of the droplets occurs after the initial saturation of the elastomer. Harrison et al (1991) studied the diffusion of water in doped (CoCl_2) plasticised PVC, the ingress is monitored by the change in absorbance (of light) through a membrane made from PVC incorporating a water sensitive dye. Figure 2.17, illustrates their results with the absorbance initially decreasing as the water diffuses into the material (A_1) until it reaches a minimum value (A_s) which corresponds to the saturated matrix. Droplets then form and the absorbance increases (A_2) due the light scattering of the droplets. The kinetics of each of these two stages are shown to be Fickian with profiles of the absorbance during the absorption process corresponding to those shown in figure 2.2. Hence Harrison et al (1991) propose that the absorption in the first stage is controlled by equation 2.3. When this reaches the saturation value the second stage of droplet formation starts which is again controlled by a constant times equation 2.3.

This approach is interesting as it splits the diffusion process into two parts A_1 and A_2 , and seems to agree with some elements of other work on the clustering behaviour when the authors say the polymer must be saturated before the clusters or droplets form. The profiling of the concentration of water in the elastomer shows the distinct two phase behaviour which differs from the kinetics assumed by Muniandy and Thomas.

Figure 2.17. Model of absorbance profile inside membrane, based on Harrison et al, 1991.



Watson and Baron (1996) take such a two phase approach to describe the water uptake of a silicone polymer using a modified Fick's second law equation 2.2.

$$\frac{\partial c_m}{\partial t} = D \frac{\partial^2 c_m}{\partial x^2} - \frac{\partial c_i}{\partial t} \quad \text{Equation 2.46.}$$

Where D is the diffusion coefficient in the pure material, c_m is the concentration of mobile or water in the matrix and c_i is the concentration of water at immobilising sites of in droplets. Cloud physics is then employed to describe the nucleation of the immobilising sites which is applied to the polymer by assuming Henry's law is being obeyed. This yields,

$$c_i = - \frac{bc_s}{\ln\left(\frac{c_m}{c_o}\right)} \quad \text{Equation 2.47.}$$

where c_s is the concentration of the immobilising sites, c_o is the maximum concentration of mobile water (i.e. the maximum c_m), and b is a material constant. This is then differentiated and applied back in to equation 2.46, to give,

$$\frac{\partial c_m}{\partial t} = D_c \frac{\partial^2 c_m}{\partial x^2} \quad \text{Equation 2.48.}$$

Where D_c is the concentration dependent diffusion coefficient and is defined as,

$$D_c = \frac{c_m \left[\ln \left(\frac{c_m}{c_o} \right) \right]^2 D}{c_m \left[\ln \left(\frac{c_m}{c_o} \right) \right]^2 + bc_s} \quad \text{Equation 2.49.}$$

There are some problems with the constant b as this is a best fit factor, it seems likely that this would relate in some way to the restraining force the material exerts on the droplet but this relationship is not speculated on here. The employment of cloud physics to describe the formation of the droplets is novel and may not be so strange as might appear as both processes involve high local concentrations being controlled by the activity of the water in the surrounding environment.

There are, however, other factors not considered within these approaches that have been identified as being important, the most notable of these is the formation of cracks (Fedors, 1980, Schirrer et al, 1992 Di Colo, 1992). Another important factor is stress relaxation (Smith and Fisher, 1984) as this will reduce the elastic restraining force; indeed for more viscous materials the stress relaxation may overshadow the elastic deformation of the material. Also the relaxation process may be increased in turn by water absorption into an elastomer (Bankovskaya et al, 1982).

2.3.6. Permeation of elastomers.

Work on the permeation of elastomers may not seem particularly relevant at this point but is considered here as it further refines the diffusion process in elastomers. When permeation is considered Fick's laws still apply (equation 2.1, and 2.2) but the solution is different as the boundary conditions and geometry are different. For one dimensional permeation through a membrane in the steady state,

$$q = P(p_1 - p_2)At / L \quad \text{Equation 2.50.}$$

where q is the amount of water passing through the membrane, P is the permeability coefficient, A is the surface area, t is time, L is thickness, p_1 and p_2 are the vapour pressures on either side of the membrane. Alternatively this may be expressed in terms of the permeation rate (Q) as,

$$Q = P(p_1 - p_2) = qAt / L \quad \text{Equation 2.51.}$$

There are different mechanisms for permeation depending on the structure and type of the media. The presence of a crack network or pore channels will all have a profound effect on the rate of permeation. Generally for homogeneous polymers and elastomers the mechanism for permeation is known as 'activated diffusion' and is divided into three stages (Cassidy et al, 1983,a). The first stage is the adsorption of the penetrant at the surface (generally too rapid to be considered as rate determining step), the second the diffusion through the membrane (dependant on concentration gradient, energy of activation and temperature), and the third the evaporation from the other surface (governed by the vapour pressure of the outgoing surface). For 'activated diffusion' the permeability coefficient is equal to the diffusion coefficient (D) times the solubility coefficient (S), (Crank, 1975).

$$P = DS \quad \text{Equation 2.52.}$$

The dependence of D and S on concentration and the formation of clusters for fluids as discussed in earlier sections complicates the situation (Cassidy and Aminabhavi, 1983,a, Favre et al, 1994). Arrhenius type and Flory-Huggins based equations are used to enable reasonable prediction of the permeation rate experienced.

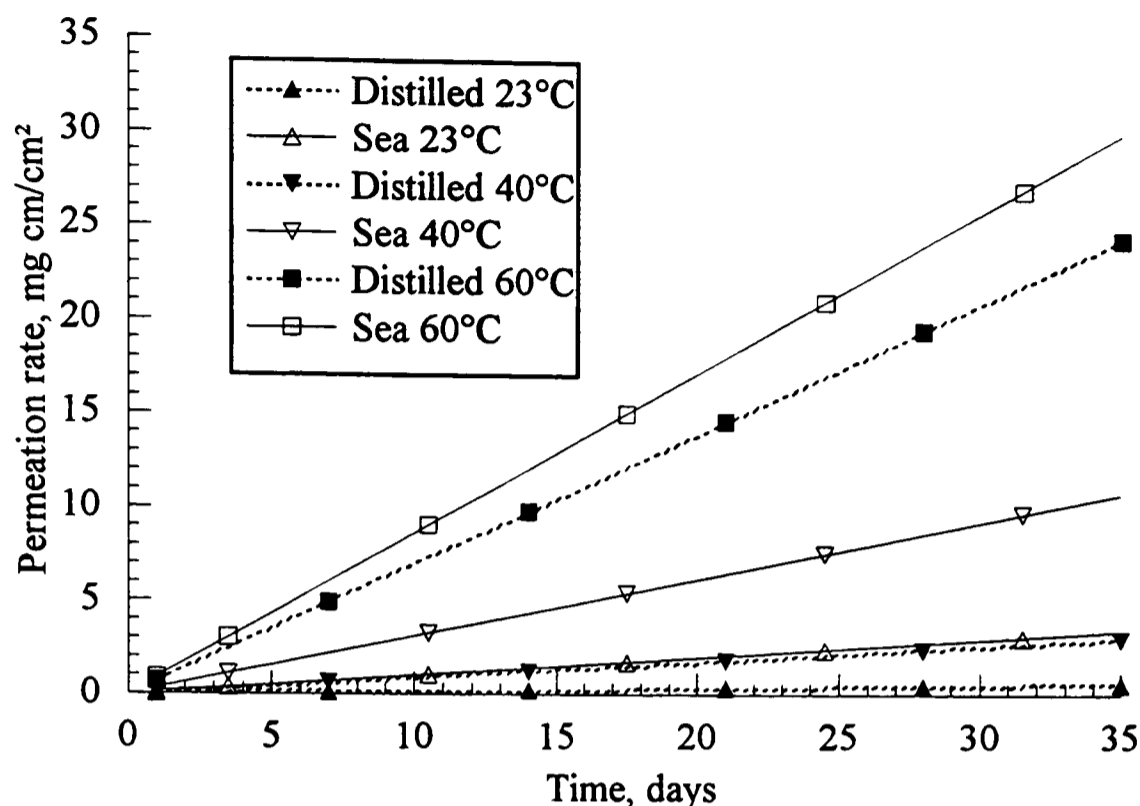
Cassidy and his colleagues published a series of papers (Cassidy et al 1983,b, Cassidy and Aminabhavi, 1986,a, Cassidy and Aminabhavi, 1986,b) on water permeation through elastomer laminates using water and a simulated sea water, 3.5 % NaCl. An interesting feature of this data being the sea water having constantly higher values of permeation through the different membranes than water, (figure 2.18). Although the magnitude of this difference does depend on the type of elastomer/laminates and temperature (at higher temperatures 60°C, there is less difference).

Cassidy does not particularly comment on this apart from saying.

'The observed higher permeation rates for salt solution could be explained on the basis of the size of the permeating molecules. Sodium and chloride ions being smaller in size than water dipoles might have moved at a higher speed than water dipoles. While doing so, the sodium and chloride ions might carry the surrounding water of hydration sheath as a whole unit and thus resulting in higher permeation rate of salt solution. Although it runs contrary to the conventional wisdom, nevertheless, this is in agreement with our earlier work.'

Cassidy and Aminabhavi, 1986,a.

Figure 2.18. Permeation rate with time for a Neoprene rubber from distilled water and simulated sea water (3.45 % NaCl) at different temperatures, based on data in Cassidy et al, 1983,b.



This does not seem to account for the data particularly satisfactorily; an alternative approach may be consider the formation of droplets within these materials. Applying the osmotic approach detailed previously, an external saline solution will decrease the osmotic gradient driving force for the absorption of water into the elastomer. Thus a lower equilibrium uptake is observed and a higher apparent diffusion coefficient. It should be noticed that the Neoprene (Dupont trade name for polychloroprene), (shown in figure 2.18) contains zinc oxide, stearic oxide and magnesium oxide, (Cassidy et al 1983). For all the samples (2 to 2.3 mm thick) a steady flow rate was observed only after a long time (25-30 days for water at 23°C) whereas this occurred more rapidly for other solutions (8-10 days for the high temperature saline solutions). As the materials were in a steady state the droplets should have already formed, so why the dramatic differences in the permeation rate? Consider the relationship $P = DS$ and the correction for s and s_0 (equation 2.37) described above which says that as the droplets grow (λ increases) the uptake of the matrix decreases. Hence if permeation is primarily conducted through the matrix the decrease in absorption would reduce the permeation rate. It is therefore feasible that the difference observed between the saline and distilled water is a function of the droplets within the polymer stressing the polymer and hence reducing the sorption and the permeability and the diffusion rate in fact is relatively constant (the system is in a steady state).

A further point is the similarity of the two solutions at higher temperatures but not at lower. Although the change in permeation with temperature depends on the permeating fluid (Urgami and Morikawa, 1992) it does not seem to apply here as water is the permeating species in both cases. As described previously the modulus and osmotic forces are in balance, the system has a modulus at 100% elongation of 9 MPa for the neoprene. Assuming that statistical theory of rubber like elasticity applies, an increase in temperature will reduce the deformation from the droplets (due to increasing the modulus) and hence the difference between the saline and distilled solutions would be reduced as s is now more similar in both solutions.

Donaldson (1991) describes the effect of an osmotic gradient (between water and a simulated body fluid) on the diffusion of water through some silicone tubes. Here the results presented seem to fit in with those of Cassidy described above.

2.4. Crack formation.

The presence or formation of cracks within a material has a profound effect on the diffusion of fluid in and out of the polymer. The tendency for some materials to form cracks during water absorption has been utilised with great effect in for drug release materials (Brook and Van Noort, 1984, Brook and Van Noort, 1985, Langer, 1990, Di Colo, 1992, Sheppard et al, 1992), to produce so called 'zero order' drug delivery devices' (Brook and Van Noort, 1984). Generally the formation of cracks is attributed to presence of soluble particles (salt, soluble drug, liquid, impurity) within the material which form solutions as previously described and then grow. The material then yields and cracks form, propagate to the surface and link up so enabling the solute solution to move out of the material via the crack network, as illustrated by figure 2.19 (Fedors, 1980, Schirrer et al, 1992). Lloyd et al (1995) support this general philosophy using H^1 NMR imaging where, after sufficient time, a water/acetone depleted region forms from the surface inwards for some polyester resins. The flow of the salt/impurity/drug is dependent on the extent of the crack network rather than on the diffusion through the matrix, indeed the crack network also increases the rate of water diffusion into the polymer (Diamant et al, 1981). This loss of the salt from within the material results in a decrease in the water uptake of the material, as shown in figure 2.20 (Di Colo, 1992). Cracking may also occur in materials as a result of gross swelling of the polymer matrix

by a good solvent, here the role of cross links and molecular weight are critical in determining the extent of the cracking (Peppas et al, 1994).

Figure 2.19. Formation of cracks within polymer due to osmotic pressure from solution droplets.

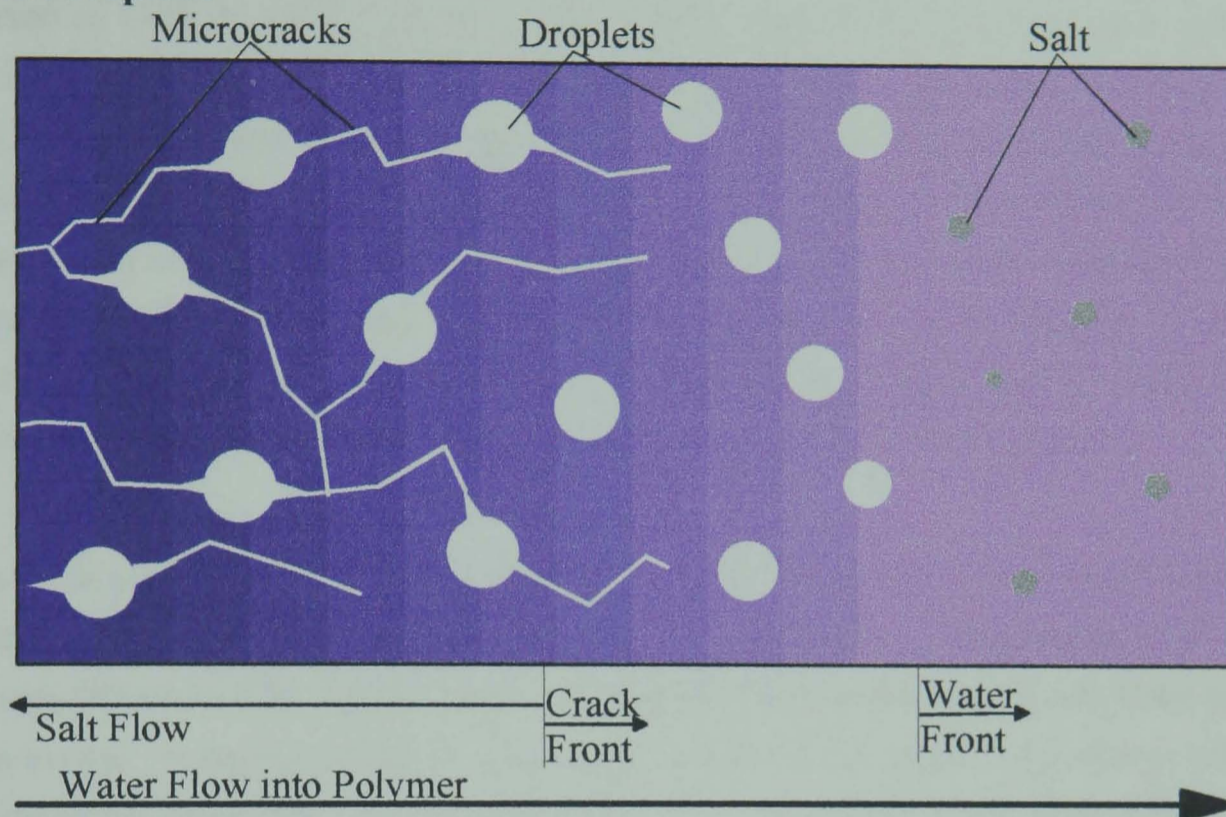
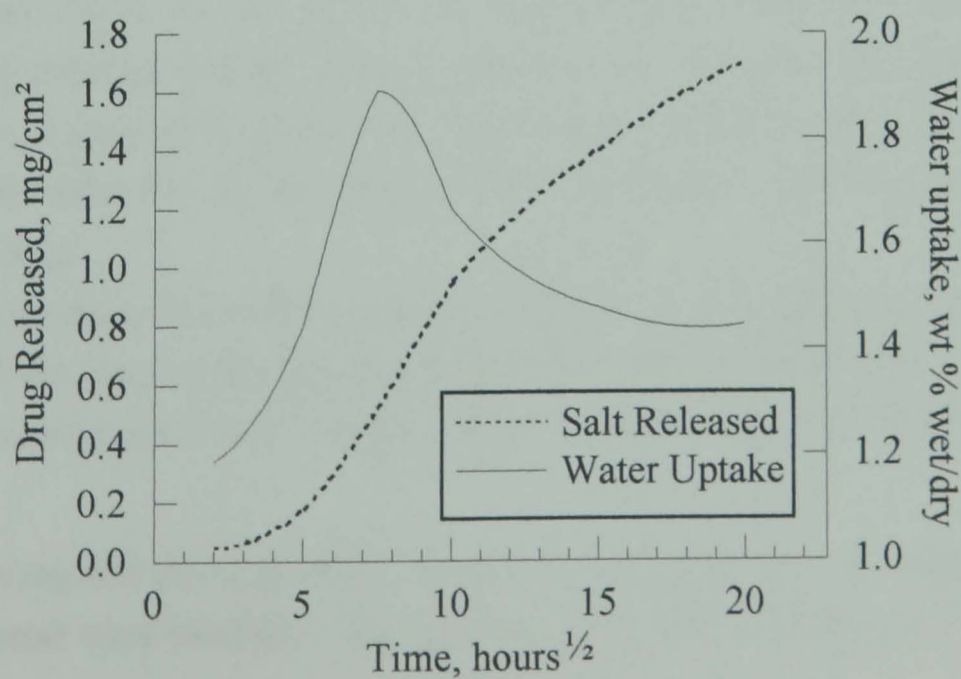


Figure 2.20. Water uptake and salt release from a silicone rubber doped with 11.5 wt% NaCl and a drug (sulphanilamide), based on Di Colo, 1992.



Schirrer et al (1992) used two silicone rubbers to model this process by doping them with NaI and KIO_3 . The KIO_3 showed a lower degree of swelling and less release from the material (attributed to the osmotic pressure of NaI being about 25 times that of KIO_3) and independence from the salt particle size. The NaI conversely was dependant on the particle size with the coarser grain size showing the greater release (as also reported by Di Colo, 1992, Lee et al, 1992). The shape of the particles is also a factor with irregular particles leading to a concentration of stresses around the droplet (Di Colo, 1992). This dependence on grain size was attributed to the larger tangential stresses from the larger grain sizes at the same osmotic pressure. The weaker (lower elongation to break) of the two materials also showed a greater release, indeed the stronger with KIO_3 showed no release indicating the droplets growth was being balanced (as previously described). This indicated that there was a critical value for rupture for the two materials below which crack formation/propagation would not occur.

Schirrer et al (1992) calculates the osmotic pressure (π_i) of the swollen droplet using equation 2.24, which if the droplet is restrained at equilibrium, will be equal to the Pressure (P) exerted by the elastomer (equation 2.25) assuming the droplets/salt particles are spherical. It therefore follows, assuming the material behaves in a perfectly elastic neo-Hookean behaviour, that if the material cracks there must be a critical pressure (P_c) at which it fails and therefore a critical extension, λ_c . Schirrer et al (1992) then utilises fracture toughness and derives an expression for λ_c in terms of the fracture toughness, tensile modulus and particle size of the salt particle. He then uses this argument to propose three possible situations in the droplet formation processes and supports them with calculations and observations.

1. λ_c exceeded before the salt has saturated and formed a saturated solution (not fully dissolved) resulting in sharp diffusion front into the materials (low fracture toughness, high tensile modulus, large grain size and high osmotic pressure).
2. λ_c exceeded after the salt has fully saturated the solution, resulting in a broader diffusion front.
3. λ_c not exceeded as the restraint offered by the material is sufficient to withstand the growth of the droplet (high fracture toughness, low tensile modulus, small grain size and low osmotic pressure). Results in almost no salt flow out of the material.

It is worth noting that this approach is continued and expressions for release rate of salt from the polymer were obtained. This approach uses a 'best fit' factor for the kinetics of

the process with very good correlation. How this 'best fit' factor relates to the diffusion coefficient etc. is unclear.

Crack formation in rigid materials takes a similar form with the first stage being the formation of clusters within the material followed by propagation of cracks from these clusters (Diamont et al, 1981, Lee et al, 1992, Bucknall et al, 1994). The ability of a material to crack or craze is therefore dependent on the clusters and the mechanical/structural restraint of the material. The presence of soluble impurities / salt (Brook and Van Noort, 1985, Lee et al, 1992 and Bucknall et al, 1994) is responsible for the formation of some cracking in some materials via a similar process as described above. Here however the solution droplets are disc shaped rather than spherical as described for elastomers, due to the difference in the physical/structure properties of the materials. The occurrence of the formation of cracks with the rigid materials occurs only after saturation with Lee et al (1992) and Bucknall et al (1994) reporting the saturation of the material (with Fickian kinetics) prior to crack formation. This was induced in some materials exhibiting no cracking by lowering the temperature to reduce the saturation limit and hence supersaturate the material. Raising the osmotic potential of the external solution reduced or prevented the onset of crack propagation (supersaturation) as found previously with the elastomers.

Lee et al (1992) also identifies another possible process for the formation of cracks due to swelling stresses and residual stresses in the polymer, similar to crazing due to solvent ingress (Kambour et al, 1974). As water enters the polymer it swells and this results in a stress between the swollen and the unswollen portion of the material. If such stresses (in conjunction with residual stresses from fabrication) are sufficient to yield the material cracking would occur before saturation of the material and accompany the advancing diffusion front. For elastomers such a mechanism is unlikely due to the possibility of larger deformations.

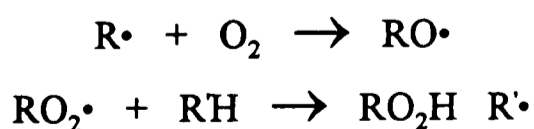
Crack healing is reported (Lee et al, 1992) when a cracked supersaturated sample is placed in a solution of high osmotic potential (low effective partial pressure) provided the polymer chains are sufficiently mobile. Water moves out of the cracks provided they are not connected to the outer surface (to establish new balance with the external solution) forcing a closure of the cracks. Thus implying that process of crack formation is reversible.

Lee et al (1992) use two approaches to describe the uptake, a thermodynamic one where the polymer is one phase and the water in the disc shaped cracks is another so the problem now becomes one of phase separation and saturation. The second an osmotic process in a similar vein to that used previously, utilising a chemical potential base. Neither of these is progressed to a conclusion but the approaches are worth noting. Bucknall et al (1994) considers the fracture properties assuming brittle fracture of the material to predict the on set of crack propagation; this approach has similarities to Schirrer et al's (1992) previously commented on.

2.5. Oxidation and diffusion.

Oxidation has been identified as a potential problem with elastomers (Briggs et al, 1962, Yashuda and Stannett, 1962, Barnard et al, 1963, Barrie et al, 1975, Tillekeratne et al, 1987, Sagripanti and Hughes-Dillon, 1994) and other materials (Wong and Broutman, 1985,a, Henry et al, 1992, Sagripanti and Hughes-Dillon, 1994) in aqueous environments. This not only weakens the material considerably but also increases the water uptake due and in an anomalous manner (Wong and Broutman, 1985,a). For latex this resulted in an upturn in the water uptake, with the newly formed groups acting to form clusters (Yashuda and Stannett, 1962).

The oxidation occurs by many different mechanisms depending on the material and the environment. Generally diene (or vinyl) bonds (Brydson, 1978) are attacked but other groups (e.g. styrene) are also prone to attack, the basic mechanism being a free radical auto catalytic process forming hydroperoxides. The reaction may be generally divided into three parts, first the initiation when the radical is formed on the polymer, this occurs by many different processes which depends on the material and its environment. The second step is propagation; this is when oxygen attaches on to the radical and the radical transfers to another chain in place of a hydrogen which completes the hydroperoxide. This propagation stage is illustrated below (Barnard et al 1963),



where \cdot indicates a radical. The final stage is termination, this can occur by many reactions involving the combination of two radicals which may result in formation of cross links if the radicals are both on polymer chains. A widely used means of preventing oxidation is to employ an antioxidant. These work in many different ways

but in general they accept the radical and trap it so the radical is no longer available to promote oxidation, typical antioxidants include 2,6-di-t-butyl-4-methyl phenol, 2,5-di-t-phenyl hydroquinone, n,n'-diphenylphenylenediamine and tris(nonylphenyl)phosphite (Nicholson, 1991). The major problem with antioxidants is their tendency to leach out of the material, also the antioxidant will eventually get used up and so the oxidation resistance has a limited life. In a biomedical application, there must also be concerns about the toxicity.

Oxidation is promoted by many factors, most commonly ultra violet light initiates the process (Brydson, 1978). There are however other mechanisms which may occur. The potential of some metal ions (particularly copper) to catalyse the formation of radicals is a well known (Barnard et al, 1963). The catalysing potential of a range of solutions was investigated by Henry et al (1992) for polyethylene, and increased rates of oxidation were observed for a range of ionic solutions most noticeably in basic conditions. pH 10 showed approximately 10 fold increase in rate of radical production compared to that in distilled water, which itself was 8.3 times greater than in hexadecane, but perhaps more significantly for biomaterials a 0.1 M NaCl showed a 4.5 fold increase compared to that of distilled water. Similar results were obtained by Tillekeratne et al (1987) for latex in air, fresh and sea water with the oxidation being accompanied by discolouration, hardening and reduced tensile strength. Malek and Stevenson (1986) conversely examined a natural rubber tyre after exposure to sea water for 42 years and found little degradation even near the iron reinforcement (which might have been expected to catalyse the oxidation). They attribute this to the low absorption of the material due the good mechanical properties particularly the modulus and the antioxidant.

Sagripanti and Hughes-Dillon (1994), investigated a range of medical polymers under different oxidising conditions (raised temperature and copper and ferrous iron ions) their results showed the materials to remain reasonably intact. However, their tests were only over 5 hours and they looked for microscopic changes, under such conditions the antioxidants may well have been sufficient to prevent the oxidation which may have been picked up by a more suitable technique such as I.R. spectrometry. They also quote some 'in use' observations which show oxidation to be a problem for PVC and polyamides particularly.

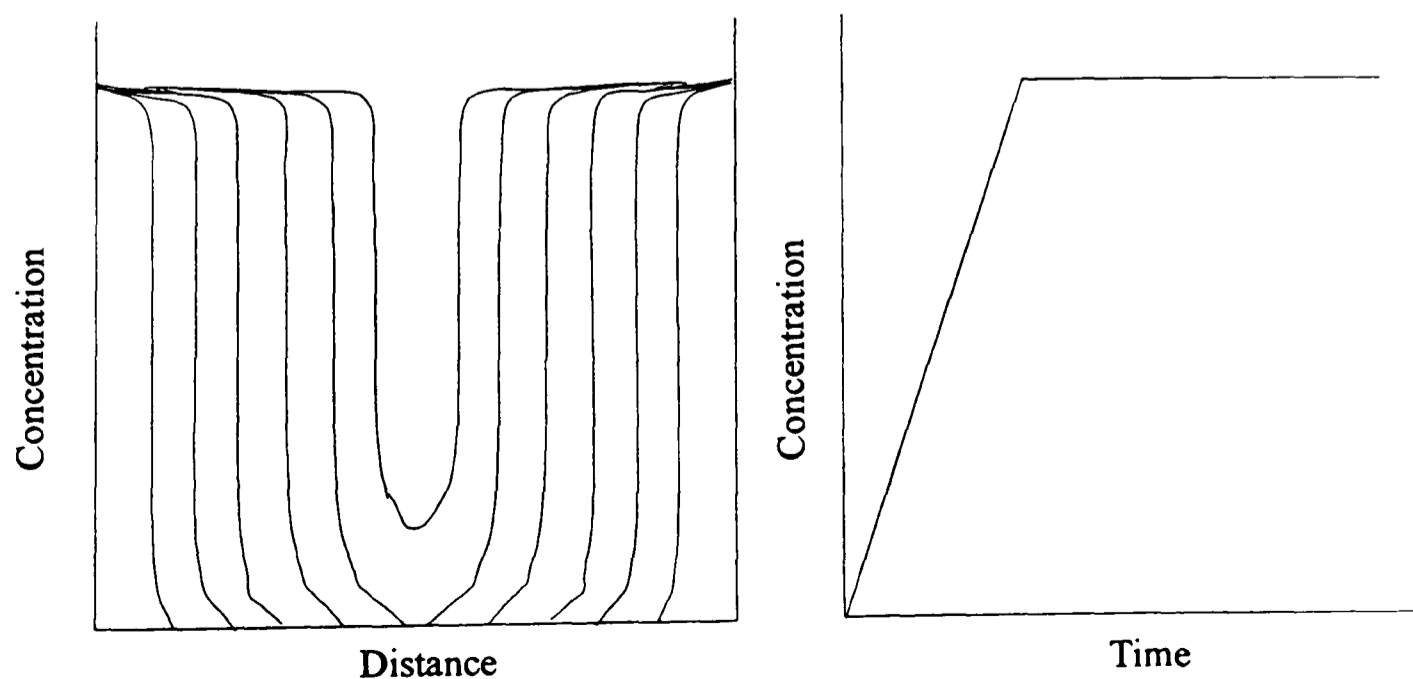
The kinetics of the absorption and oxidation process are complex as the ingress of water and ions promotes the oxidation of the material which in turn promotes the water uptake, a vicious circle rapidly becomes apparent. There have been a few approaches on this

area with modified chemical rate and diffusion equations being combined (Andrews and Braden, 1961, Neilsen and Valladen, 1985, Berlin, 1991). However the overall situation is not really adequately described, and the influence of antioxidants and cluster formation further complicates the application of any chemical reaction/diffusion theory to the oxidation of elastomers in aqueous media.

2.6. Case II diffusion.

Case II diffusion is probably the most well reported non Fickian diffusion of a fluid into a polymer, it occurs in many different polymer/solvent systems (i.e. when the fluid is methanol, ethanol or acetone). It is characterised by a very steep concentration gradient along the diffusion front and a linear dependence with time (linear kinetics) rather than a with $t^{1/2}$ as with the Fickian. Although it is of little direct relevance to the study of water diffusion in to elastomers, the approach used to model it is interesting and worth noting. The theory of case II diffusion modelling is excellently dealt with by Thomas and Windle (1982) in a summary of many years work, which forms the basis of the subsequent description. The model predicts results of the type shown in figure 2.21, which are consistent with the experimental results of case II diffusion. It is worth noting that the diffusion front is headed by a small Fickian region and there is a slight concentration gradient between the diffusion front and the surface.

Figure 2.21. Type of results obtained for case II diffusion into polymer in terms of concentration with distance into polymer and time.

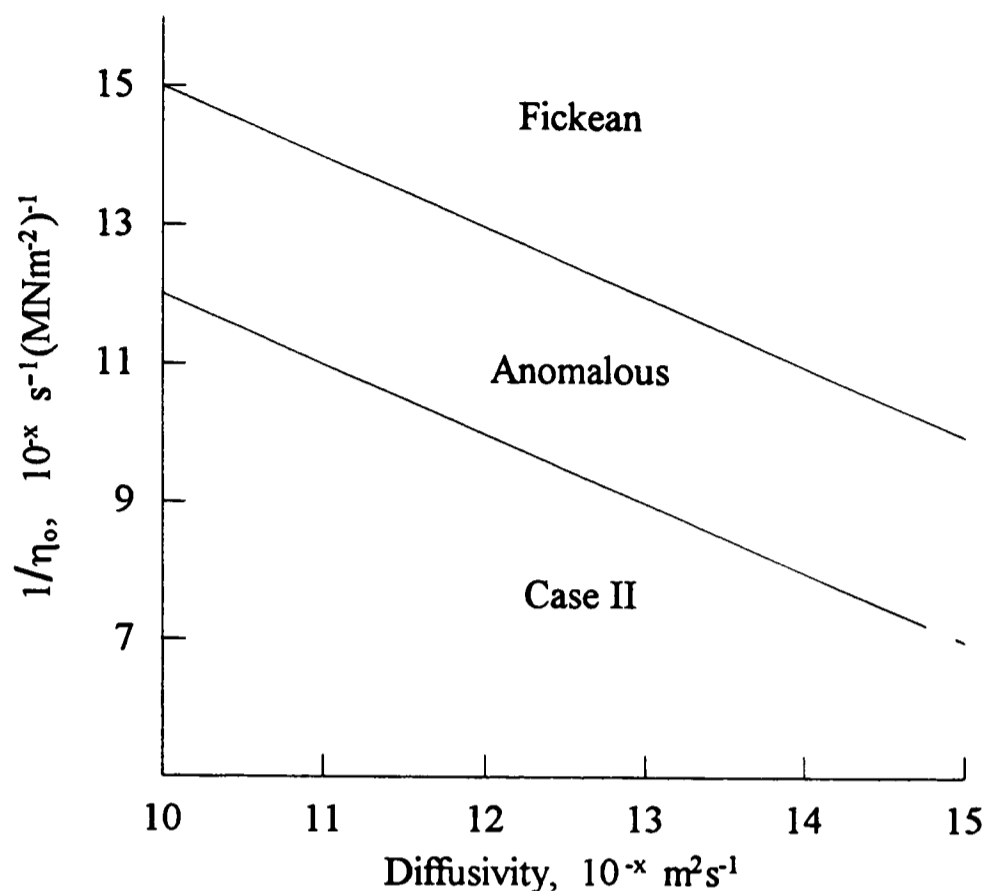


The basic premise made is that some molecular relaxation is primarily responsible for controlling the velocity of the diffusion front. This molecular relaxation may be a crazing type of process or a swelling of the material by solvents. Hence the rate controlling step is time dependence of the mechanical deformation of the polymer in response to thermodynamic swelling. The model based around this theory then forms in three parts. First is the relationship between pressure, concentration and activity (for the chemical interaction of the polymer and solvent) for the liquid swelling the polymer (this is considered on a thermodynamic based alone). Secondly the kinetics of the swelling process for a slice of the material which is thin enough so that the effect of diffusional resistance is insignificant. Here the rate determining step is seen as the mechanical viscous resistance and modelled using assumptions involving the plasticising effect of the solvent. Finally the different elements are combined to predict mass uptake and concentration profiles using numerical solutions. The overall approach is based largely on using chemical potential rather than the concentration gradient and utilises the same variation of Fick's first law as Muniandy and Thomas (see earlier section) as shown by Park (1950) shown in Equation 2.31.

Whether case II or Fickian diffusion occurs depends largely on the relative values of the viscous flow rate ($1/\eta_0$, where η_0 is the intrinsic viscosity of the unswollen polymer) and the diffusivity (using the thermal diffusion coefficient) of the penetrant in the polymer. Figure 2.22 shows the limiting values for the change of Fickian to case II diffusion with a region of anomalous diffusion which is undefined forming a zone between the two. From this we can see that the change from case II to Fickian occurs only when the relaxation (represented by $1/\eta_0$) is greater than the diffusivity. This assumes isothermal conditions and no major changes in the polymer properties like the T_g , if a sample goes through the T_g due to the effect of plasticisation by the solvent the relaxation will no longer be represented by the initial viscosity (as the assumptions made to account for the plasticisation assumes it to be a progressive consistent effect). Above the T_g the material is in the elastomeric state and so is capable of much faster relaxation, the diffusion will therefore be Fickian.

A great deal of the work has utilised NMR (see appendix III.a) as a means to study the diffusion of solvents particularly methanol (Weisenberger and Koenig, 1989, 1990,a, and 1990,b, Grinstead and Koenig, 1992, Grinstead et al, 1992) and acetone (Weisenberger and Koenig, 1990, Grinstead and Koenig, 1992) into polymers. An attractive feature of these solvents is the much slower T_2 times which are around 10 to 20 ms for methanol and 100 to 400 ms for acetone, thus reducing the problems experienced for water.

Figure 2.22. Change of case II to Fickian, based on Thomas and Windle, 1982.



Whilst much of this work has yielded some excellent results, its applicability here is limited, it is worth however considering the elements of the results reported. The difference between Fickian and case II diffusion has been widely reported with authors also reporting a brief Fickian diffusion front preceding that of the case II (Weisenberger and Koenig, 1989) as predicted in the Thomas and Windle (1982) model. This sort of Fickian preceded case II was found to become Fickian when the rate of polymer relaxation (not the NMR relaxation times) is greater than the diffusion rate (Weisenberger and Koenig, 1990,a, Grinsted and Koenig, 1992). This is indicated by the T_2 time being unaffected by the concentration gradient across the sample (as the polymer can relax faster than the diffusing solvent), whereas for true case II diffusion there is a gradient in the T_2 (to shorter times) values across the imbibed region due to the rate of polymer relaxation being slower than the rate of ingress (Weisenberger and Koenig, 1990,a, Grinsted and Koenig, 1992). This was also observed for increasing water content (Grinsted et al 1992). This effect has been attributed to the effect of the solvent plasticising the polymer to below its T_g . The desorption of such systems is purely Fickian controlled although the T_2 values indicate that the surface and outer layers act as though a case II diffusion process was occurring (Weisenberger and Koenig, 1990,b).

These results clearly contradict those of Fyfe et al (1993) where a decreasing T_2 was found for decreasing concentration for the Fickian diffusion of water as shown in figure 2.10. The reason for this is unclear but may stem from the possibility of H-bonding with the water molecules and not for the solvent.

The change from case II to anomalous and Fickian diffusion is taken further by Korsmeyer et al (1986,a), Hayes and Cohen (1992) and Wu and Peppas (1993), who consider the change in relaxation of a hydrophilic polymer in water during the absorption process due to swelling of the polymer. Kosmeyer et al (1986,a) developed a series of models for different conditions where the swelling and diffusion coefficient's dependence on concentration of penetrant were the major feature. Here, depending how the system was defined, case II like, anomalous or broadly Fickian diffusion was observed. This was then verified in a follow up paper Kosmeyer et al (1986,b), based on drug release from hydrogels of different compositions. Hayes and Cohen (1992) used a similar hydrogel, drug delivery type of system and combined it with aspects of the Maxwell and Kelvin-Voigt model for viscoelasticity to determine the relaxation time.

An interesting point here is that the model predicts 'shocks' (a front of high water content) in the concentration at the rubber transition front as it moves through the material, with the diffusion in the glassy hydrogel being predominately case II and in the rubbery material Fickian based. Wu and Peppas (1993) adopted a similar method which resulted in the prediction of these 'shocks' at the rubbery transition here particular emphasis being placed on the Deborah number (the ratio of diffusion time to relaxation time) and χ (polymer solvent interaction parameter) which controls the penetrant equilibrium concentration and hence the transition. Indeed Lloyd et al (1995) found something that looks like these shocks (high concentration moving in to the polymer) using NMR imaging. Peppas et al (1994) indicate that in some systems the disassociation of intra molecular bond and entanglements may be as important in determining the nature of the uptake as the viscosity of the polymer of some solvent/polymer systems.

If however we think about applying this to the diffusion of water into a hydrophobic rigid polymer such as PMMA, which has a apparent viscosity of approximately $2 \times 10^{14} \text{ Nsm}^{-2}$ at 24 °C (Thomas and Windle, 1982) and a diffusion coefficient of approximately of order of $10^{-9} \text{ cm}^2\text{s}^{-1}$ (Braden, 1963). The prediction of this data from figure 2.22 is that the diffusion should be Fickian as expected; it is however worth noting how close this is to the change between Fickian and anomalous diffusion.

Various solutions and other modifications have been published on case II diffusion using Thomas and Windle's model (Hui et al, 1987,a, 1987,b, Lasky et al, 1987) but the basic model seems valid as confirmed by work on the NMR.

2.6.1. Hydrogels and ionizable gels.

The work detailed at the end of the previous section by Korsmeyer et al (1986,a and 1986,b), Hayes and Cohen (1992) and Wu and Peppas (1993) on hydrogels attributes elements of their uptake to case II and the anomalous region between case II and Fickian. The effect of increasing the cross link density of poly HEMA (hydroxyl ethyl methacrylate) decreases its absorption and swelling (Kabra et al 1991) and this reduces the extent of the Fickian diffusion of the rubbery state. Some of these results for hydrogel systems indicate that the diffusion may appear Fickian from gravimetric studies (Migliaresi, et al 1984, Kabra et al 1991, Rathna et al, 1994) but this can only be best described as pseudo-Fickian due a very steep absorption front within the material. The effect of having part of the material in a glassy state and part in a swollen rubbery state leads to stresses within the material, these stresses can also effect the absorption process and can limit the absorption in the rubbery phase by putting it in compression (Kabra et al, 1991).

The introduction of ionizable groups into a material (e.g. HEMA, MMA, BMA or other materials) increases the absorbed volume in the material, this is attributed to it increasing the osmotic swelling pressure (similar to the osmotic pressure with droplet formation in elastomers) due to the ions present (Firestone and Siegal, 1991, Kabra et al 1991). Different components are susceptible to ionisation, for example methacrylic acid or acrylic acid which ionise due the carboxylic acid groups becoming COO^- . The ionisation is promoted by strong anions (i.e. Na^+), dilute ionic solutions with high pH's (Firestone and Siegal, 1991, Khare and Peppas, 1993). The ionisation of the groups results predominately in a large increase in the free water within the material compared to the bound water (Khare and Peppas, 1993). The resulting water uptake is generally anomalous (Hariharan and Peppas, 1996) with a diffusing front much like those described previously for the hydrogels and case II with the relation between relaxation and diffusion coefficient being important, although the ionisation process does alter the kinetics of this process (Firestone and Siegal, 1991)

A feature of such hydrogel and ionizable systems worth noting is the increase in diffusion coefficient with increased water content (Khare and Peppas, 1993) as previously seen for water/solvent ingress (figure 2.6. and 2.7), as opposed to the reduction of diffusion coefficient seen previously when droplet/cluster formation occurs (figure 2.8 and 2.16).

2.7. Monte-carlo simulation.

There are of course many other theories of water uptake into polymers, one of the most notable being the Monte-Carlo or random walk simulation (Majerus et al, 1984) which was originally applied to diffusion problems in the 1950's. The motivation behind this approach is to enable modelling of the kinetics of the diffusion process encompassing different types of interactions between the polymer and water rather than the uniformity assumed in Fickian diffusion. The major draw back of this approach being the time required for the calculations. If the model uses a 3 D lattice (of a small manageable size e.g. 20 x 20 x 20), of which, at equilibrium, 6% of these contain a particle then 480 particles for each iteration (one jump per particle) must be generated for each step and 4900 iterations are required for this lattice to reach equilibrium. The number of iterations also rises with the increase in the number of trapped particles.

The approach utilises aspects of the dual-sorption model in that there is a homogeneous lattice with specific sites (randomly distributed) of a specified capacity (i.e. reduced chance of leaving the site during the iteration, known as reversibility, of 0.25 by Majerus et al, 1984). In order for it to be applied the proportion of water in the bulk, trapped (at specific sites), number of sites (hence the capacity of each site) and first row concentration (equal to the absorption in the bulk) must be known. Each particle moves in a random direction along an axis of the lattice (defined by an integer 1 to 6), after each movement the first row is back to equilibrium. There is another factor, the results generated are in terms of units of $steps^{1/2} / lattice\ size$ and so must be converted to $minutes^{1/2} / cm$. This is done by using a conversion factor (temperature dependent) based on the initial slope of the sorption curves. A similar curve fitting exercise is also performed to determine the reversibility. A similar process may be applied to desorption.

The results presented for an epoxy showing deviation from a Fickian model showed very good correlation with the model for absorption. The difficulty in determining values and performing the simulation make such experiments unattractive and the curve fitting

approach to link the theoretical to the experimental data makes the approach unattractive. The results are however good and it avoids many of the problems associated with Fickian diffusion, and as such it may yet prove a valuable tool in the predication of the data. It is possible that if this technique could be placed into a context with absorption it may overcome some of the limitations of the Fickian model. Best et al (1993) attempted to correlate a model similar to Majerus et al (1984) to the normal sort of dual sorption model as previously detailed. Here he used infra red profiles of D₂O to back up his findings of the profiles predicted by the modelling, the results show the dual sorption approach predicting the uptake better than simple Fickian kinetics.

Tamai et al (1994) used molecular dynamics (bond angles, energies, distances) to predict the behaviour of methane, ethanol and water in a silicone polymer and polyethylene. The modelling they accomplished is certainly one of the most encompassing, if not the most complex. A dual sorption type view is within the bounds of the model with a diffusion coefficient for the bound and free water being determined separately. The model does however make assumptions (e.g. no cross-links) which would limit its applicability even if the computing power was available to perform the calculations. It does however represent a new analysis tool which is certain to be more utilised as the computing power required becomes more available.

2.8. Drug delivery.

There are a number of advantages in using a drug delivery system in that a long term sustained release or high localised concentration may be achieved (Langer, 1990, Petrak, 1990). The number of drug delivery materials is rapidly rising with much work being focused in this area over the last 15 years. The number of these materials and their applications will undoubtedly increase. Already in dentistry fluoride release (Rawls, 1991) from filling materials (glass ionomers and composites) is receiving considerable interest. Indeed the control of candida albicans is another area where such materials are being used as they negate the need for repeated mouthwashes (Addy and Handley, 1981, Wilson and Wilson, 1993), as well as the development of new materials for release in the wider context such as in implants, polymer beads (Lee, 1984) and pills (Khan, 1995).

The water absorption characteristics of the polymer is critical in determining the drug delivery potential of the material. Indeed, the ability of a material to crack or swell

excessively is advantageous in some respects as it can promote/enable the release of drugs from the material. The advancement of water absorption and diffusion theories is clearly relevant to future of these materials. Many of the recent advancements in water absorption has come from research specifically aimed at understanding the release of drugs from a material, particularly the formation of cracks and hydrogels/ionizable materials. Biodegradable polymers form a major part of the research effort into drug release materials; here the release characteristics tend to be governed by the degradation process (Göpferich and Langer, 1993) although the diffusion into the polymer is still important in determining some of it's characteristics. Here the possibility of bonding the drug within the polymer chain makes for some interesting and prolonged release characteristics (Petрак, 1990).

Drug release from non degradable materials occurs through a number of mechanisms. The simplest involves the surface for a hydrophobic polymer where the drug is relatively insoluble, here the drug simply dissolves from the surface (Downes, 1991). Alternatively the drug may diffuse through the matrix (Brook and Van Noort, 1984, Lee, 1984, Schweneman et al, 1992), while this works well for drugs of a relatively low molecular weight or modified polymer resins (Mazan, 1993), large drug molecules do diffuse through the matrix but the rate is considerably slower (Langer et al, 1980). Typically the release kinetics being $t^{1/2}$ (Rawls, 1991) although zero order (t) release is also possible (Yoshida et al, 1991). For such systems increasing the hydrophilicity, (e.g. increased content of HEMA or ionizable components) and swelling increases the release rate of the drug. The ionisation characteristics can be formulated so it is responsive to enzymes in its environment to promote release (i.e. materials responsive to the gastric enzymes to promote release in the stomach, Monthéard et al, 1988). An alternative to environmentally sensitive materials is using a degradable coating on the drug implant which degrades when a specific enzyme is present (as with morphine triggered release, Roskos et al, 1993). The release from such systems also shows linear dependence on the osmotic pressure generated by the soluble drug/salt (Gale et al, 1980). The water uptake of many of the hydrophilic drug release polymer systems is case II or anomalous (initial case II then as polymer softens change to anomalous or Fickian diffusion).

Modified silicone polymers with silane side groups can be used and by controlling the silane side group's type and density in conjunction with the cross link density (also for PVA based materials, Korsmeyer and Peppas, 1981). The release characteristics may be controlled (Mazan et al, 1993) as well as the diffusion into the material (Compañ et al, 1996). The modulation of the release characteristics of the material (containing a magnetic filler) by applying a oscillating magnetic field offers a non invasive way to alter

the release from these material (Langer et al, 1980, Edelman et al, 1985, Edelman and Langer, 1993).

Generally, for the more hydrophobic polymers the incorporation of a hydrophilic drug or hydrophilic release promoting agent (such as a salt or soluble liquid) can act to promote release of the drug via the an existing crack network (Di Colo, 1992, Sheppard et al, 1992), or cracking the materials as previously discussed (Brook and Van Noort, 1984, Brook and Van Noort, 1985). Hydrophobic materials may also release the drug, possibly in this manner if it is prone to clustering (Patel and Braden, 1991, Patel et al, 1994, Di Silvio et al, 1994), here the mechanism is unclear but is likely to be due at least in part to the unusual diffusion characteristics of the polymer. The solubility of the drug in the water and polymer will also govern the release and the distribution of the drug in the polymer, here solubility parameter data may be used to predict the relative solubility of different drugs in polymers with a reasonable accuracy (Bao et al, 1988).

Chapter 3.

Methodology.

3.1. Sample preparations.

For each material the components were compounded to form a mouldable gel or paste, for some of the silicone materials two pastes were formed which when blended together formed a room temperature curing (RTV) material. Once the gel was formed the materials were all processed in the same way, based on conventional dental technology for the application of a soft lining material.

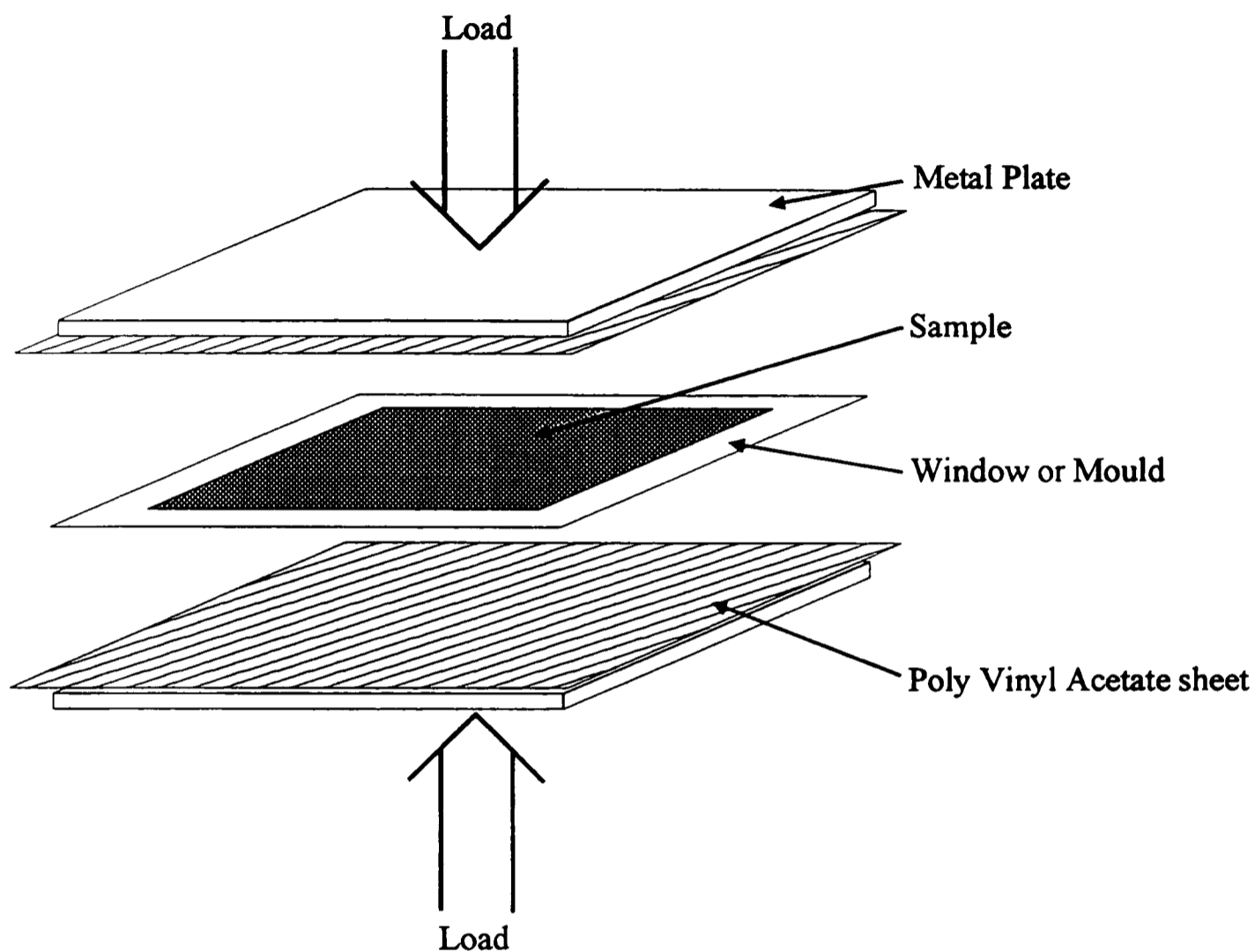
The samples were made in the form of sheets, approximately 1 mm thick, by placing about 8 grams of the gel in the centre of a mould comprising 1 mm thick window which was sandwiched between two metal plates lined with poly vinyl acetate sheets (figure 3.1). When necessary the poly vinyl acetate sheets were painted with mould release (which was then allowed to dry) to prevent the material sticking to the sheet. The mould was closed under pressure in a dental hydraulic press increasing the pressure slowly over 1 hour to a maximum force of 200 bar which was then held for 1 hour. The plates mould was then removed from the press (still with the sample in between) and placed between two dental flasks in a dental clamp. This was then placed in a bucket of cold water and heated gently until boiling (approximately 30 minutes) and then left to boil for a further 30 minutes to ensure polymerisation). If the material was a RTV silicone it was left in the press for at least 18 hours before it was moved to the clamp and boiled as with the other materials. The sample sheet was then removed from the mould and marked appropriately until it was used. If mould release was used the sheet was washed with cold water to remove any residual mould release from the surface.

3.2. Tensile strength.

Dumb-bell shaped specimens were stamped out of the 1 mm sheets with a gauge cross section of 3.3 mm and length of 30 mm. These were then marked with two fluorescent dots 20 mm apart along the middle of the gauge length as seen in figure 3.2. The dumb-bell was then mounted using self tightening grips on a J&J M30K tensile machine fitted with an infra red extensometer. The infra red extensometer was used rather than the machine's internal extensometer to enable an accurate measure of the extension over a specific gauge length. The test was then performed at a speed of 500 mm/minute with the load and extension being continuously recorded. Unfortunately the ambient temperature of the laboratory was not constant during all the tests and fluctuated

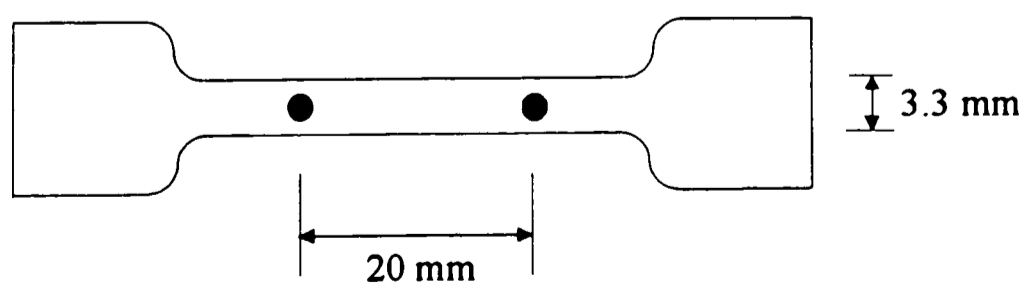
between 16 and 23°C although the temperature was constant for each individual group of materials.

Figure 3.1. Moulding of a sample between two plates.



Mooney Rivlin plots used to calculate the modulus for specific materials were based on the data from these tensile tests. It is recognised that this is not ideal but it is felt this should be a guide to the modulus at 37 °C.

Figure 3.2. Schematic of dumb-bell used in tensile tests.



3.3. Water absorption.

Two specimens 20 mm by 40 mm were cut from the 1 mm thick sheets for each absorption test. The thickness was measured with a micrometer and the samples placed in an pre-conditioning oven at 37 °C which contained a silica gel desiccant. After 1 week the samples were weighed (to 4 decimal places) and placed into 100 ml of distilled water at 37 °C. The weight of the samples was then recorded at 5, 15, 30 and 60 minutes and then at 2 hours, 1 day and 1 week. After the first week measurements were made every week until approximately 6 months. One sample was then removed from the water and placed into desorption in the pre-conditioning oven at 37 °C, weight measurements were made at the same time intervals as for before with the absorption. The other sample was left in the water and readings were continued as before. Once the desorped sample had reached a equilibrium (the samples were left for at least two weeks to ensure this) they were placed back into the same water and a second absorption cycle was recorded using the same time intervals between the measurements.

The absorption data is quoted as the percent increase from the initial weight, as is the solubility which was calculated from the weight at the end of the desorption cycle. The diffusion coefficient was calculated using the semi infinite media solution of Fick's second law, (equation 2.2),

$$\frac{M_t}{M_\infty} = 2 \sqrt{\frac{Dt}{\pi l^2}} \quad \text{Equation 3.1.}$$

by regressing M_t/M_∞ against $t^{1/2}$ using values of M_t/M_∞ of less than 0.5. The gradient

being equal to $2 \sqrt{\frac{D}{\pi l^2}}$ enabling the determination of the diffusion coefficient.

3.4. Other tests.

Infra red spectroscopy was performed on some of the materials used in this study as required using a Perkin and Elmer 882 dispersion infra red spectrophotometer. Typically this was performed over the wave number range 400 and 4,000 cm^{-1} in transmission using KBr plates with a film of sample in between.

C^{13} NMR spectrometry was performed on the condensation silicone leachant by Mrs J.Hawkes at Department of Chemistry, King's College, London, using a Bruker AMX 400.

The H^1 NMR imaging and spectroscopy was performed at Department of Chemistry, Queen Mary and Westfield College, London, under the supervision and guidance of Dr. P.Kinchesh, using a Varian / Siemens 200 NMR. The methodology used here is described in detail in chapter 7 along with the results obtained.

Chapter 4.

Silicone Polymers.

4.1. Introduction.

In addition to their role as soft lining materials silicone polymers have become widely employed as biomaterials in other areas of medicine and dentistry. Their uses are wide ranging encompassing hydrophalus shunts (for draining excess cerebrospinal fluid) (Frisch, 1983), nerve end caps (Swanson et al, 1977), artificial urethra (Quinn and Courtney, 1988), prosthetic finger joints (Swanson, 1968), breast implants either filled with silicone fluid or saline solution (Williams, 1972), maxillofacial prosthetics (Borghouts and Otto, 1978, Quinn and Courtney, 1988) and drug delivery systems, including Norplant (contraceptive) implants and transdermal patches (Folkman and Long, 1964, Ma et al, 1988, Mazan et al, 1993). These applications all involve the pre fabrication of the implant but silicone elastomers may also cure in situ for room temperature vulcanising (RTV) systems, in this form they are used for treating chronic pancreatitis, embolization of arteries in kidneys, filling balloon catheters in neurosurgery (Yuzhelevskii, 1991) and maxillofacial surgery (Polyzois et al, 1994).

There have of course been problems, notoriously with breast implants where some implants were prone to 'bleed', and leaching of the fluid leading to constrictive fibrosis around the implant (Brody, 1977). Concerns are also raised over the biocompatibility / toxicity of silicones in general (Rees, 1965, Polyzois et al, 1994). Some of these concerns seem to stem from the poor wetting characteristics of silicone polymers, while the leaching (particularly for some RTV systems) is another problem (Vassilakos et al 1993, Polyzois et al, 1994). Low grade silicone oligomers and polymers have also been suspected of causing failure of these implants (Quinn and Courtney, 1988).

Although there are concerns over some aspects of silicones as a biomaterial they seem to function well in some applications without any problems indeed they are frequently quoted as being biologically inert, resisting attack by the body (Braley, 1970) and promoting a minimal host response (Quinn and Courtney, 1988, Yuzhelevskii, 1991, Polyzois et al, 1994). Tests on maxillofacial silicones have shown variability in their long term performance with some remaining unaffected by exposure to a range of ageing conditions whereas other show considerable degradation (Haug et al, 1992).

4.2. Curing of silicone polymers.

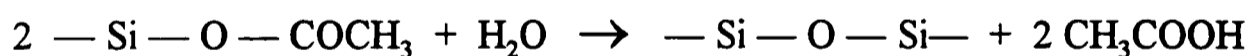
It is generally convenient to distinguish between the different types of silicone polymers on the basis of their curing reaction. There are basically four ways a silicone may be cured;

1. Acetoxy cure; this relies on water penetrating the material to initiate the curing reaction, with the evolution of acetic acid.
2. Condensation curing; the material cures by the action of a catalyst on alkyloxy and hydroxyl/silanol groups within the material which evolves a alcohol.
3. Peroxide addition cure; this involves free radical polymerisation.
4. Hydrosilylation; another type of addition cure using a vinyl and hydrogen terminated siloxane and catalyst.

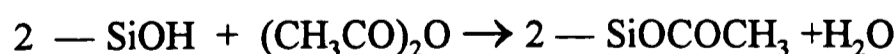
There are additional ways to cure a silicone polymer such as radiation (Vokál et al, 1986, Ma et al, 1988) but these are unsuitable for dentistry as the hazards or high temperatures involved would be beyond the scope of a dental laboratory or destroy the PMMA.

4.2.1. Acetoxy curing silicones.

The acetoxy cure silicones cure by abstracting water from the atmosphere and evolving acetic acid, as shown below (Rochow, 1987).



The acetoxy groups are produced by the reaction of acetic anhydride with silanol groups, as shown below.



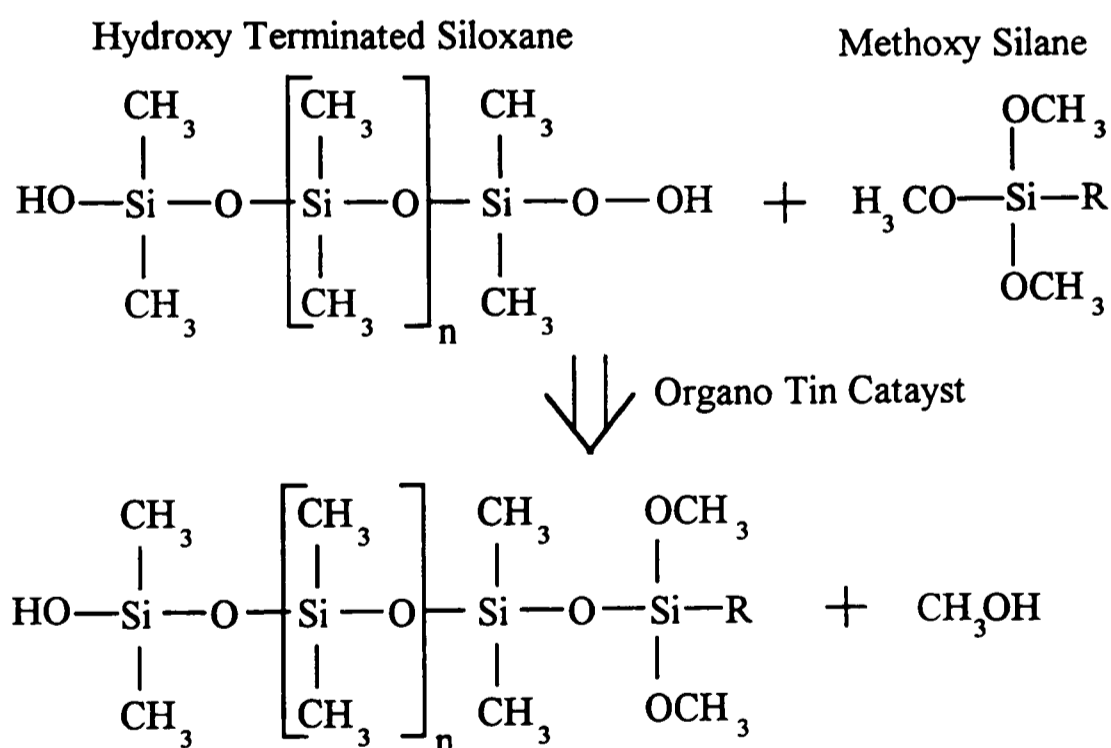
Other methods of curing are available such as using ethoxy or propenoxy groups rather than the acetoxy groups illustrated above. A small quantity of organo tin catalyst is also present to initiate this reaction when exposed to the water. However the nature of this type of polymerisation process means it is dependent on water ingress into the material

(Beers 1968), while this may be suitable for thin sections thicker sections are questionable.

4.2.2. Condensation silicone polymers.

The condensation silicones are characterised by the reaction of a silanol terminated siloxane polymer and an alkoxy functional silane or siloxane in the presence of a catalyst, typically an organo tin (stannous 2-ethyl hexanoate, di butyl tin di laurate or di octyl tin di laurate). An alkyloxy functional silane is normally used as the multi functionality enables the cross linking of the siloxane chains. Figure 4.1 shows a schematic representation of this reaction (Dolgov, 1977). The evolution of alcohol from the polymerisation and its subsequent loss by evaporation or leaching by a solution results in weight loss and polymerisation shrinkage (Braden, 1992).

Figure 4.1. Typical condensation curing reaction.



Silanes have the general formula $X_n\text{SiR}_{(4-n)}$ where the X corresponds to the alkyloxy group, n is a number between 1 and 4, and R represents an organic group.

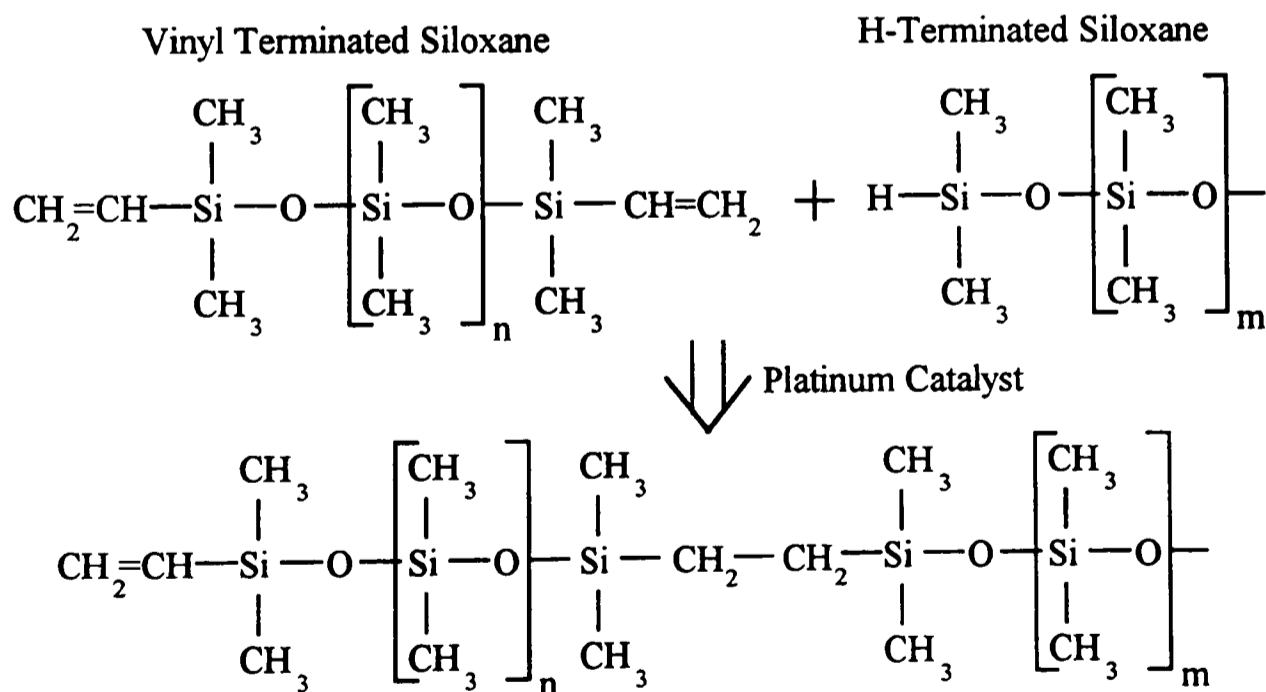
4.2.3. Peroxide addition.

Peroxide cure silicones use a free radical polymerisation route in which the initiator is used to oxidise CH_3 groups on neighbouring chains to form $\text{Si-CH}_2\text{-CH}_2\text{-Si}$ cross links between the chains (Rochow, 1987). The curing temperature is dependent on the initiator used, the usual agents being benzoyl peroxide (70 - 100 °C) (Simpson, 1967) or bis (2,4-dichlorobenzoyl) peroxide (120 - 130 °C) (Creamer, 1970).

4.2.4. Hydrosilanised silicones.

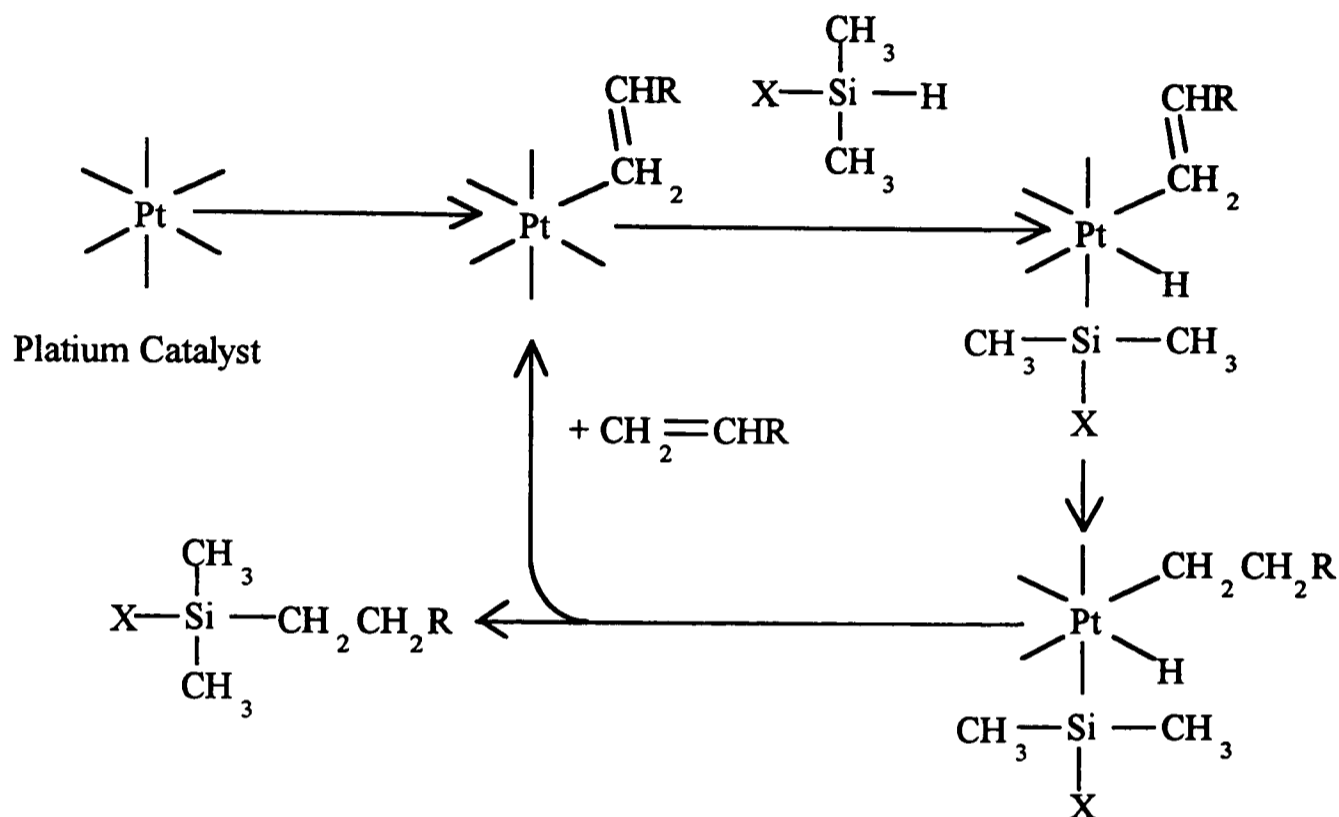
Hydrosilation is an alternative method of curing which involves the polymerisation of a vinyl terminated siloxane and a H-terminated siloxane. The curing occurs via the end groups in the presence of a platinum complex (Bontems et al, 1993) catalyst as shown in figure 4.2. Cross linking is introduced to the system by using a branched siloxane (usually the H-terminated siloxane).

Figure 4.2. Hydrosilation curing reaction.



The platinum catalyst is typically chloro platinumic acid although platinum siloxane complexes are also available and are widely used. The mechanism for the catalyst to polymerise the silicone has been shown by Kohjiya et al (1991) and is illustrated in Figure 4.3.

Figure 4.3. Action of platinum catalyst .



There are many different types of catalyst available to initiate the reaction mostly forming an RTV material; initially finely ground platinum metal or chloro platinumic acid were used (General Electric Co., 1967). This was later joined by platinum complexes such [PtCl₂.C_nH_{2xm}]₂ or H[PtCl₂.C_nH_{2xm}] (Modic, 1970); alternatively rhodium complexes may also be used (Heidingsfeldová and Capka, 1985). Heat polymerisation may be achieved by using a inhibitor such as 1,3-bis(methphenylethynylvinyl)disiloxane (Feng and Du, 1991) although this actually only slows the hydrosilation at room temperature to improve the processing time and is believed to be attributable to the presence of phenyl groups (Yuan and Li, 1988). Alternatively the catalyst may be incorporated in a finely ground material which softens at a desired temperature so releasing the catalyst to cure the material (Leverkusen et al, 1984, Schlak, 1984, Shimizu and Sakuma, 1991). Hydrosilanised catalysts can however be poisoned by presence of amines or sulphur (present in some rubber gloves) which results in poor elastomeric properties and retarded polymerisation (Warrick et al, 1979), this is particularly relevant when employed as drug

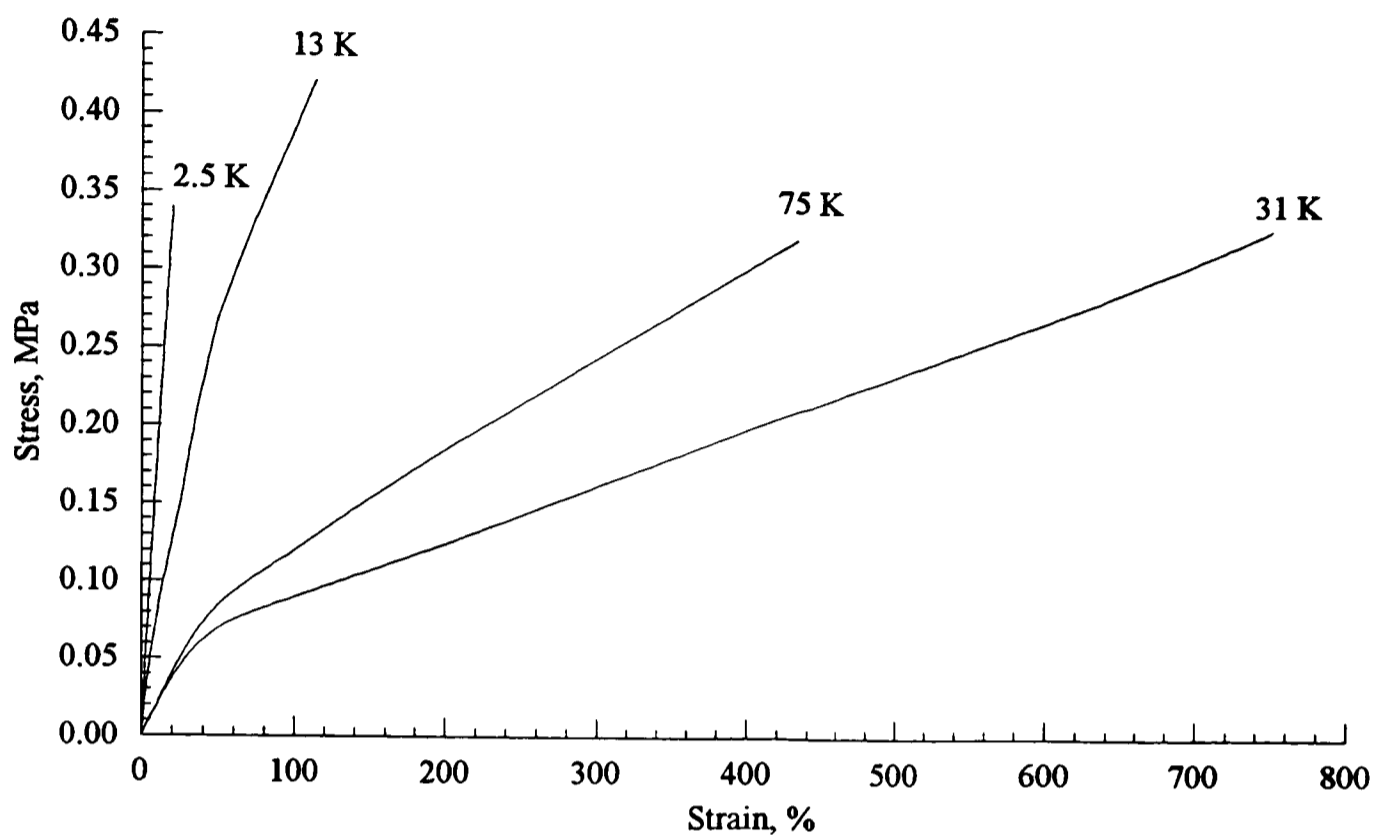
release materials when amine groups are frequently found on the drug (Pfister et al, 1985).

4.3. General formulation of silicone polymers.

The inherent strength of silicone rubber is normally low with an UTS of around 0.2 and 0.7 MPa (Heidingsfeldová et al , 1991, Bontems et al, 1993). The strength of the rubber is controlled in part by the distance between cross links. For the hydrosilanised materials the molecular weight of the siloxane fluid determines distance between cross links as cross linking usually occurs at the H-terminated siloxane (Valles and Macosko, 1979). Figure 4.4 shows the influence of different molecular weights of vinyl terminated siloxane on the final properties of the silicone polymer for a stoichiometrically balanced hydrosilanised silicone. The balance between the vinyl and Si-H groups for hydrosilanised silicones also plays an important role in determination of the properties, with an excess of Si-H generally producing the better material although too much will weaken the material (Heidingsfeldová et al, 1991). In general such silicone materials show very close agreement to classical elasticity theories with deviation generally being attributed to chain entanglement, this is demonstrated by almost linear and horizontal Mooney Rivlin plots (Valles and Macosko, 1979).

The degree of reaction is an important consideration and shows a dependence on the molecular weight of the siloxane (with the unreacted proportion increasing with molecular weight) and the balance between vinyl and Si-H, the proportion of the unreacted groups is known as the sol % (Valles and Macosko, 1979, Heidingsfeldová et al , 1991, Bontems et al, 1993). A high sol % will decrease the tensile strength and the mechanical properties generally as well as increasing the leachability.

Figure 4.4. Relationship between stress/strain curves and molecular weight of unfilled vinyl siloxane polymer of a hydrosilanised silicone ($k = 1000$) based on Bontems et al 1993.



4.3.1. Fillers for silicone polymers.

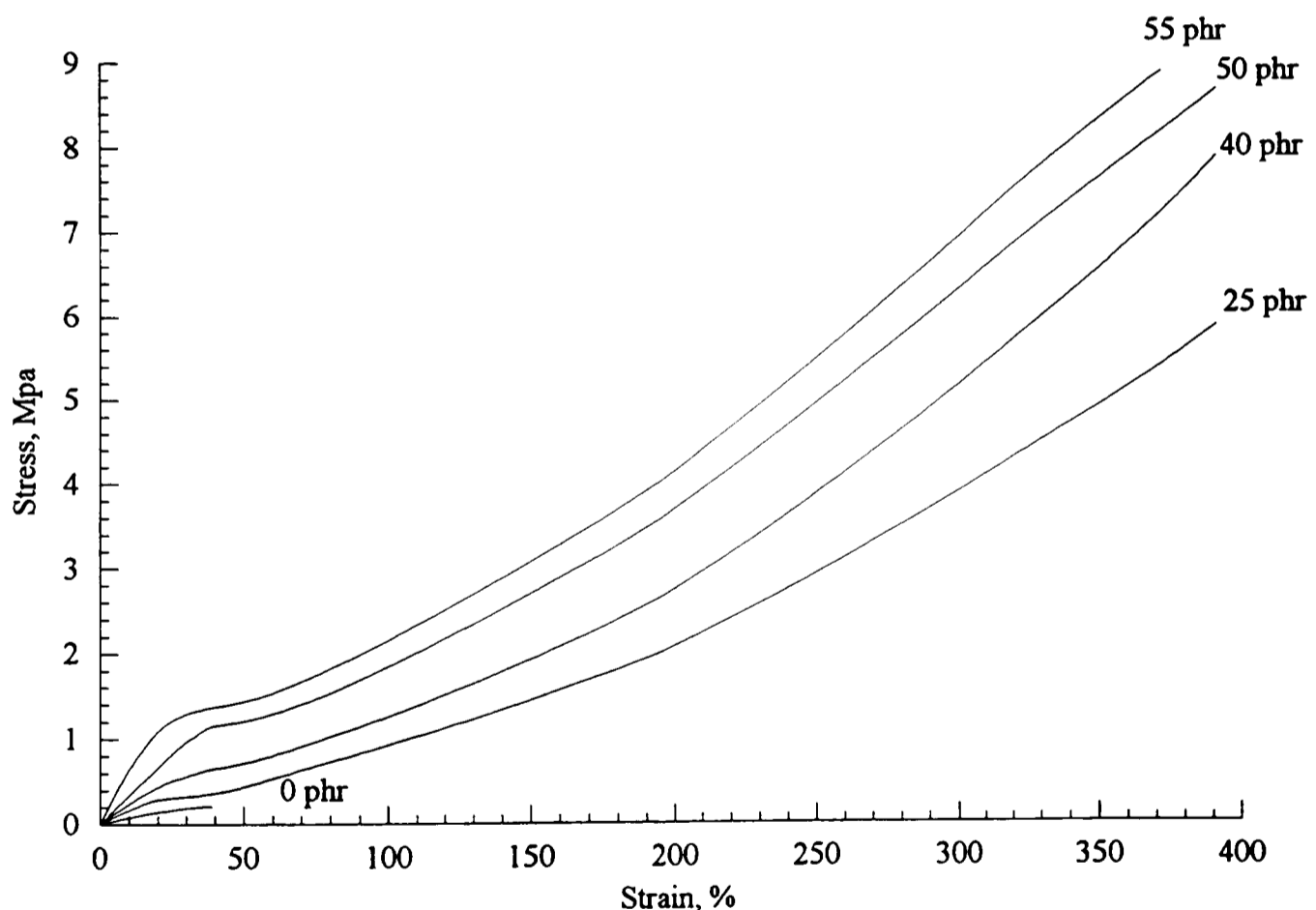
To improve the strength of silicone polymers fillers are used; these can take many forms and have a profound influence on the properties of the material. A wide variety of fillers are used such as calcium carbonate, aluminium oxide (Beers, 1969), polymer powders such as poly (vinyl chloride) (Beers, 1968) or poly (methylmethacrylate) (Van Handel, 1971), quartz (Shingledecker, 1991) or silicas (Rochow, 1987, Okal and Waddell, 1995). Generally the silicas are the most successful and are capable of improving the UTS to around 8-9 MPa (Rochow, 1987).

There are two basic types of silica available to reinforce silicone polymers. These are precipitated and fumed or pyrolytic silica. The difference between them is the order of the particle size. Generally the particle size is given in terms of surface area as, particularly the fumed silicas, are too small to be able to measure the particle size directly. The way silica reinforces the silicone is controlled by a number of factors, the

most important being the loading, particle size and surface condition. The influence of loading is demonstrated by figure 4.5, with the strength increasing dramatically with increased loading. The formation of a yield point at low strains for the highly reinforced silicones is attributed to the presence of silica networks or aggregates within the material. These yield when a sufficient shear stress is applied to enable movement of the polymer chains (Cochrane and Lin, 1993).

The silica also acts to increase the viscosity of silicone fluids by the same aggregation of the silica particles. This results in a paste that exhibits shear thinning gradually hardening with time as the silica network forms. This networking of the silica is normally known as *crépe* hardening.

Figure. 4.5. Effect of silica (200 m²/g) loading (parts per hundred) on peroxide cured silicone (based on Cochrane and Lin, 1993).



The surface of silica is covered in silanol groups (Degussa, 1993,a, 1993,b), these may exist in different states, (figure 4.6). The different types of silanol groups on the surface have different affinities for interaction with other silanol groups on other silica particles or dipoles on the siloxane chain, with the free silanol groups being most active. These free silanol groups on the surface form hydrogen bonds with silanol bonds on other silica

particles resulting in the agglomeration, networking which causes the yielding and is partially responsible for the crêpe hardening. Alternatively the siloxane groups may hydrogen bond to the siloxane backbone as shown in figure 4.7 (Cochrane and Lin, 1993) which is the primary cause of crêpe hardening.

Figure 4.6. The possible orientation and surface states of silica.

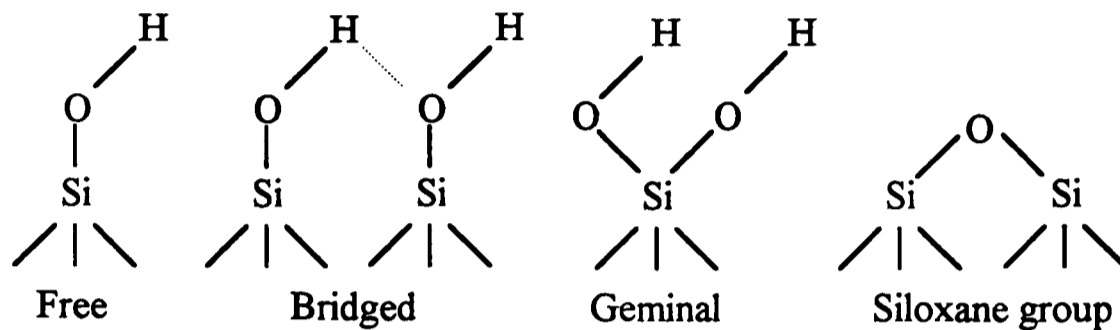
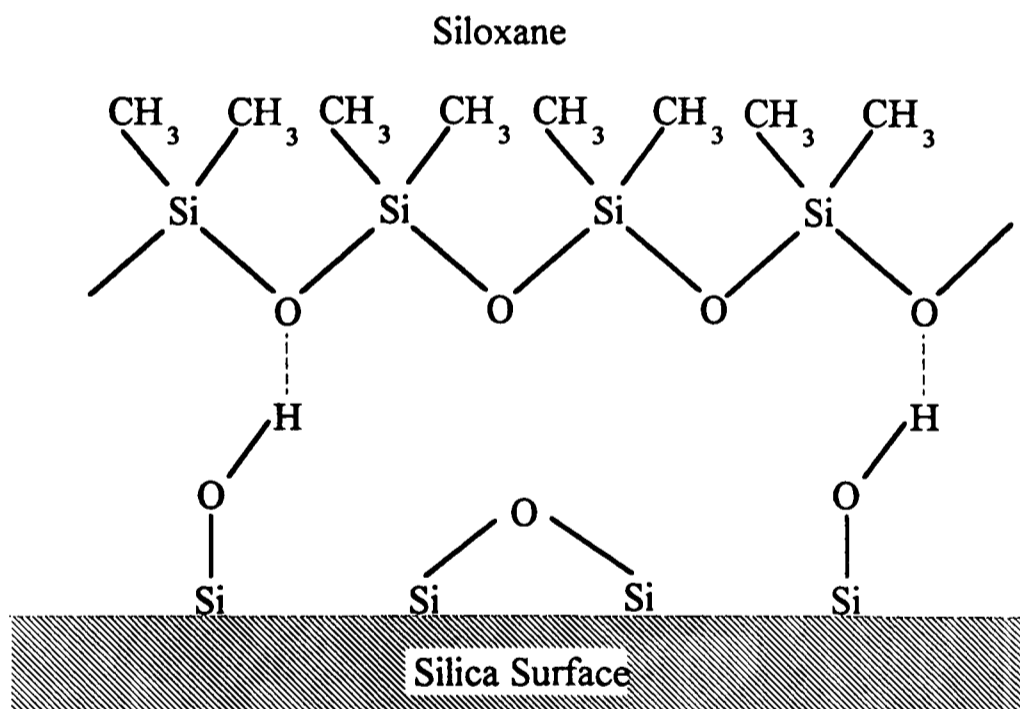


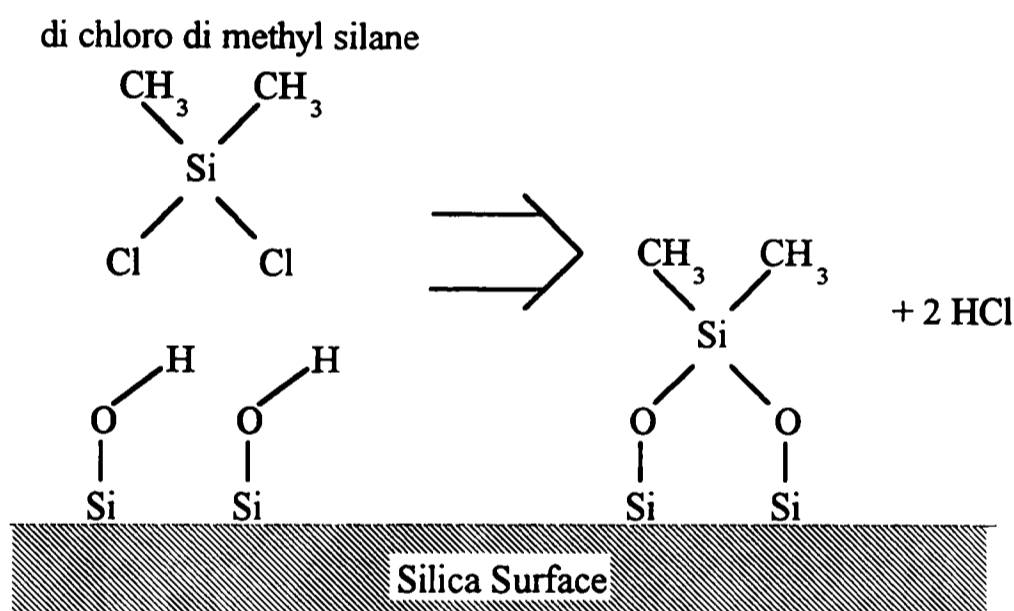
Figure 4.7. Hydrogen bonding of siloxane to silica surface.



Whilst such interaction between the silica and siloxane may be advantageous in terms of the strength of the silicone polymer it's effect on the processability/mouldability of the polymer is a major problem. This may be improved in two ways, surface treatment of the silica or using a processing aid. A processing aid is a low molecular weight siloxane or silicone oil which preferentially adsorbs or chemically bonds to the silica surface. This prevents the interaction of the high molecular weight siloxane and silica thus reducing the overall paste viscosity and crêpe hardening (Cochrane and Lin, 1993).

Surface treatment of silica may be achieved in different ways which include low molecular weight cyclo siloxanes (Yu-Fu et al, 1981) or more commonly silanation (Millar and Ishida, 1984, Girard and Cohen-Addad, 1991, Wang and Wolff, 1992, Söderholm and Shang, 1993). Silanation involves the condensation reaction of a silanol group on the silica and a hydrolysed silane which results in a siloxane bridge between the silica and silane (Ishida and Koenig, 1978). There are many different types of silane but the basic formula is $X_nSiR_{(4-n)}$, where n is an integer between 1 and 3, X is the organic group and R is normally an alkyloxy group but can also be chloride. It is the alkoxy groups that bond to the particles, these are usually methoxy groups although ethoxy groups are also common. All of these hydrolyse under wet conditions releasing hydrochloric acid (HCl), methanol (CH_3OH) or ethanol (C_2H_5OH), (Miller and Ishida, 1984). Figure 4.8, illustrates the silanation of a silica surface with di chloro di methyl silane (Degussa, 1993,b).

Figure 4.8. Silanation of a silica.



The surface coverage by the organic groups hinders the hydrogen bonding influence of the remaining silanol groups and thus prevents particle agglomeration and hydrogen bonding to the siloxane fluid (Cochrane and Lin, 1993). Such surface treatments also have a dramatic effect on the water adsorption characteristics of the powder making them hydrophobic rather than hydrophilic (due to the silanol groups). Many of these treated silica's are known commercially as hydrophobic silica (Degussa, 1993,b).

The presence of water on the surface of the silica during polymerisation has been shown to have a detrimental effect on the properties as it is hydrogen bonds to the silanol groups on the surface (Cochrane and Lin, 1993). Although this prevents the crépe

hardening as it acts as a surface coating, in the same way the processing aid does, it does not bond to the siloxane on polymerisation as with the processing aid and hence can drastically weaken the silicone rubber by preventing a good contact between matrix and reinforcement.

4.3.2. Degradation of silicone polymers.

Silicone polymers are generally regarded as stable inert polymers. Although they do exhibit excellent resistance to a wide ranging conditions they can degrade if exposed to certain conditions. Silicone polymers degrade slowly under a range of conditions by hydrolytic decomposition (Vondráček and Gent, 1982), which results in the breakage of the siloxane bridge forming silanol end groups (Stein and Prutzman, 1988).



The reaction is catalysed normally by an organo tin which is used in the production of condensation and acetoxy cure silicones (Stein and Prutzman, 1988, Stein and Leonard, 1990). Although it is believed this type of reaction occurs when the materials is exposed to different types of Lewis acid (Stein, 1994). The reaction is reversible with bond scission and recombination occurring simultaneously, many tests fail to detect and degradation as the effect is masked by the recombination. Stress relaxation being the most successful method for studying this process as it enables the degree of the chemical relaxation to be determined (Stein and Prutzman, 1988, Stein and Leonard, 1990).

The process shows a dependence on environmental factors with an increased rate being observed with humidity (Stein and Prutzman, 1988, Gambogi and Blum 1993), temperature (Stein and Leonard, 1990) and ammonia rich atmospheres (Vondráček and Gent, 1982). The degradation may be reduced by reducing the initial silanol group concentration in the matrix and filler (Vondráček and Gent, 1982), increasing the degree of cross linking (Yu-Fu et al, 1981, Stein and Leonard, 1990) and extraction of the organo tin catalyst (Stein and Prutzman, 1988, Stein and Leonard, 1990).

Silicone rubbers may degrade through other mechanisms particularly when exposed to high temperatures (Yu Fu et al 1981) or high intensity X-rays (Tóth et al 1993) but these are not included as they are unlikely to be a factor for a soft lining material.

4.4. Development of silicone polymers.

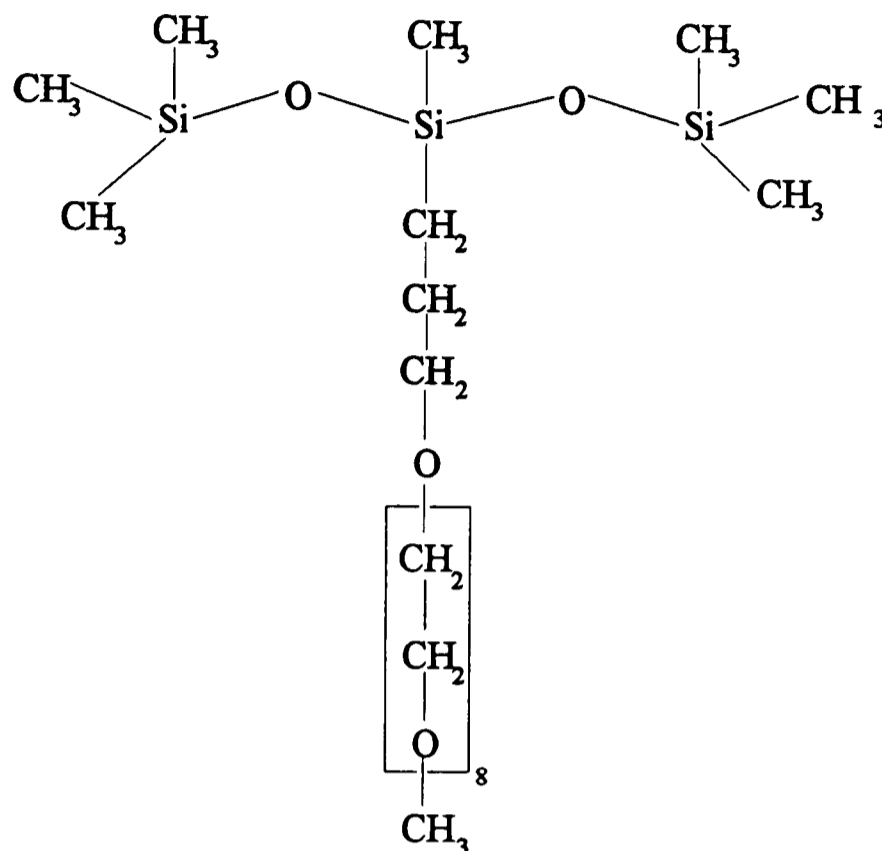
Traditional silicone manufacture often involves a post cure of the material which involves heating the material in excess of 150°C; this helps to ensure complete polymerisation and maximum strength. The potential use of these materials as dental soft lining materials prevents the use of this as the effect on the PMMA would be detrimental. Hence none of the materials detailed below were post cured although they were boiled in water at 100°C in line with current dental techniques.

Table 4.1, details the codes and suppliers of the silicone polymers used within this study. The basic method of formulation was the same for all materials. Namely, batch the components in one of two parts as required and dilute with chloroform to form a slurry this ensured components such as BP and HPT were uniformly distributed throughout the polymer and prevent loss of the fumed silica during mixing. The pastes were then left to evaporate off the chloroform before they were milled on a paste mill to ensure homogeneity of the blend. For the two part formulations the materials were re-milled when mixed prior to moulding.

Table 4.1. Codes for the materials used in the formulation of silicone polymers.

Code	Material	Supplier
SOH	Hydroxyl terminated siloxane, viscosity 20,000 cp.	Jamak Fabrication Europe Ltd.
SCC	Vinyl terminated siloxane, viscosity 60,000 cp.	V 60 K, OSi Specialities.
SCC-L	Vinyl terminated siloxane, viscosity 2,000 cp.	V 2 K, OSi Specialities.
SHT	Hydrogen terminated siloxane.	Y12135, OSi Specialities.
BTL	Di butyl tin di laurate.	Aldrich.
OTL	Di octyl tin di laurate.	Pfaltz and Bauer Inc.
BP	Benzyol Peroxide.	Aldrich.
HPT	Hydrogen chloroplatinic acid.	Aldrich.
VPT	Organo platinum complex.	V-CAT-RT, OSi Specialities.
MPS	γ -methacryloxypropyl trimethoxy silane.	A174, Ambersil.
VS	Vinyl trimethoxy silane.	A171, Ambersil.
PMMA	Poly (methylmethacrylate).	Bonar Polymers.
S150	Fumed silica, surface area 150 m ² g ⁻¹ .	Aerosil 150, Degussa AG.
S200	Fumed silica, surface area 200 m ² g ⁻¹ .	Aerosil 200, Degussa AG.
S300	Fumed silica, surface area 300 m ² g ⁻¹ .	Aerosil 300, Degussa AG.
R972	Fumed silica, surface area 130 m ² g ⁻¹ , treated with di methyl di chloro silane.	Aerosil R972, Degussa AG.
R974	Fumed silica, surface area 200 m ² g ⁻¹ , treated with di methyl di chloro silane.	Aerosil R974, Degussa AG.
C717	Fumed silica, surface area 200 m ² g ⁻¹ , treated with VS	Central Chemicals Ltd.
CS	Calcium Stearate.	Aldrich.
L77	See Figure 4.9.	L77, OSi Specialities.

Figure 4.9. The structure of L77.



4.5. Condensation silicone polymers.

4.5.1. Formulation of condensation silicone polymers.

The formulation of the condensation silicones was based on that of Molloplast B, possibly the most successful soft lining material, as described in US Patent 3,785,054 (Appendix I). Table 4.2, details a selection of the formulations of these materials which will be used in the forthcoming discussion. The curing chemistry is detailed in section 4.2.2., MPS was chosen as the silane as it was felt that the presence of the methacrylate group would aid the adhesion to the denture base (PMMA), and the PMMA added to the silicone as a filler.

The silica fillers used for all these formulations were supplied by Degussa AG. The number quoted refers to the surface area of the silica used (i.e. silica 150 has a surface area of 150 m²g⁻¹). The silica R972 refers to Degussa's Aerosol R972 which is a hydrophobic silica that is made by treating with di chloro di methyl silane. The siloxane used was silanol terminated poly dimethyl siloxane.

Table 4.2. Composition of condensation silicones, based on SOH.

Code	Silica, %	MPS, %	PMMA, %	Catalyst
CB972	R972	20	12	3 BTL
CB P5	R972	20	12	5 BTL
CB P0	R972	20	12	0 BTL
CB150	S150	20	12	3 BTL
CO150	S150	20	12	3 OTL
CO200	S200	20	12	12 OTL
CO300	S300	20	12	12 OTL

These materials were formulated as two part pastes which were mixed together, in equal parts by weight, to give the overall composition detailed table 4.2. An example of how the formulations were divided is shown in table 4.3, the critical factor being the separation of the MPS and the catalyst (BTL or OTL) to prevent polymerisation of the material.

Table 4.3. Composition of CB972 as two part paste.

Component	Part 1, Wt%	Part 2, Wt%	Total, Wt%
Siloxane	25.6	38.4	64
MPS	12	-	12
Silica R972	9.4	10.6	20
PMMA	3	-	3
BTL	-	1	1

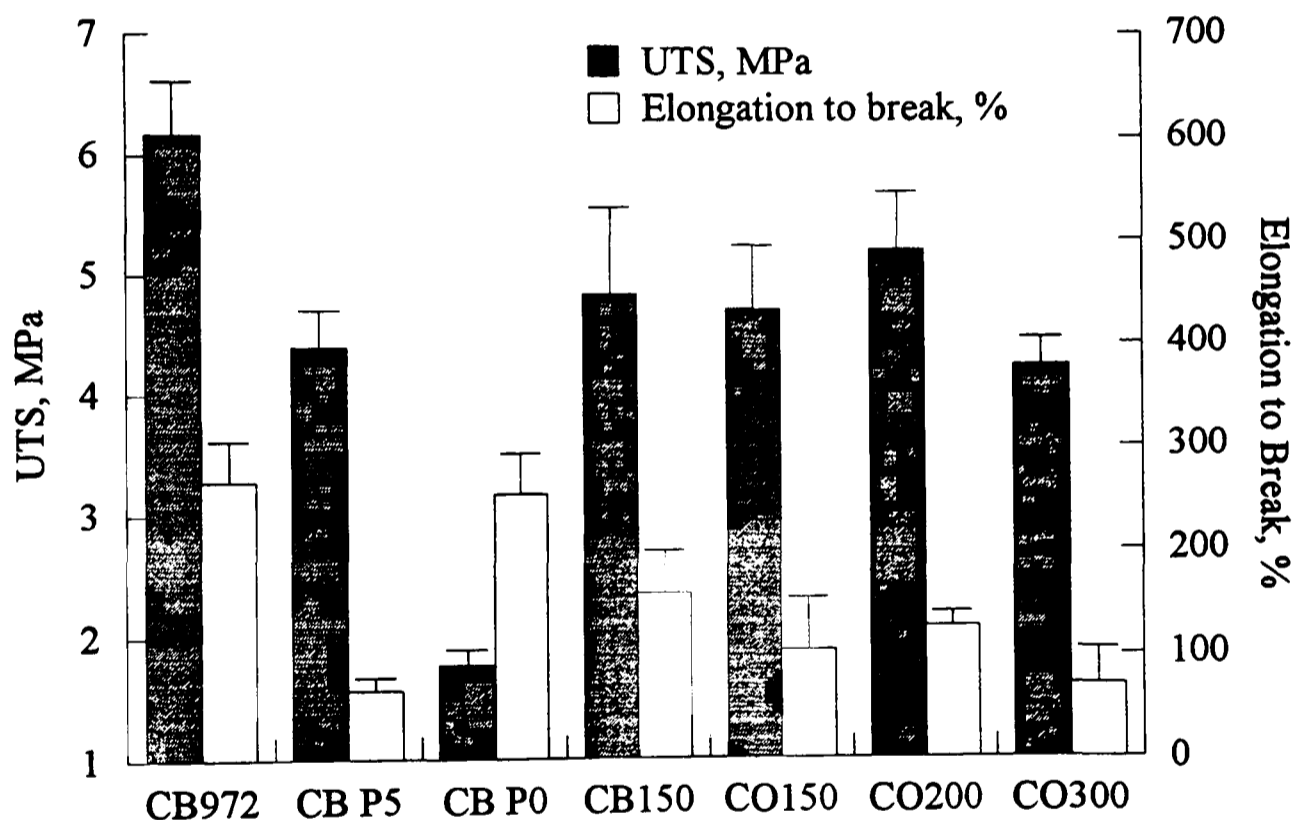
4.5.2. Results for the condensation silicone materials.

Tensile results for the condensation silicones are shown in figure 4.10. It is apparent from these results that the UTS of these materials shows a great dependence on the PMMA present within the material, CB972 (having 3 % PMMA) has a higher UTS than both the CB P5 (5% PMMA) and CB P0 (no PMMA). The PMMA should strengthen the material as it should bond with the MPS so reinforcing the material. However, too

high a PMMA level is liable to weaken the material as the PMMA particles would tend to agglomerate together.

The type of silica only has a slight influence on the strength of the material, with the CB972 having a slightly higher UTS than the CB150. The reason for this is likely to be the homogeneity of the pastes. The S150 is covered in silanol groups rather than the methyl groups as with the silica R972; this makes the S150 much more wettable by the siloxane which causes an increase in the viscosity. This makes blending the pastes together more problematic and leads to a non uniform distribution of catalyst and silane in the material.

Figure 4.10. UTS results for the condensation silicones.



The results show little dependence on the type of catalyst used to initiate the reaction with the CB150 and CO150 having a very similar UTS. The particle size of the silica is important for the UTS with the CO200 being stronger than the CO150. This is expected from the literature previously detailed as the finer silica provides a more effective reinforcement. The CO300 however shows a decrease in UTS and elongation to break which is attributable to the thixotropic nature of the pastes due to the S300 making blending difficult leading to problems of inhomogeneity.

On the basis of these results two samples were placed in water, the CB972 and the CO200. The absorption results for these materials are shown in figure 4.11, and summarised in table 4.11

Figure 4.11. Absorption results for condensation silicones.

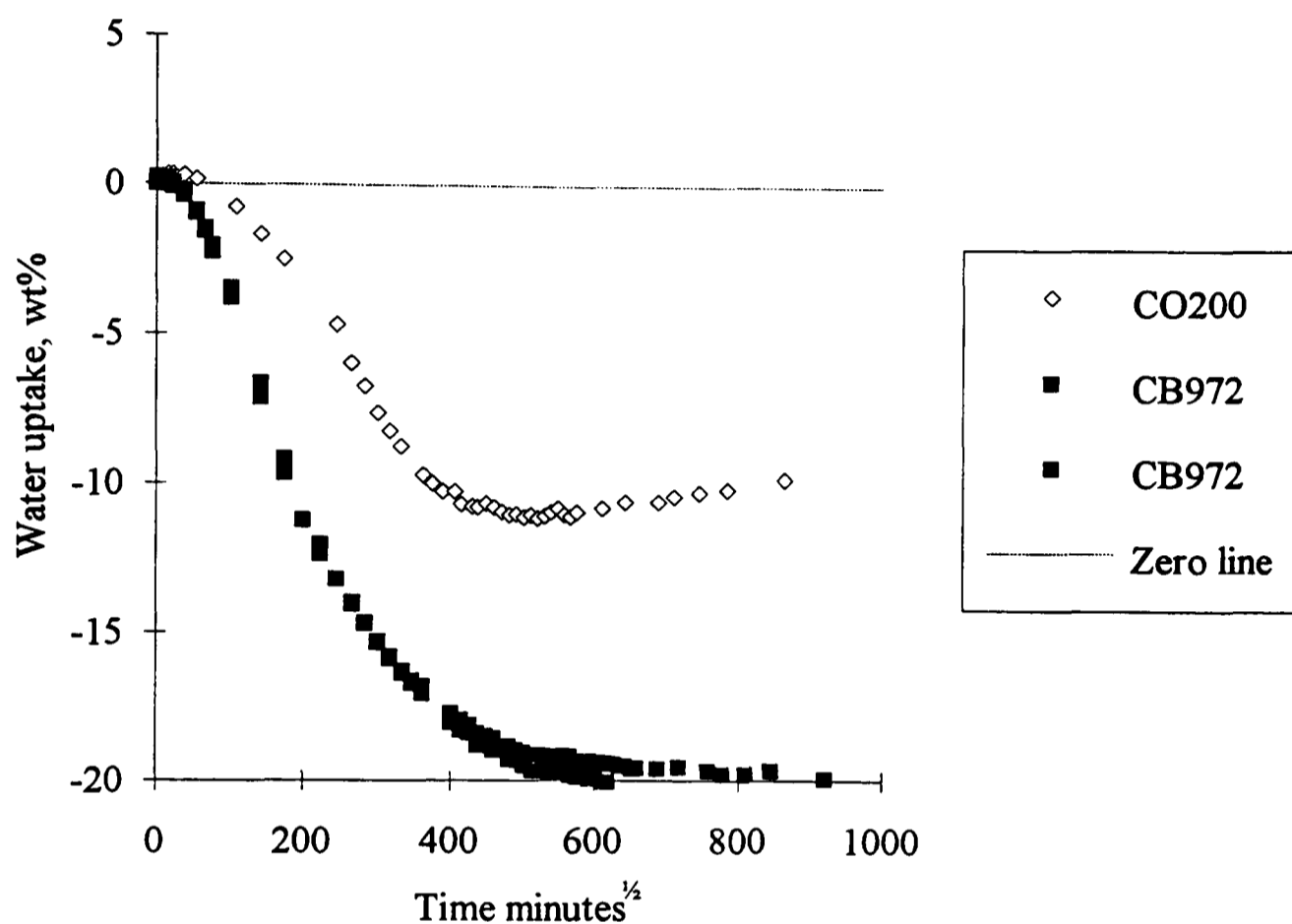
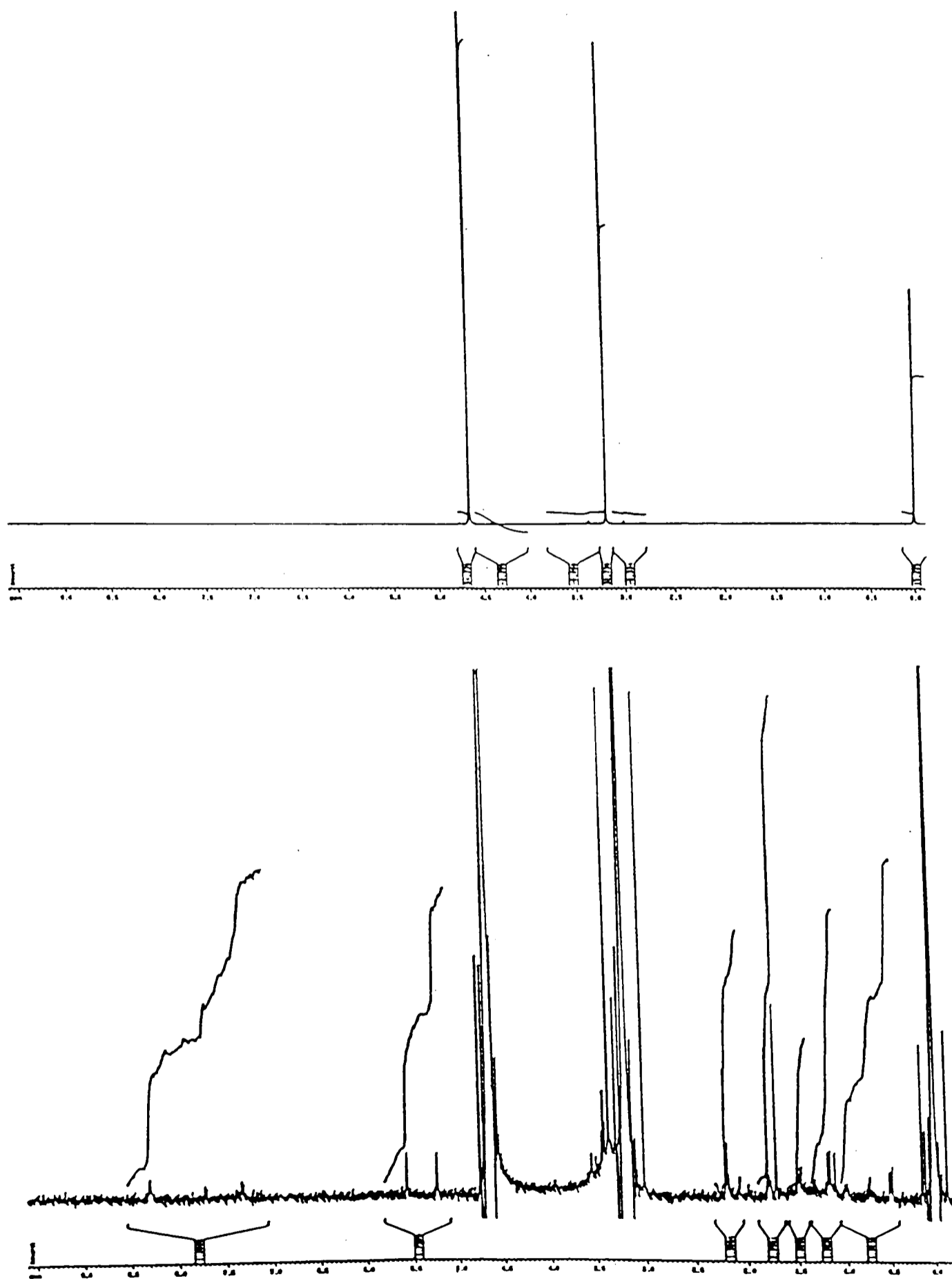


Table 4.4. Summary of absorption data for condensation silicones.

Code	Water Uptake, After, wt %	Weight Loss on Desorption, wt %	Solubility, wt %	D_{des} , m^2s^{-1}
CO200	-9.80	-	-	-
CB972	-20.06	1.17	18.89	6.79×10^{-9}

Both of these materials, rather than showing a positive weight change, exhibit a large weight loss of up to 20 % for the CB972. This weight loss is accompanied by hardening and embrittlement of the material. To establish what materials were being lost CB972 was immersed in D_2O rather than water so that the leached material could be analysed by nuclear magnetic resonance (NMR). These results are shown in figure 4.12, the lower figure showing the low intensity lines.

Figure 4.12. C^{13} NMR spectrum of leached from CB972, scan performed by Mrs J. Hawkes, Department of Chemistry, King College London. The lower spectrum is a magnification of the low intensity peaks.



From the spectra we can see a large peak corresponding to the hydrogen in H₂O at 4.66 ppm, CH₃OH at 3.19 ppm and CH₃-Si at 0 ppm. The lower part of figure 5 is a magnification of the low intensity peaks of the upper figure. The peaks at 8.5 to 7 ppm are attributed to hydrogen atoms in the BTL which are in the proximity of the tin. The two distinctive equal sized peaks at 5.57 and 5.25 ppm are the CH₂ of the methacrylate group of the MPS. The range of peaks between 2.2 and 0.4 ppm correspond to CH₂ and CH₃ groups in a carbon chain, these may stem from either the MPS or BTL. These peaks indicate that only a very small amount of BTL and MPS had leached out of the material during absorption.

The larger peaks may be used to calculate the relative proportions of the different molecules in the solution by dividing the intensity of the peak by the number of hydrogen ions within the molecule contributing to each peak as shown in Table 4.5. The CH₃-Si peak is calculated on the basis of being CH₃-Si-CH₃ as the bond is likely to have come from any siloxane leached out of the material. The large amount of H₂O within the D₂O is misleading as it is likely to be due to the hygroscopic nature of the D₂O absorbing atmospheric H₂O rather than the leachant. The CH₃OH and CH₃-Si-CH₃ are however likely to be the majority of the leachant. The intensities of these peaks show there is approximately 4.5 times as much CH₃OH than CH₃-Si-CH₃. The CH₃-Si-CH₃ is likely to be in the form of unreacted or broken down siloxane chain. As these chains tend to be very large molecules it would take only a few of these chains to account for the CH₃-Si peak at 0 ppm. The majority of the leachant is therefore taken to be methanol.

Table 4.5. Intensities of NMR spectra from CB972 leachant from D₂O.

Identification	PPM	Intensity	No. of molecules	Proportion, %
H ₂ O	4.66	48.19	24.10	72.86
CH ₃ OH	3.19	22.00	7.33	22.17
CH ₃ -Si-CH ₃	0	9.86	1.64	4.97

To determine where the CH₃OH and CH₃-Si-CH₃ have come from we must consider the curing reaction and the post cure stability of the materials. From the curing behaviour (shown in a previous section) we know that methanol will be produced as a by-product of the curing cycle. This methanol will have evaporate off during the preconditioning (at 37 °C) of the material prior to the absorption and so is unlikely to account for the large weight loss during the absorption.

The nature of the loss, with a slow decrease in weight (figure 4.11) over 250 days (600 minutes^{1/2}), implies the leached material is due to a chemical change within the material. The stability of the condensation silicones has been questioned by Stein (1988 and 1990) and Kohjiya et al (1991) by monitoring the stress relaxation for organo tin catalysed materials in water. The results showed that the silicone was prone to an increased relaxation when both the water and organo tin was present. This was attributed to the bond scission and recombination of the siloxane bonds and silanol bonds in the presence of both BTL and water as previously discussed.

This type of bond scission and recombination would account for the siloxane being present in the leached material, as the bond scission would enable the less tangled chains to detach from the material and so enter the solution. This would also account for the hardening of the material as the bonds break and reform so increasing the cross link density and lowering the molecular weight between cross links. The amount of methanol present in the leachant seems too high to have been due to the methoxy groups on the MPS. It therefore seems that there is another reaction also taking place which involves the methyl on the siloxane chains being replaced by cross links to other siloxane chains, which could evolve methanol.

The activity of organo tin catalysts will decrease with time (Stein, 1988) and hence the rate of bond scission and recombination would be reduced over time. This would explain the decrease in rate of weight loss over time, as the catalyst becomes deactivated.

Figure 4.11, shows a marked difference in the percentage loss of CB972 and CO200; this may be due to the hydrophilic silica 200 absorbing more water than the silica 972. This is unlikely as the CO200 loses 10% less material than CB972, and the silica 200 should absorb no more than 1.5 % (this will be further explained later). It is therefore concluded that OTL deactivates faster than BTL or is less capable of bond scission.

These results indicate that the problems of the water loss on absorption may be limited by using different catalysts and possibly by reducing the amount of MPS. The problems associated with the nature of the curing reaction (weight loss) would be likely to remain it was therefore concluded that an alternative curing method would be more suitable.

4.6. Peroxide silicone polymers.

4.6.1. Formulation of peroxide silicone polymers.

The peroxide cure materials are single component systems which cure when heated due to the presence a peroxide initiator. The initiator used is typically di cumyl peroxide (initiates ~120°C) or benzol peroxide (BP), for this study BP was used as this initiates at around 70°C making it suitable for conventional dental technology (boiling in water, 100°C). Lauryl peroxide was also tried as a initiator but this failed to cure the silicone polymer (believed to stem from its lower activity) despite its success with the methacrylate materials (shown in later sections). All the compositions detailed here where made using 2.5wt% BP as an initial study indicated this was the preferred level in terms of strength of the material. Above this level the BP tended to precipitate out of the material and below this level the strength of the material was reduced.

The siloxane used in all these formulations was SCC. SOH and SCC-L was also used to make peroxide silicones but these materials were weaker than the SCC due to the lower molecular weight (demonstrated in terms of the lower viscosity of the fluid) in accordance with the general theory. Hydroxyl terminated siloxanes are reported to have some advantages over the vinyl in terms of the thermal stability for peroxide cure silicones. This however was not the case with these materials due primarily to the absence of a post cure and lower curing temperature making the thermal stability less important. It is anticipated that a hydroxyl terminated siloxane of the same molecular weight should basically be the same as the SCC used in this study. The formulation of the materials detailed in this section are given in table 4.6.

Table 4.6. Formulation of peroxide cure silicone polymers, the siloxane used was SCC.

Code	Silica,	%	Addition	%
P200	S200	20	-	-
P200 25	S200	25	-	-
P974	R974	20	-	-
P974 25	R974	25	-	-
P717	C717	20	-	-
P200 H	S200	20	SHT	1.8
P974 L1	R974	20	L77	0.1
P974 NF	R974	20	NaF	0.5
P200 CS	S200	20	CS	3.75
P200 LCS	S200	20	CS	0.6
P974 .5CS	R974	20	CS	0.5
P974 .1CS	R974	20	CS	0.1

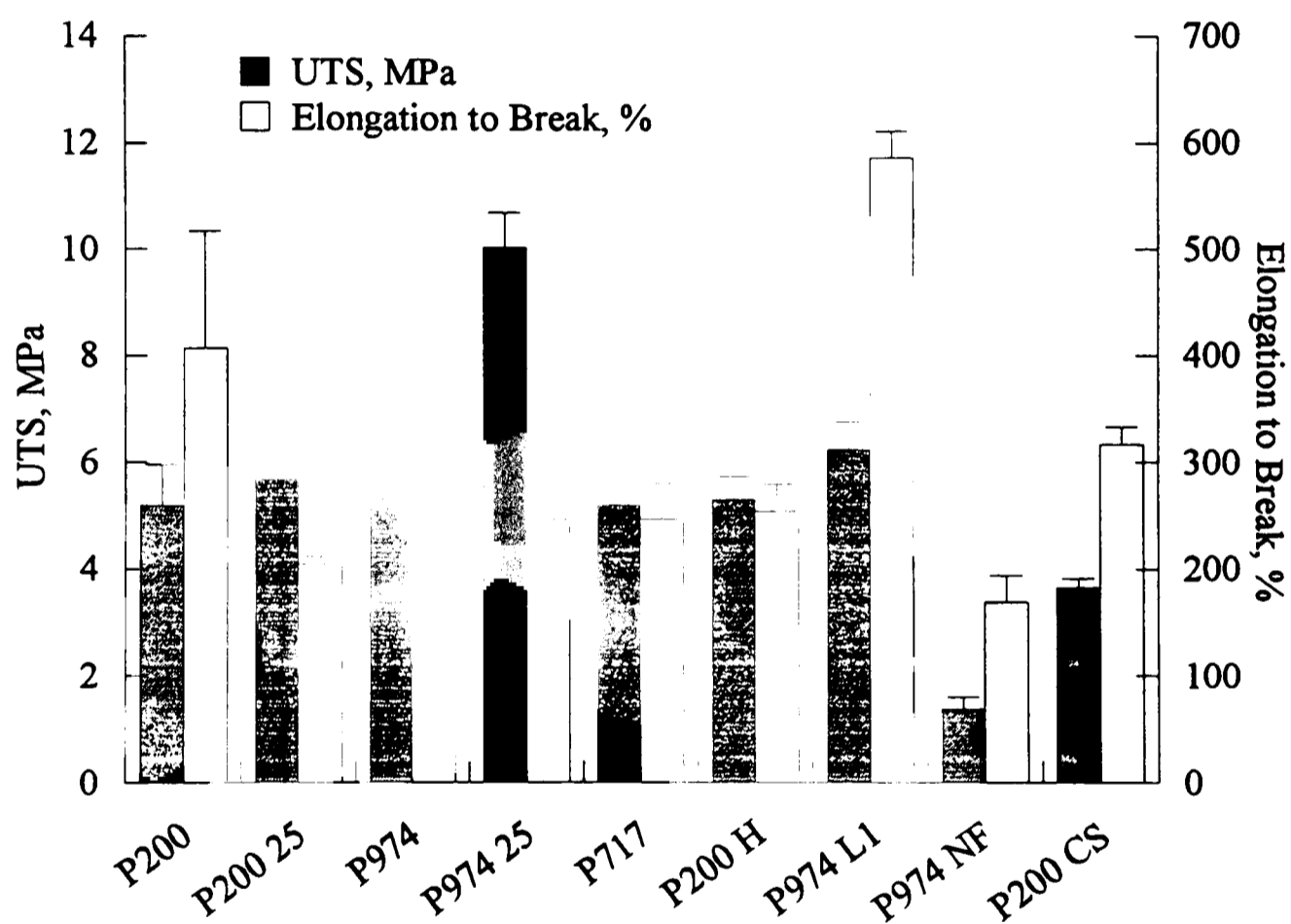
4.6.2. Results for the peroxide silicone polymers.

The tensile strengths of the peroxide cure silicones are shown in figure 4.13, the UTS of the materials typically being just over 5 MPa. The exceptions being P974 NF and P200 CS where the UTS is considerably lower this is due to the CS and NaF. The NaF was added to the material as crushed crystals, these it is felt will act to concentrate stresses at the crystals whereas the shear magnitude of the CS probably accounts for its poor performance. For P974 L1 the improvement in strength may relate to the improved wetting of silicas by the siloxane fluids.

The similarities between the different types of silica is interesting considering the different types of surface coating. S200 is covered in silanol groups which it might be thought would bond with the silicone matrix and provide a more effective reinforcement than the R974. This seems not to be the case and may be attributed to the state of the silica used. The silanol groups on the surface are capable of different states as previously detailed, water (from the atmosphere) may also be adsorbed or chemisorbed on to the surface of the silica forming a 'bound water shell' around the silica particle (this was confirmed by a larger OH peak, 3600 to 4000 cm^{-1} , on IR trace for the older samples). This is supported by the results from fresh S200 samples typically exhibiting a higher

strength than those shown in figure 4.13, prepared from older batches of S200. The water on the S200 surface can be driven off by heating (at 500-600°C) when this was performed the OH peak on the IR trace diminished, however the particles at this temperature tended to agglomerate resulting in a larger particles which resulted in poor reinforcement. When C717 was used (P717) the presence of the vinyl groups made little difference to the strength of the material, hence it was concluded that the vinyl groups were not participating in the polymerisation.

Figure 4.13. Tensile properties of peroxide cure silicone polymers.



The rheology of the pastes plays an important role in the results and explains the differences seen for S200 and R974. When the proportion was increased to 25 %, where R974 25 is noticeably stronger than P200 25. P974 25 shows improvement in UTS compared to P974 in line with the expected theories. S200 is more thixotropic than R974 due to the more wettable nature of its surface, and will also agglomerate together, crépe hardening the paste. This tendency to cluster together makes the paste shear thin as the loose bonds between the agglomerated silica particles break. It is felt these

rheological characteristics of the P200 25 paste make producing an homogenous sample effectively impossible, thus accounting for its poor performance compared to P974 25.

The water absorption results for these materials are shown as a series of figures (4.14, 4.15, 4.17, and 4.20) each showing the first absorption cycle for a few selected materials with the details of the absorption cycles given in table 4.7 and 4.8. The diffusion coefficients for all the materials show a faster desorption coefficient (typically of the order of $10^{-8} \text{ m}^2\text{s}^{-1}$ the generally regarded diffusion coefficient of silicone polymer) than absorption coefficient. This indicates that the diffusion coefficient is indeed concentration dependent as expected. The diffusion coefficient calculated for the second absorption cycle is slower than that of the desorption cycle but is faster than the original absorption cycle. This indicates that the inherent absorption characteristics of the materials have changed during the first absorption cycles. It seems most likely that crack formation is responsible for this increase in rate as the materials now have channels along which water can penetrate the material.

Figure 4.14, shows the first absorption of the silicone materials with 20 % of the different silica fillers. The results here are somewhat surprising with the water uptake of P974 being the highest, although P200 was higher prior to 111 days (400 minutes^{1/2}). However taking the solubility of the materials into account (table 4.7) reveals the overall absorption (water uptake plus the solubility) of the P200 (11 %) to be greater than the P974 (0.73%). It is important to note that P974 has a long protracted uptake with the absorption not seemingly reaching equilibrium during the course of the experiment. This is believed to be due to the presence of benzoic acid (from the benzoyl peroxide) which is soluble at 37 °C and hence will cause droplets to form within the material as previously described, this also accounts for the very slow diffusion coefficient ($10^{-13} \text{ m}^2\text{s}^{-1}$), as the formation of droplets reduces the apparent diffusion coefficient. Why this does not show up in P200 is probably due to the greater solubility of the material overshadowing this effect, the reason for the solubility for P200 is unclear. Comparison with P717 shows another trend with the material showing a negative absorption from an early stage with the overall uptake being only 0.48 wt %.

The effect of different types of silica is complex as different interactions between the initiator (benzoyl peroxide) and the silica surface seem to be taking place. The solubility of R974 (P974) is noticeably less than with S200 (P200) and C717 (P717), apart from B974 NF where the solubility is due to the NaF. R974 will be less likely to become involved in the polymerisation (due to the surface covering of methyl groups) than S200

(covered in silanol) and C717 (covered in vinyl). Exactly how this happens is not known but it does seem to explain deviations between the materials with the lower uptake (P974 and P717) being due to the more hydrophobic (R974 and C717) silicas. However the lower solubility and the more protracted uptake of the P974 is attributed to the difference in the polymerisation from the interaction between the initiator and silica surface.

Figure 4.14. The effect of hydrophilic and hydrophobic fillers on the water uptake of peroxide silicone polymers.

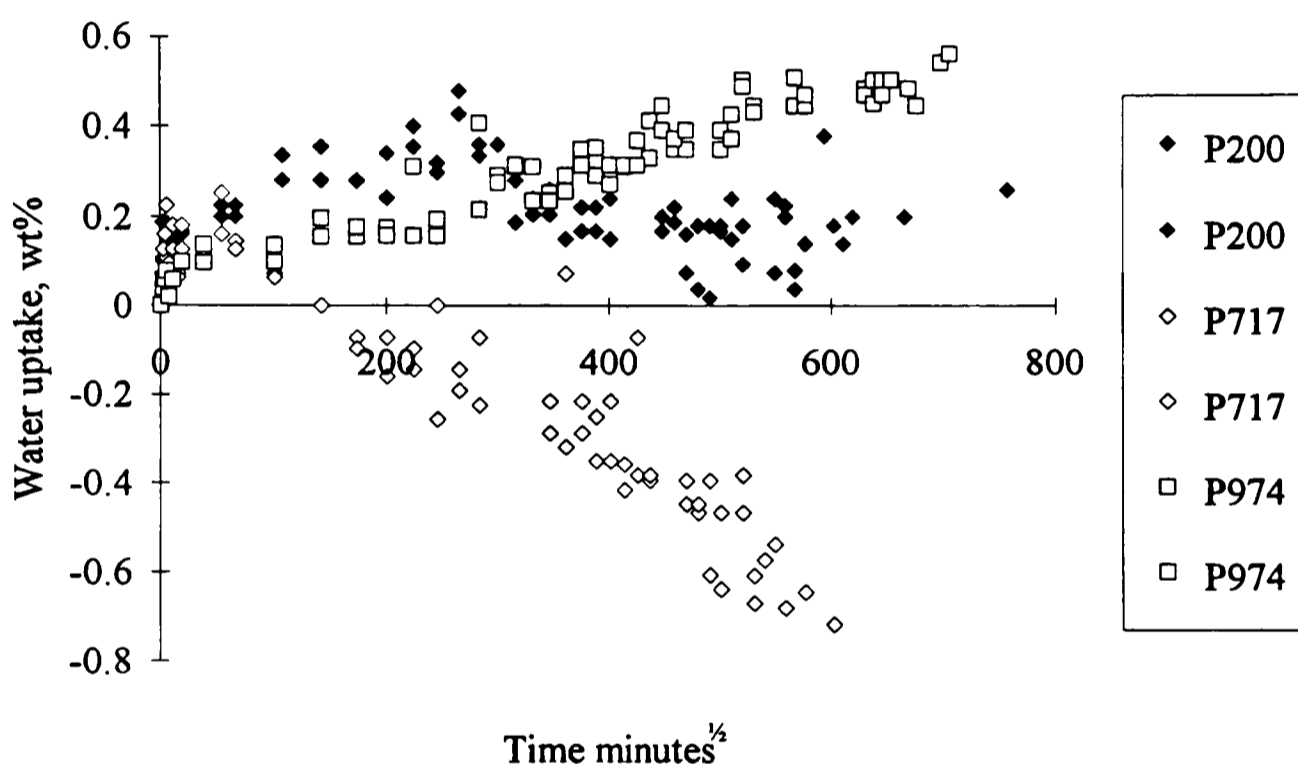


Figure 4.15. presents a somewhat clearer picture with the addition of CS to P200 showing an increase in water uptake with increasing proportion of CS, 3.75% CS (P200 CS) having 7.83 wt% absorption and the 0.6 % CS (P200 LCS) having 2.97wt% compared to the P200 absorption of 1.10 wt%. This is in agreement with the theories on the addition of soluble agents to elastomeric materials as previously detailed, however trying to apply the theories of the kinetics of the process soon runs into difficulties. The shape of the initial period of water uptake is generally linear with reference to $t^{1/2}$ as shown figure 4.16 hence it seems reasonable to calculate the diffusion coefficient. The diffusion coefficient for the first absorption cycle for P200 is $3.68 \times 10^{-11} \text{ m}^2\text{s}^{-1}$ which is greater than that for the P200 CS ($2.05 \times 10^{-11} \text{ m}^2\text{s}^{-1}$) and for the P200 LCS ($5.95 \times 10^{-11} \text{ m}^2\text{s}^{-1}$), hence is in conflict with the expected results. Again this seems to be due to the

presence of the benzoic acid in the material and how the filler affects the polymerisation process.

Figure 4.15. The effect of additives on the water absorption of P200.

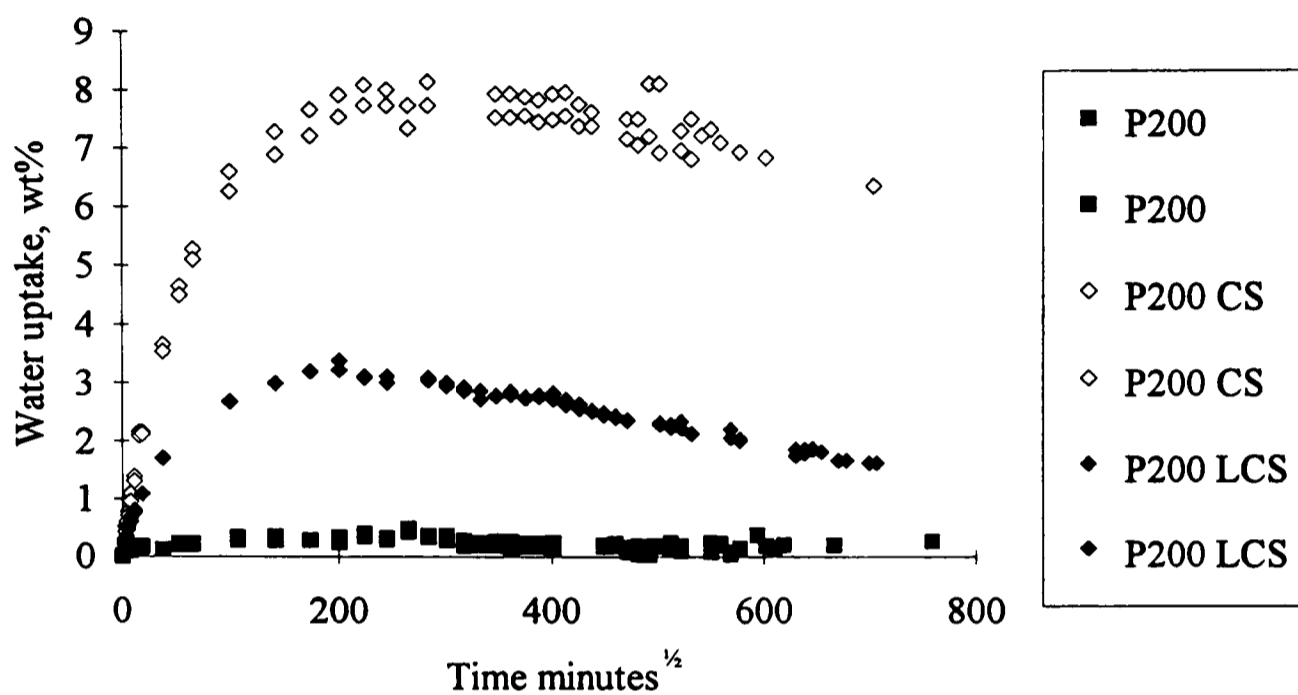


Figure 4.16. Initial period of the uptake of P200 based CS doped materials.

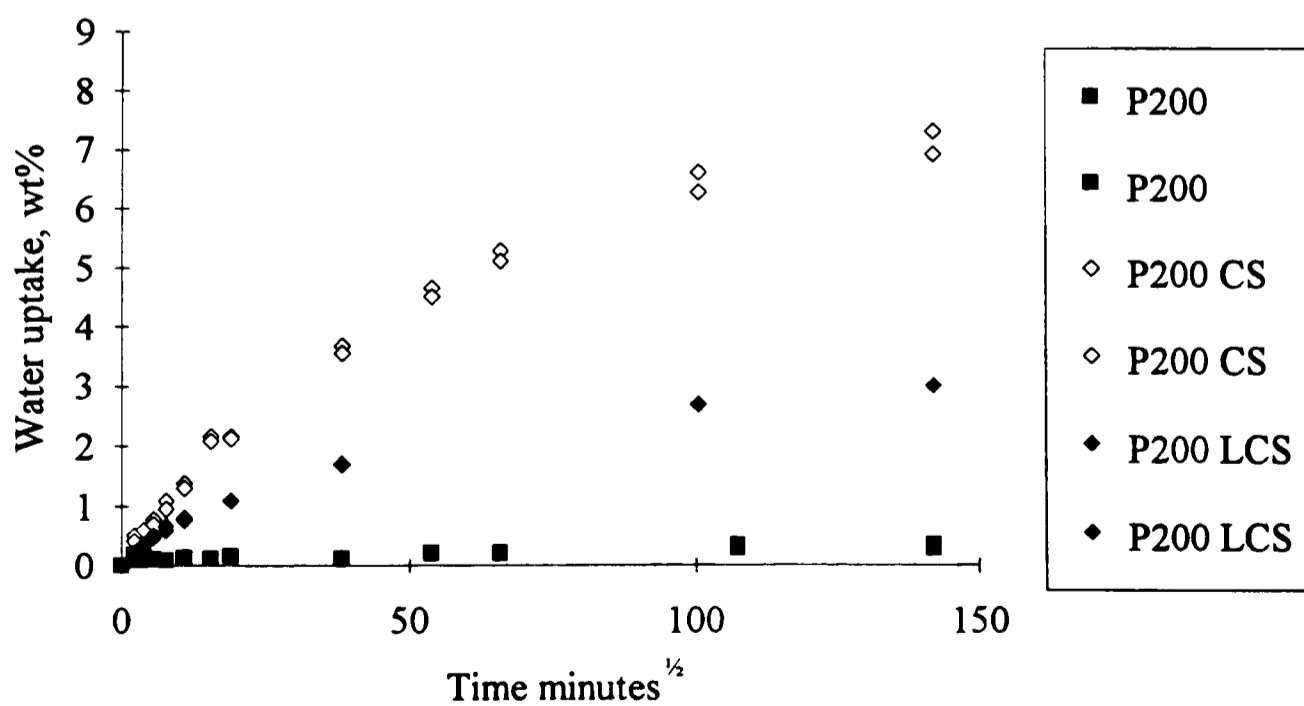
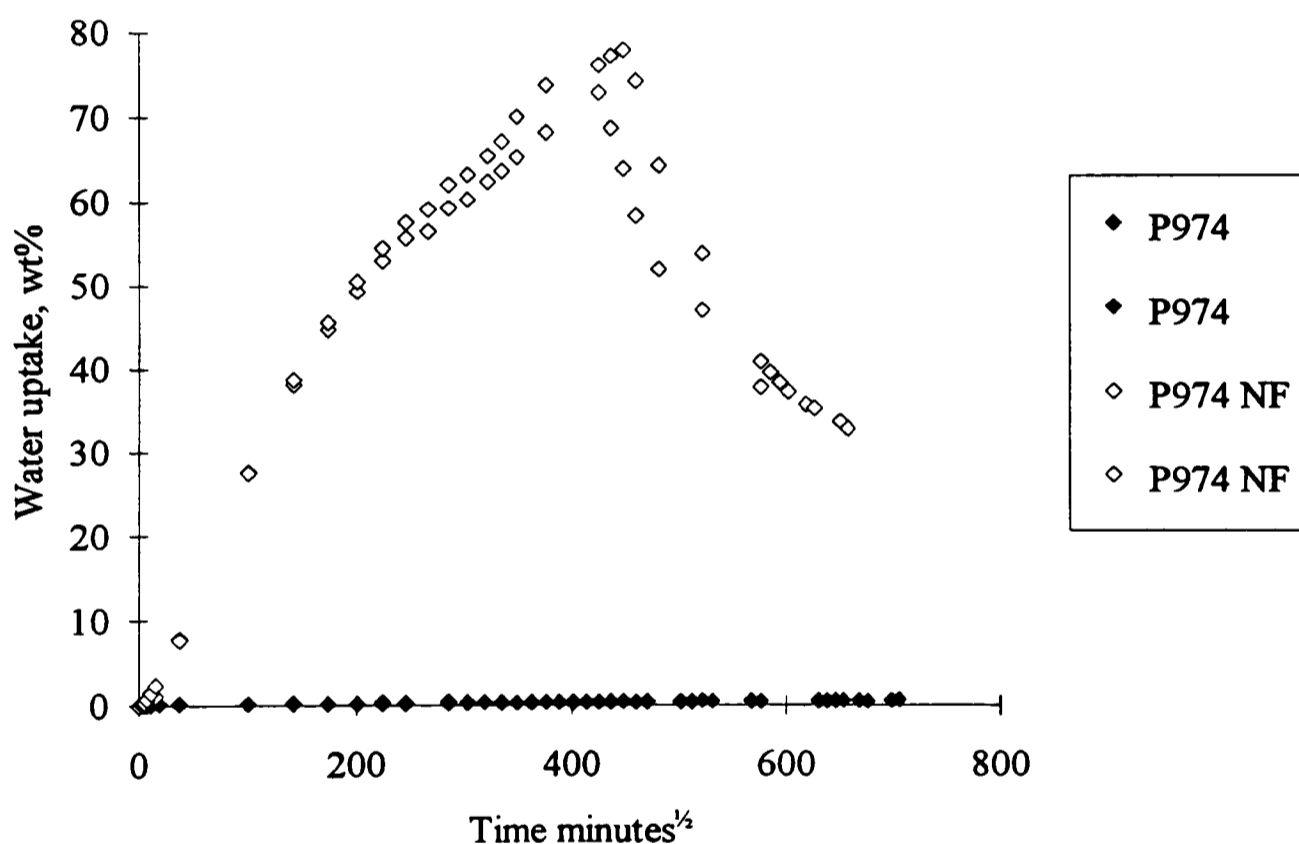


Figure 4.17, clearly shows the influence of 0.5 % NaF with a massive uptake of over 70 wt% then a subsequent loss. This loss is attributed the formation of a crack network, as described in a previous section, with NaF causing the formation of droplets within the material, these then reach such a size that the principle extension ratio (λ) exceeds the critical extension ratio for fracture (λ_{1C}). When this happens a crack network spreads throughout the material and when this reaches the surface the solution inside the material is released and the water uptake of the material decreases due to the change in chemical potential.

Figure 4.17. The effect of NaF on water uptake of P974.



Closer inspection of the P974 NF data is very interesting, with the first and second absorption cycles plotted against $t^{1/2}$ shown in figure 4.18. Here we can see that the water uptake is linear with respect to $t^{1/2}$ for the second absorption cycle (as previously seen in figure 4.16) but not for the first (although at longer times this too is linear with $t^{1/2}$). If this data is re-plotted with respect to t , as shown in figure 4.19, the first cycle is now linear and the second is not. This may seem a surprising result, but consider case II diffusion when the material's relaxation determines the uptake of the material and the kinetics are linear with time. When the salt is initially wetted by the water diffusing into the material, there will be a relatively large change in volume due to the change in state.

How the material restrains this large initial change is therefore critical in determining the initial kinetics of the water uptake. If the relaxation of material is such that the magnitude of the relaxation associated with the change in state of the salt is greater than the time required for enough water to diffuse into the material, then a change in state to case II situation may be reasonable.

Figure 4.18. Initial period of the water uptake of P974 NF plotted against time $^{1/2}$ for the first and second absorption cycles.

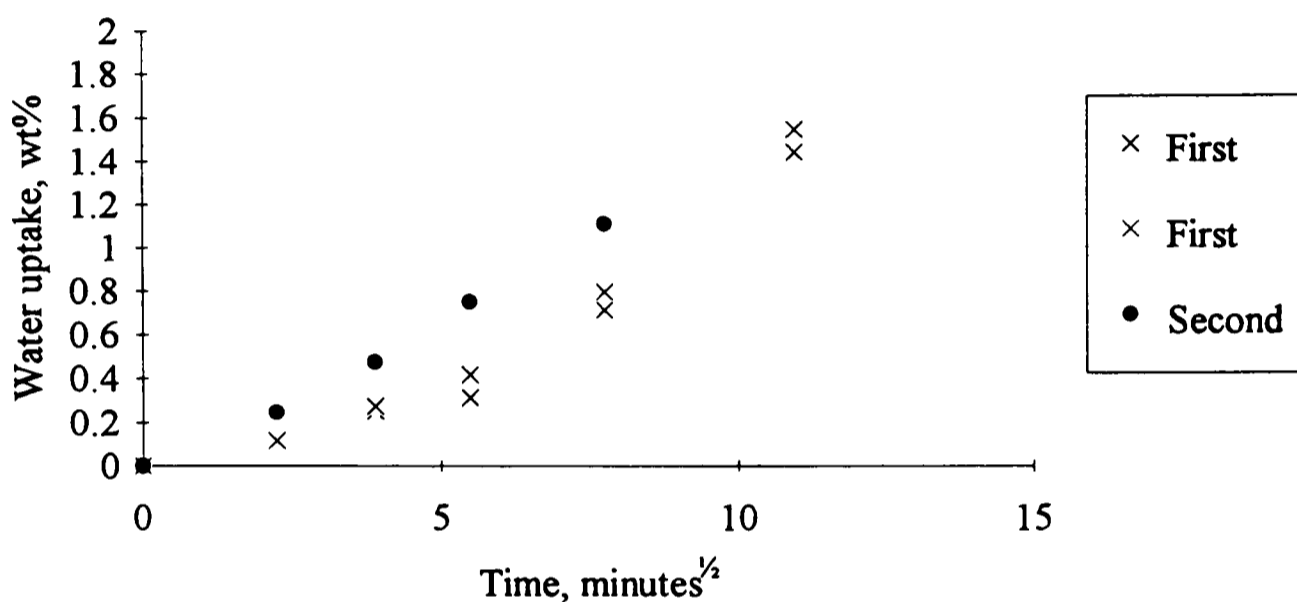
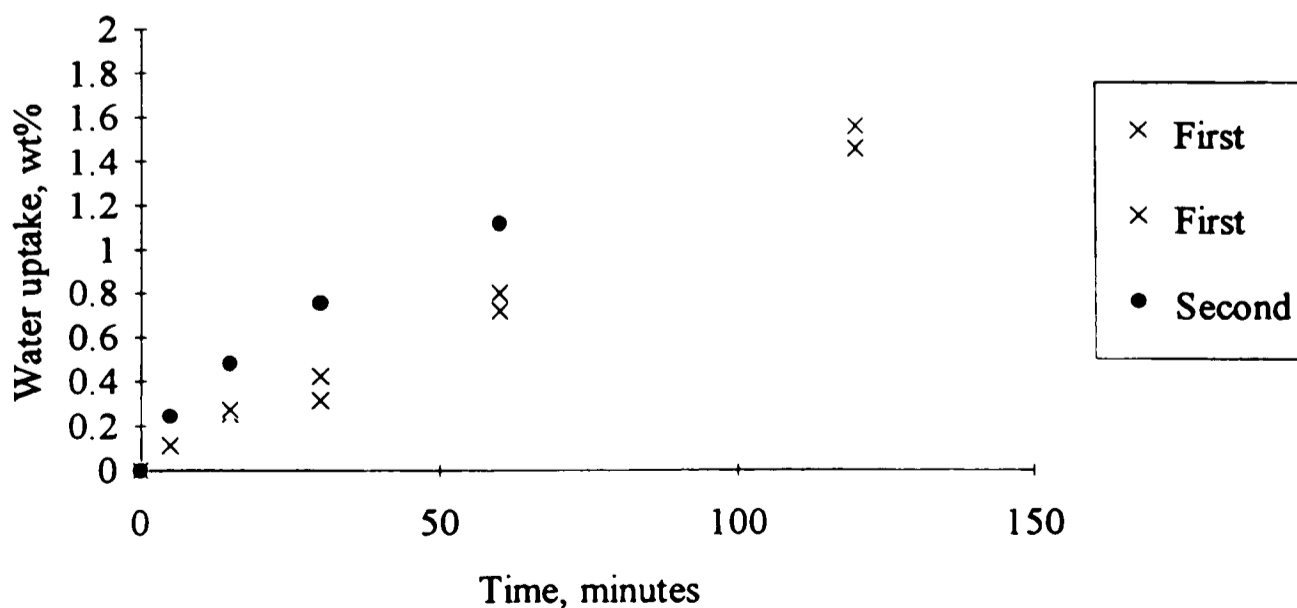


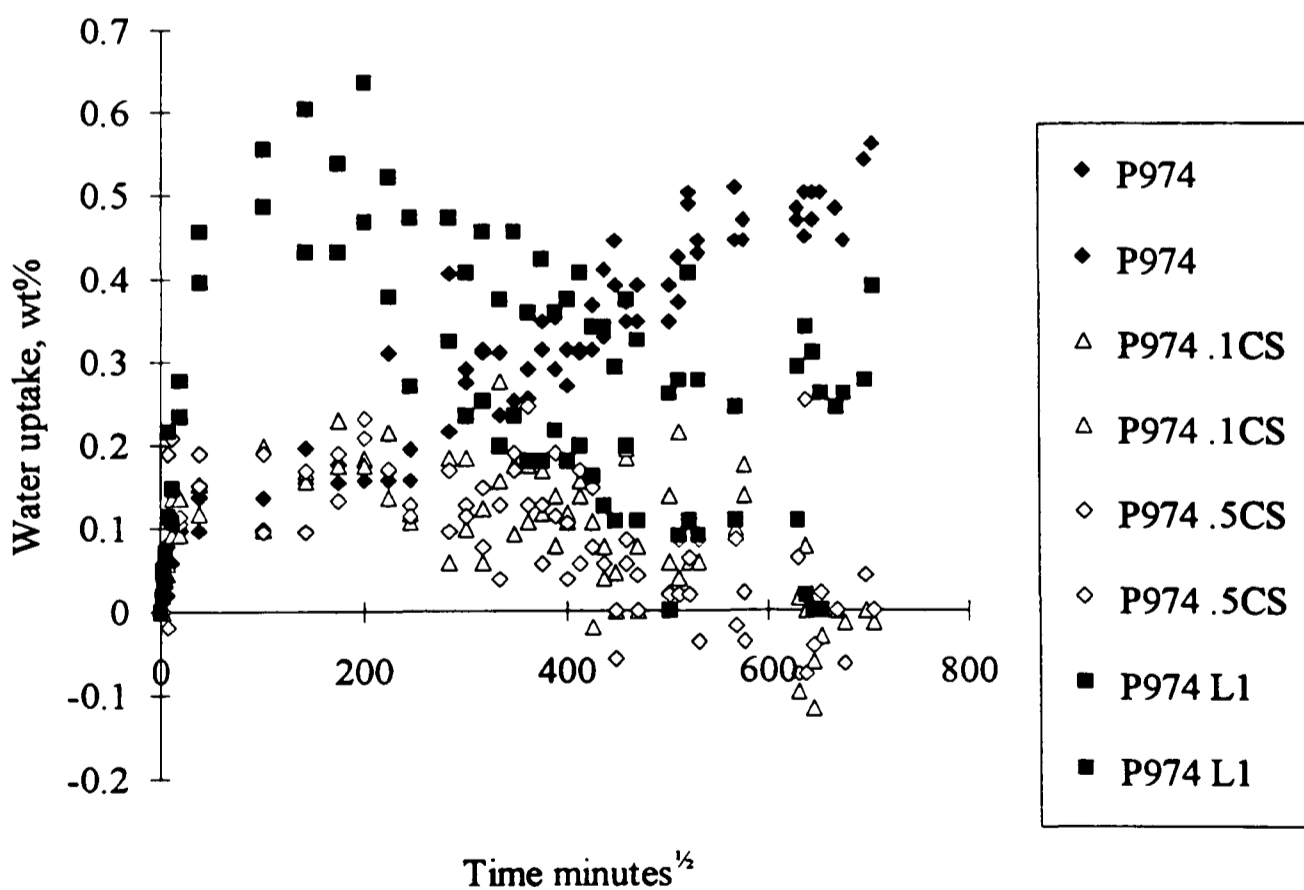
Figure 4.19. Initial period of water uptake of P974 NF plotted against time for the first and second absorption cycles.



This would explain the results shown in figures 4.18, and 4.19, as the salt goes into solution the relaxation of the material determines the ingress. Once the salt is in solution Fickian kinetics take over and so the uptake is linear with $t^{1/2}$. For the second absorption cycle the material has already forced solutions from the salt particles hence the initial wetting of the salt requires little further deformation of the material (as the solution droplets open up again). Hence the kinetics this time are Fickian as the initial deformation no longer plays a important role in the uptake of water.

The effect of other additions, CS and L77, on P974 is shown in figure 4.20. Here the picture is again confused with P974 showing the highest uptake of these materials which is in conflict with what would be expected from the theories. Again no satisfactory explanation may be brought forward to explain this. It is however worth comparing the two levels of CS which seem to fit in with the expectations, the higher percentage 0.5 % (P974 .5CS) has the higher uptake).

Figure 4.20. The effect of additives on the water uptake of P974.

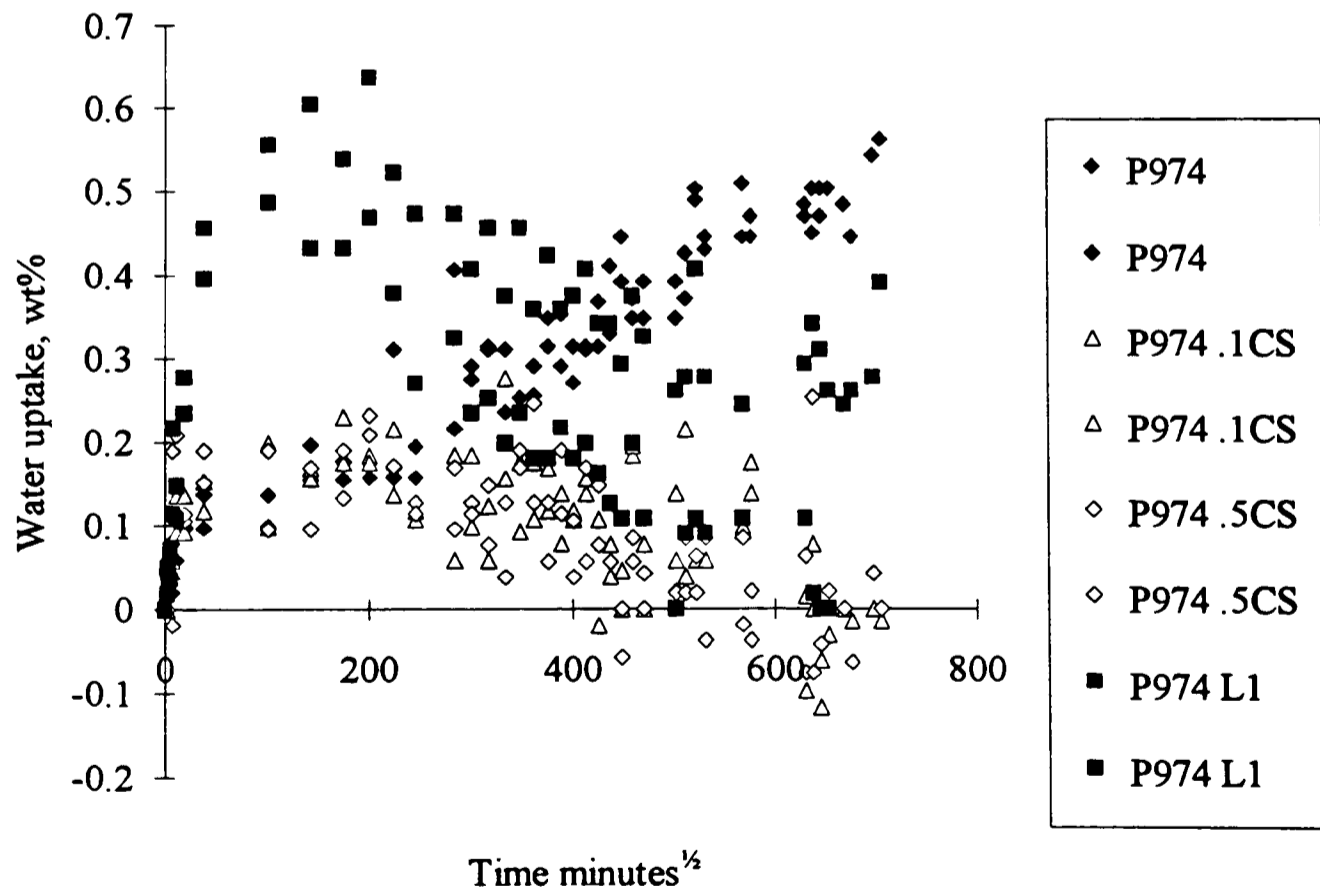


The L77 doped sample (P974 L1) shows a high initial uptake then a loss of water from the material. The L77 should distribute it self evenly throughout the material and as such

This would explain the results shown in figures 4.18, and 4.19, as the salt goes into solution the relaxation of the material determines the ingress. Once the salt is in solution Fickian kinetics take over and so the uptake is linear with $t^{1/2}$. For the second absorption cycle the material has already forced solutions from the salt particles hence the initial wetting of the salt requires little further deformation of the material (as the solution droplets open up again). Hence the kinetics this time are Fickian as the initial deformation no longer plays a important role in the uptake of water.

The effect of other additions, CS and L77, on P974 is shown in figure 4.20. Here the picture is again confused with P974 showing the highest uptake of these materials which is in conflict with what would be expected from the theories. Again no satisfactory explanation may be brought forward to explain this. It is however worth comparing the two levels of CS which seem to fit in with the expectations, the higher percentage 0.5 % (P974 .5CS) has the higher uptake).

Figure 4.20. The effect of additives on the water uptake of P974.



The L77 doped sample (P974 L1) shows a high initial uptake then a loss of water from the material. The L77 should distribute it self evenly throughout the material and as such

its effect on the water uptake would be expected to be subtly different to that of the CS and NaF. L77 increases the water uptake due to the presence of the hydroxyl and other hydrophilic groups on the surfact. The amount of water absorbed by P974 L1 (0.1 % L77) is greater than that by P974 .5CS (0.5 % CS). This seems to indicate that L77 is either forming clusters within the material or the distribution of L77 throughout the matrix results in the formation of an even distribution of water throughout the material as with hydrogels. Figure 4.21, shows the the initial period of the absorption of these materials which seems generally linear with respect to $t^{1/2}$ (apart from P974 .5CS where the spread of the data in this initial period is large). The diffusion coefficients calculated for the absorption, desorption and 2nd absorption of P974 L1 are much closer than those calculated for the other materials with droplets forming during the absorption (i.e. P974 .1CS, P974, P200 LCS and P200 CS). The diffusion coefficient therefore does not display the same level of concentration dependence as the droplet forming materials. It therefore seems likely that the water is uniformly distributed throughout the material rather than being attributed to clusters within the material. It should be pointed out that the benzoic acid within the material will still have an effect on the water uptake and hence droplet formation associated with this will further obscure what processes are occurring.

Figure 4.21. Initial water uptake of P974 based doped materials.

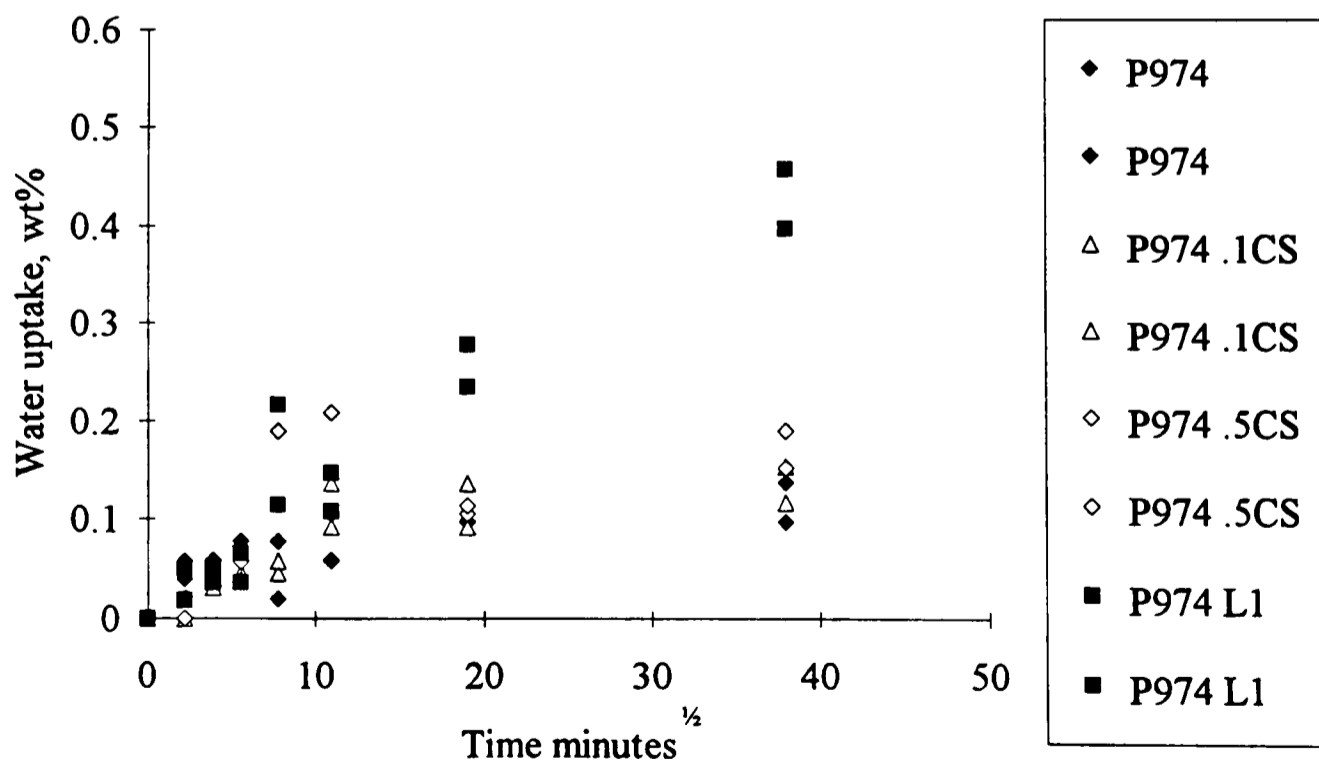


Table 4.7. Summary of absorption data for the peroxide cured silicone polymers.

Code	Abs, wt %	D_{abs} , m^2s^{-1}	At, Days	Sol., Wt%	D_{des} , m^2s^{-1}	Max Abs, wt %	Overall Abs, Wt%
P200	0.04	3.68×10^{-11}	224	1.06	1.64×10^{-9}	0.43	1.10
P200 CS	6.84	2.05×10^{-11}	196	0.99	1.97×10^{-9}	7.76	7.83
P200 LCS	1.86	5.95×10^{-11}	290	1.11	5.52×10^{-9}	3.39	2.97
P974	0.47	7.82×10^{-13}	290	0.26	1.29×10^{-8}	0.47	0.73
P974 NF	38.18	-	231	0.88	7.11×10^{-10}	74.30	39.06
P974 L1	0.00	1.85×10^{-10}	297	0.67	8.28×10^{-9}	0.49	0.67
P974 .5CS	0.00	-	290	0.34	2.97×10^{-8}	0.21	0.34
P974 .1CS	-0.12	9.28×10^{-10}	290	0.39	2.83×10^{-8}	0.18	0.27
P717	-0.67	-	196	1.15	1.57×10^{-8}	0.22	0.48

Table 4.8. Summary of second absorption data for the peroxide cured silicone polymers.

Code	2nd Abs Wt %	D_{2nd} m^2s^{-1}	At, Days
P200	0.73	2.08×10^{-10}	165
P200 CS	5.97	8.69×10^{-11}	140
P200 LCS	1.65	6.12×10^{-10}	49
P974	0.59	8.37×10^{-11}	49
P974 NF	26.43	-	56
P974 L1	0.76	7.15×10^{-10}	49
P974 .5CS	0.30	-	49
P974 .1CS	0.33	6.42×10^{-9}	49
P717	0.16	1.27×10^{-9}	140

4.7. Hydrosilanised silicone polymers.

4.7.1. Formulation of hydrosilanised silicone polymers.

Hydrosilanised silicone polymers come in many different varieties with a range of catalysts available to initiate the curing reaction as previously detailed. For the purpose of this study hydrogen chloroplatinic acid (HPT), which is probably the cheapest and certainly the more traditional, and a platinum siloxane complex (VPT) which represents a more recent development in catalysts were used. Both of these catalysts operate at room temperature, the materials are therefore formulated as two pastes which are mixed together prior to use. In theory they may also be reformulated using one of the heat sensitive catalysts to form a single component system.

The initial basis of the formulations was a stoichiometrical balanced formulation, so the material had an equal number of hydrogen and vinyl groups. Using the data supplied by OSi Specialities (OSi Specialities, 1991) on the siloxanes, the ratio of 1.25 g of SHT to 100g g of SCC was used. For the lower molecular weight material SCC-L this was changed to 4.6g of SHT per 100 g SCC-L. Using these ratios as an initial basis, a series of materials were made using 16 % silica filler, this was then varied as detailed in table 4.9, an example of exact batching of H974 V is shown in table 4.10.

Table 4.9. Formulations of Hydrosilanised materials.

Code	Component, %,					Catalyst
	SHT	Filler	Additive			
H Un low	4.4	-	-	-	-	HPT
H Un high	1.2	-	-	-	-	HPT
H974 V	1.0	R974	16	-	-	VPT
H200 V	1.0	S200	16	-	-	VPT
H974 H	1.0	R974	16	-	-	HPT
H974 CS	1.0	R974	16	CS	0.6	VPT
H200 2.5	2	S200	20	-	-	VPT
H200 5	4	S200	20	-	-	VPT
H200 10	8	S200	20	-	-	VPT
H717 5	4.2	C717	20	-	-	VPT

Table 4.10. Formulation for 20g of H974 V as two part paste.

Component	Part 1	Part 2	Overall
SCC	8.4 g	8.2 g	16.6 g
SHT	-	0.2 g	0.2 g
R974	1.6 g	1.6 g	3.2 g
VPT	0.05 ml	-	0.05 ml

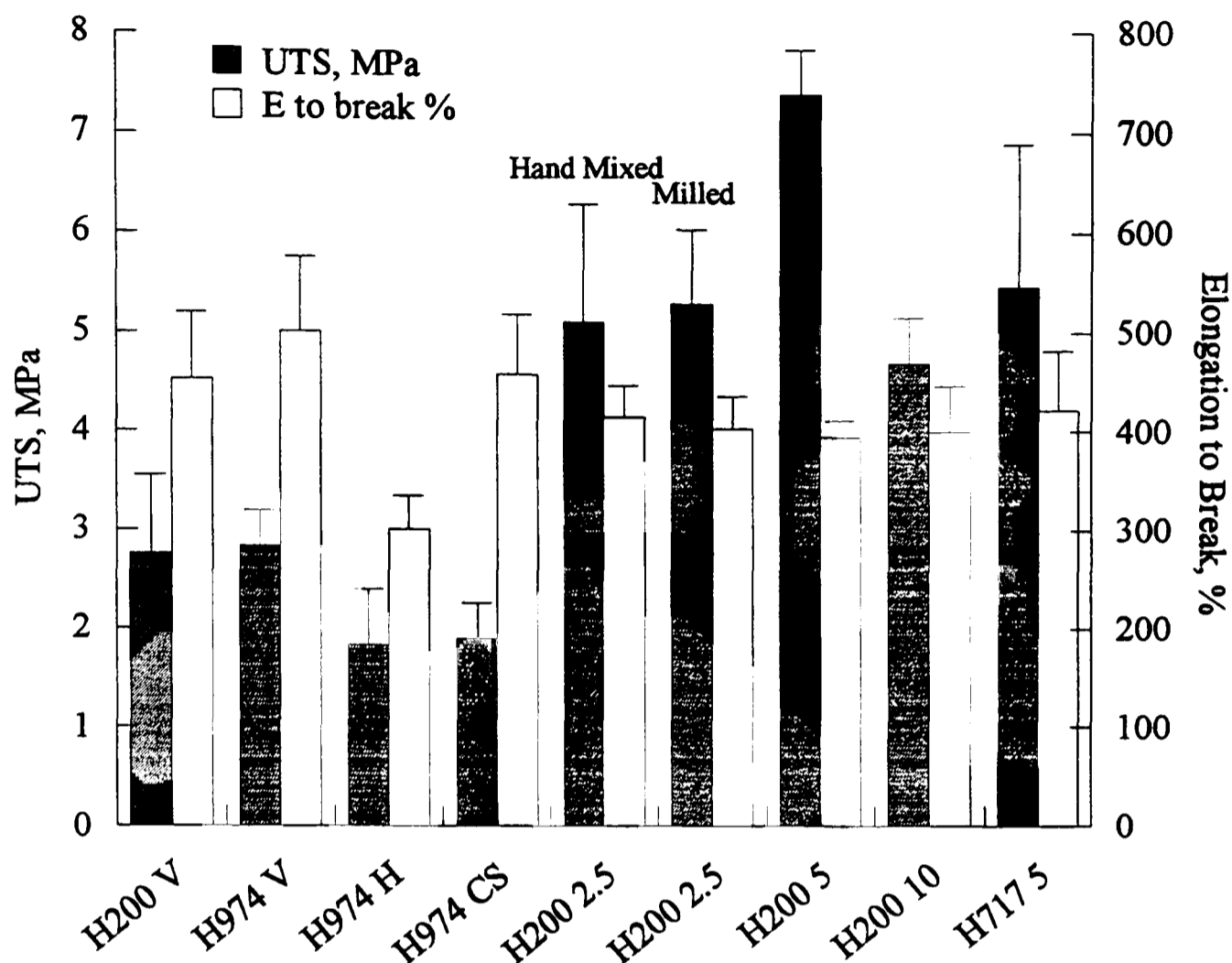
4.7.2. Results for the hydrosilanised silicones.

The strength results for the hydrosilanised materials are shown in figure 4.22. Here the results show H200 V and H974 V to be very similar (as with the peroxide materials) in terms of the tensile properties and H974 CS to be somewhat lower, attributed to the action of the CS as a poor filler. H974 H however is noticeably weaker than H974 V, although the reason behind this is not clear. It is likely to be due to inhomogenities in the polymerisation due to the catalyst being non uniformly distributed. Historically, this was one of the major driving forces behind the development of the organo platinum complex catalysts.

When a sample of C717 reinforced material based on the same stoichometric formulation was prepared, the resulting material could best be described as a viscous paste (much like the start material). This it seemed was due to the vinyl groups on the silica particles being active in the polymerisation process. Hence the material did not contain a sufficient proportion of SHT to enable enough polymerisation to occur to form an elastomeric material. A similar situation seemed apparent when the level of S200 in the material was increased to 20 % indicating the silanol groups on the surface are also capable of reacting with the siloxanes during polymerisation.

When a series of S200 based materials was made up using increased levels of SHT a maximum strength was found at 5 % SHT. The higher level (10% SHT) seemed to have an excess and the lower level (2.5 % SHT) insufficient to ensure maximum bonding of the silica to the siloxane. When a C717 based material (H717 5) was made using an increased level of SHT (5%) the result was a reasonable material of similar strength to the H200 2.5.

Figure 4.22. Tensile strength of hydrosilanised silicone materials.



In order to establish whether the rheological properties of the pastes were suitable for hand blending (as the materials were normally milled on a paste mill) a sample was mixed by hand. As the results show for the hand mixed and milled sample of H200 2.5 there is little difference in the properties of the material obtained, therefore it may be assumed reasonable homogeneity is obtained by hand mixing. Therefore the material should be suitable use in conventional dental laboratories.

The absorption of the silicone polymer H974 V is very low as shown in figure 4.23 with the initial period being linear (figure 4.24). The apparent absorption is ~ 0.18 wt%, although the solubility of 0.13 wt% increases the overall uptake to 0.31 wt% (table 4.24) which is noticeably lower than P974 (table 4.7). It should be noted the solubility of all the hydrosilanised materials, excluding the unfilled samples, are comparable at 0.10 to 0.13 wt % (this is noticeably lower than that with the peroxide materials) this leaching is believed to be due to residual unreacted siloxane fluid. The two unfilled samples show similar pictures in that they both loose weight (table 4.24) and have a slower rate of absorption than might be expected (this may be attributed to the HPT as will be

discussed later). The very low strength of the H Un low made the material difficult to handle, the material eventually tore during a measurement and the sample had to be discarded hence the lack of desorption data. H200 V has a maximum uptake of about 1.4 wt% and a overall uptake of 1.52 wt%, this increase over the H974 V is be attributed to the presence of a hydrophilic filler. Although the silica S200 is effectively insoluble and incapable of forming solution droplets, it is hydrophilic due to its surface coating of silanol (Si-O-H) groups which will adsorb water onto its surface.

Figure 4.23. Water absorption of the stoichiometrically balanced silicone materials.

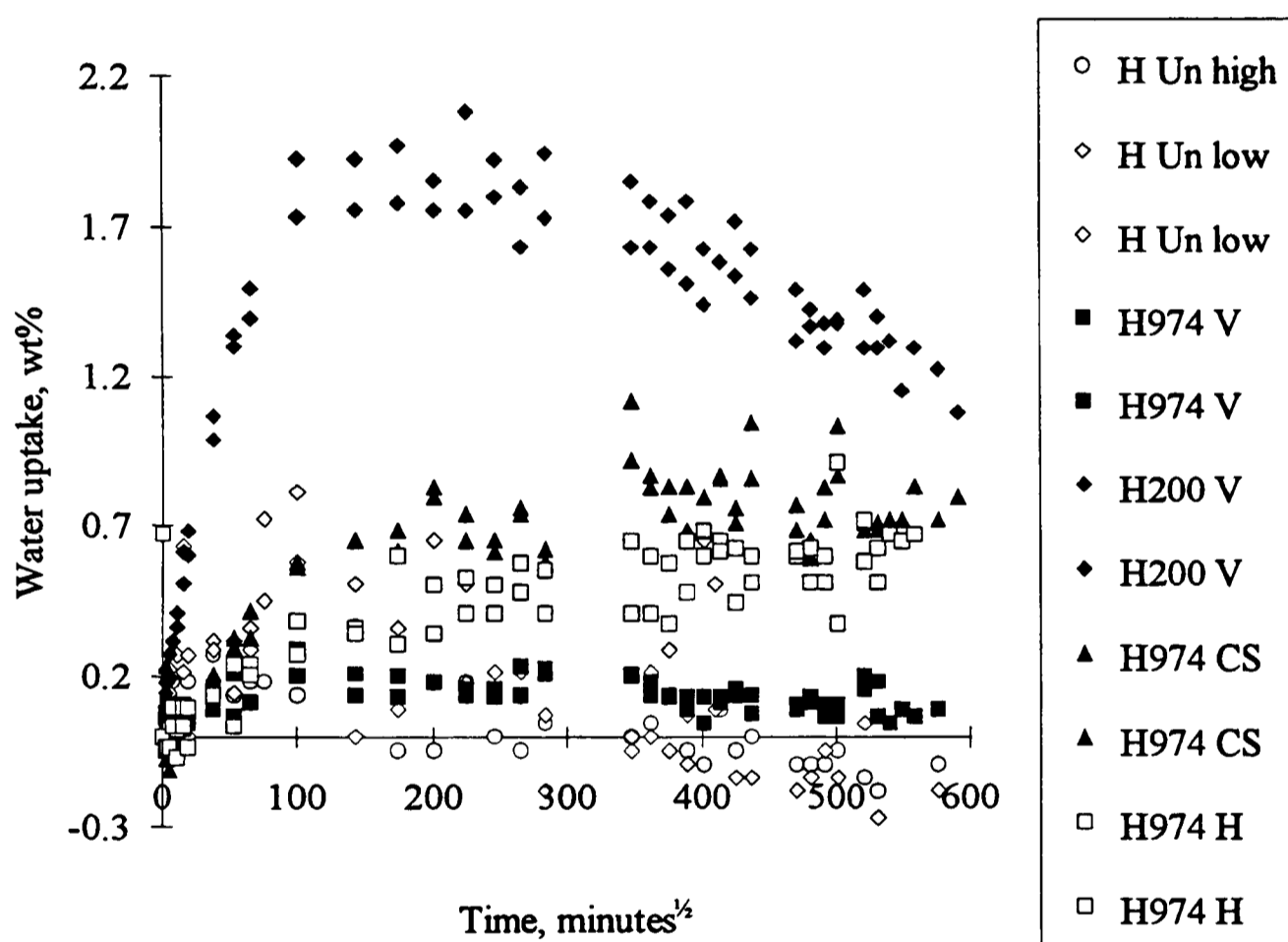


Figure 4.24. Initial period of water absorption of the stoichiometrically balanced silicone materials.

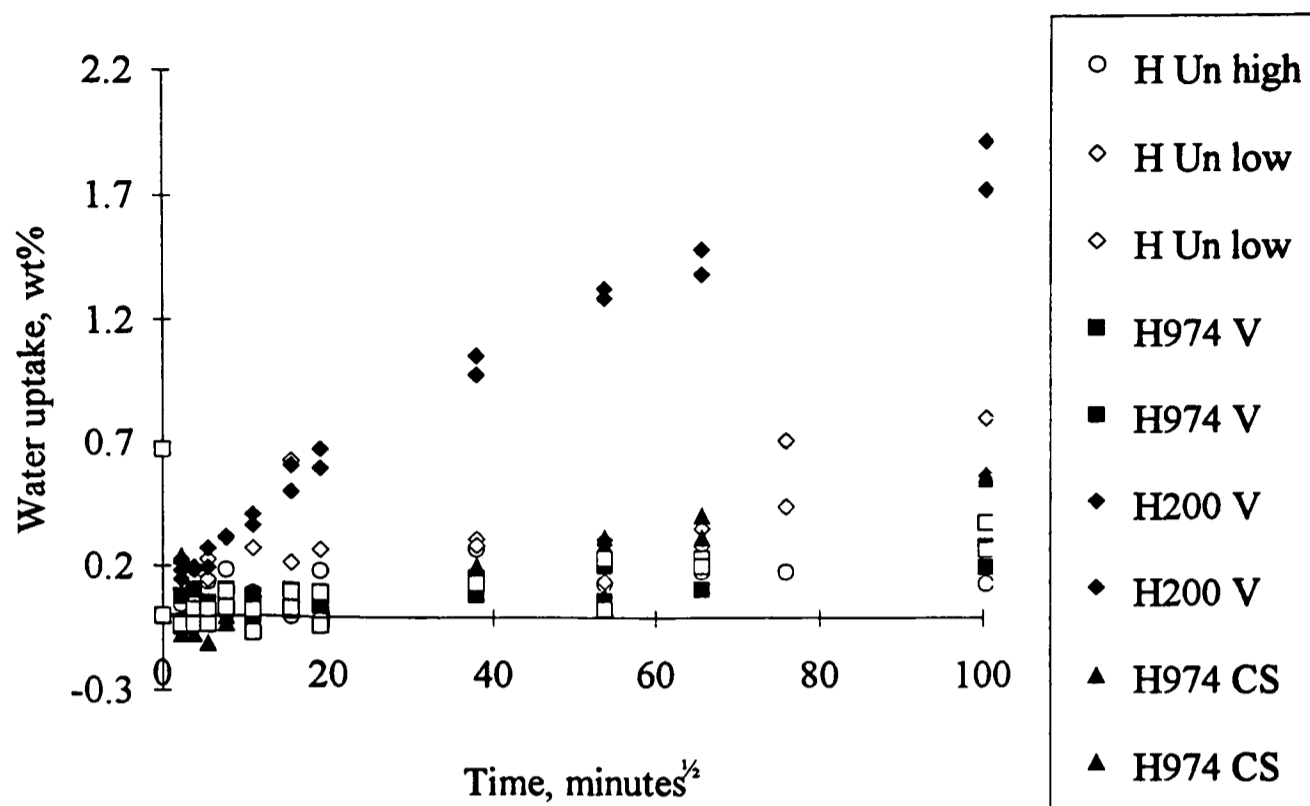


Table 4.11 Summary of absorption data of hydrosilanised silicone polymers at 196 days.

Sample Code	Absorption, wt%	Solubility, wt%	Overall Uptake, wt%	$D_{Abs\ 1st}$, m^2s^{-1}	D_{Des} , m^2s^{-1}	$D_{Abs\ 2nd}$, m^2s^{-1}
H Un low	-0.23	-	364	1.73×10^{-10}	-	-
H Un high*	-0.18	0.27	0.09	1.07×10^{-9}	2.79×10^{-8}	-
H200 V	1.41	0.11	1.52	3.18×10^{-11}	1.39×10^{-8}	5.86×10^{-10}
H974 V	0.18	0.13	0.31	2.71×10^{-10}	3.29×10^{-8}	8.97×10^{-10}
H974 H	0.51	0.10	0.61	4.41×10^{-12}	2.02×10^{-8}	1.12×10^{-10}
H974 CS	0.71	0.12	0.83	4.69×10^{-12}	1.29×10^{-8}	8.31×10^{-11}
H 200 5	0.18	0.19	0.37	1.57×10^{-9}	1.92×10^{-8}	1.52×10^{-8}

* Sample desorped at 357 Days.

The surface chemistry of silica is fairly complex with the silanol groups on the surface of the S200 existing in different forms as previously shown. Water becomes physically adsorbed onto the surface of the silica via the silanol groups. Water can also become chemisorbed onto the surface of the silica via the siloxane bonds. As previously stated the effects of chemisorption will not be prevalent in these experiments as the silica was not pre treated before formulation at a temperature sufficient to remove the chemisorbed water (above 500°C). The physical absorption of water onto the silica surface is

dependent on the relative proportions of silanol group on the surface. This depends largely on the prior treatment of the silica, the highest proportion of free silanol groups existing immediately after manufacture and then decreasing with age. The decrease in weight after 60 days (≈ 300 minutes^{1/2}) for the H200 V cannot be attributed to the leaching of the filler (as the solubility is only 0.11 wt%) and seems to stem from bridging or loss of some of the free silanol groups present on the silica surface. This removal of free silanol groups changes the chemical potential driving the absorption which effectively causes water to migrate out of the polymer as the material is already in a state of equilibrium.

The actual absorption attributed to the silica may be calculated by comparison with H Un high silicone which has an overall uptake of 0.09 wt%. By calculating the amount of matrix and silica in the material (84 wt % and 16 wt % respectively) and subtracting the amount attributed to the matrix (0.84 x absorption of unfilled) from the overall. This results in a value of 9.01 wt% (table 4.12) when expressed as water on silica for the H200 V material. This figure compares favourably to the value of about 10 wt% given for the absorption of hydrophilic silica (Deggusa, 1993). Table 4.12, also gives a value of 1.48 wt% for the R974 based on the H974 V material. While R974 is generally considered hydrophobic the silanation of the silica with di chloro di methyl silane does not remove all the silanol groups present on the surface. The silanol surface density is reduced from 2.65 nm⁻² (after a years storage) to 0.39 nm⁻² (Degussa, 1993). The silica is therefore still slightly hydrophilic and so will account for the absorption of some water into the material.

Table 4.12. Water absorption attributed to different elements of the composition for the stoichiometrically balanced Hydrosilanised silicone polymers.

Sample Code	Total Absorption, wt%	Element of composition	Absorption attributed to, wt %	Expressed as wt % of element.
H200 V*	1.52	S200	S200 1.44	9.01
H974 V*	0.31	S974	S200 0.24	1.48
H974 H†	0.61	HPT	HPT 0.30	15030.40
V974 CS†	0.83	CS	CS 0.52	86.5

* Using unfilled as matrix.

† Using V974 as matrix.

The uptakes of H974 H and H974 CS are very similar with both showing a much slower rate of uptake to a higher level than the V974. Both of these materials contain soluble, hydrophilic agents (HPT or CS) which will form solution droplets as previously described and results in a slower uptake. It should be noted that the VPT used in H974 V is a siloxane platinum complex and insoluble. Table 4.12, shows the proportion of the total absorption of each these materials that can be attributed to the soluble agent but, rather than using the unfilled material as a reference, V974 is used as this would be the effective matrix for the droplets. Expression of the attributed uptake in terms of wt % of the element incorporated in the material reveals the HPT to have a much larger effect on the absorption than the CS. This may be attributed to the difference in water solubility of each of the constituents, which in Weast (1977) are given as $4 \times 10^{-6} \text{ kg l}^{-1}$ for the CS and 'very soluble' for the HPT.

The unfilled sample of the silicone polymer was initiated by HPT (rather than VPT) and so it would be reasonable to expect that some proportion of its uptake could be attributed to this highly soluble agent; this is supported by the slower diffusion coefficient calculated for the 1st absorption than found for desorption (table 4.11). The absorption of the unfilled sample however shows that the uptake reaches a maximum at 0.18 wt% (figure 4.23) and then decreases. As the total absorption (table 4.11) of the unfilled sample is only 0.09 wt%, the higher value at shorter time periods seems attributable to HPT. It seems probable that HPT is leached out of the sample during immersion in water, therefore the overall uptake should be a measure of the inherent absorption of the material. For the H974 material the leaching of HPT should not take place as the material is considerably stronger than the unfilled material so better restrains droplet growth and the time of immersion is less (196 days as compared to 357 days for the unfilled material).

$$c_w - s = c_i (\lambda^3 - 1) \frac{\rho_w}{\rho_i} \quad \text{Equation 4.1.}$$

An idea of the extent of the droplet formation and the localised stressing of the material may be obtained from applying equation 4.1, and re-arranging to yield a value of the principle extension ratio, λ (assuming spherical droplets). From table 4.12 it is clear that for both the silica filled materials the λ value is small, this is consistent with an insoluble particle. For CS a λ of 1.27 equates to a strain of 27% around the droplet assuming the material is Hookean. For HPT a λ of 7.12 is considerably higher and indicates that the material will not be behaving in a Hookean manner, indeed it seems likely that the

material will have failed around the droplet considering the elongation to break of the material is 460 % (figure 4.22).

It should be noted that in order to calculate values of λ we have to assume that the value s_0 is effectively the same as s as, in order to calculate s from s_0 (equation 4.2), λ has to be known. If we assume that $s = s_0$ this problem is avoided, this is reasonable as the influence of equation 4.2, should result in a very small difference between s and s_0 . For V974 CS M_i is 0.60704 kg/mole and for H974 the λ of 7.124, means in both cases the correction divider may be taken as 1 within the experimental error in the study, therefore $s=s_0$.

$$s = \frac{s_0}{1 + \frac{M_w \rho_i}{M_i \rho_w} \frac{1}{(\lambda^3 - 1)}} \quad \text{Equation 4.2.}$$

The diffusion coefficients calculated in table 4.11, show that the diffusion though the silicone is very rapid with all the materials having a D_{Des} of the order of $10^{-8} \text{ m}^2 \text{ s}^{-1}$. This is a measure of the inherent rate of diffusion though the silicone polymer. Comparison with results obtained by other authors shows a good level of agreement with the values obtained in this study.

Table 4.13. Mechanical properties of matrix relative to droplet for the H974 H and H974 CS.

Sample Code	Element of composition	λ around droplet.	E, from Mooney Rivlin Plots, Pa	Density, Kgm^{-1}	Material behaviour at λ
H974	HPT	7.124	332486	1052	Failed
V974 CS	CS	1.271	221974	1065	Hookean

Using V974 as matrix.

When equation 4.3, is applied to V974 CS (using the D_{Abs} of V974 as the materials true diffusion coefficient) a good level of agreement is obtained (Table 4.14).

$$D_a = \frac{(\lambda^3 + A - 1)(\lambda^3 - 1)}{\left[(\lambda^3 + A - 1)^2 + \frac{s_0 A}{kc_i} \right]} \left[\frac{K_2}{(\lambda^3 - 1)^2} + K_1 \left(\frac{1}{\lambda^4} + \frac{1}{\lambda^7} \right) \right] \quad \text{Equation 4.3}$$

The soluble component of V974 CS is calcium stearate which has a solubility of 4 kg m^{-3} this means the droplet that forms should be restrained elastically as confirmed by the low value of λ .

The conditions of the Muniandy and Thomas's theory are met and hence there is good agreement between the experimental and calculated diffusion coefficients.

Table 4.14. Diffusion Coefficients calculated from Muniandy and Thomas for the H974 H and H974 CS.

Sample Code	Element of composition	M_i (effective), kg/mol.	D_{Abs} Calc, m^2s^{-1}	D_{Abs} Expt, m^2s^{-1}
H974	HPT	0.51792	1.31×10^{-13}	4.41×10^{-12}
V974 CS	CS	0.60704	5.47×10^{-12}	4.69×10^{-12}

Using D_{Abs} for V974 as D_t .

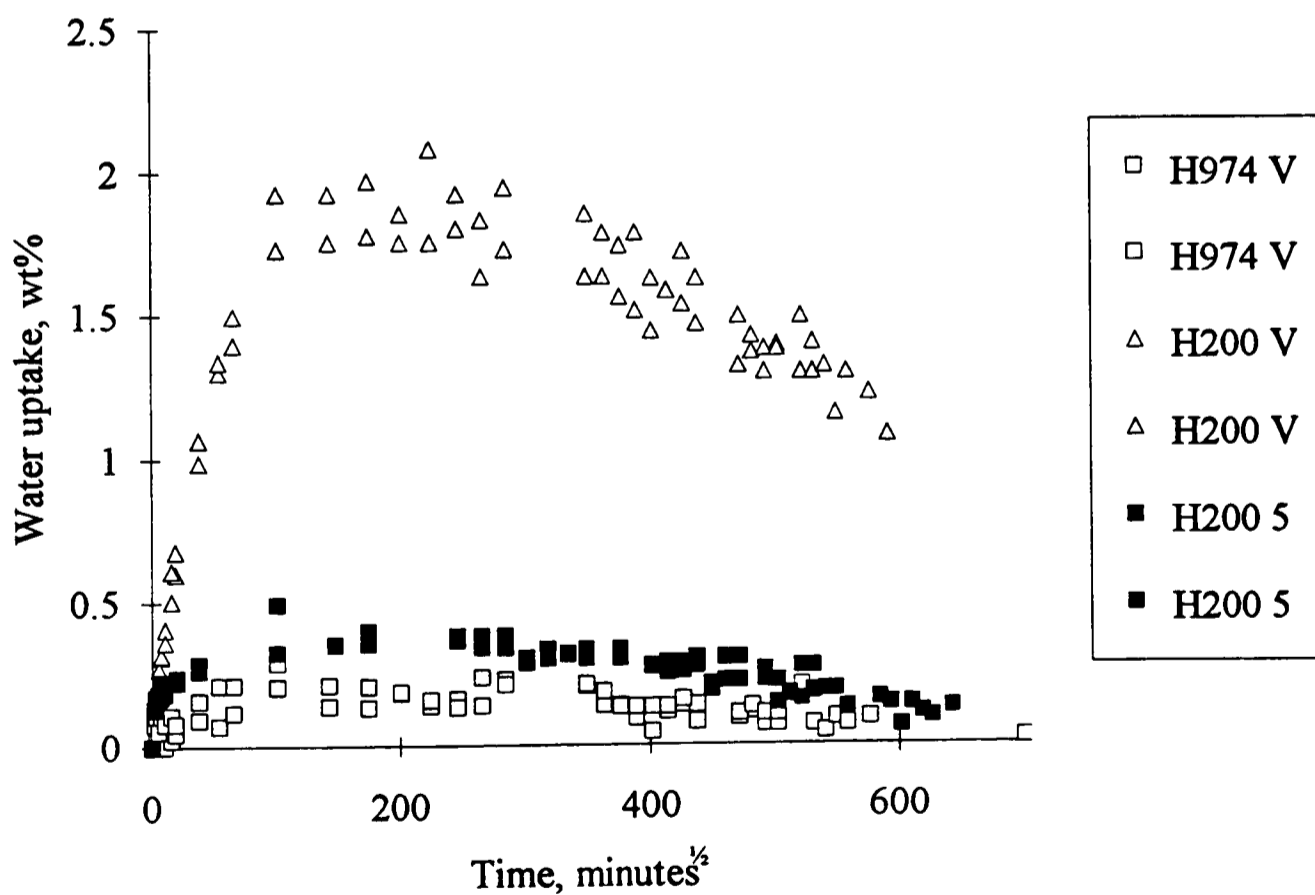
The application of this theory to H974 reveals a different situation. HPT is very soluble and the material is no longer restraining the droplet elastically as shown by the value of λ exceeding the strain required to fracture the material. This leads to internal plastic deformation of the material which is likely to result in the formation of cracks within the material. Hence the D_{calc} is lower than the D_{expt} as the cracking increases the rate of water uptake. The ability of a material to restrain a droplet arising from a soluble particle depends on the properties of the material and the particle. The greater solubility of the HPT places a greater strain on the surrounding matrix, this then exceeds the critical value of λ for crack propagation. This leads to an increased rate of absorption as the restraining force being applied around the droplet is relaxed. The cracking of the material may also give rise to a crack network within the material which can act as a pathway for diffusion, hence further increasing the diffusion coefficient.

Schirrer et al 1992 looked at the salt release from two silicone polymers and showed the critical value of λ for rupture of the matrix depended on the size of the particle present in the material, the value he obtained for a $40 \mu\text{m}$ particle was 3.6. Whilst this approach was not attempted here the critical value he found in this instance agrees with the λ data calculated here and the way the Muniandy and Thomas's model predicts the diffusion coefficient of the H974 H and H974 CS.

Applying the Muniandy and Thomas theory to H200 V and H974 V is impossible as the driving force behind the absorption has changed from an osmotic solution to adsorption on the surface of the silica. It is therefore necessary to develop a new approach which uses the chemical potential associated with the adsorption process of the water on to the silica rather than from the osmotic solution.

Figure 4.25 shows the water uptake of the H200 5 material, here the absorption is very different to the H200 V, in fact it is similar to the H974 V. This agrees with the theory postulated for the strength data with the increased SHT proportion enabling bonding between the silanol groups and the matrix. The removal of the silanol groups reduces the silica's tendency to adsorb water hence the lower uptake. The exact reaction occurring is not known but is likely to involve the platinum catalyst removing the hydrogen from the SHT as seen in the curing reaction proposed by Kohjiya et al (1991). This then reacts with the silanol group on the surface of the silica if no vinyl groups are available to the platinum catalyst.

Figure 4.25. Water absorption characteristics of H200 5.



The reaction does seem to prefer vinyl groups of siloxane (or of the silica as the stoichiometrically balanced C717 reinforced material failed to cure) to the silica's silanol

groups, as the stoichiometrically balanced H200 V has a much greater uptake. Whether the silanol group loses a hydrogen or the full OH is unclear (either H₂ or H₂O will be the by-product), it seems more probable that just the hydrogen will come off as this would lead to the formation of the more stable Si-O-Si link rather than a Si-Si. The diffusion coefficient determined for H200 5 is very rapid (table 4.11) as would be expected from a pure silicone material with no hydrophilic agents, the solubility is very low as with all hydrosilanised materials.

4.8. Summary of silicone polymer results.

The water uptake of silicone polymers demonstrates many different aspects of water uptake. The hydrosilanised materials demonstrate that the application of Muniandy and Thomas's theories to these materials demonstrates the benefit and limitations of the approach they adopted. The relationship of λ and crack formation indicates a limit of the Muniandy and Thomas theories which was widely predicted by other authors but largely overlooked (for the purpose of simplicity). There is a limiting value of λ for the safe application of Muniandy and Thomas 's theories which depends on the material system being used. The links with this and λ_{IC} are apparent as noted by Schirrer et al (1992) but the full nature of this is unclear as the local geometries of the material around the droplet are not known.

The influence of the impurities on the material's uptake is complex, the interactions between filler, impurity and initiator all play a role in the uptake seen. These interactions are difficult to quantify as the overlap between the different contributing factors overshadow each other. The sensitivity of the materials to slight unknown impurities, such as HPT, also complicates the uptake. Indeed the presence of such agent may account for a few of the cluster forming polymers.

The sensitivity of the gravimetric test method is impressive showing differences between some very low water uptakes. A point should however be noted the very rapid diffusion coefficient of the order of $10^{-8} \text{ m}^2\text{s}^{-1}$ is only going to be a guide as the lack of measurements when the value of M_t/M_∞ is less than 0.5 (i.e. suitable for regression). These absorption/desorption cycles are complete within 15 minutes hence the regression is performed on only the zero and 5 minute value and therefore open to a significant error. A more frequent sampling during the early stage would overcome this but would

still present problems as would increase the time out of the controlled environment (water or conditioning cabinet at 37°C).

Chapter 5.

Elastomer / Methacrylate Materials.

5.1. Overview.

Elastomer / methacrylate materials as previously stated (see introduction) overcome many of the problems associated with plasticised methacrylates. Previous authors have shown that these materials have considerable potential as soft lining materials but the water sorption characteristics give cause for concern.

These materials were developed from those developed by Dr S.Parker in conjunction with Professor M.Braden in the early 80's (although the history of these materials does go back further as described in the introduction). The initial work was conducted on natural rubber being dissolved in different methacrylate monomers containing an initiator and cross linking agent. These proved to have excellent strength and adhesion to the denture bases, but had an excessively high water uptake due to proteins and other impurities in the natural rubber. The type of rubber was then changed to synthetic elastomers, butadiene / acrylonitrile and butadiene / styrene copolymers. Many interesting points are raised by Dr S.Parker's PhD thesis (1982) which in part focuses on these materials. There are also a series of papers following up on this work (Parker and Braden, 1990, Parker 1993).

The monomers used in this part of the study were 2-ethyl hexyl methacrylate (EHM), hexyl methacrylate (HM), tridecyl methacrylate (TDM) and 2-ethoxy ethyl methacrylate (EOEM), as these are all soft and elastomeric at 37°C and so would help to soften the overall materials formed. 1% Benzol peroxide was used as a initiator and 10 % ethylene glycol dimethacrylate was also used in these materials as a cross linking agent. The materials generally proved unsuitable on grounds of the water uptake (due to soluble agents in the natural rubber) and biologically suspect (again due to the impurities) or too hard a material was produced.

In order to obtain a purer elastomer, synthetic elastomers were tried as an alternative, all of these were available in powder form to enable gelling of the methacrylate and the elastomer particles. Initially both butadiene / acrylonitrile and butadiene / styrene rubbers were used. The butadiene / acrylonitrile elastomers were found only to gel with the EOEM rather than any of the other higher methacrylates, the reason being the polar nature of the EOEM and butadiene / acrylonitrile elastomer making them mutually miscible. The strength of these material was adequate (5.9 MPa and elongation to break of 320 %) as well as the tear resistance and adhesion to the PMMA denture. The water absorption characteristics were of cause for concern with uptakes of 4-16 wt% and 4.6

to 8.6 wt % solubility. The main problem of this system was however the toxicity as both the acrylonitrile component and EOEM (Aiken, 1988, ICI) have been proven to be biologically suspect.

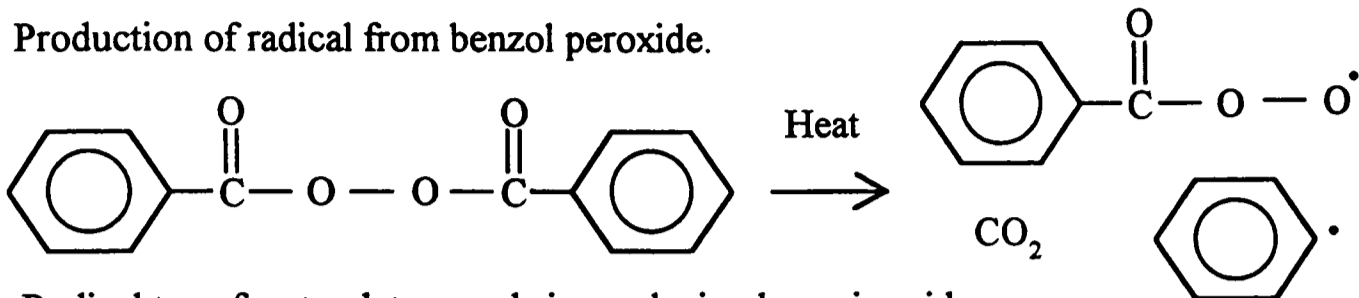
The butadiene / styrene elastomers gelled with all the monomers previously detailed, and generally the materials looked promising. One source of the powdered elastomer demonstrated a problem with using these materials by displaying an excessively high water uptake. The production of a powdered elastomer involves the grinding (below the T_g so the material is rigid) of a bale of elastomer. During this process a separating agent or partitioning agent is added to the elastomer, this prevents the elastomer agglomerating together once the material is above the T_g . Separating agents are typically soluble (e.g. Talc) with act to form droplets within the material once the material is in an aqueous environment (Parker and Braden, 1982, Parker 1993).

The level of cross linking agent used in these materials was originally 10 to 30 wt% but later this was found to be unnecessary as 1 to 2 wt% was found to be sufficient in a later study (Parker, 1993).

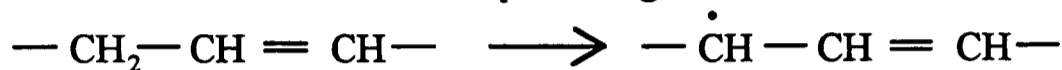
The initiation of the benzoyl peroxide results in the formation of two radicals (Allen, 1963) which can then react with the materials in different ways as illustrated in figure 5.1. The methacrylate may polymerise or the elastomer cross link (Bateman et al, 1963) alternatively, as all the elastomers used by Parker and Braden are unsaturated, they are susceptible to methacrylate grafting during initiation.

The nature of the material formed was also identified by Parker (1982) by looking at the effect of varying the proportion of the elastomer (a natural rubber, Pulvatex) with different methacrylates. Figure 5.2, is an illustration of this, with a distinct discontinuity being observed for the shear modulus at approximately 0.3 g of 'Pulvatex' to 0.7 ml of nonyl methacrylate. This transition is attributed to the state of the material changing from a continuous nonyl methacrylate matrix with discontinuous 'Pulvatex' to a continuous 'Pulvatex' phase and discontinuous nonyl methacrylate. The importance of the relative solubility of the monomer and the elastomer is noted, with the EHM being the less paraffinic ester (higher solubility parameter, appendix IV) exhibiting this transition at a higher powder / monomer ratio. The more paraffinic TDM exhibits such a transition at a lower level. Such gelling characteristics are also supported by the inability of some of the elastomers used to form a gel with some of the monomers used.

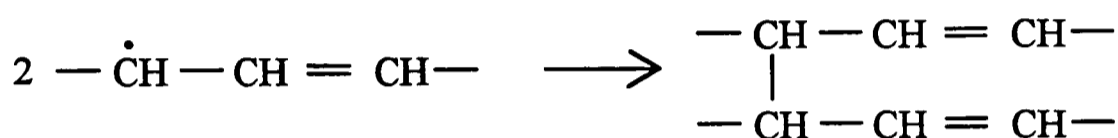
Figure 5.1. Possible reactions of the methacrylate monomer and elastomer within due to the peroxide radical.



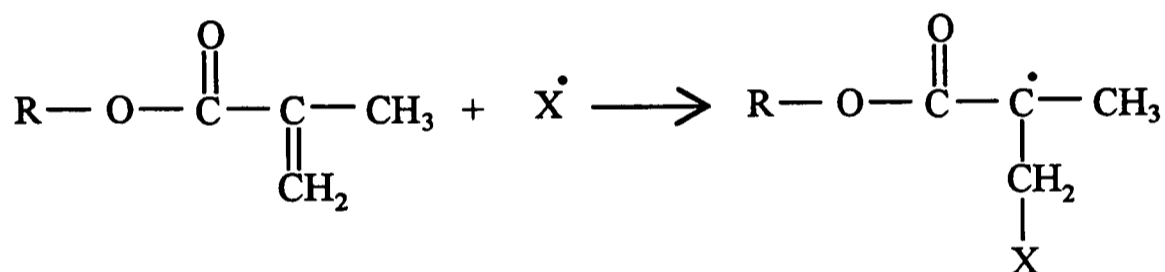
Radical transfers to elastomer chain producing benzoic acid.



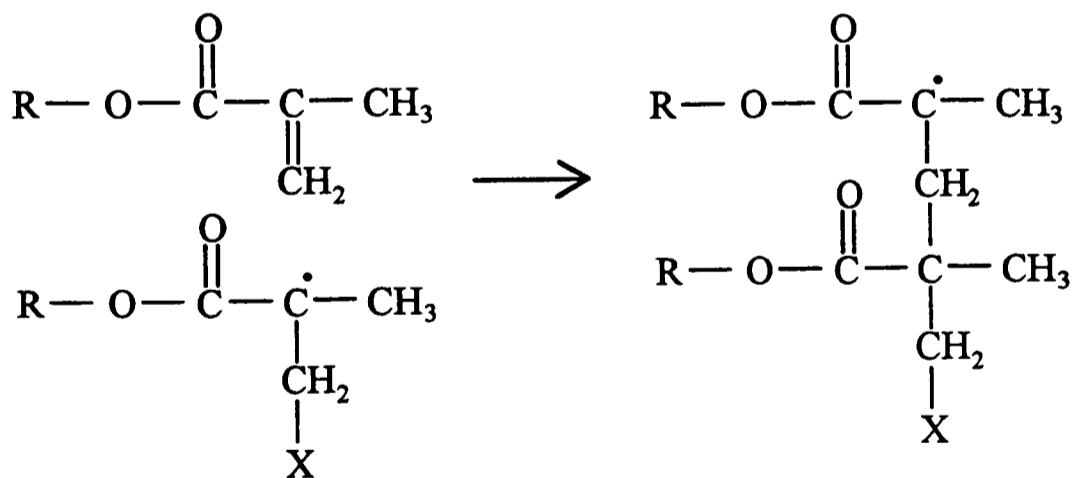
Cross linking of elastomer.



Radical transfers to a methacrylate group.



Polymerising with methacrylate.



Grafting of the elastomer to methacrylate group.

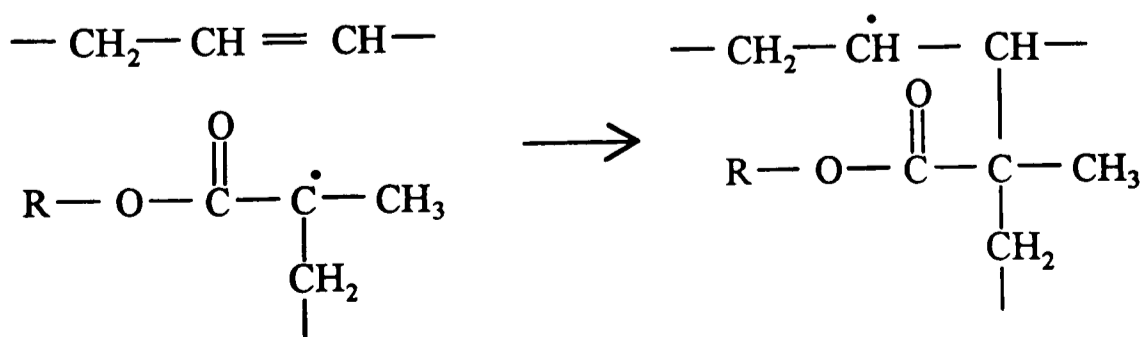
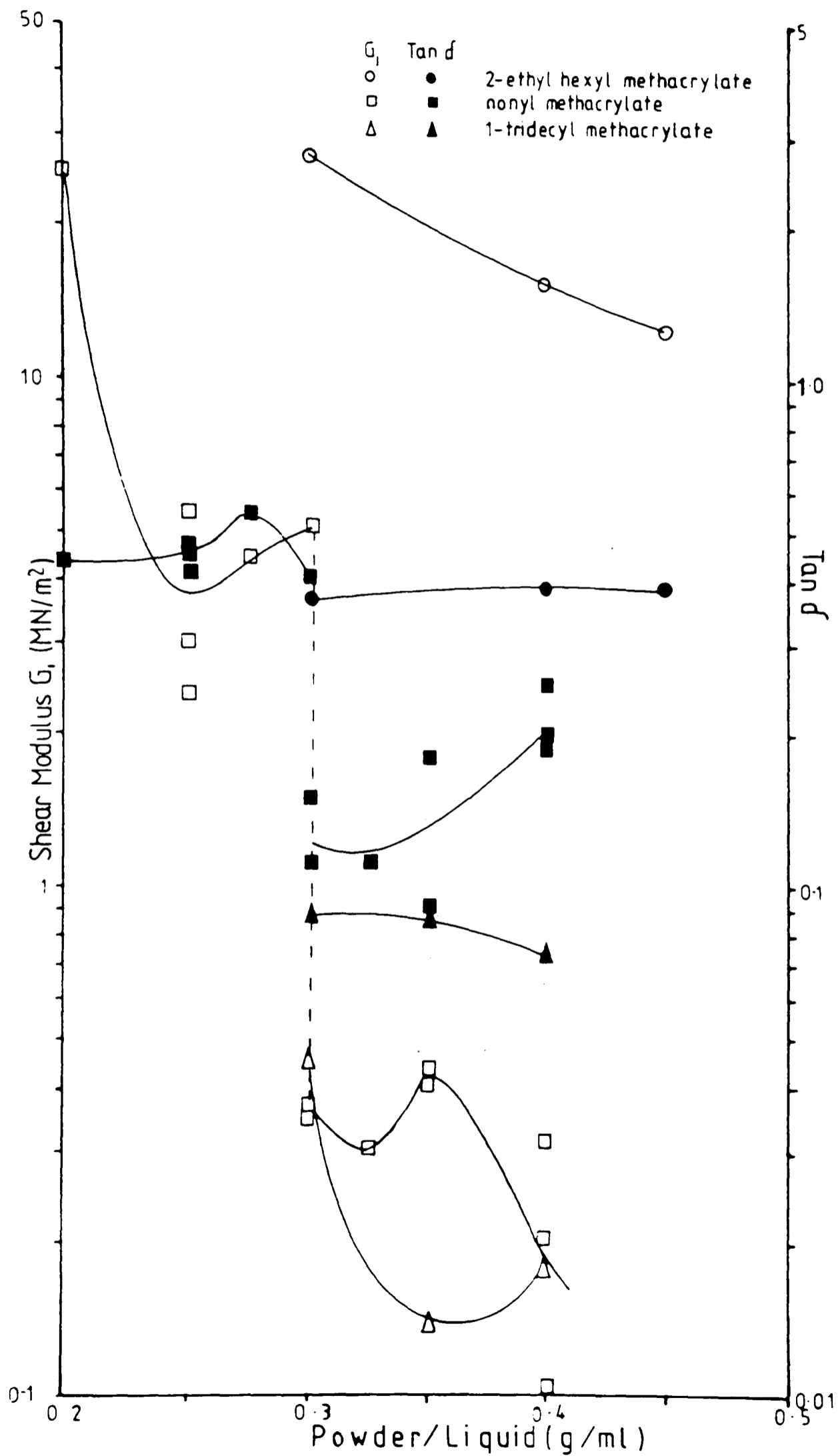


Figure 5.2. The effect of powder liquid ratio on the viscoelastic properties of Pulvatex based materials. Reproduced from Parker (1982), figure 4.2 page 124, or Parker and Braden, 1990.



5.2. Methacrylates.

The mechanical properties of the elastomeric methacrylates was investigated by Davy and Braden (1987), who used a series of linear alkyl methacrylates as defined by the length of the carbon side chain i.e. hexyl methacrylate is C6 and tridecyl methacrylate is C13. The effect of increasing the cross link density of these materials was also investigated and the results are presented in terms of energy to rupture (w) for increasing cross linking agent as reproduced in figure 5.3. There is a dramatic decrease in the energy to rupture with increasing alkyl group length but the effect of cross linking is somewhat more complex. The C6 showing a decrease with increasing EGDM and the C8 showing a increase, other materials showed a peak value as seen for the C13 where as others go through a minima C5 this in spite of the cross link density increasing linearly with increasing addition of the EGDM (apart from the C8). They recommend a level of 0.5 % cross linking agent as an initial starting point for studies on the mechanical properties of soft methacrylates used.

A series of water absorption measurements were made on a range methacrylate monomers (some of those in table 1.1) which were made by dissolving 1 % lauryl peroxide initiator into the methacrylate. This was then injected between two lined (poly vinyl acetate) glass plates via a rubber gasket spacer (1 mm thick). The material was then cured under a pressure of 2 bar for at least 4 hours at 90°C. C17.4 M is a mixture of high molecular weight monomers with a average chain length of 17.4 (hence the name) this is due to the difficulties in separating and purifying high molecular weight monomers. It is believed that the range of chain lengths ranges from C13 to C22 with most being around C18.

Figure 5.3. Plot of energy to rupture (w) as a function of concentration of the cross linking agent, for a series of elastomeric poly (alkyl methacrylate)s. Reproduced from Davy and Braden (1987).

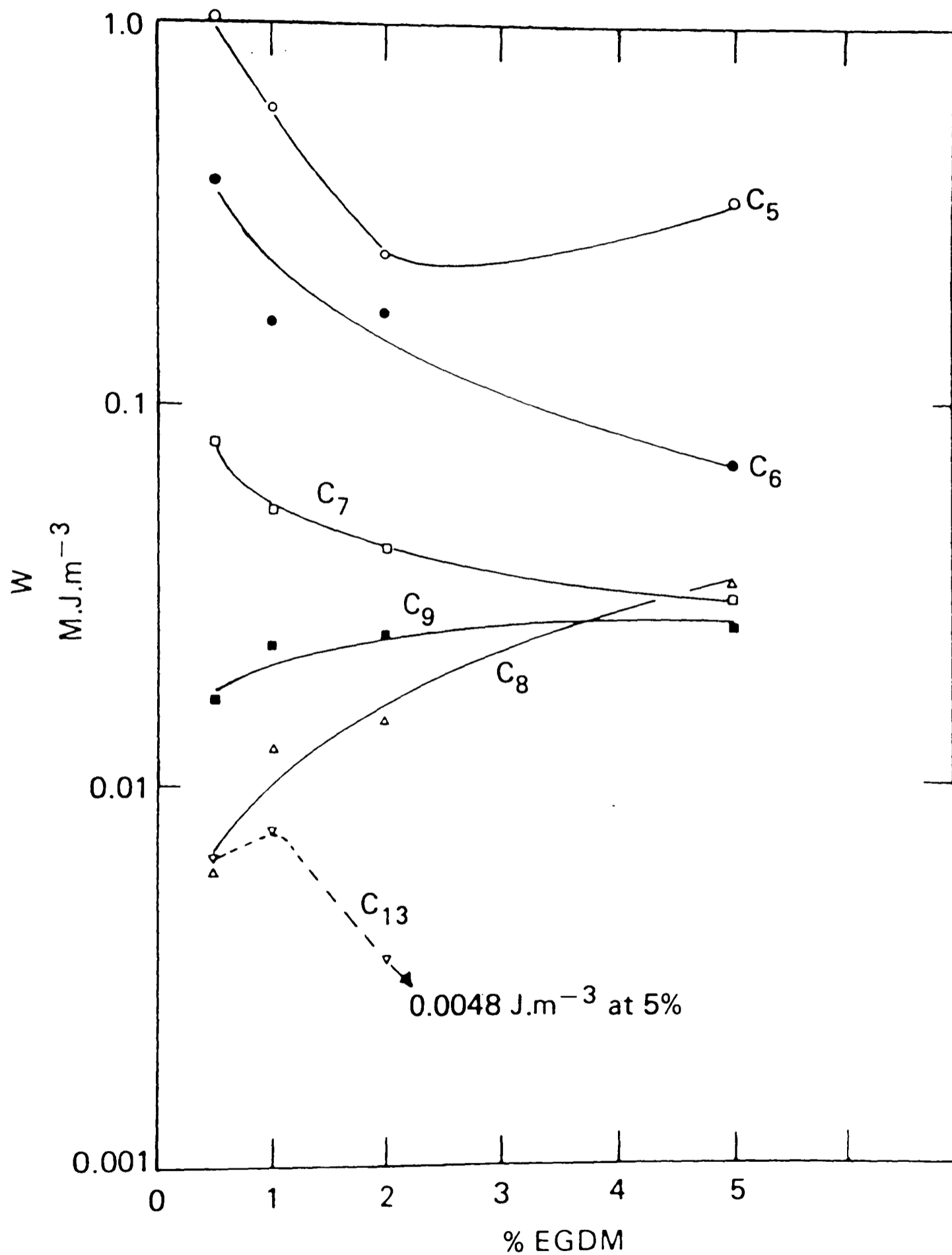


Table 5.1. The codes of the methacrylates used.

Code	Methacrylate	Molecular weight, g	Side chain length, C units.	Supplier
MM	Methyl	100.1	1	Bonar polymers.
EM	Ethyl	114.1	2	Bonar polymers.
BM	n-butyl	142.2	4	Bonar polymers.
HM	n-hexyl	170.3	6	Bonar polymers.
EHM	2-Ethyl hexyl	198.3	8	Bonar polymers.
TDM	Tri decyl	268.0	13	Bonar polymers.
C17.4M	C17.4	330.0	17.4	Hüls Chemicals.
<u>Dimethacrylates,</u>				
EGDM	Ethylene glycol di	198.2	2	Bonar Polymers.
HDM	1,6-hexandiol di	254.3	6	Hüls Chemicals.
DDM	1,12-dodecandiol di	338.5	10	Hüls Chemicals.

5.2.1. Water uptake of the methacrylate homopolymers.

The water uptake of the some of the higher methacrylate polymers are shown in figure 5.4. However a more complete picture of the absorption characteristics of the polymers may be seen in table 5.2, as the effect of the large solubility overshadows the absorption. The first point to be realised is that the water uptake of the soft methacrylates (HM, EHM, TDM and C17.4M) is very low and generally decreases with increasing length of side chain as noted by Kalachandra and Kusy (1991) for the rigid methacrylates tested. They did however find that the higher methacrylates did not fit in with this trend with the water uptake for HM he found was 6.9 wt % with is clearly in conflict with the results presented here when the HM has a total uptake of 0.22 wt%. As both these tests were performed with a similar method at the same temperature (37°C) although they were polymerised differently. The gamma irradiation performed by Kalachandra and Kusy should ensure that no soluble agents were incorporated into the material this way, as had happened with the peroxide cured silicone materials. It seems therefore likely that the methacrylate used by Kalachandra and Kusy was infiltrated with a soluble agent, which forms droplets. This is also supported by the diffusion coefficient which quoted as $5.19 \times 10^{-11} \text{ cm}^2\text{s}^{-1}$ or $5.19 \times 10^{-13} \text{ m}^2\text{s}^{-1}$ (although in the paper this is quoted as 519×10^8

cm^2s^{-1} which is believed to be a mistake) and therefore in line with the theories on the effect of droplet formation on diffusion coefficient.

Figure 5.4. Water uptake of soft mono methacrylates.

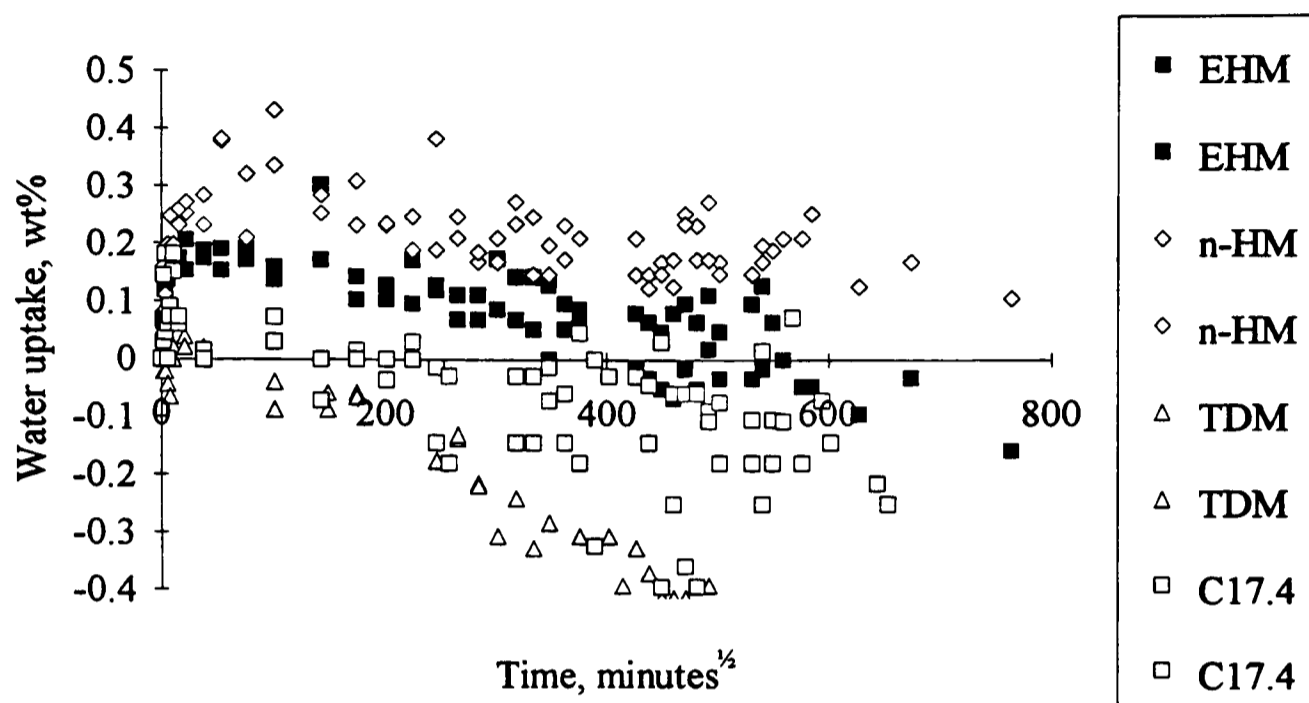


Table 5.2. Summary of water uptake of methacrylates.

Code	Abs, wt %	Sol, wt %	Total, wt%	D_{des} , m^2s^{-1}	D_{abs} 1st, m^2s^{-1}	D_{abs} 2nd, m^2s^{-1}	2nd Abs, wt%
<u>Mono methacrylates</u>							
HM	0.20	0.02	0.22	3.78×10^{-8}	1.28×10^{-9}	4.65×10^{-9}	0.33
EHM	-0.17	0.68	0.51	8.95×10^{-10}	8.40×10^{-10}	-	-
TDM	-0.50	0.92	0.42	8.79×10^{-12}	-	-	-0.02
C17.4M	-0.11	0.44	0.33	3.38×10^{-9}	-	-	0.06
<u>Di methacrylates</u>							
EGDM	3.08	1.73	4.82	1.08×10^{-9}	1.96×10^{-9}	-	-
HDM	0.39	0.58	0.97	9.03×10^{-10}	4.68×10^{-10}	4.88×10^{-10}	0.93
DDM	0.63	0.21	0.84	1.18×10^{-9}	1.38×10^{-9}	3.63×10^{-9}	0.42

An interesting point is the similarity of all the diffusion coefficients (for absorption, desorption and second absorption) for the materials when they could be determined. TDM and C17.4 M showed so small an uptake with too great a spread of data during the initial period that no meaningful coefficient could be determined. For EGDM the absence of a second absorption cycle is due the sample crazing (followed by shattering) excessively during desorption so only small fragments of the sample remained. The magnitude of the uptake and rate of desorption would lead to tensile stresses in the surface material which would lead to crazing the magnitude was however surprising. TDM seems to deviate from the model of the uptake decreasing with increasing side chain length with a higher than expected uptake being observed. This may relate to the purity of the monomer, as the monomers get larger they become increasingly difficult to purify. This type of argument is supported by the slow diffusion coefficient calculated.

Water uptake of the dimethacrylates (figure 5.5) fits the pattern that increasing the distance between the methacrylate groups decreases the water uptake (i.e. the series goes EGDM, HDM and DDM). Here however the water uptake seems higher than that which would be expected from the mono methacrylates detailed above as the DDM should have a similar density of O groups as HDM but has a higher uptake.

Figure 5.5. Water uptake of di methacrylates.

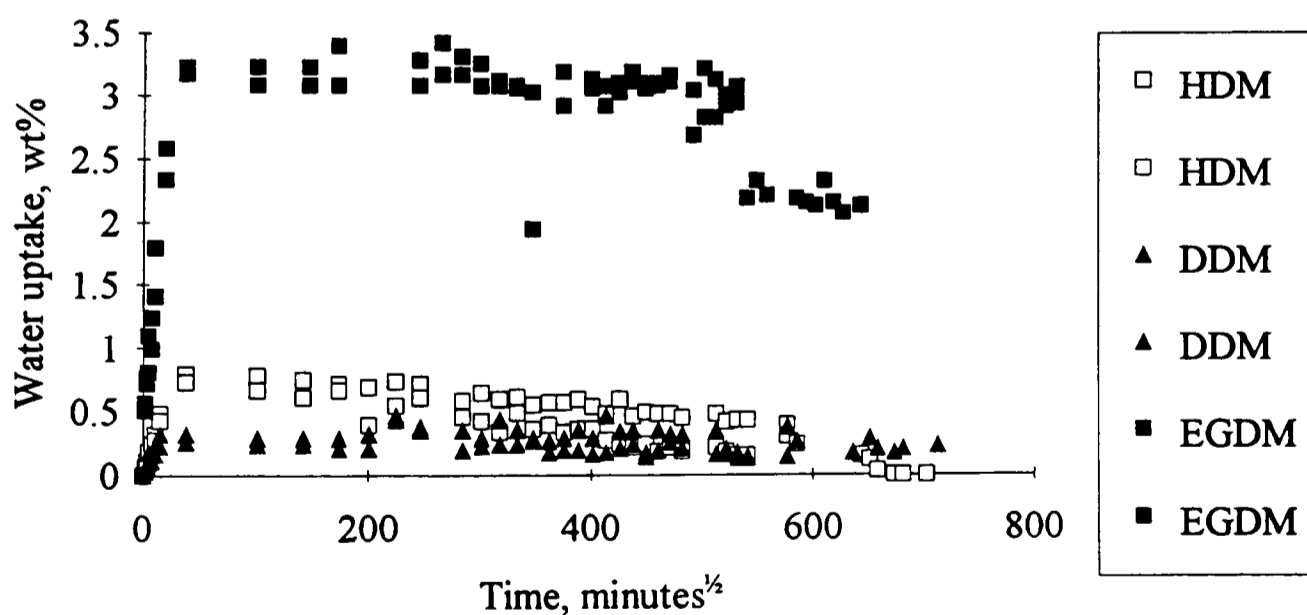


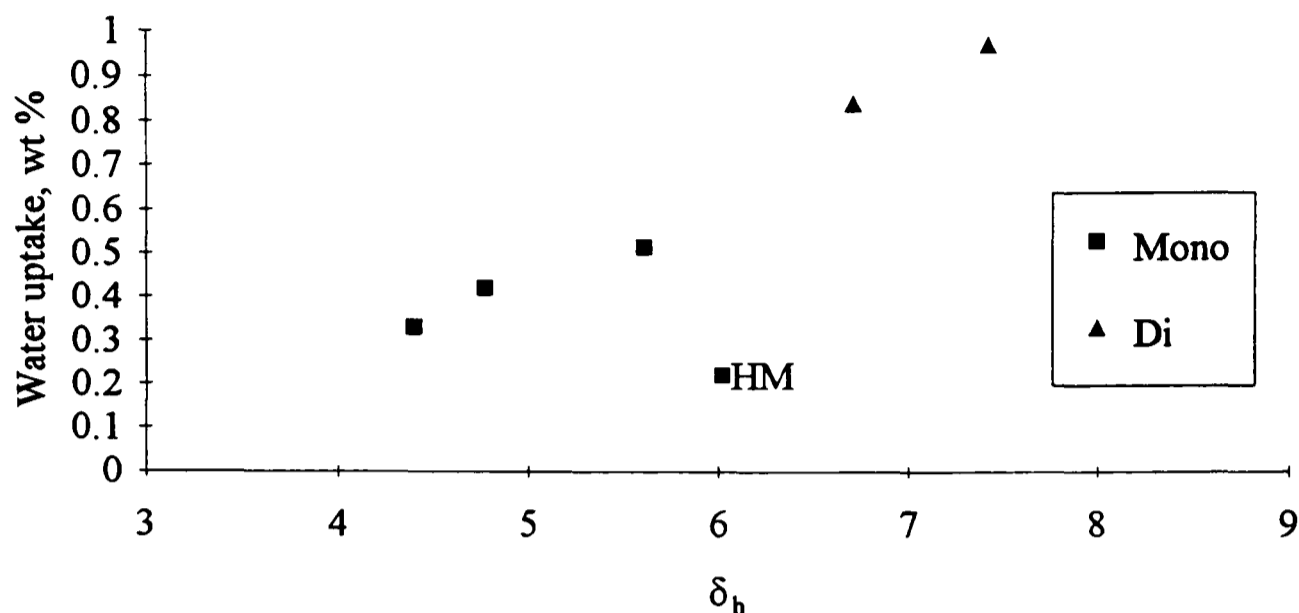
Table 5.2, details the absorption characteristics of the materials as can be seen for all the materials. Where similarity between the diffusion coefficients calculated for the cycles (absorption, desorption and second absorption) for each material indicates that these materials are behaving in a fairly ideal Fickian manner. The uptake is therefore driven by the the matrix rather than any soluble particles present in the material.

The approach of Kalachandra and Kusy of looking at the O group density for the methacrylates is somewhat simplistic in terms of attributing the water uptake to these groups. From the literature we know other groups can also have a profound influence on uptake (i.e. amine groups), therefore the simple O group density is not entirely applicable. The application of dual sorption theories (Flory Huggins and Langmuir) will certainly enable a level of prediction but the relationship of constants is complex and they can not be determined from the available data. The Flory Huggins interaction parameter (χ) is related to the solubility parameter (δ) but this relationship is limited by the polarity of the solvent and polymer. Appendix IV details the theoretical background and calculation of the δ , the splitting of this up into dispersive (δ_d), polar (δ_p) and the hydrogen bonding component (δ_h) of δ . The effect on the O density on δ_p , polar δ_h for the methacrylates used here is illustrated in appendix IV, the O density relationship noted for the methacrylates by Kalachandra may be altered in terms of δ_h .

Figure 5.6, shows a plot of the water uptake from the methacrylate materials against δ_h (based on calculation from the monomer) which shows a linear relationship as described by Kalachandra and Kusy for the O density. The deviation of HM is unclear it may relate to an impurity acting to cross link the material so lowering the uptake as previously reported. The other exception is EGDM which exhibited a much higher uptake, this is likely to be due to another process occurring.

While this indicates the relationship is valid and in some ways vindicates the dual sorption theories, it does not provide sufficient information to explain the processes occurring. The contribution of the hydrogen bonding of the water to the polymer will undoubtedly control the uptake as demonstrated by figure 5.6, it is important but will not be the complete picture as the polarity would also have a significant influence on the water uptake.

In terms of the water uptake in the elastomer methacrylate materials the influence of hydrogen bonding will be limited as the influence of the soluble agents within the material will more significant.

Figure 5.6. Equilibrium water uptake of the methacrylate materials against the δ_h .

5.3. Powdered butadiene styrene samples (PBS).

A powdered butadiene styrene rubber (PBS) was used as a base material as this had been previously used by Dr S.Parker, and could be used to characterise the uptake with reference to changes in the structure and composition. Initially three different elastomer (g) to monomer(ml) ratios 50:50, 60:40 and 70:30 were used using three monomer HM EHM and TDM. The PBS used was supplied by the Performance Polymers Division of Plascoats Systems Ltd. For each of the monomers three different initiators were tried 'Lucidol', LB, (supplied by AKZO chemicals), a 50 % benzol peroxide and 50 % di cyclohexyl phthalate as previously by Parker (1993), the di cyclohexyl phthalate acts to stabilise the benzol peroxide and prevents the need for damping of the benzol peroxide to prevent combustion. Lauryl peroxide (LP) which initiates in a similar way to the benzol peroxide but forms lauric acid rather than benzoic acid which is considerably less soluble. Azo iso butyl nitrile, AZBN, (BDH Ltd) was also used as this is a free radical initiator but is slightly different as the initiation process evolves nitrogen as shown in figure 5.7. Table 5.3, details the formulations used during the initial study for the formulation of the materials.

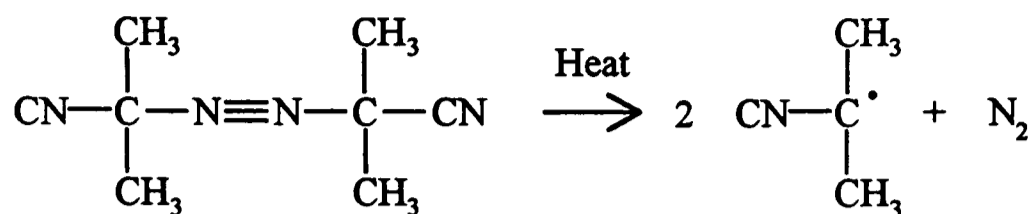
Figure 5.7. Breakdown of AZBN.

Table 5.3. Initial formulation of the PBS based materials, the percentages are expressed in terms of the monomer. These monomer formulations were then mixed with the elastomer to monomer in the ratio's 50:50, 60:40 and 70:30.

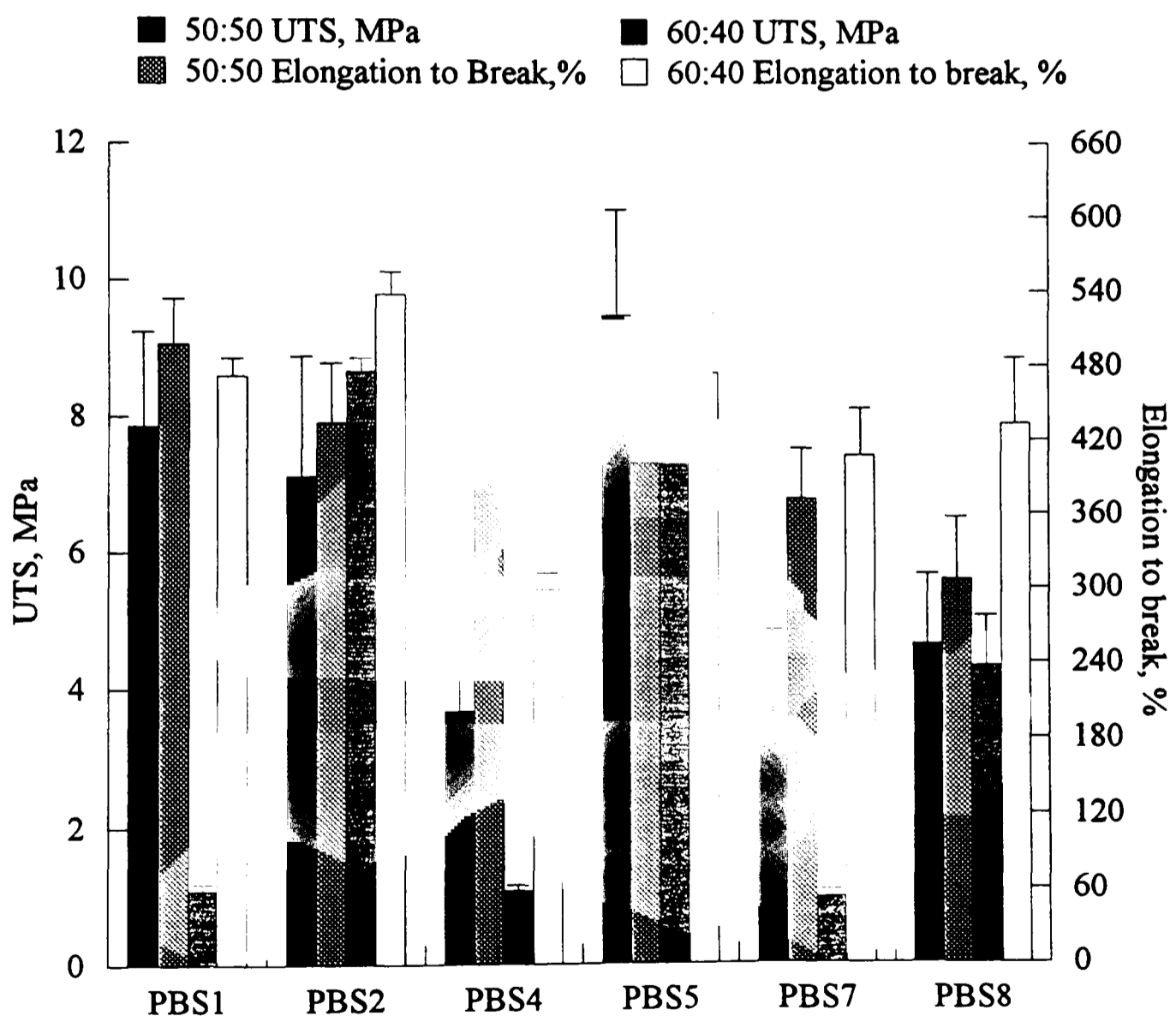
Code	Monomer	EGDM, %	Initiator	%
PBS1	HM	0.5	LB	1
PBS2	HM	0.5	LP	1
PBS3	HM	0.5	AZBN	1
PBS4	EHM	0.5	LB	1
PBS5	EHM	0.5	LP	1
PBS6	EHM	0.5	AZBN	1
PBS7	TDM	0.5	LB	1
PBS8	TDM	0.5	LP	1
PBS9	TDM	0.5	AZBN	1

At this stage it became apparent that the 70:30 polymer/monomer blends were unusable as gels because there was insufficient monomer to dissolve the polymer. AZBN also proved to be insoluble in TDM and unstable in the EHM at room temperature. Despite this the samples made from the AZBN using HM and EHM contained lots of evenly distributed gas bubbles. These bubbles were due to the evolution of N₂ from the breakdown of AZBN during initiation (shown in figure 5.7). LB (benzoyl peroxide) does evolve CO₂ (figure 5.1) which does not cause the same bubbling this seems to be due the better solubility of CO₂ in the material compared to N₂.

5.3.1. Tensile strength of PBS based materials.

Ultimate tensile strength and elongation to break were used as the preliminary selection criteria as this should maximise the restraining force exerted by the material and so limit water uptake. Figure 5.8, shows the tensile results from those initial formulations which formed testable materials. These results show the 50:50 mixes to have a greater ultimate tensile strength than the comparable 60:40 mix with the exception of the LP initiated HM. The study was therefore restricted to the 50:50 mixes. The difference between the two initiators shows LP to produce a superior material in terms of the UTS of the material for all the materials apart from the 50:50 HM based materials.

Figure 5.8. Summary of the strength data for of the initial formulations of the PBS materials.

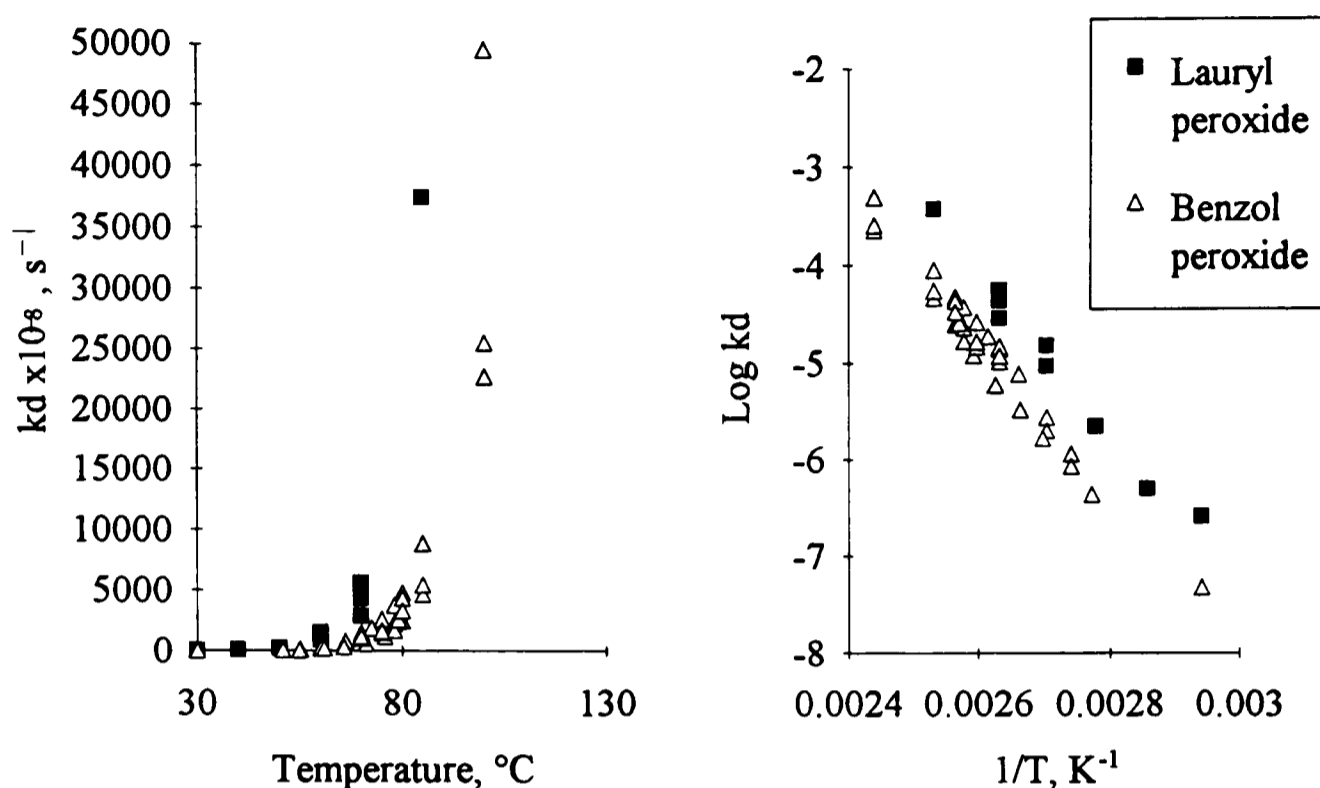


EHM can also be seen as the preferred monomer as this proved to produce the strongest material (PBS5) although there is little difference between this and HM. TDM as predicted from Davy and Braden (1987), figure 5.3, is the weakest of the materials tested, the strength of EHM is not predicted by this work as no branched alkyl methacrylates were used.

The behaviour of the initiators at different levels of elastomer is interesting as for all the 60:40 LB samples the strength was much lower than the equivalent 60:40 LP samples, whereas at the 50:50 level this difference had much less. Indeed the 60:40 LB samples all have a UTS of around 1 MPa. This result is interesting in considering the state of the material formed and seems to fall into a similar pattern to Dr. S. Parker's results shown in figure 5.2, where increase of the elastomer content produced a discontinuity in the viscoelastic properties of the 'Pulvatex' / nonyl methacrylate based material. Why such a discontinuity should be observed for LB but not LP initiated materials seems to stem from the initiation characteristics resulting in differences in the material.

The different initiators will lead to a different number of radicals being produced during heating of the material and will result in different chain lengths between the cross links and grafting onto the elastomer. The effect of antioxidant on the elastomer will also play a role as it will 'mop up' the radicals as they are produced. Without a full study on the energetics of the initiation, polymerisation, grafting and oxidation retarding process it is impossible to describe the process in the any detail. Figure 5.9, shows how the initiation rates of benzol and lauryl peroxide alter with temperature (Bandrup and Immegut, 1975), from this we see that lauryl peroxide initiates at a faster rate at lower temperatures than benzol peroxide (the activation energies are similar with values between 120 and 133 kJ mol⁻¹ being quoted). Thus there should be a high concentration of radicals in the lauryl peroxide initiated samples, due the lower initiation temperature and high percentage of lauryl peroxide in the materials (as Lucidol is used which is only 50 % benzol peroxide). How the polymerisation rate influences the solubility parameter (or the paraffinic nature) and how this fits in with the previous work of Dr. S.Parker is unclear. It is possible that the LP initiates with a greater degree of grafting (due to the higher radical concentration) onto the elastomer or less interference from the antioxidant than the LB. The difference in polymerisation characteristics between benzol peroxide and lauryl peroxide has already been noted for the peroxide cure silicone polymers where LP failed to polymerise the material, but the full reason for this remains unclear.

Figure 5.9. Initiation rates of benzol peroxide and lauryl peroxide in benzene, based on data in Brandrup and Immegut, 1975.



The effect of composition on strength was further investigated by the formulation of second set of 50:50 based materials. This second set of formulations are shown in table 5.4 and were all based on EHM as this showed the most promise from the initial results.

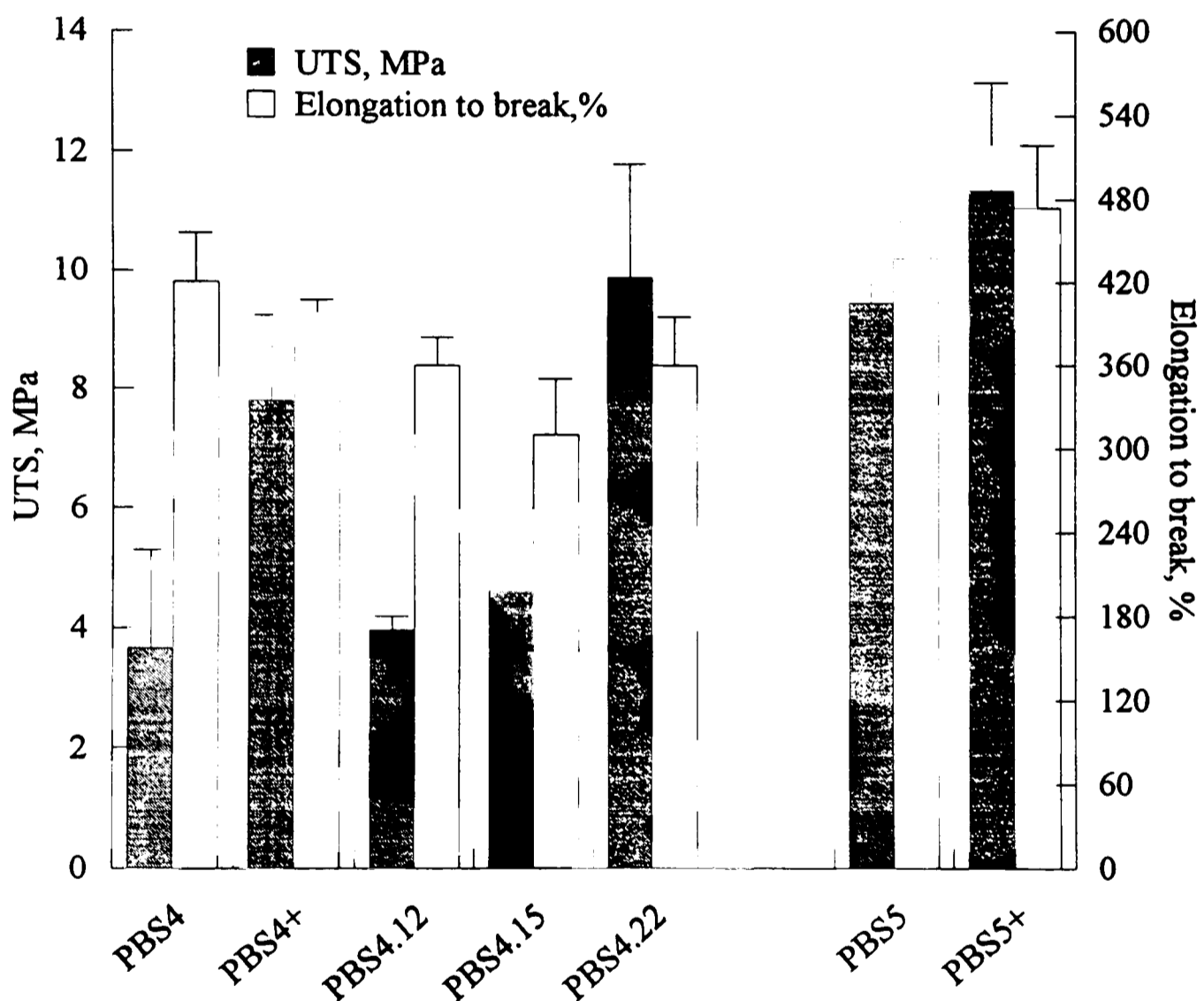
Table 5.4. Second formulations based on the PBS elastomer and EHM monomer 50 : 50 ratio.

Code	Initiator, %	EGDM, %
PBS4	LB 1	0.5
PBS4+	LB 1	1
PBS4.12	LB 1	2
PBS4.15	LB 1	5
PBS4.22	LB 2	2
PBS5	LP 1	0.5
PBS5+	LP 1	1

Figure 5.10, shows the effect of increasing of the percentage of EGDM with a maximum in the UTS occurring at approximately 1 % then decreasing. Such behaviour is observed

by Davy and Braden (1987), figure 5.3, the reason for this complex behaviour is unclear. The decrease in elongation to break with cross link density is easily understood as the increase number of cross links will restrict chain movement and hence the elongation. When the initiator level (LB) was raised to 2 % (PBS4.22) there was an increase in the UTS but not the elongation to break (comparison to PBS4.12). The increase in the initiator will have decreased the average length of chain produced but probably more significantly the grafting to the elastomer (see figure 5.1). Increasing the cross linking for the LP initiated samples also improved the strength of the samples (PBS5+).

Figure 5.10. Strength of 50:50 PBS and EHM based materials.



5.3.2. Water uptake of PBS materials.

From these tensile results a series of formulations, shown in table 5.5, were selected for the initial water absorption study.

Table 5.5. PBS based materials for absorption.

Code PBS	Monomer	Initiator	%	EGDM %
PBS1	HM	LB	1	0.5
PBS2	HM	LP	1	0.5
PBS4+	EHM	LB	1	1
PBS5	EHM	LP	1	0.5
PBS5+	EHM	LP	1	1

Figure 5.11, 5.12, and 5.13, shows the water uptake of these materials. The increase in the water uptake of the PBS1 at long time periods is due to oxidation of the elastomer and will be dealt with in a later section. Ignoring the effect of oxidation it is clear that the water uptake is non-Fickian, the plot being non linear as illustrated by figure 5.12, although the initial period seems to be as shown in figure 5.13. There is a strong correlation of the uptake with the strength of the material, the similar strength PBS1 and PBS2 show similar uptakes. This is repeated for the similar strength PBS4+ and PBS5 despite the difference in the cross linking (figure 5.8, 5.10, 5.12, and table 5.6). The strongest PBS5+ shows the lowest uptake, noticeably lower than that from PBS4+, material despite the similar cross linking (judging by the results of PBS1 and PBS2). The reason for this strength dependence is clearly due to greater restraining force exerted by the stronger material preventing the expansion of the droplets due to a higher modulus.

The driving force behind the uptake is the separating agent, added to the elastomer to prevent agglomeration as previously described, acting to form droplets within the materials. It is interesting to note that the benzol peroxide does not seem to have a noticeable effect with the uptake of these materials, (unlike the peroxide cure silicones). This seems to be an overshadowing effect of the separating agent and far less being present in the material. From the previous work on monomers we know that the water uptake attributable to the monomer will be relatively small at 0.11 wt% for HM and 0.26 wt% for EHM (half of the values given in table 5.2). The water uptake of the PBS elastomer is shown in figure 5.14, with the material having a water uptake in excess of 15 wt% without any sign of equilibrium being reached.

Figure 5.11. Water uptake of PBS based materials.

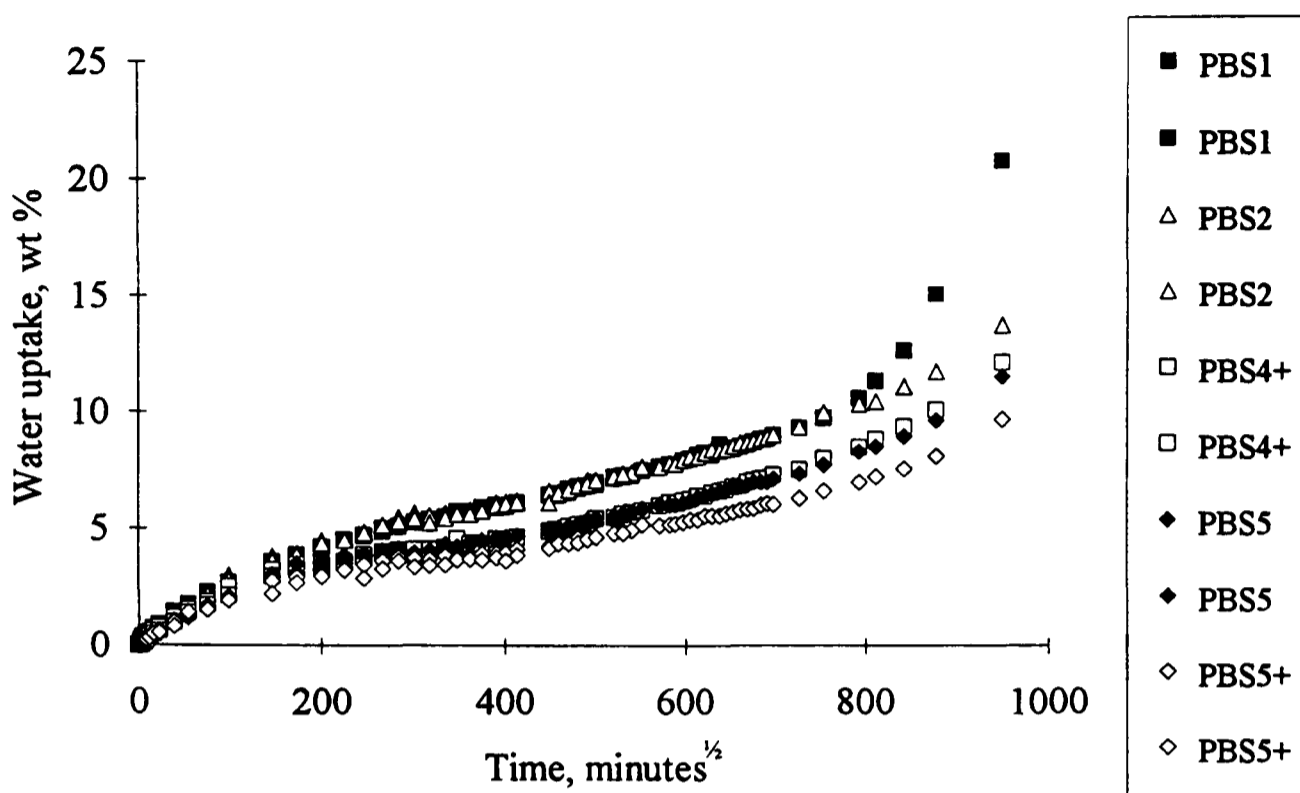


Figure 5.12. Water uptake of PBS based materials up to 10 wt%.

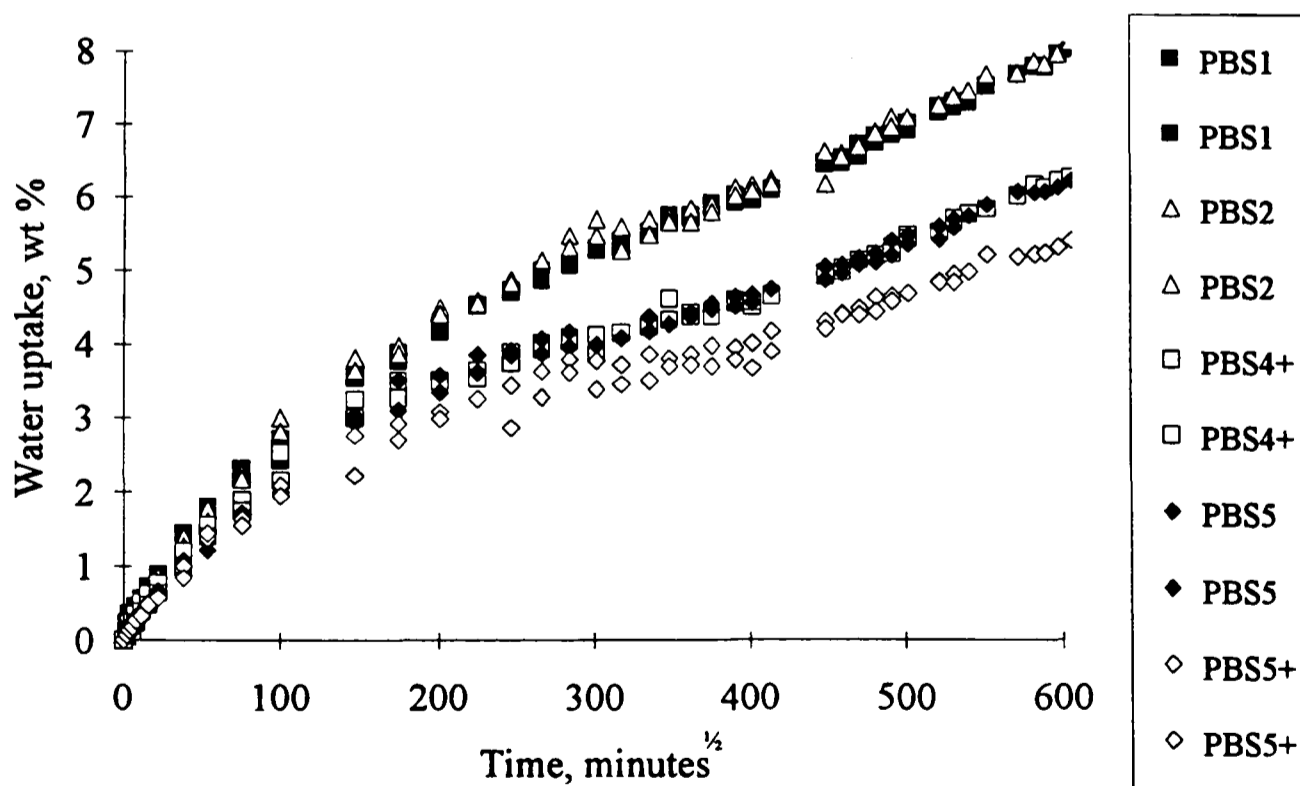
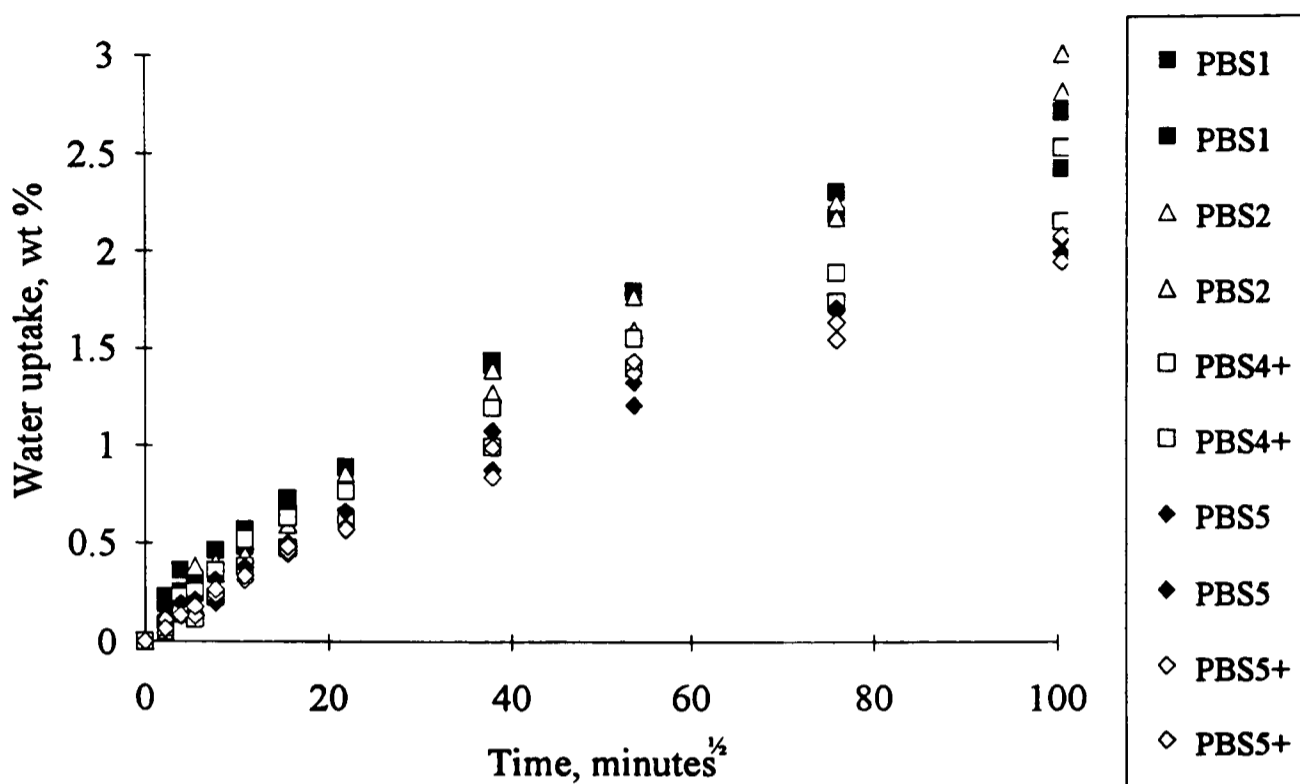
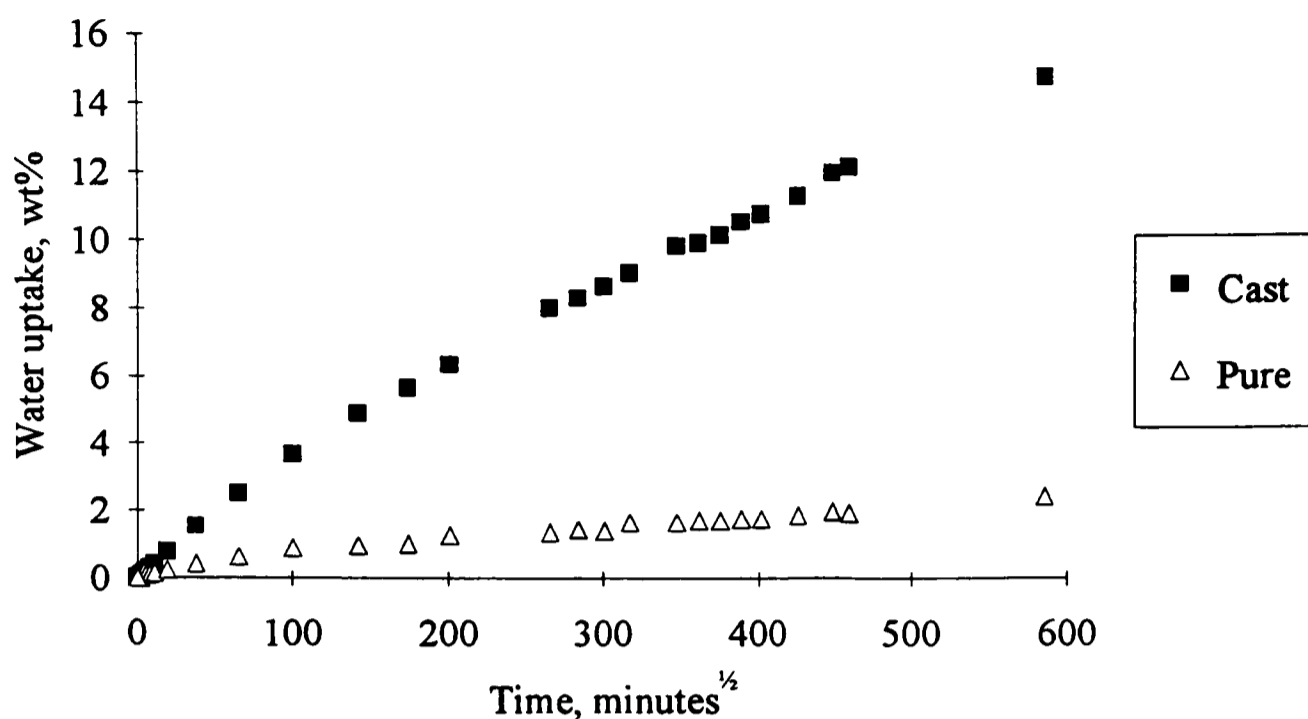


Figure 5.13. Water uptake of the PBS materials over the initial period.**Table 5.6. Summary of the first absorption and desorption results for the PBS samples after 196 days.**

Code	Water uptake, wt%	Solubility, wt%	Total uptake, wt%	D_{des} , m^2s^{-1}
PBS1	7.33	0.25	7.58	3.00×10^{-10}
PBS2	7.39	0.31	7.70	3.16×10^{-10}
PBS4+	5.71	0.45	6.16	3.25×10^{-10}
PBS5	5.58	0.39	5.97	3.23×10^{-10}
PBS5+	4.84	0.38	5.22	3.28×10^{-10}

The sample was made by dissolving the elastomer in chloroform so it formed a viscous liquid which was then poured into a 'Petri' dish and the chloroform allowed to evaporate slowly to prevent the formation of bubbles within the material. A second sample was also dissolved in chloroform so forming a low viscosity liquid, this was then centrifuged to remove the separating agent (the separating agent being assumed to have a higher density). The upper portion of this centrifuged mixture was then decanted off and cast in the same was as the previous sample. This pure sample showed a considerably lower uptake of approximately 1.5 to 2 wt% as seen in figure 5.14, the profile here is not Fickian indicating that some of the separating agent is still present in the elastomer.

Figure 5.14. Water uptake of the cast and purified PBS.

The quantity of the separating agent was determined by performing an ash test on the material in a furnace up to 700 °C, this assumed the agent was inorganic and stable which in this case seemed reasonable. This was determined to be 1.73 wt% which for a 50:50 based material translates too 0.87 wt% in the materials tested. X-ray diffraction was performed on the PBS ash but this was unsuccessful in determining the agent used as an amorphous pattern was obtained.

The desorption however followed classical Fickian characteristics as demonstrated by figure 5.15. The diffusion coefficients calculated from the desorption are all very similar as seen in table 5.6, and of the same order as the EHM diffusion coefficients shown in table 5.2. The second absorption cycle of these materials is shown in figure 5.16, 5.17, 5.18, and 5.19, here the uptake is higher and faster for all the materials than for the first absorption. This may be attributed to damage due to permanent deformation around the droplets during the first absorption cycle.

Figure 5.15. Desorption of the PBS materials after 196 days.

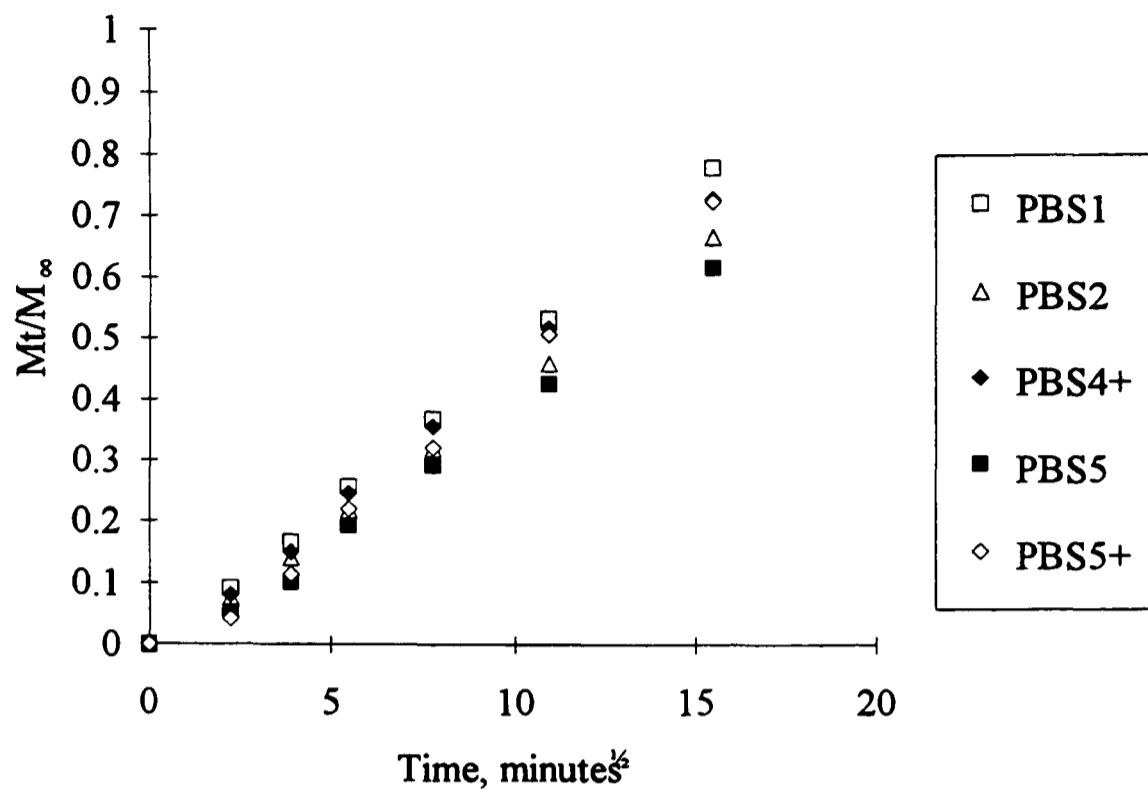


Figure 5.16. First and second water uptakes of the HM based PBS materials removed from the first absorption after 196 days.

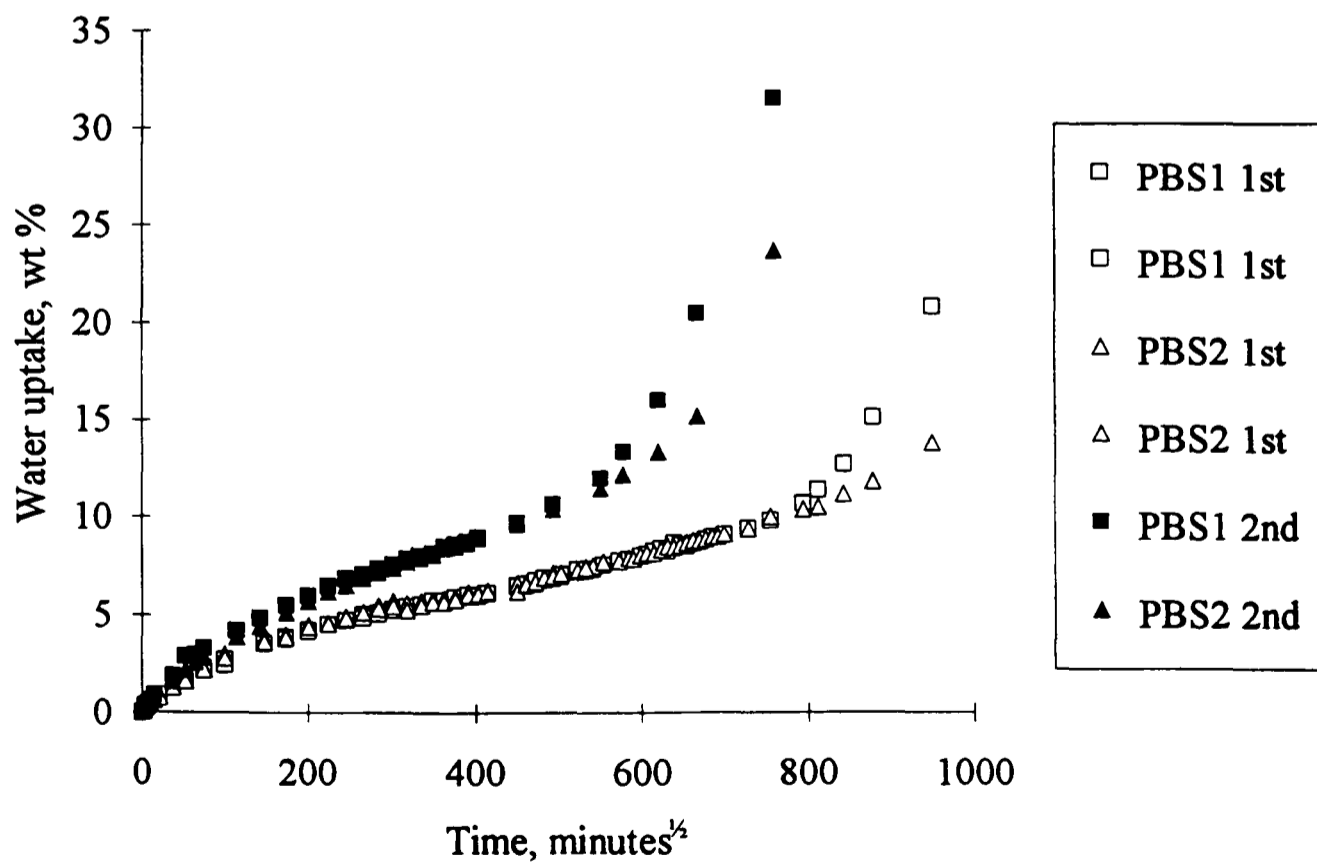


Figure 5.17. Initial period of first and second water uptakes of the HM based PBS materials removed from the first absorption after 196 days.

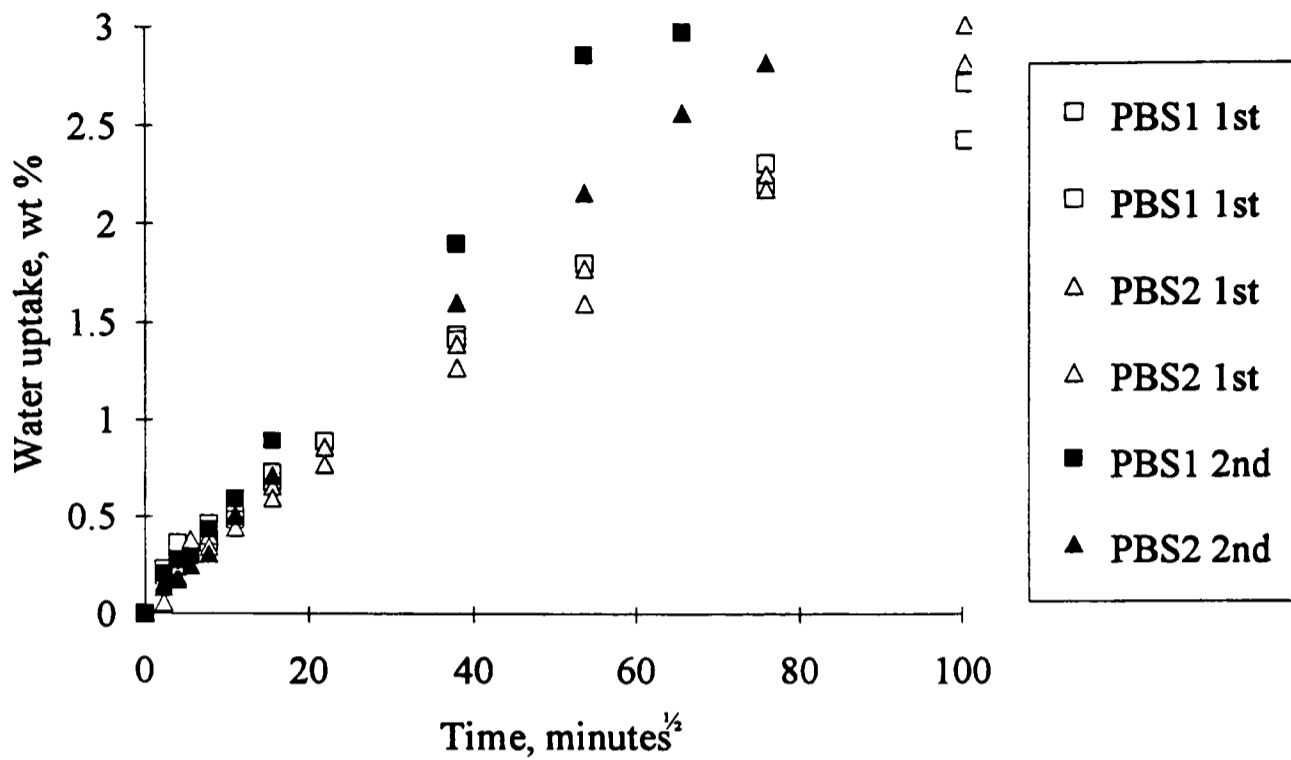


Figure 5.18. First and second water absorption of EHM based PBS samples of the samples removed from first cycle after 196 days.

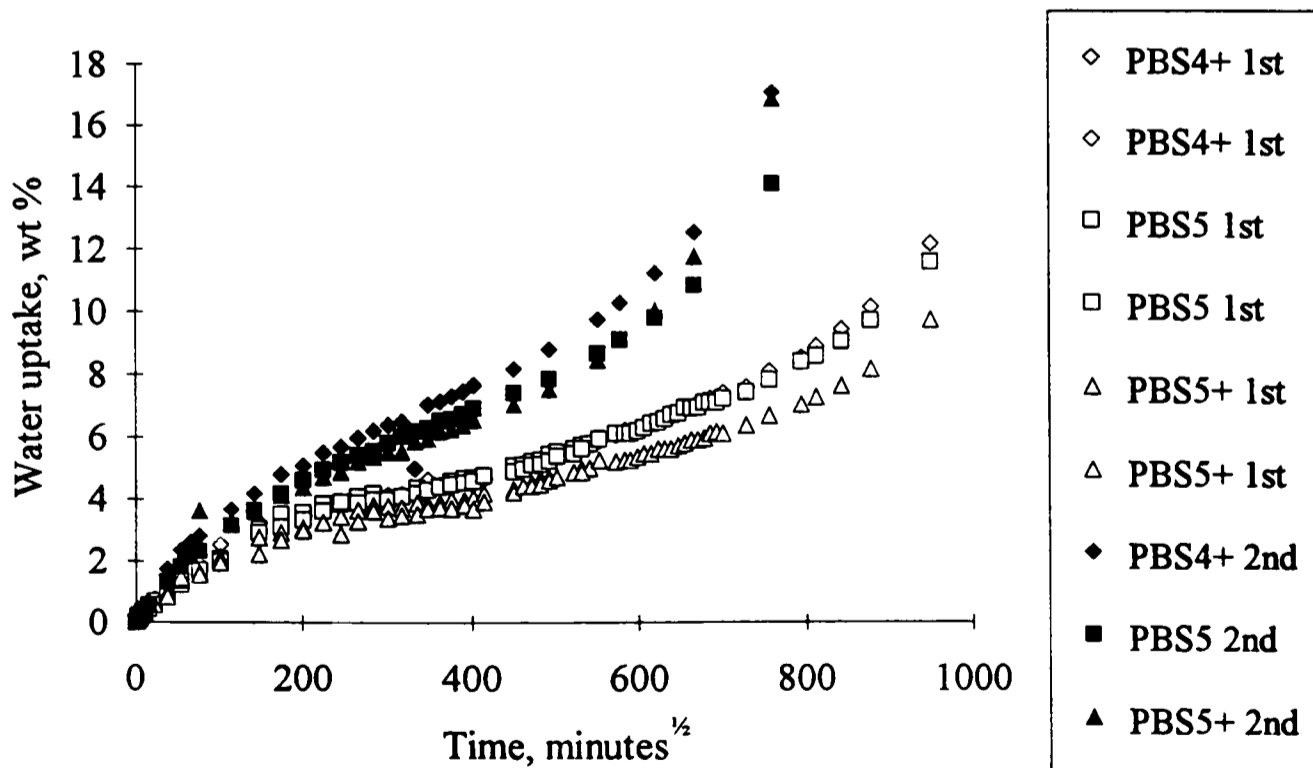
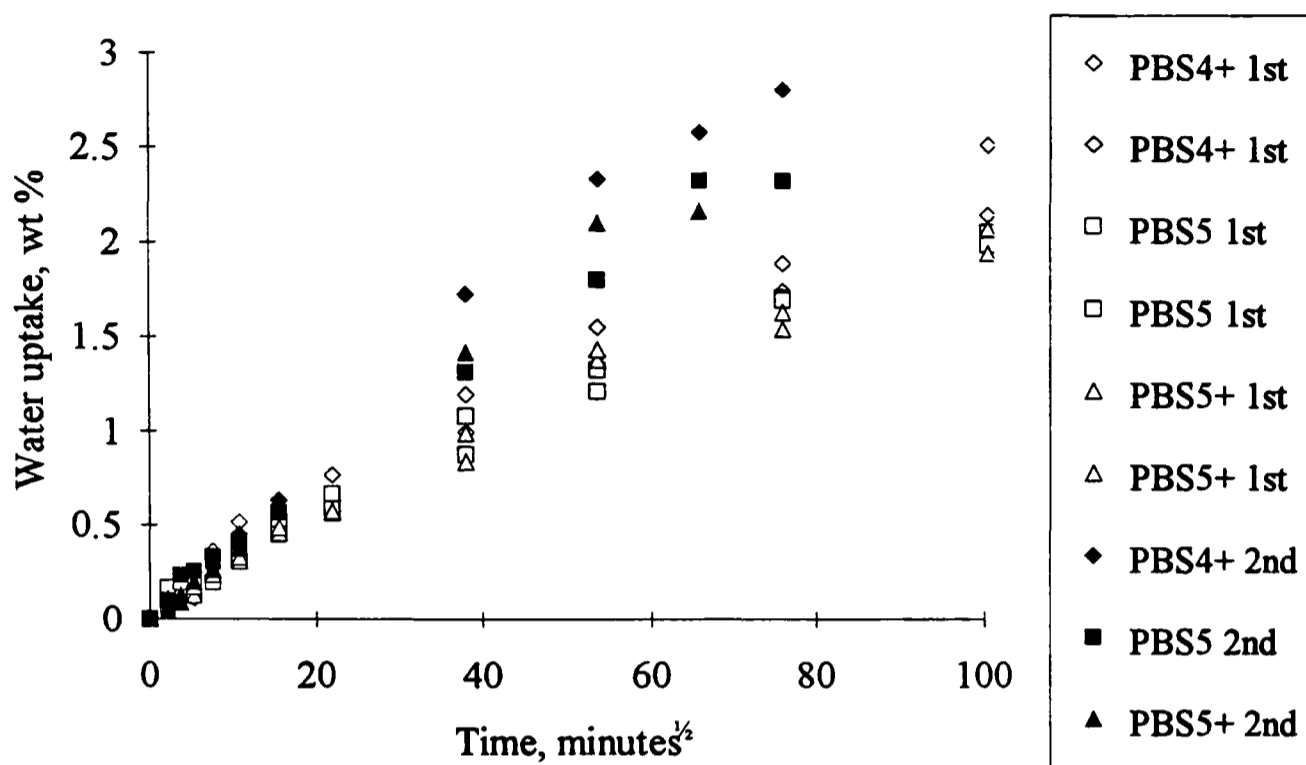


Figure 5.19. Initial period of first and second water absorption of EHM based PBS samples of the samples removed from first cycle after 196 days.



5.4. Water uptake of PBS materials from solutions of differing osmotic pressures.

As previously described the balance between the restraining force and the osmotic force is dependent on the osmolarity of the external solution as well as the internal solution droplets. Previous studies by Muniandy and Thomas and others as discussed in the literature review, have detailed the effect of different osmolarities on the absorption characteristics of the material. Clinically, soft lining material are not used in water but in saliva which is a blend of different ionic and organic components, this has an osmotic potential associated with it. Therefore a series of solutions, NaCl (strong electrolyte), glucose (carbohydrate) and an artificial saliva, was used to evaluate the materials.

5.4.1. Formulation of an artificial saliva.

Saliva is a complex solution made up from ionic and organic components which varies between individuals. The use of natural saliva is impossible as collecting a few hundred millilitres, sterilising and then keeping it free from micro bacterial or fungal growth

makes this problematic and hazardous. There are many artificial saliva's available commercially for clinical use, these are typically used to relieve problems associated with a dry mouth, particularly when the patient is using dentures. Such salivas have been used for in vitro testing of dental materials, but there is a wide range available and the formulations are unknown. Comparison of the behaviour of orthodontic elastomeric chains (used in some orthodontic braces) showed different behaviour in the different salivas used (Von Fraunhofer et al, 1992). Hence the effect of these commercial salivas would be difficult evaluate (due to the unknown composition) and may not necessarily reflect the behaviour in vivo. There are also concerns over the long term (over 1 year) viability of such formulations due to the organic elements of the composition. It was therefore decided to formulate an artificial saliva based on literature available.

Shellis (1978) conducted a detailed study on the formulation of an artificial saliva and forms one of the most detailed studies on saliva, and the complete formulation (apart from enzymes) of an artificial saliva. Over 40 components including salts, vitamins and amino acids make up this saliva which seems to behave in a similar way to natural saliva in many ways although Shellis does state that no artificial saliva can duplicate natural saliva in all respects. The key issue therefore is to use an artificial saliva which is similar to natural saliva in the most important aspects. From our understanding of elastomers in water the ionic elements will predominately determine the osmotic potential of the solution, although the lower molecular weight organic elements will also have a influence. The ionic components (particularly the cationic i.e. X^+) would also be responsible for the promotion of oxidation (see section 2.5). The organic components of saliva are going to be responsible for bacterial or fungal growth therefore the absence of such elements would be preferable. It was therefore decided to use a purely ionic composition for the artificial saliva.

A purely ionic composition of a saliva is given by Avidson and Johansson (1985) who used it for testing the galvanic currents between dental amalgams. Söderholm et al (1995) used this formulation for long term testing on the stability of dental composites. It was therefore decided to use this formulation as shown in table 5.7, a small portion of thymol was added to the solution to prevent any microbiological activity. Kazanji and Watkinson (1988) used a similar approach using the inorganic portion of the formulation given by of Shellis's (1978) to study the water uptake of a series of commercial soft lining materials.

Table 5.7. Composition of artificial saliva as used by Avidson and Johansson (1985).

Component	Quantity
KH_2PO_4	2.5 mM/l
Na_2PHO_4	2.4 mM/l
KHCO_3	15 mM/l
NaCl	10 mM/l
MgCl_2	1.5 mM/l
CaCl_2	1.5 mM/l
Citric acid	0.15 mM/l
<u>pH adjusted to 6.7 by NaOH or HCl</u>	

There were however problems with this formulation in practice, in that after mixing (which involved dissolving each element up in a small amount of water before making the total solution) a precipitate appeared in the solution. The identity of this precipitate is unknown, it is felt that this may relate to the water used (distilled and so will contain some ions). What it does mean is the osmolarity of the solution is unknown due to the precipitation of some of the ions from the solution.

5.4.2. Behaviour of PBS based materials in NaCl solutions.

The absorption characteristics of the PBS based materials (PBS1, 2 and 5+) was investigated in a range of NaCl solutions (0.9, 0.45, 0.225 and 0.1125 M). The absorption studies were conducted in the same way under the same conditions as those used for uptake from distilled water as previously detailed. The results of PBS5+ are shown for the first absorption in figure 5.20, with the osmotic solutions showing considerably lower uptake than those from water. The upturn in the latter part of the higher NaCl solutions (particularly the 0.9 M) is attributed to oxidation and will be discussed fully in a later section. The reduction in the water uptake is not surprising bearing in mind the osmotic potential of the solutions used. Similar results are also seen for PBS1 (figure 5.21) and PBS2 (figure 5.22) when these are placed in NaCl solutions. Again the upturns are believed due to oxidation during the absorption process.

Figure 5.20. Water uptake of PBS5+ from NaCl solutions.

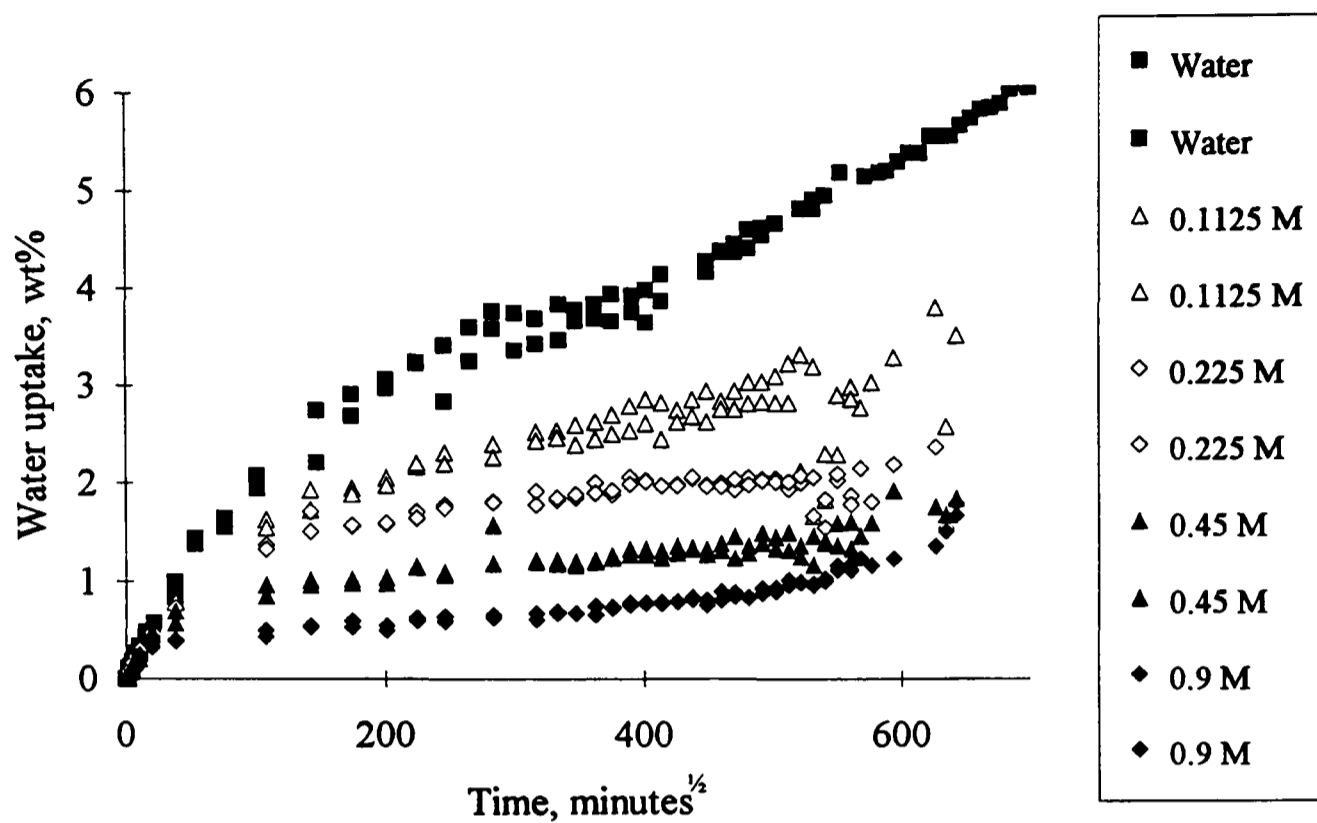


Figure 5.21. Water uptake of PBS1 from NaCl solutions.

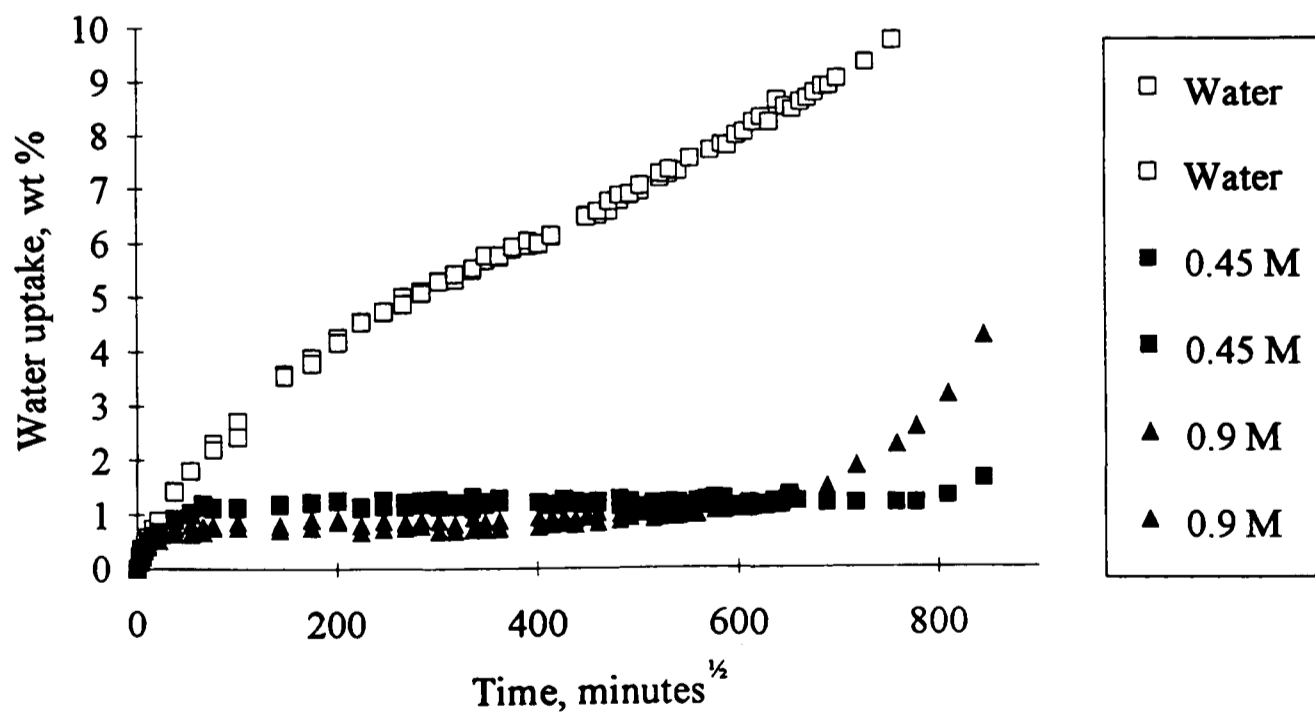
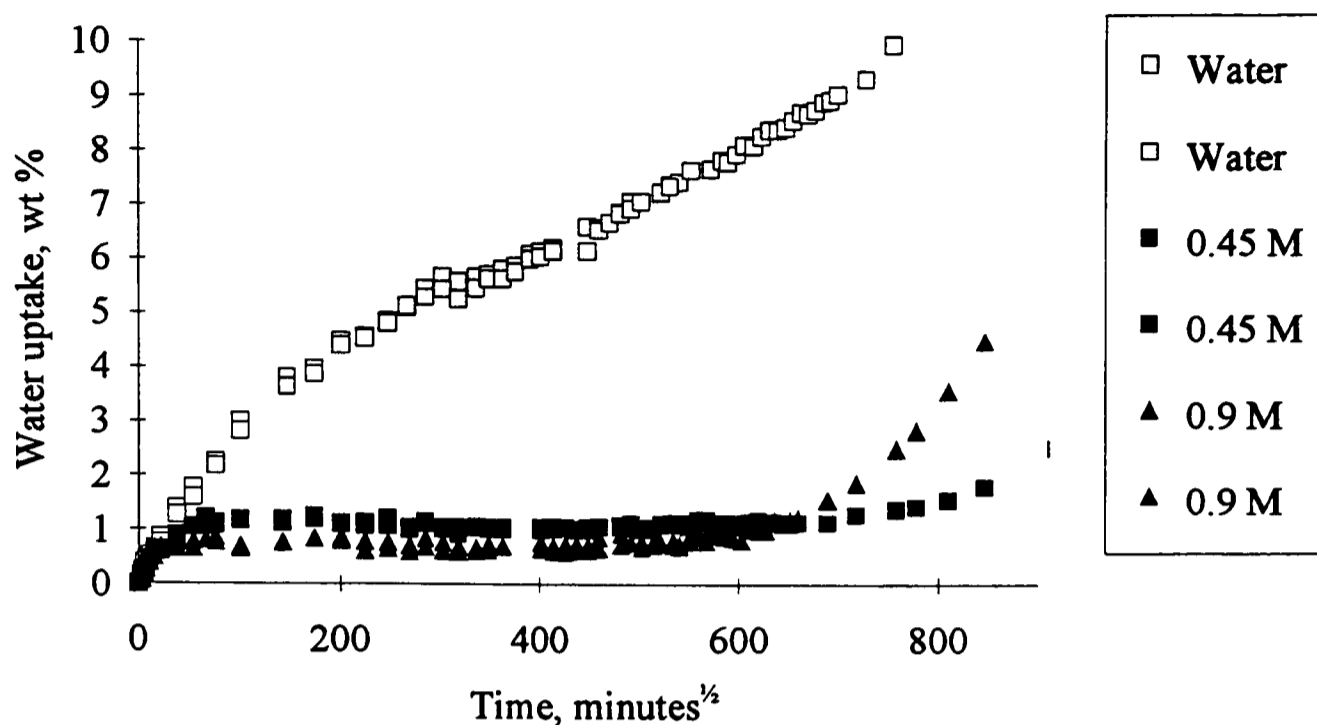


Figure 5.22. Water uptake of PBS2 from NaCl solutions.

The equilibrium seen for the 0.45 M, 0.9 M and 0.225 M prior to the onset of oxidation enables the diffusion coefficient for the absorption to be calculated (as there is a value for M_{∞} before the oxidation). This along with the other relevant data is shown in table 5.8, for PBS5+ and Table 5.9, for the PBS1 and PBS2. This shows that not only does the water uptake decrease with increasing the concentration of the external solution but the diffusion coefficient also increases. This behaviour is predicted by Muniandy and Thomas as previously described with the diffusion coefficient increasing with decreasing concentration. It's worth noting the similarity of the diffusion coefficients in solutions of the same molarity for the HM based materials whereas PBS5+ is somewhat slower. It is also worth noting that the diffusion coefficient obtained for HM is slower than that of EHM (table 5.2), but not for the desorption diffusion coefficients calculated for the PBS system (table 5.6, 5.8, and 5.9).

The solubility of the materials is also interesting as the higher molarity solutions display a negative solubility, a gain in weight during the absorption cycle. There are two possible explanations for this, the first is the diffusion of the salt into the material. Whilst this is possible, and indeed some diffusion will certainly occur, the magnitude of the difference between the solubility of the PBS5+ in water (0.37 wt%) and 0.9 M NaCl (-0.42 wt%) implies that approximately 0.79 wt% NaCl has diffused into the sample (although the leeching is likely to be less in the saline solutions due to the lower uptake). Alternatively the increase in mass is due to the oxidation of the material, due to the addition of oxygen

to the polymer during the oxidation process. This seems the most likely and will be returned to in light of results presented later.

Table 5.8. Summary of absorption data of PBS5+ from NaCl solutions.

NaCl, moles	Uptake, wt%	Solubility, wt %	D_{des} , m^2s^{-1}	Total, wt%	days,	Equilibrium, wt%,	Equ.	D_{abs} , m^2s^{-1}
Water	4.89	0.37	3.28×10^{-10}	5.26	196	5.27	No	-
0.1125	2.95	-0.13	1.27×10^{-9}	2.81	218	2.82	No	-
0.225	2.07	-0.12	1.20×10^{-9}	1.95	91	1.97	Yes	4.58×10^{-11}
0.45	1.47	-0.30	1.72×10^{-9}	1.18	28	1.01	Yes	1.32×10^{-10}
0.9	1.14	-0.42	2.66×10^{-9}	0.72	28	0.52	Yes	2.62×10^{-10}

Table 5.9. Summary of absorption of PBS1 and PBS2 from NaCl solutions.

NaCl, moles	Uptake, wt%	Solubility, wt %	D_{des} , m^2s^{-1}	Total, wt%	days,	Equilibrium, wt%,	Equ.	D_{abs} , m^2s^{-1}
PBS1								
Water	7.33	0.25	3.00×10^{-10}	7.58	196	7.58	No	-
0.45	1.27	0.21	1.32×10^{-9}	1.29	28	1.23	Yes	2.42×10^{-10}
0.9	1.10	-0.39	2.06×10^{-9}	0.70	28	0.91	Yes	7.29×10^{-10}
PBS2								
Water	7.39	0.31	3.16×10^{-10}	7.70	196	7.70	No	-
0.45	1.14	0.15	1.26×10^{-9}	1.29	28	1.12	Yes	1.39×10^{-10}
0.9	0.99	-0.17	1.42×10^{-9}	0.83	28	0.87	Yes	6.68×10^{-10}

5.4.3. Behaviour of PBS5+ in other solutions.

PBS5+ was placed in glucose solutions and the results (figure 5. 23 and table 5.9) show a similar trend as observed with NaCl solutions, with the water uptake decreasing and the absorption diffusion coefficient increasing as osmolarity rises. It should be noted that there is no upturn in the water uptake due to oxidation as previously seen during the latter stages of the absorption. The result for artificial saliva are somewhat surprising showing a higher uptake than that from the water (figure 5. 23 and table 5.9), although in the latter stage it does drop off and lose water, it is also slightly less than the sample in deionised (rather than distilled) water. The reason behind the use of deionised water is primarily to investigate the role of ions during the oxidation process, (as indicated by the

oxidation of the NaCl samples but not the glucose samples) which will be discussed later. The differences between these samples in water may be due to differences in the material as the sample placed in the distilled water was made from a different batch of the material than the other samples which may explain the discrepancy.

Figure 5.23. Water uptake of PBS5+ from different solutions.

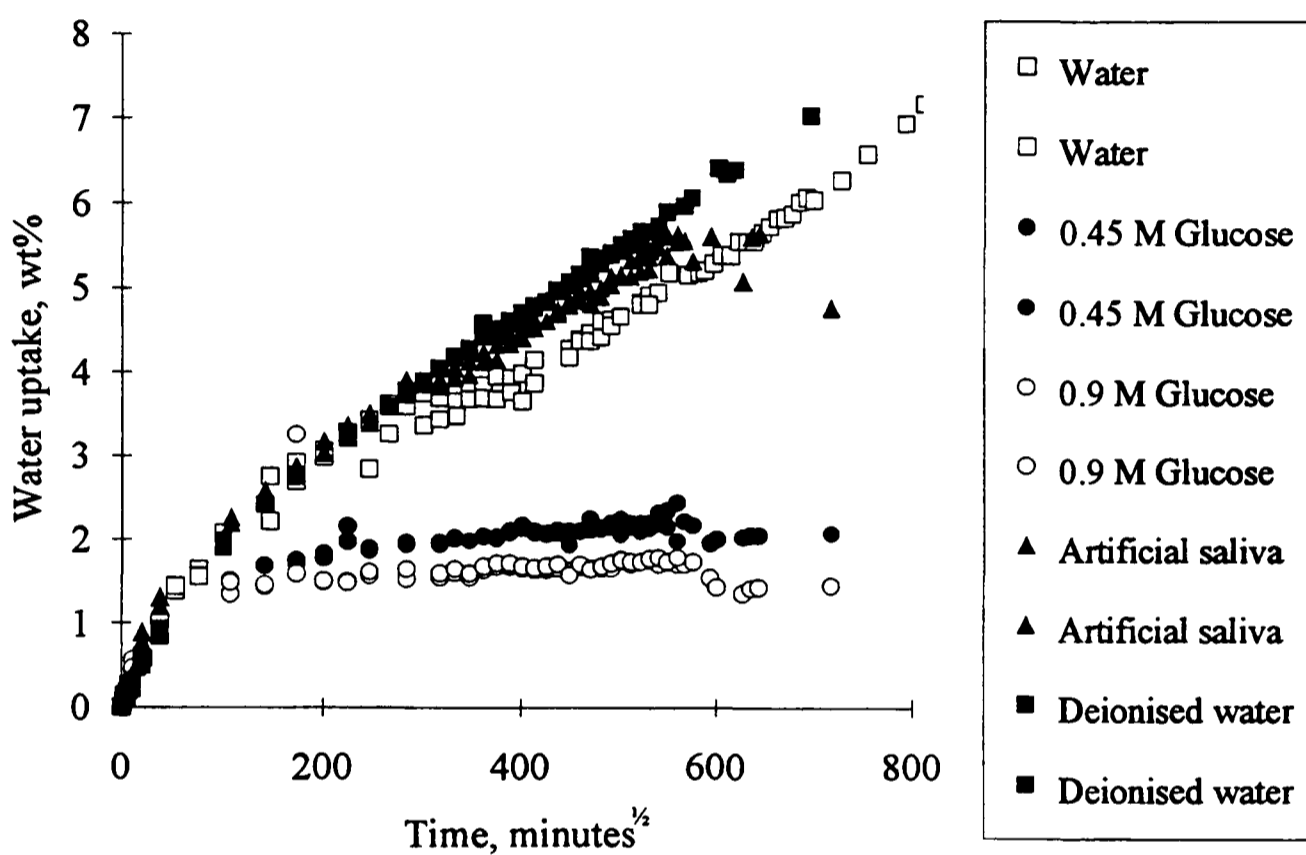


Table 5.10. Summary of absorption data of PBS5+ from different solutions.

Solution	Uptake, wt%	Solubility, wt %	D_{des} , m^2s^{-1}	Total, wt%	days,	Equilibrium wt%,	Equ. D_{abs} , m^2s^{-1}
Water	4.89	0.37	3.28×10^{-10}	5.26	196	5.27	No -
0.45 M Glucose	2.26	0.00	7.92×10^{-10}	2.26	91	2.04	Yes 4.43×10^{-11}
0.9 M Glucose	1.76	-0.05	7.22×10^{-10}	1.70	91	1.67	Yes 7.44×10^{-11}
Artificial Saliva	5.63	0.02	6.54×10^{-10}	5.64	218	5.63	No -
De-ion. Water	5.77	0.44	5.58×10^{-10}	6.20	218	5.76	No -

5.5. Osmotic pressure and the small strain theory.

The behaviour of the PBS materials in osmotic solutions (NaCl and glucose) enables a considerably more in-depth approach to the understanding the absorption process. The PBS system contains a proportion of an unknown soluble agent and (in the osmotic solutions) behaves in a manner as predicted by formation of droplets within elastomers. There is, however, insufficient information (molecular weight of impurity, density of impurity etc.) to be able to utilise these equations. The development of a simplified version to enable the application these theories to practical experimental systems is therefore beneficial. This is achieved by assuming the deformation around the droplet is small i.e. only subject to a small strain.

5.5.1. Small strain theory for droplet formulation.

The development of the small strain theory from those previously seen in section 2.3.5. basically involves the application of the constraint that the droplets are only subject to a small strain, at such strains the extension ratio, λ , is equal to $1 + \varepsilon$ where ε is the strain. This constraint does restrict the applicability of the equations but does enable the solving of the osmotic balance at equilibrium ($P = \pi_i - \pi_o$), using,

$$c_w - s = c_i (\lambda^3 - 1) \frac{\rho_w}{\rho_i} \quad \text{Equation 5.1.}$$

Which is re written in terms of ε , as,

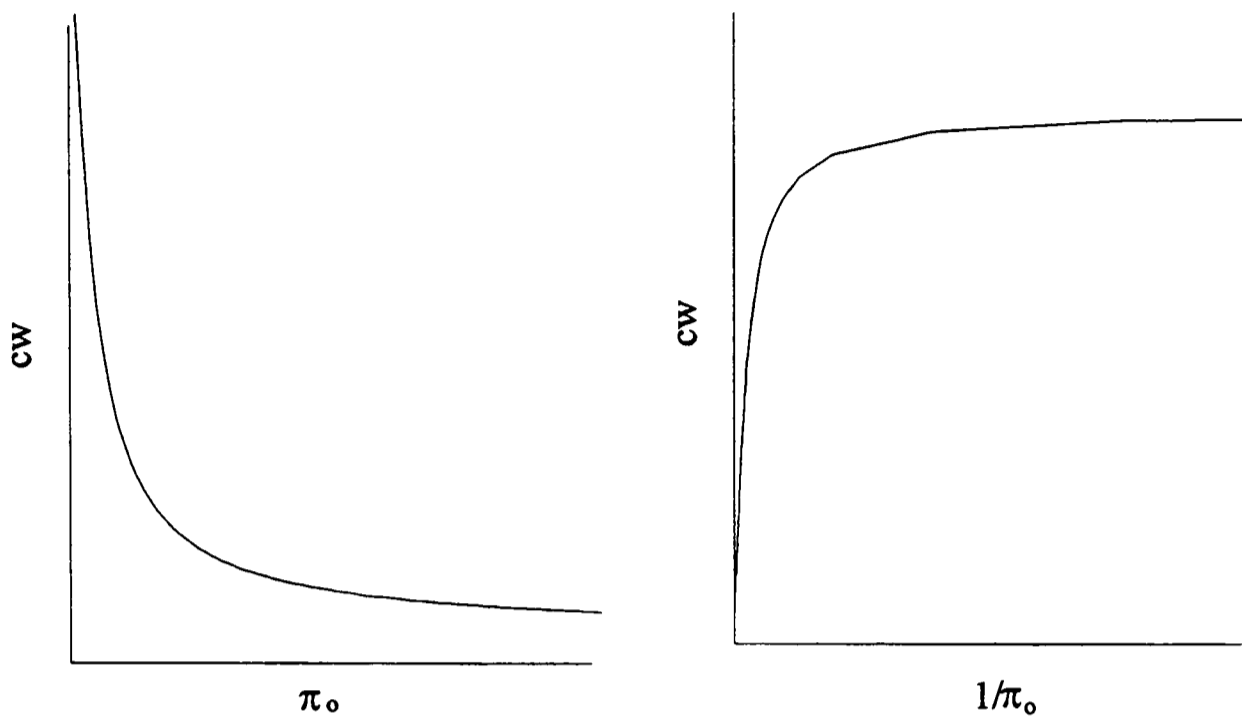
$$c_w - s = c_i \left((1 + \varepsilon)^3 - 1 \right) \frac{\rho_w}{\rho_i} \quad \text{Equation 5.2.}$$

With the assumption that values of ε^x will be insignificant compared to ε , which is reasonable considering the constraint imposed on the process is that small strains apply, it can then be shown (appendix V) that,

$$c_w = \frac{3c_i \rho_w \pi_o}{8G\rho_i} \left\{ \left[1 + \frac{16RTG\rho_i}{3M_i \pi_o^2} \right]^{\frac{1}{2}} - 1 \right\} + s \quad \text{Equation 5.3.}$$

Which is graphically represented in figure 5.24, and shows a linear dependence on $1/\pi_o$ during the initial period and a strong dependence on the osmolarity of dilute solutions.

Figure 5.24. Graphical representation of equation 5.3.



The accuracy of this equation 5.3, in comparison with the full theory (equation 5.1, and 5.4) is illustrated in figure 5.25, the data being that of H974 CS. The experimental figure for c_w is 8.847 kg m^{-3} whereas the value calculated using the full theory is 15.59 kg m^{-3} and for the small strain version 10.266 kg m^{-3} . Both of the calculated values predict that the material should absorb 8.847 kg m^{-3} when the osmotic pressure of the external solution is between 290,000-310,000 Pa (approximately 0.12 moles of NaCl) depending on how it is calculated.

$$\frac{G}{2} \left(5 - \frac{4}{\lambda} - \frac{1}{\lambda^4} \right) = \frac{c_i RT \rho_w}{(c_w - s) M_i} - \pi_o \quad \text{Equation 5.4.}$$

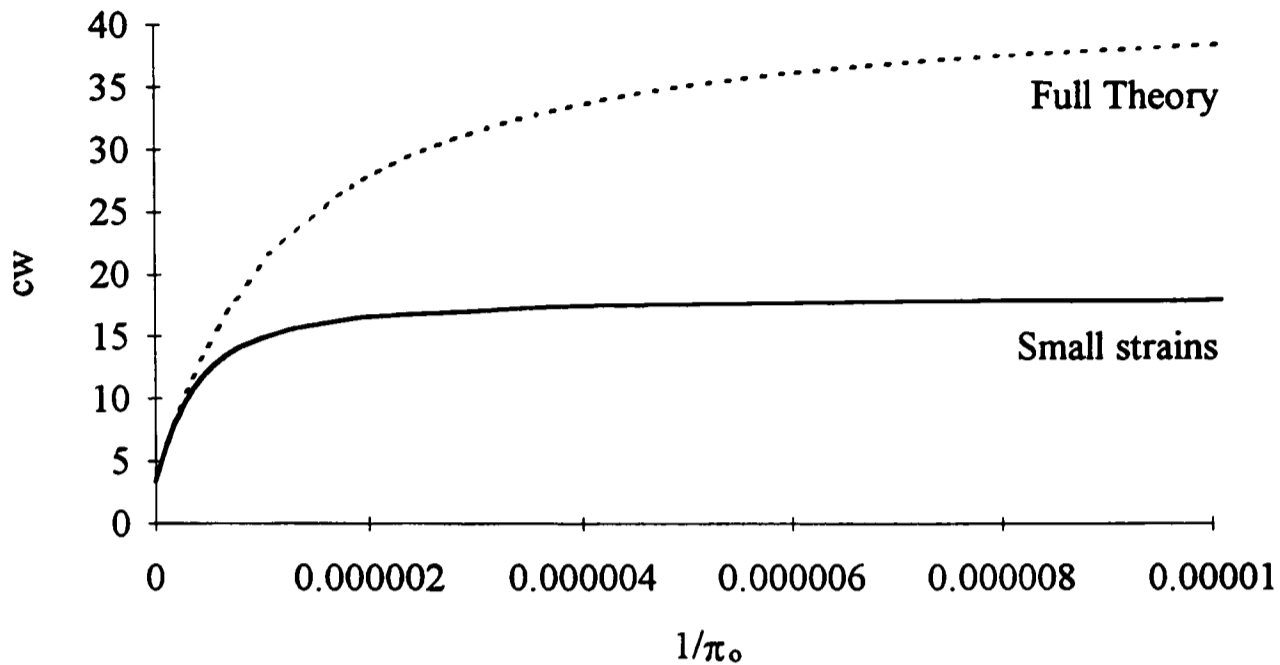
This small strain approach may be further developed to consider the boundary conditions i.e. concentrated osmotic solutions and dilute solutions to predict the limits of the absorption. The first condition used is when π_o tends to zero (i.e. infinite dilution's) then

$\frac{16RTG\rho_i}{3M_i\pi_o^2}$ becomes much greater than 1 hence we ignore the first term of equation 5.3,

which can then be shown (appendix V) to be equal to,

$$c_w = \frac{c_i \rho_w}{2} \left[\frac{3RT}{M_i G \rho_i} \right]^{\frac{1}{2}} + s \quad \text{Equation 5.5.}$$

Figure 5.25. Small strain theory in comparison with predicted values of c_w from small strains theory equation 5.3, and the full theory i.e. equations 5.1. and 5.4.



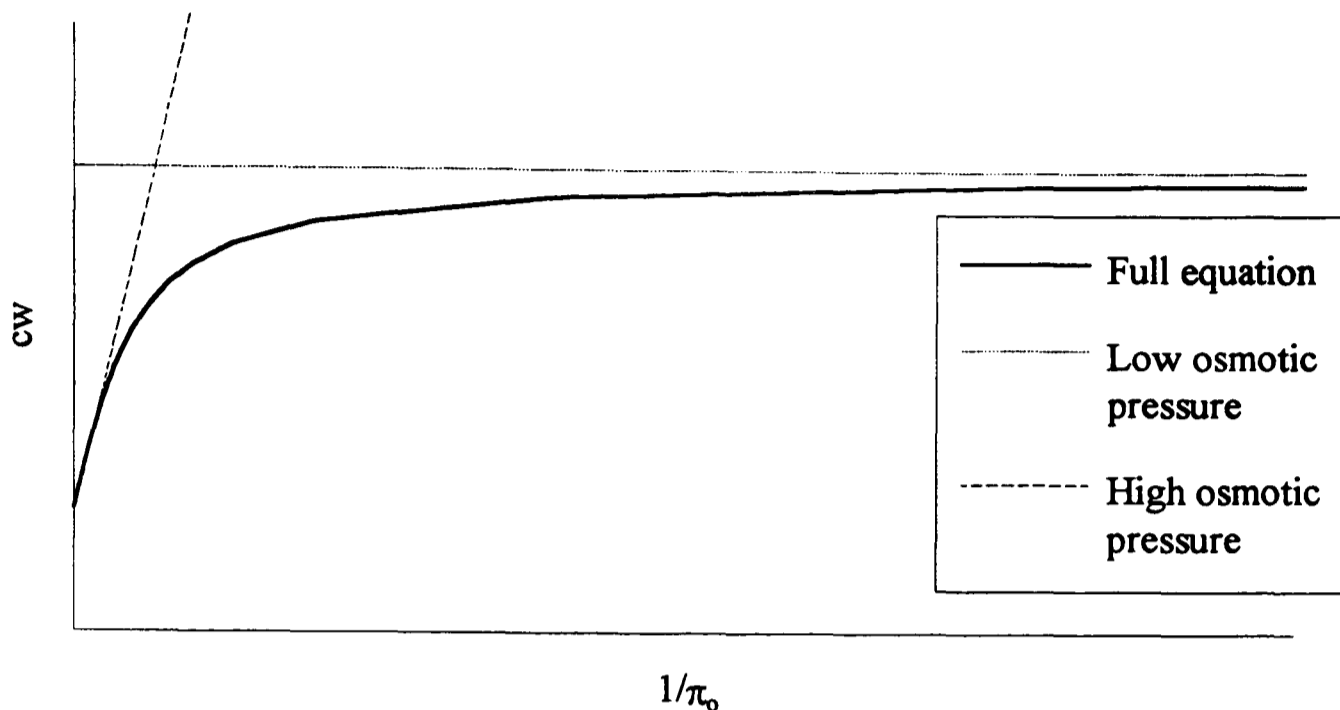
Alternatively if π_o tends to high osmotic pressure then $\frac{16RTG\rho_i}{3M_i\pi_o^2}$ becomes very small

(i.e. $\ll 1$), then equation 5.3, may be expanded by a rational index which is approximated to the first term (appendix V) so,

$$c_w = \frac{RTc_i\rho_w}{M_i} \frac{1}{\pi_o} + s \quad \text{Equation 5.6.}$$

Figure 5.26, illustrates this breakdown of equation 5.3, into equation 5.5 and 5.6, showing excellent agreement with equation 5.6, from high π_o solutions. This is the same region that showed the best agreement with the normal unconstrained approach as shown in region (5.25).

Figure 5.26. Comparison of equation 5.3, 5.5 and 5.6, for predicting the c_w dependence on π_o .



5.5.2. Application of the small strain theory to the PBS based materials.

Small strain theory predicts that c_w should show a linear dependence on $1/\pi_o$ at high osmolarity, figure 5.27 and table 5.11, demonstrates this dependence for PBS5+. The osmolarity of the 0.1125 M NaCl is insufficient to show this linear dependence and non-equilibrating. The 0.9 M glucose solution illustrates another factor as it is believed that the glucose at this high level does not go fully into solution hence uptake is higher than might be expected. The linearity of this data for the 0.9, 0.45, 0.225 M NaCl and the 0.45 M glucose indicates that the small strain theory most notably the high concentration version should apply (equation 5.6). Table 5.13, gives this calculated data with the s being 0.024 kg m^{-3} or 0.025 wt% which it should be said seems low bearing in mind the values of the absorption of EHM (0.51 wt%).

The data for the HM based materials is shown in table 5.12, which is used to calculate the variables shown in table 5.13. The values of these HM based materials are somewhat different, with s being 5.75 or 6.16 kg m^{-3} these compare very favourably to the value which is estimated from the hydrogen bonding component of the solubility parameter (δ_h) shown in figure 5.6, (approximately 0.6 wt%). The molecular weight of the separating

agent impurity (M_i) shows a similar disparity with that calculated for the PBS5+ being less than the PBS1 and PBS2. The correlation of these regressed lines is shown in figure 5.28, by regressing all the points for all the materials. A further set of data is obtained with an s value of 5.04 kg m^{-3} and also agrees with the 0.1125 M NaCl , PBS5+ sample. Initially this combination data seems more attractive as the s of the EHM is now close to that would be expected.

Figure 5.27. PBS5+ equilibrium uptake from different solutions.

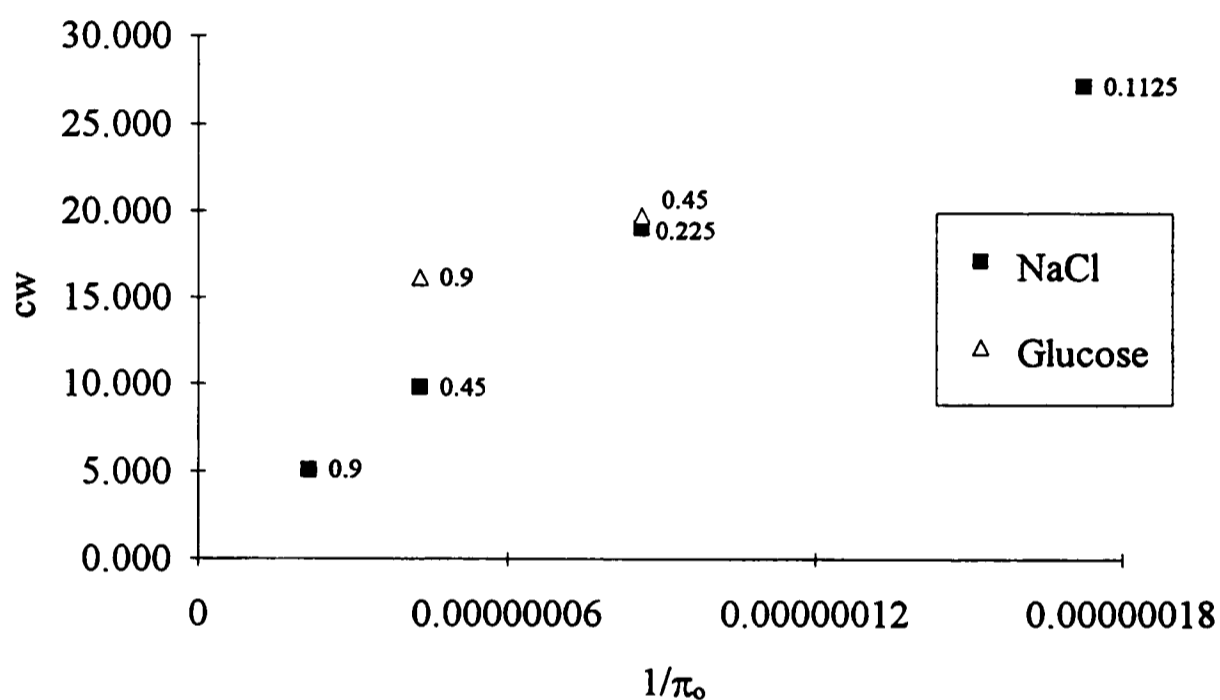


Table 5.11. Summary of PBS5+ data from different solutions.

Solution	c_o , kg m ⁻³	π_o , Pa	Value at, Days	c_w , kg m ⁻³	Equilib- rium.	D_{abs} , m ² s ⁻¹
Water	0	0	196	51.21	No	-
0.1125 M NaCl	0.66	5799015	218	27.16	No	-
0.225 M NaCl	1.31	11598030	91	19.67	Yes	4.58×10^{-11}
0.45 M NaCl	2.63	23196060	28	9.58	Yes	1.32×10^{-10}
0.9 M NaCl	5.26	46392120	28	5.08	Yes	2.62×10^{-10}
0.45 M Glucose	8.11	11598030	91	19.62	Yes	4.43×10^{-11}
0.9 M Glucose	16.21	23196060	91	16.18	Yes	7.44×10^{-11}
Artificial Saliva	-	-	238	54.85	No	-
De ion. water	0	0	238	60.28	No	-

Using the density of 972.05 kgm^{-3} .

Table 5.12. Summary of PBS1 and PBS2 data from different solutions.

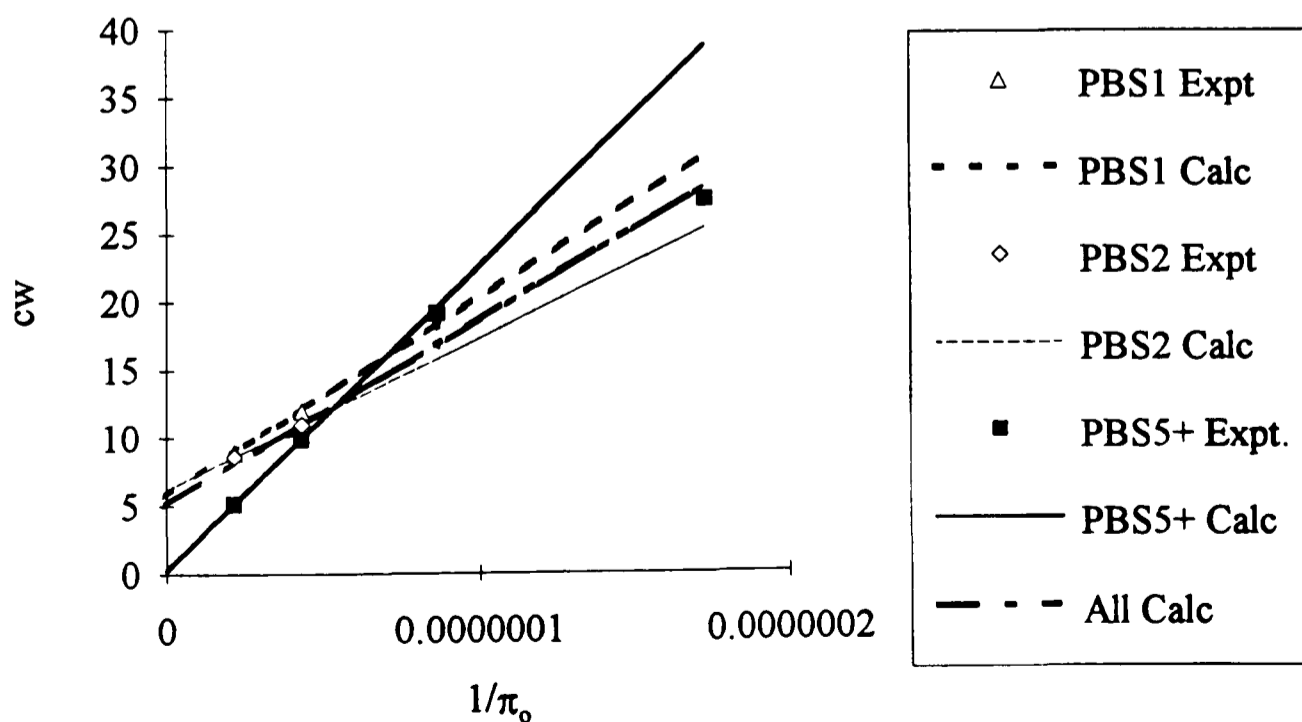
Solution	c_o , kg m ⁻³	π_o , Pa	Value at, Days	c_w , kg m ⁻³	Equilb- rium.	D_{abs} , m ² s ⁻¹
PBS1						
Water	0	0	196	73.65	No	-
0.45 M NaCl	2.63	23196060	28	11.95	Yes	2.42x10 ⁻¹⁰
0.9 M NaCl	5.26	46392120	28	8.85	Yes	7.29x10 ⁻¹⁰
PBS2						
Water	0	0	196	75.48	No	-
0.45 M NaCl	2.63	23196060	28	10.95	Yes	1.38x10 ⁻¹⁰
0.9 M NaCl	5.26	46392120	28	8.56	Yes	6.68x10 ⁻¹⁰

Using the density of 980.21 kg m⁻³ for PBS1 and 976.37 kg m⁻³ for PBS2.

Table 5.13. Values calculated from small strains theory using equation 5.6, from PBS based materials.

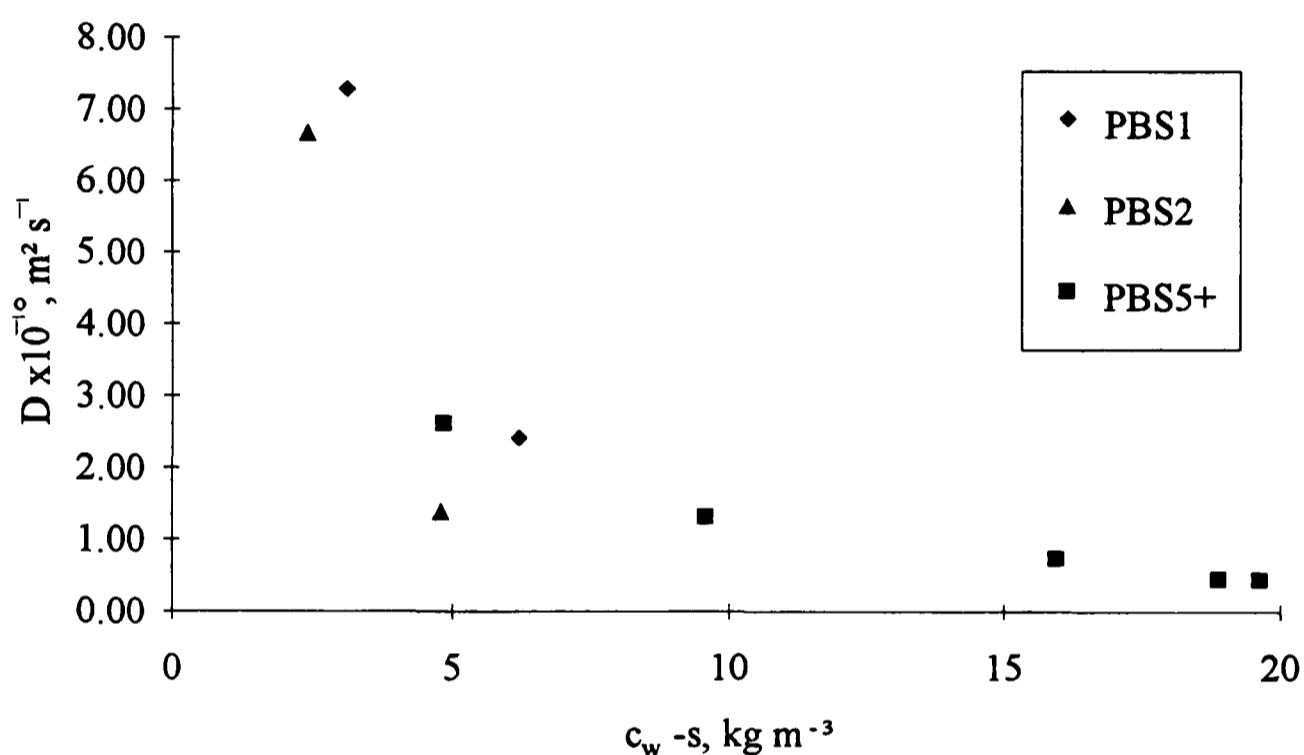
Variable	units	PBS1	PBS2	PBS5+	ALL
ρ	kg m ⁻³	980.21	976.37	972.05	-
c_i^*	kg m ⁻³	8.33	8.30	8.26	8.30
s	kg m ⁻³	5.75	6.16	0.24	5.04
M_i^*	kg mol ⁻¹	0.1483	0.1925	0.0954	0.1577

* Based on the ash from 700°C of 1.7 wt%.

Figure 5.28. Correlation between data and calculated figures.

When the diffusion coefficient is plotted against the concentration of water in the droplets (c_w -s, using the s for the specific material) at equilibrium a clear relationship is seen as shown in figure 5.29. It is worth noting that the 0.9 M glucose is also included in the data as the lower than expected osmolarity won't effect the relationship between water concentration and diffusion coefficient. If this is re-plotted using the s from all the materials there is no relationship apart from within each particular material.

Figure 5.29. Relationship between D_{abs} size of droplets c_w -s.



This relationship may be further explored by plotting the $\log D$ against $\log (c_w$ -s) as seen in figure 5.30, which shows a linear relationship. This relationship is similar to that described by Muniandy and Thomas (1987) as seen in figure 2.15, for the elastic and osmotically restrained region where the full equation applies. A simple linear regression of the linear part of this log relationship for all the PBS materials and the PBS5+ data is shown in table 5.14. Here the equation is of the form of $\log D = \log c + k \log (c_w$ -s) which would relate to the equation $D = c (c_w$ -s) k where c and k are constants. The c corresponds to common factors within Muniandy and Thomas's equation 2.40. and 2.45.

which may be moved outside the factors dependent on λ , (i.e. $c = D_i \frac{Vs_o}{kc_i}$). The k

value however is simply an approximation of this linear region and is used simply as a guide here. The agreement with the data points when the regression is performed on all

the data (PBS1, PBS2 and PBS5+) or that just from the PBS5+ data shows a high level of agreement all with the data points. Table 5.14, gives the values of c and k from this regression and also illustrates the regression of the PBS5+ using $\log c_w$ as opposed to $\log(c_w - s)$, which may be compared to the calculated values based on Barrie's data (1975) and the data of the PBS5+ material, using the assumed density of 1500 kg m^{-3} (which seems a plausible value for an inorganic compound). These calculated values are significantly different to those calculated from the experimental data, most noticeably the k value.

Figure 5.30. Relationship between $\log D$ against $\log c_w - s$.

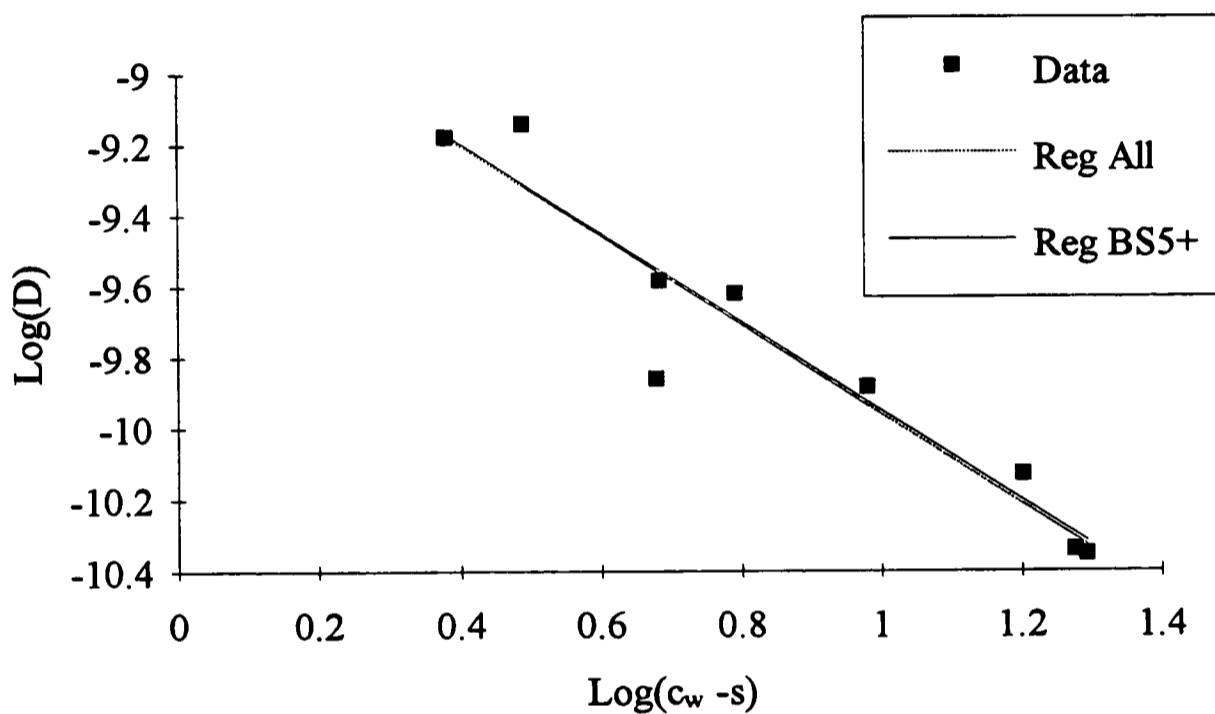


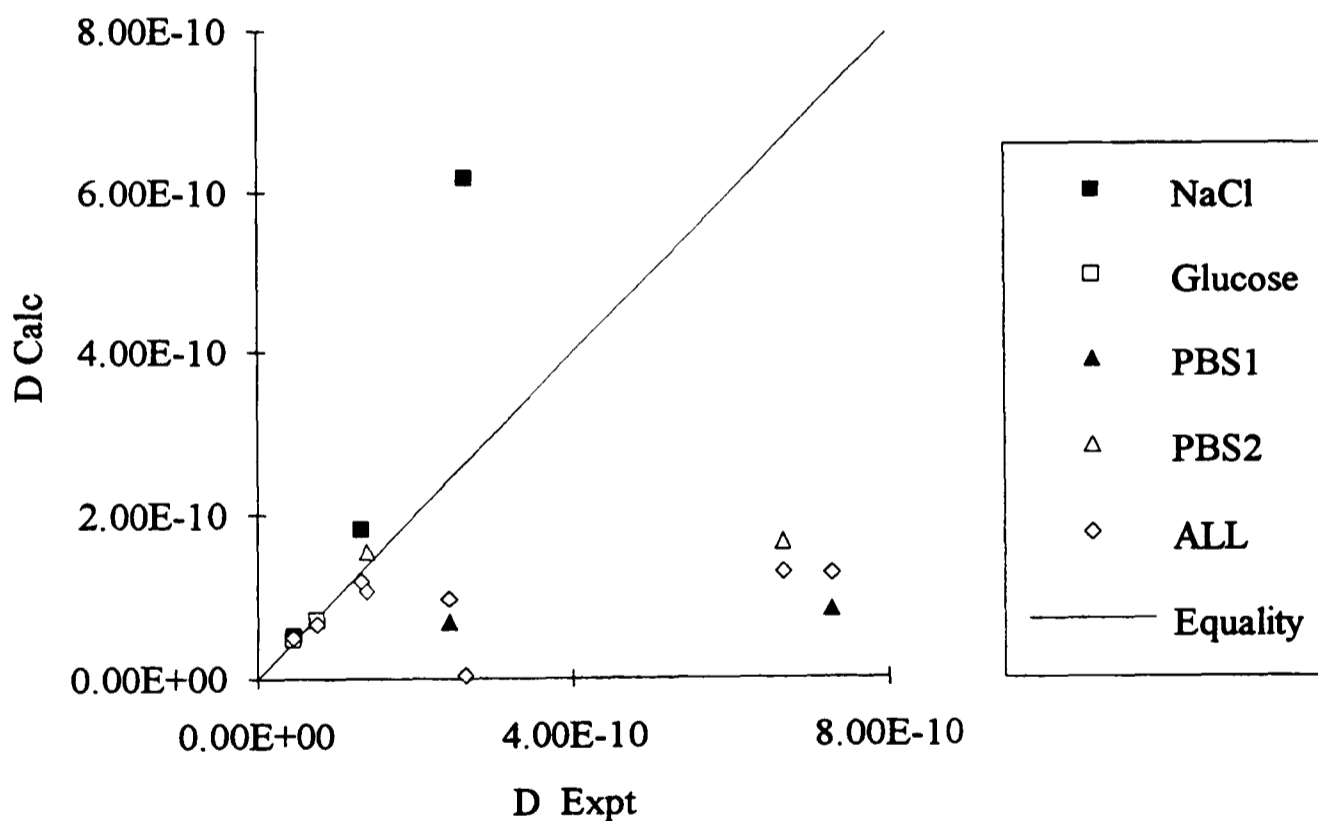
Table 5.14. Regression of \log diffusion coefficient against concentration of water within the polymer.

	Using	Intercept, $\log k$	Gradient, c
ALL	$c_w - s$	-8.693	-1.264
PBS5+	$c_w - s$	-8.688	-1.258
PBS5+	c_w	-8.638	-1.292
<u>Predictions based on,</u>			
Barrie's data	c_w	-10.445	-1.974
PBS5+ data	c_w	-7.866	-1.890

PBS5+ data as previously given and using $G = 1.56 \text{ MPa}$ (based on Mooney Rivlin plots). and an estimated density of 1500 kg m^{-3} . Barrie's data (1975) as used for figure 2.16.

This may also be illustrated by using these figures to calculate values of D_a from Muniandy and Thomas's equation as performed for the H974 CS material in the previous chapter. Here the correlation is shown in figure 5.31, using the data calculated from the small strains theory, and modulus of 0.68 MPa for PBS1, 1.2 MPa for PBS2 and 1.56 MPa for PBS5+ calculated from Moony Rivlin plots. The thermodynamic or inherent diffusion coefficient is taken to be $5 \times 10^{-8} \text{ m}^2\text{s}^{-1}$ which seems a reasonable estimate of the what the diffusion coefficient would be in the pure material based on the desorption diffusion coefficient and the diffusion coefficients for the pure monomers. The graph shows good correlation at small diffusion rates (high uptakes) but not at the lower levels with the diffusion coefficient for the 0.9 M NaCl PBS5+ being over predicted and the HM based materials under predicted.

Figure 5.31. Correlation between the experimental and calculated diffusion coefficients.



The desorption and absorption coefficients of the pure monomers seen in table 5.2, show the diffusion coefficient for HM to be of the order of $10^{-8} \text{ m}^2\text{s}^{-1}$ whereas EHM was $10^{-10} \text{ m}^2\text{s}^{-1}$. This seems to suggest at the low uptake levels (when s is approaching that for the pure monomer) the value tends to the value from monomer. It should be noted if a value of D_T of the order of $10^{-10} \text{ m}^2\text{s}^{-1}$ (as seen for the pure monomer) is used rather than the estimated value of D_i of $5 \times 10^{-8} \text{ m}^2\text{s}^{-1}$ for the PBS5+ data the correlation shown in figure

5.31, is lost completely as the diffusion coefficient calculated is now of the order of 10^{-12} m^2s^{-1} . This seems to imply the relationship described by Muniandy and Thomas breaks down at the lower concentrations as the inherent material properties become dominant. This process seems to indicate a distinct difference in the thermodynamic and observed diffusion coefficient for the elastomer.

Going back to figure 5.30, this seems to be contradictory as the regression is good for all the data of the D_a and c_w -s, Here the gradient (k) differs to that expected from the equation (table 5.14) thus indicating that the actual relationship is flawed. This in conjunction with figure 5.31 implies the Muniandy and Thomas's equation predicts the observed behaviour reasonably well over a range of data but fails to when c_w is small as the kinetics of the absorption process into the pure material are not satisfactorily accounted for in this approach.

Chapter 6.

Development of the Elastomer / Methacrylate Materials.

6.1. Introduction.

The previous chapter described in detail the water absorption characteristics of a series of elastomer / methacrylate materials using the PBS elastomer which contained a separating agent. This separating agent acted to form droplets inside the material and drive the water uptake of the materials. Whilst purification of the elastomer is possible (by centrifuging a dilute solvent solution of the elastomer) it would be preferable to obtain an elastomer without this agent added during the production. There are separating agents available which are fairly insoluble, unfortunately these tend to be less effective and have to be added in larger quantities. PVC is one such separating agent which was tried by Dr S.Parker as an alternative but was found to unduly harden the elastomer / methacrylate material.

The PBS elastomer used previously was an emulsion polymerised material which was then ground and separating agent added to prevent agglomeration of the particles. Two groups of elastomers are available without separating agent these are either bulk (or bale) elastomers which, rather than being a powder, are solid uncrosslinked rubbers, or solution (rather than emulsion) polymerised elastomers. These solution elastomers are available as either bales or pellets which do not cluster together as the particles tend to preferentially orient polar groups towards surface.

In order to simplify the evaluation of the elastomers the 5+ (EHM 1% EGDM and 1% lauryl peroxide) 50 % elastomer 50 % monomer liquid formulation was used as a basis. Further formulations with different monomers and crosslinking agents were then used to further evaluate the potential of these elastomers.

6.2. Comparison of different elastomers.

Three different butadiene styrene and one isoprene styrene copolymers were selected as alternatives to the PBS as previously used. One was a 'Hot' emulsion polymerised butadiene styrene supplied by Shell Chemicals Ltd, (S-1013) and is referred to as HBS, the specification is shown in table 6.1. The 'Hot' emulsion process is free radical initiated conducted at around 50 °C and tends to produce a random branched butadiene styrene elastomer (Brydson, 1978). Alternatively, when the polymerisation is performed at 5 °C (known as the 'Cold') a linear material is produced the degree of conversion here is slightly lower at typically 60 % compared to 72 % for the 'Hot' process (Brydson, 1988). The 'Hot' elastomer was chosen for this reason.

Table 6.1. Specification of HBS elastomer, supplied by Shell chemicals Ltd.

Volatile matter, max.	1.0 %
Total ash, max.	0.8 %
Organic acid	3.5-5.5 %
Soap, max.	0.3 %
Bound styrene	41.5-44.5 %
Density	960 kg m ⁻³

The other materials were all solution polymerised (table 6.2). The butadiene styrene co-polymer was supplied by Enichem Elastomers Ltd, (Europrene 1205) as a bale and is referred to as EBS and Shell Chemicals Ltd (Kraton D-1101) as porous pellets referred as SBS. The isoprene styrene co-polymer was also supplied by Shell Chemicals Ltd (Kraton D-1111C) as porous pellets containing 0.2 wt% silica as adjusting agent and is referred to as SIS. The SIS was unfortunately not available without this dusting agent but it was felt that the silica was present at a low level and as it is insoluble should have negligible influence on the uptake. Both of the Shell elastomers have FDA (Food and Drug Administration, of USA) approval for contact with food and have previously been employed in medical devices. The solution polymerised materials were anionically initiated in a solution (hexane) forming partial block copolymers, i.e. for the EBS 17 % of the total 25 % styrene was in blocks, this is due the butadiene preferentially polymerising in the initial stage.

Table 6.2. Specification of EBS, SBS and SIS elastomers, supplied by Enichem elastomeric Ltd and Shell chemicals Ltd.

	EBS	SBS	SIS
Volatile matter, max.	-	0.3	0.3 %
Total extractable, max.	-	1 %	1 %
Silica	-	-	0.2 %
Styrene content	25 wt%	31 wt%	22 wt%
Solution	Hexane	-	-
Antioxidant	0.5 % BHT	1.4% min. BHT	1.4% min. BHT
Initiator	Butyl lithium	Alkyl lithium	Alkyl lithium
Density	-	940 kg m ⁻³	930 kg m ⁻³

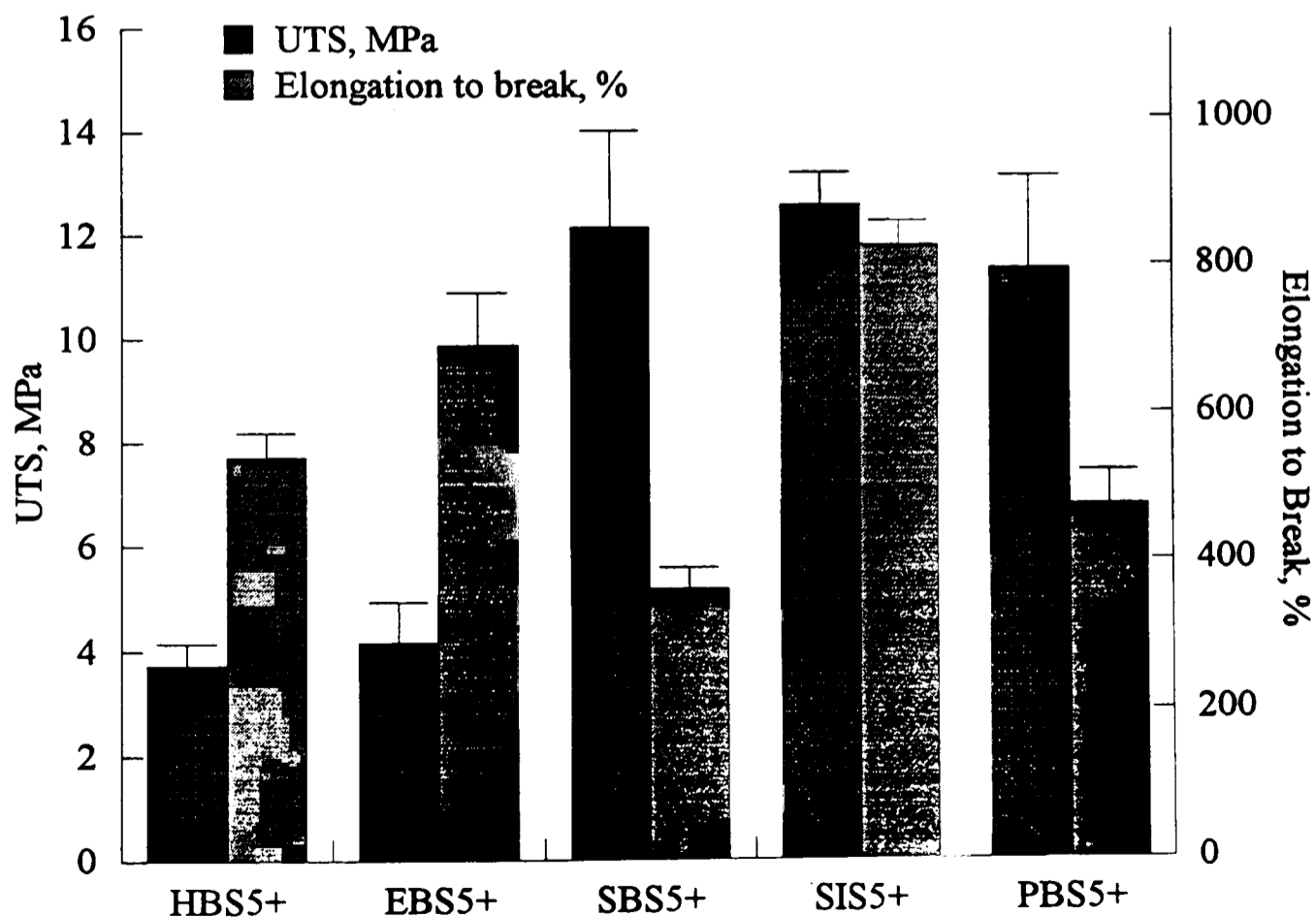
BHT Butadiene hydroxyl toluene (Ionel).

The elastomers supplied came as bales (HBS and EBS) had to be cut into small particles (5 mm^3) in order to be dissolved in the monomer. The porous pellets were approximately 3-5 mm diameter which was small enough to form a gel quite readily with the monomer.

6.2.1 Tensile results from the different elastomers.

Figure 6.1, shows the tensile results for these new elastomers with similar strengths for SBS5+ and SIS5+ to that previously achieved for PBS5+. EBS5+ and HBS5+ were however considerably weaker than PBS5+. The reason for this is unknown as it may relate to the many factors such as additives (inhibitors) added to the elastomer during production or molecular weight of the elastomer, but the susceptibility to grafting of methacrylate to the elastomer or the homogeneity of the material seem most likely as the EBS and HBS have different structures (as the HBS is branched).

Figure 6.1. Strength results for the elastomers.



6.2.2. Water uptake of emulsion elastomer based materials (HBS).

The water uptake of the emulsion polymerised HBS is interesting with differing trends to those seen for PBS, figure 6.2 and table 6.3. HBS5+, as may be expected from the absence of separating agent, shows a lower uptake than PBS5+ and seems to level off indicating the material is reaching equilibrium. A similar picture is also seen for the pure elastomer sample in figure 6.3. The absence of the separating agent gave a lower uptake so the material behaves in a more ideal manner. The level of uptake still seems rather high with an absorption of 3.84 wt%, this is likely to be due to the production process of the elastomer. From table 6.1, we can see that there is a portion of soap and organic acid (3.5 - 5.5 %) listed and this will undoubtedly increase the water uptake. The second absorption of HBS is massively increased over the first and shows no sign of equilibrating (figure 6.4), this is attributed to oxidation of the material as little else seems to be able to account for such a large increase.

Figure 6.2. First absorption of emulsion elastomer based materials.

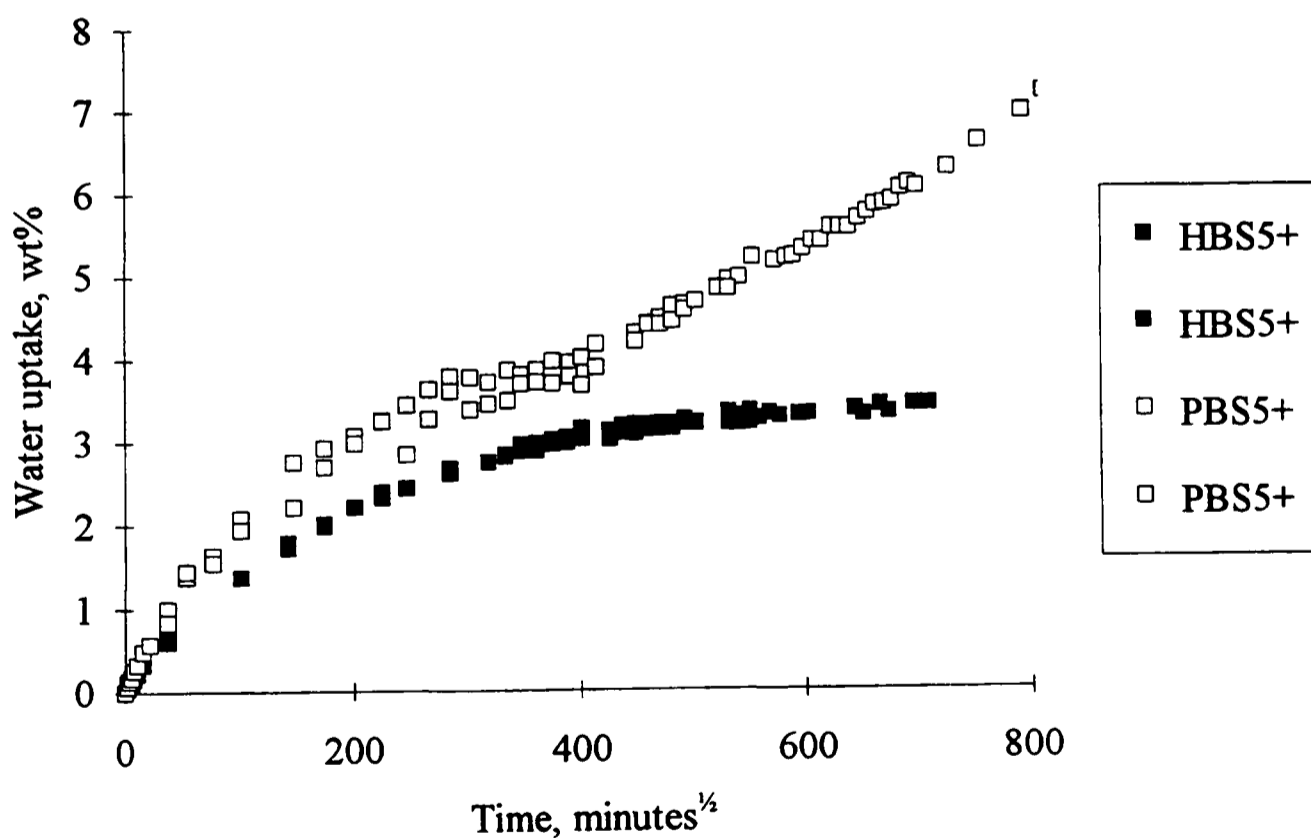


Table 6.3. Summary of water uptake for the elastomer based materials.

Material	Absorption, wt%	Solubility, wt%	At, days	Total Uptake, wt %	D_{des} , m^2s^{-1}	2nd abs, wt %	At, days
HBS5+	3.22	0.62	210	3.84	5.31×10^{-10}	6.70	126
EBS5+	8.71	0.00	203	8.71	3.41×10^{-10}	20.40	238
SIS5+	5.96	0.14	217	6.11	7.69×10^{-10}	4.40	49
SBS5+	11.08	-2.95	217	8.13	-	8.54	49
PBS5+	4.84	0.38	196	5.22	3.28×10^{-10}	16.87	399

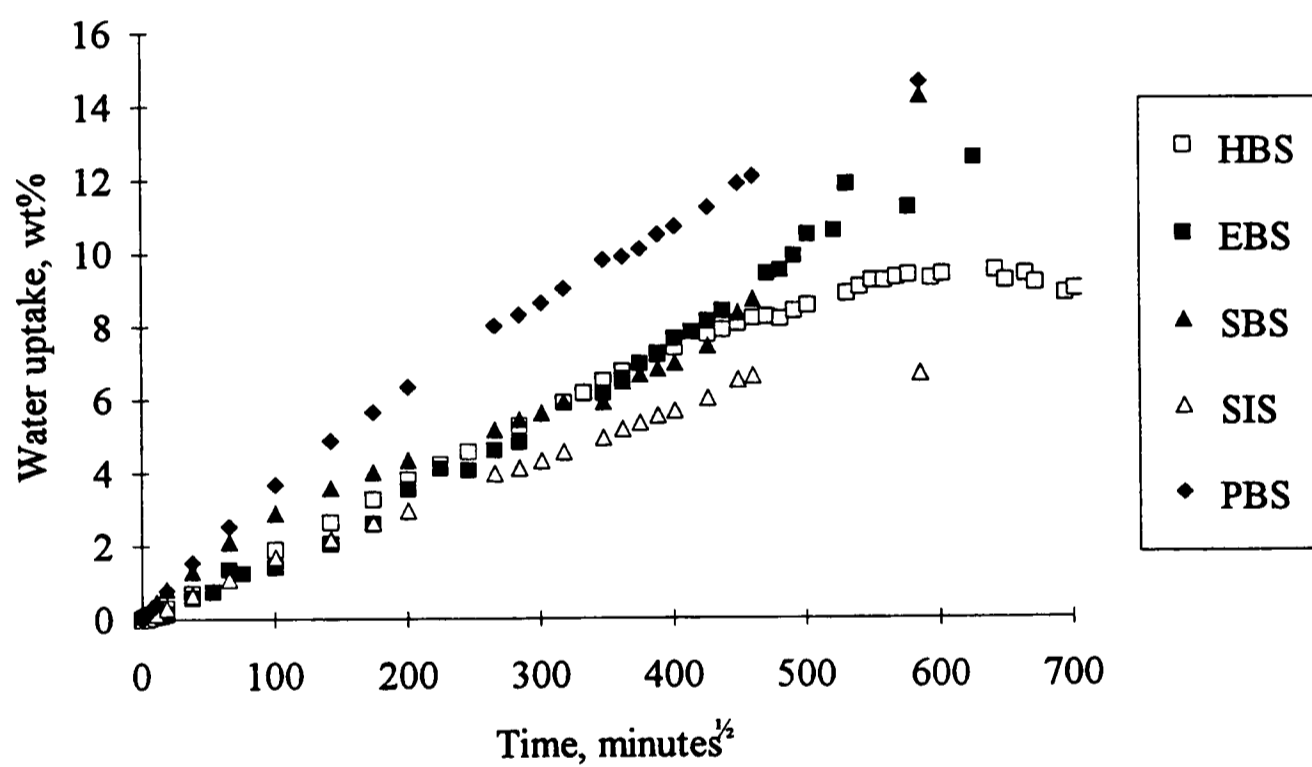
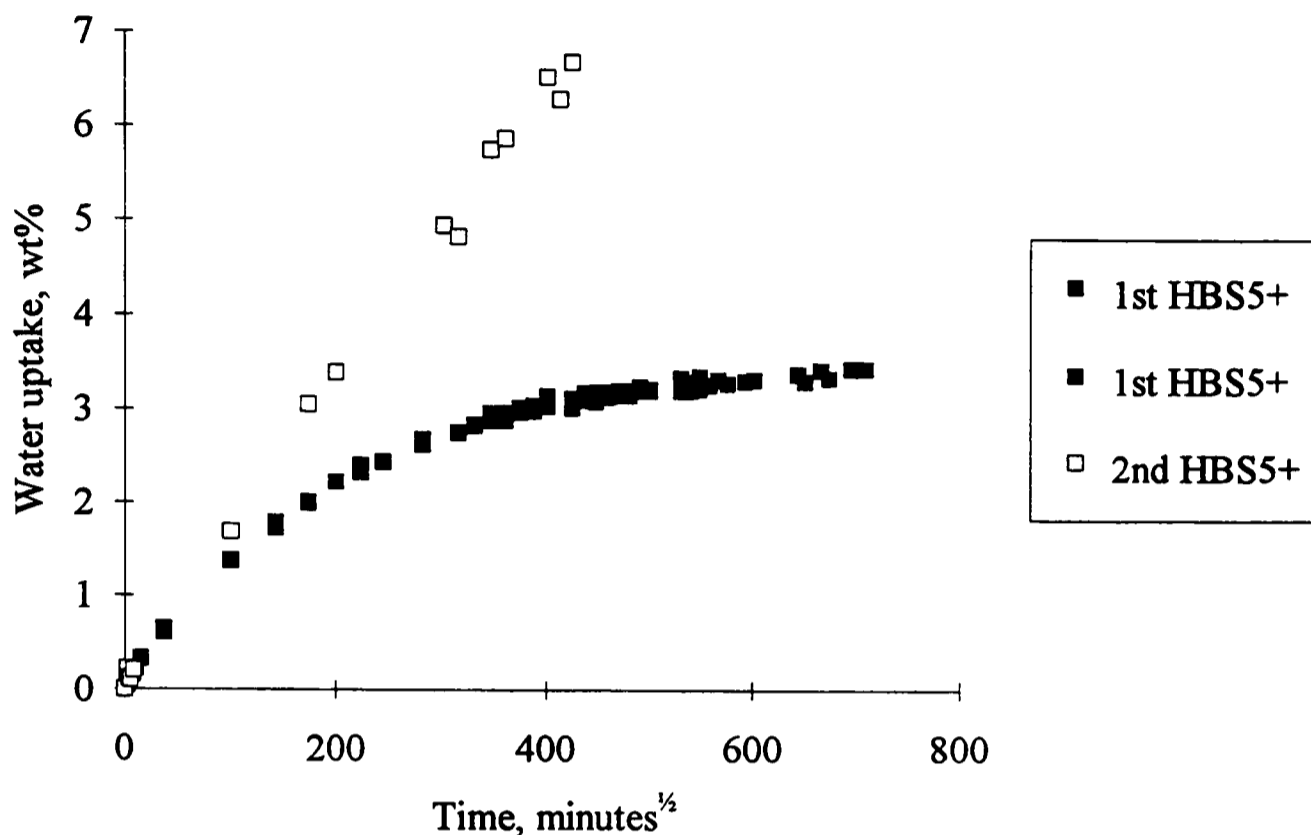
Figure 6.3. Water uptake of the pure elastomers.

Figure 6.4. Comparison of the first and second absorption cycles for the emulsion polymerised elastomer based materials.



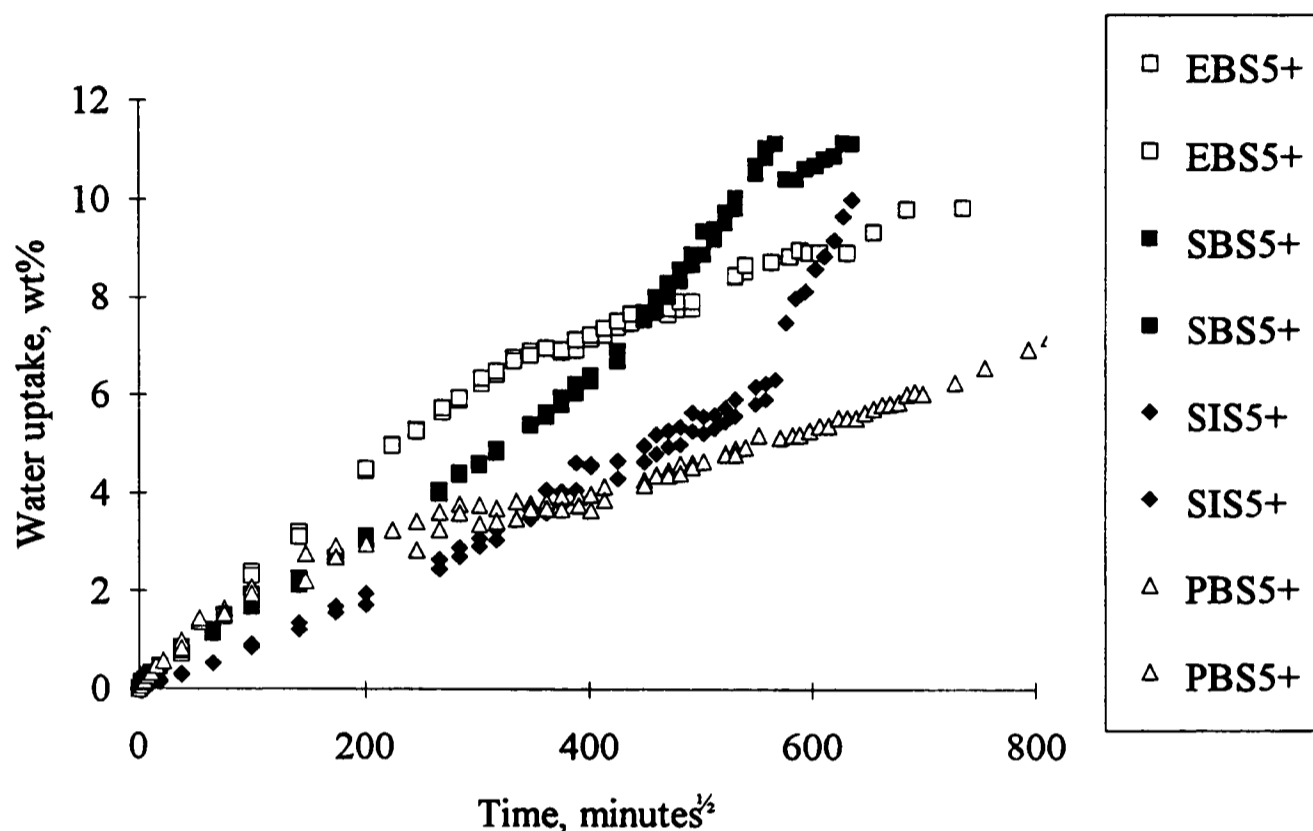
6.2.3. Water uptake of the solution polymerised elastomers.

Water uptakes of the solution polymerised materials is however noticeably different (figure 6.5) as they all show a higher eventual uptake than the PBS5+, although SIS5+ is initially lower. The latter stages when there is an upturn in the water uptake of SBS5+ and SIS5+ is due to oxidation of the elastomer, but the initial uptake and that of the EBS5+ must be due to another factor.

These solution polymerised materials are generally regarded as cleaner (less impurities) than the emulsion polymerised materials as they don't contain the organic acids and impurities introduced during the initiation process. However they are anionically polymerised which will leave active radicals at the chain ends after polymerisation. These are then available to form hydroxyl groups if exposed to water or, perhaps more likely, carboxylic acid if exposed to carbon dioxide. It is the presence of such groups

that prevent the agglomeration of the porous particles of the SBS and SIS in the absence of a separating agent.

Figure 6.5. Water absorption of solution polymerised elastomer based materials.



These carboxylic acid and hydroxyl groups will have an effect on the water uptake. There will be other components within the polymer which may influence the water uptake such as the antioxidant and the initiator (e.g. alkyl lithium compounds such as butyl lithium). It is however felt that the action of these elements which will be present at low levels (under 2 % for the antioxidant, BHT, and much less for the initiator) will be insufficient to account for the water uptake of over 6 % (as they are organic rather than inorganic) observed for the for these materials (which is higher than the PBS5+ material containing the seperating agent). SBS5+ and SIS5+ have is higher proportion of BHT (table 6.2) than EBS5+ yet show a lower uptake. This supports the hypothesis that the BHT is not responsible for this uptake. It is therefore felt that the water uptake for the solution polymerised materials is due primarily to the carboxylic acid and hydroxyl end groups on the elastomer.

The uptake of water into the elastomers was accompanied by opacity, indicating the formation of droplets within the material. In the absence of a satisfactory hydrophilic constituent a clustering of these hydrophilic groups seems the most probable. Such mechanisms have been noted during the literature review. If the groups were acting

independently the uptake would be expected to be uniform and hence the material would remain transparent.

Figure 6.3, shows the uptakes of the cast elastomers, where there are striking similarities between all the elastomers (apart from the later stages where oxidation seems to predominate) except the PBS which shows a slightly higher uptake. This is in contrast to the results of the 5+ samples figure 6.2, and 6.5, where different absorption characteristics are seen for the different materials. This may be attributed to the uncrosslinked nature of the elastomer and the different nature of hydrophilic agents. This seems to imply that the driving force behind the water uptakes are similar, suggesting the restraining force exerted by HBS5+ is superior to EBS5+ (as it shows a lower uptake). The strength results imply this is not the case as EBS5+ exhibits a slightly higher UTS (figure 6.1) so another factor seems responsible. It is impossible to know what is driving the uptake and why they differ but a few points can be made.

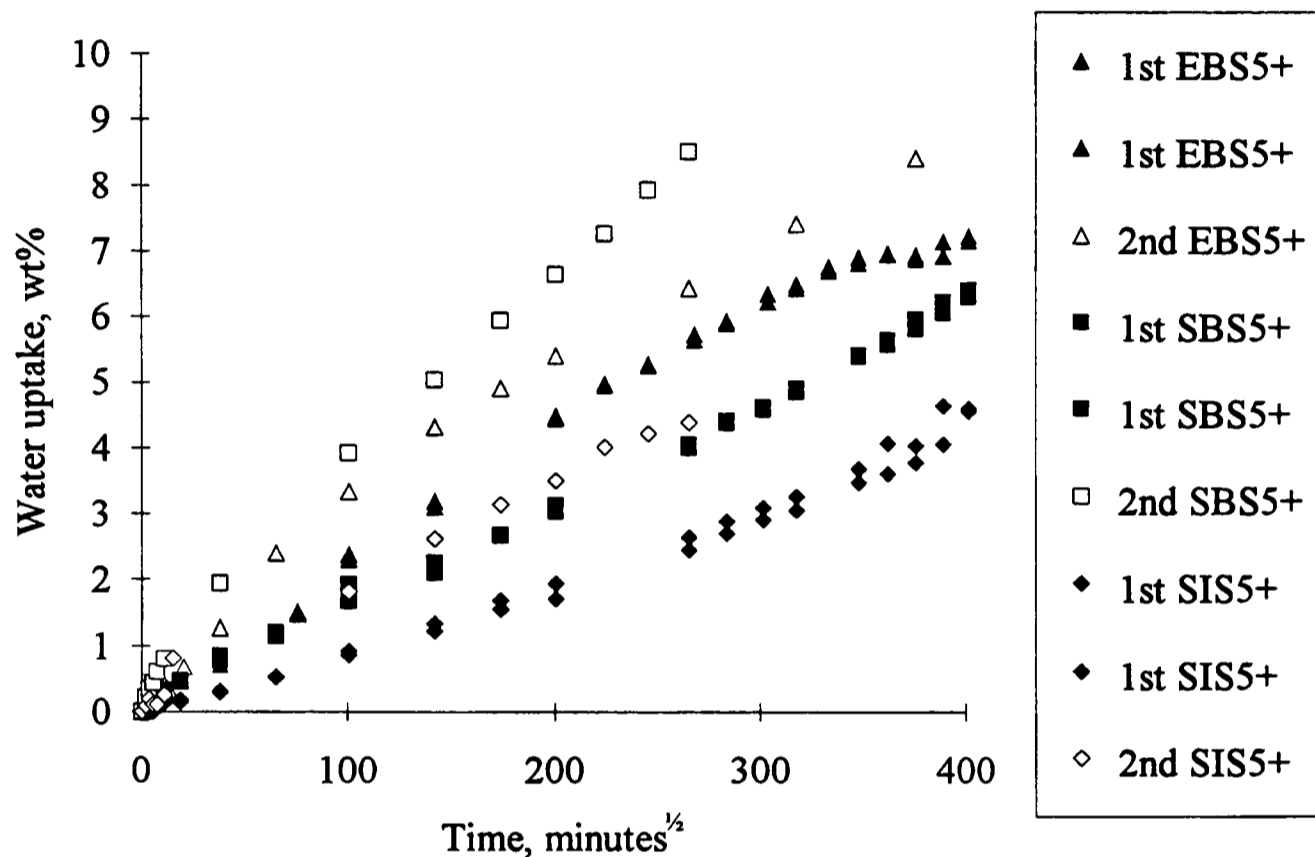
The pure cast elastomers are uncrosslinked and so will flow, whereas the 5+ samples will be slightly cross linked hence should creep less. Stress relaxation will decrease the restraining force and so increase the effective driving force behind the uptake. As the uptake occurs over an extensive period it is likely that the restraining force will be insufficient to prevent the continued growth of the droplets. The absorption will then become more dependent on the rate of transfer of water into the material as the driving force is sufficient to ensure that this rate of ingress is determined by the diffusion coefficient. The nature of the impurity will also be less important as it does not have to overcome the restraining force. It is therefore proposed that HBS5+ contains an impurity which generates a less effective driving force than EBS5+ hence is more readily restrained. When the materials are uncrosslinked this difference is less significant as the absence of an effective restraining force makes the nature of the driving force less important.

A summary of the absorption data for the solution polymerised materials is shown in table 6.3, with EBS5+ and SIS5+ having very low solubilities compared to the HBS5+ and PBS5+. SBS5+ shows an increase in weight after desorption, indeed the weight increases during the desorption cycle with a minimum solubility of -0.85 wt% being indicated. This behaviour seems to be due to oxidation of the elastomer.

The second absorption cycles for these materials, figure 6.6, show the familiar pattern with the water uptake being higher and more rapid. This is due to the deformation

around the droplets which occurred during the first sorption cycle making the growth of these droplets easier. The oxidation of SBS5+ has caused a massive increase in rate and quantity of water absorbed into the polymer due to the hydrophilic nature of the groups produced.

Figure 6.6. Comparison of first and second absorption cycles of solution polymerised elastomers.



6.3. Oxidation of the elastomers.

Elements of the water absorption process have been attributed to oxidation of the materials. Indeed all of the elastomer based materials so far described show some signs of the oxidation process in the different environments although some show a greater resistance than others. In addition to the oxidation process being accompanied by an increased water uptake there was a discolouration (yellow to brown) of the sample, this initially occurred at the edges then slowly moved throughout the sample, a hardening of the material was also observed.

Figure 6.7. Infra red spectra of PBS1 from different environments, range 400 to 2000 cm^{-1} .

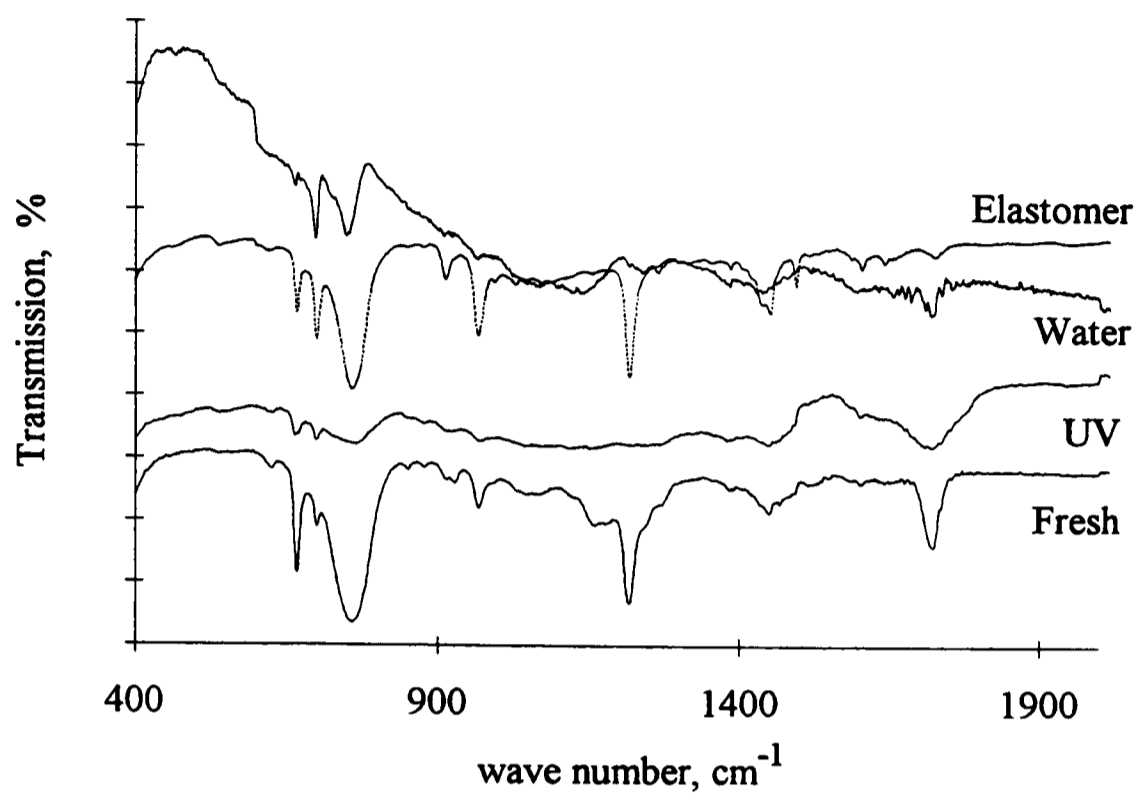
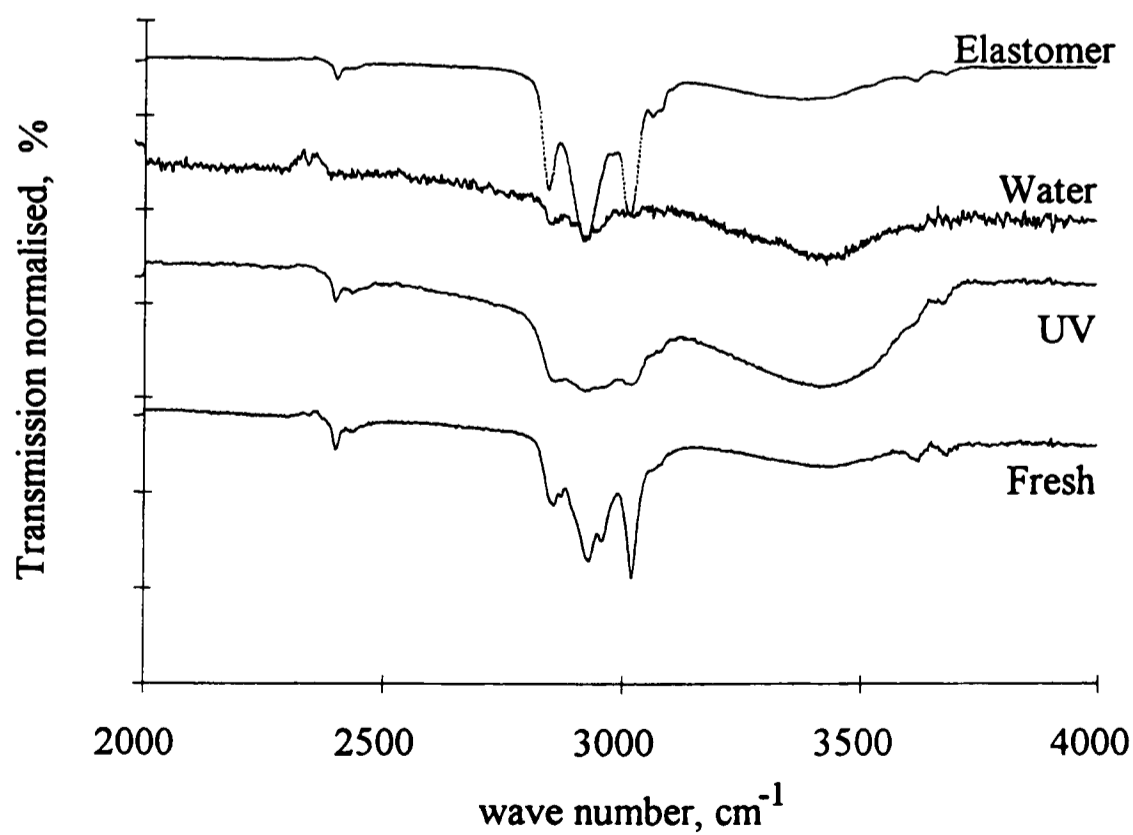
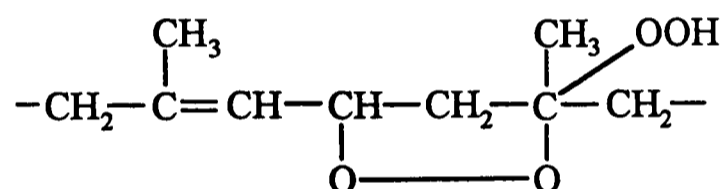


Figure 6.8. Infra red spectra of PBS1 from different environments, range 2000 to 4000 cm^{-1} .



Infra red spectrometry was performed on samples of PBS1 in different states by drying the samples in an oven and then swelling in chloroform so a soft gel was formed. This was then squeezed between potassium bromide plates so a transmission spectra could be produced. Figure 6.7, and 6.8, illustrate the oxidation of PBS1 using infra red spectrometry with fresh PBS1 and the pure elastomer showing a comparatively small broad OH peak at around $3,400\text{ cm}^{-1}$ compared to the UV and sample stored in water. A similar pattern is repeated for the carboxylic peak at around $1700 - 1720\text{ cm}^{-1}$. A problem with these spectra is the absorbance of the material due to clouding of the sample during the absorption process making it difficult to obtain a good spectra.

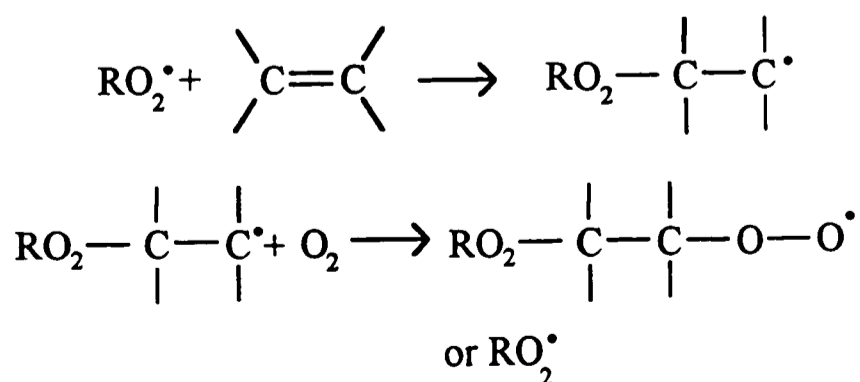
A possible mechanism for the oxidation of butadiene is illustrated in figure 6.9, this would result in crosslinking to the material which would account for the hardening observed but not the increase in the hydroxyl groups seen in figure 6.8. Another mechanism of oxidation of a poly isoprene is also described by Brydson (1978) with forms a diperoxide - hydroperoxide structure seen below, the route to its formation is a little more open to debate with different mechanisms being proposed.



A combination of different oxidation reactions seems the most likely explanation of what occurs with the butadiene styrene and isoprene styrene materials with the formation of crosslinks and hydrophilic groups which drive the water uptake into the materials.

SBS5+ was chosen to study the role of the external environment on the oxidation process as it displays the greatest tendency to oxidation from distilled water (table 6.3).

Figure 6.9. Oxidation of butadiene, as illustrated by Brydson (1978).



6.3.1. Oxidation of SBS from different environments.

Water uptake of SBS5+ in different saline solutions (figure 6.10, and 6.11) show a similar trend to that of the PBS based materials described in 5.4.2., with absorption decreasing with osmolarity prior to the onset of oxidation. This is quite an interesting result as it indicates that the clustering behaviour of SBS is dependent on the osmolarity of the external solution, the clusters having a chemical potential associated with them.

The actual oxidation in the saline solution occurs first for the 0.9 M NaCl solution then the 0.45 M with the 0.225 M and 0.1125 M remaining unoxidised. Table 6.4, confirms this with the 0.9 M and 0.45 M showing an increase in weight during absorption which further increases during the desorption process, as seen in distilled water, whereas the 0.225 M and 0.1125 M do not. This seems to imply that the oxidation is dependant on two interrelated factors, the ionic concentration and water uptake in the material with a certain water uptake being required for the oxidation which decreases as the osmolarity increases. The increase in weight is due to the combining of oxygen into the polymer increasing the mass, the increase observed during desorption indicates the weight gain is due oxidation and that the radicals formed during absorption are active.

Table 6.4. Summary of water absorption data for SBS5+ in different solutions.

	Abs., wt%	At, days	Sol., wt%	Min. Sol., wt%	Abs	D_{des} , m^2s^{-1}	2nd abs, wt%	At, days
Water	11.08	217	-2.95	-0.85	8.13	-	8.54	49
De Ionised	3.85	203	0.29	-	4.14	6.24×10^{-10}	5.71	112
0.1125 M NaCl	2.04	203	0.41	-	2.45	7.66×10^{-10}	2.75	112
0.225 M NaCl	1.53	203	0.41	-	1.93	1.13×10^{-9}	1.74	112
0.45 M NaCl	6.80	189	-7.66	-3.75	-0.86	-	3.91	147
0.9 M NaCl	5.68	189	-7.11	-3.59	-1.42	-	3.53	89
Artificial Saliva	11.49	218	-1.84	-0.92	9.65	-	16.10	216

Figure 6.10. Water uptake of SBS5+ in NaCl solutions.

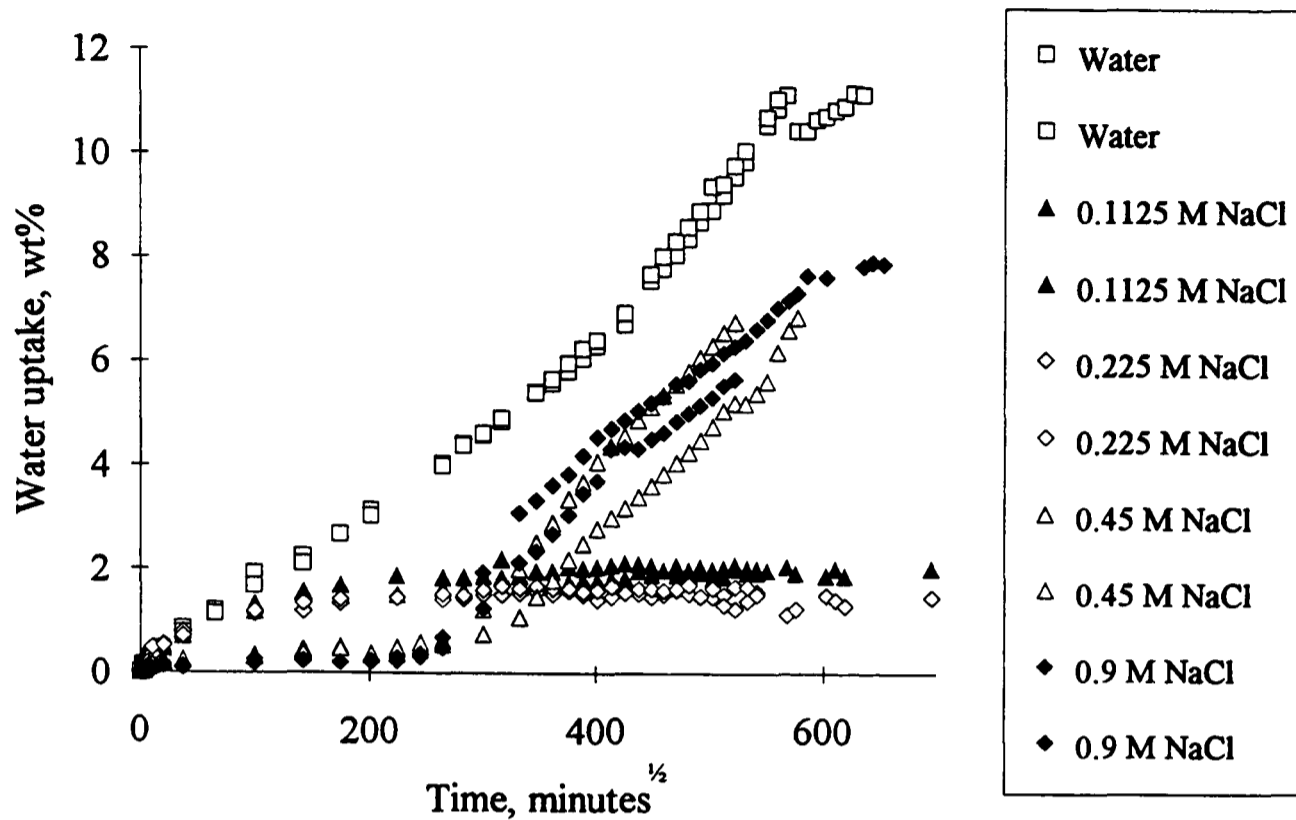


Figure 6.11. Initial water uptake of SBS5+ in NaCl solutions.

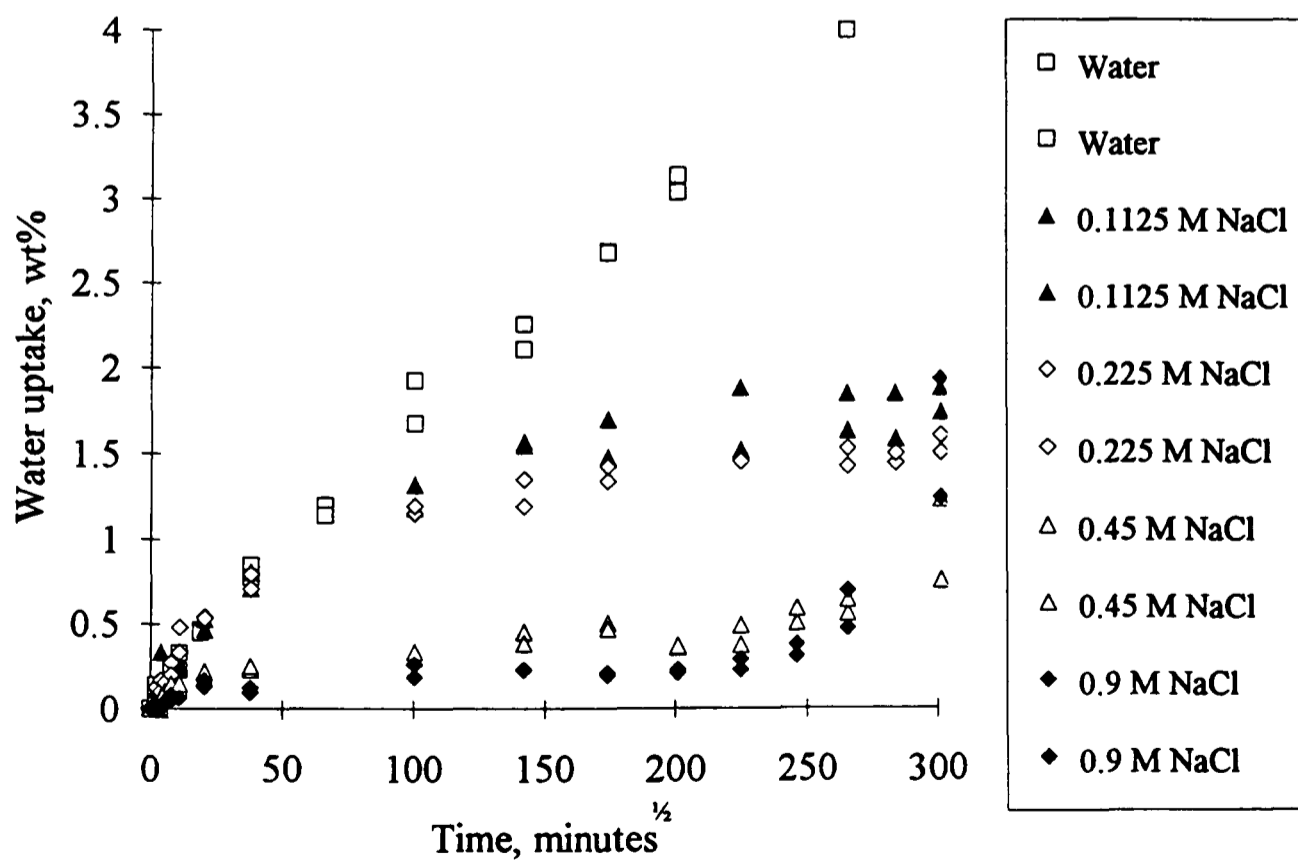
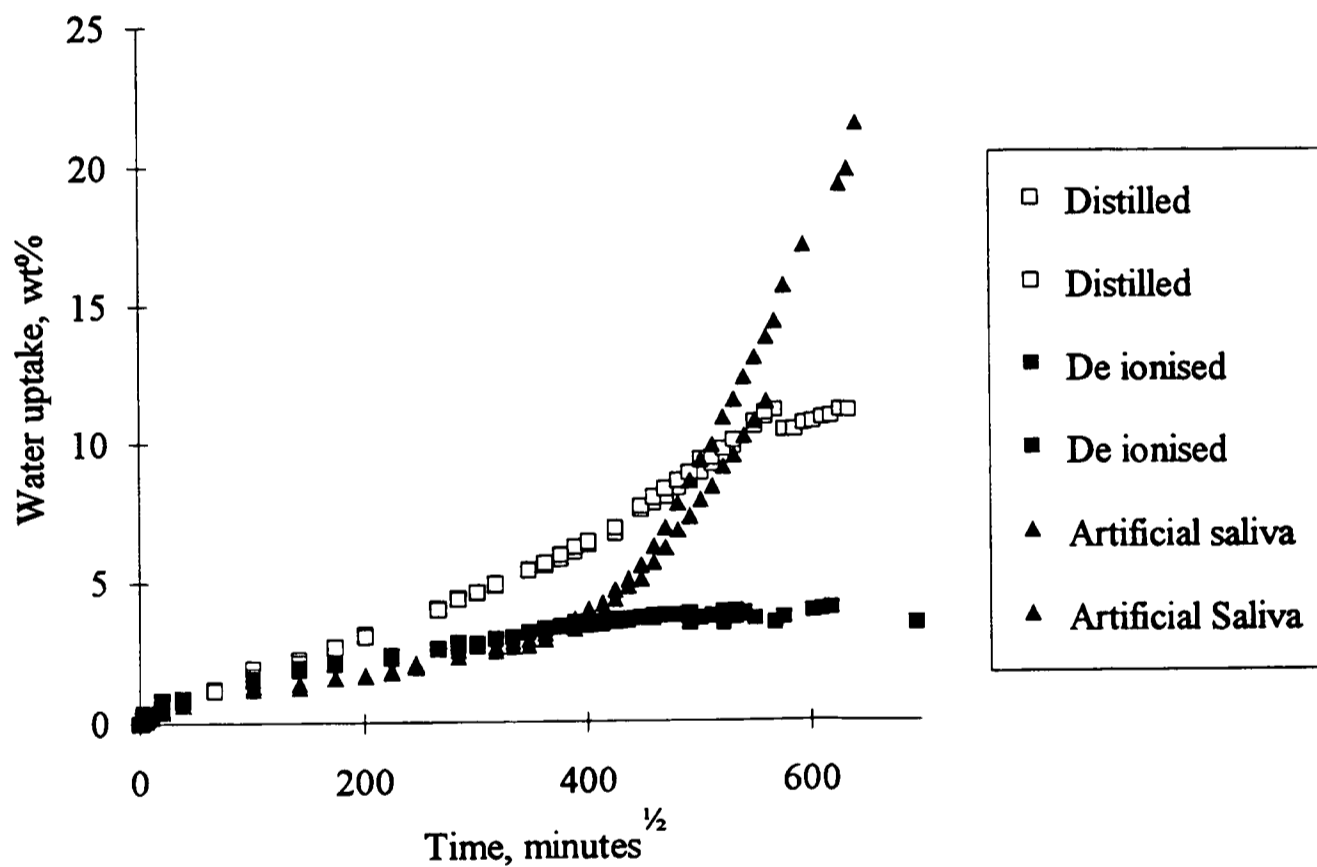


Figure 6.12, shows the oxidation of SBS5+ from de ionised water as opposed to the usual distilled. The lower uptake in deionised water implies a proportion of the uptake from distilled water is due to the oxidation of the elastomer. This oxidation is attributable to ions in the distilled (domestic) water which have been previously noted to have degrading effect Simmons (1988). The absence of oxidation enables a solubility and desorption coefficient to be calculated (table 6.4) and comparison to the EBS5+ and SIS5+ (table 6.3) shows strong similarities as might be expected. The diffusion coefficients calculated for desorption of the de ionised, 0.1125 and 0.225 M NaCl samples also fit in with the general pattern as seen for the PBS materials previously.

Figure 6.12. Water uptake of SBS5+ from artificial saliva and de ionised water.



Perhaps most worrying is the result from artificial saliva which shows a very high uptake and oxidation. This fits into the general pattern of the results with the anions present within the solution promoting the oxidation which is rapid due to the comparatively high uptake from the artificial saliva.

6.3.2. Acetone extraction of the materials.

In order to further explore the suitability of the materials in terms of stability and susceptibility to leaching a sample of SIS5+, HBS5+ and PBS5+ was placed in acetone at approximately 25°C for 48 hours to swell the polymer and promote the leaching of extractable organic components. The loss of material during the extraction is shown in table 6.5, where HBS5+ shows the greatest loss and SIS5+ the least. Although the residual monomer will be extracted, the differences between the materials are thought to stem from the elastomer component. There are many possibilities for the extraction process, the antioxidant, soaps and waxes (for the emulsion polymerised), initiators and processing aids. HBS would be expected to contain the highest portion of extractable and indeed shows the highest loss indeed the general pattern agrees with the expected trends with the more pure SIS showing the least extractable components.

Table 6.5. Summary of the acetone extraction samples and the ash testing of the elastomer materials.

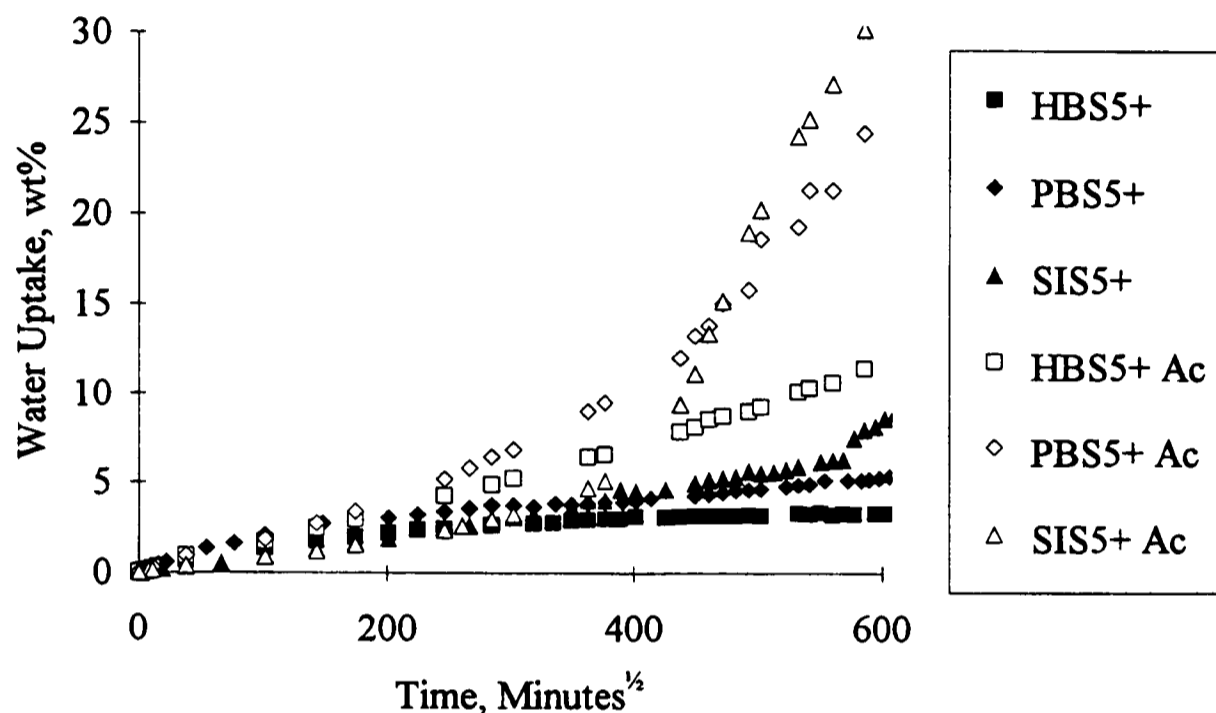
Material	Loss on acetone extraction of 5+ formulation, wt%	Ash of pure elastomer, wt%
SIS	1.46	0.30
HBS	4.94	0.02
PBS	2.49	1.73

The pure elastomers were also ashed at 700°C to check that no inorganic matter was in these materials. Table 6.5 shows this to be the case with very little ash being present from either the SIS (0.2 wt % of the SIS ash content may be attributed to the silica present as a dusting agent on the elastomer) or the HBS compared to the separating agent containing PBS.

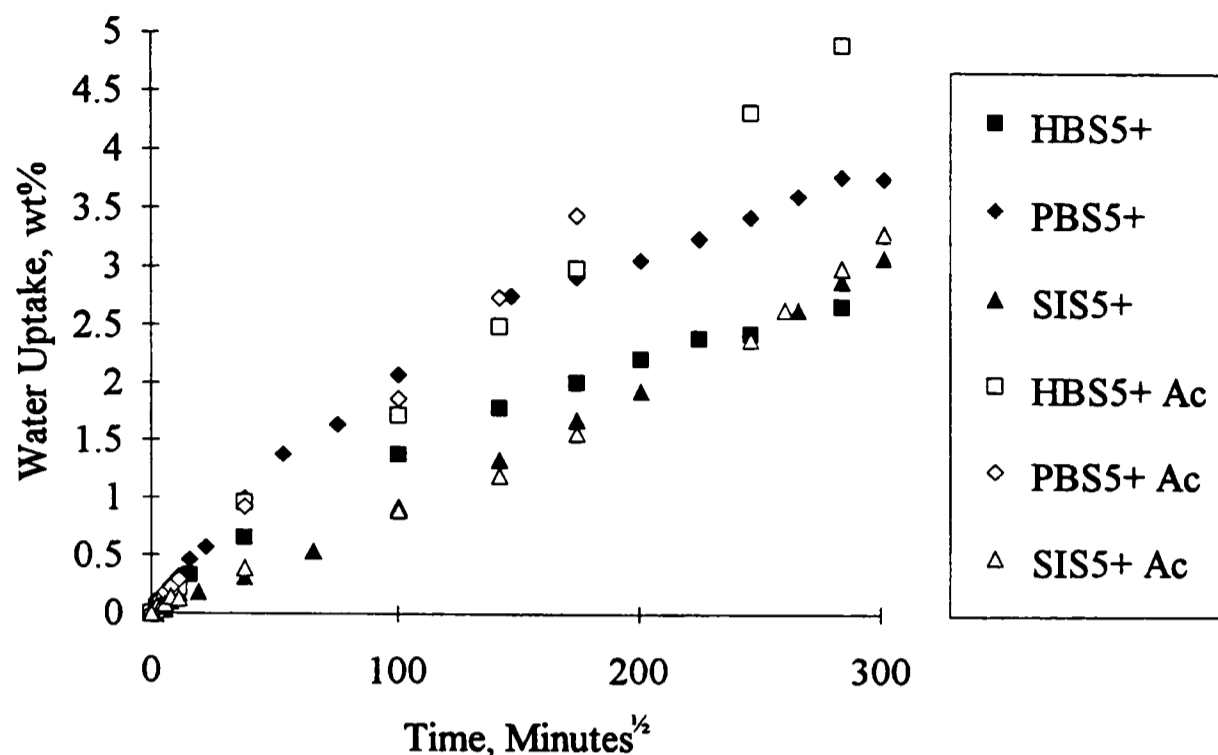
When placed in water at 37°C, considerably higher water uptakes were seen for all these materials (figure 6.13) although their initial uptakes are similar (figure 6.14). Three factors should alter the uptakes of these materials. The swelling will have damaged the structure of the material hence the restraining force might be less capable of restraining the droplets, this would increase the rate of the uptake. The extraction of hydrophilic components from the material should lower the uptake by reducing the overall concentration of hydrophilic/soluble agents. Lastly the extraction of the antioxidant from the elastomer would increase the tendency towards oxidation and so increase the uptake.

Residual acetone in the material left over after the extraction could also affect the uptake but as the materials were placed in the preconditioning oven (at 37 °C) prior to absorption for over a week this should have been minimised.

Figure 6.13. Water uptake of acetone extracted samples.



For PBS5+ little of the separating agent should have been removed as it is inorganic and a very similar uptake is seen until approximately 7 days (≈ 100 minutes^{1/2}) which implies the structural damage is not as bad as might be thought (this is also indicated by similarity of the SIS5+ samples). However, after this initial period uptake is higher which seems to stem from the extraction of the antioxidant, the extracted material also showed rapid discolouration and hardening. A similar pattern is observed for SIS5+ with oxidation occurring more rapidly for the extracted sample, although here there is little change in the uptake of the two samples until 60 days (≈ 300 minutes^{1/2}). The HBS5+ exhibits a greater uptake for the extracted sample as it seems to oxidise almost immediately which seems to be again due to the removal of the antioxidant.

Figure 6.14. Initial water uptake of acetone extracted samples.

6.3.3. Suitability of the elastomer methacrylates.

There are a number of concerns that are apparent from the results of the elastomer methacrylate based materials not least the tendency to oxidise. The presence of the antioxidant can prevent this process by neutralising the radicals produced, but the antioxidant will eventually be used up and so only delay the onset of the oxidation. The antioxidant is also a cause for concern in its own right as its extraction may lead to the toxicological problems. Although initial cell culture tests have shown little effect of the PBS and SBS based material indicating it might not be a problem (Hardie, 1982, Wright, 1995).

Emulsion polymerised elastomers have attracted a reasonable level of concern over their potential toxicity (due to their high extractable content) and are generally regarded as less suitable for food and medical uses than the solution polymerised alternatives (Groß, 1980). Indeed the portion extracted from the emulsion polymerised HBS by acetone was considerably higher than that from the solution polymerised SIS (table 6.5). For this reason, despite the promising water uptake and relative resistance to oxidation, the HBS was thought to be unsuitable as a potential soft lining material.

It is interesting to note that the samples which were desorbed and then placed back into a solution were more prone to oxidation than those which remained in solution. The reason for this is unknown but it may be possible that antioxidant was carried out of the material during the desorption cycle.

The solution polymerised materials exhibited a surprisingly high water uptake and the butadiene based materials (SBS) showed a strong tendency to oxidise when exposed to a ion containing solution. However, they are thought better from a biological context and the SIS seems to be less prone to oxidation even when the antioxidant is extracted. Comparison between the SBS and SIS is interesting as both contain the same proportion of antioxidant (table 6.2) but the SIS shows a much slower rate of oxidation (figure 6.5). This is thought to be the sterical hindrance of the extra methyl group on the isoprene compared to the butadiene. It is also worth noting that the acetone extracted sample of SIS5+ exhibits the same uptake (figure 6.13) as the normal sample in spite of the extraction process which is likely to have removed the antioxidant (seen from the earlier oxidation of the sample). This further supports the theory that it is clustering within the material that is driving the uptake of water rather than any soluble element (i.e. the antioxidant or the residual initiator). It was therefore felt further refinement of the SIS based materials should be the focus of the investigation.

There is an alternative course of action which is to use an elastomer without diene bonds and so should not oxidise. Two major types of elastomer seem most suitable, styrene ethylene butylene rubbers and butyl rubbers. A styrene ethylene butylene was tried but it refused to form a gel with the EHM and other methacrylate monomers, due in part to its thermoplastic nature and solubility parameter. The butyl based materials did form gels with the methacrylate monomers, and have proven to be one of the most stable (oxidation resistant) elastomers available (Groß, 1980, Simmons, 1988).

6.4. Butyl elastomers.

Butyl elastomers are saturated polymers which are renowned for their resistance to oxidation and weathering and have a low permeation (Brydson, 1988). They are produced by a cationic initiation process using a Lewis acid at very low temperatures (-100°C) in the presence of a co-catalyst, typically water, in an ionic (0.2 % aluminium chloride) methyl chloride solution. The monomer isobutene is normally reacted with a

small proportion of isoprene (1 to 4.5 %) which leads to a small unsaturated portion of the polymer chain backbone (Brydson 1978).

The major variation on the butyl elastomers is halogenation (chlorine or bromide) which is performed primarily to raise the polarity of the chain to promote adhesion to different substrates and improve the compatibility with other polymers when forming blends. This may be achieved through substitution or an ionic mechanism involving the unsaturated isoprene link (Brydson 1978).

Three elastomers were chosen for comparison, a butyl elastomer, PB (Polysar butyl 103-3), a chlorobutyl, PCB (Polysar chlorobutyl 1255), and a bromobutyl, PBB (Polysar bromobutyl X2), all supplied by Bayer AG. Table 6.6, shows the details of these materials supplied by the manufacturer, all these materials are pharmaceutical grade and passed by the FDA for food contact and the PB is used as the basis of some chewing gum. The stabiliser is added primarily to improve the stability when exposed to higher temperatures during production, as degradation of the residual vinyl bonds may occur.

As with the solution and emulsion polymerised materials the 5+ formulation, namely 50 g of elastomer with 50 ml of monomer liquid which is EHM containing 1% EGDM and 1% lauryl peroxide was used. As all the butyl elastomers were supplied as bales the gels were milled on a paste mill for 5 to 10 minutes to ensure homogeneity at least 48 hours prior to the moulding and curing of the sample. Although all these butyl based elastomers gelled with the EHM and a consistent gel was produced the PB5+ refused to produce a bubble free sample after mixing, this is thought to relate to the solubility of the PB in the EHM, a sample could however be produced by placing the sample in a pressure cooker as for the pure monomers (section 5.2). The PBB and PCB both gelled and formed samples without any problems.

Table 6.6. Composition of butyl based materials.

	PB	PCB	PBB
Residual diene, mol %	1.70	-	-
Halogen content, %	-	1.25	2.00
Stabiliser	None	Hydroquinone 0.2-0.3 %	Hydroquinone 0.2-0.3 %
Density, kg m ⁻³	920	920	930

6.4.1. Tensile strength of butyl based materials.

Only the PCB5+ and PBB5+ ^{were} tested (table 6.7) as the problems with forming a bubble free sample of PB5+ which lead to the use of an alternative curing cycle would make the results misleading. The results compare well with those of the HBS5+ and EBS5+ (figure 6.1) but noticeably less than the PBS5+, SBS5+ and SIS5+ (figure 6.1). This may be attributed to lack of grafting of the methacrylate to the butyl elastomers due to their low degree of saturation as postulated earlier for the difference between the results of the HBS5+ and EBS5+, and PBS5+, SBS5+ and SIS5+. The slightly better performance of the PBB5+ (than PCB5+) may relate to the crosslinking of the elastomer during polymerisation. Bromobutyl elastomers may be crosslinked by peroxide radicals whereas chlorobutyl and butyl elastomers cannot (Brydson, 1988), indeed butyl rubber degrades when exposed to peroxide radicals (Brydson, 1978).

Table 6.7. Tensile strength of butyl based materials.

	UTS, MPa	± S.D.	Elongation to break, %	± S.D.
PCB5+	3.09	0.12	797	17
PBB5+	3.90	0.36	599	13

6.4.2. Water uptake of butyl based materials.

Water uptake of the butyl materials, including the PB5+ which was cured under pressure, are shown in figure 6.15. Water uptake of PB5+ and PBB5+ is less than that of the other elastomers, apart from HBS5+ (table 6.8 and table 6.3). The solubility and the desorption diffusion coefficient of the butyl based materials are comparable to the other elastomer / methacrylate materials used.

The butyl based materials do not show any sign of oxidation throughout the absorption cycles (figure 6.15 and 6.16). This is expected as these materials have a very low unsaturated content, indeed when PCB5+ was acetone extracted, as performed previously on the other materials (shown in figure 6.13) did not show any difference between the unextracted and the extracted samples (figure 6.17). Also the loss during this extraction was only 0.65 % which is less than that from the other materials (table 6.5).

Figure 6.15. Water uptake of butyl based materials.

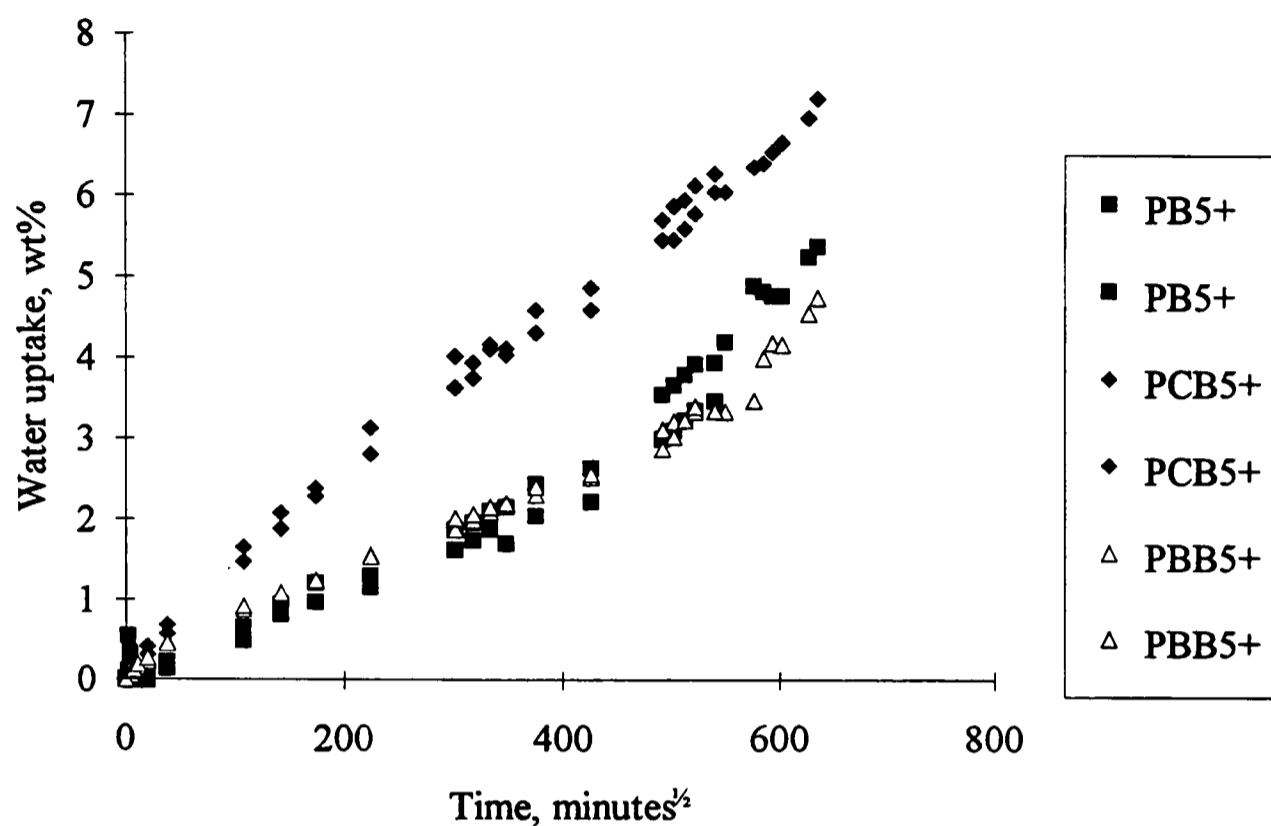


Table 6.8. Summary of water uptake of butyl based materials.

	Abs., wt%	Sol., wt%	at, days	Total, wt%	D_{des} , m^2s^{-1}	2nd abs, wt%	at, days
PB5+	3.49	0.41	203	3.89	6.62×10^{-10}	3.30	42
PBB5+	3.37	0.31	203	3.68	6.10×10^{-10}	3.40	42
PCB5+	6.31	0.15	203	6.46	1.38×10^{-10}	4.00	42

The question as to what is driving the water uptake in the butyl materials is interesting as the hydroquinone (added as stabiliser, table 6.6) seems to have little effect judging by the similar uptakes of PB5+ and PBB5+. The increase in polarity due to halogenation of the butyl elastomer has increased the water uptake of PCB5+ as might have been expected from the data on the pure monomers where the increase in the polar group density increased the uptake. The PBB5+ sample shows a slightly different trend as here the uptake is the same as the PB5+ sample in spite of the increase in the polarity of the elastomer. This might be due to any crosslinks formed in the PBB5+ as a result of the peroxide initiation restraining the expansion due to the hydrophilic bromide groups, which themselves are less polar than the chloro groups.

Figure 6.16. First and second water uptake of butyl based elastomers.

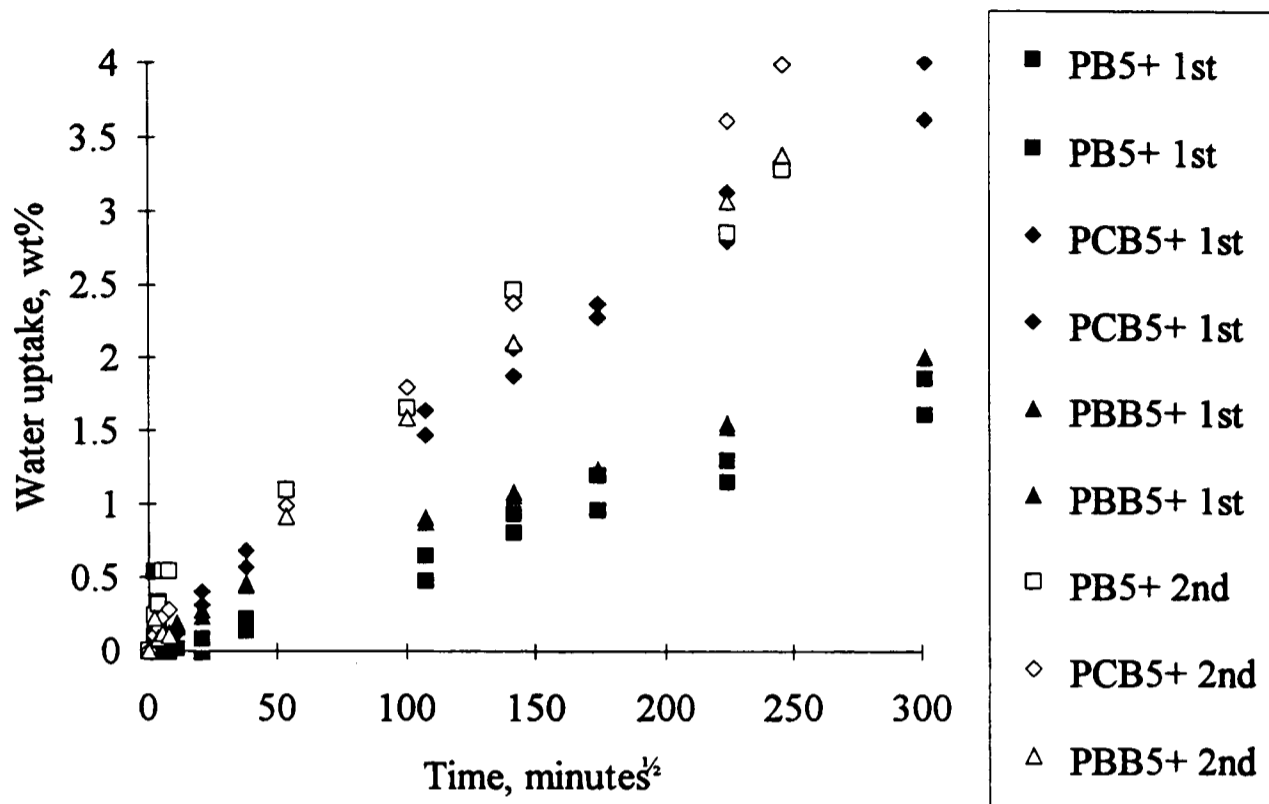
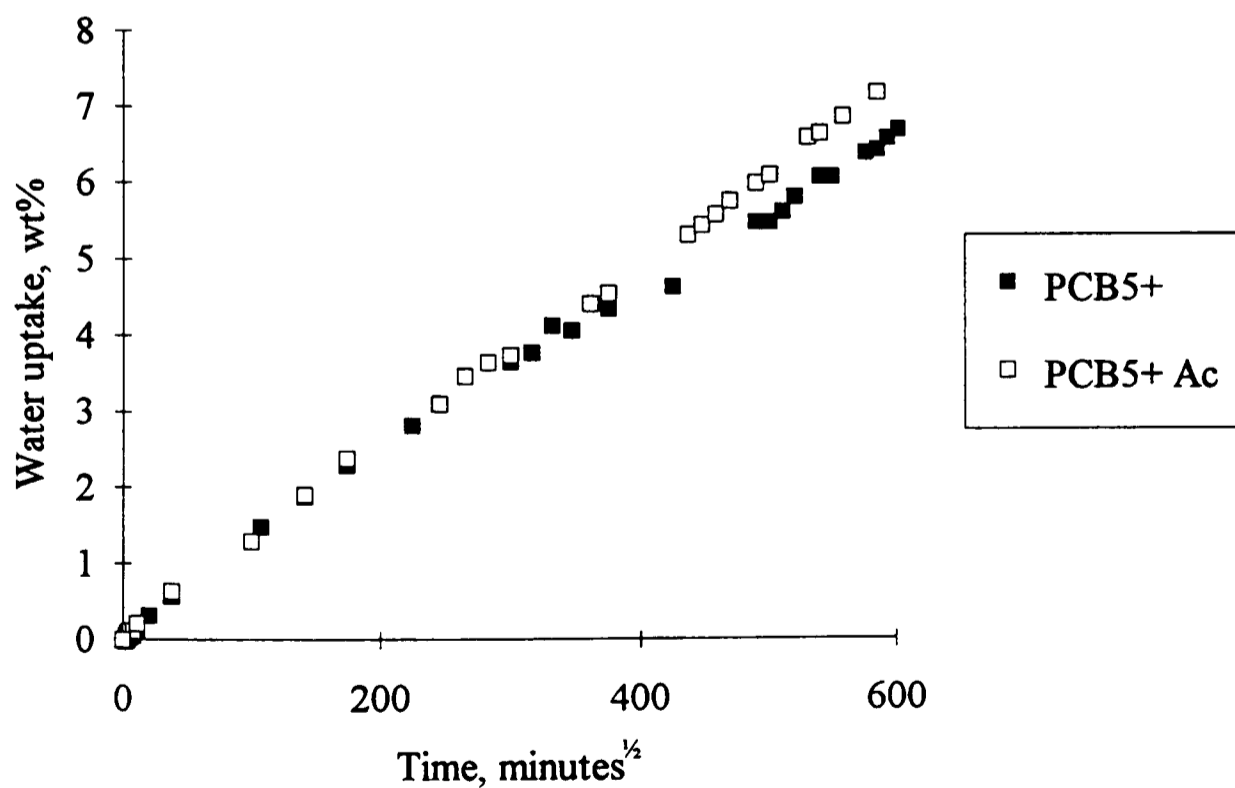


Figure 6.17. Comparison of acetone extracted and normal PCB5+.



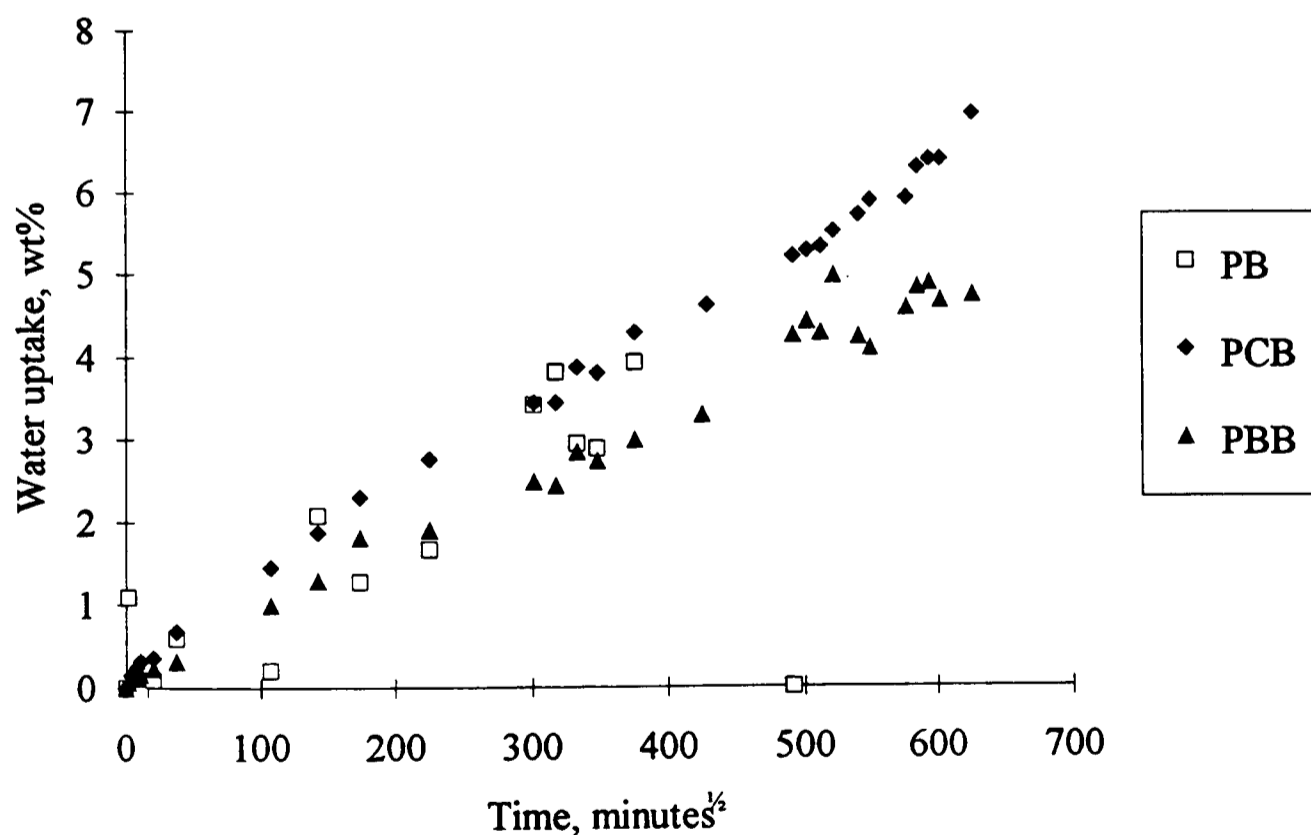
The uptake of the PB5+ is higher than that which might be expected which seems to suggest another contributing factor. There are two possibilities; firstly the cationic

catalyst is acting in a similar way to the anionic catalyst used in solution polymerisation (as previously described for EBS, SBS or SIS) to form hydrophilic carboxylate or hydroxyl groups. Secondly residual aluminium chloride (or other ionic salt) from the ionic methyl chloride solution used in production is left within the material and is forming solution droplets.

The second absorption cycle (figure 6.16) shows the familiar pattern of a faster rate of water uptake compared to the first cycle due to the damage caused to the material during that cycle. It is however interesting to note the similarities of all the materials during this second cycle.

The results from the pure elastomer samples (figure 6.18) demonstrates a similar trend to that already seen for PBB5+ and PCB5+ with the polar nature of the halogen group accounting for the difference in the uptake.

Figure 6.18. Water uptake of pure butyl elastomers.



The PB sample however presents a somewhat more confused picture with a wide spread in the data initially. The sample became what can only be describe as a lump of chewing gum rather than a sheet and so was unmeasurable. This is not surprising when we

consider that fundamentally the PB is a lump of chewing gum without the flavour, hence when pure without the methacrylate it acts as such. The PB then spreads out forming a layer on the surface of the water, which is soft and extremely tacky. This seems to imply that the uptake is being driven by hydrophilic groups on the chain rather than residual salt, as residual salt when the material is in such a state would be available to the solution which is not the case. This therefore implies that the hydrophilic groups on the polymer are responsible for driving the uptake by what seems to be a clustering mechanism as the water uptake into these materials is accompanied by clouding which is normally associated with clustering or droplet formation.

6.5. Re formulation of the elastomer methacrylate materials.

So far only the 5+ and pure samples of these new elastomers have been considered with the monomer phase EHM. There are many possibilities for refinement of the materials including employing fillers, using different monomers and increasing the crosslink density by using a increased level of EGDM and other dimethacrylates.

6.5.1. Reinforcement of elastomer by silica fillers.

The reinforcement of elastomers is normally achieved by carbon black, which is unsuitable the materials detailed here as a black materials would be aesthetically unacceptable. It was therefore decided to employ fumed silica as was previously used with the silicone materials. One advantage of using the silica is that it could act as a separating agent for the elastomer rather than the soluble agents normally used used, as with the PBS. This will enable grinding of the elastomer to form a powder (like the PBS) without including a soluble separating agent which would drive the uptake.

^a As previously described (4.3.1) there are many different states for the silica surface which will effect the water uptake of the elastomers in different ways as seen in chapter 4 on the silicone polymers. It was decided to explore the effect of the different surface treatments rather than the surface area of the silica on the water uptake of EBS5+ using the silicas detailed in Table 6.9. All these silicas were added to the material at the 5 % level which corresponds to a 10 % by wt level on the powder and should be more than adequate to prevent the agglomeration of the elastomer particles. C200 was also used at

a higher 20 % by weight of powder level. The codes used are shown in table 6.10, with the formulations keeping the 50/50 balance between the monomeric and elastomer components of the system.

Table 6.9. Silicas used for reinforcement of elastomers.

Code	Type of silica	Supplier
S200	Fumed silica, surface area 200 m ² g ⁻¹ .	Aerosil 200, Degussa AG.
R974	Fumed silica, surface area 200 m ² g ⁻¹ , treated with di methyl di chloro silane.	Aerosil R974, Degussa AG.
C687	Fumed silica, surface area 200 m ² g ⁻¹ , treated with MPS	Central Chemicals Ltd.

MPS, γ -methacryloxypropyl trimethoxysilane (supplied by, Union Carbide, A174).

Table 6.10. Formulation of EBS 5+ materials with a 50/50 ratio of monomer to elastomer.

Code	Silica	Overall, wt %
EBS5+ S5	S200	5
EBS5+ R5	R974	5
EBS5+ C5	C687	5
EBS5+ C10	C687	10

6.5.2. Results from the filled EBS5+ samples.

The tensile properties of the filled EBS5+ are very similar as seen in figure 6.19, with the filled samples generally slightly stronger. The water uptake results are very different with considerable differences being observed for the different materials figure 6.20. EBS5+ C10 shows a low uptake which equilibrates with a total uptake of 1.24 wt % (table 6.11), the EBS5+ C5 shows an uptake somewhere between this and EBS5+. The exact value of the uptake of the EBS5+ C5 is a little confused as the material shows a solubility weight gain of 1.24 wt %, this is unlikely to be oxidation as there is no upturn in the uptake in the first or second water uptakes (figure 6.21 and 6.22). The magnitude of this second uptake is very similar to the first (table 6.11), indicating the driving force has not noticeably altered. What is happening with this sample is therefore unclear with

no satisfactory reason being apparent for this solubility value. The equilibrium observed with EBS5+ C10 sample enables a diffusion coefficient to be determined (table 6.11), with a familiar pattern of a faster diffusion coefficient in desorption than absorption and slightly faster second absorption than the first.

Figure 6.19. Tensile strength of filled EBS5+ materials.

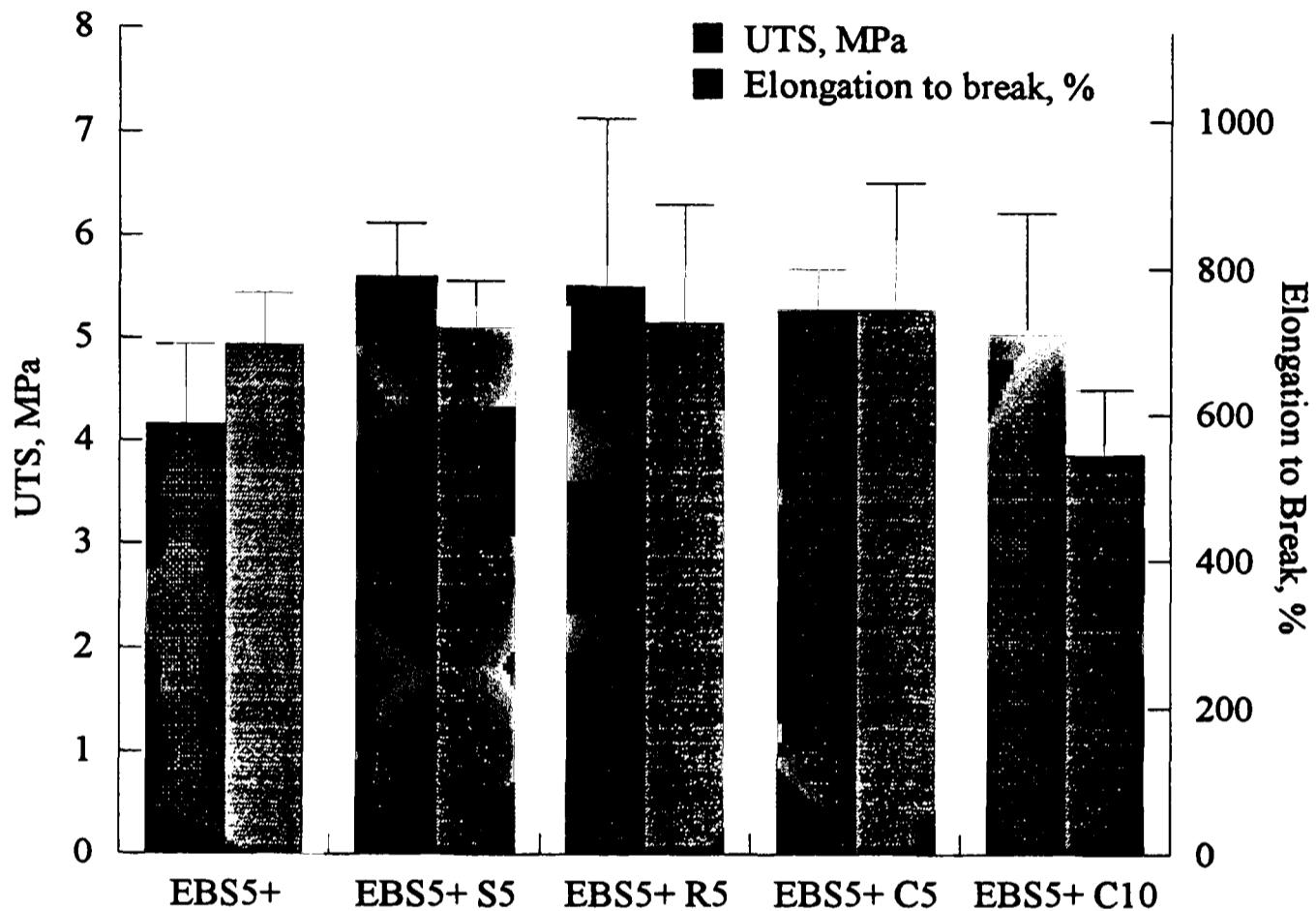


Table 6.11. Summary of water absorption data for the reinforced EBS5+ materials, first absorption values at 203 days and 2nd absorption value at 238.

	Abs, wt%	Sol, wt%	Total, wt%	D_{des}, m^2s^{-1}	D_{1st}, m^2s^{-1}	D_{2nd}, m^2s^{-1}	2nd abs, wt %
EBS5+	8.71	0.00	8.71	3.41×10^{-10}	-	-	20.40
EBS5+ S5	3.04	0.45	3.49	7.20×10^{-10}	1.05×10^{-11}	3.00×10^{-11}	3.28
EBS5+ R5	5.47	-0.04	5.43	3.93×10^{-10}	-	-	6.06
EBS5+ C5	3.19	-1.24	1.95	8.43×10^{-10}	-	-	2.94
EBS5+ C10	1.15	0.09	1.24	1.42×10^{-9}	6.4×10^{-11}	5.90×10^{-10}	1.24

Figure 6.20. Water uptake of filled EBS5+ materials.

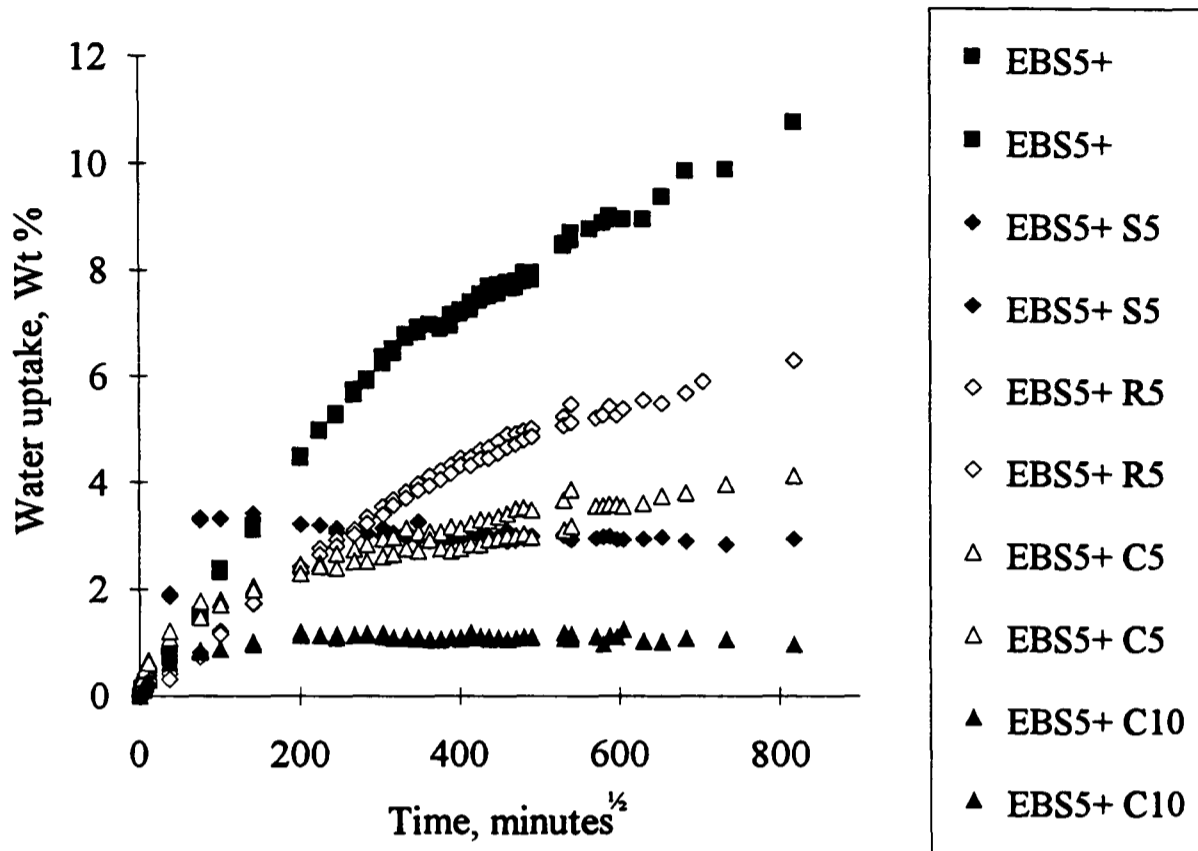


Figure 6.21. First and second absorption of filled EBS5+ materials.

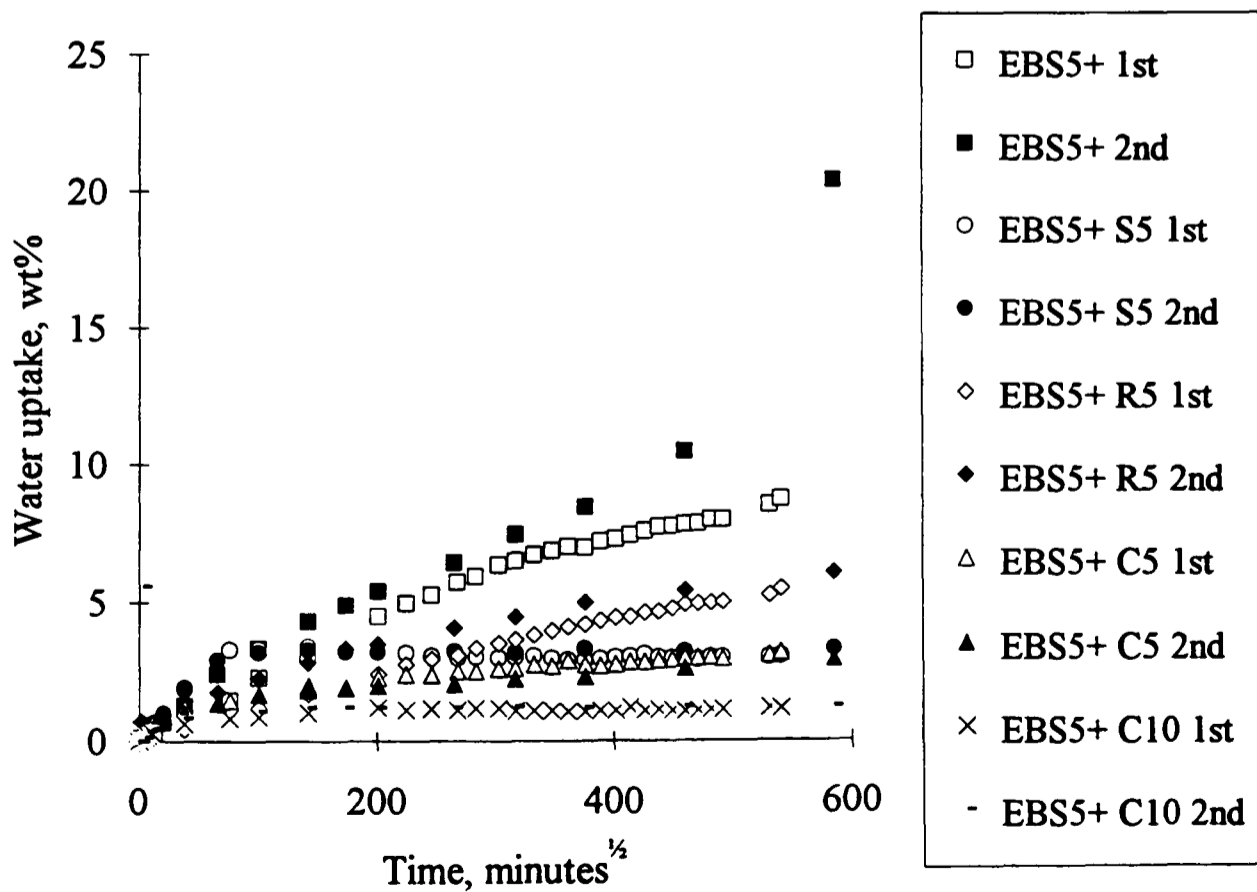
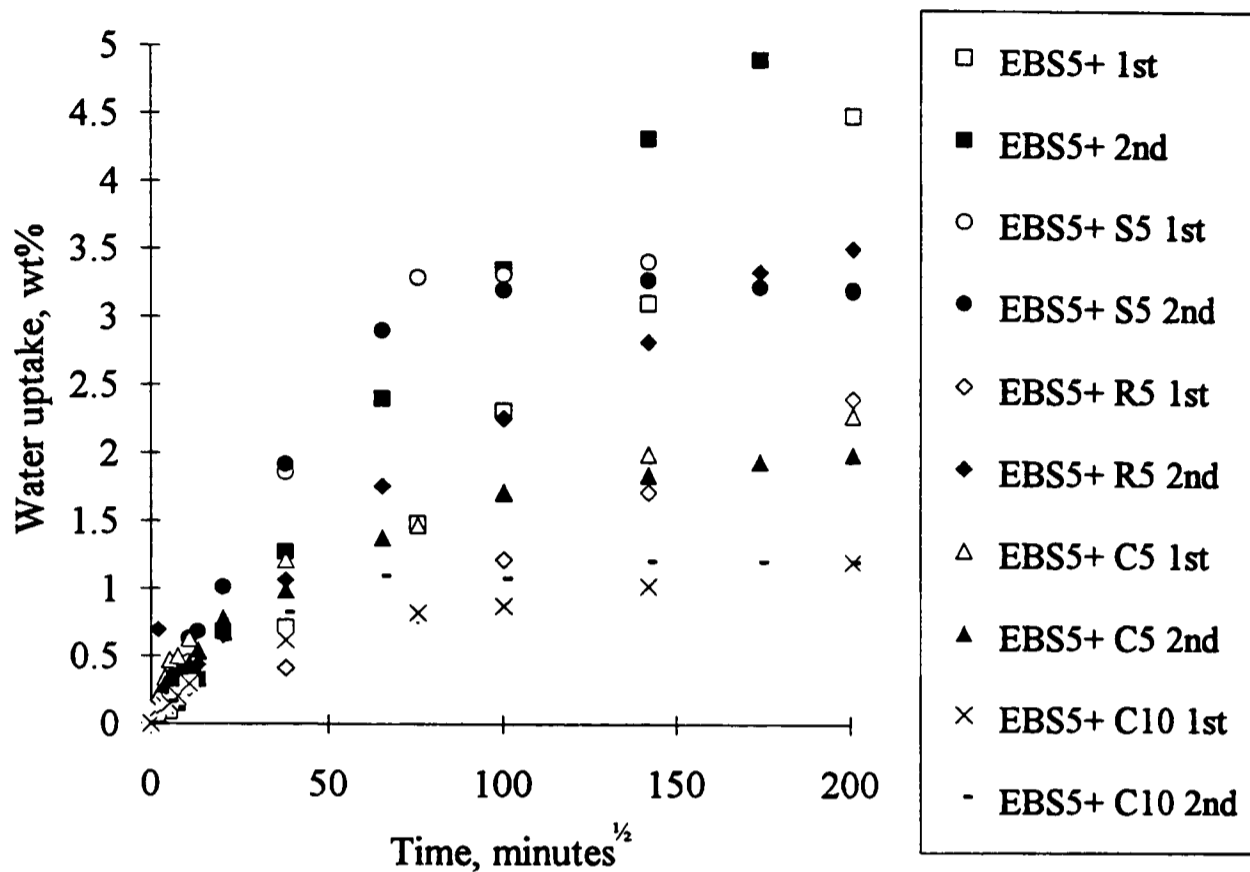


Figure 6.22. Initial first and second absorption of filled EBS5+ materials.

The lower uptake of these C687 filled materials may be attributed to the reinforcing effect of the silica with the methacrylate groups on the surface of the silica (from the MPS) bonding to the methacrylate matrix effectively increasing the crosslink density. This improves the restraining force exerted by the material on the droplets and is also shown as an increase in storage modulus (table 6.12) of the material. These results were obtained in conjunction with Dr S.Kalachandra and Dr D.Xu of Virginia Tech., Blacksburg Virginia, USA, who used a Perkin and Elmer DMA 7 in a compressive mode at a frequency of 1 hertz.

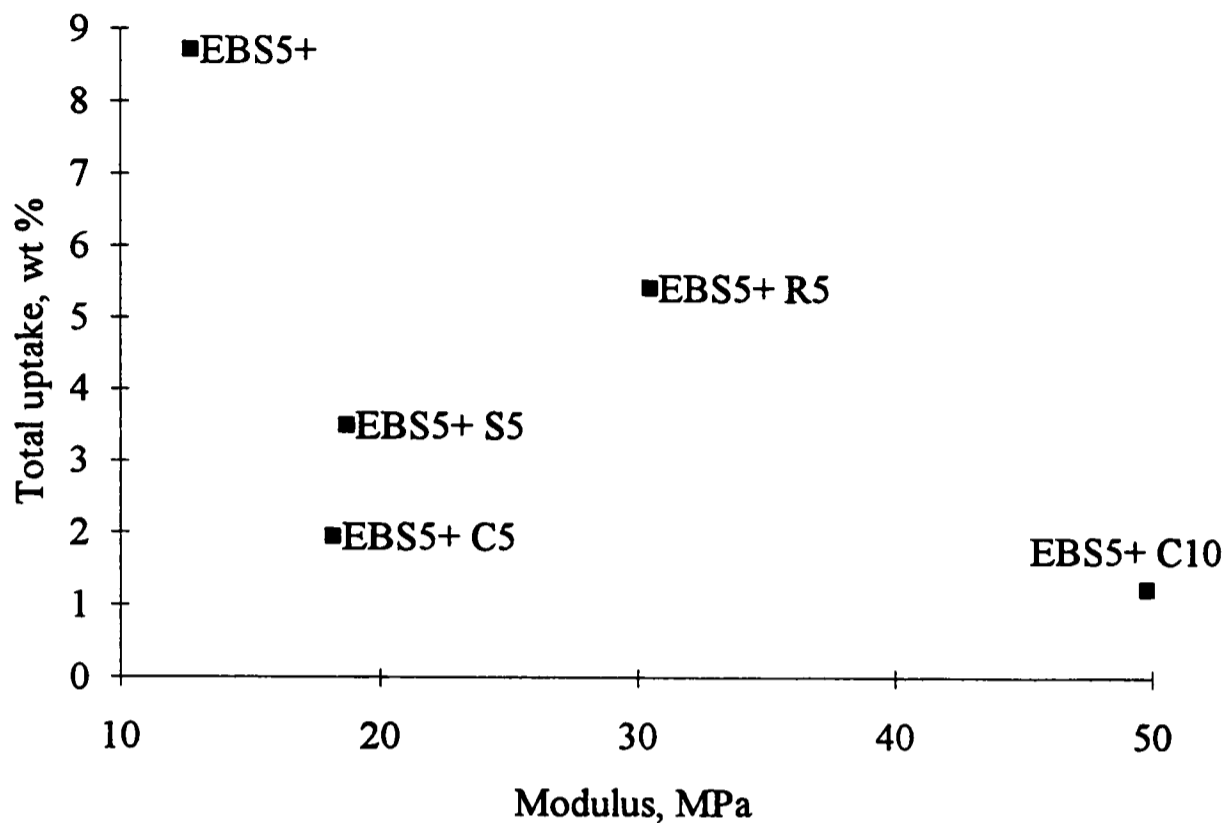
Table 6.12. Modulus and $\tan \delta$ of filled EBS5+ materials at 37 °C, data supplied by S.Kalachandra and D.Xu.

Code	Modulus, MPa	Tan δ
EBS5+	12.7	0.538
EBS5+ R5	30.5	0.386
EBS5+ C5	18.2	0.430
EBS5+ C10	49.8	0.393
EBS5+ S5	18.7	0.426

The R974 filled sample EBS5+ R5 demonstrates a slightly different picture with a slower initial rate of absorption (figure 6.19 and 6.22) but a higher eventual uptake compared to the EBS5+ C5. This is attributed to the R974 (which is covered in methyl groups) being incapable of bonding to the matrix which leads to the more prolonged uptake.

EBS5+ S5 is another case which shows a different trend with a very rapid uptake and then a slow decrease in the level of the uptake, seen for both the first and second cycles (figure 6.19, 6.21, and 6.22). This is difficult to explain as the S200 might be expected to increase the uptake by approximately 10 % of the weight of the silica in the material, i.e. about 0.5 wt%, and then decrease over time due to the bridging of the silanol groups as reported in chapter 4. While this explains the decrease observed over time it does not explain the kinetics of the diffusion. The lower uptake than EBS5+ S5 indicates the S200 is reducing the uptake more than the R974 in spite of its greater hydrophilicity. It is proposed that the silanol groups of the silica bonds to some extent with the matrix as with the C687. The hydrophilic nature of the silanol groups and the carboxylic groups (from the solution polymerisation) may interact together to prevent the protracted uptake of the other materials which leads to a fast uptake with a similar diffusion coefficient to that of EBS5+ C10 (table 6.11).

Figure 6.23, illustrates the relationship between water uptake and storage modulus as found by Dr S.Kalachandra and Dr D.Xu, shown in table 6.12. From the theories previously described it might be expected that the water uptake would decrease with increasing modulus. This is indeed seen but the relationship is more complicated. It is believed that this deviation between the C687 and R974 is attributable to creep around the droplets of the R974 allowing the slow expansion whereas the C687 reinforces the matrix and prevents much of this creep. The S200 is another case and probably in some part relates to reinforcement as for the C687 but the exact nature of this unclear.

Figure 6.23. Relationship between modulus and the water uptake.

6.5.3. Re formulation of SIS based materials.

SIS was chosen as the most suitable unsaturated elastomer to form a basis for a new soft lining material due its slightly better resistance to oxidation and lower water uptake. Initially the reformulation focused on evaluating TDM and the elastomer monomer ratio, then crosslink density became of primary interest the formulations and codes are shown in table 6.13. There are many subtleties with these formulations as for example a if TDM and EGDM was used as the basis of the monomer component rather than TDM, EHM and EGDM as with the SIS TGE the gel would phase separate and a there would be a gel and liquid component rather than a single homogeneous gel. Whereas other gels would form but would excessively bubble during the polymerisation (for example a pure EGDM SIS based sample). The reason for this is believed to stem from the differences in the solubility parameters of the different monomers and the elastomers.

Table 6.13. Re formulation of SIS based materials formulations.

Code	Elastomer, (g) to monomer (ml) ratio	Monomer,	%	EGDM, %	Filler,	%
SIS5+	50/50	EHM	99	1	-	-
SIS5+ C5	50/50	EHM	99	1	C687	5
SIS8+ 5/5	50/50	TDM	99	1	-	-
SIS8+ 6/4	60/40	TDM	99	1	-	-
SIS8+ 6/4 C5	60/40	TDM	99	1	C687	5
SIS TGE	50/50	TDM	50	-	-	-
		EHM	25			
		EGDM	25			
SIS TDE	50/50	TDM	50	-	-	-
		EHM	25			
		DDM	25			
SIS TDE C	50/50	TDM	50	-	C687	5
		EHM	40			
		DDM	10			
SIS HD	50/50	HD	100	-	-	-
SIS DD	50/50	DD	100	-	-	-
SIS M	50/50	MM	100	1	-	-

All initiated by 1% lauryl peroxide.

6.5.4. Results of the SIS based materials.

The tensile results (figure 6.24) show there is a reduction in strength when the monomer used is changed from EHM (SIS5+) to TDM (SIS8+) as might have been predicted from the results of the PBS based samples previously described in chapter 5. There is also a decrease in the UTS and elongation to break when the elastomer monomer ratio was increased for the TDM (SIS8+) materials from 50/50 to 60/40 which was not the case for the PBS materials. The addition of the filler C687 weakened the SIS5+ but strengthened the SIS8+ 6/4 as it did with the EBS5+ (figure 6.19). The greater strength of the SIS 5+ compared to both the SIS8+ 6/4 and the EBS5+ may account for this difference in behaviour, although this is not clear.

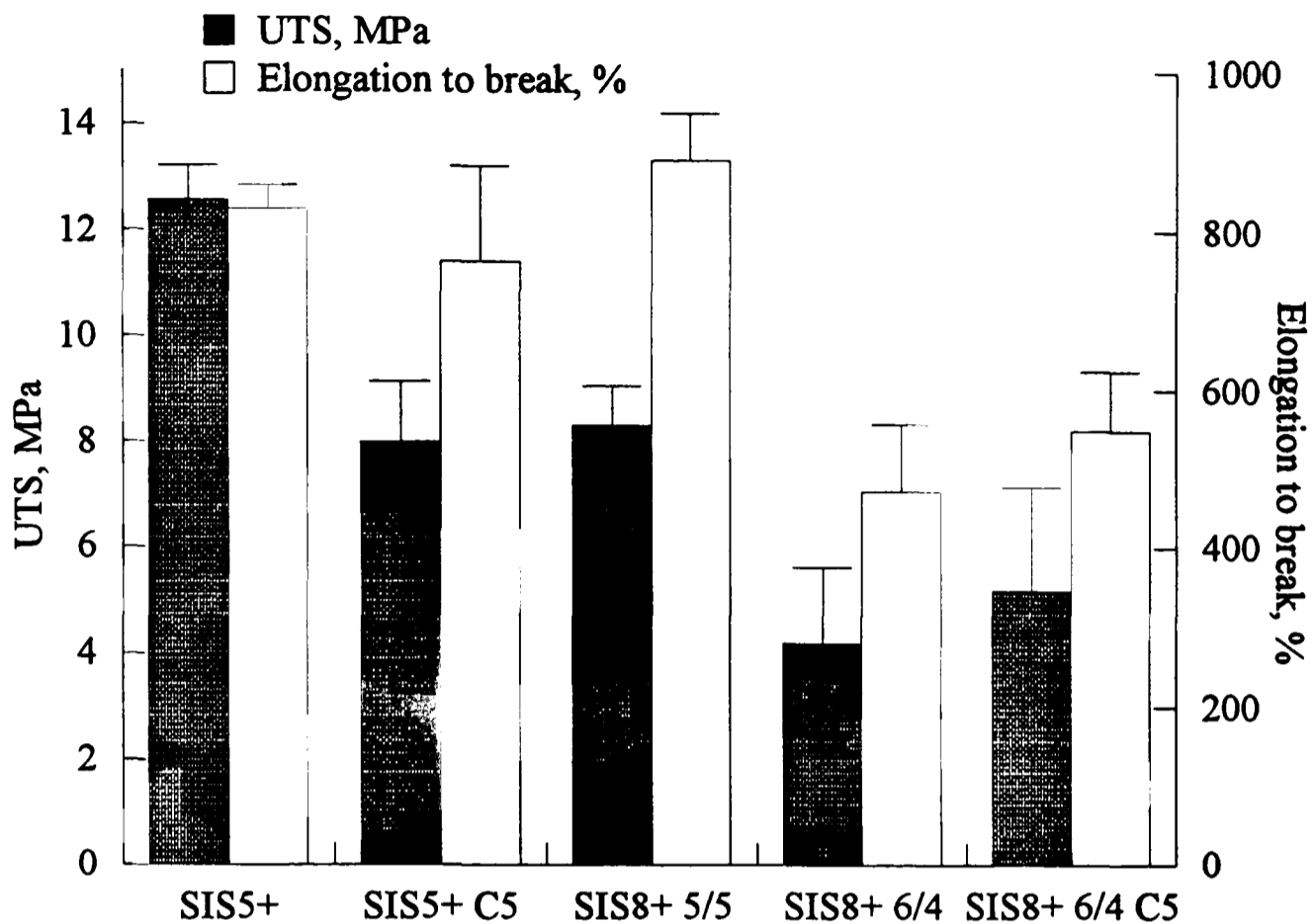
Figure 6.24. Tensile strength of SIS based materials reformulations: Part I.

Figure 6.25 and 6.26, illustrate the water uptake of these materials with the TDM based materials (SIS8+) showing a higher water uptake than the EHM based material (SIS5+). This can be attributed to lower strength of the TDM based materials as seen in figure 6.24. It is interesting to note that the onset of oxidation occurs sooner for the TDM based materials (judging by the upturn in the uptake) this probably relates to their higher uptake as seen previously with the quantity of water uptake being linked with the onset of oxidation. SIS8+ 6/4 shows the same level of uptake as SIS8+ 5/5 despite a higher content of the hydrophilic groups driving the water uptake and lower tensile strength. This seems to imply a surprising insensitivity to the proportion of elastomer, although this does effect the onset of the oxidation as expected with an earlier onset of the oxidation for the SIS8+ 6/4. The addition of the filler C687 (SIS5+ C5 and SIS 8+ 6/4 C5) to the materials lowers the uptake as previously seen for the EBS5+ based materials (figure 6.20) which is attributed to crosslinking across the silica.

Figure 6.25. Water absorption of SIS based materials: Part I.

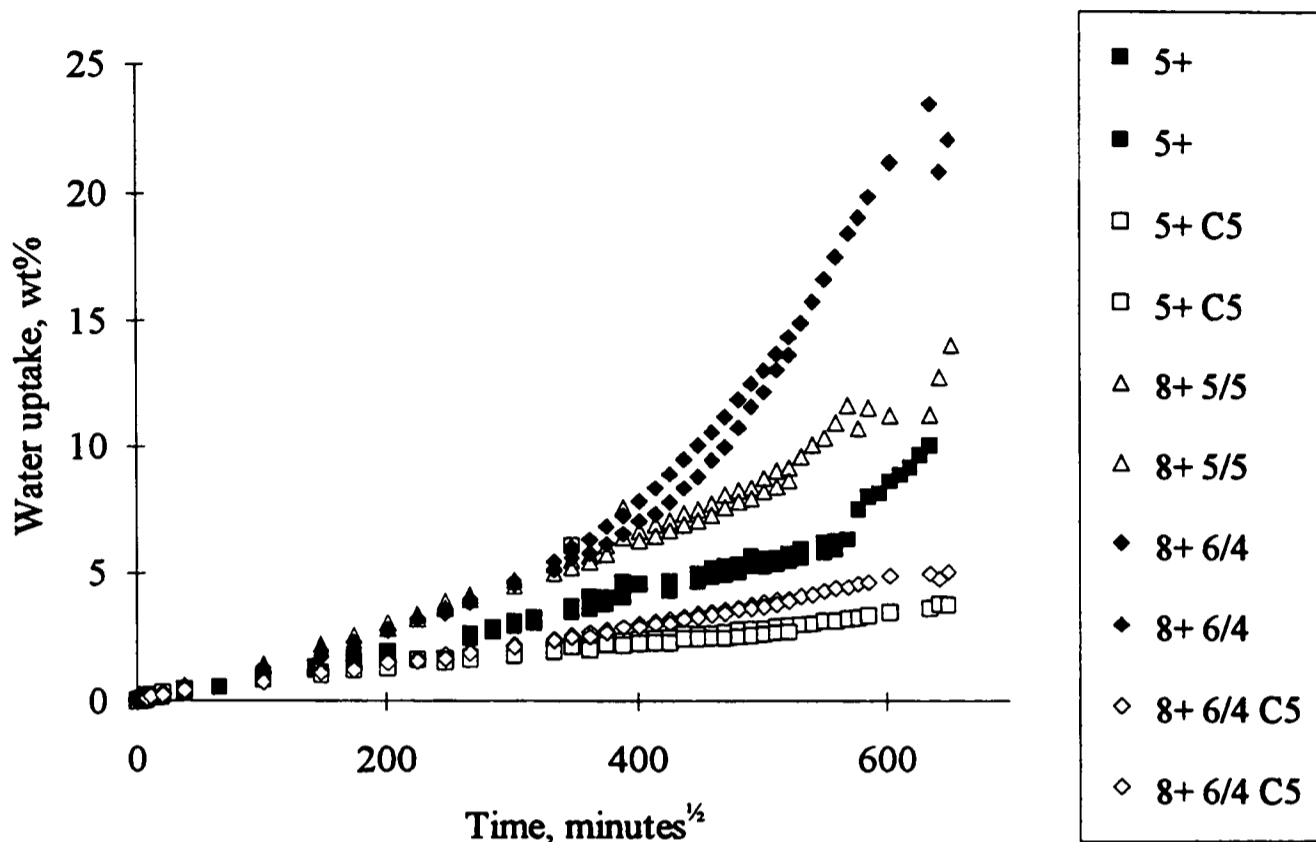


Figure 6.26. Initial water absorption of SIS based materials: Part I.

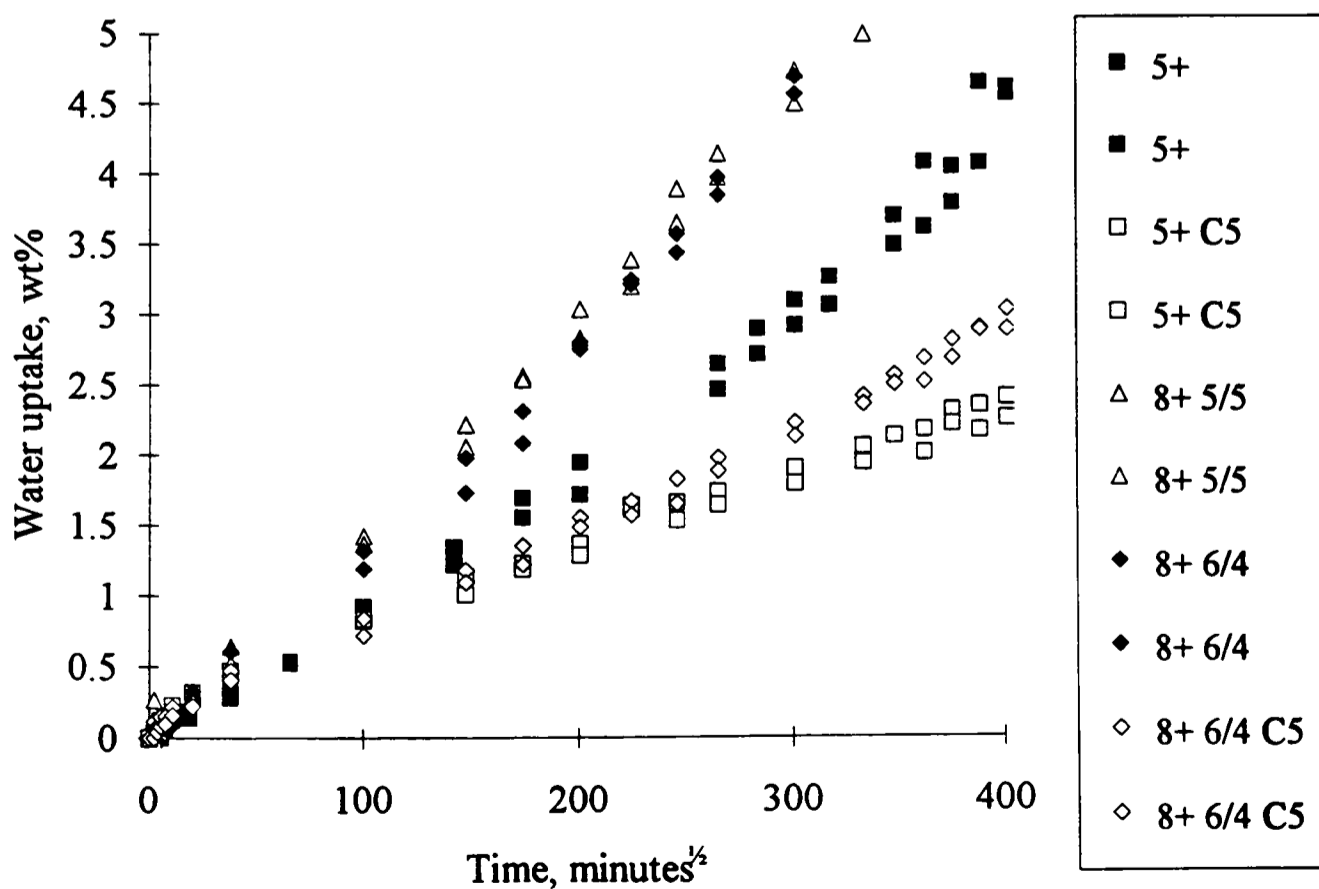
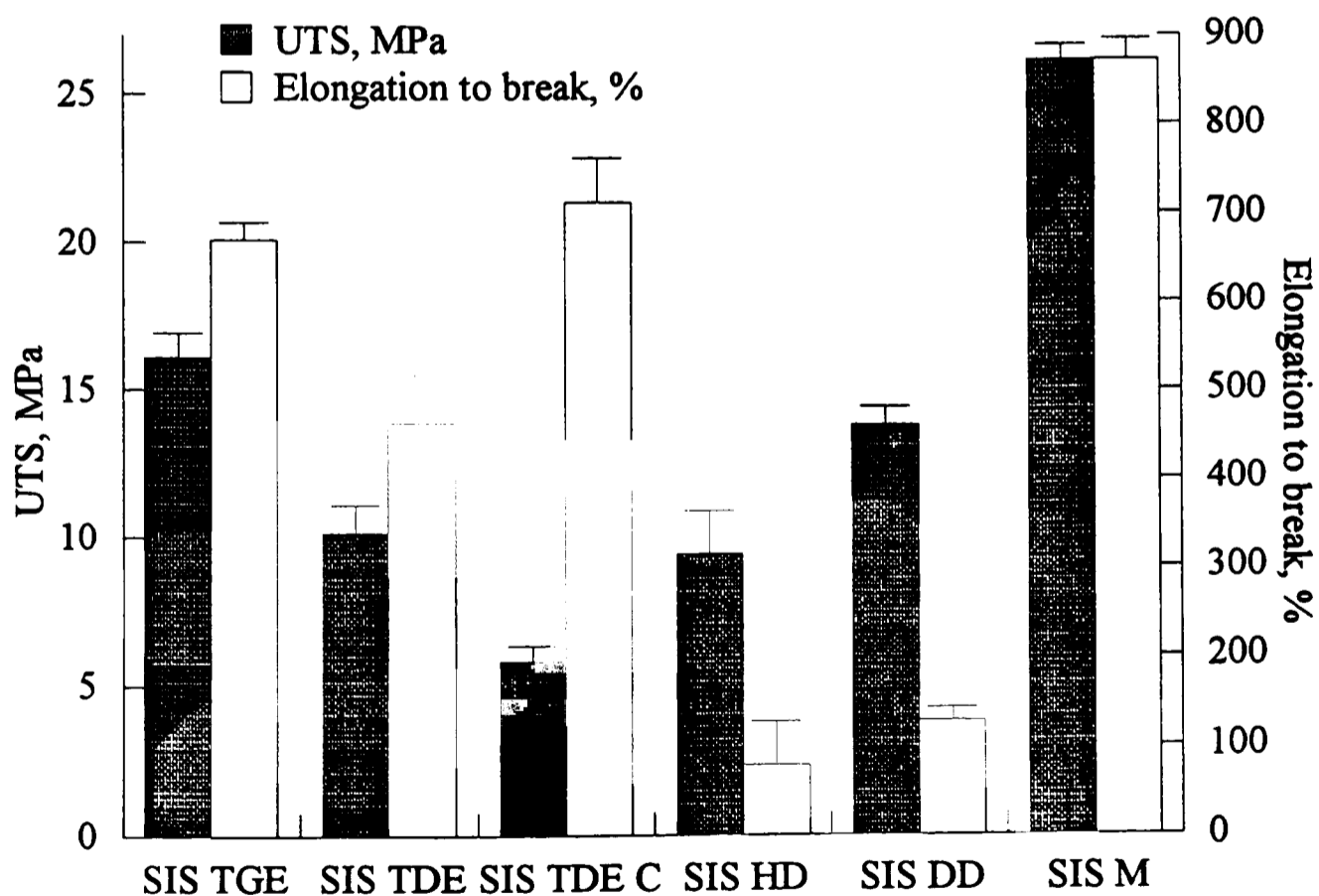


Figure 6.27 shows the results of the other SIS based materials with some large improvements in the tensile strength being seen most noticeably the SIS M which has a UTS of 26.13 MPa. This is double that for the SIS5+, This may be due to the increase in the number of the methacrylate groups increasing the degree of grafting to the elastomer chain or may simply relate to poly MM being stronger than poly EHM. The heavily crosslinked SIS HD and SIS DD were fairly hard and relatively inextensible materials (extension between 100 and 200 %) and showed a lower UTS than might have been expected. When the high portion of dimethacrylate was used in conjunction with other mono methacrylate monomers (SIS TGE and SIS TDE) a softer more extensible material was produced. The SIS HD being most heavily crosslinked materials produced the least extensible and lowest UTS followed by the second most crosslinked SIS DD. The SIS TGE proved to be the most extensible and strongest. The SIS TDE was less extensible and weaker, than both the SIS TGE and SIS 5+, this may relate to the varying nature of the relationship between crosslink density and strength as previously seen with the elastomeric higher methacrylates (described in chapter 4).

Figure 6.27. Tensile strength of SIS based materials reformulations: Part II.



It is difficult to be sure about the effect of the C687 on the SIS TDE C as the DDM was lower than the SIS TDE. The extension is however greater than any other reinforced

materials (SIS5+ C5 and SIS8+ 6/4 C5) but UTS seems to fall mid way between these reinforce materials. This implies the increased crosslinking due to the 10 % DDM is increasing the elongation but not the UTS this is contradictory to the results described above. Clearly the effect of reinforcement and crosslink density is complex and requires further study to achieve a better level of understanding.

The water uptake of the heavy crosslinked elastomers was very low with the SIS HD and SIS DD showing a total uptake of 0.68 and 0.45 wt % respectively (figure 6.28, and table 6.14). These are lower than the absorption from the pure monomers which were 0.97 wt% for the HDM and 0.84 wt% for the DDM. This implies that clustering which it seen for the other SIS based materials is not taking place (note the similarity of the absorption and desorption coefficients) due the restraint of the heavily crosslinked matrix. The level of the uptake for these materials is just over half that of the monomer indicating it is the methacrylate which is now driving the bulk of the uptake into the material. The clustering of the elastomeric groups accounting for only a fraction of the uptake this being attributable to the hydrophilic nature of these groups rather than there clustering behaviour.

Figure 6.28. Water absorption of SIS based materials: Part II.

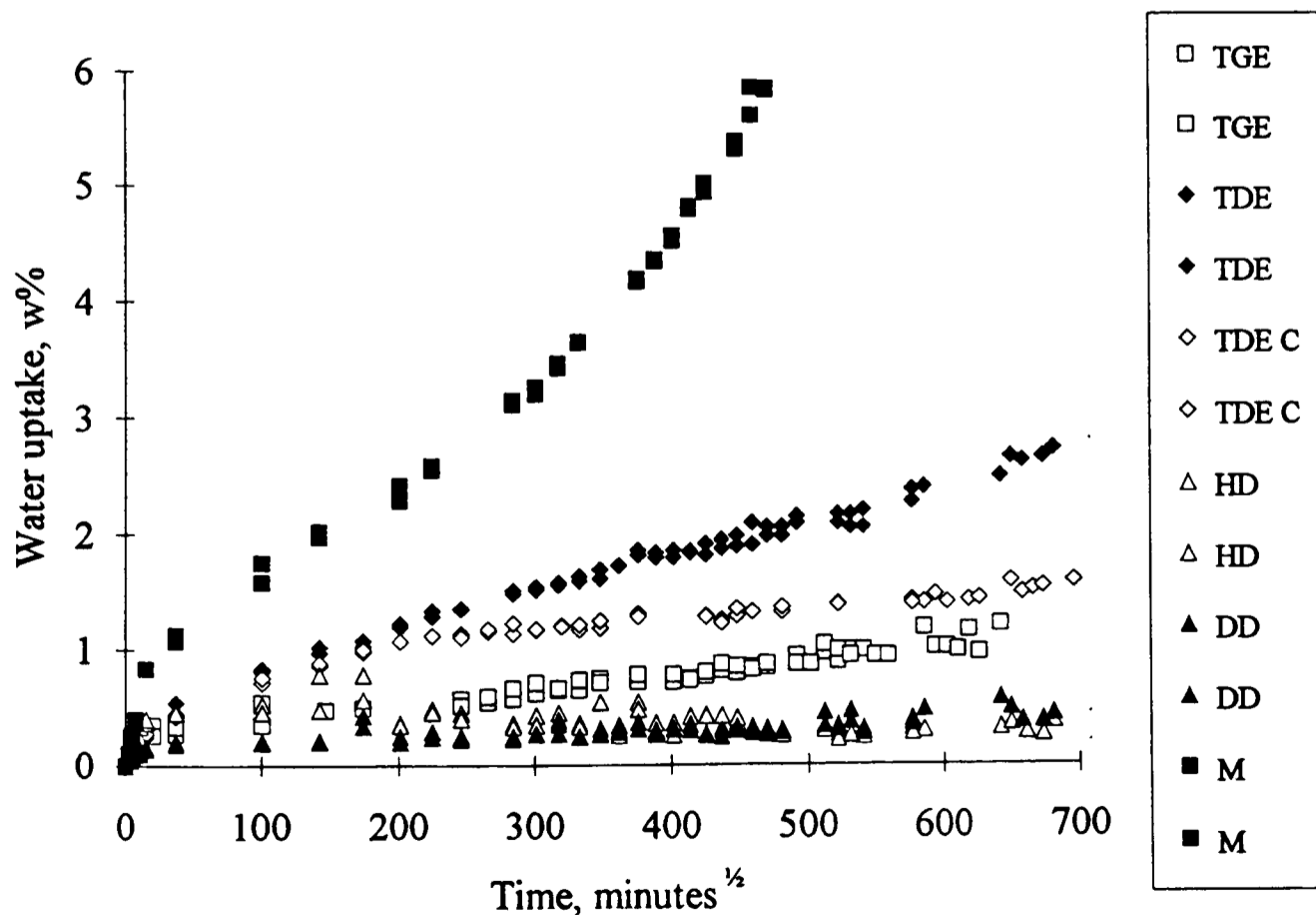


Table 6.14. Summary of water uptake of SIS based materials.

	Uptake, wt %	at, days	Sol., wt %	Total, wt %	D_{des} , m^2s^{-1}	D_{abs} , m^2s^{-1}
SIS5+	5.96	217	0.14	6.11	7.69×10^{-10}	-
SIS5+ C5	2.70	189	0.10	2.80	4.74×10^{-10}	-
SIS8+ 5/5	8.68	189	0.56	9.24	2.52×10^{-10}	-
SIS8+ 6/4	13.73	189	-3.44	10.29	3.38×10^{-10}	-
SIS8+ 6/4 C	2.70	189	0.10	2.80	4.74×10^{-10}	-
SIS DD	0.36	231	0.10	0.45	1.51×10^{-9}	2.69×10^{-10}
SIS HD	0.27	231	0.40	0.68	9.26×10^{-10}	4.82×10^{-10}
SIS TDE	2.27	231	0.26	2.53	4.03×10^{-10}	-
SIS TGE	0.94	196	0.30	1.24	6.89×10^{-10}	-
SIS TDE C	1.40	231	0.43	1.83	7.65×10^{-10}	2.4×10^{-11}
SIS M	5.84	154	0.18	6.02	2.40×10^{-10}	-

SIS TGE and SIS TDE have a lower uptake than SIS 5+ due to the increased crosslinking (figure 6.28, and table 6.14). Here the more crosslinked SIS TGE has the lower uptake as expected although neither of these materials reached equilibrium which might have been expected from increasing the crosslink density. The SIS TDE C does not reach equilibrium (which is lower than SIS TDE and contains 7.5 % more DDM than SIS TDE C) which implies the addition of the C687 (present at 5 %) is more effective in lowering the uptake than simply increasing the crosslink density. This may relate to the number of the methacrylate groups on the surface of the creating a centre of a number of crosslinks rather than a crosslink bridge as with a di methacrylate.

The absorption of SIS M (figure 6.28, and table 6.14) is greater than that of SIS5+ at 154 days, SIS5+ uptake is 4.98 wt% and SIS M is 5.84 wt%. The mechanical properties around the clusters within the material should be as good as (if not better) than that of the SIS5+ (figure 6.27) so the material might be expected to absorb less water. The nature of the matrix has now however changed from SIS / EHM to SIS / MM, which will increase its hydrophilicity as poly MM absorbs typically 2 wt% water and the EHM approximately 0.5 wt%. The increase in absorption may therefore be attributed to increase water in to the matrix rather than increased growth of the cluster while they still account for the majority of the uptake.

6.5.5. Re formulation of PBB based materials.

The PBB elastomer material was chosen as the most promising type of butyl elastomer. It was reformulated in line with that used previously for the SIS based materials. The PBB elastomer is however quite different and did not gel with the monomers that gelled the SIS, particularly with the dimethacrylates. When the PBB was used with a mix of monomers which contained a high proportion of a di methacrylate (e.g. as used for the SIS TGE) the material did not gel properly but instead phase separated to form a gel and a liquid. Even when the dimethacrylate was milled into the gel using the paste mill it would separate after a few days. It was therefore concluded that the di methacrylates (at high concentration) were unusable with the PBB system. Similarly the MM could not be persuaded to gel with the PBB and separated into a swollen particles and a liquid. This is thought to relate to the higher solubility parameter of MM and the dimethacrylates. BM did however form a reasonable gel and hence was used as the basis for the reformulation with PBB.

Table 6.15, gives the formulations of the materials used within this part of the study. The major feature of them being the increase in the elastomer content from 50 % to 80 %, and the use of the reinforcing filler C687.

Table 6.15. Formulation of the PBB and BM based materials.

	PBB to BM ratio	C687, %
PBBB 50/50	50 : 50	-
PBBB 60/40	60 : 40	-
PBBB 70/30	70 : 30	-
PBBB 80/20	80 : 20	-
PBBB C2.5	50 : 50	2.5
PBBB C5	50 : 50	5
PBBB C10	50 : 50	10
PBBB 80/20 C2.5	80 : 20	2.5

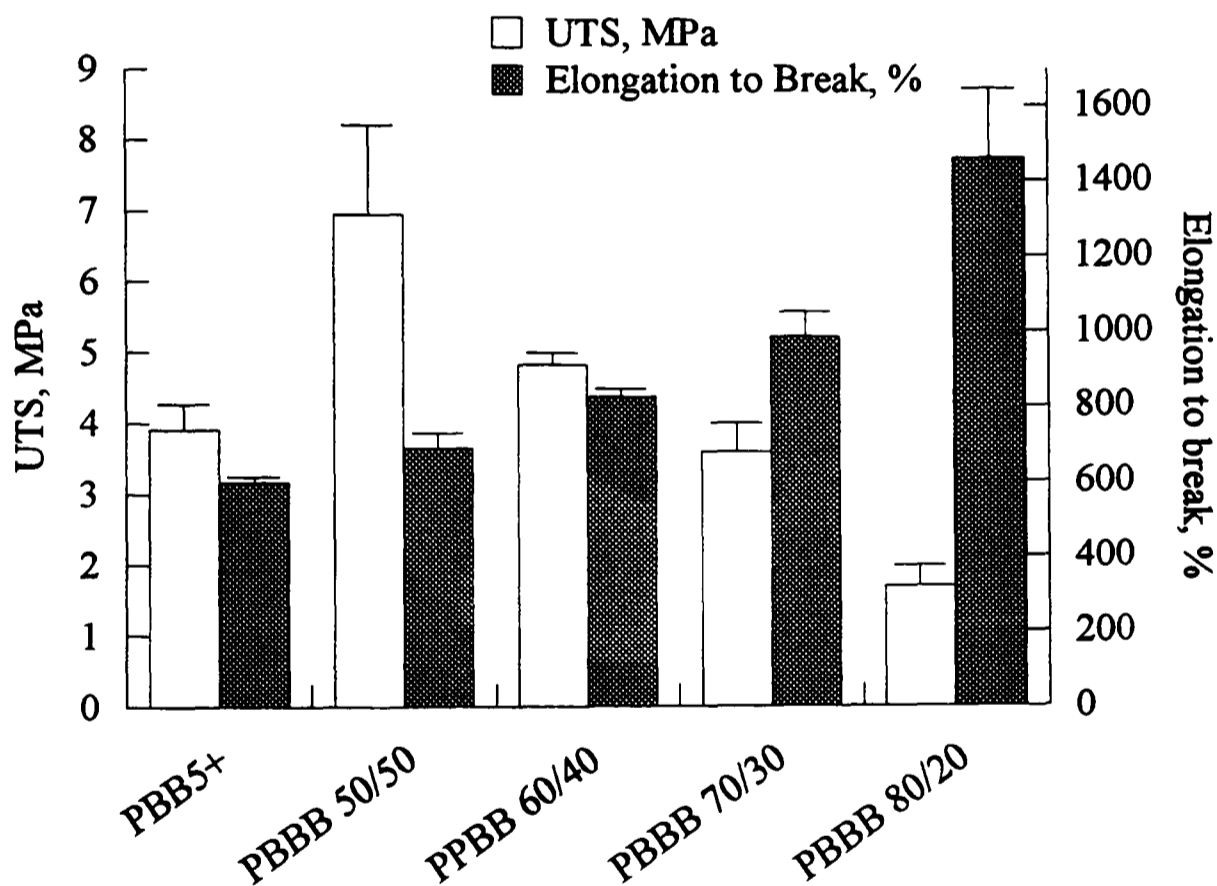
All materials contained 1 % lauryl peroxide and 1% EGDM in the monomer component.

6.5.6. Results of the reformulated PBB based materials.

The change in monomer from EHM (PBB5+) to BM (PBB B 50/50) produced a noticeable increase in strength (figure 6.29) although not as dramatic improvement as

seen for the SIS5+ to SIS M. This improvement may be attributed to poly BM being stronger than the EHM used in PBB5+. The lack of grafting on to the PBB elastomer due to its saturated nature does however mean that the increased methacrylate density (which increased grafting in the SIS M) produces no effect. When the elastomer content was increased the UTS decreased correspondingly in a seemingly linear manner, conversely the elongation to break increased again in a near linear manner. This may be attributable to the inherent nature of the two parts of the material with each part's properties being proportional to it's fraction in the overall composition. Indeed the relationship is such that it suggests little or no interaction between the two components while they form an interpenetrating network.

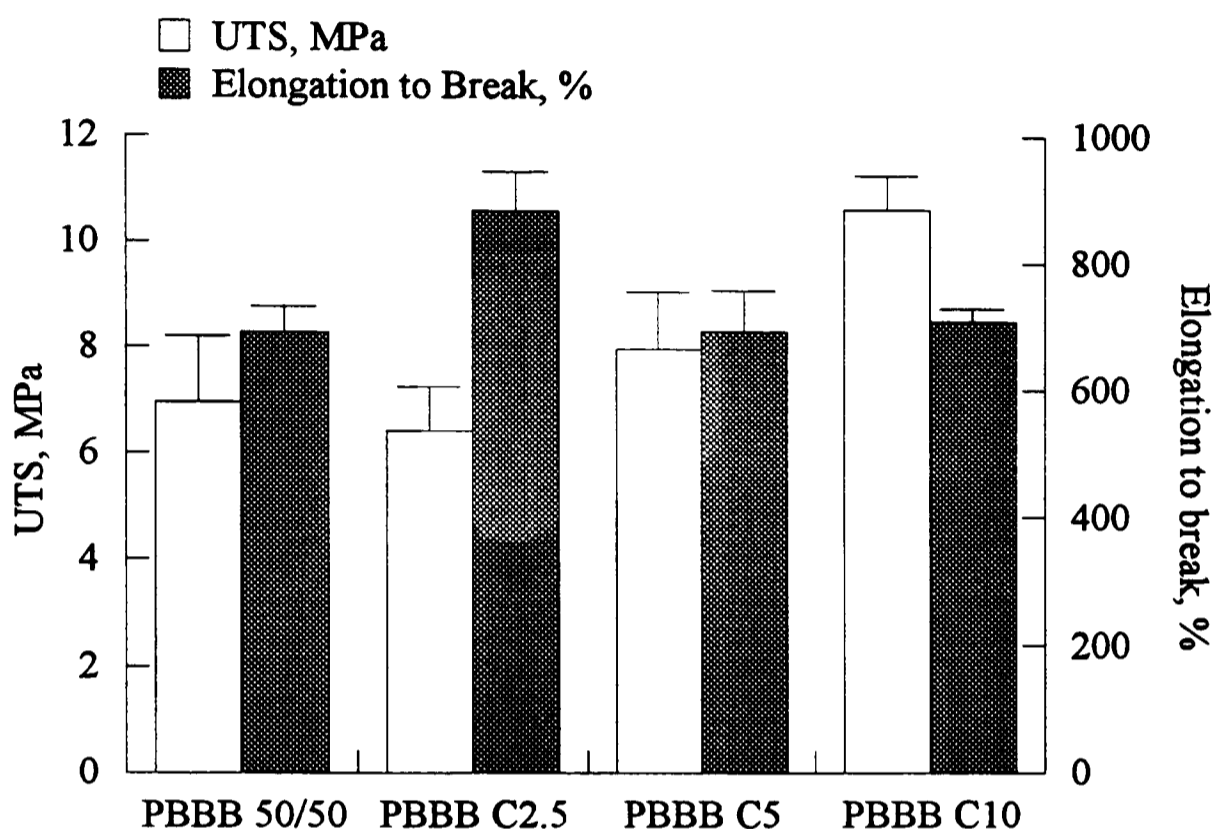
Figure 6.29. Tensile strength of the PBB B based materials with different levels of elastomer.



There is little difference in the tensile strength by reinforcing PBB B 50/50 with C687, as seen in figure 6.30. PBB B C2.5 does have a slightly longer elongation and PBB B C10 a higher UTS but generally the changes are small as with the EBS based materials. The PBB B 80/20 C2.5 is different and illustrates the viscoelastic nature of these materials figure 6.31. None of the PBB B 80/20 C2.5 samples broke during the testing but instead exhibited a maximum stress at particular elongation dependent on the loading rate. The relationship here shows a decrease in stress and increase in the elongation

when a slower loading rate was used. This may be visualised in terms of plastic and elastic deformation with the slower loading rates enabling more plastic deformation at the same elongation so lowering the stress.

Figure 6.30. Tensile strength of the reinforced PBB B based materials.



The water uptake of all the reformulated PBB materials was higher than that of the PBB5+ (figure 6.32 and table 6.16) which may be attributed to BM's greater hydrophilicity compared to the EHM. It is interesting to note that here there is no difference in the absorption for the increase in the elastomer content (although there is a reduction in the solubility) as seen for the SIS8+ samples (figure 6.25 and 6.26). Whereas rather than reducing the uptake as with the EBS and SIS materials the C687 increases the uptake noticeably.

These materials are viscoelastic rather than elastic as illustrated in figure 6.31, and so will show a strong dependence on the loading rate used. When the material is strained by the growth of the droplets (which will grow very slowly) the resultant stress will be much lower than that indicated by the tensile test loading rate (500 mm / minute) would illustrate. The restraint offered by the material to the growth of the droplets will therefore be much smaller. The other materials where the methacrylate grafted onto the elastomer behaved in a more ideal elastic manner and an effective restraining force could

be developed. The butyl elastomers are incapable of developing the restraining force and so the water moves in driven by the osmotic gradient without the restraint. While the addition of the C687 will bond to the methacrylate the lack of grafting does not prevent the plastic flow of the material around the droplets. Indeed the addition of the C687 only increases the uptake by adsorbing water onto the surface. This plastic flow or creep around the droplets is apparent in the shape of the uptakes with the butyls showing a linear uptake, which is similar to that of the uncrosslinked pure elastomer samples used in the study.

Figure 6.31. The loading rate dependence of the strength of PBB B 80/20 C2.5.

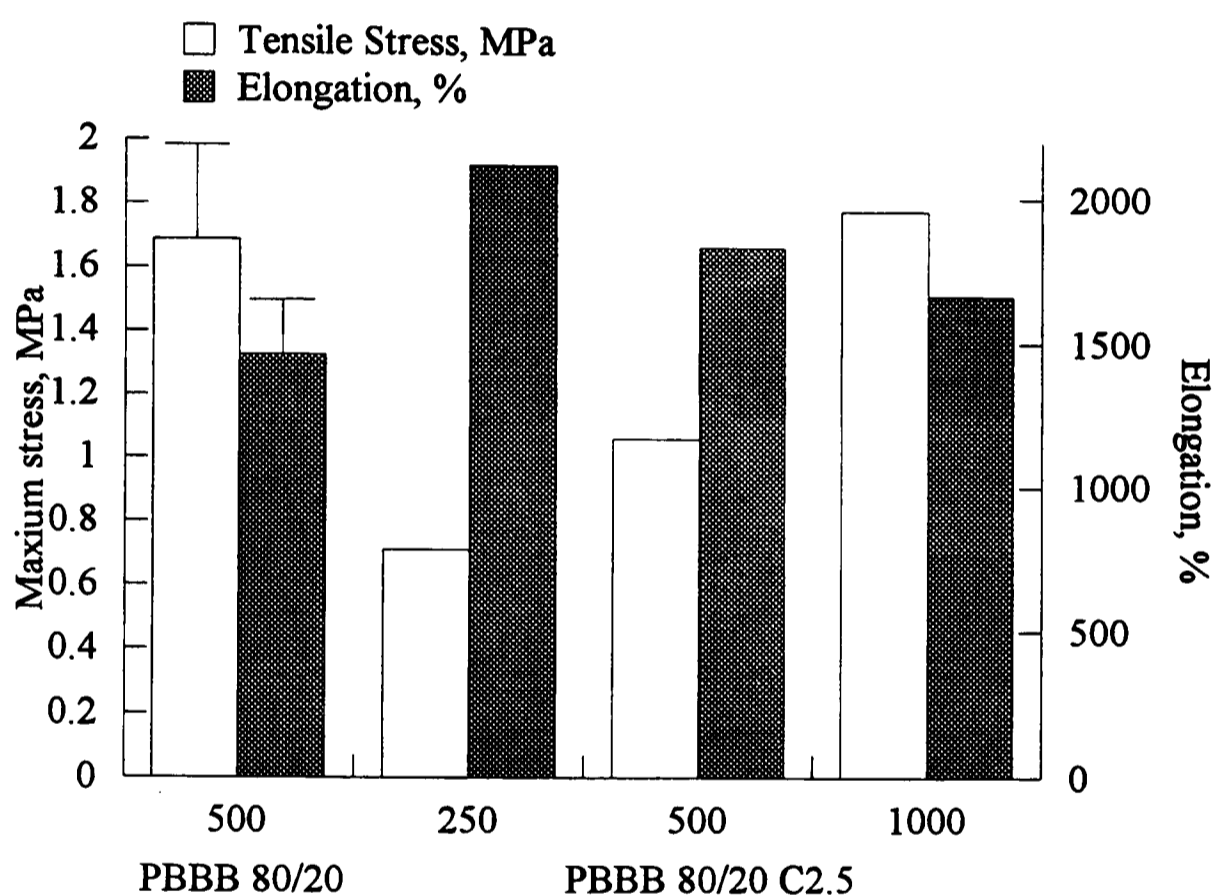
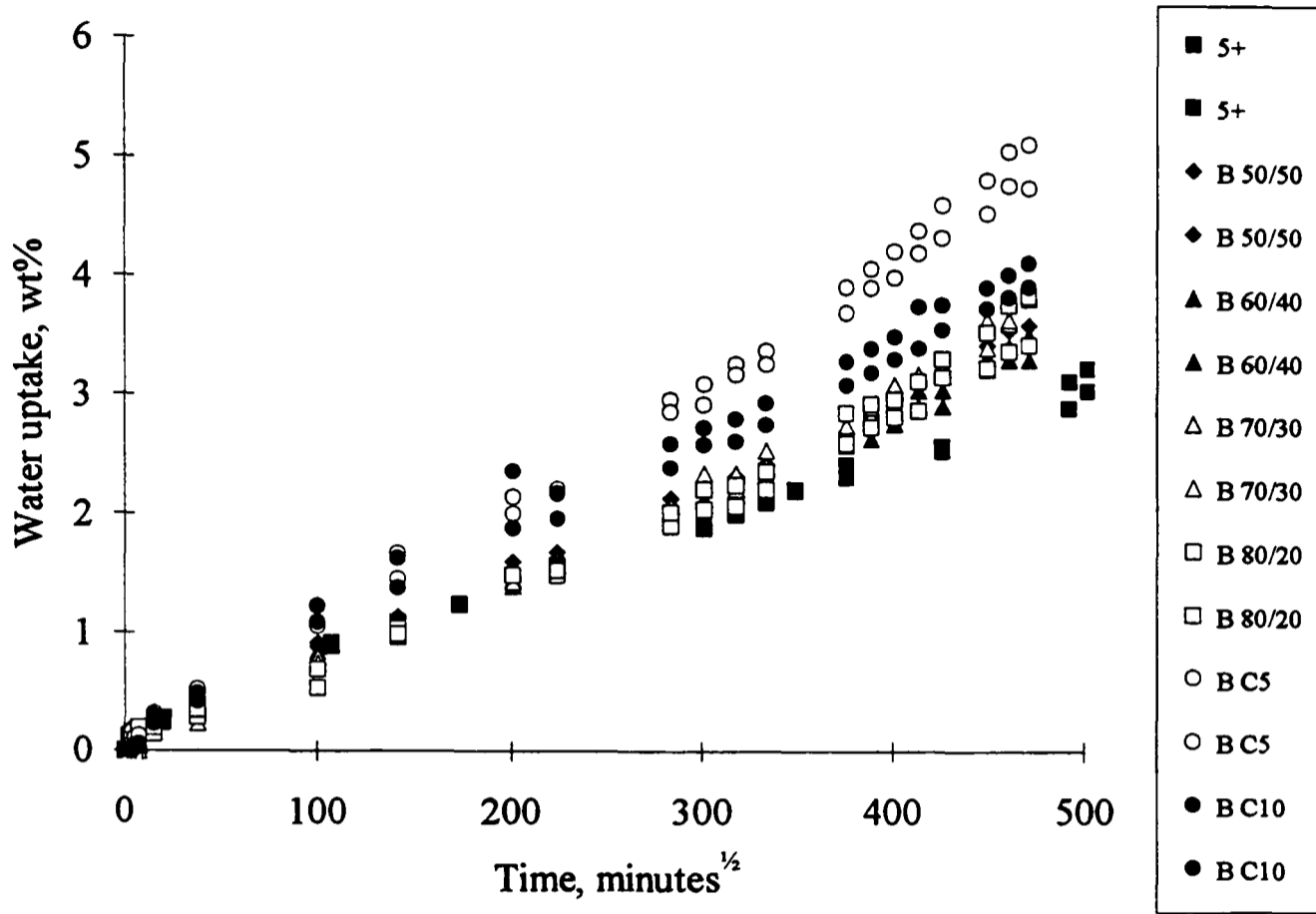


Table 6.16. Summary of absorption of PBB B based materials.

	Uptake, wt%	at, days	Solubility, wt%	Total abs, wt%	D_{des} , m^2s^{-1}
PBB5+	3.37	203	0.31	3.68	6.10×10^{-10}
PBBB 50/50	3.60	154	0.31	3.92	1.80×10^{-10}
PBBB 60/40	3.51	154	0.28	3.79	1.06×10^{-10}
PBBB 70/30	3.83	154	0.23	4.06	2.01×10^{-10}
PBBB 80/20	3.84	154	0.11	3.96	4.83×10^{-10}
PBBB C5	4.75	154	0.21	4.96	8.41×10^{-11}
PBBB C10	3.92	154	0.26	4.18	9.52×10^{-11}

Figure 6.32. Water absorption of PBBB based materials.



Chapter 7.

Nuclear Magnetic Resonance Imaging.

7.1. Introduction.

As previously described nuclear magnetic resonance (NMR) has proven a valuable tool in the study of diffusion of water and other fluids into polymers. Appendix II.2, briefly describes the operation of the NMR in relation to H^1 imaging, there are of course many other possible methods such as H^1 and C^{13} spectroscopy. H^1 NMR imaging was the only methods employed within this part of the study but it is recognised that other methods of imaging and spectrometry may be interesting and reveal more about the absorption process.

The equipment used in this part of the study was a Varian / Siemens-200 with a magnetic field strength of 4.7 T situated in the Department of Chemistry, Queen Mary Westfield, Mile End, London, under the guidance of Dr P. Kinchesh. The testing methodology used in this study was a compromise between what could be achieved on this NMR and that which ideally would have been attempted, as the acquisition time T_e and spatial resolution are limiting factors. From previous authors (Blackband and Mansfield, 1984, Blackband and Mansfield 1986, Artemov et al, 1988, Fyfe et al, 1993) the relaxation time of water in a polymer is short at 0.5 to 3 ms and will depend on how the water and polymer interact. The shortest T_e time possible on the NMR used is 2.5 ms which uses a T_1 image with a 1 ms gaussian pulse and has a resultant slice thickness resolution of about 2 mm. This leads to the conclusion that this NMR is unsuitable for imaging of water diffusion into the polymer matrix.

This however does not rule out the NMR as a potential technique for elastomers as comparatively little water is absorbed by the matrix compared to that in solution droplets. The water in these solutions will be comparatively freer and so have a longer relaxation time, pure water typically has a relaxation time over one second. This water would therefore be detectable at a much slower T_e giving more reproducible T_2 images rather than T_1 images. In order to maximise the development of droplets and minimise the water absorbed by the matrix a series of doped, unfilled, stoichiometrically balanced hydrosilanised (catalysed by VPT) silicones were prepared as samples for the NMR.

7.2. Methodology.

Five cylinders 15 mm diameter and 50 mm length were made up, 4 of which were doped with 1% of a different hydrophilic agents as given in table 7.1. These, it is felt (based on the experience of chapter 4), represented a range of different absorption characteristics.

The Si NB A used ground NaBr rather than the crystals used in Si NB B, thus the NaBr in Si NB A will be more uniform and have smaller particle size. The Si NB B had also been previously used in a preliminary study to determine a suitable technique for observing the formation of the droplets in the material. In this study this sample was immersed in water for 1 month, then desorbed so it was dry again for the start of this study.

Table 7.1. Formulation of unfilled stoichiometrically balanced silicone polymers catalysed with VPT.

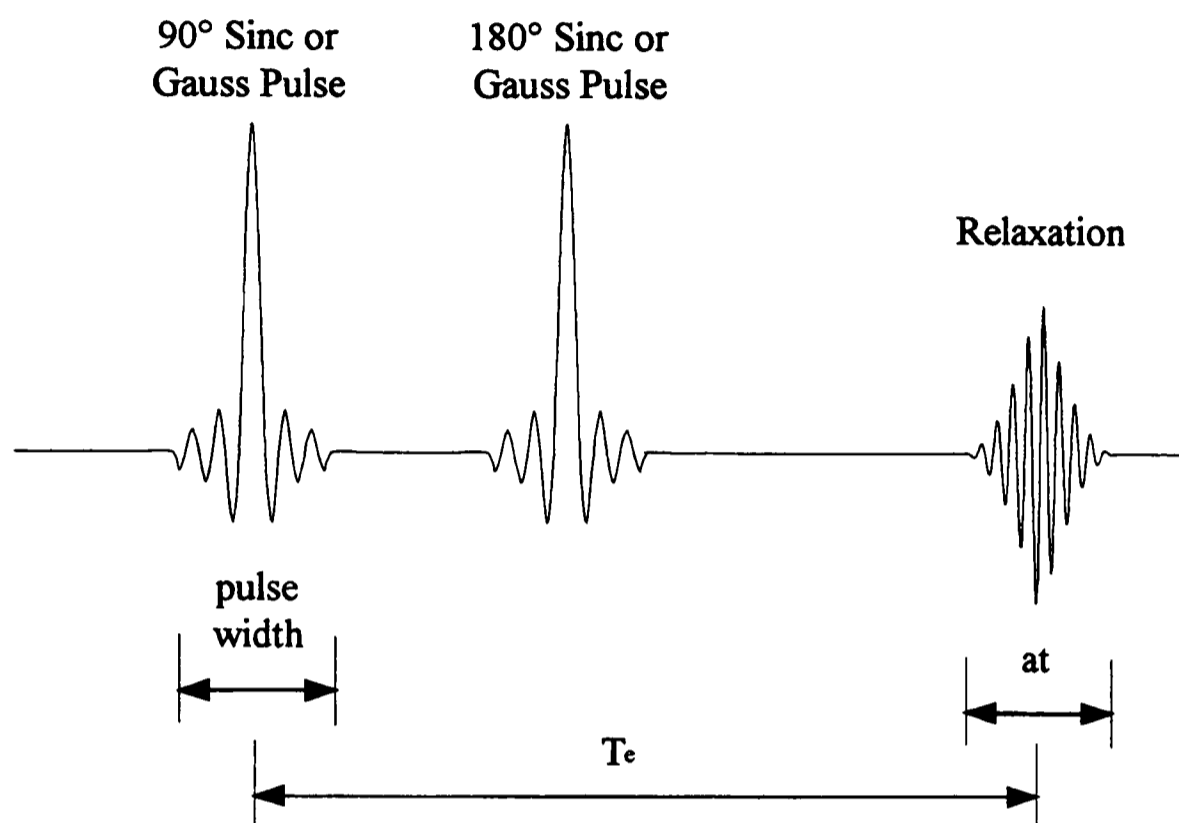
Code	Agent	%
Si Pure	-	-
Si L77	L77	1
Si CS	Calcuim Stearate	1
Si NB A	Na Br (ground)	1
Si NB B	Na Br (crystals)	1

There are practical problems associated with performing the tests, the NMR facility being a couple of miles from the site of the St. Bartholomew's and the Royal London School of Medicine and Dentistry, the tests typically taking 24 hours to complete and the lack of temperature control the temperature within the NMR. Temperature plays an important role in the absorption process, the diffusion coefficient increasing with temperature. Thus a decision had to be taken at which temperature to perform the tests, bearing in mind that it would not be possible to keep the samples at one specific temperature throughout the absorption process. It was decided to keep the samples at 37°C between measurements with the samples being left at ambient for approximately one day during each series of NMR measurement. While this is not ideal, it was the same for all the samples and should have kept the overall kinetics similar to those previously observed at 37 °C.

Figure 7.1, illustrates the basic pulse sequence used for the NMR with a 90° pulse being applied then the 180°, and time T_e after the initial pulse the relaxation is monitored by the detector. Details of the parameters used and the pulse sequences are shown in table 7.2, figure 7.2 and figure 7.3. The X, Y and Z lines below that of the pulse sequence relate to the gradients applied to select a specific volume of the material during the pulse

sequence. In the initial part of the sequence there is 'v5=0?' this relates to an event timing feature of this type of NMR experiment which was not used in this study.

Figure 7.1. Simplified pulse sequence of H^1 NMR used in imaging experiments.



The shape of the pulse controls the shape of the slice of the material selected, as the slice shape is the Fourier Transform of the pulse, i.e. a sinc pulse activates a rectangular slice of the material. A sinc pulse was used in the T_e 40 ms experiment and took 5 ms to apply (shown in figure 7.1). In order to minimise T_e for the 9 ms experiment the pulse type was changed to a Gaussian which only took 3 ms (figure 7.2) hence shortening the time required for the imaging pulses. It is important to realise however that the Fourier Transform of a Gauss is another Gauss and so the slice of the sample selected will be a Gauss rather than a rectangle as with the sinc pulse. This is not ideal but the use of a gauss enables the shorter T_e time and so represents a reasonable compromise.

Table 7.2. Selective parameters used in the imaging experiments.

	T_e , 40 ms experiment	T_e , 9 ms experiment
Slice thickness	0.546 mm	1.092 mm
Resolution	0.027 mm	0.054 mm
at, acquisition time	2.9 ms	1.4 ms
np, number of points (real and imaginary)	512	256
ni, phase encoding steps	256	128
p1, 1st pulse type	sinc	gauss
p1, 1st pulse width	5 ms	3 ms
pw, 2nd pulse type	sinc	gauss
pw, 2nd pulse width	5 ms	3 ms
total time for experiment	25 min	12 hours
nt, number of repetitions	48	8

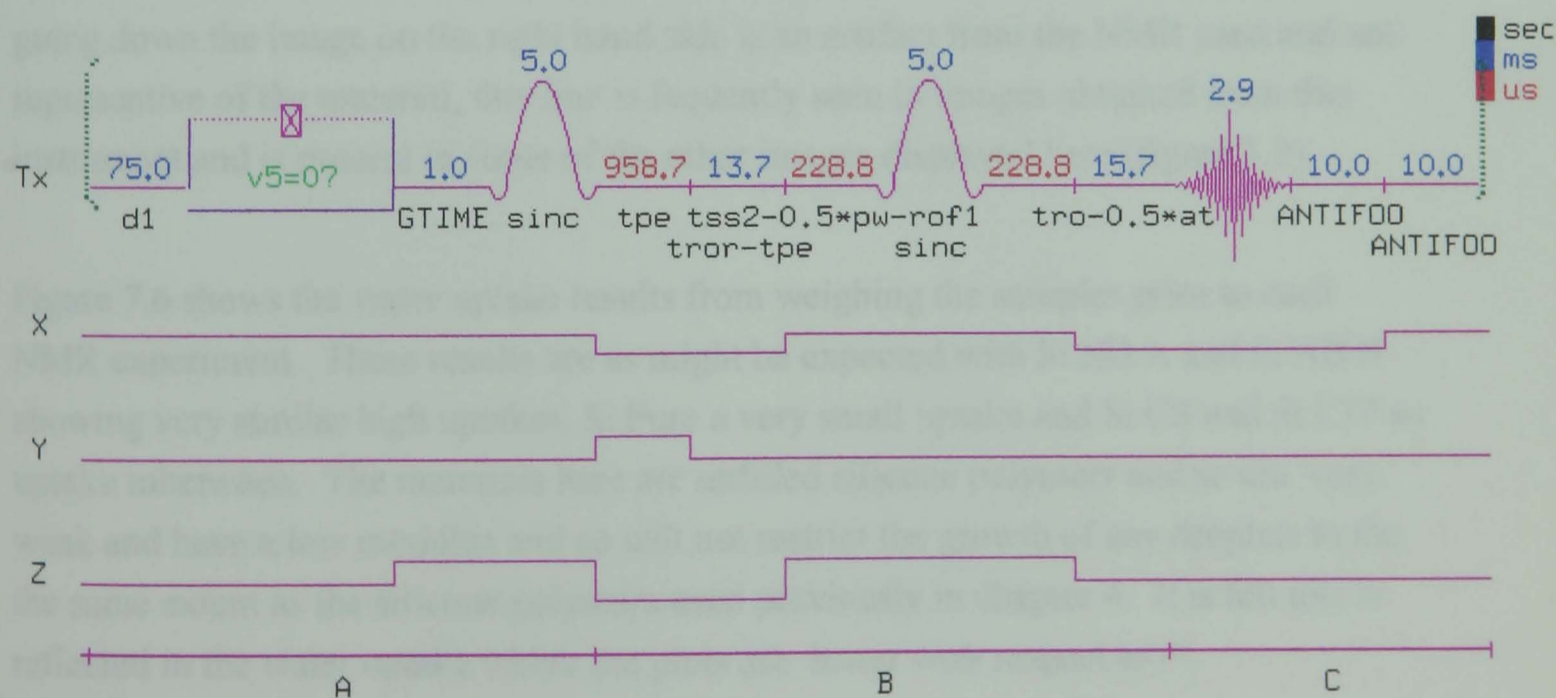
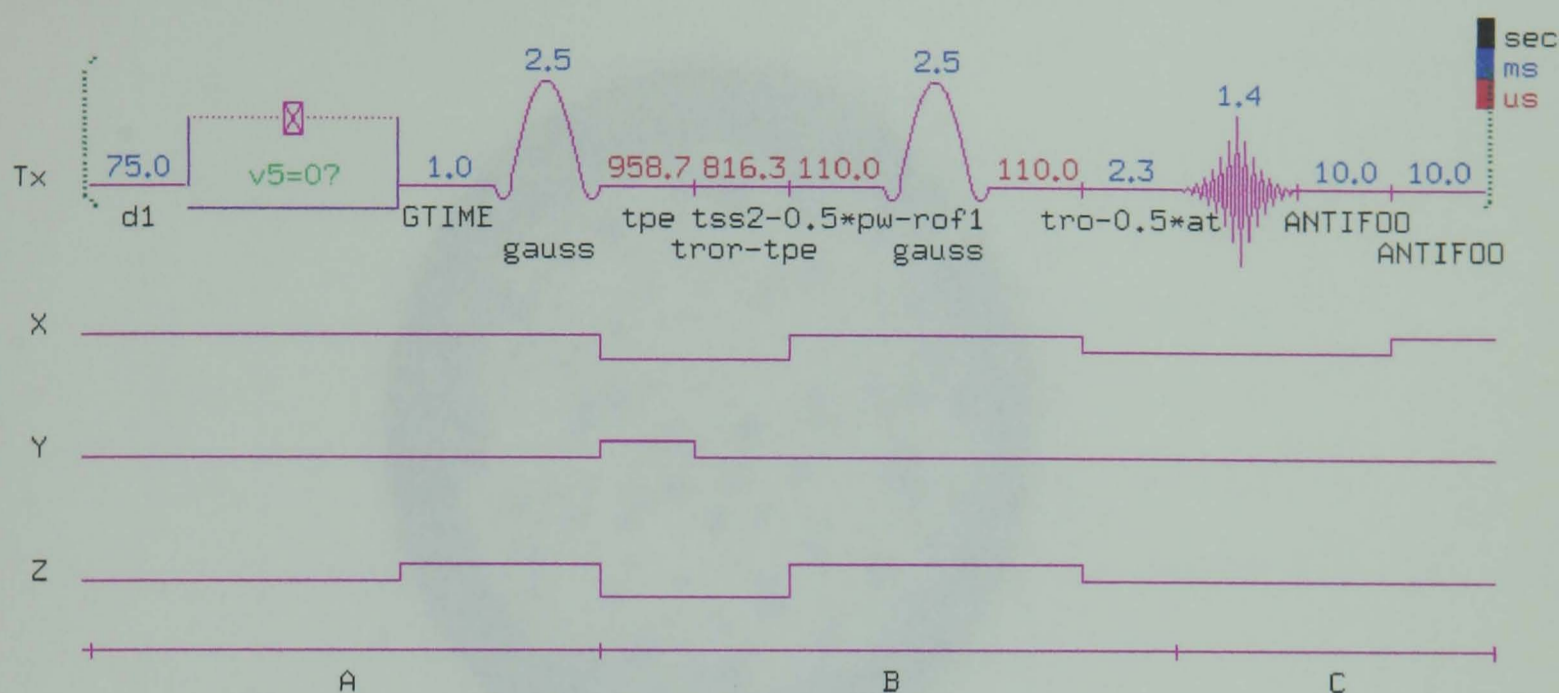
Figure 7.2. NMR Pulse sequence for T_e 40 ms experiment.

Figure 7.3. NMR Pulse sequence for T_e 9 ms experiment.

7.3. Results of NMR imaging experiments.

Figure 7.4 is an image obtained on the NMR and clearly shows the formation of droplets within one of the NaBr doped silicone samples (Si NB B). The sample (the lighter region) is situated in a tube and is surrounded by water (the blue / purple area around the outside) with droplets (blue / purple areas) within the elastomer. The line going down the image on the right hand side is an artifact from the NMR used and not representative of the material, this line is frequently seen in images obtained from this instrument and is present in some of the other images displayed here (figure 7.5).

Figure 7.6 shows the water uptake results from weighing the samples prior to each NMR experiment. These results are as might be expected with Si NB A and Si NB B showing very similar high uptakes, Si Pure a very small uptake and Si CS and Si L77 an uptake inbetween. The materials here are unfilled silicone polymers and so are very weak and have a low modulus and so will not restrict the growth of any droplets to the the same extent as the silicone polymers used previously in chapter 4. It is felt this is reflected in the water uptake where the plots are linear with respect to $t^{1/2}$.

Figure 7.4. Image of droplets within a NaBr doped silicone sample at approximately 6 months.

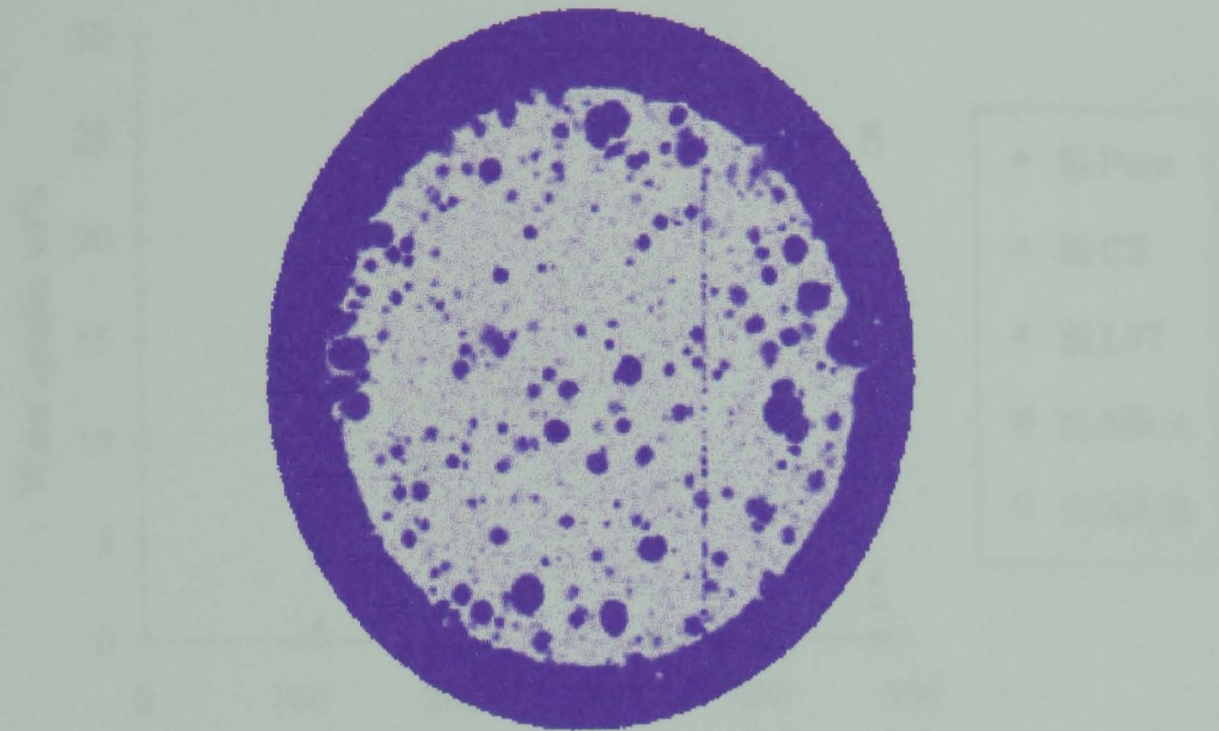


Figure 7.5. Initial image of the samples before immersion in water (t_e 40 ms).

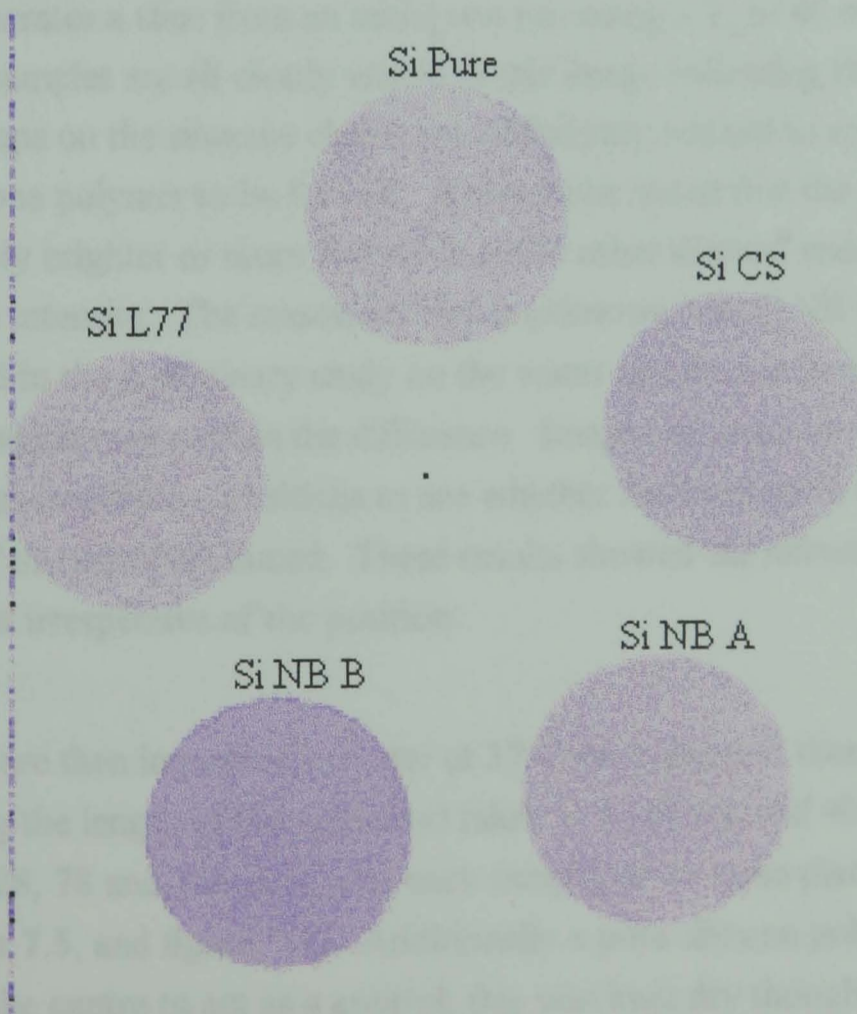


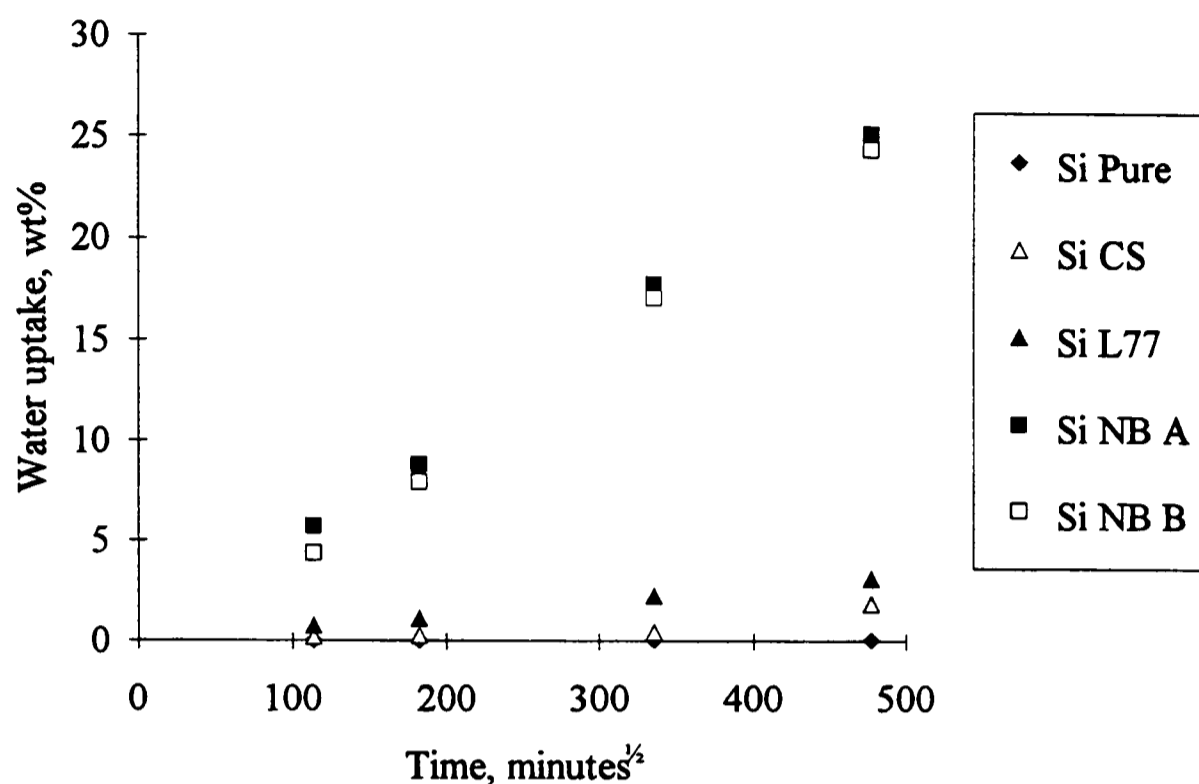
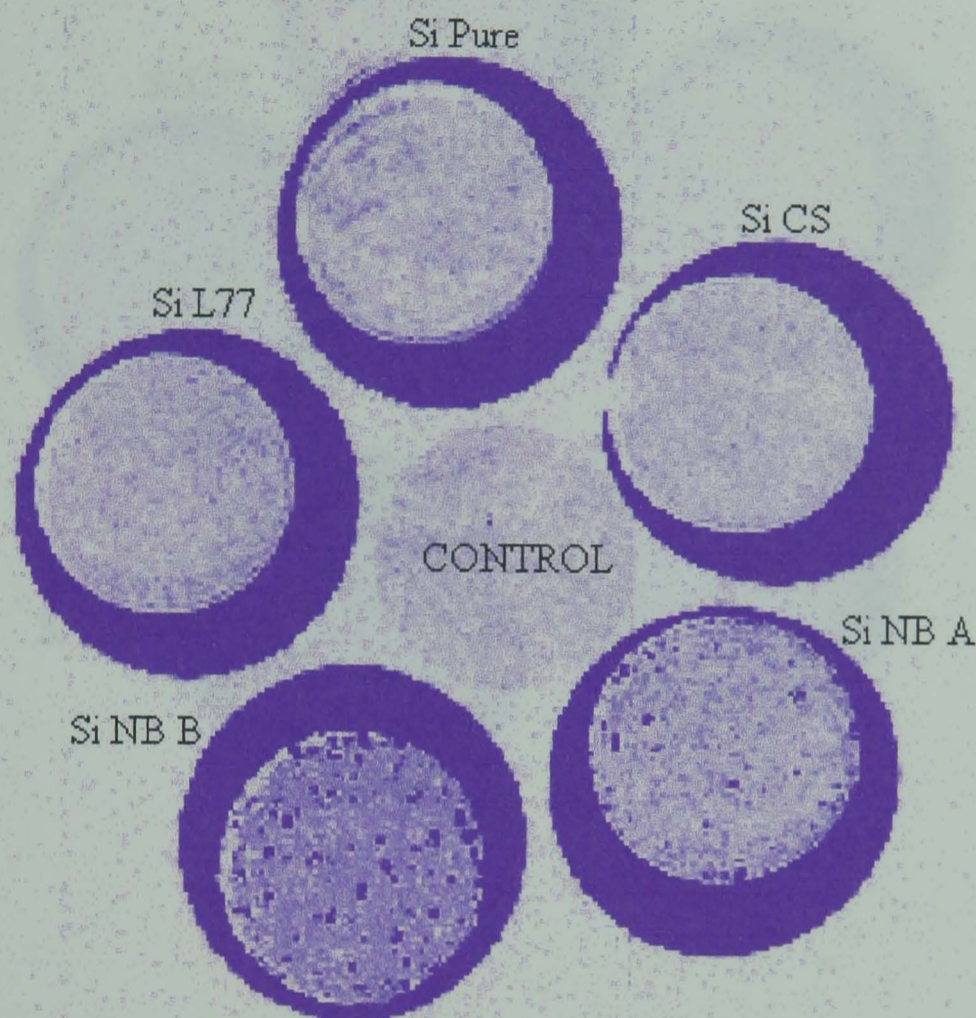
Figure 7.6. Water uptake of the silicone cylinders used in this study.

Figure 7.5, illustrates a slice from an initial test run using a T_e of 40 ms on dry desorbed samples. The samples are all clearly visible in this image indicating that the hydrogen of the methyl groups on the siloxane chains are sufficiently relaxed to enable an image of the actual silicone polymer to be formed. It should be noted that the Si NB B sample was considerably brighter or more intense than the other silicone materials which were of about the same intensity. The reason for this is unknown; the Si NB B sample was previously used in the preliminary study on the water uptake and hence made at a different time which may explain the difference. Images of these samples were taken with the samples in different positions to see whether the location in the NMR affected the intensity of the signal produced. These results showed the intensity of the samples to remain constant irrespective of the position.

The samples were then immersed in water at 37°C for 1 day and then a series of images (30 slices along the length of the cylinders) taken at T_e (9 ms, and 40 ms). This was repeated at 9, 28, 78 and 158 days with each sample in the same place in the coils (as shown in figure 7.5, and figure 7.7). Additionally a pure silicone polymer of 9 mm length was placed in the centre to act as a control, this was kept dry throughout the experiment. An example of the images obtained is seen in figure 7.7, with the control visible in the centre, and the samples in tubes surrounded by water as for figure 7.4. Solution droplets

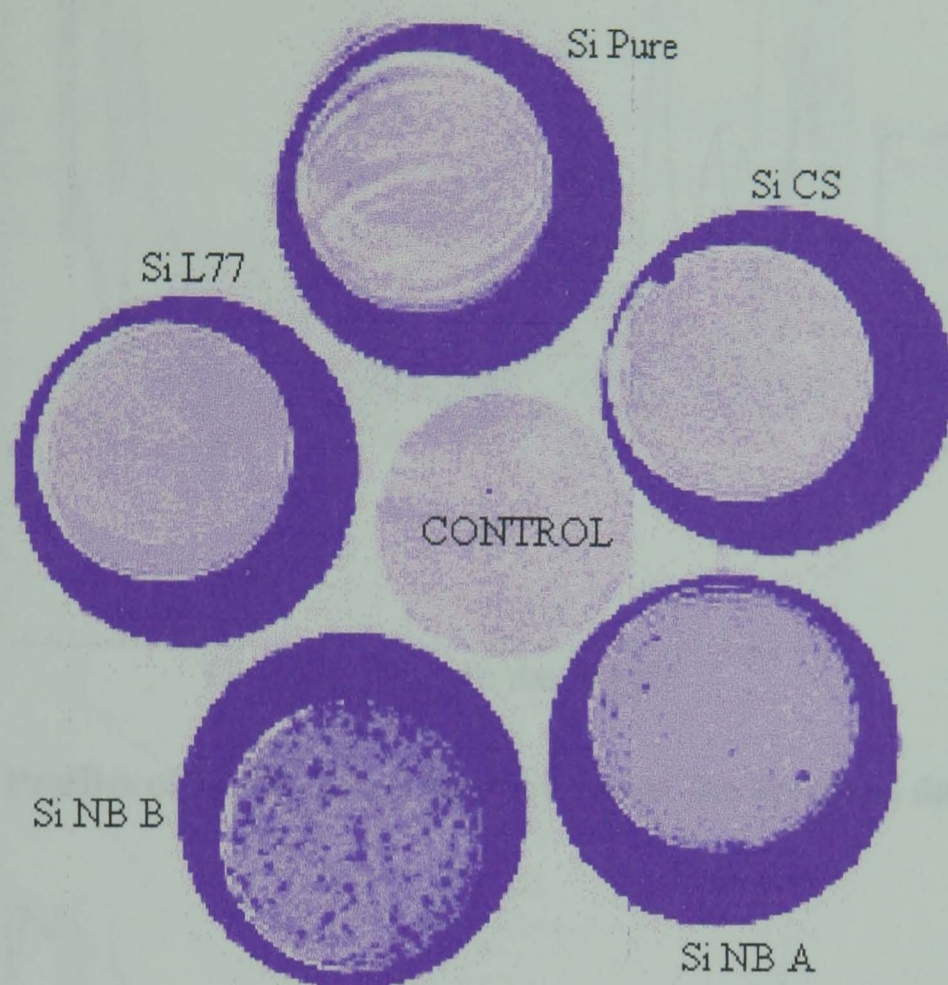
within the material are visible in both the Si NB A and B samples at this early stage but not in any of the other samples, indeed no solution droplets were observed for any of the other material throughout the study.

Figure 7.7. Image of samples after 9 days immersion in water (t_e 40 ms).



In order to try and quantify the NMR images an average image was made by adding 8 individual slices (an example of which is figure 7.7) to form a new image seen figure 7.8. The control sample (in the center of the image) was always placed approximately half way along the length of the other cylinders. By averaging the slices containing the image of the control sample, a similar portion of each sample was being taken each time. From these averaged images profiles may be taken of the intensity of signal through the sample hence the concentration of water through the sample.

Figure 7.8. Average of samples 8 slices of the samples after 9 days immersion in water (t_e 40 ms).



7.3.1. The kinetics of the absorption.

Figure 7.9, shows the profile of the average images of Si NB A at different times using T_e of 40 ms. From this we can see that the intensity of the signal (counts) increases with time, there is however a lot of variation on each line through the sample. The averaging of 8 slices will reduce the intensity of the variation through the sample due to the droplets but it does not get rid of it completely. Hence the variation may be attributed to the droplets present in the sample. Figure 7.10, shows the profiles of the same sample at a T_e of 9 ms, here their lines are much smoother. This is due to greater slice thickness used in the 9 ms experiment (slice thickness 1.092 mm for 9 ms experiment and 0.546 mm for T_e of 40 ms) giving to a better averaging of the 8 slices through the sample.

Figure 7.9. Profiles of Si NB A at different times of the averaged t_e 40 ms experiment.

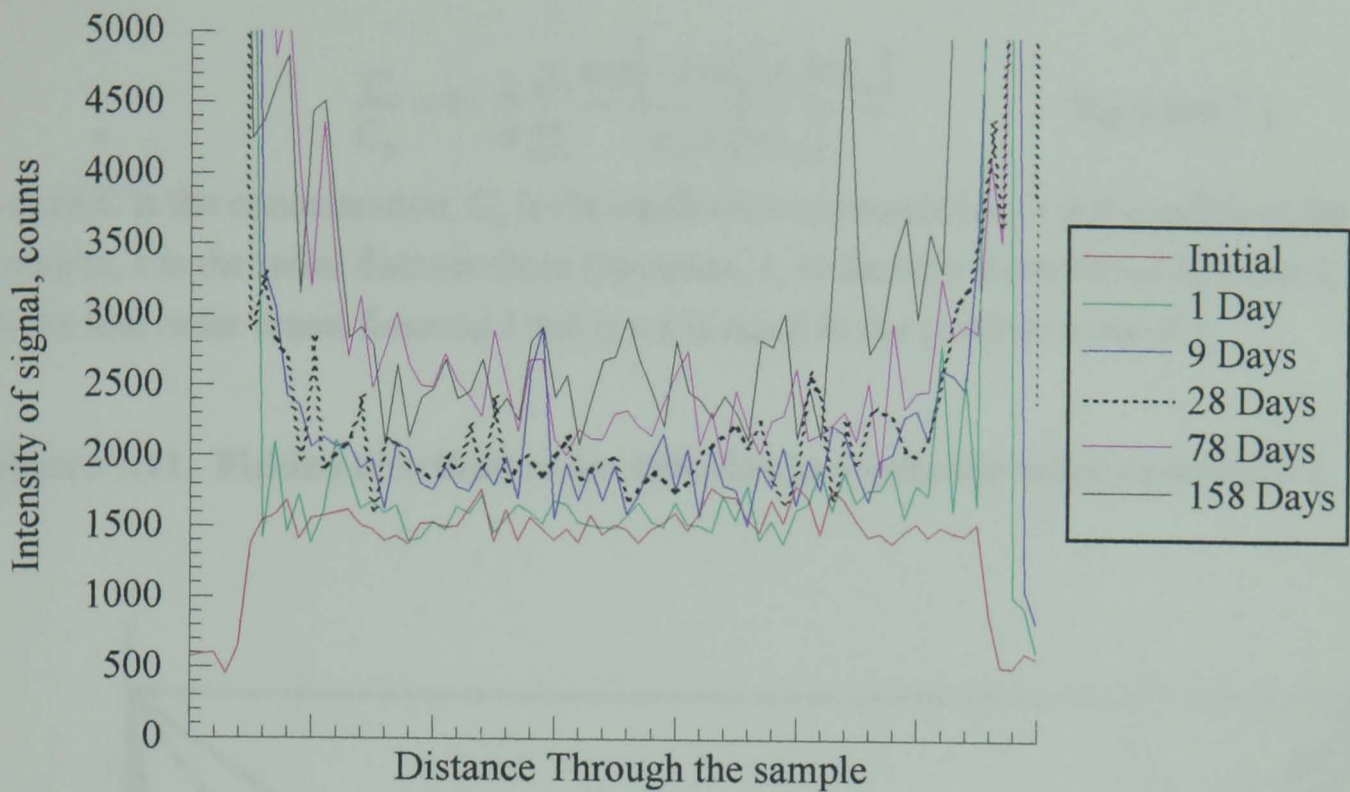
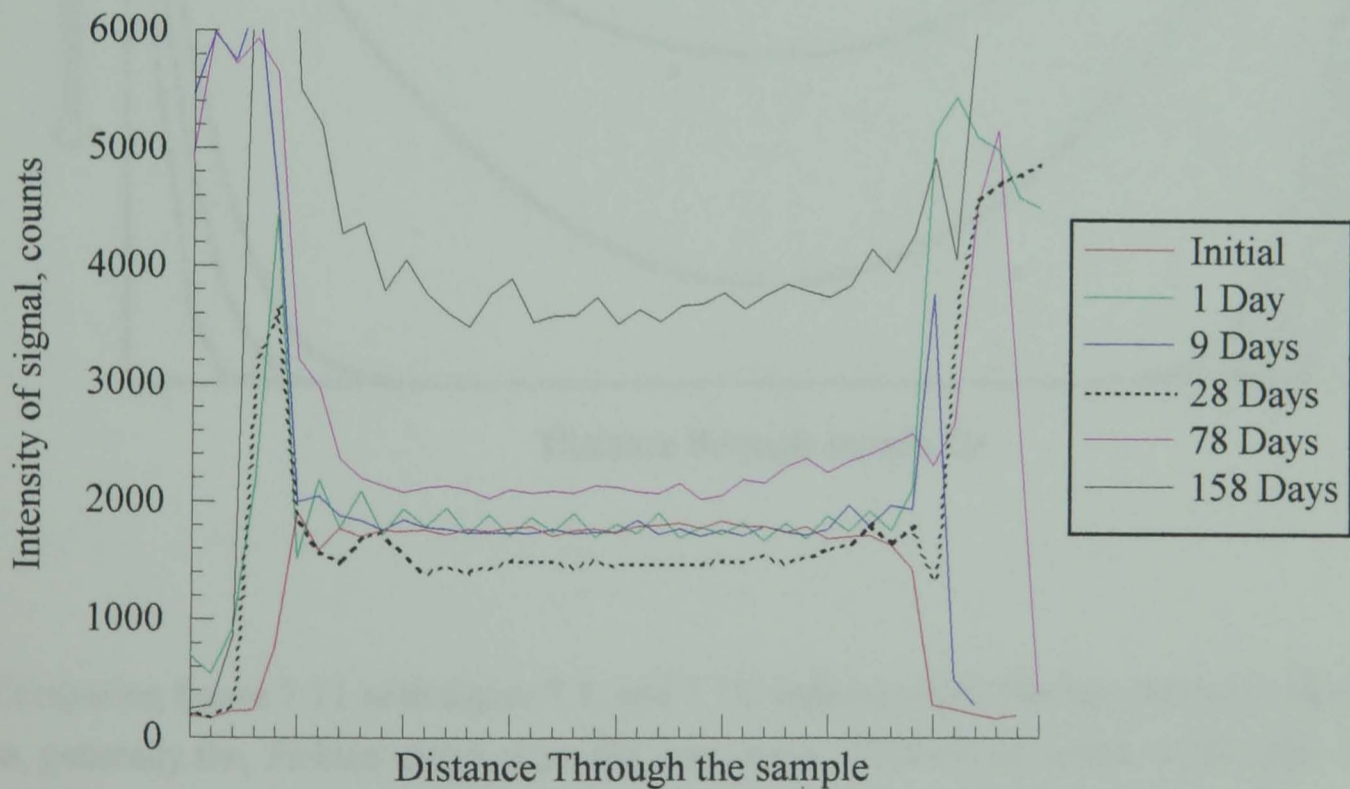


Figure 7.10. Profiles of Si NB A at different times of the averaged data t_e 9 ms experiment.



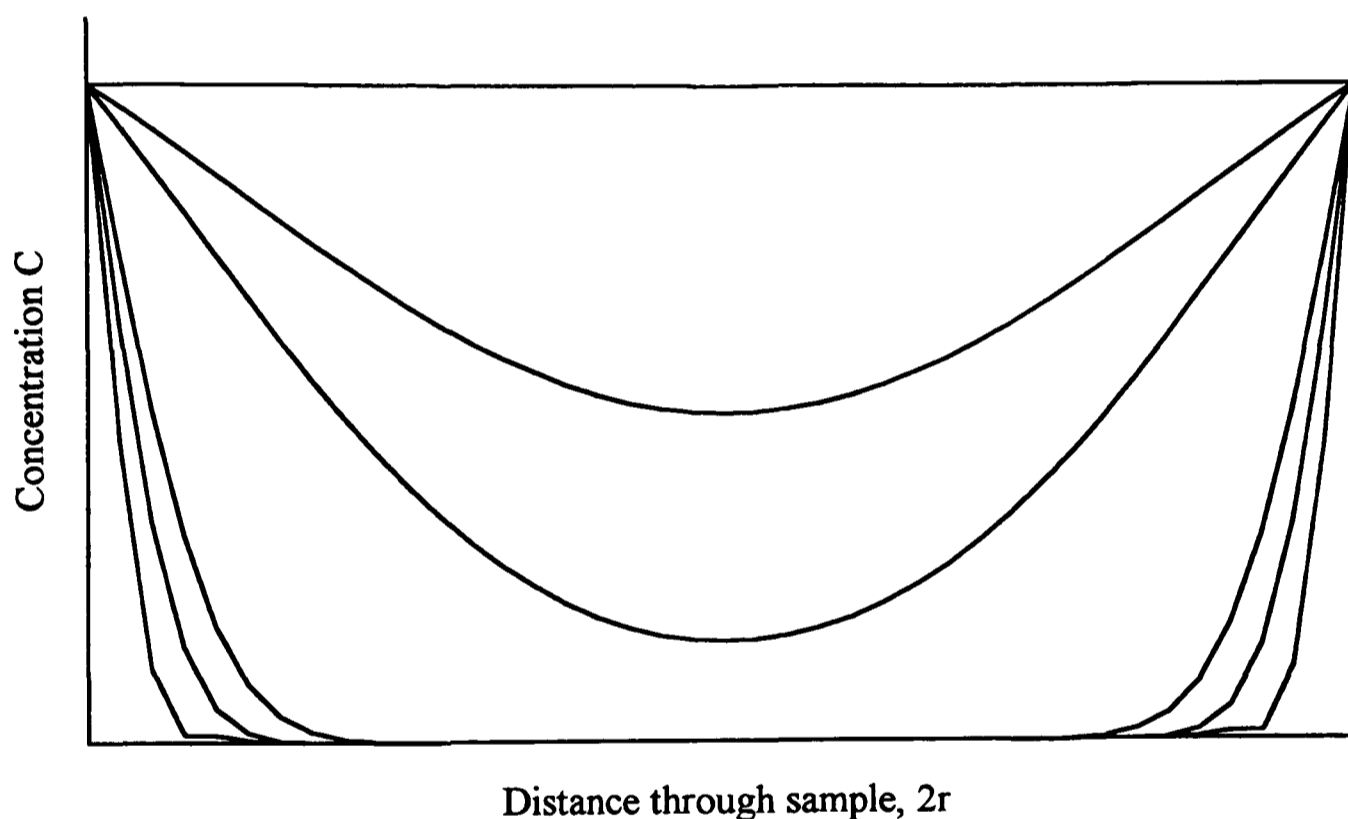
The question then arises over the shape of the profile. Muniandy and Thomas assumed that there would be a gradient in the concentration of water with the greater concentration being at the surface in a classical Fickian manner as shown in figure 7.11. This profile is described by the solution of Ficks second law for diffusion into a cylinder

where the surface is in equilibrium with the external solution (i.e. at the surface $C = C_o$). Namely (Crank, 1975),

$$\frac{C}{C_o} = 1 - \frac{2}{a} \sum_{n=1}^{\infty} \frac{\exp[-D\alpha_n^2] J_0[r\alpha_n]}{\alpha_n J_0[\alpha a]} \quad \text{Equation 7.1.}$$

where C is the concentration, C_o is the equilibrium concentration, a is the radius of the cylinder, r is the radial distance from the center, J_0 is the zero order Bessel function J , J_1 is the first order Bessel function J and $\alpha \times a$ is equal to the positive roots of J_0 .

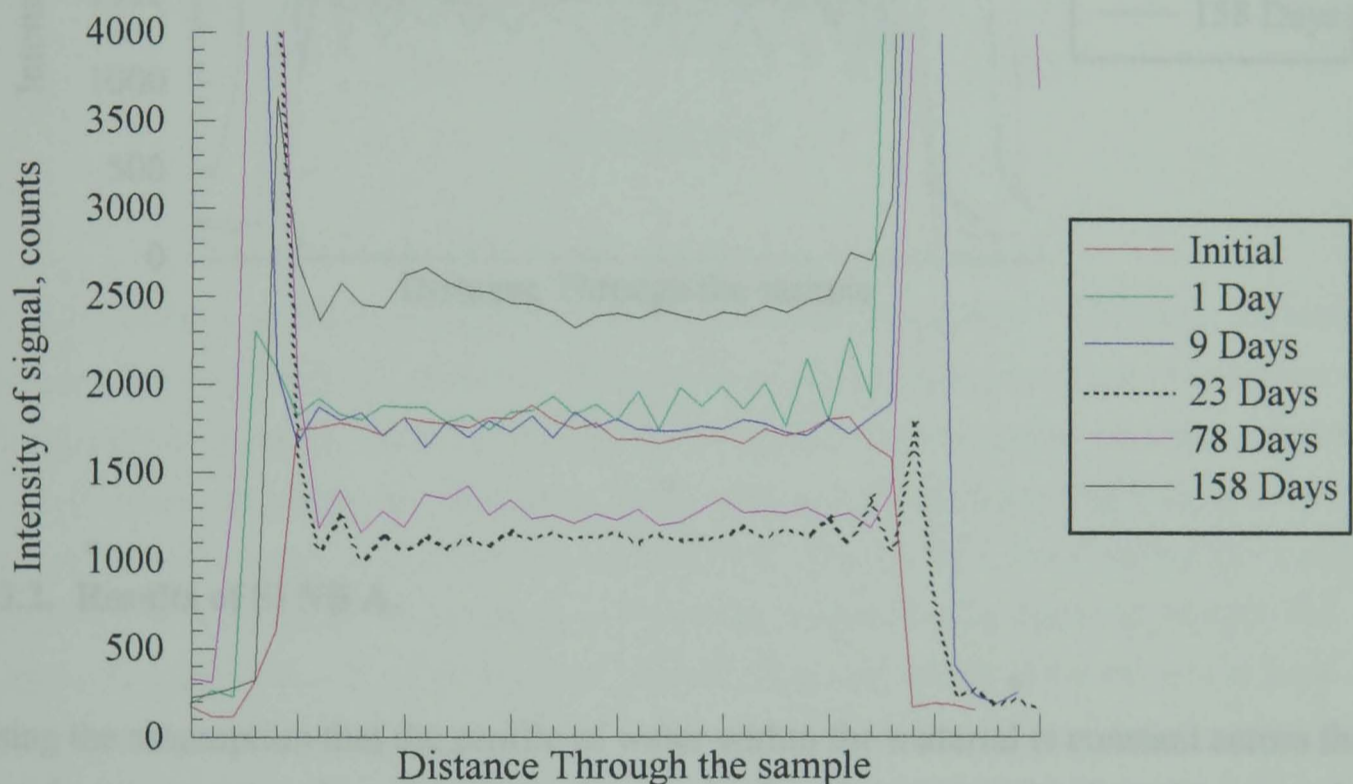
Figure 7.11. Fickian distribution for diffusion in a cylinder using equation 7.1.



Comparing figure 7.11 with figure 7.9, and 7.10, indicates that this assumption is flawed as, generally the, Fickian shape of profile is not seen. There is an upturn at the edge of the sample, particularly during the later stages, which looks as if it could be an early Fickian front but this is unlikely for two reasons. Firstly the time period for the formation of this front is very slow, and secondly there is growth of the droplets in the center of the material (i.e. a increasing intensity) which is not predicted in the earlier stages of the uptake.

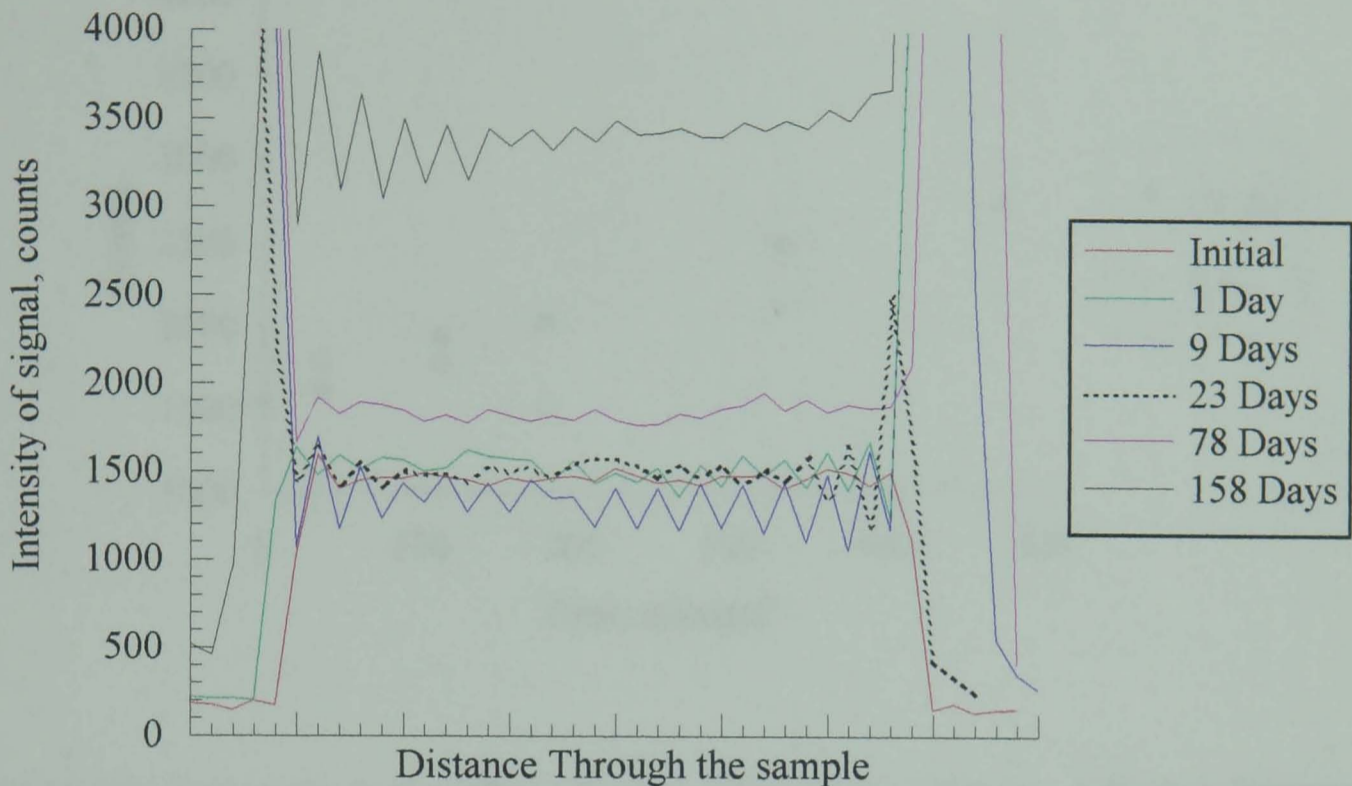
There is another possibility in that the balance between the droplets and the restraining force is not being achieved and therefore the droplets keep growing at the surface resulting in the surface front. This is contradicted by the second point and the results from the other materials which also show the level across the sample as illustrated by figure 7.12, and 7.13. This seems to suggest that the absorption is a two stage process as described Harrison et al (1991) and Watson and Baron (1996). With the water diffusion through the material wetting the entire material and then the growth of the droplets.

Figure 7.12. Profiles of Si CS at different times of the averaged data t_e 9 ms experiment.



The upturn at the edge may be explained by considering the restraining force, at the edge the geometry is different from the bulk and the restraining force developed may be substantially lower. Indeed the droplets in figure 7.4, are spherical in the centre of the material but near the surface they bulge out towards the surface as would be expected with a less effective restraining force at the surface.

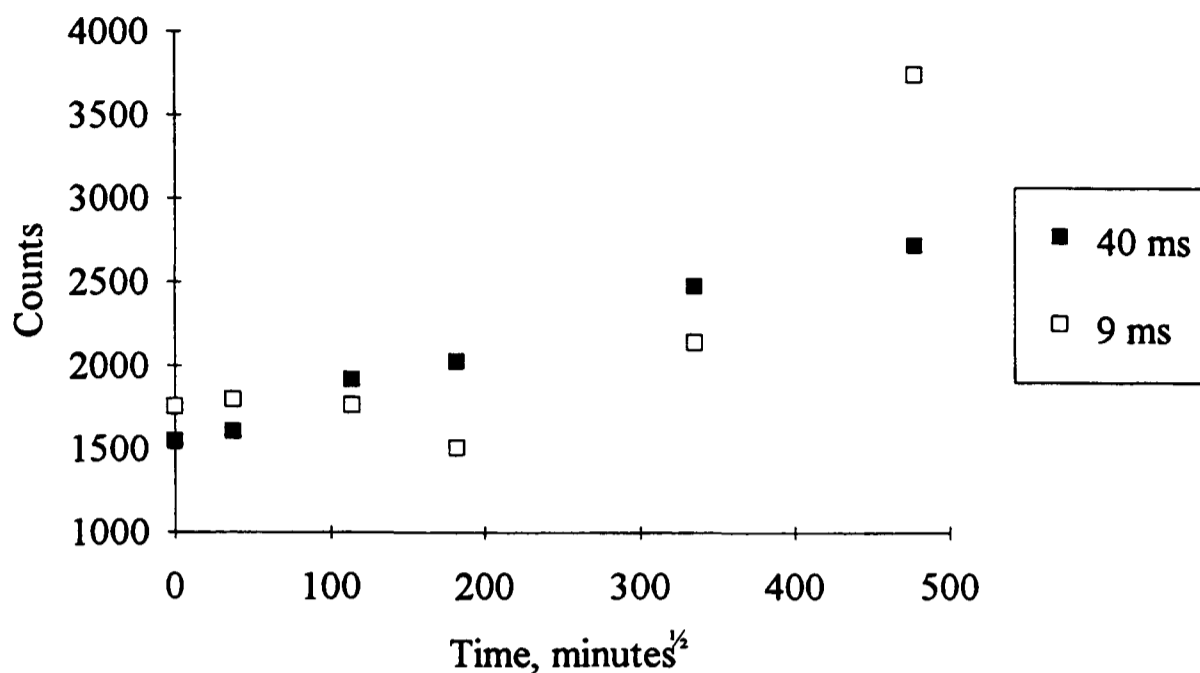
Figure 7.13. Profiles of Si L77 at different times of the averaged data t_e 9 ms experiment.



7.3.2. Results of Si NB A.

Using the assumption that the profile of water within the material is constant across the sample, an average value of the intensity may be found, ignoring the values near the surface where the forces surrounding the droplet will be different. Figure 7.14, illustrates the increase of the average value of the intensity from the profile of the Si NB A as seen in figure 7.9, and 7.10. From this we can see an increase of intensity with time, clearly for the T_e 40 ms but not so well for the T_e 9 ms experiment. The reason for this seems to stem from the NMR itself with a fluctuation in the intensity of both the control and Si Pure samples being observed (table 7.3) this is noticeably more pronounced for the T_e 9 ms experiment than the T_e 40 ms experiment. The reason for this is unknown as it is unlikely that the material will have changed during the course of the experiment indeed the fluctuations are consistent at a test age.

Figure 7.14. The intensity of the value calculated from the averaged images of Si NB A.



A possible explanation is the effect of temperature on the polymer. Although the room housing the NMR was air conditioned it seems probable there was some temperature fluctuation in the room over the course of the 6 months of the study. It seems probable that at lower temperatures the protons (hydrogens) on the siloxane and indeed in the water will relax faster than when they are warmer. At a T_e of 9 ms it seems likely more signal will be remaining when warmer than if the sample is cold, hence producing the higher intensity. At a T_e of 40 ms, most of the relaxation of the polymer would have already occurred hence there would be a smaller change with temperature. As the water relaxation time is much greater than that of the polymer and indeed in excess of 40 ms the intensity of this should be much less affected by the change in temperature.

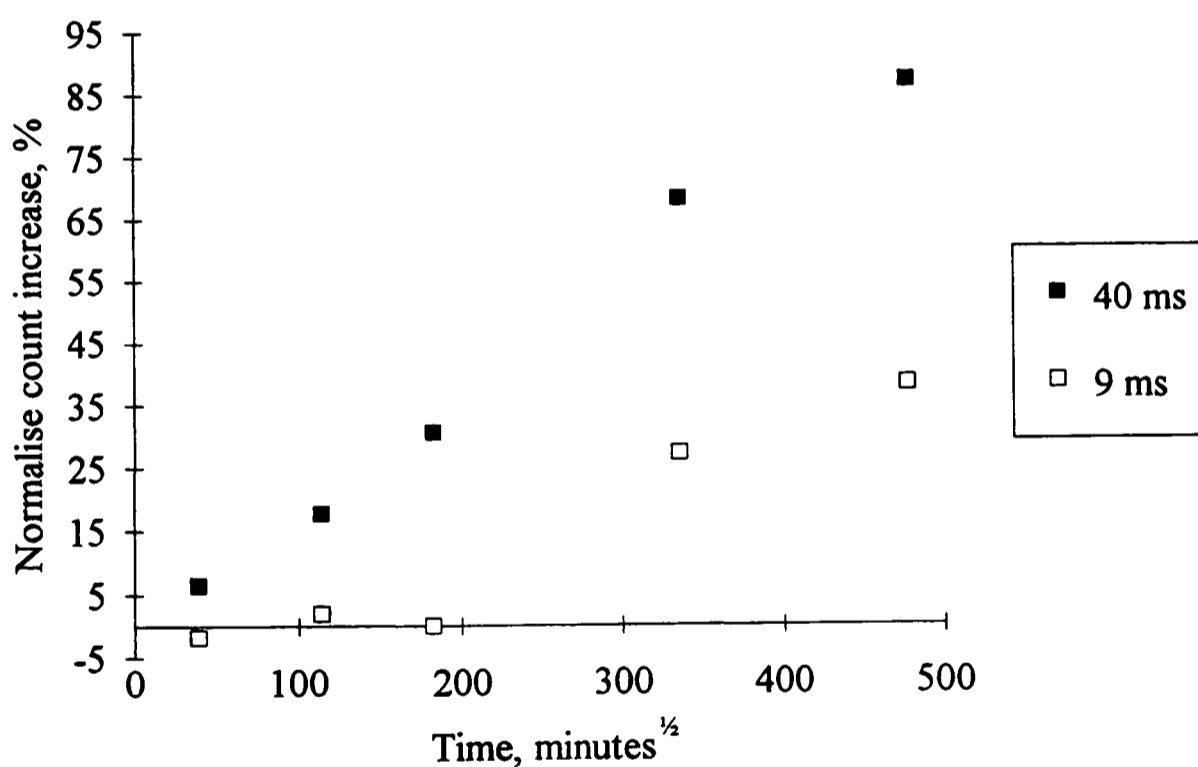
Unfortunately no measurements were made of the ambient temperature of the NMR laboratory but the dates given in table 7.3, will give some guide.

A normalisation procedure was applied to the data which involved taking an average of the values of the pure sample at the different times and then finding the shift associated at each time which could be attributed to the effect of temperature on the polymer. This figure was then applied to all the data at that age so removing the contribution of temperature on the polymer. The value at a particular age was then expressed as a percentage of that sample initially, as shown in figure 7.15, for Si NB A.

Table 7.3. Averages of the Control and Si Pure profile data at different times during the experiment.

Days	Date	T_e 9 ms		T_e 40 ms	
		Control	Si Pure	Control	Si Pure
0	6/2/96	1527	1590	1342	1342
1	13/2/96	1604	1732	1300	1520
9	21/2/96	1501	1586	1440	1499
23	6/3/96	1285	1395	1355	1431
78	7/5/96	1393	1599	1231	1454
158	26/8/96	2792	3000	1191	1291

Figure 7.15. The normalised intensity of the value calculated from the averaged images of Si NB A.



The correlation seen in figure 7.15, is better than that of figure 7.14, for the both the T_e 9 and 40 ms experiments. The T_e 40 ms forms a linear relationship, the T_e 9 ms also forms a linear relationship but only after 28 days with some of the initial points being less than the initial value. The reason for the behaviour when the T_e was 9 ms is unknown.

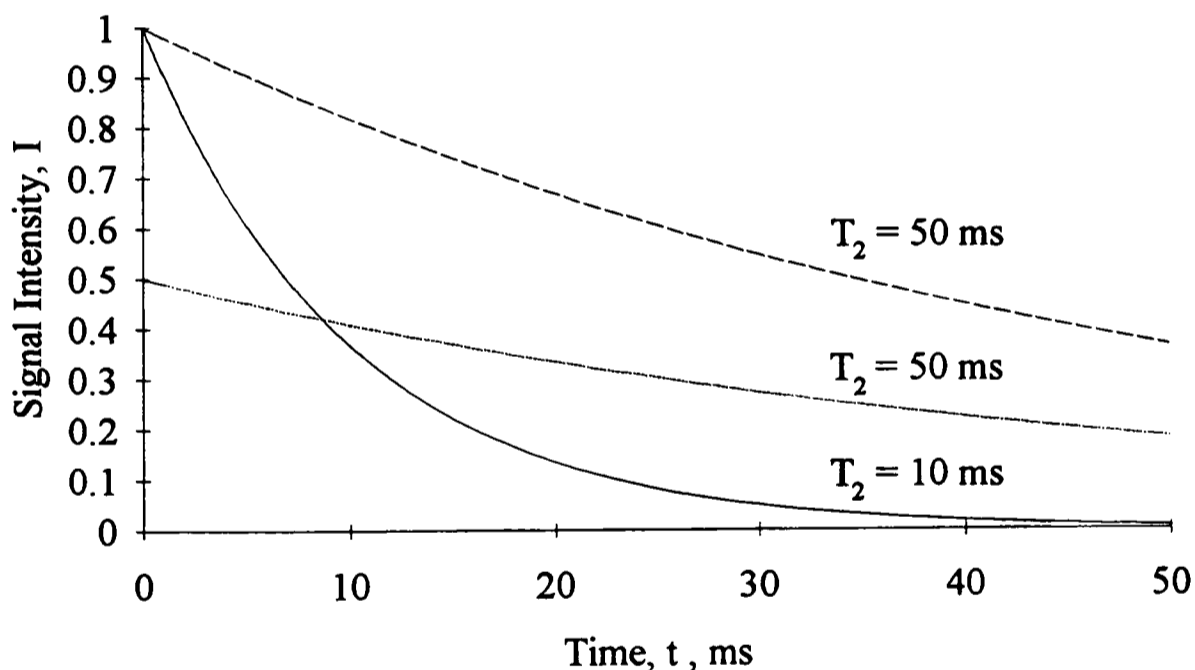
7.3.3. Correlation of the intensity with water uptake.

It is important to realise that what is actually being measured in these experiments is the intensity of the NMR signal at time T_e , not the actual concentration of the water. The intensity (I_t) at time t is related to the initial intensity (I_0), which is directly related to the concentration of water, by,

$$I_t = I_0 e^{-t/T_2} \quad \text{Equation 7.2.}$$

Figure 7.16, illustrates this for a few different situations, the intensity of the signal decreasing faster for the shorter T_2 time. The importance of this is demonstrated by altering the concentration (I_0) where the high concentration ($I_0 = 1$) but faster relaxing line ($T_2 = 10$ ms) shows a lower intensity than the lower concentration ($I_0 = 0.5$) slower relaxing ($T_2 = 50$ ms) after approximately 9 ms.

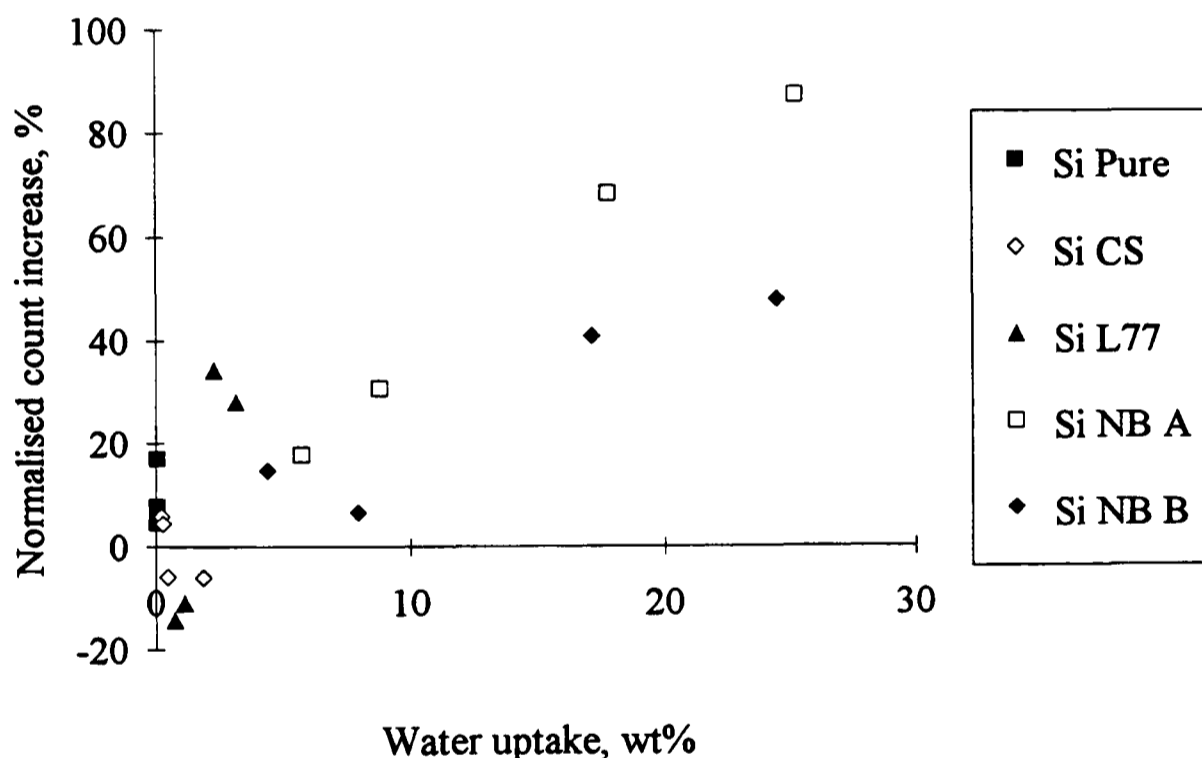
Figure 7.16. Decay of NMR signal intensity with time.



A certain degree of caution should be applied when correlating the observed intensity and the concentration of water particularly between the differently doped materials as the T_2 of the water in the material will depend on how it is bound. Even when looking at the results of the same material at different ages this should be considered as the T_2 time may vary with the dilution in the droplets depending on the type of the additive. Tests were performed to look at the effect of increasing the concentration of NaBr on the T_2 time of a solution, here there was no real observable difference in the T_2 time. Hence the NaBr results might be expected to correlate well although this may not be true for the other doping agents.

Figure 7.17, and 7.18, illustrate the correlation of the NMR intensity with the water uptake. The correlation for Si NB A for the T_e 40 ms experiment is very good as expected from the previous graph, the T_e 9 experiment similarly shows such a correlation. The results from the Si NB B sample are a little more spread but show the same sort of pattern as seen for the Si NB A sample. This may be attributable to the increased particle size of the salt leading to more variation within sampled volume. The Si Pure material shows only a small increase in intensity with time irrespective of the T_e as might be expected (figure 7.17, 7.18, and 7.19) and gives some measure of the overall accuracy of the experiment.

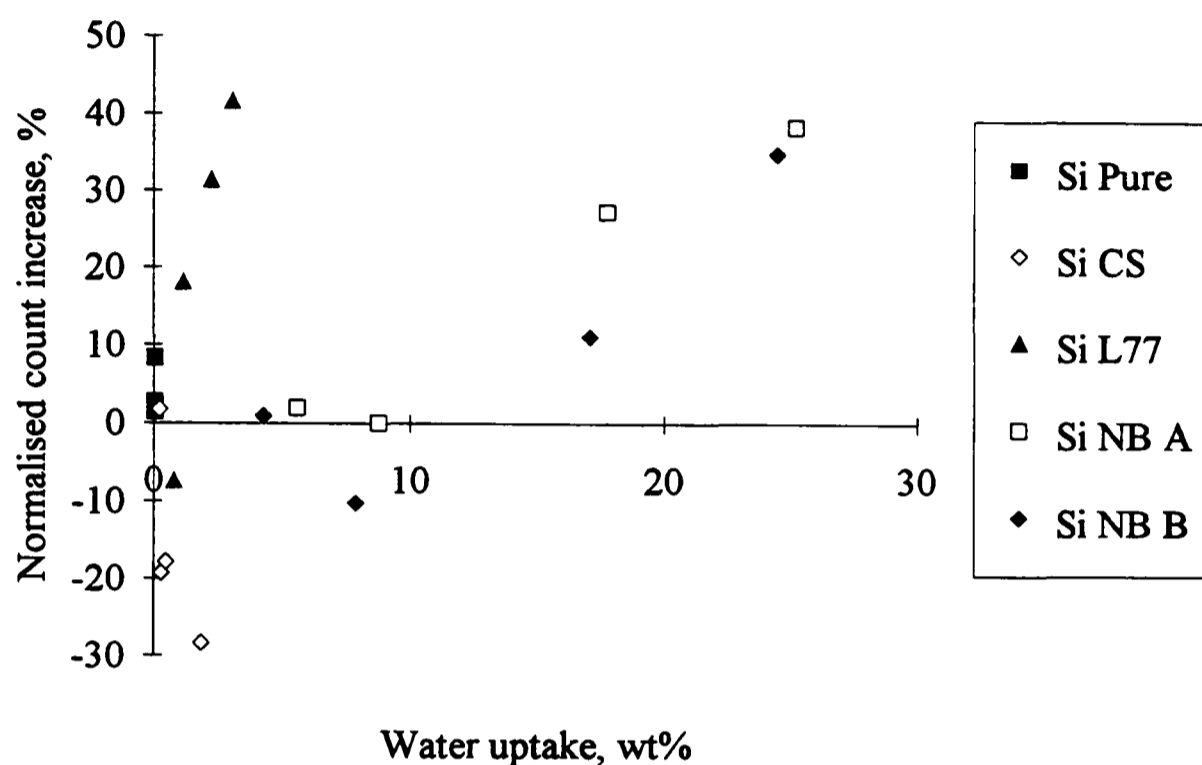
Figure 7.17. Correlation between average intensity for the T_e 40 ms experiment and water absorption.



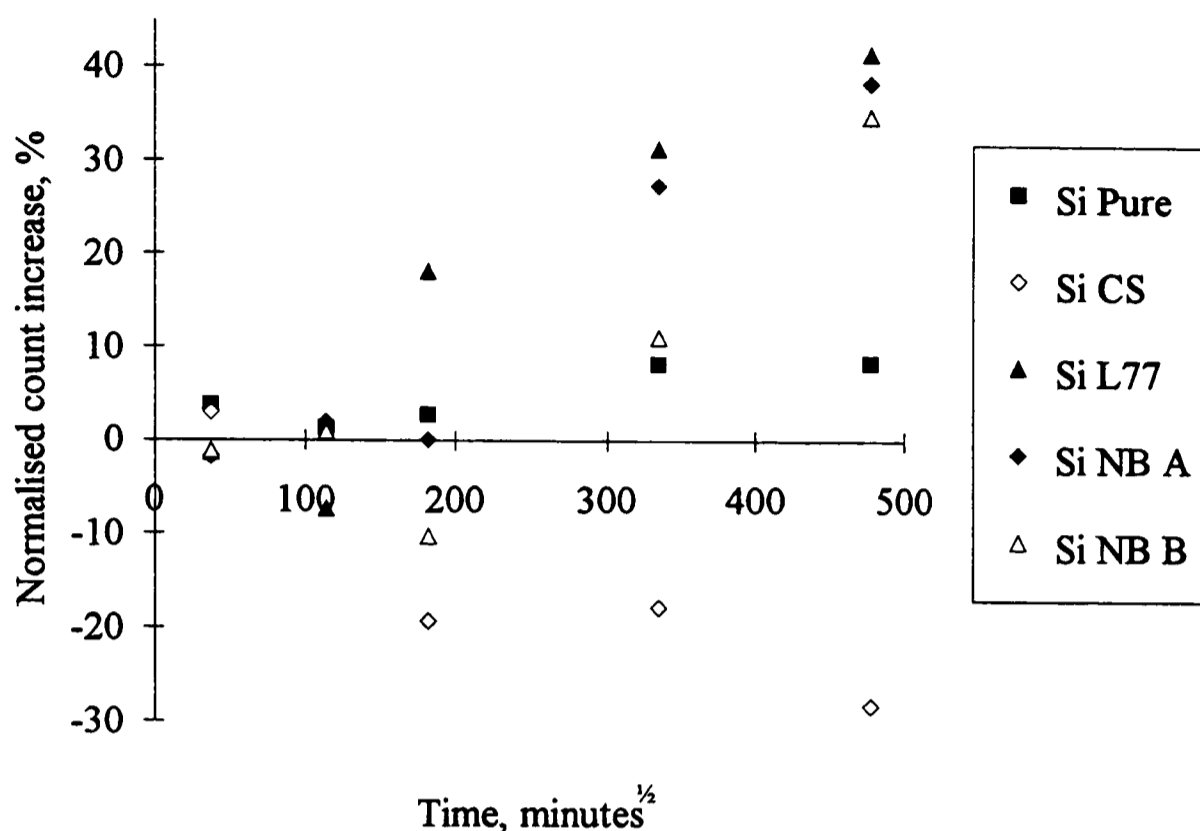
The Si L77 is somewhat different with a strong correlation existing for the T_e 9 ms experiment but not for the T_e of 40 ms. This seems to relate to the nature of the absorption in the polymer by the L77. In chapter 4 the effect of L77 on water uptake was investigated and it seemed that the distribution of water was uniform throughout the matrix based on the diffusion coefficient data for the P974 L1 material. This would explain the correlation seen as initially the water diffusing into the sample would be tightly bound by the L77. As more water diffuses in it will become freer as there is already water associated with the hydrophilic groups. Hence the 9 ms is sufficiently short a time to be able to show the relaxation but it has occurred before 40 ms hence little is seen. The last two readings do show a value for the T_e 40 ms experiment which may

relate to the water associated with these hydrophilic groups being sufficiently relaxed to be observed at the slower T_e . The increase in the T_e 9 ms experiment is linear with time (figure 7.19) as seen previously with the Si NB A sample.

Figure 7.18. Correlation between average intensity for the T_e 9 ms experiment and water absorption.



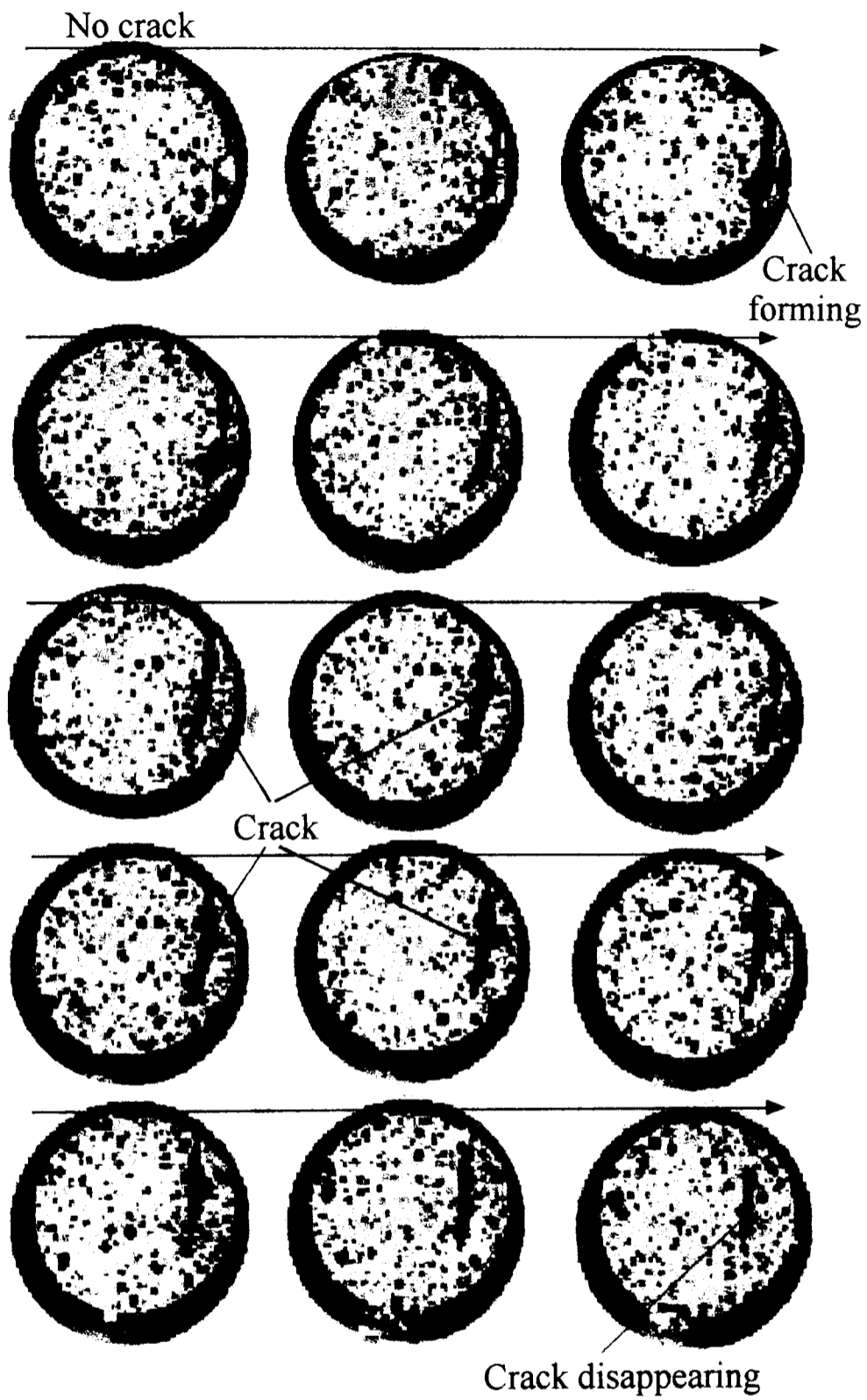
The Si CS sample is very different from the materials describe above with a decrease in the normalised count with increasing water uptake (figure 7.17, and 7.18) indeed this decrease seems fairly linear with time (figure 7.19). Why this should occur is unknown and seems to go against every thing seen for the other materials. An interaction between the CS and the polymer could be a possible explanation but the results in chapter 4 seems to go against this hence no satisfactory explanation is forthcoming.

Figure 7.19. Normalised intensity at T_e 9 ms against time.

7.3.4. Crack Formation.

Figure 7.20, shows the presence of a crack in the Si NB B sample at 158 days, this crack was not present in the images from the earlier tests (1, 9, 23 and 78). The figure shows a series of images along the length of the cylinder. A large crack may be seen on the right hand side of the cylinder, this moves deeper into the sample as we move along the sample indicating it is at an angle to the surface of the material. The mechanism by which such cracks form has been previously discussed, the magnitude of this crack is likely to stem from the poor tear resistance of the silicone and the high osmolarity of the solution droplets which form as a result of the inclusion of the NaBr crystals.

Figure 7.20. Formation of crack in the Si NB B sample shown as a series of slices along the sample at 158 days with a T_e of 40 ms.



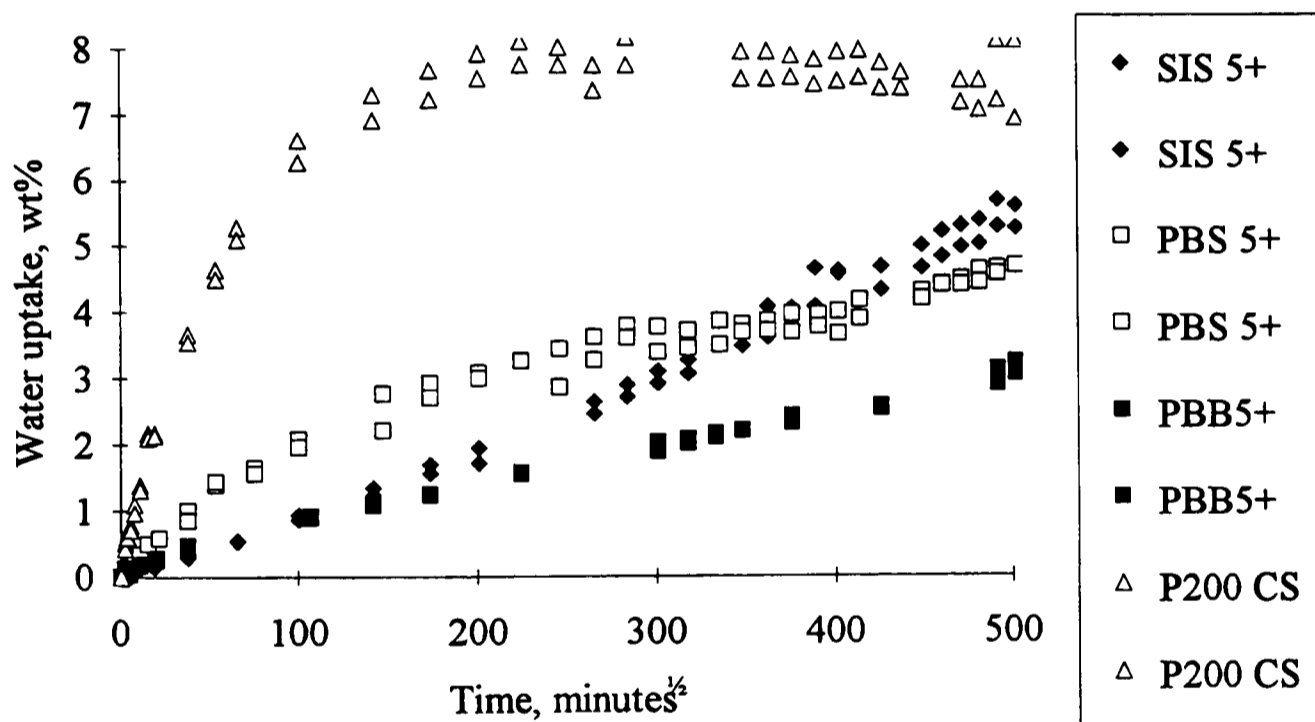
Chapter 8.

Discussion and Conclusions.

8.1. Stress relaxation, creep and the restraining force.

Generally the elastomer / methacrylate materials did not reach an equilibrium water uptake in the time scale of the experiments as would be predicted by the theories of Muniandy and Thomas (where the overall kinetics remain Fickian) and shown by the silicone materials which reached equilibrium (provided crack formation did not occur) as illustrated in figure 8.1. It should be remembered from chapter 6 that when the crosslink density was increased for the SIS based materials (SIS HD and SIS DD) an equilibrium was also achieved.

Figure 8.1. Comparative water uptake of materials of different types.



This seems to stem from the physical restraining force exerted by the material on the solution droplets as the elastomer is assumed to behave as a ideal rubber (i.e. only deform elastically) in Muniandy and Thomas's (and other authors) theories. When the material's behaviour is close to ideal as with the silicone polymers or the crosslinked poly isoprene materials (as used by Muniandy and Thomas) this seems to be true (at least in part). Many elastomers do not behave in this ideal manner and are prone to substantive creep or stress relaxation processes, which would effect the balance between the restraining force and the osmotic driving force. Stress relaxation around the droplet would reduce the effective restraining force and lead to an increase in water uptake as the droplets expand until the effective restraining force is in balance again. An

alternative way of looking at this process would be that the material creeps around the droplet so expanding it and the stress remains constant. In practice both situations are likely to occur as for the creep the movement of water in (controlled by the rate of diffusion) would be sufficient to enable the creep rate to determine the rate of growth, whereas in stress relaxation the rate would be determined by the diffusion rate of water into the droplets rather than the relaxation.

Table 8.1, illustrates the storage modulus and $\tan \delta$ (the loss tangent) of some of the material used in this study at 37 °C, these results were obtained by Dr S. Kalachandra and Dr D. Xu of Virginia Technology College, Blacksburg, Virginia, USA. The silicone based materials have a very low $\tan \delta$ and will therefore show the close to ideal behaviour (ideal behaviour being when the $\tan \delta$ is zero). The PBS based materials conversely have a much higher $\tan \delta$ and so might be expected to creep more than the silicone material.

Table 8.1. Dynamic mechanical properties of some materials at 37°C, data obtained by Dr. S. Kalachandra and Dr. D.Xu, using a frequency of 1 Hz.

Material	Modulus, MPa	Tan δ
P200	22.0	0.01
PBS 1	14.0	0.25
PBS 2	19.2	0.21
PBS 5+, Dry	20.9	0.37
PBS 5+, Wet	16.0	0.29

For unfilled elastomers well above their T_g , Gent (1962) noted a semi-empirical relationship between creep rate and $\tan \delta$ as,

$$C = \frac{1}{\varepsilon_0} \frac{\partial \varepsilon}{\partial (\log_{10} t)} = \frac{2(\ln 10)}{\pi} \text{Tan} \delta \quad \text{Equation 8.1.}$$

where C is the creep rate, ε_0 is the original strain and $\partial \varepsilon$ is the increase in strain. This was later shown (Braden and Wilson, 1982) to have a theoretical base. Re-ordering yields,

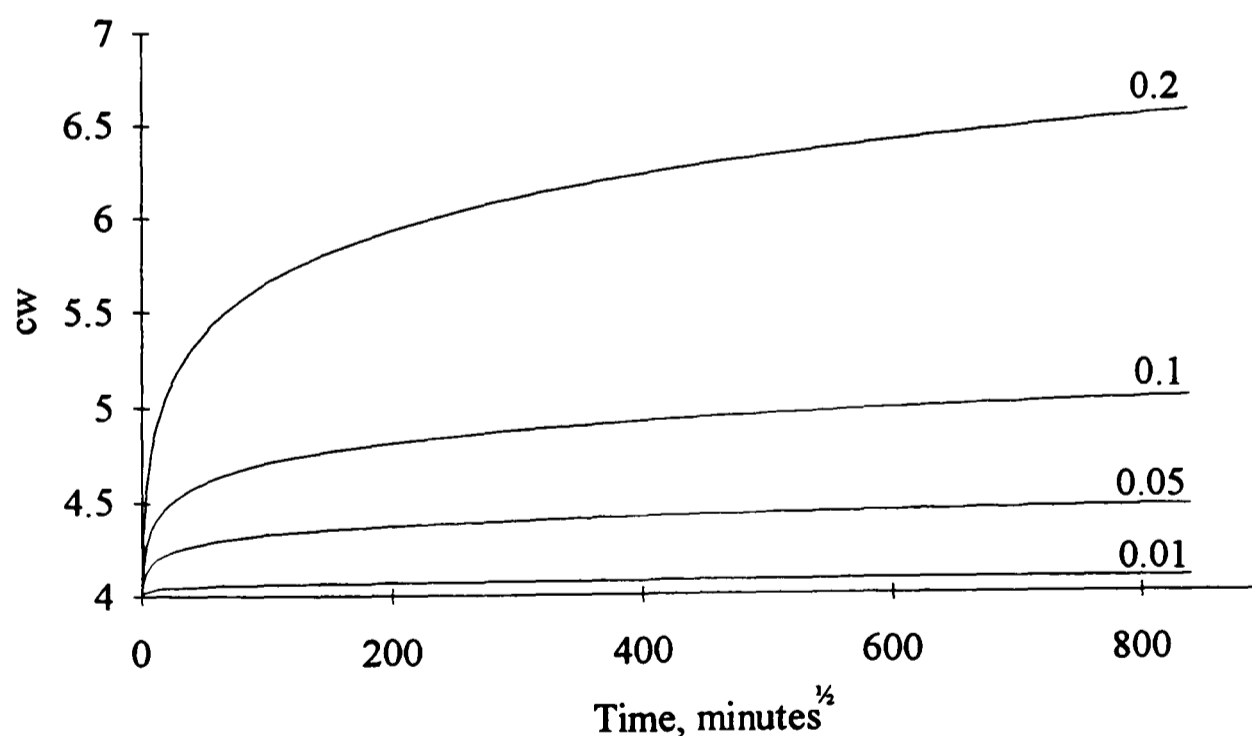
$$\frac{\partial \varepsilon}{\varepsilon} = \frac{2(\ln 10)}{\pi} \text{Tan} \delta \log_{10} \frac{t}{t_0} = 1.466 \text{Tan} \delta \log_{10} \frac{t}{t_0} \quad \text{Equation 8.2.}$$

This can then be used in conjunction with,

$$c_w - s = c_i (\lambda^3 - 1) \frac{\rho_w}{\rho_i} \quad \text{Equation 8.3.}$$

by using assumption that $\lambda = 1 + \epsilon$ (which is valid for small strains), to predict the effect of creep on the absorption of a doped elastomer, as seen in figure 8.2, with a continuous non equilibrium uptake as seen for the elastomer / methacrylate materials. Here only the effect of creep around the droplets, with the uptake initially assumed saturated (i.e. the osmotic force being balanced by the restraining force) is seen without the kinetics of diffusion into the polymer. The effect of frequency on $\tan \delta$ and the other dynamic properties means the data reported in table 8.1 would not relate very well to those properties needed to describe qualitatively the uptake of the individual material. Additionally the diffusion of water into the materials will alter the $\tan \delta$ as seen for the EBS5+ (table 8.1), therefore the influence of this would also have to be incorporated in an overall theory.

Figure 8.2. Relationship between $\tan \delta$ (0.2, 0.1, 0.05 and 0.01) and water uptake as predicted by equation 8.2, and 8.3, assuming small strains applies (i.e. $\lambda = 1 + \epsilon$).



It is interesting to note that the heavily crosslinked SIS (SIS HD and SIS DD), filled EBS5+ (EBS5+ C10) and the PBS samples in osmotic solutions reached an equilibrium in what appears a Fickian manner. In the case of the crosslinked SIS and the filled EBS this may be attributed to the effect of the increase in crosslinking decreasing the extent of

creep seen. The $\tan \delta$ values for the EBS5+ C10, described in 6.4.2, are misleading here as Gent's relationship assumes that the storage modulus (E') and the loss modulus (E'') are frequency independent and so excludes filled rubbers. For the PBS materials in osmotic solutions the reduction in the osmotic driving force reduces the forces involved and reduces the creep observed. Indeed the sample in the 0.1125 M NaCl exhibits a slow increase with time (compared to the samples in pure water) which would be accounted for by the reduction in creep rate due to the reduction in the driving force.

8.2. The desorption diffusion coefficient.

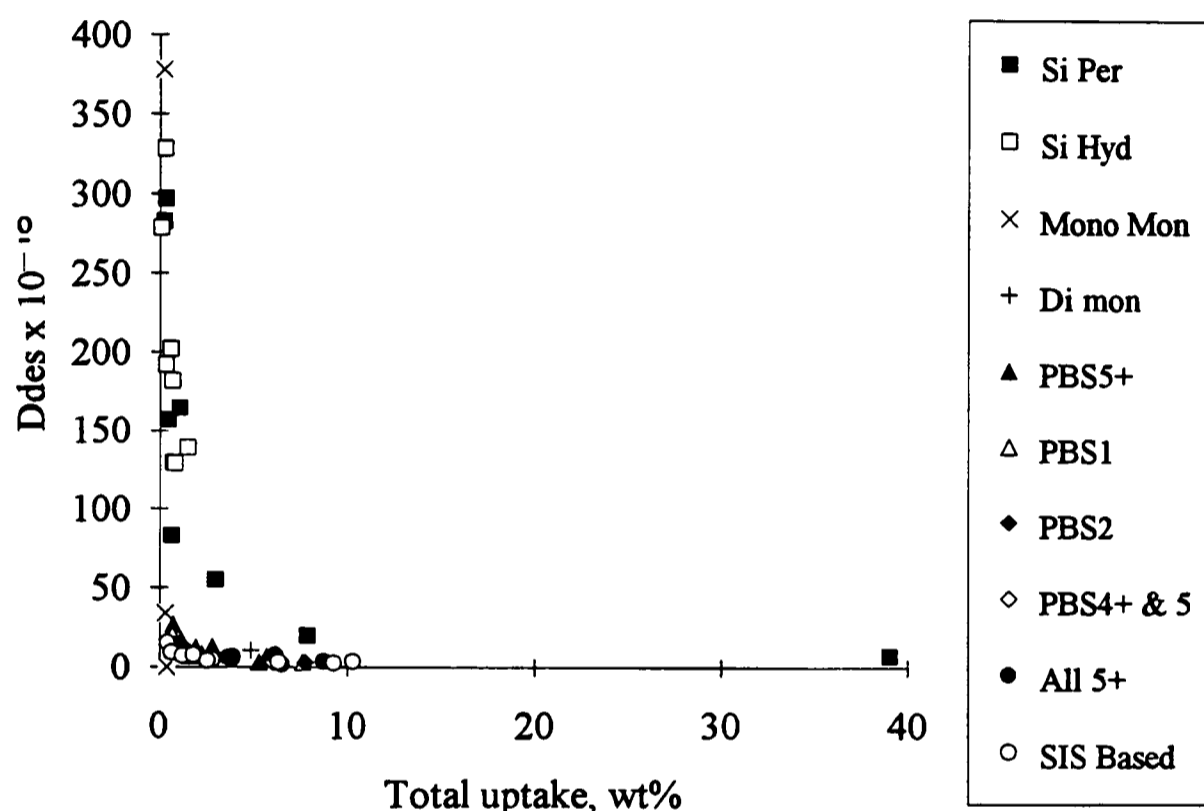
The desorption diffusion coefficient is an alternative approach of looking at the kinetics of the diffusion process of water in elastomers. The desorption results of most of the materials fit the basic Fickian linear $t^{1/2}$ dependence and so a diffusion coefficient may be calculated from the data. It has been recognised that the diffusion coefficient of non-equilibrated materials were not valid as the concentration of water in the material would not be uniform across the sample. This is certainly true for materials that absorb water in a true Fickian manner, but the doped (either purposely or by impurities) elastomers do not absorb water in the Fickian manner. From the NMR profiles (chapter 7) we found that the water was uniformly distributed and that the growth of the droplets occurred at the same rate throughout the material, rather than with a Fickian profile as seen in figure 2.1. Therefore on a macroscopic scale in desorption the Fickian kinetics (of uniform concentration) are met and a meaningful desorption diffusion coefficient may be calculated when $M_t/M_\infty < 0.5$ using the semi infinite media approximation.

Consider desorption from an elastomer rather than absorption. The rate determining step now being the diffusion process itself, as the external medium is air (or a vacuum) and the restraining force will be acting to drive the desorption along with the chemical potential gradient between the internal droplet and external (air) solution. This also has the advantage in that any non-ideal behaviour, such as stress relaxation and crack growth (provided the network is limited i.e. not connected up, especially to the surface) should not play a significant role in the overall diffusion process.

Figure 8.3, 8.4 and 8.5, show the relationship between the desorption diffusion coefficient and the total uptake of the material. The relationship here for each particular group of materials (silicones and elastomers) is very similar to that previously seen for

the PBS based materials in osmotic solutions for the absorption coefficient. The exception being the results of the pure methacrylate materials (both for the mono and di methacrylates), here the inherent diffusion characteristics of the material dominate rather than the droplets present in the material.

Figure 8.3. The relationship between total water uptake and desorption diffusion coefficient.



Indeed when this is re-plotted as log total uptake against log diffusion coefficient a linear relationship is seen for each set of materials (figure 8.6). The results of the regression of this data shown (table 8.2) show generally a gradient of -0.7 to -0.8 irrespective the actual data used. The regression on the hydrosilanised silicones and that from all the 5+ samples do deviate from this but the range of the data of these materials is comparatively small hence may not reflect the true trend. The intercept is different for the two sets of materials, with the silicones having a intercept of about -7.9 and the elastomers of -8.8. This seems to relate to the material's inherent properties, i.e. the diffusion coefficient through the material (or D_d) and the absorption of the matrix (or s), as these will be similar for all the silicone materials and the elastomers based (the variation between the HM and EHM, and the different types of elastomer is not sufficient to show up in this data).

Figure 8.4. The relationship between total water uptake and desorption diffusion coefficient, ignoring extreme point.

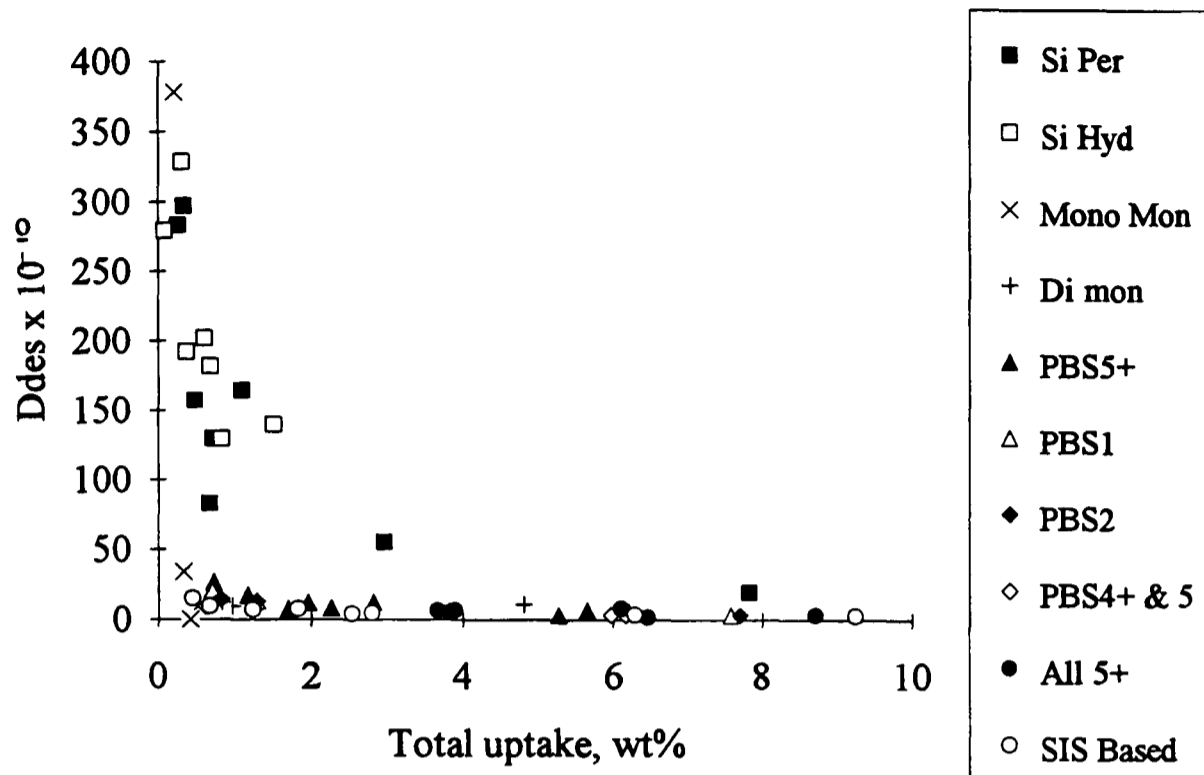


Figure 8.5. The relationship between total water uptake and desorption diffusion coefficient, for the slower diffusion materials.

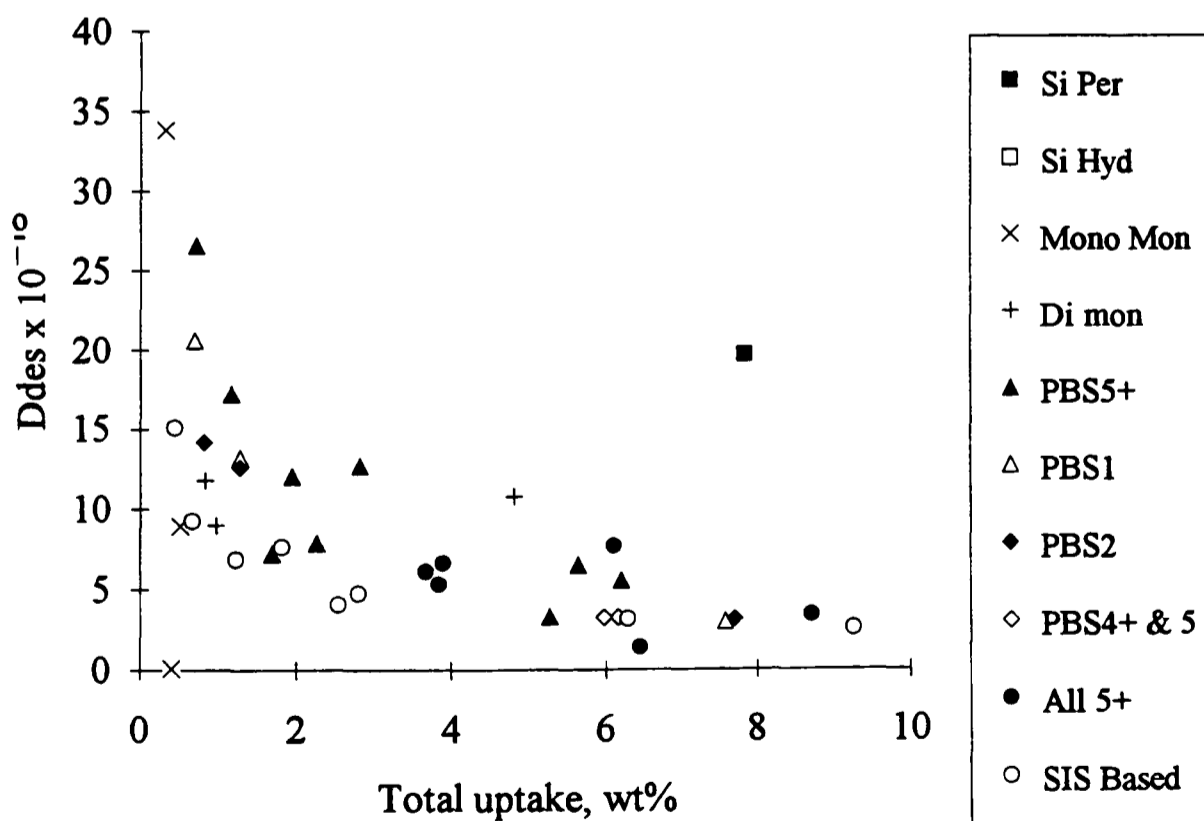
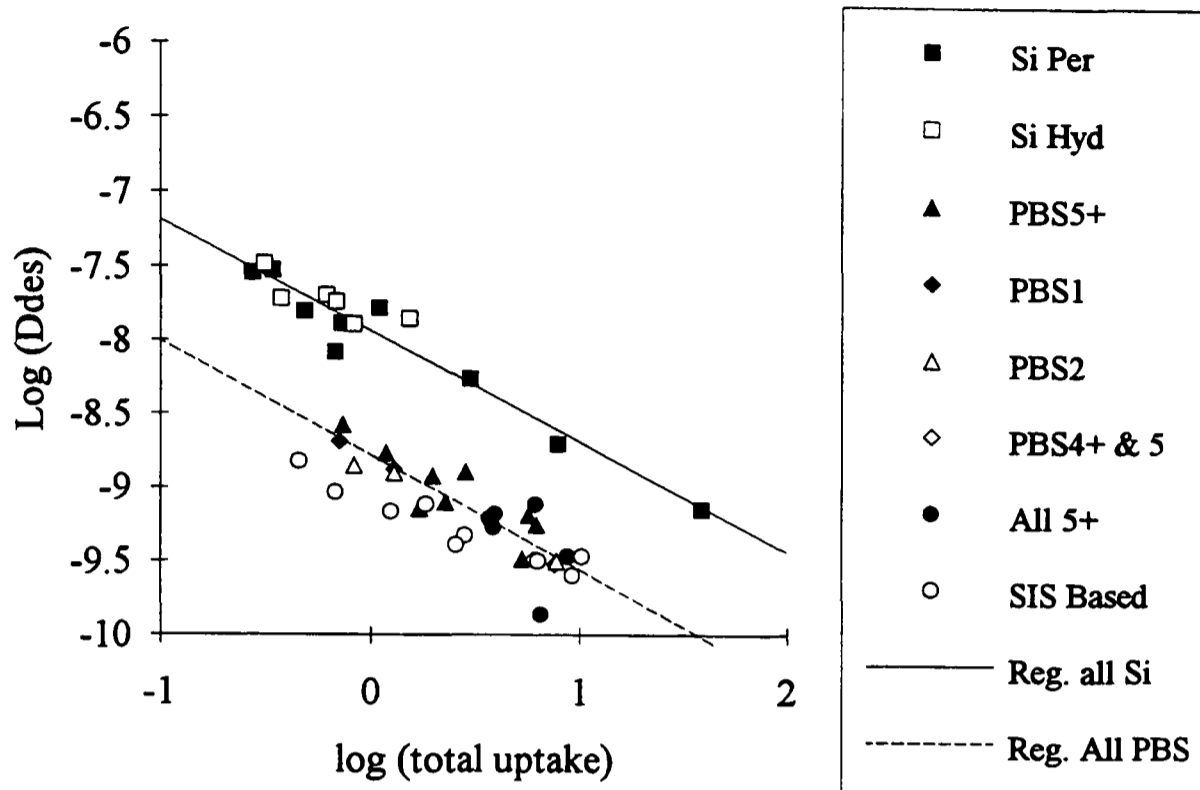


Figure 8.6. The relationship between total water uptake and desorption diffusion coefficient, as a logarithmic relationship.



This implies that there is a power law relationship between the diffusion coefficient and the water uptake, i.e.,

$$D_{des} = A(c_w)^n \quad \text{Equation 8.4.}$$

as,

$$\log D_{des} = \log A + n \log c_w \quad \text{Equation 8.5.}$$

where n is the gradient in table 8.2, and A is the intercept in table 8.2. Caution should be applied to this relationship as it makes assumptions about the process and has no theoretical bases. It is however an interesting and valuable relationship in understanding the diffusion process and comparing families of materials. The value of the intercept being between -7.8 and -8.9 gives the order of magnitude of the diffusion coefficient when the material absorbs no water, it should be noted that these values are very close to those normally taken for the inherent diffusion coefficient of the materials i.e. for the silicones approximately $10^{-8} \text{ m}^2\text{s}^{-1}$ and $10^{-9} \text{ m}^2\text{s}^{-1}$ for the other elastomers.

The SIS based materials present a slightly different picture as here the matrix is changing and the driving force behind the uptake is remaining constant. The results shown in figure 8.6, illustrates a slightly different gradient compared to that of the all the 5+ elastomers formulations and the silicone material. As the nature of the matrix is changing (from TDM/SIS to HDM/SIS) within the group it might be expected that the inherent diffusion coefficient and the concentration of water in the matrix (s) would change (section 5.2.1). Hence it might be expected that the change in characteristic

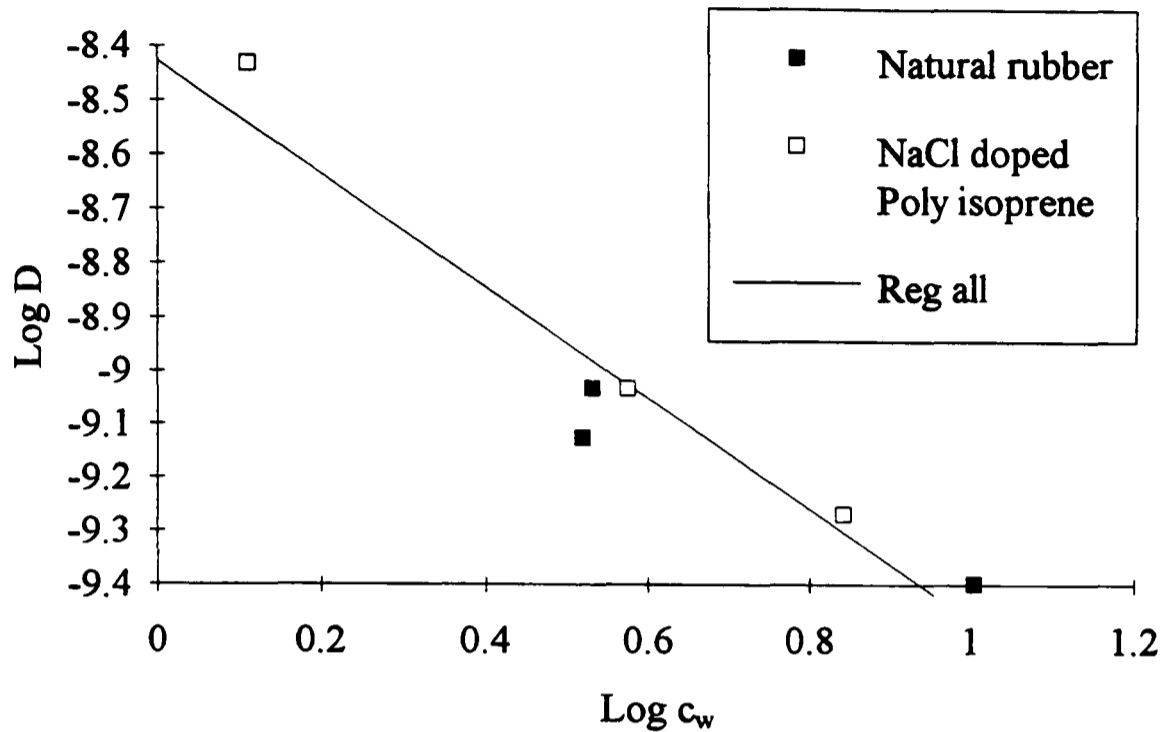
absorption of the matrix would alter the relationship between the apparent diffusion rate and total water content.

Table 8.2. Summary of logarithmic (base 10) regression data for the relationship between desorption diffusion coefficient and total absorption.

Data used	Gradient	\pm SD	Intercept	\pm SD
Si peroxide	-0.74	0.07	-7.97	0.05
Si hydro.	-0.47	0.17	-7.83	0.05
All Si	-0.74	0.06	-7.94	0.03
PBS5+	-0.73	0.17	-8.75	0.08
PBS1	-0.82	0.02	-8.80	0.01
PBS2	-0.70	0.09	-8.87	0.04
All PBS	-0.78	0.08	-8.78	0.04
All 5+	-0.92	0.77	-8.70	0.56
All elastomers	-0.79	0.09	-8.78	0.06

Comparison to Southern and Thomas's (1980) desorption data is interesting (figure 8.7) here we can see the same logarithmic relationship as the data presented here irrespective of the agent driving the water uptake (impurities or NaCl). However the gradient is different, with the regression coefficient of the data being -1.04 (with an intercept of -10.19) rather than the -0.7 and -0.8 as found with the data presented here. There are a number of possible reasons for this, such as the relative humidity and temperature of the desorption environment (as Southern and Thomas's results were at 25 °C).

Figure 8.7. The logarithmic relationship between total water uptake and desorption diffusion coefficient of Southern and Thomas (1980) for natural rubber and NaCl doped poly isoprene from NaCl solutions.



8.3. The absorption coefficient.

The absorption coefficient is a more complex issue as the process is dependent on more factors. However looking at $\log c_w$ versus $\log D$ plots trends are still apparent within the groups of materials. Indeed previously in section 5.5.3, such a relationship was observed for the PBS based materials in osmotic environments. Figures 8.8, 8.9, and 8.10, show this relationship for the silicone materials which equilibrated during absorption. The hydrosilanised materials show a considerable spread which seems to be attributable to the different surface states of the silica obscuring the effect of the formation of droplets within the material. The absorption of the hydrosilanised materials showed a dependence on type of silica used whereas the peroxide cured did not due the effect of the benzoic acid in the material. It is therefore proposed that the relationship observed with data of the hydrosilanised silicones reflects this difference in the silica.

Figure 8.8. The relationship between total water uptake and absorption diffusion coefficient for silicone materials.

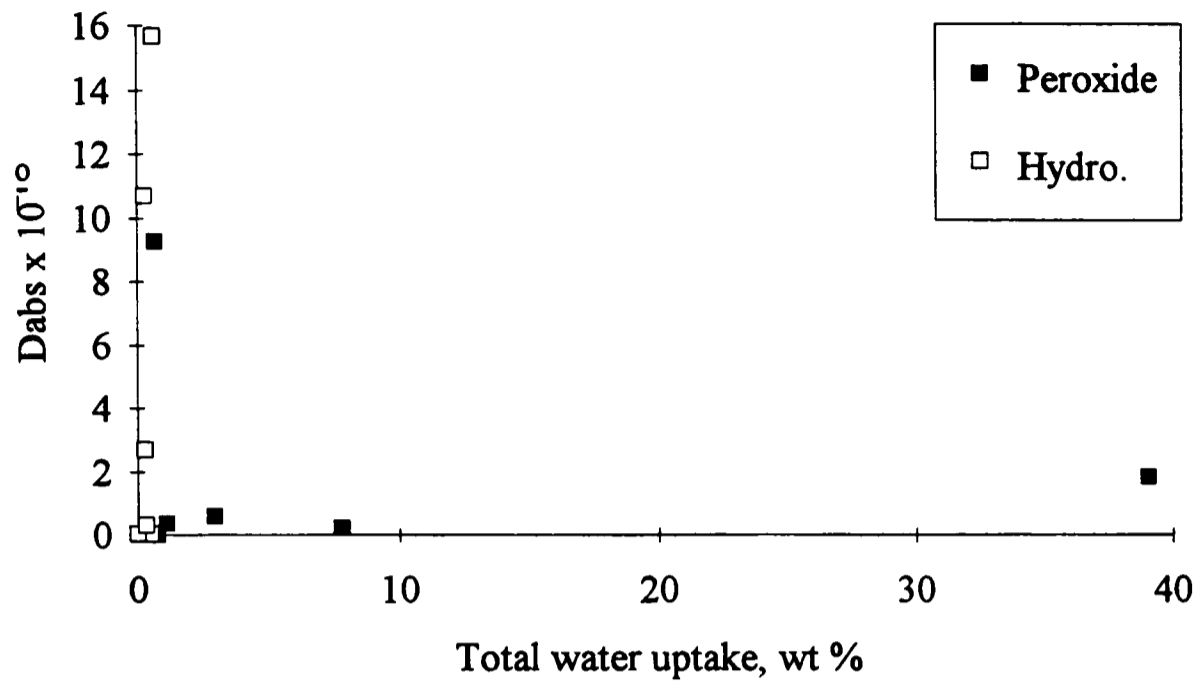


Figure 8.9. The relationship between total water uptake and absorption diffusion coefficient for silicone materials, enlargement of the lower absorbencies.

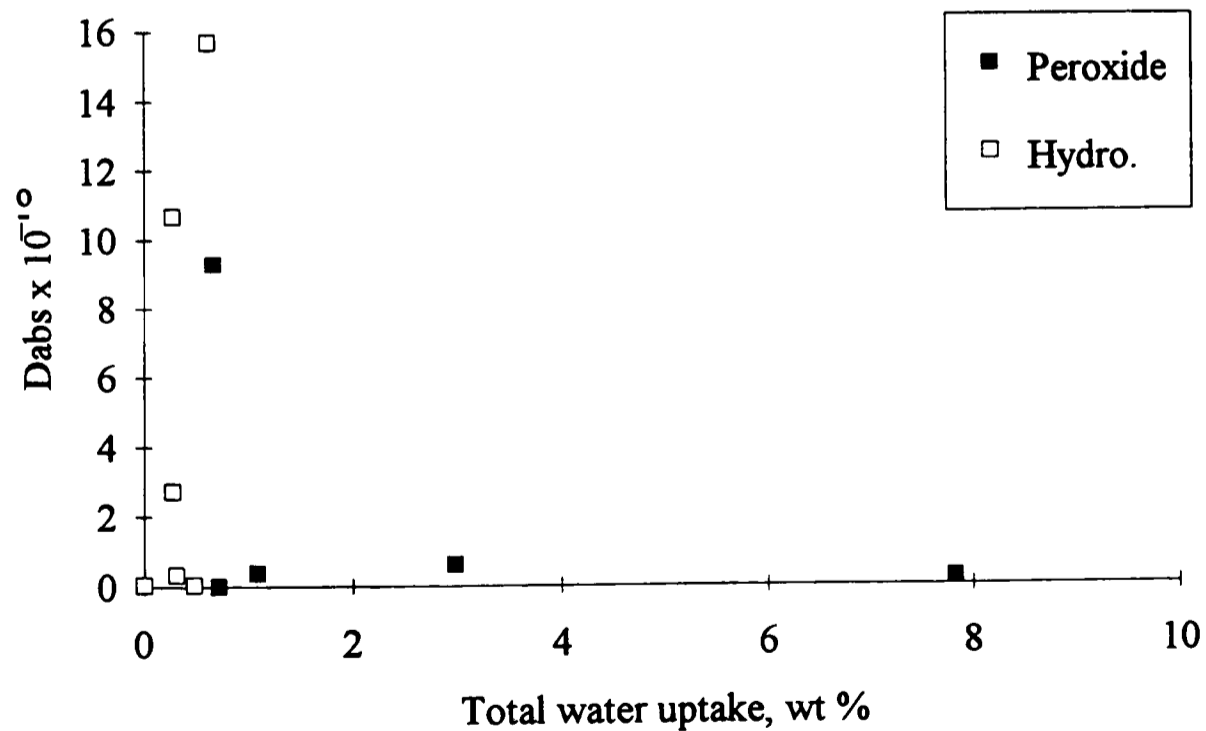
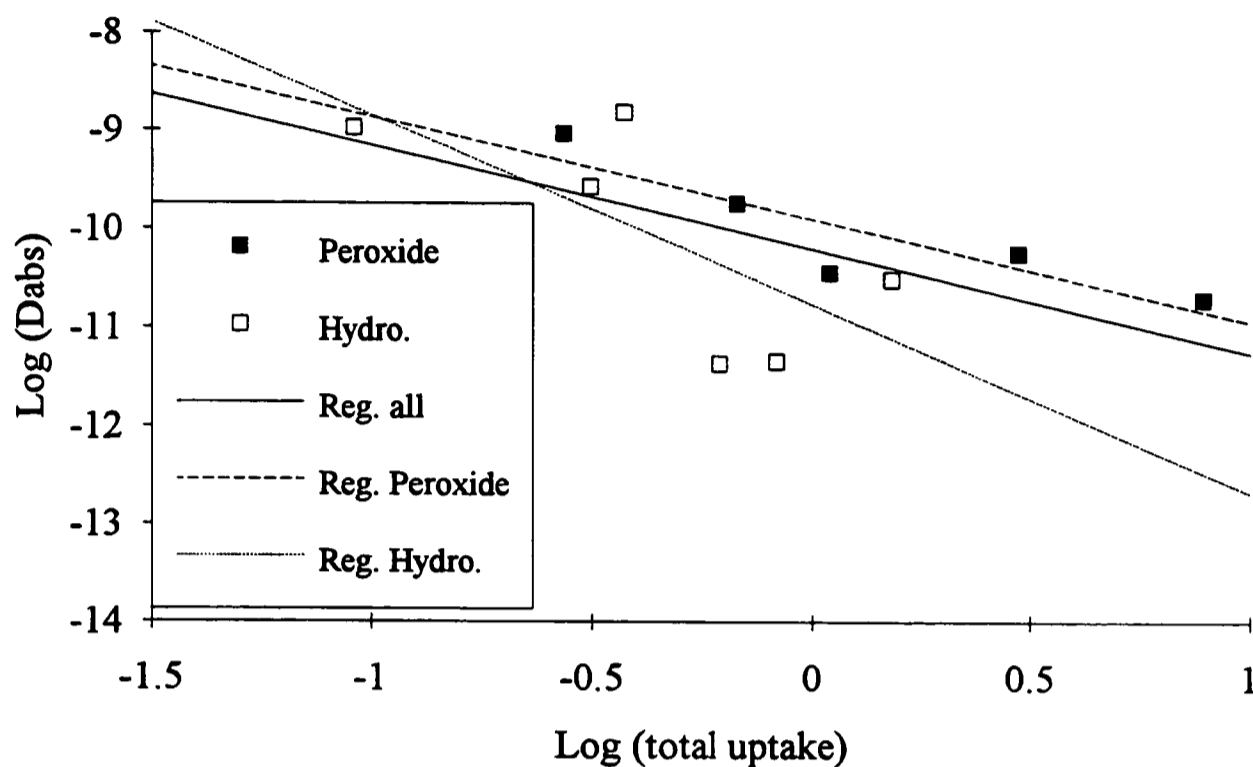


Figure 8.10. The relationship between total water uptake and absorption diffusion coefficient for silicone materials, as a logarithmic relationship.



The results from the regression of the silicones are shown in table 8.3; this may be compared to the results for the gradient from the PBS materials (approximately 1.2 to 1.3) and Barrie's data (1975) or that quoted by Muniandy and Thomas of 2. The variation is clearly wider than that seen in the desorption cycle where a fairly consistent value was seen for all the materials within the study. In absorption the restraining force will play a much more central role in determining the uptake of the material as this will balance the the osmotic force. As previously stated the restraint offered and the creep associated with it will undoubtedly effect the rate at which the material reaches equilibrium. The role of the matrix absorption also seems to play a role in determining the rate at which equilibrium is reached as shown by the silicone materials but this is a little more confused.

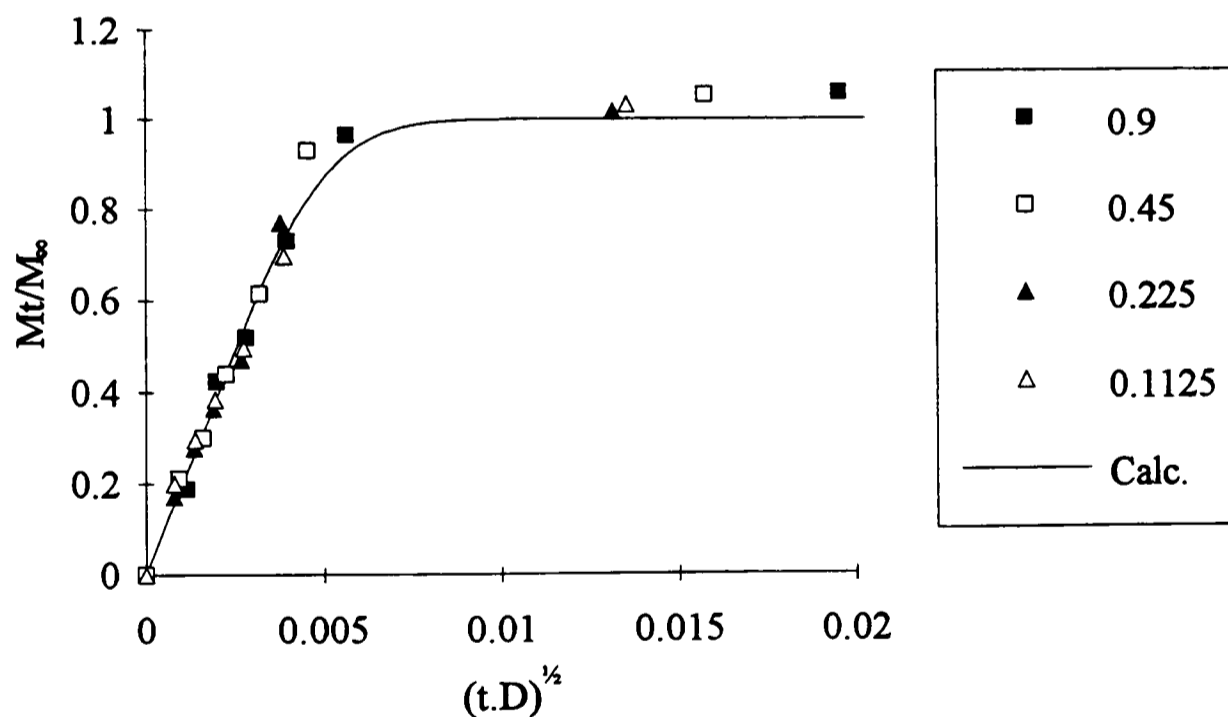
Further investigation of the difference between the absorption and desorption kinetics is interesting. Taking the PBS5+ materials in saline as a example, their kinetics have been compared to those associated with Fickian diffusion. Here M_t/M_∞ is plotted against $(t.D)^{1/2}$ so only the shape of the curve will be seen enabling comparison between each other. Figure 8.11, illustrates the desorption process where the kinetics for all the samples are very close to the Fickian prediction. The absorption however shows a considerable deviation during the later stages, figure 8.12. The early stages of the

absorption however shows the linear relationship necessary for the calculation of the diffusion coefficient from the semi infinite media solution to Fick's second law. The deviation from this behaviour seems to start later in the absorption process as the osmolarity of the saline solution increases.

Table 8.3. Summary of logarithmic (base 10) regression data for the relationship between absorption diffusion coefficient and total absorption for the silicone materials.

Data used	Gradient \pm SD	Intercept \pm SD
Si peroxide	-1.03 0.31	-9.89 0.16
Si hydro.	-1.91 0.96	-10.75 0.50
Si all	-1.04 0.46	-10.19 0.24

Figure 8.11. Comparison of observed desorption data (M_t/M_∞) against normalised time ($[t.D]^{1/2}$) for the PBS5+ material in saline solutions.



A similar picture is seen for the P200 CS material (figure 8.13) despite being a low creep material as described in section 8.1. The magnitude of the deviation from the Fickian line is somewhat less than that seen for the PBS5+ materials which could well relate to the hydrophilicity of the soluble agent in the material.

Figure 8.12. Comparison of observed absorption data (M_t/M_∞) against normalised time($[t.D]^{1/2}$) for the PBS5+ material in saline solutions.

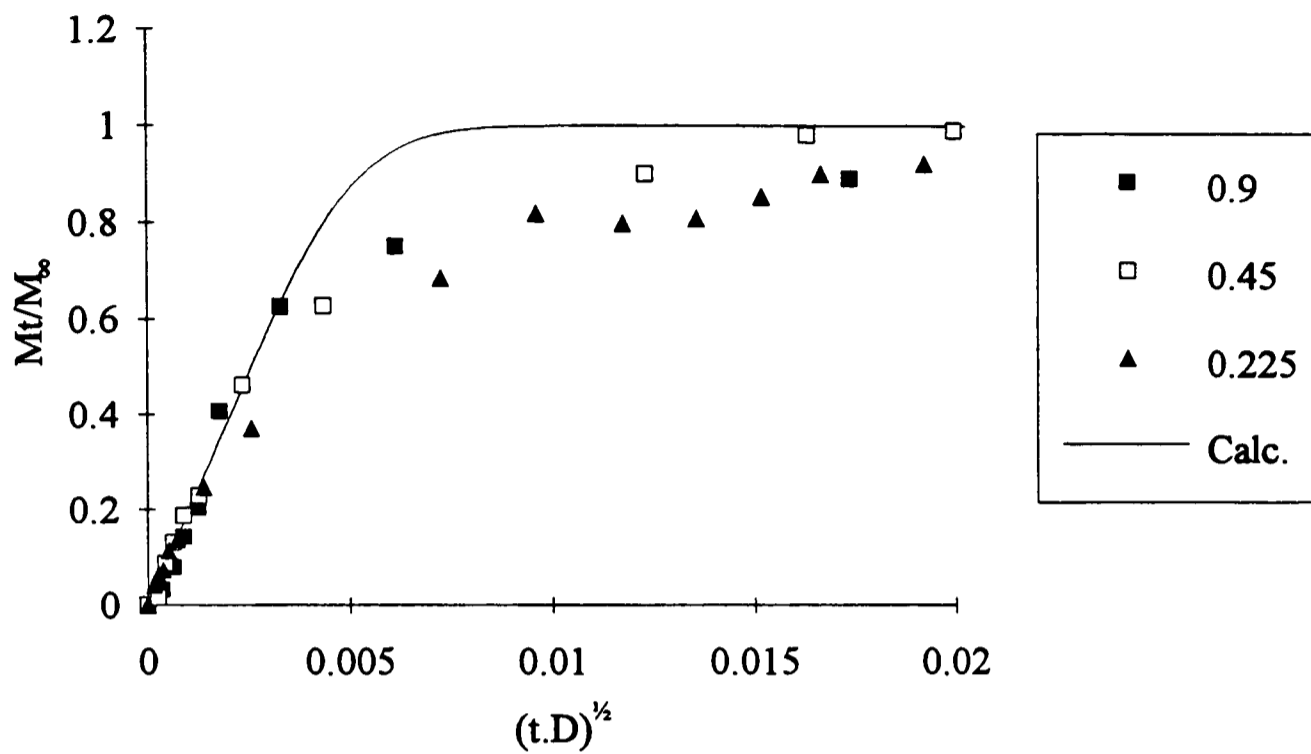
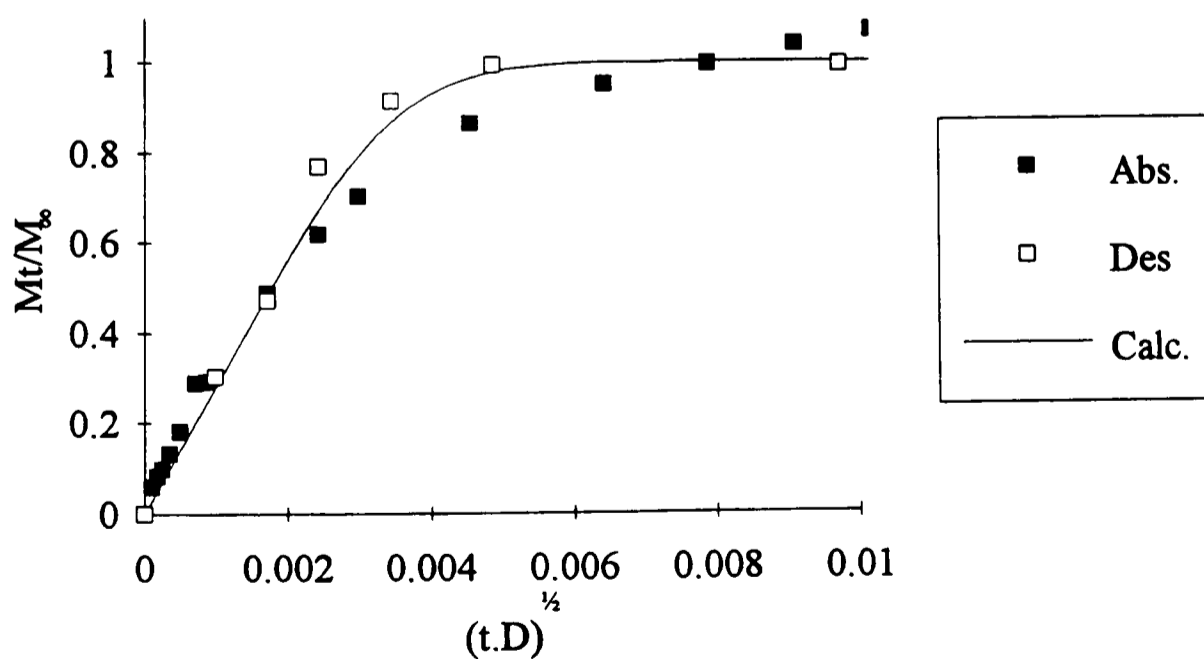


Figure 8.13. Comparison of observed absorption and desorption data (M_t/M_∞) against normalised time($[t.D]^{1/2}$) for the P200 CS material.



The lack of diffusion coefficients from many of the non equilibrating samples restricts future analysis of the materials. A possible way round this is to use an approximation of the first term for the of the infinite series of the solution into a plane sheet (equation 2.6) i.e,

$$\frac{M_t}{M_\infty} = 1 - \frac{8}{\pi^2} \sum_{n=0}^{\infty} \frac{1}{(2n+1)^2} \exp\left[\frac{-\pi^2 D(2n+1)^2 t}{4l^2}\right] \quad \text{Equation 8.6.}$$

which becomes,

$$M_t = M_\infty - \frac{8M_\infty}{\pi^2} \exp\left[\frac{-\pi^2 Dt}{4l^2}\right] \quad \text{Equation 8.7.}$$

then differentiate with respect to t so,

$$\frac{\partial M_t}{\partial t} = \frac{8M_\infty D}{4l^2} \exp\left[\frac{-\pi^2 Dt}{4l^2}\right] \quad \text{Equation 8.8.}$$

Taking natural logarithms of each side we get.

$$\ln \frac{\partial M_t}{\partial t} = \ln \frac{8M_\infty D}{4l^2} - \frac{\pi^2 Dt}{4l^2} \quad \text{Equation 8.9.}$$

Therefore by plotting the ln of the rate of change in weight with time against t we can

find the diffusion coefficient from the slope $\left(-\frac{\pi^2 Dt}{4l^2}\right)$ and the intercept $\left(\ln \frac{8M_\infty D}{4l^2}\right)$.

This does however assume that the other terms in the infinite series are insignificant, while this is alright for the latter part of the diffusion process this is not the case in the early stages. Hence a diffusion coefficient may be calculated without knowing the equilibrium uptake value (M_∞), provided the approximation to the first term is valid.

A similar result is shown by Passiniemi (1995) as,

$$\ln(\Delta M_{(t)}) = -\gamma_1 Dt + k \quad \text{Equation 8.10.}$$

where $\Delta M_{(t)}$ is the rate of change in weight at t, k is a constant and γ_1 is the first eigen function corresponding to the geometry (for a plane sheet $\gamma_1 = (\pi/2l)^2$). This is therefore analogous to equation 8.9, despite being derived for a general case by applying eigen functions to solve Fick's 2nd law.

Figure 8.14, demonstrates the inaccuracy of this prediction of D as initially neither the gradient nor intercept of the line (theory) relate to the data as calculated from equation 2.6. In fact a accurate prediction of 2.6. is only seen when M_t/M_∞ is around 0.4 to 0.5,

hence a considerable portion of the absorption cycle is unusable. The question then arises of over what range equation 8.9 may be used to predict the diffusion coefficient with a reasonable degree of accuracy. By using the theoretical data from equation 2.6, as the data set and regressing over a series of different M_t/M_∞ ratios (using a diffusion coefficient of $1 \times 10^{-8} \text{ m}^2\text{s}^{-1}$) some estimate may be obtained. Table 8.4 illustrates the limitations of equation 8.9 with accurate values of D being obtained during the later stages and reasonable values obtained when the M_t/M_∞ is greater than approximately 0.4. Below this value the prediction becomes increasingly inaccurate.

Figure 8.14. Correlation of equation 8.9 and the true data as calculated from equation 2.6.

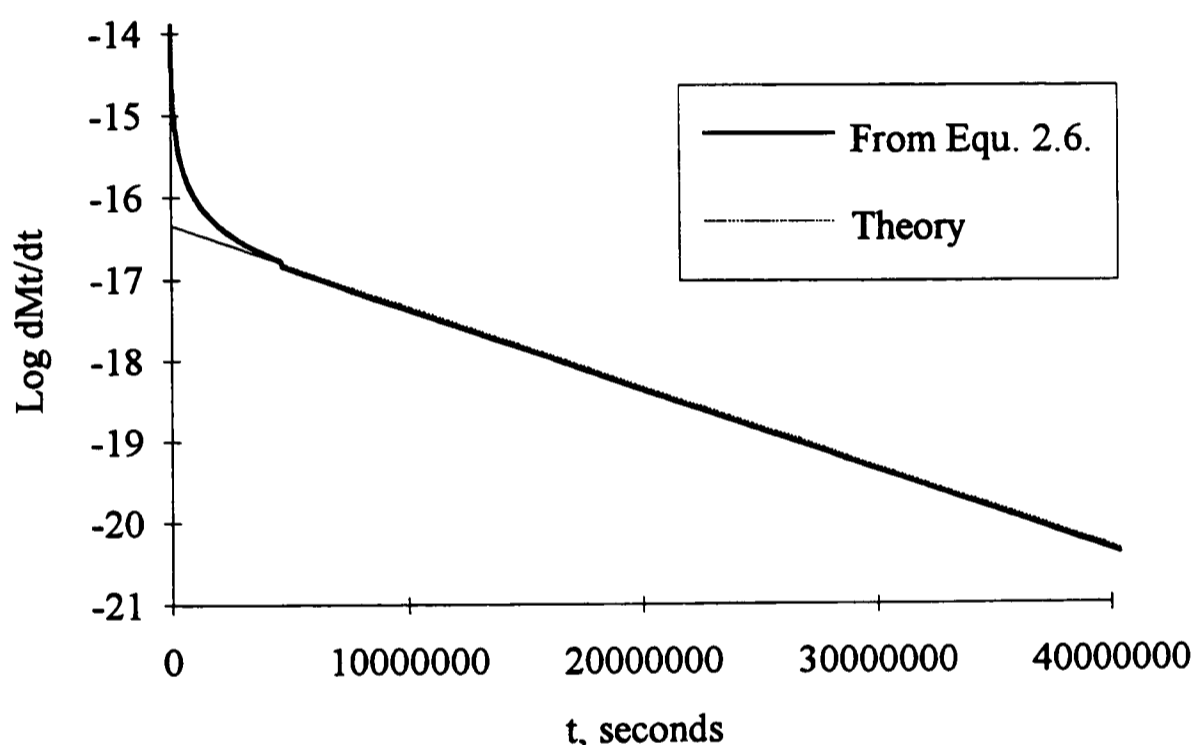


Table 8.4. Prediction of the diffusion coefficient from equation 8.9 using theoretical data.

Range of M_t/M_∞ used,		D Calc.,
From	To	m^2s^{-1}
0.82	1.00	1.00×10^{-8}
0.65	0.82	1.00×10^{-8}
0.42	0.65	1.10×10^{-8}
0.22	0.42	2.20×10^{-8}
0.11	0.22	-1.50×10^{-8}

The results of applying equation 8.9 to the experimental data obtained from the PBS 5+ material in the saline solutions are shown in table 8.5. Here there is generally a slowing of the calculated rate of diffusion in the later stages as the M_t/M_∞ values used for the calculation increases, as might be predicted from figure 8.12. The problem with this data is the lack of suitable data points (from the later part of the diffusion cycle) for the

regression which increases the uncertainty of the calculated diffusion coefficient, this is illustrated by the values calculated from the desorption cycle which might be expected to be constant (based figure 8.11).

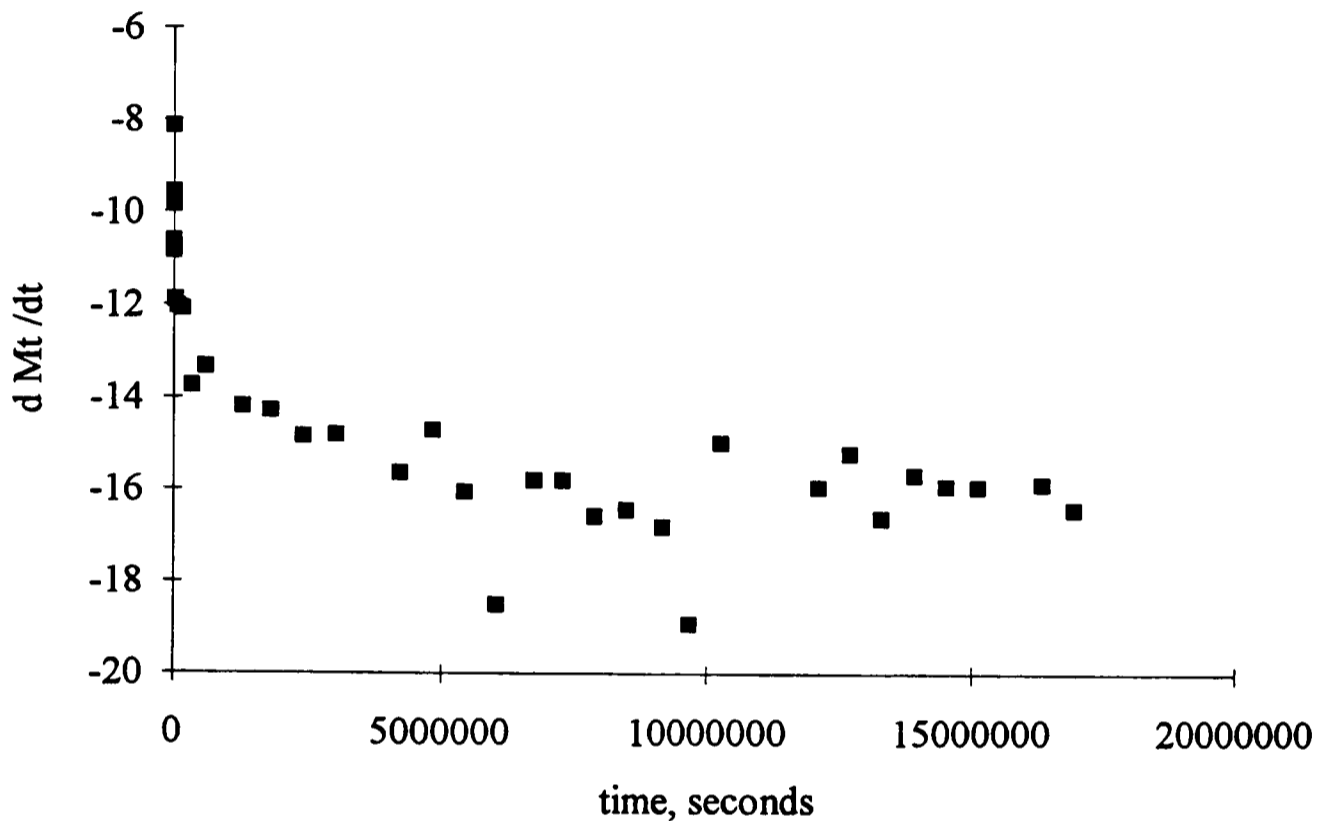
Table 8.5. Prediction of diffusion coefficient from different time periods for the PBS5+ materials in different solutions.

Solution, NaCl,	Range of M_t/M_∞ used,		D, m^2s^{-1} ,
	From	To	
<u>0.9 M</u>			
Absorption	Semi infinite		2.62×10^{-10}
	0.63	0.83	4.29×10^{-11}
	0.22	1.02	2.75×10^{-11}
	0.22	0.63	5.17×10^{-10}
Desorption	0.83	1.02	8.73×10^{-12}
	Semi infinite		2.66×10^{-9}
	0.42	0.98	1.86×10^{-9}
<u>0.45 M</u>			
Absorption	Semi infinite		1.32×10^{-10}
	0.23	0.99	2.89×10^{-11}
	0.23	0.63	1.72×10^{-10}
	0.63	0.99	2.21×10^{-11}
Desorption	Semi infinite		1.72×10^{-9}
	0.30	1.05	4.49×10^{-10}
	0.30	0.61	1.42×10^{-9}
	0.61	1.05	4.33×10^{-10}
<u>0.225 M</u>			
Absorption	Semi infinite		4.58×10^{-11}
	0.25	1.00	5.32×10^{-12}
	0.25	0.68	2.66×10^{-11}
	0.68	1.00	2.63×10^{-12}
	0.68	0.85	1.26×10^{-11}
Desorption	Semi infinite		1.20×10^{-9}
	0.28	1.02	8.01×10^{-10}
	0.28	0.47	3.31×10^{-9}
	0.47	1.02	5.28×10^{-10}

The correlation of this theory to the non equilibrating PBS5+ sample in water is seen in figure 8.15. Here shape is similar to figure 8.14, with the graph being reasonably linear after approximately 300,000 seconds although there seems to be a discontinuity at about 8,500,000 seconds. The diffusion coefficient calculated was $6.30 \times 10^{-13} m^2s^{-1}$ (between 345,600 and 16,934,400 seconds) although the regression before the discontinuity

produced a value of $2.00 \times 10^{-12} \text{ m}^2\text{s}^{-1}$ (between 345,600 and 16,934,400 seconds). The very slow diffusion rate is not surprising as it is implied by the non equilibrating nature of the uptake. It is felt however that this does not reflect the initial kinetics of the diffusion of water into the material considering the uptakes seen in chapter 5 and the diffusion coefficients calculated previously.

Figure 8.15. Correlation of equation 8.9, and PBS5+ absorption data from water.



8.4. The nature of the water uptake into elastomers.

The formation of droplets within the material is well documented and is seen in the images produced from the NMR for the NaBr doped silicone material. The kinetics and driving force for their formation is however open to debate. The materials described show a significant deviation from the Fickian kinetics, with many materials not reaching equilibrium. Indeed those that do equilibrate show a lower 'observed' diffusion coefficient in the later stages of the absorption. If Fickian kinetics are applied (as assumed by Muniandy and Thomas) this would indicate concentration dependence of the diffusion coefficient, which seems reasonable. The action of creep (as previously described) would also extend the absorption process by relaxing the restraining force. This would explain the observed uptake, but other factors should also be considered.

Looking at the profiles of the NMR we see a uniform level across the sample as opposed to the Fickian profile which would be expected. This implies that the kinetics are not Fickian and indicates that water moves into the material reaches a uniform level and then this increases as the droplets grow. Such a two stage process of water diffusing in and then growth of the droplets is described by Harrison et al (1991) as previously discussed section 2.3.5. Indeed the idea of a two stage absorption is well accepted with the dual absorption theories being widely used as discussed in section 2.3.4.

8.4.1. The initial kinetics.

Consider the initial stage when water moves into the material, at this stage the polymer matrix rather than the salt/impurity may be assumed to determine the rate of ingress. This however is an assumption. The NaF doped silicone P974 NF, demonstrated a case II type uptake rather than the expected Fickian type uptake. Other materials (when the matrix is the same or similar, i.e. within each group of materials, PBS or silicone) show some variation in this initial period rather than identical kinetics, implying dependence on the impurity.

Kinetics of the P974 NF seem to be case II initially and then changing to Fickian during the absorption. Consider water moves into the material reaching a salt particle which will initially absorb a certain amount of water of crystallisation before forming a solution. For case II kinetics the front of the diffusing water should be steep and the process be determined by a rate of a relaxation process rather than the rate of diffusion into the polymer. It is interesting to note that a similar situation is seen by Mirza (1995) when looking at the water uptake of a NaF (1%) doped poly (tetra hydrofurfuryl methacrylate / poly ethyl methacrylate), (THFM/PEM) water uptake.

The similarity between the behaviour seen for P974 NF and these rigid samples (THFM/PEM) is not seen for the other samples used within this study. This implies that the NaF is controlling the absorption in the early part of the cycle whereas the other soluble hydrophilic agents added during this study had a less significant effect during this initial period. This may be attributed to the greater osmotic potential of the NaF itself (compared to an agent like calcium stearate) which has a greater osmotic (and so chemical) potential during the initial stage and so might be expected to play a more dominant role. For case II type kinetics we would expect that the diffusion coefficient is

not determining the rate of water ingress as for normal case II (described in section 2.6), the relaxation process of the polymer determines the rate of the ingress.

For the NaF case II the question arises as to what is the controlling factor. There is no easy answer to this. It is possible that the relaxation process is creep in a similar way to that seen in section 8.1. with the material creeping around the salt so enabling the formation of a droplet before the front can progress. However the P974 NF is an elastomer and might therefore be expected to deform elastically. Crack formation is another possible explanation, with the expansion around the salt being sufficient to form local cracks around the droplet. Again the elastic nature of P974 NF makes this unlikely.

The wetting of salts is complex and this initial absorption behaviour could be a possible explanation but then why doesn't the P974 NF show the same dependence on the second absorption process that it did on the first. This implies that some aspect of polymer relaxation is indeed important in determining the behaviour as the relaxation will have already occurred for the second uptake, clearly this phenomena requires further study to detail a reasonable explanation of relationship between the polymer and the salt.

None of the other materials used within this study exhibited this case II behaviour, but no other material contained such strong electrolyte as NaF. Some of the samples used for the NMR did contain NaBr but the initial kinetics of the absorption process were not recorded. This seems to support the idea that the inter relationship between the material and electrolytic characteristics of the salt/impurity is critical in determining the initial nature of the uptake.

The initial uptakes of the other materials tend to show a comparatively small variation (compared to that at longer times) within each group of materials (figure 4.21, 5.13, 5.19, and 6.6) provided the matrix remains the same. This implies that although the formation of the solution droplets does influence the rate of the water uptake it is primarily the matrix which determines the rate during the initial period. This indicates that the water will diffuse into the material and wet the soluble particles forming the solutions and then continue the diffusion process into the material. Once the diffusion fronts meet (i.e. all the material now contains some water) the diffusion of water into the droplets start to dominate the absorption process. How does this relate to the P974 NF as described above ?

These results seem to indicate that type of initial uptake will depend on the type of the salt / impurity and the relative hydrophilicity of the matrix. For the strongly electrolytic (NaF) controls the uptake over the effect of the matrix. Where as for the weaker electrolytes (impurities or CS) the matrix dominates and the soluble particles play secondary role. It seems that the change in chemical potential associated with the water moving in to the soluble particles or the matrix dictate which one will control the process.

8.4.2. The later stages of water absorption.

The majority of the water uptake of the elastomers used here generally occurs into the water droplets once the water has moved through the polymer. During this process the concentration gradient between the internal droplets and the external solution will drive the uptake into the polymer. There will also be a gradient between droplets within the polymer of different concentrations. It is difficult to be exact about the shape of the concentration profile that will develop as a result of this gradient, but a guide may be taken from the NMR images.

From the NMR images we can see a uniform concentration from early in the absorption process which is very different to that predicted by Fickian kinetics. There are a few possible problems with these results which should be realised. The first concerns the method used with the effect of T_2 and concentration obscuring the true concentration of water within the material (as described in section 7.2.3), but this should not effect the shape of the observed profile. Secondly, the material itself is a very low modulus unfilled silicone polymer thus any droplets formed may be expected to grow relatively unrestrained within the material indeed the absorption data for the doped samples show no sign of a equilibrium. The question arises as to what are we seeing here, is it the elastic restraint by the material of the droplets or is it creep around the droplets (after the balance has been achieved) ?

If it was creep a uniform concentration might be expected as the relaxation around the droplets determines the uptake. But if this was the case the balance between the osmotic and elastic restraining force would have to be achieved before the readings at 9 days or even 1 day (as there is a absence of any concentration profile in these images). This seems unlikely, as from the experience of the other materials this would not be expected

so rapidly, indeed we would expect the low modulus unfilled silicone to show a longer uptake than the other materials. This implies that the profiles seen are representative of those which might be expected for diffusion into elastomers in general especially as the same sort of profile is seen for all the differently doped materials. It is accepted that the action of creep and perhaps more importantly crack formation (particularly in the NaBr doped material) will also be playing an important role in what is observed.

8.4.3. Free energy and water absorption.

The division of the water uptake into two parts, the matrix and the droplets, enables a level of understanding and visualisation but the division is unlikely to be observed so distinctly in practice. The recognition that the process of absorption is driven by the chemical potential change is very important as it enables the two parts of the process to be divided. As the water moves into the polymer there will be a corresponding decrease in the free energy associated with absorption into the matrix. This has been described by the Flory Huggins equation and the dual sorption models previously described in section 2.3.4. The energy associated with the droplets and the wetting is more complex.

Consider if the soluble agent absorbs a specific amount of water before dissolving to form a solution droplet; there will be a free energy change associated with water moving into the soluble agent, during the change from an absorbing solid to a dissolved solid, the dilution of the concentrated solution droplet and the dilute solution droplet where Raoult's law will apply (as used in section 2.3.5). This will be further complicated by the material's elastic restraint (allowing for the creep) around the droplet which will reduce (make less negative) the free energy change of the water moving into the droplet.

Assuming Flory Huggins equation predicts the water absorption of the matrix reasonably accurately (although it is recognised that the Flory Huggins equation is unsuitable for poor solvents) can find the change in chemical potential ($\mu_1^0 - \mu_1$) associated with this using (see section 2.3.4).

$$\mu_1 - \mu_1^0 = RT \left(\ln v_1 + (1 - v_1) + \chi(1 - v_1)^2 \right) \quad \text{Equation 8.11.}$$

where v_1 is the volume fraction of the water and χ is the interaction parameter between the water and the polymer. From section 2.3.5, we also have an expression for the osmotic pressure (π) of the water within the polymer (assuming a dilute solution), which may be re expressed in terms of the change in chemical potential as,

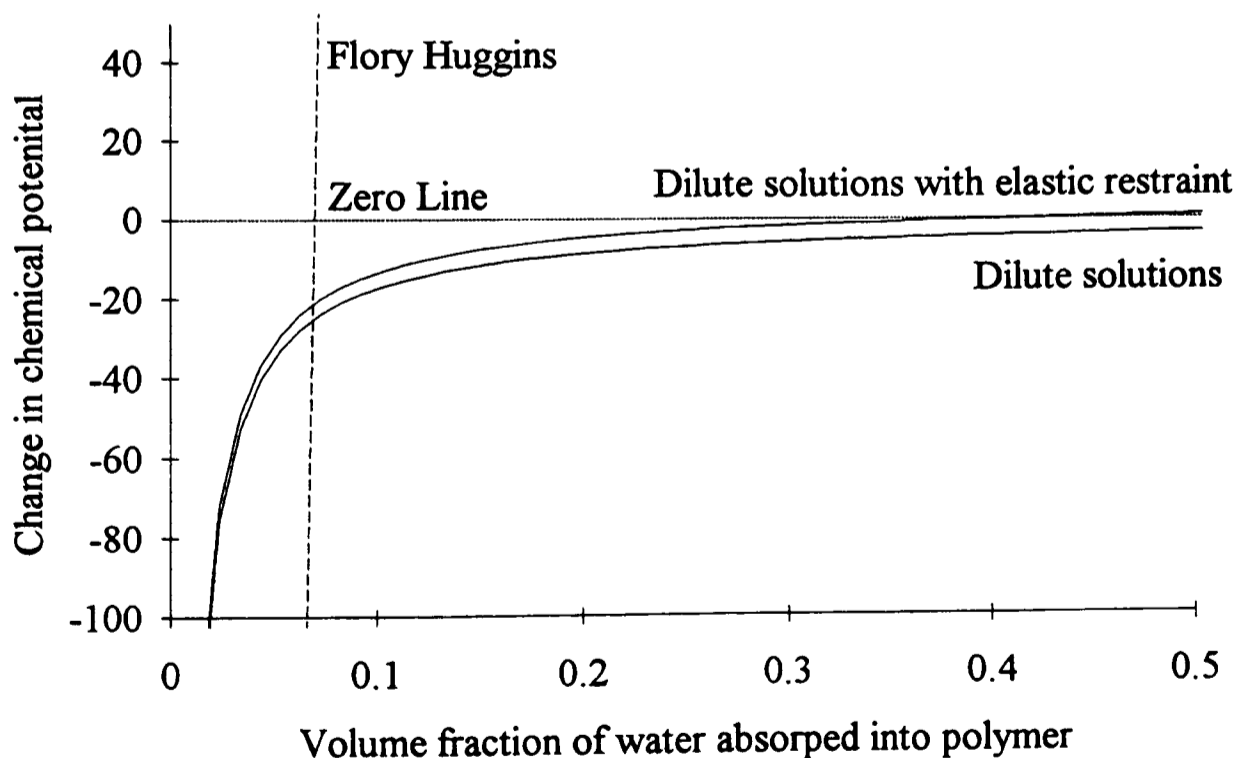
$$\mu_1 - \mu_1^0 = -V_1 \pi_i = \frac{-V_1 c_i R T \rho_w}{(c_w - s) M_i} \quad \text{Equation 8.12.}$$

The actual driving force for the uptake is the difference in the osmotic potential of the internal droplet and external solution minus the elastic restraining force around the material. Hence if the external solution is pure water this may be expressed as,

$$\mu_1 - \mu_1^0 = -V_1 \left[\frac{c_i R T \rho_w}{(c_w - s) M_i} - \frac{G}{2} \left(5 - \frac{4}{\lambda} - \frac{1}{\lambda^4} \right) \right] \quad \text{Equation 8.13.}$$

where V_1 is the molecular volume of the water, c_i is the concentration of the impurity, c_w concentration of water in the polymer, s is the water absorbed by the polymer, M_i is the molecular weight of the impurity, G is the shear modulus and λ is the extension ratio. Figure 8.16 illustrates equations 8.11, 8.12 and 8.13, using χ of 2, c_i of 1 kg m^{-3} , M_i of $0.0265 \text{ kg mol}^{-1}$ (NaCl), ρ_i of 2200 kg m^{-3} (NaCl), V_1 of $0.000018 \text{ m}^3 \text{ mol}^{-1}$, G of 0.1 MPa and taking the $c_w - s$ to be equal to the volume fraction of water divided by the water's density (i.e. $(c_w - s)/\rho_w$).

Figure 8.16. The change in chemical potential with the increasing volume fraction of water as predicted by equations 8.11, 8.12 and 8.13, using χ of 2.



The water will move into either the matrix or droplets depending on which produces the greatest reduction in the chemical potential. The prediction here is similar to that seen in

the results described previously with the chemical potential associated with the absorption into the matrix being greatest at low water volume fractions (the early stage of water absorption) and that into the droplets at higher fractions (the later stages). It should be realised that for any given chemical potential change the total water content in the polymer will be that volume fraction in the matrix required for that change plus that volume fraction in the droplet to produce that change in the chemical potential. This implies that during the initial stage the water will diffuse primarily into the polymer matrix, with only a small portion being associated with the droplets, and then, once the matrix has become almost saturated, it is the diffusion into the droplets that determines the uptake.

Favre et al, 1994, quotes a value of χ for water and a silicone polymer of 5.31, this is very high and represents its hydrophobic nature. When this value is used (keeping the other factors constant) the prediction is figure 8.17, the lines are very similar during the initial period with the droplet term now dominating at low volume fractions. This implies that the droplets are determining the early absorption as well as that at longer times. The numbers used here are similar to those of the P974 NF material and thus this is in agreement with the previous observations when relaxation around the droplets was determining the early absorption kinetics. If the impurity is changed to calcium stearate (M_i of $0.607 \text{ kg mol}^{-1}$ and ρ_i of 1221 kg m^{-3}) as seen in figure 8.18, the same pattern is seen as in figure 8.16, this would be expected from the results of the silicone chapter.

It is recognised that the predictions shown here relied heavily on the ability of the Flory Huggins equation and the dilute concentrations term predicting the behaviour outside their well accepted limits. The results are however interesting and agree surprisingly well with the results presented in this thesis, their significance should therefore not be ruled out but care should be taken in not to over estimate them.

Figure 8.17. The change in chemical potential with the increasing volume fraction of water as predicted by equations 8.11 and 8.13, using χ of 5.31 for silicone and water (Favre et al, 1994) with NaCl as the impurity.

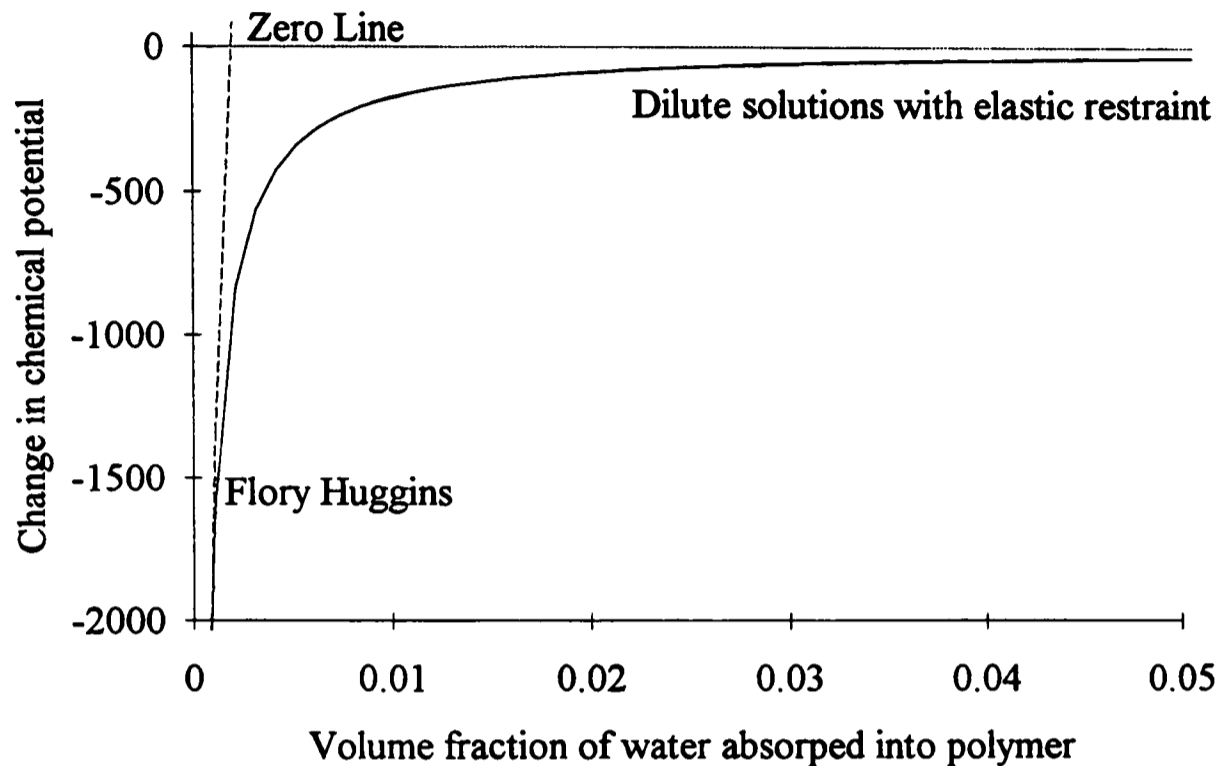
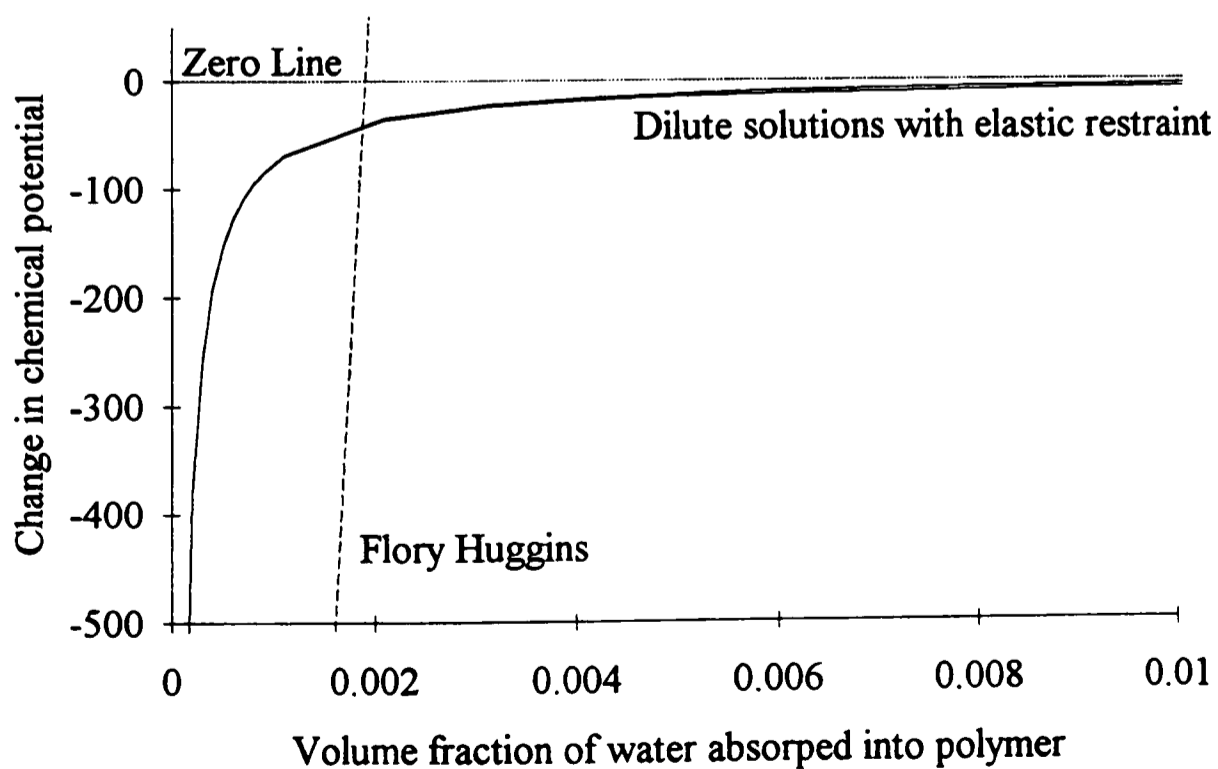


Figure 8.18. The change in chemical potential with the increasing volume fraction of water as predicted by equations 8.11 and 8.13, using χ of 5.31 for silicone and water (Favre et al, 1994) with calcium stearate as the impurity.



Consider applying these results into the chemical potential variation of Fick's 1st law namely,

$$F = -\frac{D_T s}{RT} \frac{\partial \mu}{\partial x} \quad \text{Equation 8.14.}$$

Here the chemical potential term (μ) would relate to either that calculated from the Flory Huggins (equation 8.11) or the term associated with the droplets (equation 8.13) depending on which one was the greater or more accurately both.

The approach combines elements of the dual sorption philosophies with a traditional Fickian model and may predict the different types of behaviour as indicated by figures 8.16, 8.17, and 8.18. The potential benefit of following through this approach in the formation of a new model (particularly when s is predicted by the Flory Huggins equation) is somewhat marred by the limitations of the dilute solutions and Flory Huggins equation but it is felt this offers a starting point for further development.

8.5. Clustering during water uptake.

The mechanism behind clustering is somewhat confused, with different authors attributing it to different factors as described in section 2.3.3. Their formation in this study for the solution polymerised elastomer materials has been attributed to carboxylic and hydroxyl groups on the elastomer which stem from the production of the elastomer (the anionic or cationic polymerisation). Similar mechanisms are described by Garcia-Ferro and Aleman (1982), Nakamura et al (1983), Lim et al (1993) and Favre et al (1994). Other authors describe a self association of water within the polymer when it enters a supersaturated state (Lee et al 1992) as the driving force behind the uptake. It is generally recognised in these studies that the clusters only start to form during the latter part of the diffusion cycle when the polymer is close to saturation (within the matrix). Indeed the results from the SBS5+ in osmotic solutions (prior to the onset of oxidation) show that the sensitivity of the formation of the clusters to the environment is very similar to that seen for PBS5+ where the absorption is driven by a soluble agent. These materials also seem to fit in with the other patterns seen for the relationship of the diffusion coefficient and the concentration of water in the polymer in desorption (figure 8.6). The general absorption of these materials shows the same sort of dependence on the strength and more particularly the modulus of the material.

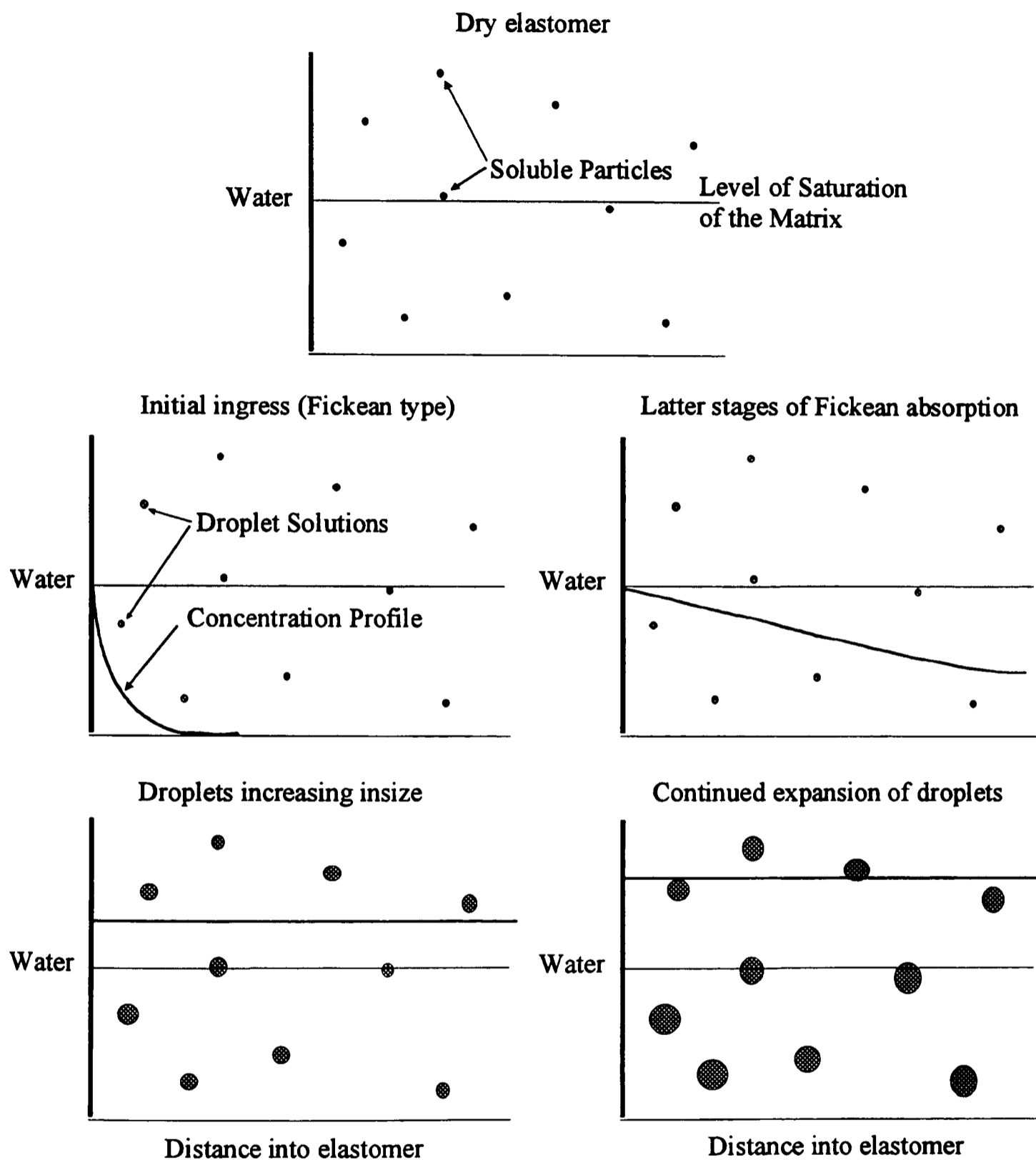
Consider the free energy for the formation of the clusters; here there is no readily available term for the chemical potential as used for the droplets, but for them to form the change must be negative. The Flory Huggins term would stay the same as that previously used. The term which could describe the clustering is more difficult; the Zimm Lundberg approach could be modified but this does not seem satisfactory as the reliance on material constants (K and B) does limit the applicability of the equation formed (equation 2.20). The actual nature of the uptake indicates that the clustering function would give a low negative value with most of the absorption in the early stage being into the matrix (as is seen in figure 8.16, and 8.18). This would account for the observed phenomena with the clusters being sensitive to the osmolarity and strength of the material, and their formation only after most of the absorption into the matrix has taken place.

The importance of relaxation in the process should also be realised as this enables the groups responsible for the clustering to move together to form the cluster itself. The materials used here were all elastomers so the chains are comparatively free to move around and so will not be restricted, but relaxation during clustering mechanisms for rigid materials will be a major factor determining whether the groups will cluster together. Similarly the intermolecular bonding of the groups will also be important as if the groups bond strongly to each other or another species in preference to the water the clustering will not occur.

8.6. Summary of diffusion into elastomers.

Water uptake into elastomers is a balance between different factors and cannot be simply described. The general form of a typical uptake is shown in figure 8.19, with water moving into the sample in a Fickian manner. The water then wets the soluble particles, there is now a dependence on the hydrophilic nature of both the soluble particle and the matrix. If the soluble particle is very soluble with a high osmotic potential and the absorbence of the matrix is very small then growth of the solutions can dominate the early absorption characteristics and result in a steep concentration front diffusing into the material. More usually the soluble particles have a lower osmotic potential associated with them so in the initial stages their effect is less, although they do slow the apparent rate of diffusion. Here a normal Fickian front moves into the material with the concentration quickly reaching what looks like near saturation of the matrix. The

Figure 8.19. Illustration of sequence of water moving into the elastomer and the concentration profile across the material.



expansion of the droplets then comes to dominate the uptake into the material, with a near uniform concentration profile across the sample, although it is recognised that there may well be some concentration gradient towards the centre of the material. The droplets will keep expanding until the restraining force exerted by the materials is equal to that resulting from the osmotic restraining force.

Clustering behaviour of groups in the matrix of the material is complex and the mechanisms are unknown, but it seems that the overall behaviour is adequately described in the above philosophy if the clusters are treated as an impurity with a low osmotic potential. This is of course a simplification and makes no account of the subtleties of the processes involved, but the general patterns seem to fit fairly well.

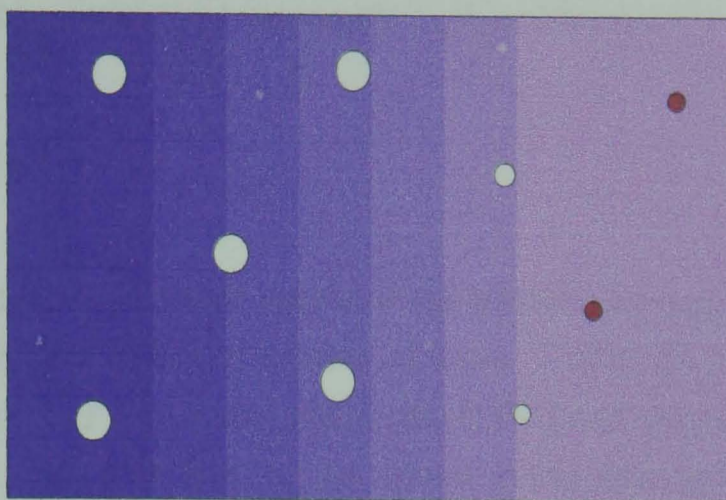
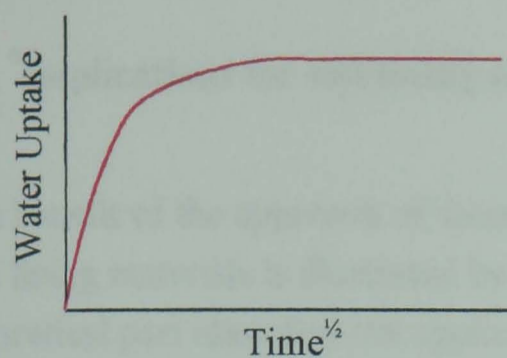
There are other factors that determine the type of the uptake, as illustrated in figure 8.20, which shows the type of uptake profile which might be expected in each case. The first is the normal elastic restraint as described above with the overall kinetics looking fairly Fickian. The second is when the material creeps (or stress relaxes) around the droplets so enabling the continued expansion of the droplets, hence a non-equilibrating protracted uptake results. Thirdly, the expansion of the droplets leads to fracturing of the material around the droplets and eventually to the formation of a crack network which, if it connects to the surface, causes an inversion in the uptake as the solution from these droplets moves out of the material along these crack channels. The last is oxidation which dramatically increases the water uptake of the material. Here the results indicate that the water must first diffuse into the material in order for the material to oxidise, the proportion being dependent on the type and concentration of ions promoting the oxidation.

The kinetics of the absorption and desorption processes were described in the early part of this chapter. The desorption of all the materials exhibit the same sort of relationship between the diffusion coefficient and the concentration of water, with the diffusion coefficient of the matrix determining the rate of transfer from the droplets (and the matrix) into the surrounding solution. The other factors such as restraining force and osmotic potential of the soluble agent (or that arising from the clusters) being insignificant (as seen in figure 8.6). For absorption the picture is more complex, as might have been predicted with all the factors coming into play. Here the chemical potential (arising from the osmotic pressure) difference, the absorption of the matrix and the restraining force all play a role in determining the relationship. Although there appears to be a relationship between the water content, diffusion coefficient and chemical potential difference between the internal and external solution similar to that observed in diffusion within each group of materials (section 5.5.3 and 8.10).

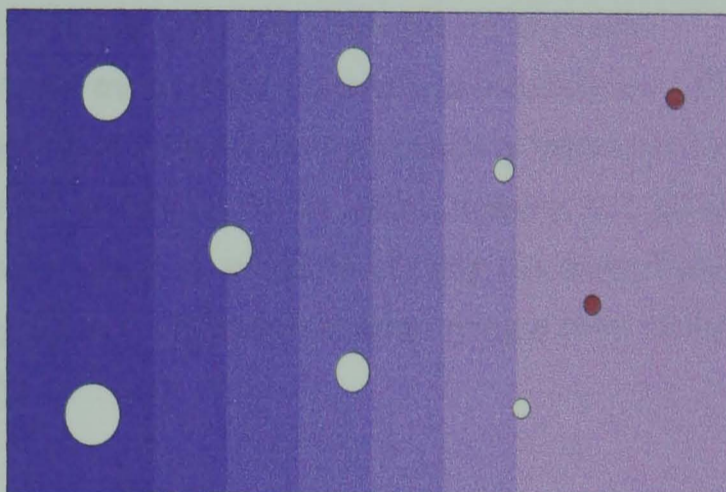
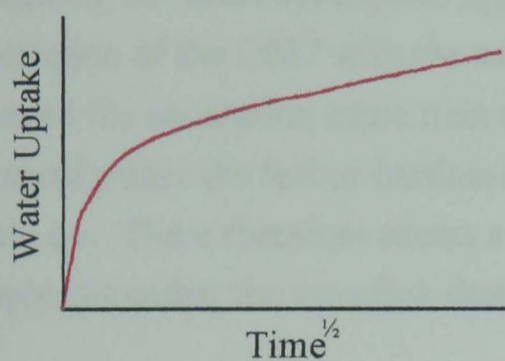
The absorption cycle of the materials is typically non Fickian with deviation at high M_t/M_∞ values, although for smaller values the agreement is good (figure 8.12 and 8.13). Indeed the non equilibrating samples also show a Fickian type of start to the uptake

Figure 8.20. Illustration of different types of water uptake into the elastomer and the subsequent mass uptake profile.

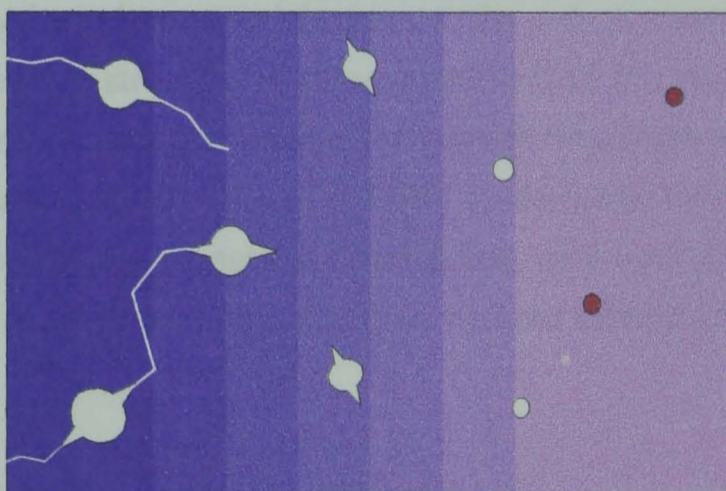
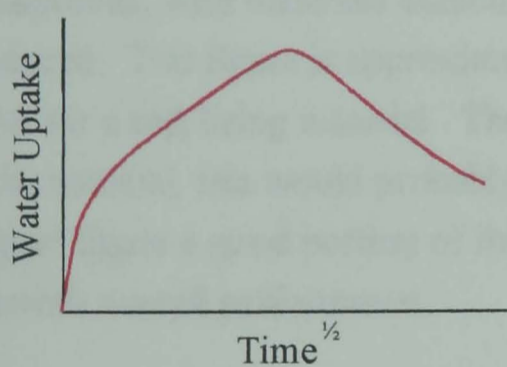
1. Droplets restrained elastically.



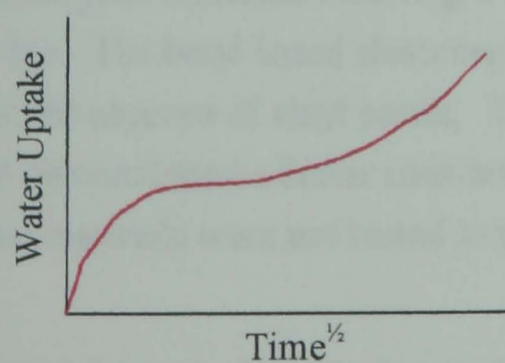
2. Material creeps around droplets.



3. Material cracks around droplets.



4. Material Oxidises.



Water diffusing into polymer with time

(figure 8.14, and 8.15) which breaks down as the absorption progresses. This again indicates the importance of the Fickian process in describing the uptake although the overall uptake may not be described adequately by keeping the Fickian kinetics.

8.7. Implications for soft lining materials.

The benefit of the approach of focusing on the water uptake in the development of new soft lining materials is illustrated by these results in a number of ways. Firstly the more theoretical part identified the application of reinforcing fillers (the C687) and increased crosslink density (e.g. SIS TGE) as a method of limiting the uptake of the elastomer / methacrylate materials. These materials exhibited a low absorption despite the containing the same hydrophilic agent that made other materials unsatisfactory. The application of the C687 with the unsaturated elastomers is particularly interesting as it lowered the absorption more than simply increasing the crosslink density, but did not drastically alter the feel or hardness of the material which increasing the cross link density could do. There therefore seems a significant advantage in employing a filler rather than simply increasing the crosslink density.

The water uptake of the elastomer methacrylate materials was not the only property to be improved, with materials demonstrating strengths of up to 26 MPa (SIS M) being produced. This figure is approximately 5 times the accepted minimum requirement (5 MPa) for a soft lining material. The application of the filler C687 could lower the uptake of the material, this would probably lower the strength somewhat but, with such a high original figure a good portion of the strength could be sacrificed without effecting the materials overall performance.

Oxidation was also identified as a major potential problem for the elastomer / methacrylate materials requiring a solution to be found before the material was employed in vivo. The butyl based elastomers demonstrate a guaranteed solution to this problem with the absence of vinyl bonds. The low absorption materials (filled or cross linked) also demonstrated a better resistance to oxidation, although it should be realised that these materials were not tested in the potent oxidising media of saliva.

The butyl (particularly the bromo butyl) based materials show considerable promise as soft lining materials as they will not oxidise, have reasonable strength (PBB B, over 6 MPa) and are widely used already in pharmaceuticals, although the water uptake is cause for some concern. The major problem here is the lack of grafting or crosslinking with

the elastomer due to its saturated nature. The application of the same procedures that helped to improve the water uptake of the unsaturated elastomers (crosslinking and fillers) do not work here which again seems to be due to the saturated nature of the elastomer. Bromo butyl can however be cross linked by sulphur, ZnO, or by peroxides (especially in conjunction with N,N'-m-1,3-Phenylenedimaleimide) Brydson (1978 and 1988). Whilst the sulphur is not suitable here the other two seem possible methods to improve the crosslinking and hence, hopefully the water uptake.

The silicone based materials generally showed a low uptake as expected, the addition of a hydrophilic or soluble agent hence raised the uptake. The extent of the problems encountered with condensation silicones was somewhat surprising, but it is felt that this class of silicone materials is always going to be prone to scission and recombination of the siloxane bond which leads to leaching of the silicones. This may account for the high water uptake and loss of Flexibase as reported by Wright (1976) in combination with a soluble agent (bearing in mind how this would effect the restraining force).

Both the peroxide and hydrosilanised silicones exhibited very low uptakes (when pure) and had reasonable strength. Probably the most interesting of these materials is the H200 5 which seems to, due to the excess of the hydrogen terminated siloxane, bond to the silica surface. This not only improved the strength of the material and further reduced the uptake but may improve the tear resistance of the material. When 'trouser' tear tests (method described in Parker, 1982) the material failed in knotty tear, the tear turned back on itself. This prevented any meaningful values of tear resistance being determined. Experience from conducting these tests and generally handling the materials indicated this material was somewhat more resistant than the other materials.

The wettability of the silicone polymers was not directly measured in this study but the investigator feels it is worth commenting on as differences were observable when different agents were added to the pure silicone polymers. Generally, out of the additives used, the calcium stearate and L77 show most promise in improving the wettability for the hydrosilanised materials. Although the increase in the excess of hydrogen terminated siloxane also seemed beneficial. The peroxide silicones did not seem to obey any such trends with little to distinguish between them, this perhaps being a reflection on the effect of residual benzol peroxide in the material. Clearly, further work on the wettability of these materials should be undertaken.

The importance of creep in determining the water uptake of the materials here has been demonstrated. This has implications for the plasticised (both the traditional and polymisable variety) acrylic materials which are widely used in dentistry. These materials tend to have a very high $\tan \delta$ (values in excess of 1 are not uncommon) which implies the materials will be prone to creep. The presence of any soluble agent (including benzol peroxide) or groups capable of clustering will increase the uptake of the material significantly with time as the polymer creeps.

The role of the osmolarity of the external solution may well explain the discrepancy between the in vivo and ex vivo results of Novus where large uptakes are observed in laboratory tests (in water) but these are not reproduced clinically. Indeed when Novus is placed in 0.45 and 0.9 M NaCl a much lower absorption is seen (Parker et al, 1995, 1997) the soluble agents driving the absorption with Novus having a high sensitivity to the external solutions.

8.8. Recommendations for further study.

The trends and observations described here seem to form a general overview of the diffusion of water into elastomers, although there is much that is left not satisfactorily explained. The work also shows the limitations of focusing too closely in one particular group of materials as this tends to exclude factors which more usually dominate in other types of materials. The application of aspects of this work to rigid and other anomalous polymer systems may well help explain their behaviour and also refine the description of the phenomena seen here.

Probably the most relevant parts are, the relationship of the water uptake (c_w) with the osmolarity (π_o) and it's basis in the small strains theory, which although not ideal does predict the type of behaviour that is seen. Further from this the logarithmic relationships between the absorption and particularly the desorption diffusion coefficient and the water uptake. The linearity enables the nature of the process to be seen and some of the factors separated.

The NMR imaging revealed much about the inherent process of the absorption into the elastomers. It also showed the potential of this technique and further study using other modes of operation, perhaps most significantly T_2 relaxation time maps of the different states of the water within the polymer. This then enables the determination of the osmolarity of the internal droplet or the association of the water with groups on the

polymer itself. Although not straight forward the appropriate selection of the material and soluble agent or hydrophilic group would enable a further insight into the process of absorption. Further potential is also seen in the determination of the change in the relaxation time of the polymer with the ingress of water. This would enable the other side of the process to be investigated, as the importance of the balance between the water and polymer is apparent. Another exciting possibility is the use of F^{19} in conjunction with H^1 imaging which could enable the location of fluorine (associated with the hydrophilic agent) and then correlate with the H^1 image. This might be particularly relevant for the drug release materials where the movement of the drug out of the polymer is the primary concern.

The link between the physical properties and the water uptake is not new but its understanding is still quite poor with different factors being important in describing the process, ideally the tensile, shear and rupture properties should all be considered with respect to time and the absorption of water. An alternative approach is dynamic mechanical analysis, although this makes many assumptions about the relationships of the materials properties it provides a simple and quick way to gauge some of them. Hence making it a useful tool in the understanding and development of materials in water.

The role of the hydrogen bond in the interaction of water with polymers is probably the major factor determining the uptake by the matrix and clusters, but comparatively little is known about it in relation to polymers. This must soon change, hydrophilic polymers are becoming increasingly important and the hydrogen bond is therefore attracting more and more interest. This work draws heavily on the work from other fields noticeably chemistry and biochemistry. Recognition of the relevance of this work to any polymers in contact with water is important but so far no research seems to have pursued this direction adequately.

Perhaps the most important aspect of the work is the recognition of the chemical potential as central to the absorption process. This enables many different aspects of the process to be incorporated in a unifying approach. Exactly how this could be developed into a usable equation is unclear and is further hampered by the absence of adequate descriptions of the different elements of the process. But it must surely be an area for considerable research activity.

References.

Addy, M. and Handley, R. The effects of the incorporation of chlorohexidine acetate on some physical properties of polymerised and plasticized acrylics. *Journal of Oral Rehabilitation*, **8**, 155-163, 1981.

Adrian, E.D., Drantz, W.A. and Ivanhoe, J.R. The use of processed silicone to retain the implant-supported tissue-borne over denture. *Journal of Prosthetic Dentistry*, **67**, 219-222, 1992.

Aiken, A. A physico-chemical and biological study of systems based on poly(2 ethoxy ethyl methacrylate) for use in oral and maxiofacial surgery. Phd, University of London, UK, 1988. D

Allen, P.W. Graft polymerisation from natural rubber. Chapter 5, Ed. Bateman, L.C. *Chemistry and physics of rubber-like substances*. Maclaren and Sons Ltd., London, 1963.

Aminabhavi, T.M., Thomas, R.W. and Cassidy, P.E. Predicting water diffusivity in elastomers. *Polymer Engineering and Science*, **24**, 1417-1420, 1984.

Andrews, E.H. and Braden, M. The reaction of ozone with surfaces of natural rubber and its dependence on strain. *Journal of Polymer Science*, **55**, 787-798, 1961.

Artemov, D.Y., Samoilenko, A.A., Iordanskii, A.L., Sibel'dina, L.A. and Kosenko, R.Y. NMR intrascopy-a new method for studying diffusion into polymers. *Polymer Science U.S.S.R.*, **30**, 1648-1650, 1988.

Arvidson, K. and Johansson, E.G. Galvanic currents between dental alloys in vitro. *Scandinavian Journal of Dental Research*, **93**, 467-473, 1985.

Auerbach, L. and Carnicom, M.L. Sorption of water by Nylon 66 and Kevlar 29. *Equilibria and Kinetics*. *Journal of Applied Polymer Science*, **42**, 2417-2427, 1991.

Ault, A. and Dudek, G.O. *NMR an introduction to proton nuclear magnetic resonance spectroscopy*. Holden-Day Inc. San Francisco, 1976.

Autian, J. Toxicity and health threats of phthalate esters: review of literature. *Environmental Health Perspectives*, June, 3-26, 1973.

Badawy, M.S. and El-Sherbiny, N. Effect of using soft liner on bone density around the abutments supporting complete lower overdenture. *Egyptian Dental Journal*, **38**, 105-112, 1992.

Baddour, R.F., Graves, D.J. and Vieth, W.R. Transmission of water and ions through crosslinked hydrophilic membranes. *Journal of Colloid Science*, **20**, 1057-1069, 1965.

- Bankovskaya, T.P., Akopyan, L.A., Nikiforov, V.P. and Bartenev, G.M. Influence of water on the relaxation properties of filled elastomers. *Journal of Soviet Materials Science*, **18**, 432-434, 1982.
- Barnard, D., Bateman, L., Cunneen, J.I. and Smith, J.F. Oxidation of olefins and sulphides. In Ed. Bateman, L. *The chemistry and physics of rubber like substances*. Maclaren and Son Ltd., 1963.
- Barrer, R.M. *Diffusion in and through solids*. Second Edition, Cambridge University press, 1951.
- Barrie, J.A. and Platt, B. The diffusion and clustering of water vapour in polymers. *Polymer*, **4**, 303-313, 1963.
- Barrie, J.A., Machin, D. and Nunn, A. Transport of water in synthetic *cis*-1.4-polyisoprenes and natural rubber. *Polymer*, **16**, 811-815, 1975.
- Barrie, J.A., Sagoo, P.S., and Johncock, P. The sorption and diffusion of water in halogen-containing epoxy resins. *Polymer*, **26**, 1167-1171, 1985.
- Bao, Y.T., Samuel, N.K.P. and Pitt, C.G. The prediction of drug solubilities in polymers. *Journal of Polymer Science: Part C: Polymer Letters*, **26**, 41-46, 1988.
- Bates, J.F. and Smith, D.C. Evaluation of indirect resilient liners for dentures: laboratory and clinical tests. *Journal of the American Dental Association*, **70**, 344-353, 1965.
- Bateman, L.C., Moore, C.G., Porter, M. and Saville, B. Chemistry of vulcanisation, chapter 15. Ed. Bateman, L.C. *Chemistry and physics of rubber-like substances*. Maclaren and Sons Ltd., London, 1963.
- Baumann, M.A., Doll, G.M. and Zick, K. Stray-field imaging (STRAFI) of teeth. *Oral Surgery, Oral Medicine, Oral Pathology*, **75**, 517-522, 1993.
- Beer, M.D. Compositions containing silanol chain stopped poly dimethylsiloxane, organosilicon process aid and curing agent. US Patent 3,382,205, 1968.
- Beers, M.D. Alkoxyhydroxy-terminated poly di organosiloxanes curable at room temperature. U.S. Patent No. 3,438,930, 1969.
- Bell, D.H. Clinical evaluation of a resilient denture liner. *Journal of Prosthetic Dentistry*, **49**, 394-406, 1970.
- Berlin, Y.U., Chekunaev, N.J. and Goldanskii, V.I. Apparent rate constant of partially diffusion-controlled chemical reactions in disordered solids. *Radiation Physics and Chemistry*, **37**, 407-410, 1991.

- Best,M., Halley,J.W. and Johnson.B. and Vallés,J.L. Water penetration in glassy polymers: experiment and theory. *Journal of Applied Polymer Science*, **48**, 319-334, 1993.
- Blackband,S. and Mansfield,P. NMR imaging and diffusion of water into Nylon. *Proceedings of the XXII nd Congress on magnetic resonance and related phenomena, Switzerland*, 516-517, 1984.
- Blackband,S. and Mansfield,P. Diffusion in liquid-solid systems by NMR imaging. *Journal of Physics: Part C: Solid State Physics*, **19**, L49-L52, 1986.
- Bontems,S.L., Stein,J. and Zumbrum,M.A. Synthesis and properties of monodisperse polydimethylsiloxane networks. *Journal of polymer science: Part A: Polymer chemistry*, **31**, 2697-2710, 1993.
- Bordeleau,A., Rousset,G., Bertrand,L. and Crine,J.P. Water detection in polymer dielectrics using photo acoustic spectroscopy. *Canadian Journal of Physics*, **64**, 1093-1097, 1986.
- Boakye,E.E. and Yeager,H.L. Water sorption and ionic diffusion in short side chain perfluorosulfonate ionomer membranes. *Journal of Membrane Science*, **69**, 155-167, 1992.
- Borghouts,J.M.H. and Otto,A.J. Silicone sheet and bead implants to correct the deformities of inadequately healed orbital fractures. *British Journal of Plastic Surgery*, **31**, 254, 1978.
- Braden,M. The absorption of water by acrylic resins and other material. *Journal of Prosthetic Dentistry*, **14**, 307-316, 1964.
- Braden,M. and Clarke,R.L. Viscoelastic properties of soft lining materials. *Journal of Dental Research*, **51**, No.6, 1525-1528, 1972.
- Braden,M., Causton,B.E. and Clarke,R.L. Diffusion of water in composite filling materials. *Journal of Dental Research*, **55**, No.5, 730-732, 1976.
- Braden,M. and Wilson,A.D. Relationship between stress relaxation and viscoelastic properties of dental materials. *Journal of Dentistry*, **10**, No.3, 181-186, 1982.
- Braden,M and Wright,P.S. Water absorption and water solubility of soft lining materials for acrylic dentures. *Journal of Dental Research*, **62**, 764-768, 1983.
- Braden,M. and Parker,S. Soft linings. *British Patent Application No. 8,302,547*, 1985.
- Braden,M. Dimensional stability of condensation silicone rubbers, *Biomaterials*, **13**, 333-336, 1992.

- Braden,M., Wright,P.S. and Parker,S. Soft lining materials - a review. *European Journal of Prosthodontics and Restorative Dentistry*, **3**, 163-174, 1995.
- Braley,S. The chemistry and properties of medical-grade silicones, *Journal of Macromolecular Science: Part A: Chemistry*, **A4**, 529, 1970.
- Brandrup,J. and Immergut,E.H. *Polymer Handbook*. 2nd Ed., John Wiley and Sons, 1975.
- Briggs,G.J., Edwards,D.C. and Storey,E.B. Water absorption of elastomers. *Proceedings of the 4th Rubber Technology Conference, London*, 362-386, 1962.
- Brody,G.S. Fact and fiction about breast implant 'bleed'. *Plastic and Reconstructive Surgery*, **60**, 615, 1970.
- Brook,I.M. and Van Noort,R. Controlled delivery of drugs, a review of polymer-based devices. *British Dental Journal*, **157**, 11-15, 1984.
- Brook,I.M. and Van Noort,R. Drug release from acrylic polymers via channels and cracks: in vitro studies with hydrocortisone. *Biomaterials*, **6**, 281-285, 1985.
- Brown,D. Resilient soft liners and tissue conditioners. *British Dental Journal*, **164**, 357-360, 1988.
- Brydson,J.A. *Rubber chemistry*. Applied Science Publishers, 1978.
- Brydson,J.A. *Rubbery materials and their compounds*. Elsevier Applied Science, 1988.
- Bucknall,C.A., Zhang,X.C. Orton,M.L. and Jackson,G.V. Water absorption and disc cracking in urethane-methacrylate resins. *Journal of Applied Polymer Science*, **52**, 457-466, 1994.
- Carslaw,H.S. and Jaeger,J.C. *Conduction of heat in solids*. Clarendon Press, Oxford, 1959.
- Cassidy,P.E., Aminabhavi,T.M. and Brunson,J.C. Water permeation through elastomers and plastics. *Rubber Chemistry and Technology*, **56**, No.3, 594-618, 1983,a.
- Cassidy,P.E. Aminabhavi,T.M. and Brunson,J.C. Water permeation through elastomer laminates I. Neoprene/EPDM. *Rubber Chemistry and Technology*, **56**, 357-366, 1983,b.
- Cassidy,P.E. and Aminabhavi,T.M. Water permeation through elastomer laminates II. SBR/EPDM. *Rubber Chemistry and Technology*, **59**, 779-786, 1986,a.
- Cassidy,P.E. and Aminabhavi,T.M. Water permeation through elastomer laminates III. Neoprene/styrene butadiene. *Polymer*, **27**, 1396-1399, 1986,b.

- Cochrane,H. and Lin,C.S. The influence of fumed silica on the processing, curing and reinforcement properties of silicone rubber. *Rubber Chemistry and Technology*, **66**, 48-60, 1993.
- Cohen,Y. and Cohan,E. Role of water in the phase transformations observed in solutions of a rigid polymer. *Macromolecules*, **28**, 3631-3636, 1995.
- Collis,J. Assessment of a recently introduced fluoroelastomeric soft lining material. *International Journal of Prosthodontics*, **6**, No.5, 440-445, 1993.
- Combe,E.C. and Grant,A.A. The selection and properties of materials for dental practice. *British Dental Journal*, **134**, 289-292, 1973.
- Compañ,V., Villar,M.A., Vallés,E. and Riande,E. Permeability and diffusional studies on silicone polymer networks with controlling dangling chains. *Polymer*, **37**, 101-107, 1996.
- Crank,J. and Park,G.S. Water in polymers. In Barrie,J.A. (Ed.), *Diffusion in polymers*, 1st Edition, New York, Academic press Inc. 259-313, 1968.
- Crank,J. *The mathematics of diffusion*. 2nd Edition. Clarendon Press, Oxford Science Publications, 1975.
- Creamer,C.E. Organosiloxane elastomers. U.S. Patent 3,696,068, 1972.
- Crowley,J.D., Teague,G.S. and Lowe,J.W. A three dimensional approach to solubility I. *Journal of Paint Technology*, **38**, 269-80, 1966.
- Crowley,J.D., Teague,G.S. and Lowe,J.W. A three dimensional approach to solubility II. *Journal of Paint Technology*, **39**, 19-27, 1967.
- Davidson,M.G. and Deen,W.M. Hindered diffusion of water-soluble macromolecules in membranes. *Macromolecules*, **21**, 3471-3481, 1988.
- Davy,K.W.M. and Braden,M. The mechanical properties of elastomeric poly (alkyl methacrylate)s. *Biomaterials*, **8**, 393-396, 1987.
- Degussa. Technical bulletin pigments No 11: basic characterisation of Aerosil. Degussa AG, 1993,a.
- Degussa. Technical bulletin pigments No.18: the use of hydrophobic Aerosil in the coatings industry. Degussa AG, 1993,b.
- Di Colo,G. Controlled release from implantable matrices based on hydrophobic polymers. *Biomaterials*, **13**, No.12. 850-856, 1992

- Di Silvio, L., Kayser, M. V. and Downs, S. Validation and optimisation of a polymer system for potential use as a controlled drug delivery system. *Clinical Materials*, **16**, 91-98, 1994.
- Diamant, Y., Marom, G. and Broutman, L. J. The effect of network structure on moisture absorption of epoxy resins. *Journal of Applied Polymer Science*, **26**, 3015-3025, 1981.
- Dolgov, O. N., Voronkov, M. G. and Grinbat, M. P. Organosilicon liquid rubbers and materials based on them. *Khimiya*, 1975, Translated by Moseley R. J., *International Polymer Science and Technology Monograph*, No. 1, RAPRA, 1977.
- Donaldson, P. E. K. Aspects of silicone rubber as an encapsulant for neurological prostheses, part 1, osmosis. *Medical and Biological Engineering and Computing*, **29**, 34-39, 1991.
- Dootz, E. R., Koran, A. and Craig, R. G. Comparison of physical properties of 11 soft liners. *Journal of Prosthetic Dentistry*, **67**, 707-712, 1992.
- Downs, S. Methods for improving drug release from poly(methyl) methacrylate bone cement. *Clinical Materials*, **7**, 227-231, 1991.
- Edelman, E. R., Kost, J., Bobeck, H. and Langer, R. Regulation of drug release from polymer matrices by oscillating magnetic fields. *Journal of Biomedical Materials Research*, **19**, 67-83, 1985.
- Edelman, E. R. and Langer, R. Optimisation of release from magnetically controlled polymeric drug release devices. *Biomaterials*, **14**, 621-626, 1993
- Edwards, D. C. Water absorption phenomena in elastomers. *Elastomerics*, **117**, 25-30, 1985.
- Ellis, B., Lamb, D. J. and Al-Nakash, S. Variations in the elastic modulus of a soft lining material. *British Dental Journal*, **149**, 79-82, 1980.
- Favre, E., Schaetzel, P., Nguygen, Q. T., Clément, R. and Néel, J. Sorption diffusion and vapour permeation of various penetrants through dense poly (dimethylsiloxane) membrane: a transport analysis. *Journal of Membrane Science*, **92**, 169-184, 1994.
- Fedors, R. F. Osmotic effects in water absorption by polymers. *Polymer*, **21**, February, 207-212, 1980.
- Feng, S. and Du, Z. Effects of some phenylethynylsilicon compounds on heat-curable silicone rubber. I. 1,3-Bis (methylphenyl ethynylvinyl) disiloxane. *Journal of Applied Polymer Science*, **43**, 1323-1326, 1991.

- Firestone, B.A. and Siegel, R.A. Kinetics and mechanisms of water sorption in hydrophobic, ionizable copolymer gels. *Journal of Applied Polymer Science*, **43**, 901-914, 1991.
- Flory, P.J. Thermodynamics of high polymer solutions. *Journal of Chemical Physics*, **10**, 51-61, 1942.
- Folkman, J. and Long, D.M. The use of silicone rubber as a carrier for prolonged drug therapy. *The Journal of Surgical Research*, **4**, 139, 1964.
- Fourier, J.B. *Théorie analytique de la chaleur*. English translation by A Reeman, Dover Publ., New York, 1955, 1822.
- Frisch, E.E. Technology of silicones in biomedical applications. In Rubin, L.R. (Ed.), *Biomaterials in reconstructive surgery*. St. Louis: C.V. Mosby Co., 724, 1983.
- Fyfe, C.A., Randall, L.H. and Burlinson, N.E. Water penetration in Nylon 6,6: Absorption desorption and exchange studied by NMR Microscopy. *Journal of Polymer Science: Part A: Polymer Chemistry*, **31**, 159-168, 1993.
- Gale, R., Chandrasekaran, S.K., Swanson, D. and Wright, J. Use of osmotically active therapeutic agents in monolithic systems. *Journal of Membrane Science*, **7**, 319-331, 1980.
- Gambogi, J.E. and Blum, F.D. Effects of water on the interface in a model polymer composite system: a nuclear magnetic resonance study. *Materials Science and Engineering*, **A162**, 249-256, 1993.
- Garcia-Fierro, J.L. and Aleman, J.V. Sorption of water by epoxide prepolymers. *Macromolecules*, **15**, 1145-1149, 1982.
- Gedde, U.W. *Polymer Physics*. Chapman and Hill, London, 1995.
- General Electric Co. Pourable curable elastomer-forming composition. U.S. Patent 1,090,958, 1967.
- Gent, A.N. and Lindley, P.B. Internal rupture of bonded rubber cylinders in tension. *Proceedings of the Royal Society of London: Series A: Mathematical and Physical Sciences*, **249**, 195, 1958.
- Gent, A.N. Relaxation processes in vulcanised rubber I. Relaxation among stress relaxation, creep and hysteresis. *Journal of Applied Polymer Science*, **6**, 433-441, 1962.
- Gettleman, L. and Gebert, P.H. Soft Denture Liner. U.S. Patent No. 4,661,065, 1987.
- Gettleman, L., Jameson, L.M. and Guerra, L.R. Interim results from a clinical trial of two permanent resilient denture liners. *Journal of Dental Research*, **66**, 134, 1987.

- Gettleman, L., Guerra, L.R. and Jameson, L.M. Clinical trials of Novus soft denture liner vs. Molloplast B: final results and four year follow-up. *Journal of Dental Research*, **69**, 458, 1990.
- Gilbert, A.S. Pethrick, R.A. and Phillips, D.W. Acoustic relaxation and infrared spectroscopic measurements of plasticization of poly(methyl methacrylate) by water. *Journal of Applied Polymer Science*, **21**, 319-330, 1977.
- Girard, O. and Cohen-Addad, J.P. Silica-siloxane mixtures: surface saturation process of particles. *Kinetics. Polymer*, **32**, 860-863, 1991.
- Gonzales, J.B. and Laney, W.R. Resilient materials for denture prostheses. *Journal of Prosthetic Dentistry*, **16**, 438-444, 1966.
- Göpferich, A. and Langer, R. Modelling of polymer erosion. *Macromolecules*, **26**, 4105-4112, 1993.
- Grinsted, R.A. and Koenig, J.L. Study of multicomponent diffusion into polycarbonate rods using NMR imaging. *Macromolecules*, **25**, 1299-1234, 1992.
- Grinsted, R.A., Clark, L. and Koenig, J.L. Study of cyclic sorption-desorption into poly(methyl methacrylate) rods using NMR imaging. *Macromolecules*, **25**, 1235-1241, 1992.
- Groß, D. Elastomere im Trinkwasserkontakt (II). *Kunststoffe*, **34**, 464-466, 1980.
- Hansen, C.M. The three dimensional solubility parameter - key to paint - component affinities. I, solvent, plasticizer, polymers and resins. *Journal of Paint Technology*, **39**, 104-117, 1967.
- Hariharan, D. and Peppas, N.A. Characterization, dynamic swelling behaviour and solute transport in cationic networks with applications to the development of swelling-controlled release systems. *Polymer*, **37**, 149-161, 1996.
- Harned, H.S. and Owens, B.B. *The physical chemistry of electrolytic solutions*. Reinhold, New York, 1958.
- Harsanyi, B.B., Foong, W.C., Howell, R.E., Hidi, P. and Jones, D.W. Hamster cheek-pouch testing of dental soft polymers. *Journal of Dentistry*, **9**, 991-996, 1991.
- Harrison, D.J. Li, X. and Petrovic, S. A detailed study of the behaviour and distribution of water inside ion selective membranes. *IEEE, Transducers '91, International conference on solid state sensors and actuators, San Francisco, June, 777-780, 1991*.
- Haug, S.P., Andres, C.J., Munoz, C.A. and Okamura, M. Effects of environmental factors on maxillofacial elastomers: part III - physical properties. *Journal of Prosthetic Dentistry*, **68**, 644-651, 1992.

- Hayes, C.K. and Cohen, D.S. The evolution of steep fronts in non Fickian polymer-penetrant system. *Journal of Polymer Science: Part B: Polymer Physics*, **30**, 145-161, 1992.
- Hardie, J.M. Examination of new soft lining materials. Internal Report, London Hospital Medical College, University of London, October, 1982.
- Heidingsfeldová, M. and Capka, M. Rhodium complex catalysts for hydrosilylation crosslinking of silicone rubber. *Journal of Applied Polymer Science*, **30**, 1837-1846, 1985.
- Heidingsfeldová, M., Schätz, M. and Capka, M. Hydrosilylation crosslinking of silicone rubber catalysed by Bis (1,5-cyclooctadiene) di- μ, μ' -chlorodirhodium. *Journal of Applied Polymer Science*, **42**, 179-183, 1991.
- Henry, J.L., Ruaya, A.L. and Garton, A. The kinetics of oxidation in aqueous media. *Journal of Polymer Science. Part A. Polymer Chemistry*, **30**, 1693-1703, 1992.
- Hernandez, R.J. and Gavara, R. Sorption and transport of water in nylon-6 films. *Journal of Polymer Science: Part B: Polymer Physics*. **32**, 2367-2374, 1994.
- Hildebrand, J. and Scott, R. The solubility of non-electrolytes. 3rd Ed., Reinhold Publishing Corp., 1949.
- Hirschinger, J., Miura, H., Gardner, K.H. and English, A.D. Segmental dynamics in the crystalline phase of nylon 66. Solid-state H NMR. *Macromolecules*, **23**, 2153-2169, 1990.
- Hoy, K.L. New values of the solubility parameter from vapour pressure data. *Journal of Paint Technology*, **42**(541), No.76-8, 115-118, 1970.
- Huggins, M.L. Solutions of long chain compounds. *Journal of Chemical Physics*, **10**, 151, 1942.
- Hui, C-Y., Wu, K-C., Lasky, R.C. and Kramer E.J. Case II diffusion in polymers. I. Transient swelling. *Journal of Applied Physics*. **61**, No.11, 5129-5136, 1987,a.
- Hui, C-Y., Wu, K-C., Lasky, R.C. and Kramer E.J. Case II diffusion in polymers. II. Steady-state front motion. *Journal of Applied Physics*. **61**, No.11, 5137-5149, 1987,b.
- Hsu, W.P., Li, R.J., Myerson, A.S. and Kwei, T.K. Sorption and diffusion of water vapour in hydrogen bonded polymer blends. *Polymer*, **34**, No.3, 597-603, 1993.
- IARC Monographs on the evaluation of the carcinogenic risks of chemicals to man. 12: Some carbamates, thiocarbamates, and carbazides. Lyon, 262.197.
- ICI Chemical safety sheet, 2 ethoxy ethyl methacrylate. ICI Chemicals Ltd.

- Ishida,H. and Koenig,J.L. Fourier transform infrared spectroscopic study on the silane coupling agents/porous silica interface. *Journal of Colloidal and Interface Science*, **64**, 555-564, 1978.
- Jepson,N.J.A., McCabe,J.F. and Basker,R.M. A new temporary soft lining material. *Journal of Dentistry*, **23**, No 2, 123-126, 1995.
- Jepson,N.J.A., McCabe,J.F. and Storer,R. Evaluation of the viscoelastic properties of denture soft lining materials. *Journal of Dentistry*. **21**, 163-170, 1993, a.
- Jepson,N.J.A., McCabe,J.F. and Storer,R. Age changes in the viscoelasticity of permanent soft lining materials. *Journal of Dentistry*, **21**, 171-178, 1993, b.
- Jepson,N.J.A., McCabe,J.F. and Storer,R. Age changes in viscoelasticity of a temporary soft lining materials. *Journal of Dentistry*, **21**, 244-247, 1993, c.
- Kabra,B.G., Gehrke,S.H., Hwang,S.T. and Ritschel,W.A. Modification of dynamic swelling behaviour of poly(2-hydroxyethyl methacrylate) in water. *Journal of Applied Polymer Science*, **42**, 2409-2416, 1991.
- Kaelble,D.H. Cavitation in a viscoelastic media. *Transactions of the Society of Rheology*, **15(2)**, 275-296, 1971.
- Kalachandra,S. and Kusy,R.P. Comparison of water sorption by methacrylate and dimethacrylate monomers and their corresponding polymers. *Polymer*, **32**, 2428-2434, 1991.
- Kalachandra,S., Minton,R.J., Takamata,T. and Taylor,D.F. Characterisation of commercial soft liners by dynamic mechanical analysis. *Journal of Material Science: Materials in Medicine*, **6**, 218-222, 1995.
- Kambour,R.P., Gruner,C.L. and Romagosa,E.E. Bisphenol-A polycarbonate immersed in organic media. Swelling and response to stress. *Macromolecules*, **7**, 248-253, 1974.
- Kawano,F., Dootz,E.R., Koran,A. and Craig,R.G. Comparison of bond strength of six soft denture liners to denture base resin. *Journal of Prosthetic Dentistry*, **68**, 368-371, 1992.
- Kawano,F., Dootz,E.R., Koran,A. and Craig,R.G. Sorption and solubility of 12 soft denture liners. *Journal of Prosthetic Dentistry*, **72**, No.4, 393-8, 1994.
- Kawano,F., Koran,A., Asaoka,K. and Matsumoto,N. Effect of soft denture liner on stress distribution in supporting structures under a denture. *International Journal of Prosthodontics*, **6**, No.1, 43-49, 1993.
- Kazanji,M.N.M., and Watkinson,A.C. Soft lining materials: their absorption of, and solubility in, artificial saliva. *British Dental Journal*, **165**, 91-94, 1988.

- Khan, M.Z.I. Recent trends and progress in sustained or controlled oral delivery of some water soluble drugs, Morphine salts, diltiazem and captopril. *Drug Development and Industrial Pharmacy*, **21**, 1037-1070, 1995.
- Khare, A.R. and Peppas, N.A. Investigation of hydrogel water in polyelectrolyte gels using differential scanning calorimetry. *Polymer*, **34**, No.22, 4736-4739, 1993.
- Kohjiya, S., Ono, A. and Yamashita, S. Hydrosilylation of mesogens having carbon-carbon double bonds with Poly(methyl hydrosiloxane)s. *Polymer Plastic Technology Engineering*, **30**, 351-366, 1991.
- Koningsveld, R. and Kleinjans, L.A. Liquid-liquid phase separation in multicomponent polymer systems. X. Concentration dependence of the pair interaction parameter in system cyclohexane-polystyrene. *Macromolecules*, **4**, 637-641, 1974.
- Korsmeyer, R.W. and Peppas, N.A. Effect of the morphology of hydrophilic polymeric matrices on the diffusion and release of water soluble drugs. *Journal of Membrane Science*, **9**, 211-217, 1981.
- Korsmeyer, R.W., Lustig, S.R., and Peppas, N.A. Solute and penetrant diffusion in swellable polymers, I mathematical modelling. *Journal of Polymer Science: Part B: Polymer Physics*. **24**, 395-408, 1986,a.
- Korsmeyer, R.W., Meerwall, E.V. and Peppas, N.A. Solute and penetrant diffusion in swellable polymers, II verification of theoretical models. *Journal of Polymer Science: Part B: Polymer Physics*, **24**, 409-434, 1986,b.
- Kutay, O. Comparison of tensile and peel bond strengths of resilient liners. *Journal of Prosthetic Dentistry*, **71**, No.5, 525-31, 1994.
- Kutay, O., Bilgin, T., Sakar, O. and Beyli, M. Tensile bond strength of a soft lining with acrylic denture base resins. *European Journal of Prosthodontic and Restorative Dentistry*, **2**, No.3 123-126, 1994.
- Labarr, E.E. and Turner, D.T. Increased water sorption of poly (methyl methacrylate) after removal of methanol. *Journal of Polymer Science: Part B: Polymer Physics*, **20**, 557-560, 1982.
- Lammie, G.A. and Storer, R. A preliminary report on resilient denture plastics. *Journal of Prosthetic Dentistry*, **8**, 411-424, 1958.
- Langer, R. Hsieth, D.S.T., Rhine, W. and Folkman, J. Control of release kinetics of macromolecules from polymers. *Journal of Membrane Science*, **7**, 333-350, 1980.
- Langer, R. Novel drug delivery systems. *Chemistry in Britain*, March, 232-236, 1990.

- Lasky,R.C. and Kramer,E.J. The initial stages of Case II at low penetrant activities. *Polymer*, **29**, 673-679, 1988.
- Lee,M.C. and Peppas,N.A. Water transport in graphite/epoxy composites. *Journal of Applied Polymer Science*, **47**, 1349-1359, 1993.
- Lee,P.I. Effect of non-uniform initial drug concentration distribution on the kinetics of drug release from glassy hydrogel matrices. *Polymer*, **25**, 973-978, 1984.
- Lee, S-B., Rockett,T.J. and Hoffman,R.D. Water-induced nucleation of disc cracks in selected thermosets. *Polymer*, **33**, 2353-2363, 1992.
- Leverkusen,O.S., Cologne,W.M. and Leverkusen,B.M. Thermosetting organopolysiloxane mixtures containing platinum catalyst dispersed in solid silicone resin. U.S. Patent 4,481,341, 1984.
- Lim,B.S., Nowick,A.S., Lee,K-W. and Viehbeck,A. Sorption of water and organic soluted in polyimide films and its effects on dielectric properties. *Journal of Polymer Science: Part B: Polymer Physics*, **31**, 545-555, 1993.
- Litchfield,J. and Wood,L.G. Improvements in or relating to synthetic resins. British Patent No. 983,817, 1965.
- Lloyd,C.H., Schimgeoug,S.N., Chudek,J.A., Hunter,G. and Mackay,R.L. Diffusion of miscible liquids in dense polymers studied by Magnetic resonance imaging. *Plastics Rubber and Composites Proceeding and Applications*, **24**, No.4, 181-188, 1995.
- Lundberg,J.L. Molecular clustering and segregation in sorption systems. *Journal of Pure and Applied Chemistry*, **31**, 261-281, 1956.
- Lytle,R.B. The management of abused oral tissues in complete denture construction. *Journal of Prosthetic dentistry*, **7**, 27-42, 1957.
- Ma,J-T., Wu,L., Qi,G-G., Lui,J-H., and Yao,K-D. Radiation crosslinked poly (vinylmethylsiloxane) for levonorgestrel delivery system. *Journal of Polymer Science: Part C: Polymer Letters*, **26**, 195-199, 1988.
- Majerus,M.S., Soong,D.S. and Prausnitz,J.M. Experimental measurements and monte-carlo simulation of water diffusion into epoxy matrices. *Journal of Applied Polymer Science*, **29**, 2453-2466, 1984.
- Malek,K.A.B. and Stevenson,A. The effect of 42 year immersion in sea water on natural rubber. *Journal of Materials Science*, **21**, 147-154, 1986.
- May,P.D., Farris,C.L. and Gettleman,L. New elastomers for soft denture liners. *Journal of Dental Research*, **60**, 437, 1981.

- Mazan,J., Leclerc,B., Porte,H. Torres,G. and Couarraze,G. Influence of network characteristics on diffusion in silicone elastomer. *Journal of Materials Science: Materials in Medicine*, **4**, 175-178, 1993.
- McKinstry,R.E. Microwave processing of permanent soft denture liners. *The Compendium of Continuing Education in Dentistry*, **XII**, 32-37, 1991.
- Migliaresi,C., Nicodemo,L., Nicolais,L. and Passerini,P. Water sorption and desorption in 2-hydroxyethyl methacrylate/methyl methacrylate copolymers. *Polymer*, **25**, 686-689, 1984.
- Miller,J.D. and Ishida,H. Quantitative monomolecular coverage of inorganic particles by methacryl-functional silanes. *Surface Science*, **148**, 601-622, 1984.
- Mirza,M.A. Analysis of water sorption and fluoride release of some poly(ethyl methacrylate) based polymers. Project for Diploma in Industrial Studies, Eastman Dental Institute, University of London, 1995.
- Modic,F.J. Platinum Catalyst compositions for hydrosilylation reactions. U.S. Patent 3,516,946, 1970.
- Monthéard,J-P., Vergnaud,J-M. and Chafi,N. Polymeric drugs carriers of methacrylic and acrylic derivatives. *Polymer Bulletin*, **20**, 177-182, 1988.
- Muniandy,K. and Thomas,A.G. Water absorption in rubbers. *Transactions of the Institute of Marine Engineers*, **97**, *Polymers in Marine Environments*, London, Conference 2, Paper 13, 87-94, 1984,a.
- Muniandy,K. and Thomas,A.G. Water absorption in vulcanised rubber. *International Rubber Conference*, Moscow, No. 1052, 1984,b.
- Muniandy,K. and Thomas,A.G. The role of hydrophilic materials in the transport of water in rubbers. *Proceedings International Rubber Technology Conference*, No 1289, 129-146, 1988.
- Nakamura,K., Hatakeyama,T. and Hatakeyama, H. Studies on bound water of cellulose by differential scanning calorimetry. *Textile Research Journal*, **51**, No.9, 607-613, 1981
- Nakamura,K., Hatakeyama,T. and Hatakeyama,H. Relationship between hydrogen bonding and bound water in polyhydroxystyrene derivatives. *Polymer*, **24**, 871-876, 1983.
- Neogi,P. A hole filling theory of anomalous diffusion in glassy polymers. Effect of microvoids. *Journal of Polymer Science: Part B: Polymer Physics*, **31**, 699-710, 1993.
- Nicholson,J.W. *The chemistry of polymers*. Royal Society of Chemistry, 1991.

Nielsen,P.H. and Valladensen,J. An analysis of the multiplicity pattern of models for simultaneous diffusion chemical reaction. *Chemical Engineering Science*, **40**, No.4, 571-587, 1985.

Nishiyama,M. and Kato,T. Properties of LTV vinyl silicone rubber-based resilient denture base liner and directions for use. *Journal of Nihon University School of Dentistry*, **29**, 100-111, 1987.

Noda,I. Plastics and rubber with water-wettable surfaces. *Chemistry and Industry*, October, 749-752, 1991.

Okel,T.A. and Waddell,W.H. Effect of precipitated silica physical properties on silicone rubber performance. *Rubber Chemistry and Technology*, **68**, 59-68, 1995.

Olge,R.E., Sorensen,S.E. and Lewis,E.A. A new visible light curing system applied to removable prosthodontics. *Journal of Prosthetic Dentistry*, **56**, 497-506, 1986.

OSi. Products for use in formulating dental impression compounds. Union Carbide, August, 1991.

Pace,R.J. and Datyner,A. Model of sorption of simple molecules in polymers. *Journal Polymer Science: Part B: Polymer Physics*, **18**, 1103-1124, 1980.

Park,G.S. The diffusion of some halo-methanes in polystyrene. *Transactions of the Faraday Society*, **46**, 684-697, 1950.

Parker,H.M. Impact reduction in complete and partial dentures. A pilot study. *Journal of Prosthetic Dentistry*, **32**, 477-491, 1966.

Parker,S. The development and evaluation of new elastomeric prosthetic materials. *Phd thesis*, University of London, 1982.

Parker,S. and Braden,M. New soft lining materials. *Journal of Dentistry*, **10**, 149-153, 1982.

Parker,S. and Braden,M. Water absorption of methacrylate soft lining materials. *Biomaterials*, **10**, 91-95, 1989.

Parker,S and Braden,M. Soft prosthetic materials based on powdered elastomers. *Biomaterials*, **11**, 482-490, 1990.

Parker,S. New soft prosthesis materials based on a butadiene/styrene co-polymer. *Journal of Dental Research*, **72 (Special Issue)**, 199, Abstract #761, 1993.

Parker,S. An experimental silicone soft lining material. *Journal of Dental Research*, **73 (Special Issue)**, 275, Abstract #1384, 1994.

- Parker,S., Riggs,P.D., Kalachandra,S., Braden.M. and Taylor,D.F. Water uptake of soft lining materials from osmotic solutions. *Journal of Dental Research*, **74** (Special Issue), 585, Abstract #1474, 1995.
- Parker,S., Riggs,P.D., Kalachandra,S., Braden.M. and Taylor,D.F. Water uptake of soft lining materials from osmotic solutions. *Journal of Dentistry*, In Press, 1997.
- Parker,S. Private communication. 1996.
- Passiniemi,P. General theory for determination of diffusion coefficient of solvents and gases in polymers. *Polymer*, **36**, 341-344, 1995.
- Patel,M.P. A physico-chemical study of hetrocyclic methacrylate polymer systems for dental and other clinical uses. Phd thesis, University of London, 1987.
- Patel,M.P. and Braden,M. Hetrocyclic methacrylates for clinical applications. III water absorption characteristics. *Biomaterials*, **12**, 653-657, 1993.
- Patel,M.P., Braden,M. and Downs,S. Hetrocyclic methacrylate-based drug release polymer system. *Journal of Material Science: Materials in Medicine*, **5**, 338-339, 1994.
- Peppas,N.A., Wu,J.C. and von Meerwall,E.D. Mathematical modelling and experimental characterisation of polymer dissolution. *Macromolecules*, **27**, 5626-5638, 1994.
- Perry,K.L., McDonald,P.J., Randall,E.W. and Zick,K. Stray filed magnetic resonance imaging of diffusion of acetone into poly(vinyl chloride). *Polymer*, **35**, No.13, 2744-2748, 1994.
- Petersen,S.B., Muller,R.N. and Rinck,P.A. An introduction to biomedical nuclear magnetic resonance. Thieme Inc., Stuttgart, 1985.
- Petrak,K. Polymers for use in drug delivery - property and structure requirements. *British Polymer Journal*, **22**, 213-219, 1990.
- Pfister,W.R., Sweet,R.P. and Walters,P.A. Silicone based sustained and controlled release drug delivery. 30 th National SAMPE Symposium, March 19-21, 1985.
- Polyzois,G.L. Adhesion properties of resilient lining materials bonded to light-cured denture resins. *Journal of Prosthetic Dentistry*, **68**, No.8, 854-858. 1992.
- Polyzois,G.L., Hensten-Pettersen,A. and Kullmann,A. An assessment of the physical properties and biocompatibility of three silicone elastomers. *Journal of Prosthetic Dentistry*. **71**, 500-504, 1994.
- Polyzois,G.L., Hensten-Pettersen,A. and Kullmann,A. Effects of RTC-silicone maxillofacial prosthetic elastomers on cell cultures. *Journal of Prosthetic Dentistry*. **71**, 505-510, 1994

- Quadah,S. Harrison,A. and Huggett,R. Soft lining materials in prosthetic dentistry: a review. *International Journal of Prosthodontics*, **3**, 477-483, 1990.
- Quadah,S., Huggett,R. and Harrison,A. The effects of thermocycling on the hardness of soft lining materials. *Quintessence International*, **22**, No.7, 575-580, 1991.
- Quinn,K.J. and Courtney,J.M, Silicones as biomaterials. *British Polymer Journal*, **20**, 25-32, 1988.
- Rathna,G.V.N., Mohan Rao,D.V. and Chatterji,P.R. Water-induced plasticization of solution cross-linked hydrogel networks: Energetics and mechanism. *Macromolecules*, **27**, 7920-7922, 1994.
- Rawls,H.R. Preventive dental materials: sustained delivery of fluoride and other therapeutic agents. *Advances in Dental Research*, **5**, 50-55, 1991.
- Rees,T.D. Local and systematic response to injectable silicone fluid. In Rubin,L,R. (Ed.), *Biomaterials in reconstructive Surgery*, St. Louis: C.V. Mosby Co., 529, 1983.
- Robinson,R.A and Stokes,R.H. *Electrolytic solutions*. Second Edition, Butterworths Scientific Publications, London, 1959.
- Robinson,J.G. and McCabe,J.F. Creep and stress relaxation of soft denture liners. *Journal of Prosthetic Dentistry*, **48**, No.2, 135-141, 1982.
- Rochow,E.G., *Silicon and Silicones*. Spriner-Verlag, 107-117, 1987.
- Roskos,K. V., Tefft,J.A. and Heller,J. A morphine-triggered delivery system useful in the treatment of heroin addiction. *Clinical materials*, **13**, 109-119, 1993.
- Rothwell,W.P. Holecek,D.R. and Kershaw,J. NMR imaging: study of fluid absorption by polymer composites. *Journal of Polymer Science: Part C: Polymer Letters Edition*, **22**, 241-247, 1984.
- Rowland,S.R. *Water in polymers*, American Chemical Society Symposium Series, American Chemical Society, Washington, 1980.
- Ryan,J.E. Twenty-five years of clinical application of a heat cured silicone rubber. *Journal of Prosthetic Dentistry*. **65**, No5, 658-661, 1991.
- Saber-Sheik.K. Private Communication, 1996.
- Sagripani,J-L, and Hughes-Dillon,K. Stability of five plastics used in medical devices to oxidation produced by copper or iron ions and reducing agents. *Polymer Degradation and Stability*, **46**, 241-246, 1994.
- Sancaktar,E. and Baechtle,D.R. The effect of stress whitening on moisture diffusion in thermosetting polymers. *Journal of Adhesion*, **42**, 65-85, 1993.

- Schneider, N.S., Dusablon, L.V., Spano, L.A. and Hopfenberg, H.B. Sorption and diffusion of water in a rubbery polyurethane. *Journal of Applied Polymer Science*, **12**, 527-532, 1968.
- Schirrer, R., Thepin, P. and Torres, G. Water absorption, swelling, rupture and salt release in salt-silicone rubber compounds. *Journal of Material Science*, **27**, 3424-3434, 1992.
- Schlak, O. Thermosetting organopolysiloxane mixtures containing platinum catalyst dispersed in solid silicone resin. U.S. Patent 4,481,341, 1984.
- Schwendeman, S.P., Amidon, G.L., Meyeyhoff, M.E. and Levy, R.J. Modulated drug release using iontophoresis through heterogeneous cation-exchange membrane preparation and influence of resin crosslinkage. *Macromolecules*, **25**, 2531-2540, 1992.
- Shellis, R.P. A synthetic saliva for cultural studies of dental plaque. *Archives of Oral Biology*, **23**, 485-489, 1978.
- Sheppard, N.F., Madrid, M.Y. and Langer, R. Polymer matrix controlled release systems: influence of polymer carrier and temperature on water uptake and protein release. *Journal of Applied Polymer Science*, **46**, 19-26, 1992.
- Shimizu, K. and Sakuma, A. Thermosetting organosiloxane composition, U.S. Patent 5,064,924, 1991.
- Shingledecker, R. Custom mixing of silicone rubber. *Rubber world*, February, 27-30, 1991.
- Simpson, V.G. Elastomeric organopolysiloxane compositions containing unsaturated alkoxy silanes. U.S. Patent No. 3 341 489, 1967.
- Small, P.A. Factors affecting the solubility of polymers. *Journal of Applied Polymer Chemistry*, **3**, 71-80, 1953.
- Smith, P.M. and Fisher, M.M. Non-Fickian diffusion of water in melamine formaldehyde resins. *Polymer*, **25**, 84-90, 1984.
- Söderholm, K.J.M. Water sorption in a bis(GMA)/TEGMA resin. *Journal of Biomedical Materials Research*, **18**, 271-279, 1984.
- Söderholm, K.J.M., Mukherjee, R. and Longmate, J. Filler leachability of composites stored in distilled water or artificial saliva. *Journal of Dental Research*, **74**(Special Issue), 90, Abstract #628, 1995.
- Söderholm, K.J.M. and Shang, S.W. Molecular orientation of silane at surface of colloidal silica. *Journal of Dental Research*, **72**, 1050-1054, 1993.
- Simmons, C.L. Effect of the additives in domestic water systems on rubber vulcanizates, *Rubber World*, **199**, 16-24, 1988.

- Sinobad,D., Murphy,W.M., Huggett,R. and Brooks,S. Bond strength and rupture properties of some soft denture liners. *Journal of Oral Rehabilitation*, **19**, 151-160, 1992.
- Southern,E. and Thomas,A.G. Diffusion of liquids in crosslinked rubbers: Part 1. *Transactions of the Faraday Society*, No. 536, **63**, Part 8, August, 1913-1921, 1967.
- Southern,E. and Thomas,A.G. Diffusion of water in rubbers. *ACS Symposium Series*, No.127, *Water in Polymers*, 375-386, 1980
- Stein,J. and Prutzman,L.C. Stress relaxation studies of model silicone RTV networks. *Journal of Applied Polymer Science*, **36**, 511-521, 1988.
- Stein,J. and Leonard,T.M. Stress relaxation studies of a model for unfilled anionically stabilised curable silicone latexes. *Polymer Degradation and Stability*, **28**, 311-322,1990.
- Stein,J. Private communication, 1994.
- Sreenivasan,K. Diffusion of water and alcohol in chemically modified polyurthethane, *Polymer International*, **30**, 363-365, 1993.
- Suchatlampong,C. and Davies,E.H. Some physical properties of four resilient lining materials. *Journal of Dentistry*, **4**, No.1, 19-27, 1975.
- Sung,Y.K., Gregonis,D.E., John,M.S. and Andrade,J.D. Thermal and pulse NMR analysis of water in Poly(2-hydroxyethyl methacrylate). *Journal of Applied Polymer Science*, **26**, No.11, 3719-3728, 1981.
- Swanson,A.B. Silicone rubber implants for replacement of arthritic or destroyed joints in the hand. *Surgical Clinics of North America*, **48**, 1113, 1968.
- Swanson,A.B., Boeve,W.R. and Lumsden,P.M. The prevention and treatment of amputation neuromata by silicone capping. *Journal of Hand Surgery*, **2**, 70, 1977.
- Takigami,S., Kimura,T. and Nakamura,Y. The state of water in nylon-6 membranes grafted with hydrophilic monomers: 2. Water in acrylic acid, acrylamide and *p*-styrenesulphonic acid grafted nylon-6 membranes. *Polymer*, **34**, No.3, 604-609, 1993.
- Tamai,Y., Tanaka,H. and Nakanishi,K. Molecular simulation of permeation of small penetrants through membranes. 1. Diffusion coefficients. *Macromolecules*, **27**,4498-4508, 1994.
- Teeter,M.M. The water structure surrounding proteins, Ed. Gierasch,L.M. and King,J. *Protein folding*. American Association for the advancement of Science, Washington, DC, 43-56, 1989.
- Thomas,A.G. and Muniandy,K. Absorption and desorption of water in rubbers. *Polymer*, **28**, 408-415, 1987.

- Thomas,N.L. and Windle,A.H. A Theory of Case II diffusion. *Polymer*, **23**, 529-542, 1982.
- Tillekeratne,L.M.K., Perera,M.C.S. and Rodrigo,H.V. Effect of fresh water and sea water on different grades of crepe rubber. *Plastics Rubber Processing and Applications*, **8**, 245-251, 1987.
- Todd,R. and Holt,J.A. Kennedy Class I removable partial denture with a resilient liner. *Journal of Prosthetic Dentistry*, **57**, 247-249, 1987.
- Tóth,A., Bertóti,I., Blazsó,G., Bánhegyi,G., Bogнар,A. and Szaplónczay,P. Oxidative damage and recovery of silicone rubber surfaces. I. X-ray photoelectron spectroscopic study. *Journal of Applied Polymer Science*, **52**, 1293-1307, 1994.
- Travaglini,E.A., Gibbons,P. and Craig,R.G. Resilient liners for dentures. *Journal of Prosthetic Dentistry*, **10**, 664-672, 1960.
- Turner,D.T. Water sorption of poly(methyl methacrylate): 1. Effect of molecular weight. *Polymer*, **28**, 293-296, 1987.
- Turner,D.T. and Abell,A.K. Water sorption of poly(methyl methacrylate): 2. Effect of crosslinks. *Polymer*, **28**, 297-302, 1987.
- Uchytíl,P., Nguyen,Q.T., Clément,R., Grosse,J.M. and Essamri,A. Diffusion of acetic acid and water through poly(vinylalcohol) membranes. Coupling effects. *Polymer*, **37**, 93-100, 1996.
- Uragami,T. and Morikawa,T. Permeation and separation characteristics of alcohol-water mixtures through poly(dimethyl siloxane) membrane by pervaporation and evapermeation. *Journal of Applied Polymer Science*, **44**, 2009-2018, 1992.
- Valles,E.M. and Macosko,C.W. Properties of network formed by end linking of poly(dimethylsiloxane). *Macromolecules*, **12**, 673-679, 1979.
- Van Krevelen, D.W. *Properties of polymers, their estimation and correlation with chemical structure*. 2nd Edition, Elsevier Scientific Publication Co., 1976.
- Van Handel,A.B. Lining for artificial dentures. US Patent 3,785,054, 1974.
- Vassilakos,N., Fernandes,C.P. and Nilner,K. Effect of plasma treatment on the wettability of elastomeric impression material. *Journal of Prosthetic Dentistry*, **70**, 165-171, 1993.
- Venz,S. and Dickens,B. NIR-spectroscopic investigation of water sorption characteristics of dental resins and composites. *Journal of Biomedical Materials Research*, **25**, 1231-1248, 1991.

- Vieth,W.R. and Sladek,K.J. A model for diffusion in a glassy polymer. *Journal of Colloid Science*, **20**, 1014-1033, 1965.
- Vieth,W.R., Frangoulis,C.S. and Rionda,J.A. Kinetics of sorption of methane in glassy polystyrene. *Journal of Colloid and Interface Science*, **22**, 451-461, 1966.
- Vokál,A., Kourím,P., Süßmilchova,J., Heidingsfeldova,M. and Kopecky,B. Comparison of thermal and radiation curing on silicone rubber. *Radiation Physics and Chemistry*, **28**, No5/6, 497-499, 1986.
- Von Fraunhofer,J.A., Coffelt,M-T.P. and Orbell,G.M. The effect of artificial saliva and topical fluoride treatments on the degradation of the elastic properties of orthodontic chains. *The Angle Orthodontist*, **62**, No.4, 265-273, 1992.
- Vondráček,P. and Gent,A.N. Slow decomposition of silicone rubber, *Journal of Applied Polymer Science*, **27**, 4517-4523, 1982.
- Wang,M-J., and Wolff,S. Filler elastomer interactions. Part V. Investigation of the surface energies of silane-modified silicas. *Rubber Chemistry and Technology*, **65**, 715-735, 1992.
- Warrick,E.L., Pierce,O.R., Polmanteer,K.E. and Saam,J.C. Silicone elastomer developments 1967-1977, *Rubber Chemistry and Technology*, **52**, 437-525, 1979.
- Watson,J.M. and Baron,M.G. The behaviour of water in poly (dimethyl siloxane). *Journal of Membrane Science*, **110**, 47-57, 1996.
- Weisenberger,L.A. and Koenig,J.L. NMR imaging of case II diffusion in glassy polymers. *Journal of Polymer Science: Part C: Polymer Letters Edition*, **27** 55-57, 1989.
- Weisenberger,L.A. and Koenig,J.L. NMR imaging of diffusion process in polymer: measurement of spatial dependence of solvent mobility in partially swollen PMMA rods. *Macromolecules*, **23**, 2445-2453, 1990,a.
- Weisenberger,L.A. and Koenig,J.L. NMR imaging study of methanol desorption from partially swollen PMMA rods. *Macromolecules*, **23**, 2454-2459, 1990,b.
- Wendt,D.C. The degenerative denture ridge. Care, treatment. *Journal of Prosthetic Dentistry*, **32**, 477-491, 1974.
- Whitsitt,J.A., Battle,L.W. and Jarosz,C.J. Enhanced retention for the distal extension - base removable partial denture using a heat - cured resilient soft liner. *Journal of Prosthetic Dentistry*, **52**, 447-448, 1984.
- Williams,J.E. Experience with a large series of silastic breast implants. *Journal of Plastic Reconstructive Surgery*, **26**, 264, 1972.

- Williamson, J.J. The effect of denture lining materials on the growth of candida albicans. *British Dental Journal*, **6**, 106-110, 1968.
- Wilson, H.J. and Thomlin, H.R. Soft lining materials: Some relevant properties and their determination. *Journal Prosthetic Dentistry*, **21**, No.3, 244-251, 1969.
- Wilson, S.J. and Wilson, H.J. The release of chlorhexidene from modified dental acrylic resin. *Journal of Oral Rehabilitation*, **20**, 311-319, 1993.
- Woelfel, J.B. and Paffenbarger, G.C. Evaluation of complete dentures lined with resilient silicone rubber. *Journal of the American Dental Association*, **76**, 582-590, 1968.
- Wong, T.C. and Broutman, L.J. Effect of stress on sorption of water in a epoxy resin. ANTEC'85, Society of the Plastic Engineering, 723-727, 1985.
- Wong, T.C. and Broutman, L.J. Moisture in Epoxy resins part I. Non Fickian sorption processes. *Polymer Engineering and Science*, **25**, 521-528, 1985,a.
- Wong, T.C. and Broutman, L.J. Moisture in Epoxy resins part II. Diffusion mechanism. *Polymer Engineering and Science*, **25**, 529-534, 1985,b.
- Wong, T.C. and Broutman, L.J. Effect of stress on sorption of water in a epoxy resin. ANTEC'85, Society of the Plastic Engineering, 723-727, 1985,c.
- Wright, P.S. Soft lining materials: their status and prospects. *Journal of Dentistry*, **4**, 247-256, 1976.
- Wright, P.S. Characterisation of the rupture properties of dental soft lining materials. *Journal of Dental Research*, **59**, 614-624, 1980.
- Wright, P.S. Composition and properties of soft lining materials for acrylic dentures. *Journal of Dentistry*, **9**, 210-223, 1981.
- Wright, P.S. Characterisation of the adhesion of soft lining materials to Poly (methyl methacrylate). *Journal of Dental Research*, **61**, 1002-1005, 1982.
- Wright, P.S. Observations on long-term use of soft-lining material for mandubular complete dentures. *Journal of Prosthetic Dentistry*, **72**, No.4, 385-392, 1994.
- Wright, P.S. Personal communication, 1995.
- Wu, J.C. and Peppas, N.A. Modelling of penetrant diffusion in glassy polymers with integral sorption Deborah number. *Journal of Polymer Science: Part B: Polymer Physics*, **31**, 1503-1518, 1993.
- Yasuda, H. and Stannett, V. Permeation, sorption and diffusion of water into some high polymers. *Journal of Polymer Science*, **57**, 907-923, 1962.

- Yoshida,R., Sakai,K., Okano,T. and Sakurai,Y. A new model for zero-order drug release I. Hydrophobic drug release from hydrophilic matrixes. *Polymer Journal*, **23**, 1111-1121, 1991.
- Yu-Fu,L., Yong-Xia,X. Dong-Peng,X. and Guang-Liang,L. Surface Reaction of particulate silica with poly dimethylsiloxanes. *Journal of Polymer Science: Part A: Polymer Chemistry*, **19**, 3069-3079, 1981.
- Yuan,Q. and Li,G. Vulcanisation kinetics of silicone rubber. *Chinese Journal of Polymer Science*, **6**, 353-358, 1988.
- Yuzhelevskii,Y.U. Elastic siloxane materials for endorosthetic applications. *Artificial Organs*, **15**, 392-396, 1991.
- Zieminski,K.F. and Peppas,N.A. Diluent diffusion in polymer-diluents systems near: T_g: migration of phthalic esters from PVC to water. *Journal of Applied Polymer Science*, **28**, 1751-1765, 1983.
- Zimm,B.H. and Lundberg,J.L. Sorption of vapours by high polymers. *Journal of Physical Chemistry*, **60**, 425-428, 1956.

Appendices.

I. The formulation of Molloplast B.

Molloplast B is probably one of the most successful of the commercially available soft lining materials. Some authors (Parker and Braden, 1982, Braden et al, 1995) have cited US Patent 3,785,054 (Van Handel, 1974) as relating to Molloplast B. This patent describes a silicone based soft lining material made by blending 2.5% PMMA with 1.22% gamma-methacryloxypropyltrimethoxysilane (Silane A174) and 0.01% titanium dioxide blended to gum colour with Washung Red. Then mixing with 96.2% silicone rubber RTV 108.

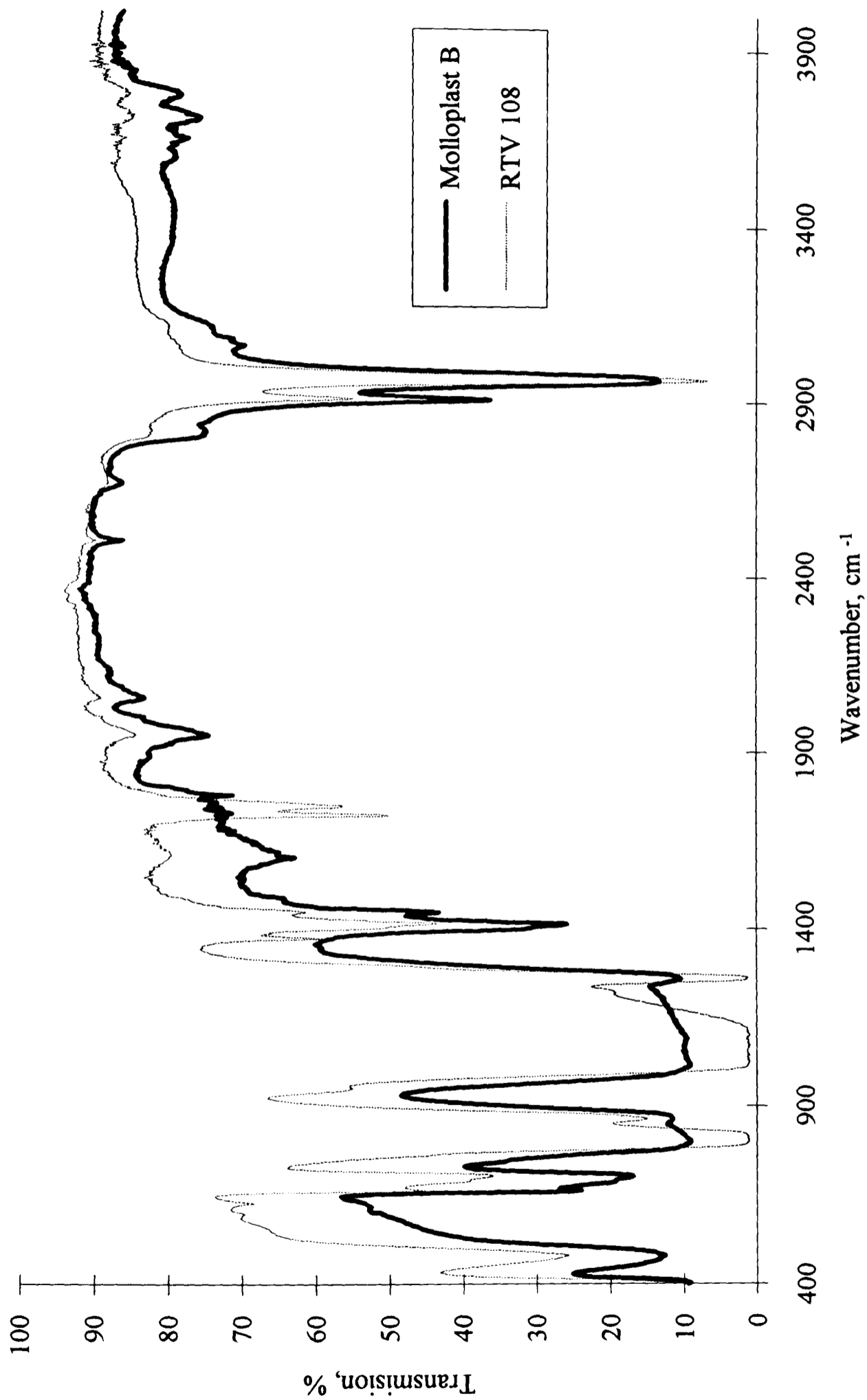
RTV 108 is produced by G.E. Silicones as a room temperature vulcanising paste which will cure on exposure to water vapour. Although the composition of RTV 108 remains unclear a guide to its composition may be gained from U.S. Patent 3,382,205 (Beers, 1968). The patent describes a organopolysiloxane which is chemically combined with an diorganosiloxy ($(R)_2SiO$) and then combined with a curing agent $(RSi(OCOR')_3)$. The patent also describes a 'processing aid' composed of the organopolysiloxane chemically combined with a organosiloxy ($RSiO_{1.5}$) and triorganosiloxy ($(R)_3SiO_{0.5}$). Exactly what the R and R' groups are is unclear but some of them at least should be acetoxy-Si-groups. These acetoxy-Si-groups react with moisture and crosslink with the curing agent (an organo tin).

Parker (1994) conducted a series of studies on the properties of RTV 108 and RTV 106 (also produced by GE Silicones and covered by US Patent 3,382,205) and Molloplast B and found them to be very similar in terms of adhesion, tensile strength and water absorption. Indeed RTV 108 and RTV 106 are quite attractive as potential soft lining materials in their own right.

A problem with US Patent 3,785,054 is that it does not produce a room temperature stable material indeed following the examples in the patent produce an RTV acetoxy cure material basically the same as RTV 108. This contradicts Molloplast B which is a stable when exposed to moisture and requires heating for polymerisation.

Infra Red studies of Molloplast B and RTV 108 (Figure I.1) have revealed them to have very similar spectra with only one major difference. The RTV 108 has a peak at 1720 wave numbers, which attributed to a carboxylic acid group and which is absent in the Molloplast B. These carboxylic acid groups are part of the acetoxy curing mechanism indicating they must have been substituted during manufacture at some stage that is not

Figure I.1. Infra red spectrum of Molloplast B and RTV 108.



described in the patent. Indeed the removal of these groups would be necessary in order for the paste to be stable.

In the processing of RTV 108 into Molloplast B there must be a reaction in order for the paste to be stable. This reaction has been suggested by Wacker-Chemie GmbH to be an exchange reaction between the acetoxy-Si-groups and methoxy-Si-groups on mixing under conditions "free of water vapour". If the methoxy-Si-groups come from the A174 there seems to be insufficient A174 (1.22%) to substitute for these groups, cross link the material and ensure bonding to the denture base.

Molloplast B cures when the material is heated but neither US Patent 3,785,054 or 3,382,205 describe any temperature sensitive initiator. There is a mention of heating for 3 hours at 100°C in water but these would serve to ensure the completion of the acetoxy curing system as previously described. Other authors (Wright, 1981, Parker and Braden, 1982, Quadah et al, 1991, Sinobad et al, 1992, Collis, 1993) describe Molloplast B as an addition silicone which uses benzoyl peroxide as the initiator, this would result in a material which polymerises in the same way a Molloplast B. This peroxide may stem from residual peroxide in the PMMA, although as the PMMA is present at only 2.5 % and is likely to contain less than 2% peroxide it seems unlikely to be sufficient to promote the cure.

A further complication arises from the chronological history of the material, US Patent 3,785,054 came out in 1974 although it was initially filed in 1971 and US Patent 3,382,205 was 1968 and filed in 1963. A problem arises in that Molloplast B is named in what appears to be its current form by Williamson, 1968, Wilson and Thomlin, 1969 and Braden and Clarke, 1972, additionally Ryan 1991 published a paper in which he describes 25 years of using Molloplast B indicating its first use in November 1963. Clearly some developmental work must have been conducted before the filing of the patent, but such publications in 1968, 1969 and 1972 treating Molloplast B as a commercial material indicate discrepancy between the Patent and the material.

There is clearly a discrepancy between the reported composition of the Molloplast B and what the material actually is. The similarities and discrepancies to the material described in the Patent and Molloplast B are apparent. The simplest answer to the problem would be to assume that the processing and formulation described in the patent is inaccurate but papers 5 and 6 years prior to the publication of the patent throw the issue open to debate.

II. Diffusion.

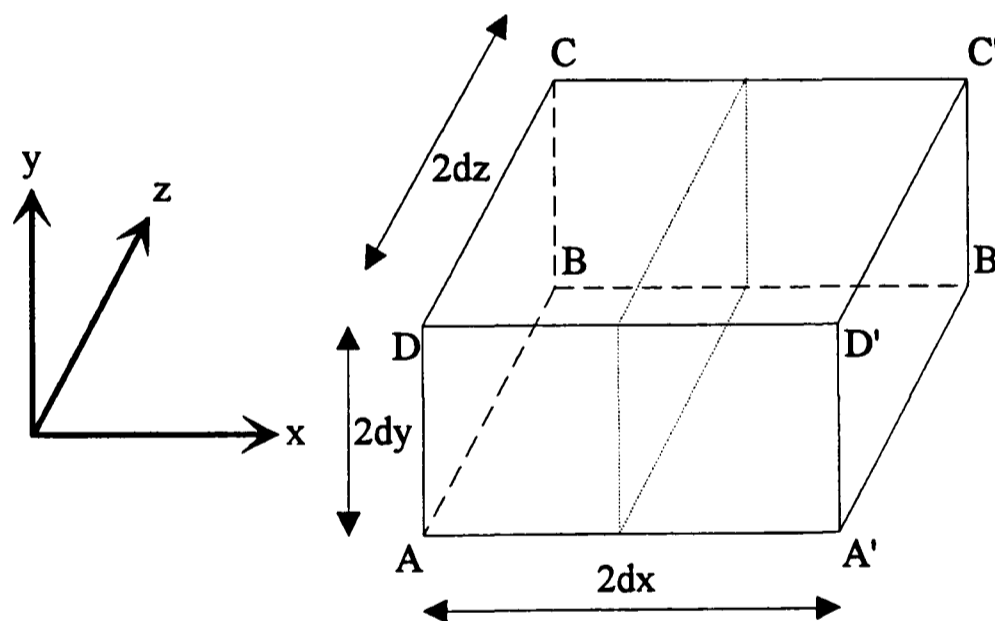
II.a. Fick's laws.

Consider the process of diffusion in an isotropic substance where the rate of diffusion or flux (F) through a section of unit area is proportional to the concentration gradient measured normal to the section (x). This gives rise to Fick's first law (equation II.1) where D is the diffusion coefficient and c is concentration.

$$F = -D \frac{\partial c}{\partial x} \quad \text{Equation II.1.}$$

It should be noted that the diffusion coefficient may be constant (i.e. dilute solutions) or may vary with the concentration (c). The negative sign within the equation is required as the direction of the diffusion is opposite to the direction of increasing concentration.

Figure II.1 Element for diffusion model.



Consider a rectangular element as shown in figure II.1. which has a two parallel faces (ABCD and A'B'C'D') separated by a distance $2 dx$ perpendicular to the x axis. As the rate of transfer of the diffusing species through a plane is F multiplied by the area, the rate of diffusion substance entering the face ABCD is given by,

$$4 dy dz \left(F_x - \frac{\partial F_x}{\partial x} dx \right),$$

where F_x is the flux in the x direction at the central plane. It therefore follows that the rate of transfer of the diffusing species through plane A'B'C'D' is given by,

$$4 \, dy \, dz \left(F_x + \frac{\partial F_x}{\partial x} dx \right).$$

Hence the rate of increase of the diffusing species in the element due to diffusion in the x direction is,

$$- 8 \, dx \, dy \, dz \frac{\partial F_x}{\partial x}.$$

This is also true for the y and z directions therefore the total rate of increase in the diffusing species in the element is,

$$- 8 \, dx \, dy \, dz \left(\frac{\partial F_x}{\partial x} + \frac{\partial F_y}{\partial y} + \frac{\partial F_z}{\partial z} \right).$$

The total rate of increase in the diffusing species is also equal to the increase in concentration with time (t) within the volume of the element, i.e.,

$$- 8 \, dx \, dy \, dz \frac{\partial c}{\partial t},$$

therefore,

$$\frac{\partial c}{\partial t} = - \frac{\partial F_x}{\partial x} + \frac{\partial F_y}{\partial y} + \frac{\partial F_z}{\partial z}. \quad \text{Equation II.2.}$$

Hence by using Fick's first law (Equation II.1.) and assuming D is consistent in all directions (as a isotropic substance) this yields,

$$\frac{\partial c}{\partial t} = \frac{\partial(D \partial c / \partial x)}{\partial x} + \frac{\partial(D \partial c / \partial y)}{\partial y} + \frac{\partial(D \partial c / \partial z)}{\partial z} \quad \text{Equation II.3.}$$

If the diffusion coefficient is constant this becomes,

$$\frac{\partial c}{\partial t} = D \left(\frac{\partial^2 c}{\partial x^2} + \frac{\partial^2 c}{\partial y^2} + \frac{\partial^2 c}{\partial z^2} \right) \quad \text{Equation II.4.}$$

and if the diffusion process is one dimensional (i.e. in the x direction only), this yields Fick's second law,

$$\frac{\partial c}{\partial t} = D \frac{\partial^2 c}{\partial x^2} \quad \text{Equation II.5.}$$

The diffusion coefficient (D) is frequently (particularly for higher polymer systems) dependent on the concentration (c) of the diffusing species (Crank, 1975), and hence also x,y,z and time (t). In order to simplify this for an isotropic substance, dT is defined as,

$$dT = D dt.$$

Hence equation II.2 becomes,

$$\frac{\partial c}{\partial T} = \frac{\partial^2 c}{\partial x^2} + \frac{\partial^2 c}{\partial y^2} + \frac{\partial^2 c}{\partial z^2} \quad \text{Equation II.6,}$$

and if the diffusion is one dimensional,

$$\frac{\partial c}{\partial T} = \frac{\partial^2 c}{\partial x^2} \quad \text{Equation II.7.}$$

II.b Solutions to Fick's second law.

In general, and particularly for the theories of diffusion into polymers, the diffusion coefficient is assumed constant with concentration of diffusing species. Whilst this is a significant assumption, and frequently not the case, it simplifies the problem to a solvable form. Fick's second law (equation II.5.) may be solved in a few ways but the most of useful (as it can yield both of the normally used solutions) employs Laplace transforms in an operator method, (where the restraints for each particular experimental geometry and system become built into the equation). Essentially a Laplace transform is applied to each side hence,

$$\int_0^{\infty} e^{-pt} \frac{\partial c}{\partial t} dt = D \int_0^{\infty} e^{-pt} \frac{\partial^2 c}{\partial x^2} dt \quad \text{Equation II.8.}$$

as the D is a constant. Here the left side integrates to,

$$c_{t=0} + p \int_0^{\infty} e^{-pt} c dt \quad \text{or} \quad c_{t=0} + pv \quad \text{Equation II.9.}$$

if we take c initially when $t = 0$ ($c_{t=0}$) to be zero this becomes pv (where v is the Laplace transform of pc with respect to c). The right of side of Equation II.8. is re written as,

$$D \frac{\partial^2}{\partial x^2} \int_0^{\infty} e^{-pt} c dt \quad \text{or} \quad D \frac{\partial^2 v}{\partial x^2}$$

as x is a dimension and so independent of time. Hence substituting back into Equation II.8. we get,

$$\frac{\partial^2 v}{\partial x^2} = \frac{p}{D} v \quad \text{Equation II.10.}$$

which if we let,

$$q = \sqrt{\frac{p}{D}} \quad \text{is} \quad \frac{\partial^2 v}{\partial x^2} = q^2 v \quad \text{Equation II.11.}$$

which is a standard differential of,

$$v = Ae^{qx} + Be^{-qx} \quad \text{Equation II.12.}$$

and,

$$v = L \cosh qx + M \sinh qx \quad \text{Equation II.13.}$$

where A,B,L and M are constants. Both of these solutions are used to derive useful diffusion equations which one is used depends on which case the resultant equation applies to.

Consider a semi infinite medium where the sample is in treated as a block of material with a fluid ingress into one face (in the x direction) only and is not impaired during the process (i.e. does not reach the other side of the block). Here we assume the concentration c to be c_0 at the surface ($x = 0$) and the concentration tends to a finite value as x tends to ∞ . Using equation II.12, we can see that as x tends to ∞ the term e^{qx} will also tend to ∞ hence to avoid this A has to equal 0, hence,

$$v = Be^{-qx} \quad \text{Equation II.14.}$$

Now consider when $x = 0$ and $c = c_0$, here the concentration is independent of time

$$\text{hence from equation II.9, where } v = \int_0^{\infty} e^{-pt} c dt \text{ becomes } v = c_0 \int_0^{\infty} e^{-pt} dt \text{ so } v = \frac{c_0}{p} .$$

Therefore,

$$v = c_0 \frac{e^{-\sqrt{\frac{p}{D}}x}}{p} \quad \text{Equation II.15.}$$

Which is the Laplace transform of the function,

$$c = c_0 \operatorname{erfc} \frac{x}{2\sqrt{Dt}} \quad \text{Equation II.16.}$$

In order to get equation II.16, in terms of mass uptake (M_t at time, t) from a solution we must integrate it with respect to x, and multiply by the area (A) of the sheet perpendicular to the direction of the diffusion.

$$M_t = Ac_0 \int_0^{\infty} \operatorname{erfc} \frac{x}{2\sqrt{Dt}} dx \quad \text{Equation II.17.}$$

This is integrated in parts by letting the $u = \text{erfc}$ function and $dv/dx = 1$ hence $v = x$. As

$\text{erfc } f(x) = 1 - \text{erf } f(x)$ and $\text{erf } nx = n \frac{2}{\sqrt{\pi}} \int_0^x e^{-(nx)^2} dx$, u may be written as,

$$u = 1 - \text{erf} \frac{x}{2\sqrt{Dt}} = 1 - \frac{2}{\sqrt{\pi}} \frac{1}{2\sqrt{Dt}} \int_0^x e^{\frac{-x^2}{4Dt}} dx \quad \text{Equation II.18.}$$

hence,

$$\frac{du}{dx} = \frac{-1}{\sqrt{\pi Dt}} e^{\frac{-x^2}{4Dt}} \quad \text{Equation II.19.}$$

therefore,

$$M_t = Ac_o \left\{ \left[\text{erfc} \left(\frac{x}{2\sqrt{dt}} \right) x \right]_0^\infty - \frac{1}{\sqrt{\pi Dt}} \int_0^\infty x \cdot e^{\frac{-x^2}{4Dt}} dx \right\} \quad \text{Equation II.20.}$$

the first term is zero when x is either zero or infinity hence,

$$M_t = Ac_o \frac{1}{\sqrt{\pi Dt}} \int_0^\infty x \cdot e^{\frac{-x^2}{4Dt}} dx \quad \text{Equation II.21.}$$

the remaining integral is solved by substituting $u = \frac{-x^2}{4Dt}$ hence $\frac{du}{dx} = \frac{-x}{2Dt}$ so M_t may be expressed as

$$M_t = Ac_o \frac{1}{\sqrt{\pi Dt}} \int_0^\infty \frac{-2Dt}{x} x \cdot e^u du = -Ac_o 2 \sqrt{\frac{Dt}{\pi}} \left[e^{\frac{-x^2}{4Dt}} \right]_0^\infty \quad \text{Equation II.22.}$$

Therefore,

$$M_t = Ac_o 2 \sqrt{\frac{Dt}{\pi}} \quad \text{Equation II.23,}$$

which predicts the mass uptake of a media with time based on the saturated surface concentration (c_o). If we then define l as the thickness of the material we can express the equilibrium uptake as $M_\infty = c_o \cdot A \cdot l$, hence,

$$\frac{M_t}{M_\infty} = 2 \sqrt{\frac{Dt}{\pi l^2}} \quad \text{Equation II.24.}$$

Consider a plane sheet, here the diffusing species moves into the material through the opposing surfaces, the edge contributions are assumed insignificant. Taking the centre of

the sheet as $x = 0$ so l is the distance from $x = 0$ to the surface (hence $2l$ is the sheet thickness). With the concentration at the surface (i.e. $x = \pm l$) the concentration (c) is equal to the saturated surface concentration (c_0). Using equation II.13,

$$v = L \cosh qx + M \sinh qx \quad \text{Equation II.13.}$$

The initial stage is to determine L , and M using the limits at the surface where $c = c_0$ hence applying a Laplace transform we get,

$$v = \frac{c_0}{P} \quad \text{when } x = \pm l \text{ and } c = c_0 \quad \text{Equation II.25.}$$

Therefore applying the limits to equation II.13, we get.

$$x = +l, \quad \frac{c_0}{P} = L \cosh ql + M \sinh ql \quad \text{Equation II.26.}$$

and,

$$x = -l, \quad \frac{c_0}{P} = L \cosh ql - M \sinh ql \quad \text{Equation II.27.}$$

Therefore subtracting equation II.26, from II.27,

$$0 = 0 - 2M \sinh ql \quad \therefore \quad M = 0 \quad \text{Equation II.28.}$$

And adding equation II.26, to II.27,

$$\frac{2c_0}{P} = 2L \cosh ql \quad \therefore \quad L = \frac{c_0}{P \cosh ql} \quad \text{Equation II.29.}$$

Therefore applying these into equation II.13, we get,

$$v = \frac{c_0 \cosh qx}{P \cosh ql} \quad \text{Equation II.30.}$$

From inversion theorem we have,

$$\text{if } v_{(p)} = \frac{f_{(p)}}{\Phi_{(p)}} \text{ then } f_{(t)} = \sum \frac{f_{(\alpha)}}{\Phi'_{(\alpha)}} \cdot e^{p\alpha} \quad \text{Equation II.31.}$$

where α denotes the value of p when $\Phi_{(\alpha)}$ is equal to zero and $\Phi'_{(\alpha)}$ is the differential of $\Phi_{(\alpha)}$. Hence $f_{(p)} = c_0 \cosh qx$ and $\Phi_{(p)} = P \cosh ql$. The first step is to determine P , when $\Phi_{(p)} = 0$ either $P = 0$ or $\cosh ql = 0$.

For $\cosh ql = 0$, $ql = \frac{(2n+1)\pi i}{2}$ (as $\cosh iz = \cos z$), hence using $q = \sqrt{\frac{P}{D}}$ (from equation II.11) we have,

$$q = \frac{(2n+1)\pi i}{2l} \quad \text{or} \quad P = -\frac{(2n+1)^2 \pi^2 D}{4l^2} \quad \text{Equation II.32.}$$

Using, $\Phi_{(\alpha)} = P \cosh \sqrt{\frac{P}{D}} l$ we get $\Phi'_{(\alpha)} = \cosh \sqrt{\frac{P}{D}} l + \frac{Pl}{\sqrt{D}} \frac{1}{2} \frac{1}{\sqrt{P}} \sinh \sqrt{\frac{P}{D}} l$ or,

$$\Phi'_{(\alpha)} = \cosh ql + \frac{1}{2} \sqrt{\frac{P}{D}} l \sinh ql \quad \text{Equation II.33.}$$

As $\Phi_{(p)} = 0$ when $q = \frac{(2n+1)\pi i}{2l}$ then $\cosh ql = 0$ hence,

$$\Phi'_{(\alpha)} = \frac{1}{2} \frac{(2n+1)\pi i}{2} \sinh \frac{(2n+1)\pi i}{2} \quad \text{Equation II.34.}$$

or by applying $\sinh iz = i \sin z$

$$\Phi'_{(\alpha)} = \frac{1}{2} \frac{(2n+1)\pi i}{2} i \sin \frac{(2n+1)\pi}{2} = \frac{1}{2} \frac{(2n+1)\pi i}{2} i (-1)^n = \frac{(2n+1)\pi (-1)^{n+1}}{4} \quad \text{Equation II.35.}$$

$f_{(\alpha)}$ is determined by applying $q = \frac{(2n+1)\pi i}{2l}$ to $f_{(p)} = c_0 \cosh qx$ so,

$$f_{(\alpha)} = c_0 \cosh \frac{(2n+1)\pi i}{2l} x \quad \text{Equation II.36.}$$

by applying $\cosh iz = \cos z$

$$f_{(\alpha)} = c_0 \cos \frac{(2n+1)\pi}{2l} x \quad \text{Equation II.37.}$$

Consider the case when $P = 0$, now $q = 0$, as $\cosh 0 = 1$ and $\sinh 0 = 0$, we get $\Phi'_{(\alpha)} = 1$, $f_{(\alpha)} = c_0$ and $e^{PT} = 1$, hence the first term in the series is c_0 .

Therefore by combining Equation II.31, II.32, II.35, and II.37, we can express,

$$c_{(x,t)} = c_0 + \sum_{n=0}^{\infty} c_0 \cos \left[\frac{(2n+1)\pi}{2l} x \right] \frac{4}{(2n+1)\pi (-1)^{n+1}} \cdot \exp \left[-\frac{D(2n+1)^2 \pi^2 t}{4l^2} \right] \quad \text{Equation II.38.}$$

Therefore,

$$c_{(x,t)} = c_0 \left\{ 1 - \frac{4}{\pi} \sum_{n=0}^{\infty} \frac{(-1)^n}{(2n+1)} \cos \frac{(2n+1)\pi x}{2l} \cdot \exp \left[-\frac{(2n+1)^2 \pi^2 Dt}{4l^2} \right] \right\} \quad \text{Equation II.39.}$$

Further as $M_t = A \int_{-l}^l c_{(x,t)} dt$ where A is the area of sample active in diffusion. So,

$$M_t = Ac_o \left\{ 2l - \frac{2.2.l.4}{\pi \cdot \pi} \sum_{n=0}^{\infty} \frac{(-1)^n}{(2n+1)^2} \left[\sin \frac{(2n+1)\pi x}{2l} \right]_{-l}^l \cdot \exp \left[-\frac{(2n+1)^2 \pi^2 Dt}{4l^2} \right] \right\}$$

Equation II.40.

As $\left[\sin \frac{(2n+1)\pi x}{2l} \right]_{-l}^l$ is 1 and -1 at the limits $x = l$ and $x = -l$ this may be rewritten as,

$$\frac{M_t}{2Alc_o} = \frac{M_t}{M_{\infty}} = \left\{ 1 - \frac{8}{\pi^2} \sum_{n=0}^{\infty} \frac{1}{(2n+1)^2} \cdot \exp \left[-\frac{(2n+1)^2 \pi^2 Dt}{4l^2} \right] \right\} \quad \text{Equation II.41.}$$

II.c. The equations of Muniandy and Thomas.

The following section is a description and possible derivation (based on that derived by Professor M. Braden) of the results of Muniandy and Thomas (although the initial paper was published by Southern and Thomas, 1980) who published a series of papers (Muniandy and Thomas, 1984,a, 1984,b, 1988, Thomas and Muniandy, 1987) on the water uptake of elastomers.

Consider an ideal elastomer containing an impurity which has reached an equilibrium water uptake. There is therefore a balance between the osmotic force to expand the droplet and the elastic restraining force. As previously described the osmotic force is attributable to the difference between the osmotic pressure of the external solution (π_o) and the osmotic pressure of the internal droplet solution (π_i). Therefore,

$$P = \pi_i - \pi_o \quad \text{Equation. II.42.}$$

where P is the pressure being applied by the droplet. Although Raoult's law is only applicable to dilute solutions it is used to calculate π_o and π_i (this seems reasonable when the system is at equilibrium, although initially at earlier times this is questionable for π_i).

Hence,

$$\pi_o = \frac{c_o RT}{M_o} \quad \text{and} \quad \pi_i = \frac{c_i RT \rho_w}{(c_w - s) M_i} \quad \text{Equation. II.43. \& II.44.}$$

where c_o is the concentration of salt in external solution, M_o molecular weight of salt in external solution, R Gas constant, T temperature, c_i concentration of impurity/salt in

rubber, ρ_w density of water, c_w over all concentration of water in material, s concentration of water in rubber matrix and M_i is the molecular weight of impurity/salt. Here, $c_w - s$, is the concentration of water in droplets within the material and so, $c_i \rho_w / (c_w - s)$, is the concentration of the impurity/salt within the droplets.

The droplets are assumed to be spherical and the rubber obey statistical theory and hence the pressure required to enlarge a spherical droplet (Gent and Lindley, 1958) is,

$$P = \frac{G}{2} \left(5 - \frac{4}{\lambda} - \frac{1}{\lambda^4} \right) \quad \text{Equation II.45,}$$

where G is the shear modulus and λ is the principle extension ratio.

It should be realised that the pressure to enlarge the droplet is equal to the restraining pressure exerted by the material. Hence substituting into Equation II.42,

$$\frac{G}{2} \left(5 - \frac{4}{\lambda} - \frac{1}{\lambda^4} \right) = \frac{c_i RT \rho_w}{(c_w - s) M_i} - \frac{c_o RT}{M_o} \quad \text{Equation II.46.}$$

Assuming the impurity/salt and the resultant droplets they produce are spherical then the volume within the material occupied by a impurity/salt is,

$$\frac{4}{3} \pi r^3 \quad \text{and the mass of these particles is} \quad \frac{4}{3} \pi r^3 \rho_i,$$

where r is the radius and ρ_i is the density of the impurity/salt. Therefore as the radius at equilibrium is going to be λr the increase in volume will be,

$$\frac{4}{3} \pi (r\lambda)^3 - \frac{4}{3} \pi r^3 \quad \text{or} \quad \frac{4}{3} \pi (\lambda^3 - 1) r^3.$$

Therefore the total increase in volume will be,

$$\frac{4}{3} \pi (\lambda^3 - 1) \sum n_j r_j^3$$

where n is the number of particles with radius r_j . Similarly the increase in mass will be,

$$\frac{4}{3} \pi (\lambda^3 - 1) \rho_w \sum n_j r_j^3$$

As the $c_w - s$ is the concentration of water in the material within the droplets this will be equal to the increase in mass of the droplets / volume of material (V), i.e.,

$$c_w - s = \frac{\frac{4}{3} \pi (\lambda^3 - 1) \rho_w \sum n_j r_j^3}{V} \quad \text{Equation II.47.}$$

As the initial volume of the impurity/salt in the material is,

$$V \frac{c_i}{\rho_i} = \frac{4}{3} \pi \sum n_j r_j^3 \quad \text{Equation II.48}$$

Therefore substituting equation II.48 into II.47 gives,

$$c_w - s = \frac{V \frac{c_i}{\rho_i} (\lambda^3 - 1) \rho_w}{V} \quad \text{Equation II.49.}$$

Which may be simplified to,

$$c_w - s = c_i (\lambda^3 - 1) \frac{\rho_w}{\rho_i} \quad \text{Equation II.50.}$$

Although assumptions are made during this derivation (that the droplets are spherical, the solutions are dilute, the volume of the material is constant and the rubber obeys statistical theory) which in the reality are unlikely to be met they establish an ideal model for the absorption process.

Muniandy and Thomas then consider the actual rate of the diffusion and define an 'apparent diffusion coefficient', based on the previously derived equations and a variation on Fick's Laws (for chemical potential), to describe the protracted uptake observed for the elastomers. The actual philosophy behind their approach assumes that there is a decrease in the droplet size with increasing depth into the material this then enables the establishing of a chemical potential gradient (stemming from the dilution of impurity/salt particles) through the material. The next part is best described in their own words;

'It is assumed that the water in the rubber phase immediately adjacent to the impurity droplet is in local equilibrium with the water in the droplet solution. The free energy of the water in the rubber phase in the neighbourhood of a droplet which in the rubber surface will be higher than that for a droplet nearer the rubber surface. Hence a free-energy gradient exists for the water dissolved in the rubber phase favouring movement of water into the body of the rubber.'

Muniandy and Thomas, (1984)

There is however a further problem the growth of the droplets gives rise to stresses in the rubber which lead to complex stress fields within the material. The effect of this stress field on the concentration of the water in the rubber is complex and avoided by using the chemical potential (μ) gradient rather than the normal concentration gradient as dealt with in the previously sections. This approach is based on a thermodynamic diffusion coefficient developed by Park (1950) using the modified expression for flux,

$$F = -D_T \left(\frac{s}{RT} \right) \left(\frac{\partial \mu}{\partial x} \right) \quad \text{Equation II.51.}$$

where s the concentration of water in the rubber phase. D_T is defined as the thermodynamic diffusion coefficient but as the concentration of water dissolved in the rubber is small it is taken to be the ordinary diffusion coefficient as defined previously by equation (Equation II.41). The problem is now somewhat simplified to determining the dependence of the chemical potential on the water present in the rubber matrix and that in the droplets.

As the system is not in a state of equilibrium equation II.42 has to be modified to,

$$P = \pi_i - \pi_o - p \quad \text{Equation II.52.}$$

where p is the elastic pressure restraining the droplet exerted by the material and P is the pressure applied by the droplet. With the chemical potential of being,

$$\mu = -PV_w \quad \text{Equation II.53.}$$

where V_w is the molecular volume of water. Equation 2.51 can therefore be written as,

$$F = D_T \left(\frac{sV_w}{RT} \right) \left(\frac{\partial P}{\partial x} \right) \quad \text{Equation II.54.}$$

The apparent diffusion coefficient (D_a) is then defined as the diffusion coefficient as for Fick's first law (equation II.1), so,

$$F = -D_a \frac{\partial c_w}{\partial x} \quad \text{Equation II.55.}$$

Hence combining equations II.54 and II.55 gives,

$$-D_a \frac{\partial c_w}{\partial x} = D_T \frac{sV_w}{RT} \frac{\partial P}{\partial x} \quad \text{Equation II.56.}$$

Which may be put in terms of the extension ratio (λ),

$$D_a = -D_T \frac{sV_w}{RT} \frac{\partial P}{\partial c_w} = -D_T \frac{sV_w}{RT} \frac{\partial P}{\partial \lambda} \frac{\partial \lambda}{\partial c_w} \quad \text{Equation II.57.}$$

There is however one further complication concerning the concentration of water in the rubber phase (s). As the rubber is stressed (under pressure) the water concentration will be less than that in the pure rubber. This is dealt with by applying Raoult's and Henry's laws assuming the system acts as a ideal gas. Raoult's Law,

$$P - \Delta P = XP \quad \text{Equation II.58.}$$

where P is the partial vapour pressure of pure liquid (water), X is the mole fraction of water and ΔP is the change vapour pressure at mole fraction X . Defining the water as the solvent (signified by N_i) and the impurity/salt as the solute (signified by N_w).

$$N_w = \frac{c_w - s}{M_w} \quad \text{and} \quad N_i = \frac{c_i}{M_i} \quad \text{Equation II.59 and II.60.}$$

Hence N_w/N_i mole fraction of water (X). Therefore,

$$\frac{P - \Delta P}{P} = 1 - \frac{\Delta P}{P} = X = \frac{N_w}{N_i} = 1 - \frac{N_i}{N_w} \quad \text{or} \quad \frac{\Delta P}{P} = \frac{N_i}{N_w} \quad \text{Equation II.61.}$$

From Henry's Law,

$$P = kX \quad \text{Equation II.62.}$$

where P is pressure, k is constant (for a particular material) and X is mole fraction, using P as the pressure of the water and for X use s and s_o as they are both proportional to the X of water in there respective materials, we get,

$$s_o = kP \quad \text{and} \quad s = k(P + \Delta P) \quad \text{so} \quad \frac{s}{s_o} = 1 + \frac{\Delta P}{P} \quad \text{Equation II.63.}$$

Therefore substituting equation II.61 into II.63 we get,

$$\frac{s}{s_o} = 1 + \frac{N_i}{N_w} \quad \text{Equation II.64.}$$

Which equation II.59 and II.60 are substituted into we get,

$$\frac{s}{s_o} = 1 + \frac{c_i M_w}{M_i (c_w - s)} \quad \text{Equation II.65.}$$

now substitute in equation II.50,

$$s = \frac{s_o}{1 + \frac{M_w \rho_i}{M_i \rho_w} \frac{1}{(\lambda^3 - 1)}} \quad \text{Equation II.66.}$$

The derivation of s in terms of s_o is problematic and can also give another equally valid solution where rather than adding the second term it is subtracted, this actually makes more sense in the derivation as equation II.63 then has a $P - \Delta P$ rather than $P + \Delta P$. It also creates a problem in that as λ tends to 1, (i.e. for increasingly pure systems) s tends to zero rather than s_o . Additionally it should be remembered that the effect of the stressing of the matrix was assumed insignificant when dealing with the difference it would have on D_T . It is therefore fairly apparent that this is a weak point in the over all argument.

Now returning to equation II.57, it is apparent that we need to find $\partial P/\partial \lambda$ and $\partial \lambda/\partial c_w$. The expression for $\partial \lambda/\partial c_w$ is derived by substituting, equation II.66 into a reordered version of equation II.50. So that,

$$c_w = \frac{\rho_w}{\rho_i} (\lambda^3 - 1) c_i + \frac{s_o}{1 + \frac{M_w \rho_i}{M_i \rho_w} \frac{1}{(\lambda^3 - 1)}} \quad \text{Equation II.67.}$$

This may then be differentiated in parts using the substitution $u=(\lambda^3-1)$ which yields,

$$\frac{\partial c_w}{\partial \lambda} = 3\lambda^2 \frac{\left\{ \frac{\rho_w}{\rho_i} c_i \left[(\lambda^3 - 1) + \frac{M_w \rho_i}{M_i \rho_w} \right]^2 + s_o \frac{M_w \rho_i}{M_i \rho_w} \right\}}{\left[(\lambda^3 - 1) + \frac{M_w \rho_i}{M_i \rho_w} \right]^2} \quad \text{Equation II.68.}$$

For the $\partial P/\partial \lambda$ equation II.52 is used and equation II.43, II.44 and II.45 (for p rather than P) substituted to yield,

$$P = \frac{c_o RT}{M_o} - \frac{c_i RT \rho_w}{(c_w - s)} - \frac{G}{2} \left(5 - \frac{4}{\lambda} - \frac{1}{\lambda^4} \right) \quad \text{Equation II.69.}$$

Then substituting in equation II.50,

$$P = \frac{c_o RT}{M_o} - \frac{RT \rho_i}{(\lambda^3 - 1) M_i} - \frac{G}{2} \left(5 - \frac{4}{\lambda} - \frac{1}{\lambda^4} \right) \quad \text{Equation II.70.}$$

This is then differentiated by parts substituting $u = \lambda^3-1$ in the first term to yield,

$$\frac{\partial P}{\partial \lambda} = \frac{-3\lambda^2 RT \rho_i}{(\lambda^3 - 1) M_i} - 2G \left(\frac{1}{\lambda^2} + \frac{1}{\lambda^5} \right) \quad \text{Equation II.71.}$$

Here the first term stems from the elastic pressure and the second from the osmotic pressure.

Equations II.68 and II.71 are then substituted into equation II.57, to give the solution for D_a as,

$$D_a = \frac{\frac{-sV_w D_T}{RT} \left[\frac{-3\lambda^2 RT \rho_i}{(\lambda^3 - 1)^2 M_i} - 2G \left(\frac{1}{\lambda^2} + \frac{1}{\lambda^5} \right) \right] \left[(\lambda^3 - 1) + \frac{M_w \rho_i}{M_i \rho_w} \right]^2}{3\lambda^2 \left\{ \frac{\rho_w c_i}{\rho_i} \left[(\lambda^3 - 1) + \frac{M_w \rho_i}{M_i \rho_w} \right]^2 + s_o \frac{M_w \rho_i}{M_i \rho_w} \right\}} \quad \text{Equation II.72.}$$

This is then simplified by defining A and k as,

$$A = \frac{M_w \rho_i}{M_i \rho_w} \quad \text{and} \quad k = \frac{\rho_w}{\rho_i} \quad \text{Equation II.73 and II.74.}$$

The s term is replaced by equation II.66, which results in

$$D_a = \frac{(\lambda^3 + A - 1)(\lambda^3 - 1)}{\left[(\lambda^3 + A - 1)^2 + \frac{s_o A}{kc_i} \right]} \left[\frac{D_T s_o V_w \rho_i}{(\lambda^3 - 1)^2 c_i k M_i} + \frac{2GD_T s_o V_w}{3c_i k RT} \left(\frac{1}{\lambda^4} + \frac{1}{\lambda^7} \right) \right] \quad \text{Equation II.75.}$$

This then simplified further by defining K₁ and K₂ as,

$$K_2 = \frac{D_T s_o V_w \rho_w}{c_i k^2 M_i} \quad \text{and} \quad K_1 = \frac{2GD_T s_o V_w}{3c_i k RT} \quad \text{Equation II.76 and II.77.}$$

Hence,

$$D_a = \frac{(\lambda^3 + A - 1)(\lambda^3 - 1)}{\left[(\lambda^3 + A - 1)^2 + \frac{s_o A}{kc_i} \right]} \left[\frac{K_2}{(\lambda^3 - 1)^2} + K_1 \left(\frac{1}{\lambda^4} + \frac{1}{\lambda^7} \right) \right] \quad \text{Equation II.78.}$$

As derived by Muniandy and Thomas, alternatively this may be expressed as,

$$\frac{D_a}{D_T} = \frac{\left[\frac{3\rho_i V_w}{(\lambda^3 - 1)M_i} + \frac{2GV_w}{RT} \left(\frac{1}{\lambda^4} + \frac{1}{\lambda^7} \right) \right] \left[(\lambda^3 - 1) + \frac{M_w \rho_i}{M_i \rho_w} \right]^3}{3 \left\{ \frac{\rho_w c_i}{\rho_i s_o} \left[(\lambda^3 - 1) + \frac{M_w \rho_i}{M_i \rho_w} \right]^2 + \frac{M_w \rho_i}{M_i \rho_w} \right\}} \quad \text{Equation II.79}$$

III. Nuclear Magnetic Resonance (NMR) Imaging.

Earlier work on water absorption by composites (Rothwell et al, 1984) recognised the benefit of using NMR imaging to determine the concentration, location, nature (whether it is free or tightly bound by H-bonded to a polar group) and mechanism behind the absorption process. The major benefit of employing the technique is that it is non-invasive and able to show regional concentrations of the fluid and its energy and see how they progress with time. In practice Rothwell et al's (1984) results also showed the dependence of the quality of the results on the equipment used. There have been great improvements in the equipment over the years and now much of the early promise of the technique is being realised although its limitations still remain.

In order to interpret the results a little background of how the image is generated is necessary, the detail of how they are generated is beyond the scope of the thesis and surplus to requirement for understanding how the technique may be applied. The basis of NMR imaging and spectrometry uses the magnetic dipoles of the proton, ^1H , although other magnetically active isotopes may also be used, such as ^{19}F , ^{31}P and ^{13}C (Ault and Dudek, 1976, Mansfield, 1988). These may orientate due to a magnetic field in two directions, a low energy (with the magnetic field) or a high energy (against the magnetic field), normally there is a balance between them with a few more existing in the lower energy state. When an electromagnetic wave (known as the radio frequency, RF, field or pulse) of the appropriate frequency is applied to the proton of the lower energy it will transfer to the higher energy (Ault and Dudek, 1976). Although the actual spins of the individual protons do not line up exactly with the applied field the overall result is a net magnetisation in the direction of the field when applied over a sample containing millions of protons. In spectroscopy the frequency is varied so different atoms and geometry excite at different times so forming a spectrum of intensity with time.

The time that the protons remain in this excited state will depend on the local magnetic and electric field conditions around the individual protons (Peterson et al, 1985, Mansfields, 1988), this relaxation time is known as T_1 . In practice this relaxation depends on the (Peterson et al, 1985);

- type of nucleus.
- resonance frequency, (field strength).
- temperature.
- mobility of observed spin.
- presence of large molecules.
- presence of paramagnetic ions or molecules.

The last 3 being dependent on the polymer / diffusing species system.

There are many different methods used in NMR imaging but the basic philosophy behind them may be described by considering the spin-lattice relaxation time, known as T_1 , a RF pulse is applied at 90° (in practice different angles are frequently used) to the magnetic field and the electron spins therefore reorient to the new direction. When the pulse is removed the spins move back to the original orientation. The intensity of the magnetic flux in the 90° direction is then measured so determining number of spins still in that direction.

Additionally a second pulse may be applied at 180° to the first pulse (again in practice this may alter) a finite time after the first pulse and this flips the spins over part way through the relaxation process. This has effect of normalising the effect of variations in the field strength within the NMR, the relaxation is now measured from this orientation in what is known as a spin-echo relaxation, T_2 .

In practice for NMR imaging there is a finite time before the detector can switch on, this is known as the acquisition time (T_e) and measured from the middle of the first pulse. Hence the spin-lattice method is capable of faster T_e times as it misses the re-focusing pulse of the spin-echo experiment, additionally it also depends on field strengths, pulse widths, pulse shape and control set up (Peterson et al, 1985). It should be realised that the relaxation may occur before the detector is on. As previously mentioned the time for this relaxation depends on the degree of mobility of the atom, a rigidly bound atom (i.e. on the chain of a glassy polymer backbone) will relax faster than a more freely bound atom (i.e. in a fluid), (Weisenberger and Koenig, 1990).

In general the application of the spin-echo method is used in the studies that have looked at diffusion as there are beneficial effects in normalising the image which outweigh the detrimental effect on T_e . There are numerous other factors affecting the imaging (such as gradients for the spatial dimensions) which are beyond the scope of this thesis. There are also many other techniques which have been applied (Weisenberger and Koenig, 1990) or could be applied that have some advantages over those briefly described above, but again space and applicability limit what is included.

A new technique that should additionally be mentioned is stray field magnetic imaging resonance imaging (STRAFI), which utilises the greater field gradients obtained outside the magnet which until recently were too unpredictably unstable to enable consistent imaging. This makes much shorter T_2 times (in the order of μs) observable when compared to the normal NMR (about 1 ms), (Baumann et al, 1993). Although this

technique has not been applied to any water absorption studies it has been used to look at the diffusion of acetone into (poly vinyl chloride), (Perry et al, 1994) where the potential of its ability to obtain very short T_2 times yielded information on the polymer dynamics (in terms of the polymer softening) during the case II absorption process.

IV. Polymer Solubility and Miscibility.

The solubility of a polymer or monomer in a solvent depends on the potential change in the free energy of the system (Brandrup and Immergut, 1975).

$$\Delta G = \Delta H - T\Delta S \quad \text{Equation IV.1.}$$

Where, ΔG is the change in gibbs free energy.

ΔH is the change in enthalpy on mixing.

T is temperature.

ΔS is the change in entropy on mixing.

For the dissolution of a polymer in a liquid the change in enthalpy is always large and positive. It is therefore the entropy term controls whether the polymer will form a solution with the solvent. Hildebrand (1949) connected the ΔH term to the energy of vaporisation of each component (ΔE_1 or ΔE_2) otherwise known as the cohesive energy and the relative volume fraction of each component (ϕ_1 or ϕ_2) in the mixture.

$$\Delta H = V_m \left[(\Delta E_1 / V_1)^{1/2} - (\Delta E_2 / V_2)^{1/2} \right]^2 \phi_1 \phi_2 \quad \text{Equation IV.2.}$$

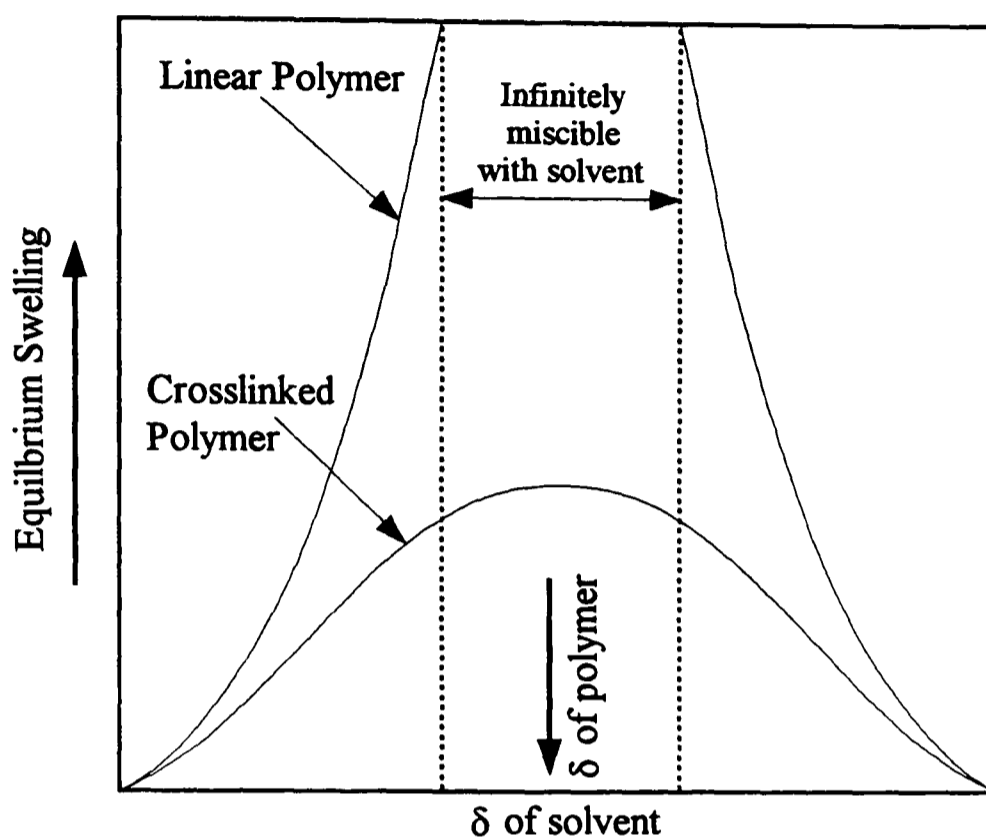
Where V is the molecular volume of each component.

V_m is the total volume of the mixture.

In order for dissolution to be favourable ΔG has to be negative, therefore ΔH should be small. From equation IV.2, we can see that the ΔH is dependent on the square of the difference between the square roots of the cohesive energy densities ($\Delta E/V$). So in order to ensure dissolution the cohesive energy densities should be as similar as possible. It is convenient to use a solubility parameter ($\delta = (\Delta E/V)^{1/2}$) with the dissolution being favoured where $(\delta_1 - \delta_2)^2$ is small.

The relationship between the solubility parameter and dissolution is demonstrated in figure IV.1 as with a linear polymer (or monomer) dissolving in a solvent of similar solubility. For crosslinked polymers the polymer can not form a infinite dissolution as with the linear polymer, due to the restraint of the crosslinks, but swells in the presence of the solvent.

Figure IV.1. Equilibrium swelling as a function of solubility parameter of the solvent for linear and cross linked polymers (Based on Fig 7.1, page 130, Van Krevelen, 1976).



Solubility parameters can be found experimentally by a number of different methods, namely, from heat of evaporation, thermal coefficients, relationship between pressure and temperature, van der Waals' Gas constant, critical pressure, surface tension and Kauri-Butanol Values (Brandrup and Immergut, 1975). They can also be calculated from the structural formula of the polymer with a reasonable degree of accuracy (Brandrup and Immergut, 1975 and Van Krevelen, 1976).

Solubility parameter calculations are based on the summation of the contribution of the different structural groups of the monomer/polymer. This is expressed in below (Brandrup 1975),

$$\delta = d \sum \Psi / M \quad \text{Equation IV.3.}$$

where, d is the density.

Ψ is the group molar attraction constant.

M is the molecular weight of the molecule.

It should be noted this approach does not apply to materials which are strongly hydrogen bonded such as alcohol's, amines and carboxylic acids.

Small (1953) and Hoy (1970) have published a list of the contributions of various groups to the solubility parameter. These are used to calculate the solubility parameter for methyl Methacrylate as shown in table IV.1. The values calculated from Small (18.78 $J^{1/2}/cm^{3/2}$) and Hoy (16.90 $J^{1/2}/cm^{3/2}$) compare fairly well to that obtained experimentally of 18.00 $J^{1/2}/cm^{3/2}$ (Brandrup and Immergut, 1975).

Table IV.1. The calculation of the solubility parameter of methyl methacrylate monomer from Small's (1953) and Hoy's (1970) group molar attraction constants.

Group	Ψ , Small	Ψ , Hoy
CH ₂ =	388.74	258.90
CH ₃ -	437.84	301.38
>C=	38.87	172.91
>C=O	562.65	538.02
-O-	143.22	235.25
CH ₃ -	437.84	301.38
δ $J^{1/2}/cm^{3/2}$	18.78	16.90

Molecular Formula CH₂=C(CH₃)-CO-O-CH₃
Molecular Weight 100.12 g/mol
Density 0.936 g/ml

Some solubility parameters of other methacrylates and other materials are shown in table IV.2, together with the solubility parameters for some other materials used within this study.

The solubility parameter is not as simple as has so far been indicated, as different solvent and polymers may have different forces that contribute to the overall solubility. So far It is assumed that the dispersion forces dominate the solubility of the solvent/polymer rather than any polar or hydrogen bonding interactions. When these are taken in to account the Cohesive energy (ΔE) becomes summation of the different forces,

$$\Delta E = \Delta E_d + \Delta E_p + \Delta E_h \quad \text{Equation IV.4.}$$

where, ΔE_d is the contribution of dispersion forces.

ΔE_p is the contribution of the polar forces.

ΔE_h is the contribution of the hydrogen bonding.

Table IV.2. Solubility parameters calculated from Small (1953) and Hoy (1970) values for the group molar attractions with comparison to experimental values where available.

Material	Monomer δ , J ^{1/2} /cm ^{3/2}			Polymer δ , J ^{1/2} /cm ^{3/2}		
	Small	Hoy	Expt	Small	Hoy	Expt
Methyl Methacrylate	18.78	16.90	18.00	19.74	20.30	17.4-27.2
Ethyl Methacrylate	18.33	16.68	16.98	19.00	19.43	15.9-27.2
n-Butyl Methacrylate	17.68	16.37	16.78	19.18	19.47	15.1-20.2
n-Hexyl Methacrylate	17.44	16.32	-	15.65	15.82	-
2-EthylHexyl Methacrylate	17.37	16.32	-	-	-	-
Octyl Methacrylate	17.45	16.46	-	-	-	-
C12 Methacrylate	17.06	16.25	-	17.33	17.38	-
C13 (1-Tridecyl) Methacrylate	17.16	16.39	-	19.24	19.65	-
C16 Methacrylate	16.86	16.17	-	17.31	17.31	-
2-hydroxyethyl methacrylate	-	19.92	-	-	-	-
2-ethoxyethyl methacrylate	18.22	17.49	-	-	-	-
Ethylene glycol di methacrylate	19.53	18.81	-	-	-	-
Water	-	-	47.88	-	-	-
70/30 butadiene styrene	-	-	-	-	-	17.35
60/40 butadiene styrene	-	-	-	-	-	17.74
poly isoprene 1,4-cis	-	-	-	-	-	16.47

And consequently the solubility parameter (δ) is,

$$\delta^2 = \delta_d^2 + \delta_p^2 + \delta_h^2 \quad \text{Equation IV.5.}$$

where, δ_d is the contribution of the dispersion forces.

δ_p is the contribution of the polar forces.

δ_h is the contribution of the hydrogen bonding.

Thus Hildebrand's (1949) equation IV.2, becomes (Van Krevelen, 1976),

$$\Delta H = \phi_1 \phi_2 \left[(\delta_{d1} - \delta_{d2})^2 + (\delta_{p1} - \delta_{p2})^2 + (\delta_{h1} - \delta_{h2})^2 \right] \quad \text{Equation IV.6.}$$

As with the single solubility parameter the greatest chance of solubility occurs when the solubility parameters are similar, i.e. $\delta_{d1} \approx \delta_{d2}$, $\delta_{p1} \approx \delta_{p2}$ and $\delta_{h1} \approx \delta_{h2}$.

Unfortunately the different contributions of the solubility parameter cannot be directly measured. There are numerous methods available for indirectly determining the different parts of the solubility parameter (Crowley et al, 1966, Crowley et al, 1967, and Hansen 1967).

The solubility parameter components may be predicted from the molecular structure. Although it should be realised that these predictions are based on localised structural information and so complicated influences of different structural on the overall polar and hydrogen bonding properties are ignored. The calculated therefore produces on a rough guide to the different components (Van Krevelen, 1976).

The predication of the solubility parameter components is based on three equations.

$$\delta_d = \frac{\sum F_{di}}{V} \quad \text{Equation IV.7.}$$

$$\delta_p = \frac{\sqrt{\sum F_{pi}^2}}{V} \quad \text{Equation IV.8.}$$

$$\delta_h = \frac{\sqrt{\sum E_{hi}}}{V} \quad \text{Equation IV.9.}$$

where F_{di} is the structural groups dispersive component.

F_{pi} is the structural groups polar component.

E_{hi} is H bonding energy of the structural group.

V is the molecular Volume.

This situation is however complicated by the effect of molecular symmetry with both the δ_p and δ_h being dependent on the number of planes of symmetry. The δ_p component is reduced by a factor of 0.5 for one plane of symmetry, 0.25 for 2 planes and 0 for more than 2 planes of symmetry. For δ_h the situation is more obscure but several planes mean the overall contribution of δ_h will be 0.

The data published by Van Krevelen (1976) can be used to calculate a the different components of δ as shown in Table IV.3. The value for the overall δ is between the two values previously calculated in Table IV.2, (16.90 and 18.78 J^{1/2}cm^{3/2}) and compares favourably with the experimental determined value of 18.00 J^{1/2}cm^{3/2}.

A summary of the calculation of the solubility parameter components is shown in table IV.4 for some other materials.

Table IV.3. Calculation of the solubility parameter components from parts based on Van Krevlen (1976).

Component	Dispersive	Polar	H Bond	Overall
Groups	F _{di}	F _{pi}	E _{hi}	-
CH ₂ =	400	0	0	-
CH ₃ -	420	0	0	-
>C=	70	0	0	-
-COO-	390	490	7000	-
CH ₃ -	420	0	0	-
δ ,	δ_d	δ_p	δ_h	δ
J ^{1/2} cm ^{3/2}	15.89	4.58	8.09	18.41

Molecular formula CH₂=C(CH₃)-CO-O-CH₃.

Molecular Weight 100.12 g/mol.

Density 0.936 g/ml.

Molecular Volume 107 ml/mol.

Table IV.4. The calculated data of the solubility parameter and its different components as calculated from Van Kevelen 1976.

Material	Monomer δ , J ^{1/2} cm ^{3/2}				Polymer δ , J ^{1/2} cm ^{3/2}			
	δ_d	δ_p	δ_h	δ	δ_d	δ_p	δ_h	δ
Methyl Methacrylate	15.89	4.58	8.09	18.41	18.6	5.81	9.11	21.54
Ethyl Methacrylate	15.83	3.94	7.50	17.95	18.0	4.81	8.29	20.45
n-Butyl Methacrylate	15.71	3.07	6.62	17.32	18.4	3.79	7.36	20.18
n-Hexyl Methacrylate	15.79	2.54	6.02	17.09	15.1	2.54	6.02	16.47
2- EthylHexyl Methacrylate	15.96	2.20	5.61	17.06	-	-	-	-
Octyl Methacrylate	16.01	2.19	5.59	17.10	-	-	-	-
C12 Methacrylate	15.92	1.67	4.89	16.74	16.8	1.82	5.10	17.74
C13 (1-Tridecyl) Methacrylate	16.07	1.59	4.77	16.84	17.1	1.75	5.00	17.97
C16 Methacrylate	15.91	1.36	4.40	16.57	16.9	1.48	4.59	17.61
2-hydroxyethyl methacrylate	16.13	5.56	14.65	22.49	-	-	-	-
2-ethoxyethyl methacrylate	16.02	3.88	7.83	18.25	-	-	-	-
Ethylene glycol Di methacrylate	16.42	1.84	8.61	18.63	-	-	-	-
1,6 hexanediol di methacrylate	16.42	1.36	7.42	18.07	-	-	-	-
do decyl di methacrylate	16.93	1.12	6.71	18.25	-	-	-	-

Appendix V. Modification of theory of water uptake into elastomers for small strains.

The modification of the equations for small strains, enables the solving of equation II.50.

$$c_w - s = c_i (\lambda^3 - 1) \frac{\rho_w}{\rho_i} \quad \text{Equation II.50.}$$

By utilises equation II.46.

$$\frac{G}{2} \left(5 - \frac{4}{\lambda} - \frac{1}{\lambda^4} \right) = \frac{c_i RT \rho_w}{(c_w - s) M_i} - \frac{c_o RT}{M_o} \quad \text{Equation II.46.}$$

Which was based on equation II.42,

$$P = \pi_i - \pi_o \quad \text{Equation II.42.}$$

and,

$$\pi_o = \frac{c_o RT}{M_o} \quad \text{and} \quad \pi_i = \frac{c_i RT \rho_w}{(c_w - s) M_i} \quad \text{Equation II.43, and II.44.}$$

This involves the modification of the term for the elastic restraint term (equation II.45).

$$P = \frac{G}{2} \left(5 - \frac{4}{\lambda} - \frac{1}{\lambda^4} \right) \quad \text{Equation II.45.}$$

By assuming the deformation around the droplet is small so,

$$\lambda = 1 + \varepsilon \quad \text{Equation V.1.}$$

where ε is the strain. Hence,

$$P = \frac{G}{2} \left(5 - \frac{4}{1 + \varepsilon} - \frac{1}{(1 + \varepsilon)^4} \right) \quad \text{Equation V.2.}$$

As $(1 + \varepsilon)^{-1} = 1 - \varepsilon$ this may be expressed as,

$$P = \frac{G}{2} \left(5 - 4 + 4\varepsilon - (1 - 4\varepsilon + 6\varepsilon^2 - 4\varepsilon^3 + \varepsilon^4) \right) \quad \text{Equation V.3.}$$

Then as small strains are assumed (i.e. ε is close to zero) the terms ε^2 , ε^3 and ε^4 terms are assumed insignificant compared to ε . Therefore,

$$P = 4G\varepsilon \quad \text{Equation V.4.}$$

Applying this into equation II.42, with II.44, gives.

$$4G\varepsilon = \frac{c_i RT \rho_w}{(c_w - s) M_i} - \pi_o \quad \text{Equation V.5.}$$

Using the same approach to equation. II.50. yields,

$$c_w - s = c_i \left((1 + \varepsilon)^3 - 1 \right) \frac{\rho_w}{\rho_i} \quad \text{Equation V.6.}$$

and expanding it out gives,

$$c_w - s = c_i \left((1 + 3\varepsilon + 3\varepsilon^2 + \varepsilon^3) - 1 \right) \frac{\rho_w}{\rho_i} \quad \text{Equation V.7.}$$

which is simplified by ignoring ε^2 , and ε^3 .

$$c_w - s = 3c_i \varepsilon \frac{\rho_w}{\rho_i} \quad \text{Equation V.8.}$$

or,

$$\varepsilon = \frac{(c_w - s)\rho_i}{3c_i\rho_w} \quad \text{Equation V.9.}$$

Applying this into equation V.5.

$$4G \frac{(c_w - s)\rho_i}{3c_i\rho_w} = \frac{c_i RT \rho_w}{(c_w - s)M_i} - \pi_o \quad \text{Equation V.10.}$$

By letting $z = c_w - s$ this may be expressed as,

$$\frac{4G\rho_i}{3c_i\rho_w} z^2 + \pi_o z - \frac{c_i RT \rho_w}{M_i} = 0 \quad \text{Equation V.11.}$$

or by multiplying by $\frac{3c_i\rho_w}{4G\rho_i}$,

$$z^2 + z \frac{3c_i\rho_w\pi_o}{4G\rho_i} - \frac{3RTc_i^2\rho_w^2}{4G\rho_i M_i} = 0 \quad \text{Equation V.12.}$$

Then let $\alpha = \frac{3RTc_i\rho_w}{4G\rho_i}$, hence,

$$z^2 + z \frac{\alpha\pi_o}{RT} - \frac{\alpha c_i \rho_w}{M_i} = 0 \quad \text{Equation V.13.}$$

Which may be solved as a quadratic equation, so,

$$z = \frac{-\frac{\alpha\pi_o}{RT} \pm \sqrt{\frac{\alpha^2\pi_o^2}{R^2T^2} + \frac{4\alpha c_i \rho_w}{M_i}}}{2} \quad \text{Equation V.14.}$$

As a negative value of z ($c_w - s$) is a nonsense hence,

$$z = -\frac{\alpha\pi_o}{2RT} + \frac{1}{2} \sqrt{\frac{\alpha^2\pi_o^2}{R^2T^2} + \frac{4\alpha c_i\rho_w}{M_i}} \quad \text{Equation V.15.}$$

or,

$$z = -\frac{\alpha\pi_o}{2RT} + \left[\frac{\alpha^2\pi_o^2}{4R^2T^2} + \frac{\alpha c_i\rho_w}{M_i} \right]^{\frac{1}{2}} \quad \text{Equation V.16.}$$

Which is equivalent to,

$$z = -\frac{\alpha\pi_o}{2RT} + \frac{\alpha\pi_o}{2RT} \left[1 + \frac{\alpha c_i\rho_w}{M_i} \frac{4R^2T^2}{\alpha^2\pi_o^2} \right]^{\frac{1}{2}} \quad \text{Equation V.17.}$$

and,

$$z = \frac{\alpha\pi_o}{2RT} \left\{ \left[1 + \frac{4R^2T^2 c_i\rho_w}{\alpha M_i \pi_o^2} \right]^{\frac{1}{2}} - 1 \right\} \quad \text{Equation V.18.}$$

therefore,

$$c_w - s = \frac{\pi_o}{2RT} \frac{3RT c_i\rho_w}{4G\rho_i} \left\{ \left[1 + \frac{4R^2T^2 c_i\rho_w}{M_i \pi_o^2} \frac{4G\rho_i}{3RT c_i\rho_w} \right]^{\frac{1}{2}} - 1 \right\} \quad \text{Equation V.19.}$$

or,

$$c_w = \frac{3c_i\rho_w\pi_o}{8G\rho_i} \left\{ \left[1 + \frac{16RTG\rho_i}{3M_i\pi_o^2} \right]^{\frac{1}{2}} - 1 \right\} + s \quad \text{Equation V.20.}$$

Alternatively this may be expressed in terms of c_o by applying equation II.44, so,

$$c_w = \frac{3RT c_i\rho_w c_o}{8G\rho_i M_o} \left\{ \left[1 + \frac{16G\rho_i M_o^2}{3RT M_i c_o^2} \right]^{\frac{1}{2}} - 1 \right\} + s \quad \text{Equation V.21.}$$

Consider when π_o tends to zero (i.e. dilute solutions), then $\frac{16RTG\rho_i}{3M_i\pi_o^2}$ becomes much greater than 1 hence we ignore the first term. Therefore,

$$c_w = \frac{3c_i\rho_w\pi_o}{8G\rho_i} \left[\frac{16RTG\rho_i}{3M_i\pi_o^2} \right]^{\frac{1}{2}} + s \quad \text{Equation V.22.}$$

or,

$$c_w = \frac{c_i\rho_w}{2} \left[\frac{3RT}{M_iG\rho_i} \right]^{\frac{1}{2}} + s \quad \text{Equation V.23.}$$

Alternatively as π_o tends to high osmolarity (large values) then $\frac{16RTG\rho_i}{3M_i\pi_o^2}$ becomes very

small (i.e. $\ll 1$), hence may be expanded by a rational index, i.e. is $\beta = \frac{16RTG\rho_i}{3M_i\pi_o^2}$,

$$\left(1 + \frac{\beta}{\pi_o^2} \right)^{\frac{1}{2}} = 1 + \frac{1}{2} \frac{\beta}{\pi_o^2} - \frac{1}{8} \frac{\beta^2}{\pi_o^4} + \frac{3}{48} \frac{\beta^3}{\pi_o^6} - \dots \quad \text{Equation V.24.}$$

Taking just the 1st term as the effect the second, third, etc will be comparatively small as π_o is large, therefore equation V.20, is,

$$c_w = \frac{3c_i\rho_w\pi_o}{8G\rho_i} \left\{ \left[1 + \frac{16RTG\rho_i}{6M_i\pi_o^2} \right] - 1 \right\} + s \quad \text{Equation V.25.}$$

Which may be simplified to,

$$c_w = \frac{RTc_i\rho_w}{M_i} \frac{1}{\pi_o} + s \quad \text{Equation V.26.}$$

Again this may be defined in terms of c_o by applying equation II.44, as,

$$c_w = \frac{c_i\rho_w M_o}{M_i} \frac{1}{c_o} + s \quad \text{Equation V.27.}$$